

Light and Heat:  
Nonlocal Aspects in Conformal Field Theories

Thesis by  
Murat Kolođlu

In Partial Fulfillment of the Requirements for the  
Degree of  
Ph.D. in Physics

**Caltech**

CALIFORNIA INSTITUTE OF TECHNOLOGY  
Pasadena, California

2019  
Defended May 20, 2019

© 2019

Murat Kolođlu

ORCID: 0000-0002-5082-8434

All rights reserved

*Aileme.*

## ACKNOWLEDGEMENTS

This thesis is the culmination of years of work and good fortune. I owe my good fortune to the many incredible individuals who have shaped me and my Ph.D. years. With customary injustice, I have attempted to condense my gratitude to the confines of a few pages.

No amount of effort would suffice to express my indebtedness to my advisor, David Simmons-Duffin. He has taught me so much physics, and provided me with endless opportunities. He has been very generous in sharing his brilliant ideas and inviting me to join in to explore them. If there is a limit to his intelligence, his ability to explain the arcane, and his humility, I am yet to find it. I could not have wished for a better advisor. I only hope that someday I will be able to advise others half as well.

I am also indebted to the members of my thesis committee, who have been constant sources of guidance, each in their individual ways. Thanks to Sergei Gukov for initiating me to the beauty of theoretical physics, and for providing me with my first projects as my unofficial advisor in the earlier years of graduate school. Thanks to Hiroshi Ooguri for his passion for sharing his vast knowledge of physics, and for providing me with crucial advice and opportunities. Thanks to Maria Spiropulu for her unabating drive for motivating and pushing me towards the milestones of graduate school.

This thesis comprises of research I have undertaken with the most talented and wonderful collaborators I could have conceived of. I would like to thank Luca Iliesiu, Petr Kravchuk, Raghu Mahajan, Eric Perlmutter, and Alexander Zhiboedov for embarking on these journeys with me. It has been a pleasure to think about physics with each of you, and I am looking forward to our future collaborations. I would like to especially thank Eric Perlmutter for his friendship, wisdom, and advice, and Petr Kravchuk and Luca Iliesiu for extended discussions on physics, and for their camaraderie.

Caltech has been my home for the years of my Ph.D. I would like to thank the physics department and the graduate office for their unmitigated support. A special thanks to Sofie Leon for guiding me through the most tumultuous times. Many thanks to Carol Silberstein for her uncanny ability to keep everything running smoothly and fix virtually any problem.

Before Caltech, I was lucky to have been a student of Steven J. Miller and David Tucker-Smith, who have introduced me to mathematical and scientific research. I

would like to thank them for preparing me for graduate school, for rooting for me, and for their wise counsel.

Graduate school would not be complete without the fellow explorers of physics and denizens of the fourth floor of Lauritsen. I am lucky to have so many to thank, who have been with me on this journey together. Let me start off by thanking Ingmar A. Saberi; his sheer brilliance and ability elucidate any topic have been an inspiration — not to overshadow his friendship. No less to mention are Tristan McKinney, long-time officemate Enrico Herrmann, Matthew Heydeman, Nicholas Hunter-Jones, Du Pei, Lev Spodyneiko, Alex Turzillo, as well as Mykola Dedushenko, Abhijit Gadde, Ying Hsieh-Lin, and Natalie Paquette, and others I am sure to have forgotten to mention. I have shared many laughs with and learned endlessly from each of them.

My days would have been bleak without the extraordinary friendship of certain exceptional individuals. The undying support and sagely advice of my old friends Marcello Halitzer, Nargis Sakhibova, and Jorge Tena have kept me going as fortunes waxed and waned. Andrei Pissarenko has been a constant friend, often against the backdrops of sea, sun, music, and beach volleyball. On the topic of volleyball, thanks to Ron Appel for endless amounts of it. Thanks to Christian Kettenbeil, Eloïse Marteau, Alysha de Souza, Thibault Filinois, John Steeves, Niccolo Cymbalist, Mélanie Delapierre, Kristina Hogstrom, Hayden Burgoyne, and the rest of Team Europe for always being up for enjoying the bountiful good weather. Thanks to Kathleen Blake for cheering me on and putting up with me through some of the hard times. Thanks to Calvin Sam and Jan Rys for many adventures in Los Angeles, and elsewhere. Also thanks to Eric Carlson for being the finest flatmate, and a finer friend.

For my oldest friend Talat A. Çıkıkçı, and for Emre Sıraçe and Hasan Sağır, and especially for my true oldest friend (the other) M. Koloğlu, I can hardly find the right words. They have been my constant connection to home, to the gentle times of childhood, to the bliss of summers ignorant of the passage of time. Nothing can replace our adventures, the banter, and the paradise that is Çeşme.

During a fortuitous escape from the demands of graduate school, I have been incredibly lucky to have met the truly special Laura Rodrigues. On a good day, her presence brings joy, on a lesser day, staunch support. Her talent and drive are inspirational. Thank you for being by my side, through the most trying of times, and for the best of times.

At the heart of it all, anything I have ever achieved is ultimately thanks to my family.

Their love, wisdom, and sacrifices have led me to the path I have taken. If I have been a wise man, they set me up for it. If I have been a fool, I could afford to by their grace. My resourceful, wise mother ıgdem, for whom no sacrifice was too big for her children, who dedicated her life to us. My brilliant, resolute father ınar, who taught me to unlock the hidden truths of the world. My joyous brother Mehmet, insightful beyond his years, who has always been the delight of our family. This thesis is dedicated to them. Sizin hakkınız lisan-ı kal ile izah edilemez.

## ABSTRACT

The majority of this thesis is dedicated to certain nonlocal aspects of conformal field theories (CFTs). Two main directions are the study of CFTs on a particular globally-nontrivial spacetime, and the study of particular nonlocal observables in CFTs.

The first aspect concerns with the study of CFTs on a spacetime with imaginary periodic time, equivalent to the study of static properties of a CFT at finite temperature. We introduce bootstrap techniques for determining finite-temperature data of CFTs, and make predictions for the 2+1-dimensional  $O(N)$  model at large  $N$  and the 2+1-dimensional Ising model.

The second aspect is the study of light-ray operators in CFTs — operators that are supported on light-like trajectories. We propose the “stringy equivalence principle,” stating that coincident gravitational shocks commute, as a generalization of the strong equivalence principle of Einstein’s General Relativity that must hold in all consistent theories of gravity. Analyzing properties of light-ray operators dual to gravitational shocks, we prove the stringy equivalence principle for holographic CFTs dual to gravity in Anti-de Sitter (AdS) spacetimes. We place stringent constraints on effective theories of gravity. We also derive an operator product expansion (OPE) for light-ray operators in CFT, by which two light-ray operators on the same light-sheet can be expanded as a sum of single light-ray operators. Light-ray operators model detectors — such as calorimeters. We use the light-ray OPE to compute event shape observables suitable for conformal collider physics in 3+1-dimensional  $\mathcal{N} = 4$  super-Yang-Mills Theory.

An additional part of this thesis determines the low energy vacua of two-dimensional maximal super-Yang-Mills theory, which describes the dynamics of stacks of D-strings in Type IIB string theory. By computing an invariant of the renormalization group (RG) flow from high to low energy — a modified thermal partition function named the refined elliptic genus — we prove the existence of multiple vacua, and identify the superconformal field theories capturing their dynamics. The vacua correspond to bound states of  $(p, q)$ -strings in Type IIB string theory. Our computation serves as a check of the strong-weak S-duality of the Type IIB string.

## PUBLISHED CONTENT AND CONTRIBUTIONS

The chapters of my thesis are adapted from the published articles [1–5] listed below. The articles [2–5] are the joint products of their respective collaborations; each author has contributed equally. The article [1] is my solitary endeavor.

- <sup>1</sup>M. Koloğlu, “Quantum Vacua of 2d Maximally Supersymmetric Yang-Mills Theory”, *Journal of High Energy Physics* **11**, 140 (2017) [10.1007/JHEP11\(2017\)140](https://doi.org/10.1007/JHEP11(2017)140), [arXiv:1609.08232](https://arxiv.org/abs/1609.08232) [[hep-th](#)].
- <sup>2</sup>L. Iliesiu, M. Koloğlu, R. Mahajan, E. Perlmutter, and D. Simmons-Duffin, “The Conformal Bootstrap at Finite Temperature”, *Journal of High Energy Physics* **10**, 070 (2018) [10.1007/JHEP10\(2018\)070](https://doi.org/10.1007/JHEP10(2018)070), [arXiv:1802.10266](https://arxiv.org/abs/1802.10266) [[hep-th](#)].
- <sup>3</sup>L. Iliesiu, M. Koloğlu, and D. Simmons-Duffin, “Bootstrapping the 3d Ising model at finite temperature”, (2018), [arXiv:1811.05451](https://arxiv.org/abs/1811.05451) [[hep-th](#)].
- <sup>4</sup>M. Koloğlu, P. Kravchuk, D. Simmons-Duffin, and A. Zhiboedov, “Shocks, Superconvergence, and a Stringy Equivalence Principle”, (2019), [arXiv:1904.05905](https://arxiv.org/abs/1904.05905) [[hep-th](#)].
- <sup>5</sup>M. Koloğlu, P. Kravchuk, D. Simmons-Duffin, and A. Zhiboedov, “The light-ray OPE and conformal colliders”, (2019), [arXiv:1905.01311](https://arxiv.org/abs/1905.01311) [[hep-th](#)].



## TABLE OF CONTENTS

|  |      |
|--|------|
| Acknowledgements . . . . .   | iv   |
| Abstract . . . . .   | vii  |
| Published Content and Contributions . . . . .  | viii |
| Table of Contents . . . . .  | ix   |
| Chapter I: Introduction . . . . .  | 1    |
| 1.1 New and Old Frontiers in Conformal Field Theories . . . . .                      | 4    |
| 1.2 Summary of this Thesis . . . . .   | 12   |
| Chapter II: The Conformal Bootstrap at Finite Temperature . . . . .                  | 18   |
| 2.1 Introduction . . . . .   | 18   |
| 2.2 CFTs at nonzero temperature . . . . .  | 23   |
| 2.3 A Lorentzian inversion formula . . . . .   | 32   |
| 2.4 Applications I: Mean Field Theory . . . . .                                      | 44   |
| 2.5 Applications II: Large $N$ CFTs . . . . .  | 48   |
| 2.6 Large-spin perturbation theory . . . . .   | 57   |
| 2.7 Conclusions and future work . . . . .  | 80   |
| Chapter III: Bootstrapping the 3d Ising Model at Finite Temperature . . . . .        | 85   |
| 3.1 Introduction . . . . .   | 85   |
| 3.2 Review . . . . .   | 86   |
| 3.3 Method and results . . . . .   | 94   |
| 3.4 Details of the computation . . . . .   | 102  |
| Chapter IV: Shocks, Superconvergence, and a Stringy Equivalence Principle . . . . .  | 121  |
| 4.1 Introduction . . . . .   | 121  |
| 4.2 Shocks and superconvergence in flat space . . . . .                              | 126  |
| 4.3 Event shapes in CFT and shocks in AdS . . . . .                                  | 148  |
| 4.4 Products of light-ray operators and commutativity . . . . .                      | 157  |
| 4.5 Computing event shapes using the OPE . . . . .                                   | 183  |
| 4.6 Discussion . . . . .   | 221  |
| Chapter V: The Light-ray OPE and Conformal Colliders . . . . .                       | 229  |
| 5.1 Introduction . . . . .   | 229  |
| 5.2 Kinematics of light-ray operators and event shapes . . . . .                     | 237  |
| 5.3 The light-ray-light-ray OPE . . . . .  | 248  |
| 5.4 Commutativity . . . . .  | 276  |
| 5.5 The celestial block expansion . . . . .  | 283  |
| 5.6 Contact terms . . . . .  | 289  |
| 5.7 Event shapes in $\mathcal{N} = 4$ SYM . . . . .                                  | 294  |
| 5.8 Discussion and future directions . . . . .                                       | 322  |
| Chapter VI: Quantum Vacua of 2d Maximally Supersymmetric Yang-Mills Theory . . . . . | 329  |
| 6.1 Introduction and summary . . . . .   | 329  |
| 6.2 The structure of vacua . . . . .   | 337  |

|                                     |   |     |
|-------------------------------------|---|-----|
| 6.3                                 | Elliptic genera of $SU(N)/\mathbb{Z}_N$ gauge theories  | 350 |
| 6.4                                 | Elliptic genus of $\text{MSYM}_2$   | 356 |
| 6.5                                 | Elliptic genera of $\mathcal{N} = (8, 8)$ sigma models  | 368 |
| 6.6                                 | Conclusions and future directions   | 375 |
| Appendix A: Appendices to Chapter 2 |   | 377 |
| A.1                                 | Estimating $b_T$ from $Z_{S^1_\beta \times S^{d-1}}$  | 377 |
| A.2                                 | One-point functions on $S^1_\beta \times \mathbb{R}^{d-1}$ from one-point functions on $S^1_\beta \times S^{d-1}$ | 380 |
| A.3                                 | Thermal mass in the $O(N)$ model at large $N$   | 382 |
| A.4                                 | Subtleties in dimensional reduction of CFTs   | 382 |
| A.5                                 | Fixed point of self-corrections of double-twist families  | 383 |
| Appendix B: Appendix to Chapter 3   |   | 385 |
| B.1                                 | Details of the Monte-Carlo simulation   | 385 |
| Appendix C: Appendices to Chapter 4 |   | 386 |
| C.1                                 | More on superconvergence in flat space  | 386 |
| C.2                                 | Noncommutativity of light-transformed scalars   | 390 |
| C.3                                 | Fourier transform of two-point functions  | 392 |
| C.4                                 | Details on the light-transform of three-point structures  | 393 |
| C.5                                 | Structures for the sum rule   | 395 |
| Appendix D: Appendices to Chapter 5 |   | 396 |
| D.1                                 | Notation  | 396 |
| D.2                                 | Representations of orthogonal groups  | 398 |
| D.3                                 | More on analytic continuation and even/odd spin   | 404 |
| D.4                                 | Checking the celestial map with triple light transforms   | 407 |
| D.5                                 | Swapping the integral and $t$ -channel sum in the inversion formula   | 411 |
| D.6                                 | Contact terms at $\zeta = 1$ in $\mathcal{N} = 4$ SYM   | 412 |
| Appendix E: Appendices to Chapter 6 |   | 415 |
| E.1                                 | Action and supersymmetry transformations of $\text{MSYM}_2$   | 415 |
| Bibliography                        |   | 419 |

*“The goal that led him on was not impossible, though it was clearly supernatural: He wanted to dream a man. He wanted to dream him completely, in painstaking detail, and impose him upon reality. This magical objective had come to fill his entire soul; if someone had asked him his own name, or inquired into any feature of his life till then, he would not have been able to answer. The uninhabited and crumbling temple suited him, for it was a minimum of visible world; so did the proximity of the woodcutters, for they saw to his frugal needs. The rice and fruit of their tribute were nourishment enough for his body, which was consecrated to the sole task of sleeping and dreaming.”*

*“In the birdless dawn, the sorcerer watched the concentric holocaust close in upon the walls. For a moment he thought of taking refuge in the water, but then realized that death would be a crown upon his age and absolve him from his labors. He walked into the tatters of flame, but they did not bite his flesh—they caressed him, bathed him without heat and without combustion. With relief, with humiliation, with terror, he realized that he, too, was but appearance, that another man was dreaming him.”*

—from *“The Circular Ruins”* by Jorge Luis Borges

*Chapter 1*

## INTRODUCTION

A crowning jewel of theoretical achievement would be to find the theory that describes the fundamental laws of nature of our universe in their entirety. A closely related achievement would be to explain *why* this theory is the correct one. Indeed, there doesn't seem to be a single self-consistent theory of physics, but many. For example, it is possible to conceive of an electron twice as massive, or a gravitational force half as strong. The known parameters of our universe — such as the masses of particles and the strengths of interactions — are set to very specific values. To understand why our universe is the particular theory that it is, we must understand where it stands in relation to other theories of physics. Perhaps, in a dream scenario, by ruling out theories of physics we can discover our universe. Therefore, it is the theorist's task to explore the *space* of theories, and tell us not just *what*, but also *where* the theory of our universe is.

The other goal of a theorist is to solve the discovered theories. Although finding and solving theories go hand in hand, solving — meaning computing all observables of a theory — requires further ingenuity. Luckily, there are many organizing principles that help us with both daunting quests.

One of the deepest insights of physics is that the description of a physical system is in terms of an effective theory capturing the dynamics of the fundamental degrees of freedom appropriate to the given scale. Let's take our universe as an example. At the distances characteristic of everyday life, the relevant forces are gravitation and electromagnetism. As we probe smaller distance scales, we observe the rich dynamics of the subatomic scale, and beyond. Yet, when we describe the macroscopic world, we don't need to worry about the details of the microscopic, only about the behavior of the collective degrees of freedom. The same is true for subsystems of our universe. Everyday materials can be modeled by theories of physics of their own; for example, everyday ferromagnets could be modeled by the Ising model. Of course, these models arise from the underlying fundamental laws, but the description of the system — once determined — can stand on its own within the range of scales it is valid.

The theories that describe our universe at all observed scales are General Relativity and the Standard Model. General Relativity is the effective theory that describes

the gravitational interaction. The Standard Model is a particular local, relativistic (Lorentz-invariant) Quantum Field Theory (QFT) that describes the known microscopic particles and their interactions, including electrodynamics as well as the subatomic weak interaction and strong interaction. Together, they are valid in a staggering range of scales, from the galactic to the subatomic. However, they are not valid at arbitrarily small distances. We are yet to find the ultimate theory of nature, valid at the smallest scales, which reproduces General Relativity and the Standard Model at larger distances.

How then are the theories describing different scales related? The resolution is that the very theory that describes a physical system dynamically evolves as one zooms out to larger distance scales. Degrees of freedom are averaged out, and new degrees of freedom emerge from their collective behavior — sometimes radically. The evolution of a theory as the scale is changed is governed by the Renormalization Group (RG) flow. RG flow dictates how the parameters  $g_i$  of a theory — such as the masses and the strengths of forces — change as the scale changes. Given an energy scale  $E \sim \mu$  — which corresponds to a distance scale  $\sim 1/\mu$  — RG flow determines the rate of change of the parameters  $g_i$  according to a set of equations,

$$\mu \frac{\partial g_i}{\partial \mu} = \beta_i(g_j). \quad (1.1)$$

The RG flow evolution stops only once it reaches a theory that is scale-invariant, one for which the parameters no longer depend on the scale. There are generically three scenarios. One possibility is that every degree of freedom is washed out, and one is left with just the vacuum. A second, less trivial possibility is that all masses and couplings vanish, and the remaining degrees of freedom freely propagate without interactions. At extremely large distances, our universe falls under this scenario. The third, nontrivial possibility is that one is left with an interacting theory that is scale-invariant.

A scale-invariant, Lorentz-invariant, local QFT often enhances to a Conformal Field Theory (CFT). CFTs are invariant under a larger group of symmetries, called conformal transformations, which include scale and Lorentz transformations. The interesting CFTs are the nontrivial, interacting ones arising from the third scenario above.<sup>1</sup> Conformal invariance has profound consequences. Due to their enhanced symmetries, CFTs are much simpler to describe than their generic QFT counterparts, and they give us a handle on QFTs. Virtually every computation of a quantity in a QFT

---

<sup>1</sup>The first two scenarios are also CFTs, in a trivial sense.

treats it as a perturbation of a CFT: the classical treatment of a Lagrangian is a perturbation around a free CFT. Astonishingly, CFTs can be defined nonperturbatively, without the use of a Lagrangian. Moreover, the abstract space of all QFT — the *theory space* — parametrized by all possible parameters  $g_i$ , is organized by RG flow lines that start and end at CFTs, stringing together QFTs at different scales in between.<sup>2</sup> In this sense, CFTs are the building blocks of the space of QFTs. In order to navigate the space of theories, we must chart its constellation of CFTs.

CFTs are ubiquitous. They make their presence in many areas of theoretical physics, from the phenomenological to the mathematical, describing many interesting physical phenomena on their own. Starting from the most practical and down-to-earth application, CFTs describe universality classes of critical systems, i.e. of continuous (second-order) phase transitions. Euclidean CFTs describe statistical critical systems, where the phase transition is achieved by tuning extrinsic parameters such as temperature and pressure. Examples include the critical point in the liquid-vapor phase transition of substances — including water! — and the ferromagnetic/paramagnetic phase transition, both described by the same 3d Ising CFT [1, 2], and the superfluid transition in  $^4\text{He}$  described by the 3d O(2) model [3]. Lorentzian CFTs describe quantum critical systems at zero temperature, which are quantum mechanical systems where the phase transition is achieved by tuning the microscopic parameters  $g_i$  of the system. An example is the 2+1d O(2) model description of thin-film superconducting phase transitions [4, 5].

Perhaps the most revolutionary application is to gravity. At first sight, QFT is not a valid description of quantum gravity. The spacetime on which the QFT lives is assumed to be static. However, certain CFTs with large numbers of degrees of freedom also describe gravitational theories in Anti-de Sitter (AdS) spacetime in one dimension higher, via the holographic AdS/CFT duality [6, 7]. In fact, CFTs provide our best understanding of quantum gravity: with fewer degrees of freedom, quantum effects begin to emerge. More generally, CFTs are also central in string and M-theory, which are candidate theories of quantum gravity. The worldsheet theory of a string is conformal, and many interesting CFTs arise from the low-energy dynamics of stacks of branes in string and M-theory. It is almost impossible not to mention the celebrated four-dimensional  $\mathcal{N} = 4$  super Yang-Mills (SYM) theory. The  $\mathcal{N} = 4$  SYM is a superconformal theory with many merits. It has a weakly-coupled Lagrangian description, which makes it easier to study. It arises from string theory as

---

<sup>2</sup>The high-energy starting point is not always a CFT. It might not even be a QFT as there could be flow lines coming from string or M-theory. Still, it is a useful paradigm in many circumstances.

the worldvolume theory of a stack of D3-branes. The AdS/CFT correspondence was first discovered with  $\mathcal{N} = 4$  SYM as an exact equivalent to string theory on  $\text{AdS}_5 \times S^5$ . It is also a supersymmetric cousin of quantum chromodynamics (QCD), the theory of quarks and gluons, therefore a prudent candidate for developing techniques to study QCD. Another highlight is the six-dimensional  $\mathcal{N} = (2, 0)$  superconformal theory describing the low-energy dynamics of M5-branes. This theory does not have *any* known Lagrangian description, but can be used to engineer a vast number of interesting QFTs in lower dimensions.

CFTs are the central focus of this thesis. We will be interested in multiple aspects of theirs; from computing their observables, to discovering their internal structure, and even to constraining theories of gravity using their properties. We now turn to a review of some salient aspects of CFTs, highlighting the directions of interest that this thesis will explore. We then follow up with a summary of the contents of this thesis.

### 1.1 New and Old Frontiers in Conformal Field Theories

Let us expand on the statement of symmetry in a QFT. A Lorentz-invariant QFT is one which is invariant under spacetime translations, rotations, and boosts. In  $d$ -dimensional Minkowski spacetime, rotations and boosts form the Lorentz group  $O(d-1, 1)$ , and together with translations they form the Poincaré group  $\mathbb{R}^{d-1,1} \rtimes O(d-1, 1)$ , which is the group of isometries of Minkowski space. In a Euclidean QFT, we instead have the group of isometries  $\mathbb{R}^d \rtimes O(d)$ .

For a uniform treatment, let  $G$  be the group of spacetime symmetries of a QFT. Invariance means that the states of the QFT, as well as the operators acting on those states, transform in representations of  $G$ . The QFT associates a Hilbert space of states  $\mathcal{H}$  to each spatial (codimension-one) slice. The Hilbert space is a unitary representation of the universal cover  $\tilde{G}$  of the group  $G$ ,

$$\pi : \tilde{G} \rightarrow U(\mathcal{H}). \tag{1.2}$$

Since  $G$  is typically a Lie group, there is an associated representation of the Lie algebra of  $G$ ,  $\mathfrak{g}$ ,

$$d\pi : \mathfrak{g} \rightarrow \text{End}(\mathcal{H}). \tag{1.3}$$

This representation maps the generators of  $\mathfrak{g}$  to self-adjoint (Hermitian) operators on  $\mathcal{H}$ . In particular, the generator of translations normal to the spatial slice is mapped

to the Hamiltonian  $H$  of the QFT quantized normal to the slice. For example, in a Lorentz-invariant theory on Minkowski space quantized on a spatial slice, the Hamiltonian is the representation of the generator of time translations perpendicular to the slice,  $d\pi(i\partial_t)$ . The requirement of energy positivity in a Lorentzian theory translates to a positive semi-definite Hamiltonian. The Hilbert space also contains a vacuum state  $|\Omega\rangle$ , which we typically take to be unique.<sup>3</sup> The vacuum state is invariant under the symmetries  $\tilde{G}$ ,

$$\pi(\tilde{G})|\Omega\rangle = |\Omega\rangle \tag{1.4}$$

More generally, we can decompose the Hilbert space into irreducible representations of  $\tilde{G}$ , which provide a convenient labeling of the states of the theory. For a QFT invariant under the Poincaré group, the irreducible representations are labeled by the mass  $m$  and the spin  $J$ . Unitarity requires that  $m \geq 0$ .

If a QFT is also scale invariant, scale transformations (also called dilatations) combine with the Poincaré group and often enhance to the larger group of conformal transformations. QFTs for which the group  $G$  of spacetime symmetries includes the conformal group are CFTs. In Lorentzian signature in  $d$  dimensions, the conformal group is  $SO(d, 2)$ , and in Euclidean signature it is  $SO(d + 1, 1)$ . The Hilbert space is therefore a representation of the relevant conformal group. We can label the states by the irreducible representations of the conformal group. These representations are partially labeled by a scaling dimension  $\Delta$  and a spin  $J$ .<sup>4</sup> The scaling dimension  $\Delta$  is the eigenvalue of dilatations of the state, where once again unitarity requires  $\Delta \geq 0$ .

In  $d = 2$  dimensions, scale-invariant QFTs enhance to a much stronger form of invariance. The spacetime symmetries of a 2d CFT are generated by the Virasoro algebra, which is an infinite dimensional algebra that includes the conformal algebra. Therefore, the study of 2d CFTs is quite different than in higher dimensions. In our discussion of CFTs below, we will focus on  $d > 2$  dimensions.

The usual paradigm of CFT is to focus on the properties of local operators. Local operators are insertions  $\mathcal{O}(x)$  supported at a point  $x$  of the underlying spacetime manifold  $\mathcal{M}$  the CFT is considered on. The simplest (and very physical) choices of

---

<sup>3</sup>It is possible to have multiple vacua; they correspond to different superselection sectors. In that case, one can study the excitations around a given vacuum, and the analysis proceeds identically. The “dynamics” of multiple vacua in the absence of excitations is captured by Topological Quantum Field Theory (TQFT).

<sup>4</sup>More generally, the representation is labeled by  $(\Delta, \rho)$  where  $\rho$  is an irreducible representation of the Euclidean group  $SO(d)$  or Lorentzian group  $SO(d - 1, 1)$ . The representation  $\rho$  itself can be labeled by  $(J, \lambda)$ , where  $J$  is the spin and  $\lambda$  is an  $SO(d - 2)$  representation.



$\mathcal{M}$  are flat ones, either Euclidean  $\mathbb{R}^d$  or Lorentzian  $\mathbb{R}^{d-1,1}$ , depending on the dynamics one chooses to study. The correlation functions of insertions of local operators on the underlying manifold

$$\langle \mathcal{O}_1(x_1) \cdots \mathcal{O}_n(x_n) \rangle_{\mathcal{M}} \quad (1.5)$$

comprise the relevant local observables of the CFT on  $\mathcal{M}$ . Typically, the treatment of local operators in CFT is given in Euclidean space, and is extended to Minkowski space by Wick rotation via the Osterwalder-Schrader theorem. We will review some relevant aspects of local operators in Euclidean signature.

In Euclidean signature, it is convenient to quantize a CFT radially on spherical slices  $S^{d-1}$ . The Hamiltonian of this quantization is given by the dilatation operator  $D$  which is the representation of the generator of radial rescaling, i.e. the normal derivative to the sphere. The eigenvalues of  $D$  are the scaling dimensions  $\Delta$ .

Given a local insertion  $\mathcal{O}(x)$  one can surround it with a sphere  $S^{d-1}$ . The insertion of  $\mathcal{O}(x)$  produces a state in the Hilbert space of the sphere  $\mathcal{H}_{S^{d-1}}$ ,

$$\mathcal{O}(x)|\Omega\rangle = |\mathcal{O}(x)\rangle. \quad (1.6)$$

This can be understood as the state produced by performing the Euclidean path integral inside the sphere with the operator  $\mathcal{O}(x)$  inserted [1]. Likewise, the vacuum state

$$|\Omega\rangle \in \mathcal{H}_{S^{d-1}} \quad (1.7)$$

can be viewed as the state produced by the path integral with nothing inserted inside the sphere. In axiomatic QFT, the existence of the vacuum state and of the operators defining the map (1.6) is taken as axioms, among others [8]. We take them to exist in any quantization of the theory, regardless of the availability of the path integral.

One of the beautiful properties of CFTs is the existence of an inverse to the map (1.6) known as the state-operator correspondence. We can use conformal symmetry to take an arbitrary state  $|\psi\rangle \in \mathcal{H}_{S^{d-1}}$  and decompose it into dilatation eigenstates,

$$|\psi\rangle = \sum_{\mathcal{O}} \psi_{\mathcal{O}} |\mathcal{O}\rangle. \quad (1.8)$$

Recall that in a unitary CFT, the generator of dilatations  $D$  is Hermitian, therefore diagonalizable, so such a decomposition is permissible. Then, we identify each eigenstate as one created by a local operator inserted at the center of the sphere

$$|\mathcal{O}\rangle \equiv \mathcal{O}(0)|\Omega\rangle. \quad (1.9)$$

This naturally associates a dilatation eigenvalue to each local operator, which we can write as

$$[D, \mathcal{O}] = \Delta_{\mathcal{O}} \mathcal{O} \quad \Leftrightarrow \quad D|\mathcal{O}\rangle = \Delta_{\mathcal{O}}|\mathcal{O}\rangle. \quad (1.10)$$

More generally, we can decompose a state  $|\psi\rangle$  into components along the irreducible representations of the conformal group appearing in the decomposition of  $\mathcal{H}_{S^{d-1}}$ . Accordingly, each local operator is labeled by an irreducible representation of the conformal group.<sup>5</sup> We can further collect each irreducible representation into a *primary*, and its *descendants* given by the spacetime derivatives of the primary. As a result, we only need to focus on primary operators, as all of their descendants are related by symmetry.

The state-operator correspondence guarantees the existence of an operator product expansion (OPE). Given an insertion of two local primary operators, we can consider the resulting state in the Hilbert state of a sphere surrounding them. So long as no other insertions are present inside the sphere, the resulting state is

$$\mathcal{O}_1(x_1)\mathcal{O}_2(x_2)|\Omega\rangle. \quad (1.11)$$

Using conformal symmetry, we can decompose this state into states created by single insertions of local operators

$$\mathcal{O}_1(x_1)\mathcal{O}_2(x_2)|\Omega\rangle = \sum_{\mathcal{O}} c_{12\mathcal{O}}(x_1 - x_2)\mathcal{O}(x_2)|\Omega\rangle. \quad (1.12)$$

The expansion is controlled by the separation  $|x_1 - x_2|$ , and converges faster when the separation is small. We can further collect the states into primaries and their descendants. Finally, we lift the equation on the states to an operator equation via the state-operator correspondence, resulting in the OPE

$$\mathcal{O}_1(x_1)\mathcal{O}_2(x_2) = \sum_k f_{12k}\mathcal{C}_{12k}(x_1, x_2, \partial_2)\mathcal{O}_k(x_2), \quad (1.13)$$

where each operator  $\mathcal{O}_i$  is a conformal primary. The coefficients  $f_{ijk}$  are called the OPE coefficients. They are the dynamical data. The differential operator  $\mathcal{C}_{ijk}$  is kinematical; it has a fixed form and serves to collect the contributions of the descendants of each primary  $\mathcal{O}_k$ . As the derivation shows, the OPE converges when acting on the vacuum.

---

<sup>5</sup>Technically, the Wightman axioms assume that operators transform in representations of the group of spacetime symmetries  $\tilde{G}$ , from which it follows that the Hilbert space is a representation of  $\tilde{G}$ . For pedagogy, we started with the Hilbert space.

Multiple insertions of local operators can be reduced to single insertions by repeated application of the OPE (1.13). Therefore the local data of a CFT consists of the spectrum of local primary operators  $\mathcal{O}_i$ , i.e. a set of irreducible representations  $(\Delta_i, \rho_i)$  of the conformal group, together with the set of their OPE coefficients  $f_{ijk}$ . It is believed that this is the defining data of a CFT.<sup>6</sup>

### 1.1.1 The Conformal Bootstrap

The primary goal of the conformal bootstrap program is to solve for the local data of a CFT by treating it as an abstract axiomatic system defined as a solution to certain consistency conditions. The consistency conditions come about from studying the OPE within four-point functions of local operators on flat-space,

$$\langle \mathcal{O}_1(x_1)\mathcal{O}_2(x_2)\mathcal{O}_3(x_3)\mathcal{O}_4(x_4) \rangle_{\mathbb{R}^d}. \quad (1.14)$$

Inside the correlator, the OPE (1.13) can be performed in different ways. For example, we can bring the operators  $\mathcal{O}_1$  and  $\mathcal{O}_2$  close to each other and take their OPE. Term by term, this OPE projects the correlator (1.14) into states organized by primaries  $\mathcal{O}$  exchanged between  $\mathcal{O}_1\mathcal{O}_2$  and  $\mathcal{O}_3\mathcal{O}_4$ . Alternatively, we could start by taking the OPE of  $\mathcal{O}_1$  and  $\mathcal{O}_4$ , obtaining a different sum for the correlator. Of course, the two sums must equal each other. This leads to the crossing equation,

$$\sum_{\mathcal{O}} \begin{array}{c} 1 \\ \diagdown \\ \quad \quad \mathcal{O} \\ \diagup \\ 2 \end{array} \begin{array}{c} 4 \\ \diagdown \\ \quad \quad \mathcal{O} \\ \diagup \\ 3 \end{array} = \sum_{\mathcal{O}'} \begin{array}{c} 1 \\ \diagdown \\ \quad \quad \mathcal{O}' \\ \diagup \\ 2 \end{array} \begin{array}{c} 4 \\ \diagdown \\ \quad \quad \mathcal{O}' \\ \diagup \\ 3 \end{array}. \quad (1.15)$$

In terms of the OPE coefficients, we can write the crossing equation as

$$\sum_{\mathcal{O}} f_{12\mathcal{O}} f_{34\mathcal{O}'} G_{\mathcal{O}}^{1234}(x_1, x_2, x_3, x_4) = \sum_{\mathcal{O}'} f_{14\mathcal{O}'} f_{32\mathcal{O}} G_{\mathcal{O}'}^{1432}(x_1, x_4, x_3, x_2). \quad (1.16)$$

The functions  $G_{\mathcal{O}}^{ijkl}$  depend only on the representations of the operators, and are called *conformal blocks*; they are the kinematical factors resulting from summing up the contributions of a primary  $\mathcal{O}$  and its descendants to the four-point function (1.14). The expansions on the left- and right-hand side of (1.15) or (1.16) are called the *s*- and *t*-channel conformal block expansions, respectively.

Crossing equations impose highly nontrivial constraints on the spectrum and OPE coefficients of a CFT [9, 10]. Specifying CFTs by solving the crossing equations is

<sup>6</sup>Up to possible choice of nonlocal data.

the conformal bootstrap. In a unitary theory, the OPE coefficients  $f_{ijk}$  are real. Consequently, when the external operators  $\mathcal{O}_{1,2,3,4}$  are identical, the coefficients in the expansion (1.16) are manifestly positive. By employing numerical algorithms that utilize this positivity, rigorous bounds have been placed on the space of allowed CFTs, ruling out large parts of the parameter space. Moreover, data of certain CFTs lying close to the boundary of the allowed region have been computed to record precision, such as the 3d Ising model and the  $O(N)$  models to name a few. For a comprehensive review, the reader is recommended to consult [11].

Solving the crossing equations analytically has proven to be a very difficult problem. Nevertheless, in recent years, much progress has been made on this front. One advent was the development of large-spin perturbation theory, which systematically solves the crossing equations in the limit of large spin of the exchanged operators [12–24]. The crucial observation is that CFT operators with large spin behave like free fields. By viewing them as perturbations of generalized free theory, large-spin perturbation theory provides a handle on interacting nonperturbative CFTs.

In a groundbreaking work [25], Caron-Huot derived an inversion formula for the crossing equation. The inversion formula solidified large-spin perturbation theory on firm footing, and opened up new horizons. Caron-Huot’s inversion formula is achieved by going to Lorentzian signature and studying the analyticity properties of the correlator

$$\langle \mathcal{O}_1(x_1)\mathcal{O}_2(x_2)\mathcal{O}_3(x_3)\mathcal{O}_4(x_4) \rangle_{\mathbb{R}^{d-1,1}}. \quad (1.17)$$

Let us briefly describe some aspects of the formula.

For simplicity, let’s restrict to scalar external operators. In Euclidean signature, one can extract terms in the  $s$ -channel expansion proportional to a given conformal block using orthogonality properties of conformal blocks under a certain integral pairing. This relation comes from performing harmonic analysis on the Euclidean conformal group  $SO(d+1, 1)$ . Schematically, one defines the function (see also [26])

$$C(\Delta, J) = \int d^d x_1 \cdots d^d x_4 \langle \Omega | \mathcal{O}_1(x_1)\mathcal{O}_2(x_2)\mathcal{O}_3(x_3)\mathcal{O}_4(x_4) | \Omega \rangle \Psi_{d-\Delta, J}(x_1, x_2, x_3, x_4) \quad (1.18)$$

The functions  $\Psi_{\Delta, J}$  are called *partial waves*; they are certain linear combinations of conformal blocks that are single-valued in the positions  $x_i$  of the operators. Via the orthogonality of partial waves, the integral in (1.18) projects onto the contribution  $\Psi_{\Delta, J}$  of a primary  $\mathcal{O}_{\Delta, J}$  in the  $s$ -channel OPE of the correlator. The function  $C(\Delta, J)$

is a meromorphic function of  $\Delta$  containing the  $s$ -channel OPE data of the correlator (1.17). Explicitly, for each nonnegative integer  $J$ ,  $C(\Delta, J)$  has poles in  $\Delta = \Delta_{\mathcal{O}}$  at the dimensions of the local operators  $\mathcal{O}_{\Delta_{\mathcal{O}}, J}$  appearing in the  $s$ -channel OPE. The residues at these poles are given by the products of OPE coefficients  $f_{12\mathcal{O}}f_{34\mathcal{O}^\dagger}$ .

So far, the integral (1.18) is an identity of the  $s$ -channel expansion, and impractical for relating the  $s$ - and  $t$ -channel expansions. The goal is to obtain an inversion formula for the  $s$ -channel OPE data  $C(\Delta, J)$  which is dominated by the  $t$ -channel expansion. To achieve this, the contour of the integral pairing in (1.18) is deformed to Lorentzian signature. The resulting Lorentzian inversion formula expresses  $C(\Delta, J)$  in terms of an integral over the “double-discontinuity” of the correlator (1.17),

$$C(\Delta, J) \propto \int d^d x_1 \cdots d^d x_4 \langle \Omega | [\mathcal{O}_1(x_1), \mathcal{O}_4(x_4)] [\mathcal{O}_3(x_3), \mathcal{O}_2(x_2)] | \Omega \rangle \times \tilde{G}_{J+d-1, \Delta-d+1}(x_1, x_2, x_3, x_4). \quad (1.19)$$

The integration is against a suitable conformal block  $\tilde{G}_{J+d-1, \Delta-d+1}$  of the exchange of a conformal primary with dimension  $J+d-1$  and spin  $\Delta-d+1$ . This Lorentzian inversion formula very efficiently decomposes a given term in the  $t$ -channel OPE into the  $s$ -channel.

An important observation is that the right-hand side of (1.19) is manifestly analytic in spin  $J$ . The poles of  $C(\Delta, J)$  lie on analytic Regge trajectories

$$\Delta = \Delta_i(J) \quad (1.20)$$

which pass through the local operators. Thereby the spectrum and OPE coefficients of local operators lie on complex curves parametrized by spin. This analyticity of CFT data points out a seeming dichotomy. In a unitary CFT, local operators are only allowed to be in non-negative (half-) integer spin representations. This can be seen as follows: by the state-operator correspondence, local operators must correspond to positive-energy states in a unitary theory. The positive energy representations of (the universal cover of) the Lorentzian conformal group  $\widetilde{SO}(d, 2)$  are classified [27], and in particular, they exclude continuous spin representations. This raises the natural question: what are the continuous-spin objects in a CFT that have the OPE coefficients that analytically continue those of the local operators? Can the operators of a CFT be analytically continued in spin? In a beautiful paper [28], Kravchuk and Simmons-Duffin answered this question by analytically continuing certain nonlocal transforms of local operators to continuous (complex) spin. These continuous-spin light-ray operators,  $\mathbb{O}_{i, J}$ , are nonlocal observables constructed from two local operators,  $\mathcal{O}_1$  and  $\mathcal{O}_2$ .

They are naturally associated to light-rays in the Lorentzian spacetime on which the CFT lives. The label  $i$  denotes a Regge trajectory (1.20). Kravchuk and Simmons-Duffin showed that the Lorentzian inversion formula of Caron-Huot [25] computes the matrix elements of light-ray operators,

$$\langle \Omega | \mathcal{O}_4 \mathbb{O}_{i,J} \mathcal{O}_3 | \Omega \rangle \propto - \operatorname{Res}_{\Delta=\Delta_i(J)} C(\Delta, J). \quad (1.21)$$

They also generalized the Lorentzian inversion formula to arbitrary representations of the external operators  $\mathcal{O}_{1,2,3,4}$ .

### 1.1.2 Nonlocal Directions in CFTs

Determining the spectrum of local operators and their OPE coefficients of any non-trivial strongly-interacting CFT in more than two spacetime dimensions is still an open question. Such an incredible feat might be sufficient to define said CFT fully, and will certainly allow computation of arbitrary correlation functions of local operators on flat-space. However, a CFT is richer still. A complete and satisfactory description of any QFT must include a treatment of the QFT placed on arbitrary spacetime manifolds  $\mathcal{M}$ . As long as the QFT is well-defined on a given manifold, its description should compute the associated observables — such as correlation functions of local operators inserted on the manifold,

$$\langle \mathcal{O}_1 \dots \mathcal{O}_n \rangle_{\mathcal{M}}. \quad (1.22)$$

A potential future goal for the conformal bootstrap is to develop methods to predict observables of CFTs on more general spacetime manifolds. This is not a purely academic pursuit either. One of the most practical and physical questions one could ask regarding a QFT is how it behaves at finite (nonzero) temperature. Studying a Lorentzian QFT at finite temperature is equivalent to considering the time direction to be imaginary and periodically identified, changing the topology of spacetime to that of a circle times space,  $S^1 \times \mathbb{R}^{d-1}$ . In the context of a CFT, even if the local data is known entirely, it is still a nontrivial task to compute observables at finite temperature, such as correlation functions

$$\langle \mathcal{O}_1 \dots \mathcal{O}_n \rangle_{S^1 \times \mathbb{R}^{d-1}}. \quad (1.23)$$

For a quantum critical system in the real world, observables measured in lab will necessarily be at finite temperature, as we cannot cool a sample to absolute zero temperature. Therefore, near the relevant quantum phase transition of the system, the

description is in terms of the Lorentzian CFT at finite temperature. Thus, computing finite-temperature CFT correlators (1.23) is important for real world applications.

Furthermore, in QFT there are nonlocal observables. It is known in many examples of QFT that two theories can have identical local observables, but differ in their spectrum of nonlocal observables [29, 30]. Novel knowledge could be attained from the properties of nonlocal observables in CFTs. Certain facts, even if determined by the local data, could be manifest in the dynamics of nonlocal observables, whilst obscured locally. For example, the features and diagnostics of causality in a gravity theory are more readily captured by gravitational shocks, which are nonlocal objects. In AdS/CFT, gravitational shocks are holographically dual to light-ray operators. What new features of CFTs could be captured by studying light-ray operators?

Finally, a CFT is more than just a blackbox that inputs a manifold and computes correlation functions on it. There is a beautiful underlying structure. Much is to be learned about both physics and mathematics by uncovering the secrets of CFTs. All of these aspects motivate the content of this thesis, which we now turn to summarize.

## 1.2 Summary of this Thesis

This thesis can be roughly viewed as consisting of three parts. The first two parts extend the study of CFTs. The first part studies CFTs on nontrivial manifolds, and the second part studies nonlocal operators in CFTs. The third part studies a family of supersymmetric QFTs arising in string theory.

In the first part consisting of chapters 2 and 3, we take a novel step in the direction of bootstrapping CFTs on nontrivial manifolds by initiating the bootstrap of CFTs at finite temperature. Utilizing the machinery we develop, we make predictions for the thermal data of the 3d Ising CFT.

In the second part consisting of chapters 4 and 5, we study light-ray operators in CFTs. Light-ray operators reveal beautiful analytic structures within CFTs. In chapter 4, we use their properties to constrain gravitational theories, and CFTs in general. In chapter 5, we derive an OPE for light-ray operators, and use it to compute certain correlators of light-ray operators called “event shapes” in  $\mathcal{N} = 4$  SYM.

The third part is in a somewhat separate vein. In chapter 6, we examine the behavior of a certain family of 1+1-dimensional theories describing the internal dynamics of D-strings as they flow from high-energy gauge theory descriptions to their low-energy vacua. An interesting connection is the existence of multiple vacua in a given theory in this family, some of which are massive and some of which are CFTs.

### 1.2.1 A hot new direction for the conformal bootstrap

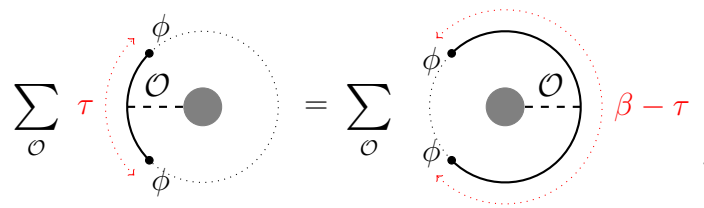
In chapters 2 and 3, we study CFTs at finite temperature  $T = 1/\beta$ . Studying the equilibrium properties of a Lorentzian CFT at finite temperature corresponds to studying it on the simplest nontrivial space,  $S^1_\beta \times \mathbb{R}^{d-1}$ , where  $S^1_\beta$  is a circle of circumference  $\beta$ . For brevity, we denote correlators on  $S^1_\beta \times \mathbb{R}^{d-1}$  by  $\langle \dots \rangle_\beta$ .

In a CFT in  $d > 2$  dimensions, scale invariance prevents local operators from having nonzero expectation values,  $\langle \mathcal{O} \rangle = 0$ .<sup>7</sup> The circumference of the circle,  $\beta$ , introduces a scale, explicitly breaking scale-invariance. As a result, local primary operators are allowed to have expectation values at finite temperature, which are determined by a single coefficient. These one-point functions are the new, thermal data of the theory: they measure the response of the CFT to finite temperature. For example, the thermal expectation value of the stress-energy tensor,  $\langle T \rangle_\beta$ , gives the free energy density of the system.

In chapter 2, we introduce novel methods to bootstrap for the finite-temperature data of a CFT. The thermal bootstrap problem is defined by the Kubo-Martin-Schwinger (KMS) condition of thermal correlators as the “thermal crossing equation.” Denoting the coordinate on the thermal circle  $S^1_\beta$  as  $\tau$ , the KMS condition requires that the thermal two-point functions of scalars,  $\langle \phi\phi \rangle_\beta$ , satisfies

$$\langle \phi(\tau)\phi(0) \rangle_\beta = \langle \phi(\beta - \tau)\phi(0) \rangle_\beta. \quad (1.24)$$

The OPE (1.13) is still valid at separation less than the size of the circle  $\beta$ . The OPE could therefore be employed to compute CFT  $n$ -point correlation functions at finite temperature in terms of one-point functions in the small separation limit. In particular, we can use the OPE to write an expansion for each side of the KMS equation (1.24). Pictorially, the resulting crossing equation could be represented as



$$\sum_{\mathcal{O}} \tau \quad \text{[Diagram 1]} = \sum_{\mathcal{O}} \quad \text{[Diagram 2]} \quad \beta - \tau \quad . \quad (1.25)$$

The two OPE channels correspond to bringing the operators close to each other on one side of the thermal circle before fusing them, or the other. The data appearing on either side are the same thermal one-point functions  $\langle \mathcal{O} \rangle_\beta$  of the local operators  $\mathcal{O}$

<sup>7</sup>Except for the unit operator,  $\mathbf{1}$ , whose expectation value,  $\langle \mathbf{1} \rangle$ , is the partition function.



appearing in the  $\phi \times \phi$  OPE. As with the vacuum crossing equation (1.15) constraining the OPE data, the thermal crossing equation places strong constraints on the thermal one-point functions. Unlike the OPE coefficients, there are no positivity conditions on the thermal one-point functions. Therefore, purely numerical approaches to the thermal bootstrap are unfeasible. Instead, we develop analytic techniques.

We derive a Lorentzian thermal inversion formula for  $\langle \phi \phi \rangle_\beta$ , which decomposes the two-point function into its constituent one-point functions  $\langle \mathcal{O} \rangle_\beta$  appearing in the OPE  $\mathcal{O} \in \phi \times \phi$ . The thermal inversion formula involves an analytic continuation of the spatial separation of the scalars to a timelike direction, justifying the name Lorentzian. As an application, we use our inversion formula to compute thermal one-point functions of higher-spin currents in mean field theory (MFT) and the 3d  $O(N)$  model at infinite  $N$ .

The thermal inversion formula, like the OPE inversion formula [25], accomplishes two powerful tasks. Firstly, it explicitly demonstrates that the thermal one-point functions are analytic in the spin  $J$  of the operators. This parallels the fact that the spectrum and the usual vacuum OPE data of a CFT is analytic in  $J$  [25, 28]. Indeed, thermal data are organized into the residues of a meromorphic function  $a(\Delta, J)$ , similar to the function  $C(\Delta, J)$  in (1.19) encoding the OPE data. The poles of  $a(\Delta, J)$  align with the Regge trajectories (1.20). Secondly, it provides a concrete map between the terms in the two OPEs related by the KMS condition. We compute this map in the limit where the scalars approach each others lightcone, and develop a perturbation theory of the thermal data in inverse large spin.

As with the local data, the large-spin perturbation theory of thermal data is a powerful tool. It provides a handle for studying strongly-interacting theories. In chapter 3, we demonstrate its power by applying our techniques to the 2+1d Ising CFT, and bootstrap the thermal expectation values of a large part of the spectrum. Our predictions, computed from first principles, are in good agreement with Monte-Carlo simulations.

### 1.2.2 A stringy equivalence principle

Chapter 4 explores constraints on gravity from gravitational shocks. The strong equivalence principle states that objects follow geodesics regardless of their polarizations or internal composition. The strong equivalence principle holds in Einstein gravity, but is violated by non-minimal (higher-derivative) gravitational couplings in its modifications, such as Gauss-Bonnet gravity. Since Einstein gravity is not a the-

ory of quantum gravity, it must arise as the low-energy description of a high-energy theory of gravity, such as string theory. Invariably, one expects that higher-derivative gravitational couplings are present at intermediate energy scales. Therefore, a natural question is, what is the principle that should generalize the equivalence principle at high energies, and reproduce it at low energies?

One consequence of the strong equivalence principle is the observation that propagation of probe particles through consecutive coincident gravitational shocks is independent of the order of the shocks. However, in the presence of non-minimal couplings, probe particles experience “gravitational birefringence” as they pass through a shock, scattering differently depending on their polarizations. This causes the ordering of the shocks to matter. Curiously, coincident shocks *do* commute in string theory, due to cancellations from stringy states. In chapter 4, we argue that consistency at high energies requires coincident gravitational shocks to commute, and claim that this “stringy equivalence principle” is the sought-for generalization of the strong equivalence principle.

In turn, the commutation of gravitational shocks imposes nontrivial constraints on low-energy effective theories. In particular, non-minimal gravitational couplings are excluded unless they are accompanied by extra degrees of freedom. As non-minimal gravitational couplings lead to non-commuting shocks, their effects must be canceled by the gravitational couplings of the extra degrees of freedom. In flat space, the cancellation is encoded in the vanishing of a certain “superconvergence sum rule.”

In AdS, gravitational shocks are holographically dual to the so-called averaged null energy (ANEC) operators, which are light-ray operators constructed by null integrals of the stress tensor. In lightcone coordinates  $ds^2 = -du dv + d\vec{y}^2$ , an ANEC operator on the null plane  $u = 0$  is

$$\mathcal{E}(\vec{y}) = \int_{-\infty}^{\infty} dv T_{vv}(u = 0, v, \vec{y}). \quad (1.26)$$

We refer to this particular null integral as a light-transform. The commutativity of coincident gravitational shocks is therefore equivalent to whether ANEC operators placed on the same null plane commute, that is

$$\left[ \int_{-\infty}^{\infty} dv_1 T_{vv}(u = 0, v_1, \vec{y}_1), \int_{-\infty}^{\infty} dv_2 T_{vv}(u = 0, v_2, \vec{y}_2) \right] = 0. \quad (1.27)$$

We prove that ANEC operators commute in any unitary CFT. This provides a strong, nonperturbative proof of the stringy equivalence principle in the holographic setting.

We also determine the conditions under which light-ray operators constructed from more general operators commute. By inserting (1.27) inside a pair of probe states, and projecting onto a complete set of states between the two ANEC operators, one obtains the analogs of superconvergence sum rules in CFTs. These are nonperturbative sum rules that constrain the CFT couplings, thereby constraining low-energy effective theories of gravity for holographic CFTs.

### 1.2.3 An OPE for light-ray operators

Chapter 5 concerns with the algebraic aspects of light-ray operators in CFTs. So much mileage has been gained by exploiting the OPE of local operators. It is natural to ask whether light-ray operators also have an OPE. In chapter 5, we once again study light-ray operators constructed from null integrals of local operators. We derive a nonperturbative OPE for such light-ray operators placed on the same null plane. The light-ray-light-ray OPE is an expansion in small transverse separation,  $|\vec{y}_1 - \vec{y}_2|$ , of the light-ray operators. Given light-transformed local operators  $\mathcal{O}_1$  and  $\mathcal{O}_2$ , of spins  $J_1$  and  $J_2$ , it takes the schematic form

$$\begin{aligned} & \int_{-\infty}^{\infty} dv_1 \mathcal{O}_{1v\dots v}(0, v_1, \vec{y}_1) \int_{-\infty}^{\infty} dv_2 \mathcal{O}_{2v\dots v}(0, v_2, \vec{y}_2) \\ &= \pi i \sum_i \mathcal{C}_{\Delta_i-1}(\vec{y}_1, \vec{y}_2, \partial_{\vec{y}_2}) \mathbb{O}_{i, J=J_1+J_2-1}(\vec{y}_2). \end{aligned} \quad (1.28)$$

The differential operators  $\mathcal{C}_{\Delta}$  are of the same form as the one appearing in the OPE of local operators (1.13), albeit in  $d-2$  dimensions, and with certain restrictions on which representations are allowed. Its appearance can be understood as follows; the light-ray operators are pointlike on the transverse space, for which the Lorentz group  $\text{SO}(d-1, 1)$  of the CFT is the conformal group. The objects appearing in the OPE are the light-ray operators  $\mathbb{O}_{i, J}$  of [28], at fixed spin  $J = J_1 + J_2 - 1$ . The label  $i$  enumerates Regge trajectories. The  $\mathbb{O}_{i, J}$  are the same light-ray operators that analytically continue the local spectrum, and the matrix elements of which are computed by the Lorentzian inversion formula [25, 28]. However, their spin is evaluated at a value for which there is no corresponding local operator that could construct it. Therefore the OPE is in terms of intrinsically non-local operators. Nevertheless, the resulting OPE is convergent.

The light-ray-light-ray OPE can be used to compute important physical observables called “event shapes” in CFTs [31]. Event shapes are correlators of light-ray operators sandwiched between two states. The states are the past and future of the event one is interested in, and the light-ray operators are inserted infinitely far away to model

detectors. For example, the ANEC operator (1.26) models an energy detector that measures the energy deposited over time at a particular transverse position at infinity. The transverse position at infinity is better thought of as the direction on the celestial sphere that a lightlike signal propagates towards — with the coordinates  $\vec{y}$  identified as the stereographic coordinates of the celestial sphere. The light-ray OPE can be used to compute event shapes in an expansion in the separation of the detectors. Using the  $d - 2$  dimensional conformal symmetry of the OPE, we derive “celestial blocks” that capture the contributions of an individual light-ray operator,  $\mathbb{O}_{i,J}$ , in the OPE to the event shape. We demonstrate the power of our approach by computing the energy correlator — event shape of two ANEC operators — in a certain state in  $\mathcal{N} = 4$  SYM theory. We are able to reproduce previous results in both weak and strong coupling, and also make new predictions for the small-angle limit at 4 loops.

#### 1.2.4 Tracking a strongly coupled theory from high to low energies, and string duality

In chapter 6, we take a somewhat different direction. Instead of studying a CFT, we study the fate of an interesting QFT under RG flow from high energy to low energy CFTs. The theory of interest is the two dimensional maximally supersymmetric Yang-Mills theory ( $\text{MSYM}_2$ ). With gauge group  $U(N)$ ,  $\text{MSYM}_2$  is the gauge theory that describes the worldsheet dynamics of a stack of  $N$  D-strings in Type IIB string theory. The strong-weak S-duality of Type IIB string theory predicts that the strong-coupling limit of the D-strings are the fundamental Type IIB string. We provide a very strong check of this duality by computing a certain invariant of the RG flow, namely a refined elliptic genus, at both high- and candidate low-energy descriptions, and matching them. The elliptic genus is a particular thermal partition function, which only counts supersymmetry-protected (BPS) states. We show that the high-energy gauge theory has a vacuum corresponding to the worldsheet theory of a stack of  $N$  free fundamental strings, described by a symmetric-orbifold sigma model CFT into the transverse target space,  $\text{Sym}^N \mathbb{R}^8$ . Moreover, S-duality also predicts the existence of bound states of fundamental strings and D-strings, the so-called  $(p, q)$ -strings. Accordingly,  $\text{MSYM}_2$  should have multiple vacua corresponding to each of these bound states. Indeed, by a careful analysis of the nonperturbative sectors of the theory, we show that the elliptic genus correctly captures all of these vacua, and determines their dynamics.

## THE CONFORMAL BOOTSTRAP AT FINITE TEMPERATURE

<sup>1</sup>L. Iliesiu, M. Koloğlu, R. Mahajan, E. Perlmutter, and D. Simmons-Duffin, “The Conformal Bootstrap at Finite Temperature”, *Journal of High Energy Physics* **10**, 070 (2018) 10.1007/JHEP10(2018)070, arXiv:1802.10266 [hep-th].

## 2.1 Introduction

One of the basic operations in quantum field theory (QFT) is dimensional reduction on a circle. When we interpret the circle as Euclidean time (and impose appropriate boundary conditions) this corresponds to studying a QFT at nonzero temperature  $T = 1/\beta$ , where  $\beta$  is the length of the circle.<sup>1</sup> When we interpret the circle as a spatial direction, this is Kaluza-Klein compactification.

In this work, we use bootstrap techniques to study conformal field theories (CFTs) on  $S^1 \times \mathbb{R}^{d-1}$ , focusing mostly on  $d > 2$ . This setting is important for several reasons. Firstly, quantum critical points always have nonzero temperature in the laboratory, so it is crucial to compute observables in this regime to make contact with experiment.<sup>2</sup> More abstractly,  $S^1 \times \mathbb{R}^{d-1}$  is perhaps the simplest manifold not conformally-equivalent to  $\mathbb{R}^d$  (when  $d > 2$ ). This poses an important challenge for bootstrap techniques. Ideally, any nonperturbative solution of a QFT should describe its observables on arbitrary manifolds.<sup>3</sup> Finally, in the context of holography [6, 7, 37], finite-temperature CFTs are dual to AdS black holes, and we obtain valuable information about both by translating between them.

CFT correlators on  $S^1 \times \mathbb{R}^{d-1}$  are a limit of correlators on  $S^1 \times S^{d-1}$ , where we take the radius of the  $S^{d-1}$  to be much larger than the length of the  $S^1$ . An advantage of this point of view is that states on  $S^{d-1}$  are understood in principle via the state-

---

<sup>1</sup>This notion of temperature is distinct from the temperature of a classical statistical theory that one tunes to reach a critical point. The latter is simply a relevant coupling in the effective action. For example, the critical  $O(2)$  model deformed by a relevant singlet describes an XY magnet (a 3-dimensional classical theory) away from criticality. However, the critical  $O(2)$  model compactified on a circle describes the nonzero temperature physics of the quantum critical point separating the superfluid and insulating phases of a thin film (a (2+1)-dimensional quantum theory) [4, 5, 32, 33].

<sup>2</sup>Note that we must analytically continue Euclidean correlators on  $S^1 \times \mathbb{R}^{d-1}$  to describe real-time correlators of a Lorentzian theory at finite temperature.

<sup>3</sup>At least when the theory on that manifold makes sense. See appendix A.4 for a discussion of subtleties that can arise in compactification on  $S^1$  and other manifolds. See [34–36] for previous work on the bootstrap in  $d > 2$  on nontrivial manifolds.

operator correspondence. However, this limit is difficult to take in practice. Current bootstrap techniques work best at small twist  $\tau = \Delta - J \sim \mathcal{O}(1)$ . However, the above limit requires knowledge of the spectrum and OPE coefficients at large dimension  $\Delta$ , which is usually out of reach. We would like an alternative approach that more directly constrains finite-temperature observables. We would also like an approach that could work for other compactifications, for instance, on the torus  $T^d$ .

In [38], El-Showk and Papadodimas identified an interesting crossing equation for a two-point function on  $S^1_\beta \times \mathbb{R}^{d-1}$  (here  $\beta$  denotes the length of the  $S^1$ ). Because this geometry is conformally flat, one can compute two-point functions using the operator product expansion (OPE), assuming the points are sufficiently close together. The new data entering this computation are thermal one-point functions. For example, the one-point function of a scalar operator is

$$\langle \mathcal{O} \rangle_\beta \equiv \langle \mathcal{O} \rangle_{S^1_\beta \times \mathbb{R}^{d-1}} = \frac{b_{\mathcal{O}}}{\beta^{\Delta_{\mathcal{O}}}} = b_{\mathcal{O}} T^{\Delta_{\mathcal{O}}}. \quad (2.1)$$

The  $\beta$  dependence of  $\langle \mathcal{O} \rangle_\beta$  is fixed by the scale symmetry, but the coefficient  $b_{\mathcal{O}}$  is not fixed by symmetry. The OPE gives an expression for a thermal two-point function that can be schematically written as:

$$g(\tau) \equiv \langle \phi(\tau)\phi(0) \rangle_{S^1_\beta \times \mathbb{R}^{d-1}} \sim \frac{1}{|\tau|^{2\Delta_\phi}} \sum_{\mathcal{O} \in \phi \times \phi} \frac{f_{\phi\phi\mathcal{O}} b_{\mathcal{O}}}{c_{\mathcal{O}}} \left| \frac{\tau}{\beta} \right|^{\Delta_{\mathcal{O}}}, \quad (2.2)$$

where  $f_{\phi\phi\mathcal{O}}$  is the OPE coefficient of  $\mathcal{O}$ ,  $\Delta_{\mathcal{O}}$  is the scaling dimension of  $\mathcal{O}$ , and  $c_{\mathcal{O}}$  is the two-point coefficient of  $\mathcal{O}$  in the vacuum.<sup>4</sup> For simplicity, we have taken the operators to be separated only in the circle direction with distance  $\tau$ . (In section 2.2 we study more general kinematics.) The KMS condition for the two-point function of identical bosonic operators separated only along Euclidean time reads

$$g(\tau) = g(\beta - \tau). \quad (2.3)$$

El-Showk and Papadodimas noted that (2.2) does not manifestly satisfy (2.3). Imposing the KMS condition therefore gives a nontrivial “thermal crossing equation.” This constrains the  $b_{\mathcal{O}}$ ’s in terms of the other data of the CFT, namely the OPE coefficients  $f_{\phi\phi\mathcal{O}}$  and dimensions  $\Delta_{\mathcal{O}}$ . Via the limit  $S^1 \times S^{d-1} \rightarrow S^1 \times \mathbb{R}^{d-1}$ , this equation can be understood as a consequence of the usual crossing symmetry for four-point functions where we sum over some of the “external” operators.

---

<sup>4</sup>It is conventional to normalize  $c_{\mathcal{O}}$  to 1. However, some operators like the stress tensor have their own canonical normalization coming from Ward identities.

As we explain in section 2.2, the one-point coefficients  $b_{\mathcal{O}}$ , together with the usual CFT data  $f_{ijk}$ ,  $\Delta_i$ , determine all finite-temperature correlators. Thus, our focus will be on computing thermal one-point coefficients using nonperturbative methods. We should note however that many interesting finite-temperature observables, like e.g. the thermal mass (discussed in section 2.2.3), are difficult to extract from thermal one-point functions. Such observables are an even more challenging target for the future.

The thermal crossing equation is problematic for numerical bootstrap techniques because the expansion (2.2) has coefficients  $f_{\phi\phi\mathcal{O}}b_{\mathcal{O}}/c_{\mathcal{O}}$  that are not sign-definite. Sign-definiteness is crucial for the linear programming-based method of [39] and its generalizations [40–43]. In this sense, the thermal bootstrap is similar to the boundary bootstrap [44–46], defect bootstrap [47–51], and four-point bootstrap in non-unitary CFTs [52, 53]. Our strategy will be to develop analytical approaches to the thermal crossing equation, with the hope of eventually applying them (perhaps in conjunction with numerics) to CFTs whose spectrum and OPE coefficients are relatively well-understood, like e.g. the 3d Ising model [20, 41, 43, 54–56].<sup>5</sup> We should note that most of our methods will apply with any choice of boundary conditions around the circle (perhaps with slight modifications). Although our focus will be on finite-temperature, one could also study supersymmetric compactifications, or compactifications with more general chemical potentials.

A general and powerful analytic bootstrap technique that can be applied to our problem is large-spin perturbation theory [13–17, 20, 23]. Large-spin perturbation theory was recently reformulated by Caron-Huot in terms of a Lorentzian inversion formula [25] (inspired by a classic formula of Froissart and Gribov in the context of  $S$ -matrix theory [57, 58]). Caron-Huot’s formula expresses OPE coefficients and dimensions in terms of an integral of a four-point function in a Lorentzian regime. Inserting the OPE expansion in the  $t$ -channel into the inversion formula, one obtains a systematic large-spin expansion for  $s$ -channel data. This process can be iterated to obtain further information about the solution to crossing symmetry [20, 24, 59–65].

In section 2.3, we derive a Lorentzian inversion formula for thermal one-point functions as an integral of a thermal-two point function. The integral is over an interesting Regge-like Lorentzian regime that is more natural from the point of view of Kaluza-Klein compactification than finite-temperature physics. Our formula is very close to the Froissart-Gribov  $S$ -matrix formula, and in fact our derivation is almost identical.

---

<sup>5</sup>Our methods share many similarities with the recent defect bootstrap analysis in [51].

However, our result relies on some (well-motivated) assumptions about analyticity properties and asymptotics of thermal two-point functions that we discuss further in sections 2.3.4 and 2.3.5. Our formula shows that thermal one-point functions in conformal field theory are also analytic in spin, in the same way as OPE coefficients and operator dimensions.

In sections 2.4 and 2.5, we apply our inversion formula in some examples, including Mean Field Theory and the critical  $O(N)$  model in  $d = 3$  at large  $N$ . We also discuss some aspects of thermal correlators in general large- $N$  theories, especially holographic CFTs with a large gap to single-trace higher-spin operators. For the  $O(N)$  model, by studying the two-point function  $\langle \phi_i \phi_i \rangle_\beta$  we derive the thermal one-point functions  $b_{\mathcal{O}}$  for all single-trace operators  $\mathcal{O}$ . This includes the singlet higher-spin currents,  $J_\ell \sim \phi_i \partial^\ell \phi_i$ , where  $\ell$  is a positive even integer. The result, which to our knowledge is new for  $\ell > 2$ , can be found in (2.104)-(2.106) and is reproduced here:

$$\frac{b_{J_\ell}}{\sqrt{c_{J_\ell}}} = \frac{\sqrt{N} 2^{\ell+1} \ell}{\ell!} \sum_{n=0}^{\ell} \frac{2^n (\ell - n + 1)_n}{n! (2\ell - n + 1)_n} m_{\text{th}}^n \text{Li}_{\ell+1-n}(e^{-m_{\text{th}}}). \quad (2.4)$$

where  $m_{\text{th}} \beta = 2 \log \left( \frac{1+\sqrt{5}}{2} \right)$  is the thermal mass of the critical  $O(N)$  model to leading order in  $1/N$ . We have normalized  $b_{J_\ell}$  by the square root of the norm of  $J_\ell$ . Interestingly, this result exhibits uniform transcendentality of weight  $\ell + 1$ , a feature that would be worth understanding more deeply. For  $\ell = 2$ , the case of the stress tensor, the result matches that of Sachdev [66]. We also derive sums of thermal coefficients for scalar composite operators with dimension  $\Delta = 2, 4, 6, \dots$

Together with the thermal mass, these higher-spin one-point functions have an interesting interpretation in the context of the holographic duality of the critical  $O(N)$  model to Vasiliev higher-spin gravity in  $\text{AdS}_4$  (see e.g. [67–69]). In particular, they determine the complete set of higher-spin charges of the putative black hole solution dual to the CFT state at finite temperature. Thus, we now have the full set of higher-spin gauge-invariant data necessary to check, or perhaps even construct, a candidate solution in the bulk.

In section 2.6, we use our inversion formula to develop large-spin perturbation theory for thermal one-point functions. This allows us to study the thermal data of arbitrary, strongly-interacting CFTs. Crucially, thermal two-point functions have different OPE channels with overlapping regimes of validity. Inverting terms in one channel to the other relates thermal coefficients of operators in the theory in nontrivial ways: one-point functions determine terms in the large-spin expansion of other one-point



functions. These relations can be posed to formulate an analytic bootstrap problem for the thermal data. The required calculations are similar to (but simpler than) those that arise in the context of vacuum four-point functions. For example, the one-point functions of low-twist operators at large spin are dominated by an analog of the double-lightcone limit, and one is interested in the discontinuity of the correlator (as opposed to the “double discontinuity” [25]) in this limit. In fact, we see that the large-spin perturbation theory of spectral and OPE data and of thermal data are intimately tied together.

As an example, we find a universal contribution to one-point functions of “double-twist” operators  $[\phi\phi]_{0,J}$ <sup>6</sup> [12–14], proportional to the free-energy density,

$$b_{[\phi\phi]_{0,J}} \sim \frac{c_{[\phi\phi]_{0,J}}}{f_{\phi\phi[\phi\phi]_{0,J}}} \frac{2^{J+1} (1 + \frac{1}{2}\gamma'(J))}{\Gamma(1 + J + \frac{1}{2}\gamma(J))} \times \left[ \frac{\Gamma(\Delta_\phi + J + \frac{1}{2}\gamma(J))}{\Gamma(\Delta_\phi)} - \left( \frac{fd \text{vol}(S^{d-1}) \Delta_\phi c_{\text{free}}}{4 c_T} \right) \frac{\Gamma(\Delta_\phi - \frac{d-2}{2} + J + \frac{1}{2}\gamma(J))}{\Gamma(\Delta_\phi - \frac{d-2}{2})} + \dots \right]. \quad (2.5)$$

Here,  $f = F/T^d < 0$ , where  $F$  is the free energy density,  $c_T$  is the stress-tensor two-point coefficient,  $c_{\text{free}}$  is  $c_T$  for a free boson, and  $\gamma(J)$  is the anomalous dimension of  $[\phi\phi]_{0,J}$ . The OPE coefficients  $f_{\phi\phi[\phi\phi]_{0,J}}$  and anomalous dimensions  $\gamma(J)$  can be computed using the lightcone bootstrap for vacuum four-point functions [13–17, 20, 23, 25].<sup>7</sup> Our precise result is that the two sides of (2.5) match to all orders in an expansion in  $1/J$ . (Our inversion formula also produces nonperturbative corrections in  $J$ .) The leading term in brackets is due to the unit operator. The stress tensor contribution is the second term in brackets, and it falls off like  $1/J^{\frac{d-2}{2}}$  relative to the leading term. The dots represent similar contributions from other operators  $\mathcal{O}$  that are suppressed by  $1/J^{\frac{\tau_{\mathcal{O}}}{2}}$  where  $\tau_{\mathcal{O}} = \Delta_{\mathcal{O}} - J_{\mathcal{O}}$  is the twist of  $\mathcal{O}$ . In particular, the stress tensor gives the next large- $J$  correction after the unit operator if it is the lowest-twist operator in the  $\phi \times \phi$  OPE (other than the unit operator).

Also in section 2.6, we discuss subtleties associated with sums over infinite families of operators, and how crossing symmetry of four-point functions is embedded in the thermal crossing equations. As an example, we apply our large-spin technology to the 3d Ising model. We conclude with discussion and comments on future directions

<sup>6</sup>The operators  $[\phi\phi]_{0,J}$  have twist  $\tau = \Delta - J = 2\Delta_\phi + \gamma(J)$ , where  $\gamma(J)$  is an anomalous dimension that vanishes as  $J \rightarrow \infty$ . They can be thought of schematically as  $[\phi\phi]_{0,J} = \phi \partial_{\mu_1} \cdots \partial_{\mu_J} \phi$ .

<sup>7</sup>Note that [13] uses the convention  $c_{\mathcal{O}} = (-\frac{1}{2})^{J_{\mathcal{O}}}$ .

in section 2.7. In appendix A.1, we pursue the independent direction of studying the partition function on  $S^1_\beta \times S^{d-1}$ , give a rough estimate of  $b_T$  in the 3d Ising model from the  $\beta \rightarrow 0$  limit, and discuss further aspects of this limit in appendix A.2. The next appendices further elaborate on technical details in the main text.

## 2.2 CFTs at nonzero temperature

### 2.2.1 Low-point functions and the OPE

Any CFT correlation function on  $\mathbb{R}^d$  can be computed using the operator product expansion (OPE). Beginning with an  $n$ -point function  $\langle \mathcal{O}_1 \cdots \mathcal{O}_n \rangle$ , we recursively use the OPE to reduce it to a sum of 1-point functions, for example

$$\begin{aligned} \langle \mathcal{O}_1 \cdots \mathcal{O}_n \rangle &= \sum_{k_1} C_{12k_1} \langle \mathcal{O}_{k_1} \mathcal{O}_3 \cdots \mathcal{O}_n \rangle \\ &= \sum_{k_1} \cdots \sum_{k_{n-1}} C_{12k_1} C_{k_1 3k_2} \cdots C_{k_{n-2} n k_{n-1}} \langle \mathcal{O}_{k_{n-1}} \rangle. \end{aligned} \quad (2.6)$$

Here the  $C_{ijk}$  are differential operators, and we have suppressed the position dependence of the  $\mathcal{O}_i$  for brevity. Each time we apply the OPE we must find a pair of operators  $\mathcal{O}_i, \mathcal{O}_j$  and a sphere surrounding them such that all other operators lie outside this sphere. This is always possible for generic configurations of points in  $\mathbb{R}^d$ . Finally, by translation invariance and dimensional analysis,<sup>8</sup> one-point functions on  $\mathbb{R}^d$  are given by

$$\langle \mathcal{O} \rangle_{\mathbb{R}^d} = \begin{cases} 1 & \text{if } \mathcal{O} = \mathbf{1}, \\ 0 & \text{otherwise.} \end{cases} \quad (2.7)$$

The same procedure works on any conformally-flat manifold  $\mathcal{M}^d$ , but with two additional complications. Firstly, non-unit operators can have nonzero one-point functions. Secondly, depending on the configuration of operator insertions, it may not always be possible to perform the OPE. More specifically, to compute  $\mathcal{O}_i \times \mathcal{O}_j$ , we must find a sphere containing only  $\mathcal{O}_i$  and  $\mathcal{O}_j$  whose interior is flat (possibly after performing a Weyl transformation). However, the geometry of  $\mathcal{M}^d$  may make this impossible.

In this work, we study CFTs on the manifold  $\mathcal{M}_\beta = S^1_\beta \times \mathbb{R}^{d-1}$ . We use coordinates  $x = (\tau, \mathbf{x})$  on  $S^1_\beta \times \mathbb{R}^{d-1}$ , where  $\tau$  is periodic  $\tau \sim \tau + \beta$ . One-point functions on  $\mathcal{M}_\beta$  are constrained by symmetries as follows. To begin, translation-invariance implies

---

<sup>8</sup>Here, we assume unitarity, which implies that only the unit operator has scaling dimension 0.

that descendant operators have vanishing one-point functions:

$$\langle P^\mu \mathcal{O}(x) \rangle_\beta = \partial^\mu \langle \mathcal{O}(x) \rangle_\beta = \partial^\mu \langle \mathcal{O}(0) \rangle_\beta = 0. \quad (2.8)$$

(The notation  $\langle \dots \rangle_\beta$  denotes a correlator on  $\mathcal{M}_\beta$ .) Thus, let us consider a primary operator  $\mathcal{O}$  with dimension  $\Delta$  and  $\text{SO}(d)$  representation  $\rho$ .

The geometry  $S^1 \times \mathbb{R}^{d-1}$  is clearly invariant under  $\text{SO}(d-1)$ . It also has a discrete symmetry under which  $\tau \leftrightarrow -\tau$ . In general, our CFT may not be parity-invariant, so to get a symmetry of the theory, we should accompany  $\tau \leftrightarrow -\tau$  with a reflection in one of the  $\mathbb{R}^{d-1}$  directions. This combines with  $\text{SO}(d-1)$  to give the symmetry group  $\text{O}(d-1) \subset \text{SO}(d)$ , where a reflection in  $\text{O}(d-1)$  also flips the sign of  $\tau$ .<sup>9</sup> For  $\langle \mathcal{O} \rangle_\beta$  to be nonzero, the restriction of  $\rho$  under  $\text{O}(d-1) \subset \text{SO}(d)$  must contain the trivial representation

$$\text{Res}_{\text{O}(d-1)}^{\text{SO}(d)} \rho \supset \mathbf{1}. \quad (2.9)$$

This implies that  $\rho$  must be a symmetric traceless tensor (STT), with even spin  $J$ . Finally, the one-point function of a spin- $J$  operator  $\mathcal{O}$  is fixed by symmetry and dimensional analysis, up to a single dimensionless coefficient  $b_\mathcal{O}$ :

$$\langle \mathcal{O}^{\mu_1 \dots \mu_J}(x) \rangle_\beta = \frac{b_\mathcal{O}}{\beta^\Delta} (e^{\mu_1} \dots e^{\mu_J} - \text{traces}). \quad (2.10)$$

Here,  $e^\mu$  is the unit vector in the  $\tau$ -direction. Here and in what follows, we are implicitly normalizing our correlators by the partition function,  $Z(\beta)$ .

We will find it convenient to study two-point functions, which encode the  $b_\mathcal{O}$ 's via the OPE.<sup>10</sup> Note that, unlike in  $\mathbb{R}^d$ , two-point functions of non-identical operators may be nonvanishing on  $\mathcal{M}_\beta$ . However, for simplicity, we focus on two-point functions of identical operators,

$$g(\tau, \mathbf{x}) = \langle \phi(x) \phi(0) \rangle_\beta. \quad (2.11)$$

The OPE is valid whenever both operators lie within a sphere whose interior is flat. In our case, the largest such sphere has diameter  $\beta$ : it wraps entirely around the  $S^1$  and is tangent to itself (figure 2.1). The condition for both  $x$  and  $0$  to lie within such a sphere is

$$|x| = \sqrt{\tau^2 + \mathbf{x}^2} < \beta, \quad (\text{OPE convergence}). \quad (2.12)$$

<sup>9</sup>In a parity-invariant theory, the rotational symmetry group would be  $\text{O}(d-1) \times \mathbb{Z}_2$ , and we would have the restriction that only parity-even operators could have nonzero one-point functions.

<sup>10</sup>For previous discussions of the OPE for CFT two-point functions at finite temperature, see [32, 70].

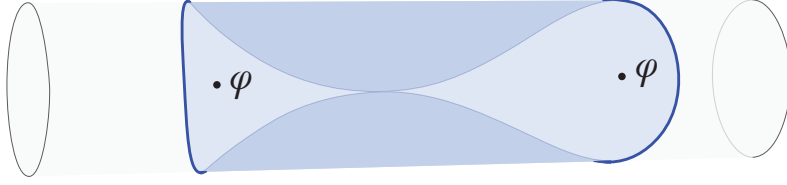


Figure 2.1: The OPE on  $S^1_\beta \times \mathbb{R}^{d-1}$  is valid if the two operators lie inside a sphere. The largest possible sphere has diameter  $\beta$ , wrapping entirely around the  $S^1$  such that it is tangent to itself. Here, we illustrate such a sphere (blue) in  $d = 2$ .

Assuming  $|x| < \beta$ , we can use the OPE to obtain

$$g(\tau, \mathbf{x}) = \sum_{\mathcal{O} \in \phi \times \phi} \frac{f_{\phi\phi\mathcal{O}}}{c_{\mathcal{O}}} |x|^{\Delta - 2\Delta_\phi - J} x_{\mu_1} \cdots x_{\mu_J} \langle \mathcal{O}^{\mu_1 \cdots \mu_J}(0) \rangle_\beta. \quad (2.13)$$

Here,  $c_{\mathcal{O}}$  is the coefficient in the two-point function of  $\mathcal{O}$ ,

$$\langle \mathcal{O}^{\mu_1 \cdots \mu_J}(x) \mathcal{O}_{\nu_1 \cdots \nu_J}(0) \rangle = c_{\mathcal{O}} \frac{I_{(\nu_1}^{(\mu_1} \cdots I_{\nu_J)}^{\mu_J)} - \text{traces}}{x^{2\Delta_{\mathcal{O}}}}, \quad I_\nu^\mu(x) = \delta_\nu^\mu - \frac{2x_\nu x^\mu}{x^2}, \quad (2.14)$$

and  $f_{\phi\phi\mathcal{O}}$  is the three-point coefficient

$$\langle \phi(x_1) \phi(x_2) \mathcal{O}^{\mu_1 \cdots \mu_J}(x_3) \rangle = f_{\phi\phi\mathcal{O}} \frac{Z^{\mu_1} \cdots Z^{\mu_J} - \text{traces}}{x_{12}^{2\Delta_\phi - \Delta_{\mathcal{O}}} x_{23}^{\Delta_{\mathcal{O}}} x_{13}^{\Delta_{\mathcal{O}}}}, \quad Z^\mu = \frac{x_{13}^\mu}{x_{13}^2} - \frac{x_{23}^\mu}{x_{23}^2}. \quad (2.15)$$

We often normalize  $\mathcal{O}$  so that  $c_{\mathcal{O}} = 1$ . Note that because descendants have vanishing one-point functions, we need only the leading (non-derivative) term in the OPE for each multiplet. Plugging (2.10) into (2.13), the index contraction is given by a Gegenbauer polynomial,<sup>11</sup>

$$|x|^{-J} (x_{\mu_1} \cdots x_{\mu_J}) (e^{\mu_1} \cdots e^{\mu_J} - \text{traces}) = \frac{J!}{2^J (\nu)_J} C_J^{(\nu)}(\eta), \quad (2.16)$$

where  $\nu = \frac{d-2}{2}$ ,  $(a)_n = \frac{\Gamma(a+n)}{\Gamma(a)}$  is the Pochhammer symbol, and  $\eta = \frac{\tau}{|x|}$ . Thus, we obtain

$$g(\tau, \mathbf{x}) = \sum_{\mathcal{O} \in \phi \times \phi} \frac{a_{\mathcal{O}}}{\beta^\Delta} C_J^{(\nu)}(\eta) |x|^{\Delta - 2\Delta_\phi}, \quad \text{where} \\ a_{\mathcal{O}} \equiv \frac{f_{\phi\phi\mathcal{O}} b_{\mathcal{O}}}{c_{\mathcal{O}}} \frac{J!}{2^J (\nu)_J}. \quad (2.17)$$

We can think of  $|x|^{\Delta - 2\Delta_\phi} C_J^{(\nu)}(\eta)$  as a two-point conformal block on  $S^1 \times \mathbb{R}^{d-1}$ .<sup>12</sup>

<sup>11</sup>When the operators in the two-point function have spin, the appropriate generalization of the Gegenbauer polynomial is described in [71].

<sup>12</sup>Note that  $a_{\mathcal{O}}$  is independent of the normalization of  $\mathcal{O}$ . We sometimes quote values for the combination  $b_{\mathcal{O}}/\sqrt{c_{\mathcal{O}}}$ , which changes sign under a redefinition  $\mathcal{O} \rightarrow -\mathcal{O}$ . We usually fix this ambiguity by choosing a sign for some OPE coefficient  $f_{\phi\phi\mathcal{O}}$  involving  $\mathcal{O}$ .

### 2.2.1.1 Free energy density

One of the most important thermal one-point coefficients is  $b_T$ , associated to the stress tensor  $T^{\mu\nu}$ . This is related to the free energy density of the thermal CFT as follows. From (2.10), the energy density is given by<sup>13</sup>

$$E(\beta) = -\langle T^{00} \rangle_\beta = -\left(1 - \frac{1}{d}\right) b_T T^d > 0. \quad (2.18)$$

In particular, note that  $b_T$  must be negative, by positivity of energy. By dimensional analysis, the free energy density  $F$  must take the form  $F = fT^d$ , where  $f$  is a dimensionless quantity. Using the thermodynamic relations  $F = E - TS = E + TdF/dT$ , we find

$$f = \frac{b_T}{d} < 0. \quad (2.19)$$

The Ward identity fixes

$$f_{\phi\phi T} = -\frac{d}{d-1} \frac{\Delta_\phi}{S_d}, \quad S_d = \text{vol}(S^{d-1}) = \frac{2\pi^{d/2}}{\Gamma(d/2)}. \quad (2.20)$$

Consequently, the coefficient of  $T$  in the thermal block expansion of  $\langle \phi\phi \rangle_\beta$  (2.17) is

$$a_T = -f S_d \frac{2\Delta_\phi}{d-2} \frac{c_{\text{free}}}{c_T}, \quad (2.21)$$

where  $c_{\text{free}} = \frac{d}{d-1} \frac{1}{S_d^2}$  is stress tensor two-point coefficient for the free boson in  $d$ -dimensions [72]. For a single free (real) scalar,  $b_T = -2d\zeta(d)/S_d$ , as can be checked by computing its free energy

$$F = fT^d = T \int \frac{d^{d-1}\mathbf{k}}{(2\pi)^{d-1}} \log[1 - \exp(-\beta|\mathbf{k}|)] = -\frac{2}{S_d} \zeta(d) T^d. \quad (2.22)$$

For the convenience of the reader, we now collect some known results for  $b_T$  in various theories.

1. For the free scalar in three dimensions, we have  $b_T^{\text{free}} = -6\zeta(3)/(4\pi) \approx -0.57394$ .
2. For the  $O(N)$  model in three dimensions at leading order in  $1/N$ ,  $b_T = 4N/5 \times b_T^{\text{free}} \approx -0.45915N$  [66, 73]. We will derive this from our inversion formula in section 2.5.1.

---

<sup>13</sup>The minus sign is because we are using conventions appropriate for Euclidean field theory. When Wick rotating from Euclidean to Lorentzian signature, it is conventional to include factors of  $i$  in the 0 components of tensor operators. This ensures that they go from tensors of  $SO(d)$  in Euclidean signature to tensors of  $SO(d-1, 1)$  in Lorentzian signature. For the stress tensor, this means  $T_{\text{Lorentzian}}^{00} = i^2 T_{\text{Euclidean}}^{00}$ , so the expectation value of  $T_{\text{Lorentzian}}^{00}$  is positive as it should be, see e.g. [1].

3. In the Monte Carlo literature, the quantity  $f$  is known as the ‘‘Casimir Amplitude.’’ For the Ising model, Monte Carlo results give  $f \approx -0.153$  [74–76], with numerical errors in the third digit. This translates to  $b_T^{\text{Ising}} \approx -0.459$ . Note that  $b_T^{\text{Ising}}$  is remarkably close to the value of  $b_T/N$  for the  $O(N)$  model at large  $N$ .<sup>14</sup>

### 2.2.1.2 Two dimensions

In  $d = 2$ ,  $S_\beta^1 \times \mathbb{R}$  is conformal to the plane, so thermal correlators on the cylinder are determined by symmetry. All one-point functions vanish except for those of operators living in the Virasoro vacuum module:

$$\langle \mathcal{O} \rangle_{S_\beta^1 \times \mathbb{R}} = 0 \quad \forall \quad \mathcal{O} \notin \{ \mathbf{1}, T^{\mu\nu}, :T^{\mu\nu}T^{\rho\sigma}:, \dots \}. \quad (2.23)$$

Likewise, two-point functions on  $S_\beta^1 \times \mathbb{R}$  are determined via a conformal transformation as

$$\langle \mathcal{O}_i(z, \bar{z}) \mathcal{O}_j(0, 0) \rangle_{S_\beta^1 \times \mathbb{R}} = \left( \frac{\beta}{\pi} \sinh \left( \frac{\pi z}{\beta} \right) \right)^{-2h_{\mathcal{O}}} \left( \frac{\beta}{\pi} \sinh \left( \frac{\pi \bar{z}}{\beta} \right) \right)^{-2\bar{h}_{\mathcal{O}}} \delta_{ij}. \quad (2.24)$$

Unlike in  $d > 2$ , two-point functions of distinct operators vanish. It follows from Virasoro symmetry and (2.23) that the right-hand side of (2.24) is the two-point Virasoro  $\times$  Virasoro vacuum block on the cylinder. By expanding (2.24) — or using formulae of section 2.3.2.2 — one may extract the (weighted) sum of one-point coefficients  $a_{\mathcal{O}}$  of all Virasoro descendants at a given level above the vacuum. These are, of course, determined by the action of the Schwarzian derivative [77–79].

### 2.2.1.3 From the sphere to the plane

Thermal correlation functions are also naturally computed on  $S_\beta^1 \times S_L^{d-1}$ , owing to the role of spherical slicing in the state-operator correspondence. Due to the presence of the  $S^{d-1}$  curvature radius  $L$ , these thermal correlators are less constrained by conformal invariance than their counterparts on  $S_\beta^1 \times \mathbb{R}^{d-1}$ . However, they must obey the flat space limit

$$\lim_{L \rightarrow \infty} \langle \mathcal{O}_1 \cdots \mathcal{O}_n \rangle_{S_\beta^1 \times S_L^{d-1}} = \langle \mathcal{O}_1 \cdots \mathcal{O}_n \rangle_{S_\beta^1 \times \mathbb{R}^{d-1}}. \quad (2.25)$$

One-point functions are fixed by dimensional analysis and spherical symmetry to take the form

$$\langle \mathcal{O}^{\mu_1 \cdots \mu_J}(x) \rangle_{S_\beta^1 \times S_L^{d-1}} = \frac{b_{\mathcal{O}} f_{\mathcal{O}} \left( \frac{\beta}{L} \right)}{\beta^\Delta} (e^{\mu_1} \cdots e^{\mu_J} - \text{traces}), \quad (2.26)$$

<sup>14</sup>We estimate  $b_T^{\text{Ising}}$  using the known part of the spectrum of the 3d Ising model in appendix A.1.

where  $f_{\mathcal{O}}(\frac{\beta}{L})$  is a function that is not determined by conformal symmetry; it obeys the boundary condition  $f_{\mathcal{O}}(0) = 1$ . On the other hand, employing radial quantization,

$$\langle \mathcal{O}^{\mu_1 \dots \mu_J}(x) \rangle_{S^1_{\beta} \times S^{d-1}_L} = \frac{1}{Z(\beta)} \sum_{\mathcal{O}'} e^{-\beta \Delta_{\mathcal{O}'}} \langle \mathcal{O}' | \mathcal{O}^{\mu_1 \dots \mu_J}(x) | \mathcal{O}' \rangle, \quad (2.27)$$

where the sum runs over all local operators  $\mathcal{O}'$  (not just primaries) and  $Z(\beta) = \sum_{\mathcal{O}'} e^{-\beta \Delta_{\mathcal{O}'}}$  is the partition function. It is useful to introduce one-point thermal conformal blocks on the sphere via

$$\begin{aligned} & \langle \mathcal{O}^{\mu_1 \dots \mu_J}(x) \rangle_{S^1_{\beta} \times S^{d-1}_L} \\ &= \frac{1}{Z(\beta)} \sum_{\text{Primary } \mathcal{O}'} f_{\mathcal{O}\mathcal{O}'\mathcal{O}'} F(h_{\mathcal{O}}, \bar{h}_{\mathcal{O}}; h_{\mathcal{O}'}, \bar{h}_{\mathcal{O}'} | \beta) (e^{\mu_1} \dots e^{\mu_J} - \text{traces}), \end{aligned} \quad (2.28)$$

where  $F(h_{\mathcal{O}}, \bar{h}_{\mathcal{O}}; h_{\mathcal{O}'}, \bar{h}_{\mathcal{O}'} | \beta)$  captures all contributions of the conformal family of  $\mathcal{O}'$  to  $\langle \mathcal{O}^{\mu_1 \dots \mu_J}(x) \rangle_{S^1_{\beta} \times S^{d-1}_L}$ . We have set  $L = 1$ , and introduced the left- and right-moving conformal weights

$$h_{\mathcal{O}} = \frac{\Delta_{\mathcal{O}} - J}{2}, \quad \bar{h}_{\mathcal{O}} = \frac{\Delta_{\mathcal{O}} + J}{2}, \quad (2.29)$$

and likewise for  $\mathcal{O}'$ . These blocks were recently computed in any  $d$ , for scalar  $\mathcal{O}$  and scalar  $\mathcal{O}'$ , in [80]. Two-point functions may also be written using the OPE and a sum over states, although we refrain from showing the details here.

Consistency of (2.28) with the flat space limit (2.10) can in principle be established by taking  $\beta \rightarrow 0$ , which involves contributions from all high-energy states. We discuss further details of this limit and thermal blocks on  $S^1 \times S^{d-1}$  in appendix A.2. The general lesson is that exact computation of  $\langle \mathcal{O} \rangle_{S^1_{\beta} \times \mathbb{R}^{d-1}}$  by passage from  $S^1_{\beta} \times S^{d-1}_L$  is challenging. Perhaps the simplest observable to compute using these methods is  $b_T$ , and we explore this possibility in appendix A.1 with the free boson and 3d Ising model as examples. The rest of this paper is devoted to developing new methods directly on  $S^1_{\beta} \times \mathbb{R}^{d-1}$ .

### 2.2.2 The KMS condition and crossing

Let us now review the derivation of the KMS condition. Consider a thermal two-point function in Euclidean time  $\langle A(\tau)B(0) \rangle_{\beta}$ , and let us assume  $\tau > 0$ . This is given by

$$\langle A(\tau)B(0) \rangle_{\beta} = \text{Tr}(e^{-\beta H} e^{\tau H} A(0) e^{-\tau H} B(0)) = \text{Tr}(e^{-(\beta-\tau)H} A(0) e^{-\tau H} B(0)), \quad (2.30)$$

where  $H$  is the Hamiltonian. Note that convergence of the exponential factor  $e^{-\tau H}$  requires  $\tau > 0$  and convergence of the exponential factor  $e^{-(\beta-\tau)H}$  requires  $\tau < \beta$ .

Thus, the above expression defines the thermal two-point function for  $\tau \in (0, \beta)$ . From cyclicity of the trace, one immediately finds that

$$\langle A(\tau)B(0) \rangle_\beta = \langle B(\beta - \tau)A(0) \rangle_\beta. \quad (2.31)$$

This is the KMS condition.

Taking  $A(\tau) = \phi(\tau, \mathbf{x})$ ,  $B(0) = \phi(0, 0)$  and  $\tau = \beta/2 + \tilde{\tau}$ , with  $\tilde{\tau} \in [-\frac{\beta}{2}, \frac{\beta}{2}]$  we get

$$g(\beta/2 + \tilde{\tau}, \mathbf{x}) = g(\beta/2 - \tilde{\tau}, -\mathbf{x}). \quad (2.32)$$

By  $\text{SO}(d-1)$ -invariance, the correlator depends only on  $|\mathbf{x}|$ , so is invariant under  $\mathbf{x} \rightarrow -\mathbf{x}$ . Thus, we can further conclude that

$$g(\beta/2 + \tilde{\tau}, \mathbf{x}) = g(\beta/2 - \tilde{\tau}, \mathbf{x}). \quad (2.33)$$

The fact that the scalar thermal two-point function is even in  $\mathbf{x}$  is built into the conformal block decomposition (2.17). Another approach to understand (2.33) is to note that Euclidean thermal correlators are computed by a path integral on the geometry  $S_\beta^1 \times \mathbb{R}^{d-1}$ , and then (2.33) is evident from the  $\text{O}(d-1)$  symmetries of the geometry discussed in section 2.2.1.

Note that the thermal conformal block decomposition (2.17) can be constrained by the KMS condition (2.33) due to the lack of manifest periodicity for the thermal conformal block, in a similar way in which the four-point functions conformal blocks are not manifestly crossing-symmetric. This constraint is well-defined within the OPE radius of convergence, whenever both  $\beta/2 + \tilde{\tau}$ , and  $\beta/2 - \tilde{\tau} \in [0, \beta]$  (2.12). Thus, in analogy to the crossing equation for vacuum four-point functions, we will interpret (2.33) as a constraint equation for all the thermal coefficients  $a_{\mathcal{O}}$  appearing in (2.17). This observation was made in [38]. The analog of expanding four-point functions around the crossing-symmetric point  $z = \bar{z} = 1/2$  is, using the reflection property (2.33), to enforce that

$$\frac{\partial^{n+m}}{\partial \tau^n \partial^m |\mathbf{x}|} g(\tau, \mathbf{x}) \Big|_{\tau=\frac{\beta}{2}, \mathbf{x}=0} = 0 \quad \text{for odd } n \text{ and even } m. \quad (2.34)$$

This philosophy extends naturally to thermal  $n$ -point functions, which are expectation



values of Euclidean time-ordered products<sup>15</sup>

$$\begin{aligned} \langle A_1(\tau_1) \cdots A_n(\tau_n) \rangle_\beta &= \text{Tr}(e^{-\beta H} T\{A_1(\tau_1) \cdots A_n(\tau_n)\}) \\ &= \text{Tr}(e^{-\beta H} A_1(\tau_1) \cdots A_n(\tau_n)) \theta(\text{Re}(\tau_1 - \tau_2)) \cdots \theta(\text{Re}(\tau_{n-1} - \tau_n)) \\ &\quad + \text{permutations.} \end{aligned} \tag{2.35}$$

The above representation of the correlator is valid if  $\text{Re}(\tau_1 - \tau_n) \leq \beta$ . If  $\tau_n$  is the earliest time, then a similar manipulation to (2.30) using cyclicity of the trace implies

$$\begin{aligned} \langle A_1(\tau_1) \cdots A_n(\tau_n) \rangle_\beta &= \langle A_n(\tau_n + \beta) A_1(\tau_1) \cdots A_{n-1}(\tau_{n-1}) \rangle_\beta \\ &= \langle A_1(\tau_1) \cdots A_{n-1}(\tau_{n-1}) A_n(\tau_n + \beta) \rangle_\beta. \end{aligned} \tag{2.36}$$

(In the second line we used that operators trivially commute inside the time-ordering symbol.) It follows that the thermal expectation value of a Euclidean time-ordered product is periodic in each of the  $\tau_i$  (since we can decrease  $\tau_i$  until it becomes the earliest time and then apply (2.36)). This is again obvious from the geometry. We may regard these periodicity conditions as crossing equations. In this work, we focus on the case  $n = 2$ . (See [81] for recent study of KMS conditions for  $n$ -point functions.)

While the KMS condition imposes constraints on the  $a_{\mathcal{O}}$ , there is an immediate obstacle to an efficient bootstrap: the OPE expansion (2.17) is linear in the OPE coefficients, nor must the  $a_{\mathcal{O}}$  be sign-definite. Thus, the resulting expression lacks manifest positivity. This is more analogous to the bootstrap in the presence of a conformal boundary or defect, rather than the vacuum four-point function bootstrap [51]. To proceed, we need to develop some complementary tools; this will be the content of section 2.3.

### 2.2.3 Away from the OPE regime

The OPE representation (2.17) comes from interpreting the two-point function  $g(\tau, \mathbf{x})$  in radial quantization around a point in  $S_\beta^1 \times \mathbb{R}^{d-1}$ . As discussed in section 2.2.1, this representation is only valid when the points satisfy  $|x| < \beta$ . Other ways of quantizing the theory give other representations with their own regimes of validity (possibly overlapping).

---

<sup>15</sup>Note that time ordering is the only sensible ordering when operators are at different Euclidean times (i.e. “imaginary” times, although here it corresponds to real  $\tau$ ). This is because if the operators weren’t ordered appropriately, the exponential factors  $e^{-(\tau_i - \tau_j)H}$  would be divergent. By contrast, if some operators are at the same Euclidean time, but different Lorentzian (“real”) times, we can consider different orderings among those operators, and these orderings correspond to different analytic continuations of the Euclidean correlator. For example, in real time thermal physics (where  $\tau_i = it_i$  with  $t_i \in \mathbb{R}$ ), one can study arbitrary orderings of the operators.

Perhaps the most familiar way to study thermal correlators is to quantize the theory on  $\mathbb{R}^{d-1}$ -slices, where  $S^1$  is interpreted as a Euclidean time direction. This quantization leads to expressions for thermal correlation functions like (2.30). It is also the most natural choice from the point of view of the limit  $S^1 \times S^{d-1} \rightarrow S^1 \times \mathbb{R}^{d-1}$  discussed in section 2.2.1.3.

Another way of quantizing the theory (that will prove useful in the next section) is to choose a direction in  $\mathbb{R}^{d-1}$ , say  $x^1$ , as the time direction. States then live on slices with geometry  $S^1 \times \mathbb{R}^{d-2}$ . This quantization is natural if we imagine a Kaluza-Klein compactification of a  $d$ -dimensional QFT on a spatial  $S^1$ . In the compactified theory, the momentum generator around the  $S^1$ , which we call  $P_{\text{KK}}$ , becomes a global  $U(1)$  symmetry with a discrete spectrum. The Hamiltonian  $H_{\text{KK}}$  generates translations in  $x^1$ . Explicitly, the generators are given by

$$\begin{aligned} P_{\text{KK}} &= \int_0^\beta d\tau \int_{-\infty}^\infty dx^2 \cdots dx^{d-1} (-iT^{10}(\tau, \mathbf{x})), \\ H_{\text{KK}} &= \int_0^\beta d\tau \int_{-\infty}^\infty dx^2 \cdots dx^{d-1} \left( -T^{11}(\tau, \mathbf{x}) - \frac{b_T}{d} \frac{1}{\beta^d} \right), \end{aligned} \quad (2.37)$$

where the factor of  $-i$  in  $P_{\text{KK}}$  and the minus sign in  $H_{\text{KK}}$  come from Wick rotation as discussed in footnote 13. Because the charges are conserved, we can evaluate them at any value of  $x^1$ . In  $H_{\text{KK}}$ , we have chosen to subtract off the vacuum energy by hand so that it annihilates the vacuum on  $S^1 \times \mathbb{R}^{d-2}$ .<sup>16</sup>

In our two-point function  $g(\tau, \mathbf{x})$ , we can use  $\text{SO}(d-1)$ -invariance to set  $\mathbf{x} = (x^1, 0, \dots, 0)$  with  $x^1 > 0$ . Interpreting the correlator in KK quantization, we obtain

$$g(\tau, x^1) = \langle 0 | \phi(0) e^{-H_{\text{KK}} x^1 + i\tau P_{\text{KK}}} \phi(0) | 0 \rangle, \quad (2.38)$$

where  $|0\rangle$  is the ground-state on  $S^1 \times \mathbb{R}^{d-2}$ . Note that  $H_{\text{KK}}$  is Hermitian and bounded from below, so the factor  $e^{-H_{\text{KK}} x^1}$  leads to exponential suppression. We discuss the regime of validity of (2.38) in section 2.3.4.

The behavior of the correlator at large  $x^1$  (with fixed  $\tau$ ) is determined by the mass gap of the compactified theory, i.e. the smallest nonzero eigenvalue of  $H_{\text{KK}}$  which we call  $m_{\text{th}}$  (the ‘‘thermal mass’’). By dimensional analysis,  $m_{\text{th}}$  is a constant times  $1/\beta$ . It is a folk-theorem that dimensional reduction on a circle with thermal boundary

<sup>16</sup>Note that the  $d-1$ -dimensional vacuum energy density, equivalently the Casimir energy density of the CFT on a circle, is simply  $\frac{b_T}{d} \frac{1}{\beta^{d-1}} = \beta F$ . In particular, it is negative since  $b_T$  is negative by the discussion in section 2.2.1.1.

conditions produces a massive theory, i.e.  $m_{\text{th}} > 0$ .<sup>17</sup> Assuming this folk-theorem is true, the correlator approaches a factorized form exponentially quickly at large  $|\mathbf{x}|$

$$g(\tau, \mathbf{x}) \sim \langle \phi \rangle_{\beta}^2 + O(e^{-m_{\text{th}}|\mathbf{x}|}). \quad (2.39)$$

Like the KMS condition, the decay (2.39) is not at all obvious from the OPE. In free theories, supersymmetric compactifications, or in the presence of nontrivial chemical potentials, we could have  $m_{\text{gap}} = 0$  and the behavior of the long-distance correlator would be different.

Finally, let us note that the representation (2.38) does not use the full  $(d-1)$ -dimensional Poincare invariance of the compactified theory. To do so, we insert a complete set of states and classify them according to their  $(d-1)$ -dimensional invariant mass and KK momentum. This leads to a version of the Källén-Lehmann spectral representation

$$g(\tau, \mathbf{x}) = \sum_{n=-\infty}^{\infty} e^{in\tau} \int_0^{\infty} dm^2 \rho_n(m^2) G_F(\mathbf{x}, m^2), \quad (2.40)$$

where  $n$  is the KK momentum and  $G_F(\mathbf{x}, m^2)$  is the Feynman propagator in  $(d-1)$ -dimensions. The decomposition (2.40) comes from going to momentum space in the compact direction, and then applying the usual Källén-Lehmann representation in each momentum sector, yielding a density of states  $\rho_n(m^2)$  for each  $n$ . For real  $\tau, \mathbf{x}$ , the expression (2.40) is valid whenever  $|\mathbf{x}| > 0$ , so it has an overlapping regime of validity with the OPE. It would be interesting to study the equality of these two representations.

### 2.3 A Lorentzian inversion formula

Inversion formulas provide an efficient way to study the operator content of vacuum four-point functions in flat space. The starting point is an expansion of the four-point function in a complete set of single-valued conformal partial waves, which are solutions to the conformal Casimir equations on  $\mathbb{R}^d$ . This basis is natural because physical four-point functions are single-valued in Euclidean space. The expansion also follows on general grounds from the Plancherel theorem for the conformal group  $\text{SO}(d+1, 1)$  [82]. One may then invert the expansion using orthogonality and completeness, to extract the exchanged operator data from integrals of the four-point function.

In [25], Caron-Huot derived a remarkable inversion formula for four-point functions that involves an integral in Lorentzian signature.<sup>18</sup> In this section, we will derive a

<sup>17</sup>We thank Zohar Komargodski for discussions on this point.

<sup>18</sup>See [26] for another derivation.

Lorentzian inversion formula for thermal two-point functions. However, our formula will not have a similarly clean group-theoretic interpretation as in the case of four-point functions. The reason is that  $C_J^{(\nu)}(\eta)|x|^{\Delta-2\Delta_\phi}$ , the two-point thermal blocks on  $S_\beta^1 \times \mathbb{R}^{d-1}$ , are not a complete set of solutions to a differential equation (for any choices of  $(\Delta, J)$ ), simply because they are not single-valued functions on  $\mathbb{R}^{d-1} \times S^1$ .<sup>19</sup> Still, we will make progress without a completeness relation by focusing on the OPE limit and writing a formula that picks out the data in this limit.

### 2.3.1 Euclidean inversion

In analogy with the conformal partial wave expansion for four-point functions, we complexify  $\Delta$ , and write the thermal block expansion (2.17) as a spectral integral:

$$g(\tau, \mathbf{x}) = \sum_{J=0}^{\infty} \oint_{-\epsilon-i\infty}^{-\epsilon+i\infty} \frac{d\Delta}{2\pi i} a(\Delta, J) C_J^{(\nu)}(\eta) |x|^{\Delta-2\Delta_\phi}. \quad (2.41)$$

For simplicity, we set  $\beta = 1$  for the remainder of the paper. The full dependence on  $\beta$  can be restored by dimensional analysis. The function  $a(\Delta, J)$  should have simple poles at the physical operator dimensions, with residues proportional to the coefficients  $a_{\mathcal{O}}$ ,

$$a(\Delta, J) \sim -\frac{a_{\mathcal{O}}}{\Delta - \Delta_{\mathcal{O}}}. \quad (2.42)$$

We also require that  $a(\Delta, J)$  not grow exponentially in the right  $\Delta$ -half-plane. When  $|x| < 1$ , we can close the  $\Delta$  contour to the right to encircle the poles clockwise (hence the minus sign in (2.42)) and recover the usual thermal conformal block decomposition. The position of the  $\Delta$  contour is arbitrary as long as the integral converges. We have chosen it to lie to the left of all physical poles, including the one from the unit operator.

It is simple to write an inversion formula that produces  $a(\Delta, J)$  from  $g(\tau, \mathbf{x})$ , by integrating against a Gegenbauer polynomial to pick out the contribution from spin  $J$ , and then Laplace transform in  $|x|$  to pick out poles in  $\Delta$ ,

$$a(\Delta, J) = \frac{1}{N_J} \int_{|x|<1} d^d x C_J^{(\nu)}(\eta) |x|^{2\Delta_\phi - \Delta - d} g(\tau, \mathbf{x}). \quad (2.43)$$

This choice of  $a(\Delta, J)$  is not unique, since we only demand that it have poles and residues consistent with (2.42). To obtain the correct poles in  $\Delta$ , it suffices to integrate

<sup>19</sup>One can restrict to a disc  $|x| < r$  and introduce boundary conditions at  $|x| = r$  to obtain a completeness relation. However, such boundary conditions are not satisfied by physical two-point functions. Alternatively, one can lift two-point functions to the universal cover of  $\mathbb{R}^{d-1} \times S^1$  and study completeness relations on this space.

$x$  over any neighborhood of the origin. We call (2.43) a ‘‘Euclidean inversion formula’’ because it involves an integral over Euclidean space. For simplicity, we have chosen to integrate over a circle with radius 1.<sup>20</sup> The factor  $N_J$  is defined by

$$\int_{S^{d-1}} d\Omega C_J^{(\nu)}(\eta) C_{J'}^{(\nu)}(\eta) = N_J \delta_{JJ'}, \quad (2.44)$$

where

$$N_J = \frac{4^{1-\nu} \pi^{\nu+\frac{3}{2}} \Gamma(J+2\nu)}{J!(J+\nu)\Gamma(\nu)^2\Gamma(\nu+\frac{1}{2})}, \quad \nu = \frac{d-2}{2}. \quad (2.45)$$

This standard normalization of the Gegenbauer polynomial is unfortunately singular when  $d = 2$ , so we will treat that as a special case.

### 2.3.2 Continuing to Lorentzian signature

The angular dependence of a two-point block on  $S^1_\beta \times \mathbb{R}^{d-1}$  is precisely the same as the angular dependence of a partial wave in a  $2 \rightarrow 2$  scattering amplitude — both are given by Gegenbauer polynomials. In the case of amplitudes, the Froissart-Gribov formula [57, 58] expresses partial wave coefficients as an integral of the amplitude over a Lorentzian regime of momenta. A standard derivation of the Froissart-Gribov formula (see e.g. [25, 51, 83]) carries over essentially unchanged to our case, where it gives  $a(\Delta, J)$  as an integral over a Lorentzian region in position space. Note that the Lorentzian region we find does not correspond to the usual real time dynamics at finite temperature (where  $\tau$  gets complexified). Instead, one of the components of  $\mathbf{x}$  gets complexified and plays the role of Lorentzian time.

#### 2.3.2.1 Kinematics

Before giving the derivation, let us discuss the Lorentzian region that will appear in our formula. Using  $\text{SO}(d-1)$  invariance, we can restrict  $\mathbf{x}$  to a line and denote the coordinate along this line as  $x_E$ . Let us introduce coordinates

$$z = \tau + ix_E, \quad \bar{z} = \tau - ix_E. \quad (2.46)$$

It will also be useful to introduce polar coordinates  $r$  and  $w = e^{i\theta}$  such that

$$z = rw, \quad \bar{z} = rw^{-1}. \quad (2.47)$$

---

<sup>20</sup>We would like to ensure that poles in  $a(\Delta, J)$  correspond only to operators in the OPE. To do this, we can restrict the range of integration to be  $|x| < r$  for some  $r < 1$ , so that the integral remains strictly inside the regime of convergence of the OPE. The only singularity in this region is the OPE singularity, and this is the only place poles can come from. We have written  $r = 1$  for simplicity, but a careful reader can imagine  $r = 1 - \epsilon$  for positive  $\epsilon$ .

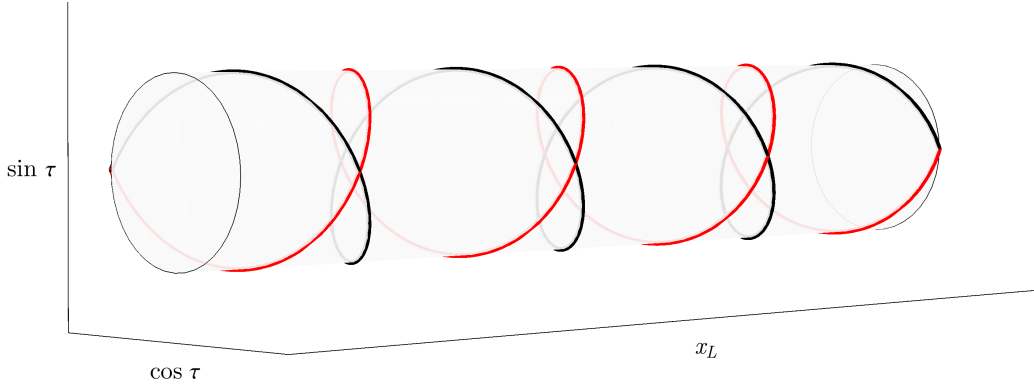


Figure 2.2: Lightlike trajectories moving in the  $x_L$  direction and around the thermal circle. One trajectory is  $z = 0$  and the other is  $\bar{z} = 0$ . Poles in the Lorentzian inversion formula come from the neighborhood of these trajectories.

In Euclidean signature,  $w$  lies on the unit circle and represents the angle of the two operators relative to the  $\tau$ -direction, and  $z, \bar{z}$  are complex conjugates of each other.

We will continue to Lorentzian signature by Wick-rotating  $x_E = -ix_L$ , so that  $z, \bar{z}$  become independent real variables. In particular, the direction  $\tau$  along the thermal circle remains Euclidean and retains the periodicity  $\tau \sim \tau + \beta$ , and  $w$  is real. This configuration is best interpreted in terms of a Lorentzian theory, one of whose spatial directions has been compactified on  $S^1$ . It is *not* the Lorentzian kinematics usually considered in thermal field theory, where one considers complex  $\tau$ . Instead,  $x_L$  plays the role of time. Poles in  $a(\Delta, J)$  corresponding to physical one-point functions will come from the regime  $z \sim 0$  or  $\bar{z} \sim 0$ , where one of the operators is following a lightlike trajectory around the thermal circle. These lightlike trajectories are depicted in figure 2.2.

The regime of small or large  $w$  will play an important role in what follows. In the limit of  $r$  fixed and  $w \rightarrow \infty$ , say, we have  $\tau \rightarrow x_L$  and  $x_L \rightarrow \infty$ . Given the periodicity  $\tau \sim \tau + \beta$ , the separation between the operators approaches a lightlike-trajectory along the cylinder at asymptotically large  $x_L$ . In terms of  $(z, \bar{z})$ , this limit corresponds to  $z \rightarrow \infty, \bar{z} \rightarrow 0$  with  $z\bar{z}$  fixed. This limit of large boost ( $w \rightarrow 0$  or  $w \rightarrow \infty$ ) is analogous to the Regge limit in flat space.

### 2.3.2.2 The inversion formula in $d = 2$

Let us first present the derivation in  $d = 2$ , where it is particularly simple. As noted in section 2.2.1.2, thermal two-point functions in  $d = 2$  are related by a Weyl

transformation to flat-space two-point functions, so this analysis is not necessary. However, the discussion in this subsection will generalize to higher dimensions.

In two dimensions, Gegenbauer polynomials are given by<sup>21</sup>

$$\cos(J\theta) = \frac{1}{2}(w^J + w^{-J}). \quad (2.48)$$

With this normalization, we have  $N_J = \pi$ . Viewed as a cylinder two-point block, the first term comes from the exchange of a vacuum Virasoro descendant having weights  $(h, \bar{h})$  and spin  $J = h - \bar{h}$ . The second term comes from the exchange of the conjugate state having weights  $(\bar{h}, h)$  and spin  $-J$ . The Euclidean inversion formula becomes

$$a(\Delta, J) = \frac{1}{\pi} \int_0^1 \frac{dr}{r} r^{2\Delta_\phi - \Delta} \oint \frac{dw}{iw} \frac{1}{2}(w^J + w^{-J}) g(z = rw, \bar{z} = rw^{-1}), \quad (2.49)$$

where the  $w$ -contour is along the unit circle as pictured in figure 2.3a. Note that  $J$  must be an integer in (2.49) in order for the integrand to be single-valued along the contour.

Now, the crucial claim is that  $g(z = rw, \bar{z} = rw^{-1})$  satisfies the following properties as a function of  $w$ :

- It is analytic in the  $w$  plane away from the cuts  $(-\infty, -1/r)$ ,  $(-r, 0)$ ,  $(0, r)$ , and  $(1/r, \infty)$ .
- Its growth at large  $w$  is bounded by a polynomial  $w^{J_0}$  for some constant  $J_0$ . Similarly, by symmetry under  $w \rightarrow w^{-1}$ , the growth at small  $w$  is bounded by  $w^{-J_0}$ .

We discuss these properties in the next section. For now, let us assume them and proceed with the derivation.

By analogy with the Froissart-Gribov formula, we now deform the  $w$  contour away from the unit circle. We must do this separately for the two terms  $w^J$  and  $w^{-J}$ . The term  $w^J$  dies as  $w \rightarrow 0$ . Assuming  $J > J_0$ , we can deform the contour towards zero for that term to obtain the contour 2.3b. Similarly, the term  $w^{-J}$  dies as  $w \rightarrow \infty$ , so we can deform the contour towards infinity for that term to obtain the contour 2.3c (again assuming  $J > J_0$ ).

---

<sup>21</sup>We are considering only external scalars, which have  $h = \bar{h}$ . Equation (2.24) explicitly shows that the correlator is symmetric under the interchange of  $z$  and  $\bar{z}$ , which gives the symmetry of the block under the exchange of  $J$  and  $-J$ . For spinning thermal correlators, a chirally-asymmetric block should be used.

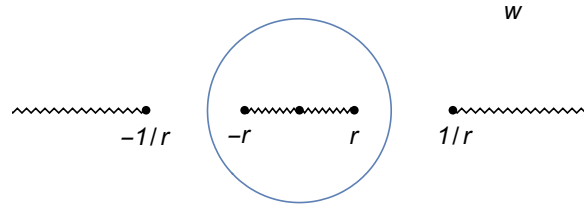
(a) Initial integration contour  $|w| = 1$ .(b) The deformed contour for terms that behave as  $w^J$ .(c) The deformed contour for terms that behave as  $w^{-J}$ .

Figure 2.3: Contour manipulations for the inversion formula in the  $w$  plane. In (a) we show the original contour which lies along the circle  $|w| = 1$ . For the  $w^J$  terms in (2.49), we deform the contour as in (b), and for the  $w^{-J}$  terms in (2.49), we deform the contour as in (c).

Let us focus on the  $w^{-J}$  term, where we deform the contour towards infinity. By our analyticity assumption, we first encounter a branch cut at  $w = r^{-1}$ , or equivalently  $z = 1$  (we comment on the contribution of the  $z = -1$  branch-cut shortly). We thus obtain an integral of the discontinuity of the two-point function  $g(z, \bar{z})$  across this cut,

$$\oint \frac{dw}{iw} w^{-J} g(z = rw, \bar{z} = rw^{-1}) \supset \int_{w=r^{-1}}^{\infty} dw w^{-J-1} \text{Disc}[g(z = rw, \bar{z} = rw^{-1})], \quad (2.50)$$

where

$$\text{Disc}[g(z, \bar{z})] \equiv \frac{1}{i} (g(z + i\epsilon, \bar{z}) - g(z - i\epsilon, \bar{z})). \quad (2.51)$$

Here, we have assumed that  $J > J_0$ , so we can drop the arcs at infinity in figure 2.3c. If instead  $J \leq J_0$ , we must keep the contribution from these arcs. The arc contributions are the analogs of finite subtractions in the case of dispersion relations for amplitudes.

Because  $g(z, \bar{z}) = g(-z, -\bar{z})$ , the branch cut from  $(-\infty, -1/r)$  contributes the same as the cut from  $(1/r, \infty)$ , up to a factor of  $(-1)^J$ . Finally, because of symmetry under  $w \rightarrow w^{-1}$ , the contribution from deforming the contour for  $w^J$  towards the origin is the same as the contribution from deforming the contour for  $w^{-J}$  towards infinity, giving an overall factor of 2.



Putting everything back in (2.49), we obtain

$$\begin{aligned}
a(\Delta, J) &= (1 + (-1)^J) \frac{1}{\pi} \int_0^1 \frac{dr}{r} r^{2\Delta_\phi - \Delta} \int_{w=r^{-1}}^\infty w^{-J-1} \text{Disc}[g(z, \bar{z})] \\
&\quad + \theta(J_0 - J) a_{\text{arcs}}(\Delta, J) \\
&= (1 + (-1)^J) \frac{1}{2\pi} \int_1^\infty \frac{dz}{z} \int_0^1 \frac{d\bar{z}}{\bar{z}} z^{\Delta_\phi - \bar{h}} \bar{z}^{\Delta_\phi - h} \text{Disc}[g(z, \bar{z})] \\
&\quad + \theta(J_0 - J) a_{\text{arcs}}(\Delta, J), \tag{2.52}
\end{aligned}$$

where

$$h = \frac{\Delta - J}{2} \quad \text{and} \quad \bar{h} = \frac{\Delta + J}{2}. \tag{2.53}$$

We have explicitly indicated the presence of non-trivial contributions from the arcs when  $J \leq J_0$ . These are given by the large  $w$  region of (2.49). Their detailed form depends on the correlator in question. We will see some explicit examples in the next section.

### 2.3.2.3 The inversion formula in $d > 2$

To perform the same derivation in  $d > 2$  dimensions, we must find the higher-dimensional analog of the decomposition  $\cos(J\theta) = \frac{1}{2}(w^J + w^{-J})$ . The role of  $w^J$  will be played by the solution to the Gegenbauer differential equation that vanishes as  $w \rightarrow 0$  (for positive  $J$ ). This is given by<sup>22</sup>

$$F_J(w) = w^{J+d-2} {}_2F_1\left(J + d - 2, \frac{d}{2} - 1, J + \frac{d}{2}, w^2\right). \tag{2.54}$$

The Gegenbauer differential equation is symmetric under  $w \rightarrow w^{-1}$  (because the equation depends only on  $\cos(\theta) = \frac{1}{2}(w + w^{-1})$ ), so the solution that vanishes as  $w \rightarrow \infty$  is  $F_J(w^{-1})$ .

Because the Gegenbauer differential equation is second-order, the two functions  $F_J(w^{\pm 1})$  span the space of solutions. In particular, a Gegenbauer polynomial can be expressed as a linear combination

$$C_J^{(\nu)}\left(\frac{1}{2}(w + w^{-1})\right) = \frac{\Gamma(J + d - 2)}{\Gamma(\frac{d}{2} - 1)\Gamma(J + \frac{d}{2})} \left(F_J(w^{-1})e^{i\pi\frac{d-2}{2}} + F_J(w)e^{-i\pi\frac{d-2}{2}}\right), \tag{2.55}$$

for  $\text{Im}(w) > 0$ . The above representation is correct for  $w$  in the upper half-plane. Because  $F_J(w)$  has cuts along  $(-\infty, -1]$  and  $[1, \infty)$  and  $F_J(w^{-1})$  has cuts along

<sup>22</sup>The function  $F_J$  is proportional to  $B_J$  defined in [26] and  $Q_J$  defined in [83]. In  $d = 3$ , it is proportional to a Legendre  $Q$ -function.

$[-1, 1]$ , the representation is different when  $w$  is in the lower half-plane (the phases in front of the two terms swap). Note that when  $w = e^{i\theta}$  is on the unit circle, the two terms are complex-conjugates of each other, so their sum is real.

Plugging this representation of the Gegenbauer polynomial into the Euclidean inversion formula (2.43), we can run the same contour argument as in  $d = 2$ . The measure contributes an extra factor of  $(z - \bar{z})^{2\nu}$ , but otherwise the derivation is essentially unchanged. We find

$$a(\Delta, J) = (1 + (-1)^J) K_J \int_0^1 \frac{d\bar{z}}{\bar{z}} \int_1^\infty \frac{dz}{z} (z\bar{z})^{\Delta_\phi - \frac{\Delta}{2} - \nu} (z - \bar{z})^{2\nu} F_J \left( \sqrt{\frac{\bar{z}}{z}} \right) \text{Disc}[g(z, \bar{z})] \\ + \theta(J_0 - J) a_{\text{arcs}}(\Delta, J), \quad (2.56)$$

where

$$K_J \equiv \frac{\Gamma(J+1)\Gamma(\nu)}{4\pi\Gamma(J+\nu)}. \quad (2.57)$$

It is easy to check that this agrees with (2.52) in  $d = 2$  after accounting for the proper normalization of the  $d = 2$  Gegenbauer polynomials.

### 2.3.3 Comments on the Lorentzian formula

Like the Froissart-Gribov formula, our Lorentzian inversion formula (3.7) has the interesting property that it can be analytically continued in spin  $J$ . As explained e.g. in [25], analyticity in spin is a consequence of polynomial boundedness in the  $w \rightarrow \infty$  limit — specifically our assumption that the correlator does not grow faster than  $w^{\pm J_0}$ . Because each partial wave with nonzero spin grows in this limit, boundedness is only possible if there is a delicate balance, due to analyticity, between each partial wave with  $J > J_0$ . This state of affairs is precisely analogous to the Regge limit of vacuum four-point functions.

The integral (3.7) is over a Lorentzian regime of the two-point function. We will see shortly that poles in  $\Delta$  come from the region  $\bar{z} \sim 0$  where the factor  $\bar{z}^{\Delta_\phi - \frac{\Delta}{2} - \nu}$  is singular. The residues are then determined by a one-dimensional integral over  $z$ . In other words, the locus that contributes to CFT one-point functions is  $\tau \sim x_L$  (cf. (2.46)), which is a lightlike trajectory moving around the thermal circle while moving forward in “time”  $x_L$ . This trajectory is pictured in figure 2.2.

The fact that physical data comes from an integral over  $z$  with  $\bar{z} \sim 0$  is also true in Caron-Huot’s Lorentzian inversion formula for four-point functions. However, in that case, the integral remains entirely within the regime of convergence of both the  $s$  and

$t$ -channel OPEs. An important difference in our case is that the  $z$ -integral extends outside the regime of convergence of any OPE. In our conventions, the  $s$ -channel OPE is an expansion around  $z = \bar{z} = 0$  and the  $t$ -channel OPE is an expansion around  $z = \bar{z} = 1$ . Their regimes of convergence are:

$$\begin{aligned} \text{s-channel OPE: } & |z|, |\bar{z}| < 1, \\ \text{t-channel OPE: } & |1 - z|, |1 - \bar{z}| < 1. \end{aligned} \tag{2.58}$$

Our integral is within the regime of convergence of the  $t$ -channel OPE for  $1 \leq z < 2$ . But for  $z > 2$ , it exits this regime. Thus, we can only obtain partial information about  $a(\Delta, J)$  from the  $t$ -channel OPE expansion alone. However, as we will see in more detail in section 2.6, corrections coming from the region  $z > 2$  are exponentially suppressed in  $J$ .

Another interesting similarity between our inversion formula and Caron-Huot’s is the significance of a double lightcone limit. We will see in section 2.6 that a systematic expansion for thermal one-point functions in  $1/J$  requires understanding the thermal two-point function in the regime  $\bar{z} \sim 0$ ,  $z \sim 1$ . This corresponds to a physical configuration where the second operator is approaching the first intersection of light rays from the first operator that wrap halfway around the thermal circle. In the context of four-point functions, the same regime  $\bar{z} \sim 0$ ,  $z \sim 1$  corresponds to all four operators approaching the corners of the square  $(z, \bar{z}) \in [0, 1]$ , and is dubbed the “double lightcone” limit.<sup>23</sup> Because our limit plays a similar role in large-spin perturbation theory, we will adopt the same terminology.

### 2.3.4 Analyticity in the $w$ -plane

To complete our derivation, we must justify the assumptions stated in section 2.3.2.3, namely analyticity of the two-point function in  $w$  outside the cuts pictured in figure 2.3, and polynomial boundedness in  $w$ . First note that convergence of the  $s$ -channel OPE guarantees analyticity in the annulus

$$r < |w| < r^{-1}. \tag{2.59}$$

Convergence of the OPE around  $z, \bar{z} = 1$  and  $z, \bar{z} = -1$  additionally guarantees analyticity in more complicated regions around  $w = \pm 1$  (figure 2.4).

---

<sup>23</sup>This is to be distinguished from the specialized terminology of [16], where “double lightcone” limit means fixed  $\frac{\bar{z}}{1-z}$ .

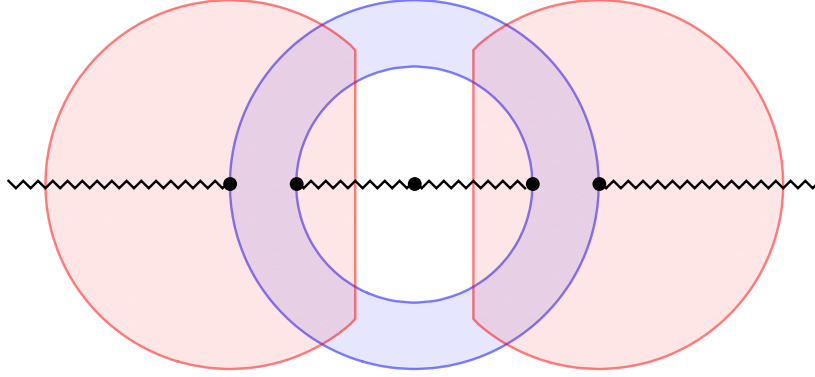


Figure 2.4: For fixed  $r \in (0, 1)$ , the  $s$ -channel OPE (expansion around  $z = \bar{z} = 0$ ) implies that the thermal two-point function  $g(z, \bar{z})$  is analytic in an annulus in the  $w$  plane between radii  $r$  and  $1/r$  (shaded blue). The  $t$ -channel OPE (expansion around  $z = \bar{z} = 1$ ), together with symmetry under  $w \leftrightarrow -w$ , implies analyticity in the red-shaded regions, except for cuts running along  $(-\infty, -1/r)$ ,  $(-r, 0)$ ,  $(0, r)$ ,  $(1/r, \infty)$  (indicated with zig-zags). In this section, we argue for analyticity everywhere in the upper and lower half planes.

To argue for analyticity in an even larger region, we will use the KK representation discussed in section 2.2.3,

$$g(\tau, x_E) = \langle \Psi | e^{-x_E H_{\text{KK}} + i\tau P_{\text{KK}}} | \Psi \rangle = \langle \Psi | e^{\frac{i}{2}(H_{\text{KK}} + P_{\text{KK}})z - \frac{i}{2}(H_{\text{KK}} - P_{\text{KK}})\bar{z}} | \Psi \rangle, \quad (2.60)$$

where

$$|\Psi\rangle = \phi(0)|0\rangle_{S^1 \times \mathbb{R}^{d-2}}. \quad (2.61)$$

Here, we have quantized the Euclidean theory on spatial slices with geometry  $S^1 \times \mathbb{R}^{d-2}$ . The Hamiltonian  $H_{\text{KK}}$  generates translations in the noncompact direction parameterized by  $x_E$ , while  $P_{\text{KK}}$  generates translations in  $\tau$  (the periodic direction). In this way of quantizing the theory, both  $H_{\text{KK}}$  and  $P_{\text{KK}}$  are Hermitian.

We first claim that  $g(\tau, x_E)$  is bounded whenever  $\text{Im}(z) > 0$  and  $\text{Im}(\bar{z}) < 0$ . Our goal will be to relate a general configuration with  $\text{Im}(z) > 0$  and  $\text{Im}(\bar{z}) < 0$  to a standard configuration where we know that the correlator is bounded. We begin by splitting the exponential into a positive Hermitian operator  $V$  and a unitary operator  $U$ ,

$$\begin{aligned} e^{\frac{i}{2}(H_{\text{KK}} + P_{\text{KK}})z - \frac{i}{2}(H_{\text{KK}} - P_{\text{KK}})\bar{z}} &= V^{1/2} U V^{1/2} \\ V &= e^{-\frac{1}{2}(H_{\text{KK}} + P_{\text{KK}})\text{Im}(z) + \frac{1}{2}(H_{\text{KK}} - P_{\text{KK}})\text{Im}(\bar{z})}, \\ U &= e^{\frac{i}{2}(H_{\text{KK}} + P_{\text{KK}})\text{Re}(z) - \frac{i}{2}(H_{\text{KK}} - P_{\text{KK}})\text{Re}(\bar{z})}. \end{aligned} \quad (2.62)$$

The Cauchy-Schwartz inequality implies

$$\begin{aligned} |g(\tau, x_E)| &= |\langle \Psi | V^{1/2} U V^{1/2} | \Psi \rangle| \leq \langle \Psi | V^{1/2} V^{1/2} | \Psi \rangle^{1/2} \langle \Psi | V^{1/2} U^\dagger U V^{1/2} | \Psi \rangle^{1/2} \\ &= \langle \Psi | V | \Psi \rangle. \end{aligned} \quad (2.63)$$

This essentially allows us to assume that  $z, \bar{z}$  are pure imaginary.

Next, we claim that  $H_{\text{KK}} \pm P_{\text{KK}}$  are bounded from below by a constant. To argue this, first let us forget about periodicity and consider a theory in  $\mathbb{R}^d$ . Then we have  $H \pm P > 0$  as a simple consequence of positivity of energy. (If either  $H \pm P$  had a negative eigenvalue, Lorentz invariance would imply the existence of a state with negative energy.)

Now consider the case where  $\tau$  is periodic. The spectrum of  $P_{\text{KK}}$  is quantized, with eigenvalues given by Kaluza-Klein (KK) momenta  $n \in \mathbb{Z}$ . In general, energies of excitations with KK-momentum  $n$  are different from energies of excitations in  $\mathbb{R}^d$  with  $|\mathbf{p}| = n$ . (For example, in the  $n = 0$  sector, the lowest nonzero eigenvalue of  $H_{\text{KK}}$  is the thermal mass  $m_{\text{th}}$ , while the Hamiltonian in  $\mathbb{R}^d$  is gapless at zero momentum.) In particular, it is not obvious whether  $H_{\text{KK}} \pm P_{\text{KK}}$  are positive operators. Positivity of  $H_{\text{KK}} \pm P_{\text{KK}}$  does not follow immediately from positivity of energy because there is no Lorentz boost relating  $H_{\text{KK}}$  and  $P_{\text{KK}}$ . However, for sufficiently large  $|n|$ , periodicity of the  $\tau$  direction becomes unimportant, and the spectrum of  $H_{\text{KK}}$  approaches the flat-space spectrum. Thus, we expect  $H_{\text{KK}} \pm P_{\text{KK}}$  are bounded from below for all  $n$  by some  $n$ -independent constant  $\lambda$ .<sup>24</sup> This is the key claim in this section, and we have not established it rigorously. However, we believe it is a physically reasonable assumption.

Thus, let us pick  $\lambda$  such that  $H_{\text{KK}} \pm P_{\text{KK}} > \lambda$ , and let  $\zeta = \min(\text{Im}(z), -\text{Im}(\bar{z}))$ . We have

$$\begin{aligned} \langle \Psi | V | \Psi \rangle &= \langle \Psi | e^{-\frac{1}{2}(H_{\text{KK}}+P_{\text{KK}})\text{Im}(z)+\frac{1}{2}(H_{\text{KK}}-P_{\text{KK}})\text{Im}(\bar{z})} | \Psi \rangle \\ &\leq \langle \Psi | e^{-\frac{1}{2}(H_{\text{KK}}+P_{\text{KK}})\zeta-\frac{1}{2}(H_{\text{KK}}-P_{\text{KK}})\zeta} | \Psi \rangle \times e^{-\frac{\lambda}{2}(\text{Im}(z)-\zeta)-\frac{\lambda}{2}(-\text{Im}(\bar{z})-\zeta)} \\ &= g(0, \zeta) e^{-\frac{\lambda}{2}(\text{Im}(z)-\zeta)-\frac{\lambda}{2}(-\text{Im}(\bar{z})-\zeta)}. \end{aligned} \quad (2.64)$$

To summarize,

$$|g(\tau, x_E)| \leq g(0, \zeta) e^{-\frac{\lambda}{2}(\text{Im}(z)-\zeta)-\frac{\lambda}{2}(-\text{Im}(\bar{z})-\zeta)}. \quad (2.65)$$

---

<sup>24</sup>Note that  $\lambda$  is not the same thing as the thermal mass. The thermal mass is a lower bound on the nonzero eigenvalues of  $H_{\text{KK}}$  in the  $n = 0$  sector, whereas  $\lambda$  is a lower bound on all eigenvalues of  $H_{\text{KK}} \pm P_{\text{KK}}$  across all sectors. Note also that it's not necessary for  $\lambda$  to be positive for the remainder of the argument in this section to work.

The correlator  $g(0, \zeta)$  is simply a Euclidean correlator at nonzero  $|\mathbf{x}|$  and time  $\tau = 0$ . This is a nonsingular configuration, so the right-hand side is bounded.

Finally, note that this derivation did not actually depend on  $\phi(0)$  being primary. Thus, it applies to all correlators of descendants of  $\phi$ , so all derivatives of  $g(\tau, \mathbf{x})$  are bounded as well. It follows that  $g(\tau, \mathbf{x})$  is analytic if  $\zeta > 0$ , i.e.  $\text{Im}(z) > 0$  and  $\text{Im}(\bar{z}) < 0$ . These conditions hold for  $w$  in the upper half-plane. Symmetry under  $w \rightarrow -w$  then implies that  $g(\tau, x_E)$  is analytic in the lower  $w$ -half-plane as well.

### 2.3.5 Behavior at large $w$

Our derivation of the Lorentzian inversion formula relies on the assumption that  $g(z, \bar{z})$  grows no faster than  $w^{J_0}$  at large  $w$  (anywhere in the upper half plane) and fixed  $r$ , for some fixed  $J_0$ . We have not been able to prove this claim or establish a rigorous upper bound on  $J_0$  (analogous to the bound on chaos for thermal four-point functions [84]). In this section, we discuss the claim in more detail.

First, one can check explicitly that thermal two-point functions in  $d = 2$ , given in (2.23), are exponentially damped at large  $w$ . Thus, our inversion formula implies analyticity in spin for all  $J \geq 0$  in 2d. This is perhaps unsurprising given that only members of the Virasoro multiplet of the identity get thermal expectation values, and such operators lie on simple trajectories as a function of  $J$ .

For  $d > 2$ , we might hope to determine  $J_0$  by studying perturbative examples. However, we should be aware that naïve perturbative expansions may not commute with the large- $w$  limit. For example, in the critical  $O(N)$  model at leading order in  $N$  (see section 2.5.1), we find  $J_0 = 0$ . However, at each order in  $1/N$  the correlator may grow more quickly.<sup>25</sup> It would be very interesting to set up a perturbative analysis specially adapted to the large- $w$  limit, perhaps analogous to [86].

Let us guess the behavior of the two-point function at large  $w$  by studying two interesting physical regimes. Firstly, consider  $w = iW$  with  $W$  large and real. This corresponds to a Lorentzian two-point function at finite temperature, in the limit where both operators are highly boosted.<sup>26</sup> In the absence of the thermal bath, such a correlator would be independent of  $W$  because a boost is a symmetry. The corre-

<sup>25</sup>Precisely this phenomenon happens for the Regge limit of four-point functions in large- $N$  theories. One can show on general grounds that the four-point function is bounded in the Regge limit [84]. However, each order in  $1/N$  contributes faster and faster growth in the Regge limit. In holographic theories, this fact is related to the necessity of regularization and renormalization in the bulk effective theory [85].

<sup>26</sup>We thank Juan Maldacena for suggesting we consider this regime.

lator can, roughly speaking, be interpreted as the amplitude for excitations created by the first operator to be absorbed by the second. There is no clear reason why this amplitude should be enhanced by the thermal bath, and thus we expect the correlator to grow no faster than  $W^0$  in this regime. In fact, we might expect that the thermal bath destroys correlations between the operators, so the correlator actually decays at large  $W$ .<sup>27</sup>

Another interesting physical regime is  $w = (1 + i\epsilon)W$  with  $W$  large and real (i.e.  $w$  on top of one of the cuts in figure 2.4). This is the configuration that appears in the Lorentzian inversion formula. It corresponds to one of the operators moving on a nearly lightlike trajectory around the thermal circle, with one of the noncompact directions as increasing Lorentzian time  $x_L$  (figure 2.2). A physical picture is that the first operator creates excitations that move around the thermal circle. They repeatedly collide at  $x_L = \beta/2, \beta, 3\beta/2, \dots$ . Finally, some of them are absorbed by the second operator. We expect each collision to reduce the amplitude for excitations to reach the second operator. Thus, we conjecture that the correlator grows no faster than  $W^0$  in this regime as well. If the collisions have a large inelastic component, the correlator should decay at large  $W$ .

These arguments are far from rigorous. It would be nice to understand — either from examples or a general argument — what the nonperturbative behavior of the two-point function can be in the entire upper half-plane at large  $w$ .

## 2.4 Applications I: Mean Field Theory

In this and the next section, we will perform some checks of the inversion formula, derive some new results and demonstrate its mechanics. We begin here with application to mean field theory.

In MFT, the operators appearing in the  $\phi \times \phi$  OPE for some scalar primary  $\phi$  are the unit operator and double-twist operators of schematic form

$$[\phi\phi]_{n,\ell} = \phi \partial^{\mu_1} \dots \partial^{\mu_\ell} \partial^{2n} \phi - (\text{traces}), \quad (2.66)$$

where  $\ell$  is even, with dimensions  $\Delta_{n,\ell} = 2\Delta_\phi + 2n + \ell$ . Note that the free theory is the MFT with  $\Delta_\phi = \nu$ , where the  $[\phi\phi]_{0,\ell}$  are identified with spin- $\ell$  currents  $J_\ell$ . The

---

<sup>27</sup>We have checked that a boundary thermal two-point function computed in AdS<sub>4</sub> using the geodesic approximation decays at large  $W$ .

thermal two-point function can be computed by using the method of images,

$$g(z, \bar{z}) = \sum_{m=-\infty}^{\infty} \frac{1}{((m-z)(m-\bar{z}))^{\Delta_\phi}}. \quad (2.67)$$

Using this, we will perform a brute-force expansion of the two-point functions into thermal conformal blocks and compare that with the thermal one-point coefficients generated by the inversion formula.

### Expanding the thermal two-point function

We start by explicitly expanding the thermal two-point function without using the inversion formula in order to provide a non-trivial check for the entire methodology. Going back to the  $\mathbf{x}$  and  $\tau$  coordinates, we can write each term in (2.67) as<sup>28</sup>

$$\frac{1}{((\tau+m)^2 + \mathbf{x}^2)^{\Delta_\phi}} = \sum_{j=0}^{\infty} (-1)^j C_j^{(\Delta_\phi)}(\eta) \text{sgn}(m)^j \frac{|x|^j}{|m|^{2\Delta_\phi+j}}, \quad (2.68)$$

where  $\text{sgn}(m) = \frac{m}{|m|}$  and  $\eta = \frac{\tau}{|x|}$ . Thus, the two-point function is

$$\begin{aligned} g(\tau, \mathbf{x}) &= \frac{1}{|x|^{2\Delta_\phi}} + \sum_{j=0}^{\infty} (-1)^j \left( \sum_{m \neq 0} \frac{\text{sgn}(m)^j}{|m|^{2\Delta_\phi+j}} \right) C_j^{(\Delta_\phi)}(\eta) |x|^j \\ &= \frac{1}{|x|^{2\Delta_\phi}} + \sum_{j=0,2,\dots} 2\zeta(2\Delta_\phi + j) C_j^{(\Delta_\phi)}(\eta) |x|^j, \end{aligned} \quad (2.69)$$

where  $\zeta(s)$  is the Riemann  $\zeta$ -function. The Gegenbauer polynomials  $C_j^{(\Delta_\phi)}(\eta)$  have an expansion in terms of the correct Gegenbauer polynomials  $C_j^{(\nu)}(\eta)$  appearing in section 2.2 for the thermal OPE on  $S^1_\beta \times \mathbb{R}^{d-1}$ ,

$$C_j^{(\Delta_\phi)}(\eta) = \sum_{\ell=j, j-2, \dots, j \bmod 2} \frac{(\ell + \nu)(\Delta_\phi)_{\frac{j+\ell}{2}} (\Delta_\phi - \nu)_{\frac{j-\ell}{2}}}{\left(\frac{j-\ell}{2}\right)! (\nu)_{\frac{j+\ell+2}{2}}} C_\ell^{(\nu)}(\eta), \quad (2.70)$$

where  $(a)_n = \frac{\Gamma(a+n)}{\Gamma(a)}$  is the Pochhammer symbol. Plugging this into (2.69), and replacing  $j = 2n + \ell$ , we get

$$g(\tau, \mathbf{x}) = \frac{1}{|x|^{2\Delta_\phi}} + \sum_{n=0}^{\infty} \sum_{\ell=0,2,\dots} \frac{2\zeta(2\Delta_\phi + 2n + \ell) (\ell + \nu)(\Delta_\phi)_{\ell+n} (\Delta_\phi - \nu)_n}{n! (\nu)_{\ell+n+1}} C_\ell^{(\nu)}(\eta) |x|^{2n+\ell}. \quad (2.71)$$

---

<sup>28</sup>Here, we use the identity  $\frac{1}{(1-2xy+y^2)^\alpha} = \sum_{j=0}^{\infty} C_j^{(\alpha)}(x)y^j$ .



This has precisely the form of the thermal conformal block decomposition given by (2.17), with support only on the unit operator and double-twist operators (2.66), whose one-point functions are given by

$$a_{\mathbf{1}} = 1 , \quad (2.72)$$

$$a_{[\phi\phi]_{n,\ell}} = 2\zeta(2\Delta_\phi + 2n + \ell) \frac{(\ell + \nu)(\Delta_\phi)_{\ell+n}(\Delta_\phi - \nu)_n}{n!(\nu)_{\ell+n+1}} .$$

In the free theory where  $\Delta_\phi = \nu$ , the spin- $\ell$  currents  $J_\ell \equiv [\phi\phi]_{0,\ell}$  have

$$a_{J_\ell} = 2\zeta(d - 2 + \ell) , \quad (2.73)$$

Note that when  $d = 3$ , the coefficient  $a_{J_0}$  is divergent. This is because the zero mode is badly behaved under dimensional reduction to  $d = 2$ , which is related to the fact that the free boson in  $d = 2$  with noncompact target space is pathological.

We can now compare the above results to those predicted by the inversion formula, starting with the case  $d = 2$  where the Gegenbauer polynomials take a simpler form.

### Inversion in $d = 2$ MFT

As required in the inversion formula (3.7), we should be looking at discontinuities across the real  $z$  axis for each term in (2.67),

$$\text{Disc} \left[ \frac{1}{((m-z)(m-\bar{z}))^{\Delta_\phi}} \right] = 2 \sin(\pi\Delta_\phi) \frac{1}{(m-\bar{z})^{\Delta_\phi} (z-m)^{\Delta_\phi}} \theta(z-m) . \quad (2.74)$$

Plugging (2.74) into the  $d = 2$  inversion formula (2.52), we find

$$a(\Delta, \ell) = \frac{(1 + (-1)^\ell)}{2\pi} 2 \sin(\pi\Delta_\phi) \sum_{m=1}^{\infty} \int_0^1 d\bar{z} \frac{\bar{z}^{\Delta_\phi - h - 1}}{(m - \bar{z})^{\Delta_\phi}} \int_m^{\infty} dz \frac{z^{\Delta_\phi - \bar{h} - 1}}{(z - m)^{\Delta_\phi}} . \quad (2.75)$$

The  $\bar{z}$  and  $z$  integrals in (2.75) are

$$\int_0^1 d\bar{z} \frac{\bar{z}^{\Delta_\phi - h - 1}}{(m - \bar{z})^{\Delta_\phi}} = \sum_{n=0}^{\infty} \frac{\Gamma(\Delta_\phi + n)}{\Gamma(n+1)\Gamma(\Delta_\phi)} \frac{1}{m^{\Delta_\phi + n}} \frac{1}{\Delta_\phi + n - h} , \quad (2.76)$$

and

$$\int_m^{\infty} dz \frac{z^{\Delta_\phi - \bar{h} - 1}}{(z - m)^{\Delta_\phi}} = \frac{\Gamma(1 - \Delta_\phi)\Gamma(\bar{h})}{\Gamma(\bar{h} - \Delta_\phi + 1)} \frac{1}{m^{\bar{h}}} , \quad (2.77)$$

respectively. As expected, (2.76) has poles at  $h = \Delta_\phi + n$ , corresponding to MFT operators (2.66). Computing the residues of each pole, we find

$$a(\Delta, \ell) = \sum_{n=0}^{\infty} \frac{-1}{\Delta - (2\Delta_\phi + 2n + \ell)} \times \left( \frac{2(1 + (-1)^\ell)\Gamma(\Delta_\phi + n)\Gamma(\Delta_\phi + n + \ell)}{\Gamma(n+1)\Gamma(\Delta_\phi)^2\Gamma(n + \ell + 1)} \zeta(2\Delta_\phi + 2n + \ell) \right) . \quad (2.78)$$

Note that we get an extra factor of two when we write the pole in  $h$  as a pole in  $\Delta$ . The thermal one-point function is minus the residue of the pole in  $\Delta$ . Thus, the thermal coefficient for double-twist operators of even spin can be read off as,

$$a_{[\phi\phi]_{n,\ell}} = 4\zeta(2\Delta_\phi + \ell + 2n) \frac{(\Delta_\phi)_{n+\ell}(\Delta_\phi)_n}{n!\Gamma(n + \ell + 1)}, \quad (2.79)$$

which is in agreement with (2.72) when  $\nu = 0$ .

### Inversion in $d > 2$ MFT

While in  $d = 2$  one can obtain the contribution of all double-twist families through simple integral manipulations, the  $d > 2$  case will require a more careful series of approximations to get the residues corresponding to each family's pole.

Plugging in the discontinuity (2.74) into the inversion formula (3.7), we are left to compute

$$\int_0^1 \frac{d\bar{z}}{\bar{z}} \int_m^\infty \frac{dz}{z} (z\bar{z})^{\Delta_\phi - \frac{\Delta}{2} - \nu} (z - \bar{z})^{2\nu} F_J \left( \sqrt{\frac{\bar{z}}{z}} \right) \frac{1}{(m - \bar{z})^{\Delta_\phi} (z - m)^{\Delta_\phi}}. \quad (2.80)$$

Again, poles for double-twist operators (2.66) come from the region of integration near  $\bar{z} \sim 0$ . So we are free to rescale  $\bar{z} \rightarrow z\bar{z}$  and set the integration range for  $\bar{z}$  back to  $[0, 1]$ , since we will obtain the same pole location with the same residue. By also rescaling  $z \rightarrow mz$ , we find

$$m^{-\Delta} \int_0^1 \frac{d\bar{z}}{\bar{z}} \int_1^\infty \frac{dz}{z} (z^2\bar{z})^{\Delta_\phi - \frac{\Delta}{2} - \nu} z^{2\nu} (1 - \bar{z})^{2\nu} F_J \left( \sqrt{\bar{z}} \right) \frac{1}{(1 - z\bar{z})^{\Delta_\phi} (z - 1)^{\Delta_\phi}}. \quad (2.81)$$

The  $z$  integral can be done explicitly, leaving the  $\bar{z}$  integral

$$m^{-\Delta} \frac{\Gamma(1 - \Delta_\phi)\Gamma(\Delta - \Delta_\phi)}{\Gamma(1 + \Delta - 2\Delta_\phi)} \times \int_0^1 \frac{d\bar{z}}{\bar{z}} \bar{z}^{\Delta_\phi - \frac{\Delta}{2} - \nu} (1 - \bar{z})^{2\nu} {}_2F_1(\Delta_\phi, -\Delta + 2\Delta_\phi, 1 - \Delta + \Delta_\phi, \bar{z}) F_J \left( \sqrt{\bar{z}} \right). \quad (2.82)$$

We can now expand in  $\bar{z}$  and get a series of poles.

Let us focus on the first sets of poles in the integrand of (2.82) corresponding to the  $[\phi\phi]_{0,\ell}$  and  $[\phi\phi]_{1,\ell}$  operators,

$$\begin{aligned} & \bar{z}^{\Delta_\phi - \frac{\Delta}{2} - \nu} (1 - \bar{z})^{2\nu} {}_2F_1(\Delta_\phi, -\Delta + 2\Delta_\phi, 1 - \Delta + \Delta_\phi, \bar{z}) F_J \left( \sqrt{\bar{z}} \right) \\ & \sim \bar{z}^{\frac{J-\Delta}{2} + \Delta_\phi} \left( 1 + \bar{z} \left( \frac{\Delta_\phi(\Delta - 2\Delta_\phi)}{\Delta - \Delta_\phi - 1} - \frac{(J+2)\nu}{J + \nu + 1} \right) + \dots \right). \end{aligned} \quad (2.83)$$

Multiplying this by the factor  $(1 + (-1)^J)2 \sin(\pi\Delta_\phi)K_J$ , left out in (2.80) for clarity, gives the full contribution of these poles to  $a(\Delta, J)$ . The first term gives a pole at  $h = \Delta_\phi$  of the form

$$\begin{aligned} a(\Delta, J) \supset (1 + (-1)^J)2 \sin(\pi\Delta_\phi)K_J \sum_{m=1}^{\infty} \frac{1}{m^\Delta} \frac{\Gamma(1 - \Delta_\phi)\Gamma(\Delta - \Delta_\phi)}{\Gamma(\Delta - 2\Delta_\phi + 1)} \frac{1}{\Delta_\phi - h} \\ = (1 + (-1)^J)\zeta(2\Delta_\phi + J) \frac{\Gamma(J + \Delta_\phi)\Gamma(\nu)}{\Gamma(\Delta_\phi)\Gamma(J + \nu)} \frac{-1}{\Delta - (2\Delta_\phi + J)}, \end{aligned} \quad (2.84)$$

where we've set  $\Delta = 2\Delta_\phi + J$  in the last step to obtain the correct value of the residue. This agrees with (2.72) at  $n = 0$ . The order  $\bar{z}$  term in (2.83) gives

$$a(\Delta, J) \supset (1 + (-1)^J)\zeta(2\Delta_\phi + 2 + J) \frac{(J + \nu)(\Delta_\phi)_{J+1}(\Delta_\phi - \nu)}{(\nu)_{J+2}} \frac{-1}{\Delta - J - (2\Delta_\phi + 2)}. \quad (2.85)$$

This agrees with (2.72) at  $n = 1$ .

Note that the unit operator pole was absent in the above manipulations. This is resolved by the presence of the ‘‘arc terms’’ in the Lorentzian inversion formula,  $a^{\text{arcs}}(\Delta, J)$ , which we have neglected here. In the limit  $|w| \rightarrow \infty$ , the MFT correlator is simply given by  $\lim_{|w| \rightarrow \infty} g(r, w) = 1/r^{2\Delta_\phi}$ . The contribution of the contours given by (2.50) precisely yields a pole corresponding to the unit operator at  $J = 0, \Delta = 0$  with residue equal to 1. We will witness a more intricate balance between the arc and non-arc contributions when studying the  $O(N)$  vector model in the subsection below.

## 2.5 Applications II: Large $N$ CFTs

Consider a CFT with large central charge  $c_T \sim N^2 \rightarrow \infty$ . In the OPE regime, we may organize two-point functions on  $S_\beta^1 \times \mathbb{R}^{d-1}$  by powers of  $1/N$ . Let us use the canonical normalization

$$\langle \mathcal{O}\mathcal{O} \rangle_{\mathbb{R}^d} \sim N^0, \quad \langle \mathcal{O}_1\mathcal{O}_2\mathcal{O}_3 \rangle_{\mathbb{R}^d} \sim \frac{1}{N}, \quad \dots, \quad (2.86)$$

where  $\mathcal{O}_i$  are single-trace operators. Then the thermal scalar two-point function  $g(\tau, \mathbf{x})$  receives the following types of contributions, organized by powers of  $1/N$  appearing in the OPE coefficients:

$$\begin{aligned} g(\tau, \mathbf{x}) \approx & \left( \langle \mathbf{1} \rangle_\beta + \sum_{n,\ell} \langle [\phi\phi]_{n,\ell} \rangle_\beta \right) + \frac{1}{N} \left( \sum_{\mathcal{O} \in \phi \times \phi} \langle \mathcal{O} \rangle_\beta \right) \\ & + \frac{1}{N^2} \left( \sum_{n,\ell} \langle [\phi\phi]_{n,\ell} \rangle_\beta + \sum_{n,\ell} \sum_{[\mathcal{O}_i\mathcal{O}_j]_{n,\ell} \in \phi \times \phi} \langle [\mathcal{O}_i\mathcal{O}_j]_{n,\ell} \rangle_\beta \right) + O\left(\frac{1}{N^3}\right), \end{aligned} \quad (2.87)$$

where we have again defined the double-trace composite operators  $[AB]_{n,\ell}$ , of schematic form

$$[AB]_{n,\ell} = A\partial^{2n}\partial_{\mu_1}\dots\partial_{\mu_\ell}B - (\text{traces}). \quad (2.88)$$

The first group of operators in (2.87) represents the two-point function of MFT, in which the  $[\phi\phi]_{n,\ell}$  appear with the MFT OPE coefficients, which can be found in [87]; the second group represents single-trace operators; the third group represents double-trace operators, including the  $1/N^2$  corrections to the MFT exchanges; and so on. However, this way of organizing the contributions is not terribly useful because the one-point functions themselves scale with positive powers of  $N$ . In particular, in the normalization (2.86), one-point functions of  $n$ -trace operators exhibit the leading-order scaling

$$\langle [A_1 \dots A_n] \rangle_\beta \sim N^n + \dots \quad (2.89)$$

This implies an infinite set of contributions to  $g(\tau, \mathbf{x})$  at order  $N^0$ , which poses an obvious challenge to computing  $g(\tau, \mathbf{x})$ , in contrast to the familiar  $1/N$  counting used in vacuum four-point functions.

We now study the inversion formula in the critical  $O(N)$  vector model, and discuss some features of its application to CFTs with weakly coupled holographic duals.

### 2.5.1 $O(N)$ vector model at large $N$

The critical  $O(N)$  model at large  $N$  has been studied in detail before [66, 88, 89]. This theory has  $c_T = Nc_{\text{free}}$  to leading order in  $1/N$ . The main feature we will need is the value of the thermal mass. In the  $O(N)$  model at large  $N$ , the thermal mass is equal to the expectation value of the IR operator  $\sigma$ , which appears in the action after applying a Hubbard-Stratanovich transformation to the  $\phi^4$  coupling:

$$\mathcal{L} = \frac{1}{2}(\partial_\mu\phi_i)^2 + \frac{1}{2}\sigma\phi_i\phi_i - \frac{\sigma^2}{4\lambda}. \quad (2.90)$$

The critical point is obtained by taking  $\lambda \rightarrow \infty$  as  $\sigma^2$  becomes irrelevant in the IR. In appendix A.3, we review the derivation of the following result [89]:

$$\langle \sigma \rangle_\beta = m_{\text{th}}^2 = \beta^{-2} \left[ 2 \log \left( \frac{1 + \sqrt{5}}{2} \right) \right]^2 + \mathcal{O}(1/N). \quad (2.91)$$

As we shall see later in this section, the above formula for the thermal mass is intimately related to correctly reproducing the  $O(N)$  singlet spectrum from the inversion formula.

Let us enumerate the  $O(N)$  singlets of the critical  $O(N)$  model whose thermal expectation values we will compute (any non-singlet has vanishing thermal one-point function). The “single-trace” singlets are the scalar  $\sigma$ , with  $\Delta = 2 + \mathcal{O}(1/N)$ , and the higher-spin currents  $J_\ell$ , with  $\ell \in 2\mathbb{Z}^+$  and  $\Delta = \ell + 1 + \mathcal{O}(1/N)$ . In the  $\phi_i \times \phi_i$  OPE, one generates the larger family of operators<sup>29</sup>

$$\ell > 0 : \quad [\phi_i \phi_i]_{n,\ell} = \phi_i \partial^{\mu_1} \dots \partial^{\mu_\ell} \partial^{2n} \phi_i \quad \text{where} \quad \Delta_{n,\ell} = 1 + 2n + \ell + \gamma_{n,\ell}. \quad (2.92)$$

where the anomalous dimensions are suppressed as  $\gamma_{n,\ell} \sim \mathcal{O}(1/N)$ . For  $n = 0$ , these operators are the slightly-broken higher-spin currents,

$$J_\ell \equiv [\phi_i \phi_i]_{0,\ell}, \quad \text{where} \quad \Delta_\ell = \ell + 1 + \mathcal{O}(1/N). \quad (2.93)$$

The families (2.93) do not analytically continue down to  $\ell = 0$ ; instead,  $\sigma$  plays the role of  $\phi_i \phi_i$  in the IR. Accordingly, the most basic scalar operators are powers of  $\sigma$ ,

$$\ell = 0 : \quad \sigma^m, \quad \text{where} \quad \Delta_m = 2m + \mathcal{O}(1/N). \quad (2.94)$$

In what follows, we will compute thermal one-point functions of  $J_\ell$  and  $\sigma^m$ , and exhibit the algorithm for computing the one-point functions of  $[\phi_i \phi_i]_{n,\ell}$  for all  $(n, \ell)$ .

As discussed below (2.87), the thermal coefficients  $a_{\mathcal{O}}$  in large  $N$  CFTs receive contributions from an infinite set of operators in the  $\phi\phi$  OPE, due to the opposite large  $N$  scaling of OPE coefficients  $f_{\phi\phi\mathcal{O}}$  and thermal one-point functions  $b_{\mathcal{O}}$ . That discussion was for single-trace operators  $\phi$ , but the same scaling holds for the  $\phi_i$  fields in the  $O(N)$  model, i.e.<sup>30</sup>

$$\begin{aligned} \frac{f_{\phi_i \phi_i \sigma^m}}{\sqrt{c_{\sigma^m}}} &\sim \mathcal{O}\left(\frac{1}{N^{m/2}}\right), \quad \frac{b_{\sigma^m}}{\sqrt{c_{\sigma^m}}} \sim \mathcal{O}(N^{m/2}), \quad \Rightarrow \quad a_{\sigma^m} \sim \mathcal{O}(1), \\ \frac{f_{\phi_i \phi_i [\phi_i \phi_i]_{n,\ell}}}{\sqrt{c_{[\phi_i \phi_i]_{n,\ell}}}} &\sim \mathcal{O}\left(\frac{1}{N^{\frac{n+1}{2}}}\right), \quad \frac{b_{[\phi_i \phi_i]_{n,\ell}}}{\sqrt{c_{[\phi_i \phi_i]_{n,\ell}}}} \sim \mathcal{O}(N^{\frac{n+1}{2}}) \quad \Rightarrow \quad a_{[\phi_i \phi_i]_{n,\ell}} \sim \mathcal{O}(1), \end{aligned} \quad (2.95)$$

where in order to derive the second set of scalings, we have used the schematic operator relation  $\partial^2 \phi_i \sim \sigma \phi_i$ . We emphasize that the computation of  $a_{\sigma^m}$  and  $a_{[\phi_i \phi_i]_{n,\ell}}$  (which we will show below) gives a window into arbitrarily high orders in  $1/N$  perturbation theory: for instance, to derive  $f_{\phi_i \phi_i \sigma^m}$  would require going to  $(m - 1)^{\text{th}}$  order in large- $N$ , which is intractable using standard perturbative methods.

<sup>29</sup>Note that, due to the equation motion for  $\sigma$ , schematically of the form  $\partial^2 \phi_i \sim \sigma \phi_i$ , the  $n > 0$  families in (2.92) may be related to families involving both  $\phi_i$  and  $\sigma$ . For instance,  $[\phi_i \sigma \phi_i]_{0,\ell} \equiv \phi_i \partial^{\mu_1} \dots \partial^{\mu_\ell} \sigma \phi_i \sim [\phi_i \phi_i]_{1,\ell}$ . There are still other families of primary singlet operators which are not of this form. For instance,  $[\phi_i \sigma \phi_i]_{n,k,\ell} = \phi_i \partial^{\mu_1} \dots \partial^{\mu_\ell} (\partial^{2n} \sigma) \partial^{2k} \phi_i$ , with  $\Delta_{n,k,\ell} = 1 + 2n + 2k + 2 + \ell$ . Note that such operators are degenerate in  $\hbar$  and  $\bar{\hbar}$  for different values of  $n$  and  $k$  and may have degenerate dimensions with some  $n > 0$  operators in (2.92); in the presence of degeneracies, the inversion method as presented here yields linear combinations of thermal one-point functions.

<sup>30</sup>We assume canonical normalization for the operators  $\phi_i$  and  $\sigma$ :  $\langle \phi_i(x) \phi_j(0) \rangle = \delta_{ij}/|x|$  and  $\langle \sigma(x) \sigma(0) \rangle = \delta_{ij}/|x|^4$ .

## Thermal two-point function review

The propagator for the field  $\phi_i$  in Fourier space is given by,

$$G_{ij}(\omega_n, \mathbf{k}) = \langle \phi_i \phi_j \rangle(\omega_n, \mathbf{k}) = \frac{\delta_{ij}}{\omega_n^2 + \mathbf{k}^2 + \sigma} = \frac{\delta_{ij}}{\omega_n^2 + \mathbf{k}^2 + m_{\text{th}}^2}. \quad (2.96)$$

At the saddle-point, the non-zero expectation of  $\sigma$  thus acts like a mass term which is absent when considering the MFT propagator considered in section 2.4. We can now use the  $G_{ij}(\omega_n, \mathbf{k})$  to express the propagator in position-space as<sup>31</sup>

$$\begin{aligned} G_{ij}(\tau, \mathbf{x}) &= \delta_{ij} \sum_{n=-\infty}^{\infty} \int \frac{d^2 k}{(2\pi)^2} \frac{e^{-i\mathbf{k}\cdot\mathbf{x} - i\omega_n \tau}}{\omega_n^2 + \mathbf{k}^2 + m_{\text{th}}^2} \\ &= \delta_{ij} \sum_{m=-\infty}^{\infty} \frac{1}{[(m-z)(m-\bar{z})]^{1/2}} e^{-m_{\text{th}}[(m-z)(m-\bar{z})]^{1/2}}. \end{aligned} \quad (2.98)$$

This is similar to the MFT propagator (2.67), but with an exponentially decaying factor multiplying each term. While in the MFT study in section 2.4, each term in (2.67) could be expanded in Gegenbauer polynomials, to our knowledge an expansion for each term in (2.98) cannot be found in the literature. Thus, we will seek to find it using the Lorentzian inversion formula.

## Inversion I: Higher-spin currents

We now use the inversion formula (3.7) to recover the thermal one-point functions of the currents  $J_\ell$ , and give implicit results for the higher families  $[\phi_i \phi_i]_{n,\ell}$  with  $n > 0$ .

First one has to understand the discontinuities along the axis  $\text{Im } z = 0$  with  $\text{Re } z > 1$  for each term in (2.98):

$$\text{Disc} \frac{e^{-m_{\text{th}}[(m-z)(m-\bar{z})]^{1/2}}}{[(m-z)(m-\bar{z})]^{1/2}} = \frac{2 \cos \left( m_{\text{th}} [(z-m)(m-\bar{z})]^{1/2} \right)}{[(z-m)(m-\bar{z})]^{1/2}} \theta(z-m). \quad (2.99)$$

---

<sup>31</sup>To derive this, we use the Poisson resummation formula to turn a sum over Matsubara frequencies  $\omega_n = 2\pi n$  into a sum over shifts in  $\tau$ :

$$\sum_{n \in \mathbb{Z}} \tilde{f}(\omega_n) e^{-i\omega_n \tau} = \int d\omega \sum_{n \in \mathbb{Z}} \delta(\omega - \omega_n) \tilde{f}(\omega) e^{-i\omega \tau} = \int \frac{d\omega}{2\pi} \sum_{m \in \mathbb{Z}} e^{-i\omega(\tau-m)} \tilde{f}(\omega) = \sum_{m \in \mathbb{Z}} f(\tau-m). \quad (2.97)$$

Here,  $\tilde{f}$  is the Fourier transform of  $f$ . Thus, we can Fourier transform  $G_{ij}(\omega, \mathbf{k})$  (treating  $\omega, k$  as continuous), which gives the Yukawa potential  $\frac{e^{-m_{\text{th}}|x|}}{|x|}$ . Then we sum over integer shifts in  $\tau$  to obtain (2.98).

We now apply the inversion formula (3.7) to get the contribution of each term in (2.98). We focus on the integral, multiplying overall factors at the end. We also denote the spin as  $\ell$ , rather than  $J$ . For terms with  $m \geq 1$  we find, following the same approximation scheme as in section 2.4 for  $d > 2$  MFT (see around (2.81)),

$$2 \int_0^1 \frac{d\bar{z}}{\bar{z}} \int_m^\infty \frac{dz}{z} (z\bar{z})^{-\frac{\Delta}{2}} (z - \bar{z}) F_\ell \left( \sqrt{\frac{\bar{z}}{z}} \right) \frac{\cos \left( m_{\text{th}} [(z - m)(m - \bar{z})]^{1/2} \right)}{[(z - m)(m - \bar{z})]^{1/2}}$$

$$\xrightarrow[\substack{\bar{z} \rightarrow m\bar{z} \\ z \rightarrow mz}]{2} \frac{2}{m^\Delta} \int_1^\infty dz z^{-\Delta} \int_0^z \frac{d\bar{z}}{\bar{z}} \bar{z}^{-\frac{\Delta}{2}} (1 - \bar{z}) F_\ell \left( \sqrt{\bar{z}} \right) \frac{\cos \left( m_{\text{th}} m [(z - 1)(1 - z\bar{z})]^{1/2} \right)}{[(z - 1)(1 - z\bar{z})]^{1/2}}. \quad (2.100)$$

Expanding the integrand in (2.100) at small  $\bar{z}$ ,

$$(1 - \bar{z}) F_\ell(\sqrt{\bar{z}}) \frac{\cos \left( m_{\text{th}} m \sqrt{(z - 1)(1 - z\bar{z})} \right)}{[(z - 1)(1 - z\bar{z})]^{1/2}}$$

$$= \frac{\bar{z}^{\frac{\ell+1}{2}}}{\sqrt{z - 1}} \left( \cos \left( m_{\text{th}} m \sqrt{z - 1} \right) + \mathcal{O}(\bar{z}) \right). \quad (2.101)$$

The  $\bar{z}$  integral at leading order gives rise to the contribution of the first double twist family with  $h = 1/2$ , via  $\int_0^z d\bar{z} \bar{z}^{-(\Delta-\ell-1)/2} = z^{\frac{1}{2}-h}/(\frac{1}{2}-h)$  with a pole at  $h = 1/2$ . Plugging this into (2.100), we now perform the  $z$ -integral to extract the residue at  $h = 1/2$ , which is found to be

$$\text{Res}_{h=\frac{1}{2}}(2.100) = -\frac{2^{\frac{5}{2}-\Delta} \sqrt{\pi}}{\Gamma(\Delta)} m_{\text{th}}^{\Delta-\frac{1}{2}} m^{-\frac{1}{2}} K_{\Delta-\frac{1}{2}}(m_{\text{th}} m), \quad (2.102)$$

where  $\Delta = 1 + \ell$  and  $K_{\Delta-\frac{1}{2}}$  is the modified Bessel function. The full result requires a sum over  $m$  as in (2.98); performing this sum, and appending overall factors from the inversion formula, we find that the thermal coefficient  $a_{J_\ell}$  for the higher-spin currents  $J_\ell$  is

$$a_{J_\ell} = (1 + (-1)^\ell) \frac{2^{-\frac{1}{2}-\ell} (m_{\text{th}})^{\frac{1}{2}+\ell}}{\Gamma(\frac{1}{2} + \ell)} \sum_{m=1}^{\infty} m^{-\frac{1}{2}} K_{\frac{1}{2}+\ell}(m_{\text{th}} m). \quad (2.103)$$

This sum can be performed to yield the following result:

$$a_{J_\ell} = \sum_{n=0}^{\ell} \frac{2^{n+1}}{n!} \frac{(\ell - n + 1)_n}{(2\ell - n + 1)_n} m_{\text{th}}^n \text{Li}_{\ell+1-n}(e^{-m_{\text{th}}}). \quad (2.104)$$

We can translate this to a result for the thermal one-point function,  $b_{J_\ell}$ , itself, using known results in the literature for the OPE coefficients  $f_{\phi_i \phi_i J_\ell}$ , together with our  $\phi_i$

normalization in footnote 30. From e.g. [90], in  $d = 3$  we have

$$\frac{f_{\phi_i \phi_i J_\ell}}{\sqrt{c_{J_\ell}}} = \frac{1}{\sqrt{N}} \Gamma\left(\ell + \frac{1}{2}\right) \sqrt{\frac{2^{\ell+1}}{\pi \ell}}. \quad (2.105)$$

Using the relation (2.17) between  $a_{\mathcal{O}}$  and  $b_{\mathcal{O}}$ , we find

$$\frac{b_{J_\ell}}{\sqrt{c_{J_\ell}}} = \frac{\sqrt{N 2^{\ell+1} \ell}}{\ell!} \sum_{n=0}^{\ell} \frac{2^n (\ell - n + 1)_n}{n! (2\ell - n + 1)_n} m_{\text{th}}^n \text{Li}_{\ell+1-n}(e^{-m_{\text{th}}}), \quad (2.106)$$

which is the ratio that is independent of the norm of  $J_\ell$ .

This is an elegant result. The case  $\ell = 2$  corresponds to the stress tensor. In this case, the sum may be further simplified to yield

$$a_T = \frac{8}{5} \zeta(3). \quad (2.107)$$

Using (2.21), we see that this agrees with a previous result of [66, 73]. For the higher-spin currents  $\ell > 2$ , we are not aware of previous results in the literature for the thermal one-point functions, so (2.106) are new. Intriguingly,  $a_{J_\ell}$  is a transcendental function of uniform transcendental weight  $\ell + 1$ , where we note that  $m_{\text{th}}$  is itself of transcendental weight one. It would be fascinating to understand this transcendental better.

As mentioned in the introduction, this result has implications for higher-spin black hole solutions of Vasiliev higher-spin gravity in  $\text{AdS}_4$ . The translation invariance of thermal one-point functions means that (2.106) are proportional to the higher-spin charges of the CFT at finite temperature. Together with the thermal mass  $m_{\text{th}} \sim \langle \sigma \rangle_\beta$ , these charges fully determine the “higher-spin hair” of the putative black hole solution dual to the CFT thermal state with vanishing higher-spin chemical potentials. This black hole has not yet been constructed, due to difficulties in interpreting and solving Vasiliev’s equations. Our result provides a benchmark, both for any explicit candidate black hole, and for a physical interpretation of proposed constructions of higher-spin gauge-invariant charges (see e.g. [91–95]).

It is not much more difficult to derive the one-point functions of the  $n > 0$  families appearing in (2.92). One simply has to keep higher orders in  $\bar{z}$  in (2.101): a term of  $\mathcal{O}(\bar{z}^n)$  gives a pole at  $h = \frac{1}{2} + n$ , i.e. for spin- $\ell$  operators with  $\Delta = 1 + \ell + 2n$ .

## Inversion II: Scalars

The above results are incomplete in the scalar sector, and present a small puzzle. Note that our final expression (2.103) was actually valid all the way down to  $\ell = 0$ ,



which would correspond to a scalar with dimension  $\Delta = 1$ , even though such an operator is absent. The same would happen for the poles with higher  $n > 0$ , which would seem to indicate the presence of spurious scalars with odd integer dimension  $\Delta \in 2\mathbb{Z}^+ - 1$ . Moreover, we did not recover the  $\Delta = 2m$  scalar poles corresponding to  $\sigma^m$  exchanges, nor the unit operator. As we now show, these issues are remedied by considering the arc contributions to the inversion formula.

Following the notation in section 2.3.2.2 where  $z = rw$  and  $\bar{z} = rw^{-1}$ , we are interested in computing the  $w \rightarrow e^{i\phi}\infty$  behavior for each term in the propagator (2.98). In this limit, the only surviving term is given by the  $m = 0$  term,

$$G_{ij}(r, |w| \rightarrow \infty) = \frac{\delta_{ij}}{r} e^{-m_{\text{th}} r}. \quad (2.108)$$

The contribution of the integral correction to the inversion formula is given by (2.52). When plugging in the asymptotic value of the propagator, this becomes

$$a^{\text{arcs}}(\Delta, \ell) = 2K_\ell(1 + (-1)^\ell) \int_0^1 dr r^{-\Delta} \oint \frac{dw}{iw} \lim_{|w| \rightarrow \infty} \left[ \left( \frac{1}{i}(w - w^{-1}) \right)^{2\nu} (F_\ell(w)e^{-i\pi\nu} + F_\ell(w^{-1})e^{i\pi\nu}) \right] \frac{1}{r} e^{-m_{\text{th}} r}. \quad (2.109)$$

The integral over  $w$  in the limit in which  $|w| \rightarrow \infty$  is trivial and simply gives a factor of  $2\pi$  when  $\ell = 0$  and 0 when  $\ell > 0$ . This indeed confirms that the thermal coefficients quoted above for the currents with  $\ell > 0$  are correct. For  $\ell = 0$ , we are left with an integral over  $r$ :

$$a^{\text{arcs}}(\Delta, 0) = \int_0^1 \frac{dr}{r} r^{-1-\Delta} e^{-m_{\text{th}} r}, \quad (2.110)$$

where we note that the factor  $4\pi K_\ell(1 + (-1)^\ell) = 2$  in the case  $\ell = 0$ . The poles in  $\Delta$  of  $a(\Delta, \ell)$  are independent of the upper bound of the integral. Changing the upper bound of the integral to  $\infty$ , we find the extremely simple formula:

$$a^{\text{arcs}}(\Delta, 0) = m_{\text{th}}^\Delta \Gamma(-\Delta). \quad (2.111)$$

Since  $\Gamma(x)$  has poles at each negative integer value of  $x$ , we can express the function  $a(\Delta, 0)$  around each  $m \in \mathbb{Z}^+$  as

$$a^{\text{arcs}}(\Delta, 0) \sim \frac{1}{\Delta - m} \frac{(-1)^{m+1} m_{\text{th}}^m}{\Gamma(m+1)}. \quad (2.112)$$

These poles do two things. First, they cancel all spurious scalar poles of  $a(\Delta, 0)$  at  $\Delta \in 2\mathbb{Z}^+ - 1$ . Second, they give the correct poles for the actual scalar operators of the theory, which have  $\Delta \in 2\mathbb{Z}^+$ , as well as the unit operator pole.

Let us first analyze the case  $m = 0$ . This simply returns a thermal one-point function of 1, corresponding to a correctly normalized unit operator.

Next we take  $m = 1$ . This pole at  $\Delta = 1$  and  $\ell = 0$  should cancel the spurious scalar pole of the previous analysis. From (2.104), we get

$$a(\Delta, 0) \sim -\frac{2\log(1 - e^{-m_{\text{th}}})}{\Delta - 1}. \quad (2.113)$$

This only cancels  $a^{\text{arcs}}(\Delta, 0)$  when

$$-2\log(1 - e^{-m_{\text{th}}}) = m_{\text{th}}. \quad (2.114)$$

The solution of this equation is uniquely given by the saddle point value of the thermal mass in (2.91)! Thus, a correct value for the thermal mass in (2.98) is what yields the precise cancellation of the  $\Delta = 1$  scalar contribution from the non-arc terms to the thermal one-point function obtained via inversion. Alternatively, this may be viewed as a novel derivation of  $m_{\text{th}}$ . Likewise, the spurious scalar poles with  $\Delta = 3, 5, \dots$  that would arise from  $n > 0$  terms in (2.100) should cancel against the  $m = 3, 5, \dots$  terms in (2.112).

Finally, by taking  $m = 2\mathbb{Z}_+$  in (2.112), we find the residue

$$\text{Res}_{\Delta=2m} a^{\text{arcs}}(\Delta, 0) = -\frac{m_{\text{th}}^{2m}}{\Gamma(2m + 1)}. \quad (2.115)$$

This gives a linear combination of the  $a_{\mathcal{O}}$  coefficients for all scalar operators  $\mathcal{O}$  of dimension  $\Delta = 2m$ . For  $m = 2$ , there is only a single operator,  $\sigma^2$ . For higher values of  $m$ , there are possible degeneracies, as briefly discussed in footnote 29.

### 2.5.2 Holographic CFTs

We now make some comments on large  $N$  CFTs in the context of AdS/CFT.

A universal set of contributions to the OPE expansion (2.87) comes from the stress tensor,  $T_{\mu\nu}$ , and its multi-traces,  $[T \dots T]$ , which necessarily appear in the  $\phi \times \phi$  OPE for any  $\phi$ . In a CFT with a weakly coupled gravity dual, these terms represent the purely gravitational interactions between the bulk field  $\Phi$ , dual to  $\phi$ , and the thermal geometry. The form of these contributions is sensitive to the gap scale to single-trace higher-spin operators ( $J > 2$ ),  $\Delta_{\text{gap}}$ . We would like to understand how.

First, consider the case  $\Delta_{\text{gap}} \gg 1$ , where the bulk dual is general relativity plus small corrections, coupled to low-spin matter [96–99]. In this case, the thermal state on  $S^1_{\beta} \times \mathbb{R}^{d-1}$  is dual to an  $\text{AdS}_{d+1}$ -Schwarzschild black brane geometry with inverse Hawking

temperature  $\beta$ ,<sup>32</sup> and the stress tensor contributions in the OPE decomposition (2.87) are dual to the exchange of arbitrary numbers of gravitons between  $\Phi$  and the black brane. In a heavy probe limit  $1 \ll \Delta_\phi \ll M_{\text{pl}} L_{\text{AdS}}$ , the connected two-point function may be computed as the exponential of a geodesic length,  $\langle \phi(x)\phi(0) \rangle_\beta \sim e^{-\Delta_\phi x}$ . The disconnected component of the correlator,  $\sim \langle \phi \rangle_\beta^2$ , is computed as an infall of each particle into the black brane horizon.<sup>33</sup> This disconnected contribution goes to a constant plus  $e^{-m_{\text{th}} x}$  corrections, and thus becomes more important at sufficiently long distances.

It is instructive to examine the classic case of strongly coupled  $\mathcal{N} = 4$  super-Yang-Mills (SYM), with  $SU(4)_R$  symmetry. The single-trace scalar spectrum consists of the Lagrangian operator, as well as the 1/2-BPS operators  $\mathcal{O}_p$  with  $p = 2, 3, 4, \dots$ , which live in the  $[0, p, 0]$  representation of  $SU(4)_R$  and have conformal dimensions  $\Delta = p$ . The  $R$ -symmetry constrains the thermal two-point functions  $\langle \mathcal{O}_p \mathcal{O}_p \rangle_\beta$  to take the form

$$\langle \mathcal{O}_p(x) \mathcal{O}_p(0) \rangle_\beta = \langle \mathcal{O}_p(x) \mathcal{O}_p(0) \rangle_\beta^{\text{MFT}} + (\text{stress tensor terms}). \quad (2.116)$$

That is, in the OPE decomposition of  $\langle \mathcal{O}_p \mathcal{O}_p \rangle_\beta$  for any  $p$ , the stress tensor terms are the *only* terms besides the MFT contributions at leading order in  $1/N$ . This follows from the absence of  $R$ -singlets in the single-trace spectrum besides the identity operator, the Lagrangian operator and the stress tensor, and the fact that the Lagrangian carries charge under an emergent  $U(1)_Y$  bonus symmetry [102]. The stress tensor contribution,  $a_T$ , exhibits a famous dependence on the 't Hooft coupling  $\lambda$  [103],

$$\frac{a_T|_{\lambda \rightarrow \infty}}{a_T|_{\lambda \rightarrow 0}} = \frac{b_T|_{\lambda \rightarrow \infty}}{b_T|_{\lambda \rightarrow 0}} = \frac{3}{4}. \quad (2.117)$$

In relating  $a_T$  to  $b_T$ , we have used that  $f_{\mathcal{O}_p \mathcal{O}_p T_{\mu\nu}}$  and  $C_T$  are  $\lambda$ -independent.

In more general theories with large  $\Delta_{\text{gap}}$  and a sparse spectrum of light operators, there can be single-trace global symmetry singlets, so contributions from operators other than the stress tensor to the scalar two-point function  $g(\tau, \mathbf{x})$  are possible. As  $\Delta_{\text{gap}}$  decreases, there are different possible sources of  $\Delta_{\text{gap}}$  corrections to thermal correlation functions. First, the low-spin OPE data receive power-law corrections in

<sup>32</sup>At infinite spatial volume, thermal AdS is thermodynamically disfavored.

<sup>33</sup>This interaction requires a nonzero cubic coupling between two gravitons and  $\Phi$ ; this is forbidden at the two-derivative level, but may appear at the four-derivative level in the form of a  $\phi C_{\mu\nu\rho\sigma}^2$  coupling, where  $C_{\mu\nu\rho\sigma}$  is the Weyl tensor (see e.g. [100] for an application). Such couplings are, however, suppressed by the mass scale of higher-spin particles in the bulk [99] and, in more general theories of gravity, by universal bounds [99, 101].

$\Delta_{\text{gap}}$ . This includes the OPE coefficients of double-trace operators (see [104] for an  $\mathcal{N} = 4$  example). In addition, there are  $e^{-\Delta_{\text{gap}}}$  corrections due to new contributions of massive string states with  $\Delta \sim \Delta_{\text{gap}}$ . At finite  $\Delta_{\text{gap}}$ , there are many possible behaviors.

Finally, note that if instead we examine thermal two-point functions of the stress tensor,  $\langle T_{\mu\nu} T_{\rho\sigma} \rangle_\beta$ , the effects of large  $\Delta_{\text{gap}}$  are more visible. For instance,  $\langle T_{\mu\nu} T_{\rho\sigma} T_{\lambda\eta} \rangle$  and  $\langle T_{\mu\nu} T_{\rho\sigma} \mathcal{O} \rangle$  couplings scale with inverse powers of  $\Delta_{\text{gap}}$  [96–99], thus suppressing various possible contributions to  $\langle T_{\mu\nu} T_{\rho\sigma} \rangle_\beta$  in the OPE limit. For many reasons, it would be interesting to extend the methods discussed herein to the case of spinning external operators, and to  $T_{\mu\nu}$  in particular; this would allow us to study the purely gravitational physics of the thermal geometry in AdS, without the need for a probe scalar field.

## 2.6 Large-spin perturbation theory

So far, our discussion of thermal two- and one-point functions has been in theories where we have enough analytic control to explicitly compute the thermal two-point functions, which we can invert to obtain one-point functions. How can we analyze theories for which we don't have any direct method of computing two- or one-point functions, such as the 3d Ising CFT? Inspired by studies of CFT four-point functions in Minkowski space, we use the inversion formula to set up a bootstrap algorithm for the thermal data in any CFT. The inversion formula takes in the two-point function, and returns its decomposition in the  $s$ -channel OPE. Crucially, any presentation of the two-point function could be inserted into the inversion formula, and its inversion would yield how the given presentation is related to the  $s$ -channel data. Here, we will invert the  $t$ -channel OPE to the  $s$ -channel data. This relates the one-point functions of operators in the theory in a highly non-trivial fashion. By iterating these relations, we solve the thermal bootstrap in an all-orders asymptotic expansion in large spin,  $J$ .

We can make explicit use of our tools in the 3d Ising model. As in MFT and the  $O(N)$  model, low-twist operators can be arranged into double-twist families with relatively small anomalous dimensions. By combining our analytic tools with previous results from the four-point function bootstrap, we will estimate the thermal one-point functions of the operators in the lowest-twist family,  $[\sigma\sigma]_0$ , as a function of  $b_\epsilon$  and  $b_T$ .

### 2.6.1 Leading double-twist thermal coefficients

Let's study the two-point function of identical scalars

$$g(z, \bar{z}) = \langle \phi(z, \bar{z}) \phi(0, 0) \rangle_\beta, \quad (2.118)$$

in some CFT at finite temperature. We want to understand the ‘‘contributions’’ to the thermal coefficients of operators in the  $[\phi\phi]_0$  family,  $a_{[\phi\phi]_0, J}$ , from other thermal data of the theory. Our starting point is the  $t$ -channel OPE ( $z \sim \bar{z} \sim 1$ ),

$$g(z, \bar{z}) = \sum_{\mathcal{O} \in \phi \times \phi} a_{\mathcal{O}} ((1-z)(1-\bar{z}))^{\frac{\Delta_{\mathcal{O}}}{2} - \Delta_\phi} C_{\ell_{\mathcal{O}}}^{(\nu)} \left( \frac{1}{2} \left( \sqrt{\frac{1-z}{1-\bar{z}}} + \sqrt{\frac{1-\bar{z}}{1-z}} \right) \right), \quad (2.119)$$

which we will systematically invert to the  $s$ -channel data  $a(\Delta, J)$ . Expanding the Gegenbauer polynomials yields a power series in  $1-z$  and  $1-\bar{z}$ :

$$g(z, \bar{z}) = \sum_{\mathcal{O} \in \phi \times \phi} a_{\mathcal{O}} \sum_{k=0}^{\ell_{\mathcal{O}}} \frac{\Gamma(\ell_{\mathcal{O}} - k + \nu) \Gamma(k + \nu)}{\Gamma(\ell_{\mathcal{O}} - k + 1) \Gamma(k + 1)} \frac{1}{\Gamma(\nu)^2} (1-z)^{h_{\mathcal{O}} - \Delta_\phi + k} (1-\bar{z})^{\bar{h}_{\mathcal{O}} - \Delta_\phi - k}. \quad (2.120)$$

For future convenience, let's define the coefficients

$$p_k(\ell_{\mathcal{O}}) \equiv \frac{\Gamma(\ell_{\mathcal{O}} - k + \nu) \Gamma(k + \nu)}{\Gamma(\ell_{\mathcal{O}} - k + 1) \Gamma(k + 1)} \frac{1}{\Gamma(\nu)^2}. \quad (2.121)$$

Massaging the inversion formula (3.7), we rewrite it as a series in  $z$  and  $\bar{z}$ ,

$$a(\Delta, J) = (1 + (-1)^J) K_J \int_0^1 \frac{d\bar{z}}{\bar{z}} \int_1^\infty \frac{dz}{z} \sum_{m=0}^\infty q_m(J) z^{\Delta_\phi - \bar{h} - m} \bar{z}^{\Delta_\phi - h + m} \text{Disc}[g(z, \bar{z})], \quad (2.122)$$

with coefficients

$$q_m(J) \equiv (-1)^m \frac{(J + 2m)}{J} \frac{(J)_m (-m + \nu + 1)_m}{m! (J + \nu + 1)_m}. \quad (2.123)$$

Let's suppose we are considering  $J$  large enough so that the contributions of the arcs in (3.7) vanish.

Before inverting the  $t$ -channel OPE into  $a(\Delta, J)$ , let's analyze a few key features of the inversion formula:

- First, as discussed previously, recall that poles of  $a(\Delta, J)$ , associated with physical operators, come from the region near  $\bar{z} = 0$ . A term like  $\bar{z}^a$  in the expansion around  $\bar{z} = 0$  inverts to terms of the form

$$\int_0^1 \frac{d\bar{z}}{\bar{z}} \bar{z}^{\Delta_\phi - h + m} \bar{z}^a = \frac{1}{\Delta_\phi + a + m - h}, \quad (2.124)$$

and gives poles at  $h = \Delta_\phi + a + m$ . Such poles represent infinite families of operators with unbounded spin  $J$  and scaling dimensions  $\Delta = 2\Delta_\phi + 2a + 2m + J$ . Of course, in interacting CFTs, operators should have anomalous dimensions. We discuss the effects that shift the locations of these naïve poles to their correct values in section 2.6.2.3.

- Next, let's imagine a term of the form  $\bar{z}^a(1-z)^c$  in  $g(z, \bar{z})$  expanded around the double-lightcone limit ( $\bar{z} = 0$  and  $z = 1$ ), and invert it. The  $z$  integral determines the residue of the poles in (2.124) as a function of  $\bar{h}$  (recall that  $\bar{h} = h + J$ ). Typical  $z$  integrals are of the form

$$\int_1^\infty \frac{dz}{z} z^{\Delta_\phi - \bar{h} - m} \text{Disc}[(1-z)^c]. \quad (2.125)$$

The discontinuity is  $\text{Disc}[(1-z)^c] = 2\sin(-\pi c)(z-1)^c$ , so the integral gives

$$2\sin(-\pi c) \frac{\Gamma(1+c)\Gamma(\bar{h}+m-\Delta_\phi-c)}{\Gamma(\bar{h}+m-\Delta_\phi+1)}. \quad (2.126)$$

Note that this is naturally a term in a large- $\bar{h}$  expansion, since

$$\frac{\Gamma(\bar{h}+m-\Delta_\phi-c)}{\Gamma(\bar{h}+m-\Delta_\phi+1)} = \frac{1}{\bar{h}^{c+1}} + \mathcal{O}\left(\frac{1}{\bar{h}^{c+2}}\right). \quad (2.127)$$

Thus, we see that terms in the double-lightcone expansion of  $g(z, \bar{z})$  correspond to power law corrections in  $1/\bar{h}$ , or equivalently in  $1/J$ , to the thermal coefficients of families of operators (in the  $s$ -channel).

- As highlighted in section 2.3.3, the  $t$ -channel OPE in (2.120) is valid for the range  $0 \leq z, \bar{z} \leq 2$ . Thus, we are only justified in integrating the  $t$ -channel OPE between  $1 \leq z \leq 2$  for the  $z$  integral. In general, we don't have an expression for  $g(z, \bar{z})$  that is valid in the region  $0 \leq \bar{z} \leq 1$  and  $z > 2$ . Luckily, for the integrands of interest, the  $z$  integral in the range  $z > 2$  is exponentially suppressed in large  $\bar{h}$ , schematically as

$$\int_2^\infty \frac{dz}{z} z^{\Delta_\phi - \bar{h} - m} f(z) \sim 2^{-\bar{h}}. \quad (2.128)$$

Therefore, we can work with the  $t$ -channel OPE, integrate it in the region of its validity (from  $z = 1$  to 2), and obtain an all-orders expansion in  $1/\bar{h}$ , with undetermined exponentially-suppressed corrections.

Now that we have oriented ourselves, let's calculate the contributions to  $a(\Delta, J)$  from a single primary operator  $\mathcal{O} \in \phi \times \phi$  in the  $t$ -channel OPE in its full glory. We take the terms in the  $t$ -channel OPE corresponding to  $\mathcal{O}$ , and invert them to the  $s$ -channel via the inversion formula. We use  $a^{(\mathcal{O})}(\Delta, J)$  to denote the contribution to  $a(\Delta, J)$  from the inversion of the contribution of  $\mathcal{O}$  in the  $t$ -channel. Then we find

$$\begin{aligned}
a^{(\mathcal{O})}(\Delta, J) &\approx (1 + (-1)^J) K_J \int_0^1 \frac{d\bar{z}}{\bar{z}} \int_1^{z_{\max}} \frac{dz}{z} \sum_{m=0}^{\infty} q_m(J) z^{\Delta_\phi - \bar{h} - m} \bar{z}^{\Delta_\phi - h + m} \\
&\quad \times \text{Disc} \left[ a_{\mathcal{O}} \sum_{k=0}^{\ell_{\mathcal{O}}} p_k(\ell_{\mathcal{O}}) (1-z)^{h_{\mathcal{O}} - \Delta_\phi + k} (1-\bar{z})^{\bar{h}_{\mathcal{O}} - \Delta_\phi - k} \right] \\
&= a_{\mathcal{O}} (1 + (-1)^J) K_J \sum_{m=0}^{\infty} \sum_{k=0}^{\ell_{\mathcal{O}}} q_m(J) p_k(\ell_{\mathcal{O}}) \\
&\quad \times \frac{\Gamma(1 + \bar{h}_{\mathcal{O}} - \Delta_\phi - k) \Gamma(\Delta_\phi + m - h)}{\Gamma(\bar{h}_{\mathcal{O}} - h + 1 - k + m)} 2\pi S_{h_{\mathcal{O}} - \Delta_\phi + k, \Delta_\phi - m}(\bar{h}).
\end{aligned} \tag{2.129}$$

In general, we will think of  $a(\Delta, J)$  as a sum of such  $a^{(\mathcal{O})}(\Delta, J)$ , up to some finite spin  $\ell_{\max}$ , plus contributions from sums over infinite families of operators with unbounded spin, so

$$a(\Delta, J) \supset \sum_{\mathcal{O} \in \phi \times \phi, \ell < \ell_{\max}} a^{(\mathcal{O})}(\Delta, J). \tag{2.130}$$

The reasoning behind separating out the sums to infinite spin will become apparent in section 2.6.2. We have defined the function

$$\begin{aligned}
S_{c, \Delta}(\bar{h}) &= \frac{\sin(-\pi c)}{\pi} \int_1^{z_{\max}} \frac{dz}{z} z^{\Delta - \bar{h}} (z-1)^c \\
&= \frac{1}{\Gamma(-c)} \frac{\Gamma(\bar{h} - \Delta - c)}{\Gamma(\bar{h} - \Delta + 1)} - \frac{1}{\Gamma(-c)\Gamma(1+c)} B_{1/z_{\max}}(\bar{h} - \Delta - c, 1+c).
\end{aligned} \tag{2.131}$$

Here  $B_{1/z_{\max}}(\bar{h} - \Delta - c, 1+c)$  is the incomplete beta function, which decays as  $z_{\max}^{-\bar{h}}$  at large  $\bar{h}$ . We have left  $z_{\max}$  generic, but for all practical purposes we will take  $z_{\max} = 2$  in our applications.

The factors  $\Gamma(\Delta_\phi + m - h)$  in the numerator in (3.19) give poles at  $h = \Delta_\phi + n$  for  $n \in \mathbb{Z}_{\geq 0}$ . Naïvely, these are the poles corresponding to the  $[\phi\phi]_n$  families, at the naïve dimensions  $\Delta = 2\Delta_\phi + 2n + J$ , without anomalous dimensions. However, the correct  $a(\Delta, J)$  has poles in  $\Delta$  at the exact dimensions, including anomalous dimensions, so our naïve poles are shifted to their correct values,

$$\frac{1}{\Delta_\phi + n - h} \rightarrow \frac{1}{\Delta_\phi + n + \delta_n(\bar{h}) - h}. \tag{2.132}$$

This has a subtle, but important effect on the thermal coefficients. When one takes the residue, there is an extra factor  $d\bar{h}/dJ$  that depends on the derivative of  $\delta_n(\bar{h})$ , since

$$\text{Res}_{\Delta=2\Delta_\phi+2n+J+2\delta_n(\bar{h})} \frac{1}{\Delta_\phi + n + \delta_n(\bar{h}) - h} = -2 \frac{1}{1 - \delta'_n(\bar{h})} = -2 \frac{d\bar{h}}{dJ}, \quad (2.133)$$

as opposed to

$$\text{Res}_{\Delta=2\Delta_\phi+2n+J} \frac{1}{\Delta_\phi + n - h} = -2. \quad (2.134)$$

Note that  $d\bar{h}/dJ = 1$  when anomalous dimensions vanish. In section 2.6.2.3, we will provide a consistency check that the poles are indeed shifted to their correct locations. In our discussion of sums over families below, we include  $\frac{d\bar{h}}{dJ}$  for two reasons: firstly, it greatly simplifies the analysis of the asymptotics of such sums; secondly, we have in mind a situation where the anomalous dimensions  $\delta_n(\bar{h})$  are known through other means (e.g. the vacuum four-point function bootstrap), and we would like to use that information in the thermal bootstrap.

Finally, evaluating the residues of  $a^{(\mathcal{O})}(\Delta, J)$  at the  $[\phi\phi]_n$  poles, we get the contribution of  $\mathcal{O}$  to the thermal coefficients of the  $[\phi\phi]_n$  family,

$$\begin{aligned} a_{[\phi\phi]_n}^{(\mathcal{O})}(J) &= - \text{Res}_{\Delta=2\Delta_\phi+2n+J} a^{(\mathcal{O})}(\Delta, J) \\ &= a_{\mathcal{O}}(1 + (-1)^J) 4\pi K_J \frac{d\bar{h}}{dJ} \sum_{r=0}^n \sum_{k=0}^{\ell_{\mathcal{O}}} q_r(J) p_k(\ell_{\mathcal{O}}) (-1)^{n-r} \\ &\quad \times \binom{\bar{h}_{\mathcal{O}} - \Delta_\phi - k}{n-r} S_{h_{\mathcal{O}} - \Delta_\phi + k, \Delta_\phi - r}(\bar{h}). \end{aligned} \quad (2.135)$$

Note that  $\bar{h}$  is implicitly defined as a function of  $J$  by  $\bar{h} = \Delta_\phi + n + \delta(\bar{h}) + J$ . As we have emphasized above, properties of using the OPE with the inversion formula, these contributions are naturally organized as power-law corrections in large  $\bar{h}$ . The function  $S_{c,\Delta}(\bar{h})$  behaves as

$$S_{c,\Delta}(\bar{h}) = \frac{1}{\Gamma(-c)} \frac{1}{\bar{h}^{c+1}} + \mathcal{O}\left(\frac{1}{\bar{h}^{c+2}}\right) \quad (2.136)$$

at large  $\bar{h}$ , and  $c_m(J)$  behaves as a constant to leading order in  $1/\bar{h}$ . So a given term in (3.21) starts at order  $\bar{h}^{-(h_{\mathcal{O}} - \Delta_\phi + k + 1)}$ . Thus, we see that the contribution of an operator  $\mathcal{O}$  in the  $t$ -channel behaves at a rate controlled by its twist. Concretely, the



leading contributions in  $1/\bar{h}$  are given by the  $k = 0$  term of the sum in (3.21),

$$a_{[\phi\phi]_n}^{(\mathcal{O})}(J) = a_{\mathcal{O}}(1 + (-1)^J) \frac{K_J}{K_{\ell_{\mathcal{O}}}} \frac{d\bar{h}}{dJ} \sum_{r=0}^n q_r(J) (-1)^{n-r} \binom{\bar{h}_{\mathcal{O}} - \Delta_{\phi}}{n-r} S_{h_{\mathcal{O}} - \Delta_{\phi}, \Delta_{\phi} - r}(\bar{h}). \quad (2.137)$$

For the leading double-twist family  $[\phi\phi]_0$ , this further simplifies to

$$\begin{aligned} a_{[\phi\phi]_0}^{(\mathcal{O})}(J) &= a_{\mathcal{O}}(1 + (-1)^J) \frac{K_J}{K_{\ell_{\mathcal{O}}}} \frac{d\bar{h}}{dJ} S_{h_{\mathcal{O}} - \Delta_{\phi}, \Delta_{\phi}}(\bar{h}) \\ &\sim a_{\mathcal{O}}(1 + (-1)^J) \frac{K_J}{K_{\ell_{\mathcal{O}}}} \frac{1}{\bar{h}^{h_{\mathcal{O}} - \Delta_{\phi} + 1}} + \dots \end{aligned} \quad (2.138)$$

In writing the last line, we have assumed that  $\delta_{[\phi\phi]_0}(\bar{h})$  grows slower than  $\bar{h}$  as  $\bar{h} \rightarrow \infty$ .

To help understand the examples that follow, let us introduce a diagrammatic language that helps keep track of terms in large-spin perturbation theory of thermal data. Our diagrams can be thought of as analogs of the four-point function large-spin diagrams for the thermal case. We do not have a rigorous definition of these diagrams or a complete set of rules for using them. Nevertheless, they will help organize the discussion.<sup>34</sup>

For example, we can understand the fact that  $\mathcal{O} \in \phi \times \phi$  in the  $t$ -channel OPE inverts to give contributions to  $a_{[\phi\phi]_n}$  proportional to  $a_{\mathcal{O}}$  via the diagrams in figure 2.5. Let's start with the  $t$ -channel diagram in figure 2.5a. We should read this diagram from left to right as two  $\phi$  operators approach each other on one side of the thermal circle (corresponding to the  $t$ -channel), and fuse into  $\mathcal{O}$ , which in turn gets an expectation value. The diagram illustrates that this process should be proportional to the three-point coefficient  $f_{\phi\phi\mathcal{O}}$  and to the one-point function  $b_{\mathcal{O}}$ , which is indeed the case by the definition of  $a_{\mathcal{O}}$ .

Now, let's relate this process to the  $s$ -channel. The diagrammatic rule relating the  $s$ - and  $t$ -channels is given by taking the two external operators to the other side of the thermal circle around opposite sides. This converts the process in figure 2.5a to the process in figure 2.5b. Reading the resulting process from right to left, we interpret it as two external  $\phi$ 's fusing into operators in the  $[\phi\phi]_n$  families, which get expectation values proportional to  $a_{\mathcal{O}}$ .

---

<sup>34</sup>Large-spin diagrams for four-point functions can be understood as physical processes in the massive 2d effective theory defined in [12]. It would be nice to develop a similar understanding of the diagrams here. For now, our diagrams are simply mnemonic devices.



Figure 2.5: An illustration of the relation between  $s$ - and  $t$ -channels in the  $\langle\phi\phi\rangle_\beta$  correlator. The two channels are related by moving the external operators around the thermal circle (gray). A single term in the  $t$ -channel OPE  $\mathcal{O} \in \phi \times \phi$  inverts to the sum over the  $[\phi\phi]_n$  families in the  $s$ -channel. Alternatively, the sum over the  $[\phi\phi]_n$  families in the  $s$ -channel reproduces the  $\mathcal{O}$  term in the  $t$ -channel.

Summarizing, we reiterate that the thermal coefficients of families of operators are organized into large-spin expansions, with the operators  $\mathcal{O}$  in the OPE contributing perturbatively at order determined by their twist. Since the unit operator has the lowest twist in any unitary theory, it gives the leading contribution for large-spin members of double-twist families. A second important contribution comes from the stress tensor  $\mathcal{O} = T_{\mu\nu}$ , which gives a universal contribution proportional to the free energy density. These two universal contributions were written in (2.5) in the introduction. Furthermore, we also see that the contribution of a given  $\mathcal{O}$  is linear in its one-point function. This greatly simplifies perturbatively solving for the one-point functions, especially when one considers the corrections from sums of families, which we shall explore below.

### 2.6.2 Contributions of double-twist families: resumming, asymptotics, and other families

We have seen that inverting any single operator  $\mathcal{O}$  in the  $\phi \times \phi$  OPE gives contributions to the one-point functions of the  $[\phi\phi]_n$  families, and only these families. But many other operators appear in the  $\phi \times \phi$  OPE, and the inversion formula must pick up their existence. How can we extract their one-point functions from  $\langle\phi\phi\rangle_\beta$ ?

As seen in section 2.6.1, any finite number of terms in the  $t$ -channel OPE have “regular”  $\bar{z}$  expansions around  $\bar{z} \sim 0$ , with integer  $\bar{z}$  powers obtained from the Taylor series of some collection of terms of the form  $(1 - \bar{z})^c$ . Inverting such terms will only give poles at  $h = \Delta_\phi + n$ , which thus correspond to the  $[\phi\phi]_n$  families. So, to obtain the necessary poles at other locations, we need to find terms in the  $t$ -channel expansion that behave as  $\bar{z}^c$  with  $c \notin \mathbb{Z}_{\geq 0}$  near  $\bar{z} \sim 0$ . Such terms invert to poles

at  $h = \Delta_\phi + c + n$ , and correspond to different families determined by  $c$ . We will call such terms “singular,” in analogy with the Casimir-singular definition of [12, 20]. Singular terms are characterized by having discontinuity around  $\bar{z} \sim 0$ , which means they would be picked up by the Lorentzian inversion formula that takes the two-point function and inverts it to the  $t$ -channel. The only way we can obtain singular terms is from tails of the infinite sums of families in the  $t$ -channel OPE, which, when summed up, will have different  $\bar{z}$  behavior compared to any finite number of terms. A related motivation for understanding this problem is to compute the contributions of the  $[\phi\phi]_n$  families to their own one-point functions.

We will now explain how to systematically compute the contributions of double-twist families to the one-point functions of operators that appear in the  $\phi \times \phi$  OPE. To begin, let’s focus on the contribution from summing the tail of the particular double-twist family  $[\phi\phi]_0$ . Once again, we start with the  $t$ -channel OPE expansion, which we now try to understand in the double-lightcone limit  $(z, \bar{z}) \sim (1, 0)$ .

Let  $\{\mathcal{O}\}$  be a set of operators in the  $\phi \times \phi$  OPE with low twist. Inverting their terms in the  $t$ -channel via section 2.6.1, we obtain from (2.138) the leading  $1/\bar{h}$  behavior of the 1-point functions of the  $[\phi\phi]_0$  family,

$$a_{[\phi\phi]_0}(J) \sim \sum_{\mathcal{O}} \frac{a_{\mathcal{O}}}{K_{\ell_{\mathcal{O}}}} (1 + (-1)^J) K_J \frac{d\bar{h}}{dJ} S_{h_{\mathcal{O}} - \Delta_\phi, \Delta_\phi}(\bar{h}). \quad (2.139)$$

Now, let’s insert this expression for  $a_{[\phi\phi]_0}$  back into the  $t$ -channel OPE, and consider the  $t$ -channel sum over the  $[\phi\phi]_0$  family

$$\begin{aligned} & \sum_{[\phi\phi]_0, J \in [\phi\phi]_0} \frac{a_{[\phi\phi]_0}(J)}{4\pi K_J} (1 - z)^{h - \Delta_\phi} (1 - \bar{z})^{\bar{h} - \Delta_\phi} \\ & \sim \sum_{[\phi\phi]_0} \sum_{\mathcal{O}} \frac{a_{\mathcal{O}}}{4\pi K_{\ell_{\mathcal{O}}}} (1 + (-1)^J) \frac{d\bar{h}}{dJ} S_{h_{\mathcal{O}} - \Delta_\phi, \Delta_\phi}(\bar{h}) (1 - z)^{h - \Delta_\phi} (1 - \bar{z})^{\bar{h} - \Delta_\phi} + \dots \end{aligned} \quad (2.140)$$

We wish to apply the inversion formula to this sum. If we naïvely invert each term in the sum, and then sum over the family, we notice that the sum over the contributions of each individual member of the family diverges. In other words, the inversion formula and the infinite sum over the family do not commute. So, we have to sum over the family first before inverting to the  $s$ -channel. This is in line with our anticipation that the poles for other families must arise from the tails of the sums over infinite families, such as  $[\phi\phi]_0$ . If the  $t$ -channel sum and the inversion integral commuted, we would only ever get poles for the  $[\phi\phi]_n$  families from the inversion formula.

### 2.6.2.1 Analytic and numerical formulae for sums over families

Let's analyze the  $t$ -channel sum over a double-twist family more carefully, in the spirit of [20]. Consider the sum over a particular term in the  $S_{c,\Delta}(\bar{h})$  expansion of one-point functions of an arbitrary double-twist family,<sup>35</sup>

$$\sum_{\bar{h}=h_f+\ell+\delta(\bar{h})} \frac{d\bar{h}}{d\ell} S_{c,\Delta}(\bar{h}) (1-z)^{h_f+\delta(\bar{h})-h_e} (1-\bar{z})^{\bar{h}-h_e}. \quad (2.141)$$

Here,  $\bar{h} = h_f + \ell + \delta(\bar{h})$  runs over the family with anomalous dimensions  $\delta(\bar{h})$ , and  $h(\bar{h}) = h_f + \delta(\bar{h})$  are the half-twists of the operators in the family. We have switched to denoting spin by  $\ell$  for sums over families, to avoid conflict with applying the inversion formula to these sums later on. We have left out the  $(-1)^\ell$  factor for now; we will return to it later. In general, this is a difficult sum to evaluate, and we don't yet know of an exact treatment. However, since anomalous dimensions  $\delta(\bar{h})$  for the families of interest are small for large  $\bar{h}$ , we can work order by order in  $\delta(\bar{h})$ . Concretely, we can split the sum over  $\bar{h}$  as

$$\sum_{\bar{h}} = \sum_{\bar{h} < \bar{h}_0 + \delta(\bar{h}_0)} + \sum_{\substack{\bar{h} = \bar{h}_0 + \ell + \delta(\bar{h}) \\ \ell = 0, 1, \dots}}, \quad (2.142)$$

for some large enough  $\bar{h}_0 = h_f + \ell_0$  such that the anomalous dimensions  $\delta(\bar{h})$  are sufficiently small for  $\bar{h} > \bar{h}_0$ , and expand the infinite sum piece in small  $\delta(\bar{h}) \log(1-z)$ ,

$$\sum_{\bar{h} = \bar{h}_0 + \ell + \delta(\bar{h})} \frac{d\bar{h}}{d\ell} S_{c,\Delta}(\bar{h}) (1-\bar{z})^{\bar{h}-h_e} \sum_{m=0}^{\infty} \frac{\delta(\bar{h})^m}{m!} \log^m(1-z) (1-z)^{h_f-h_e}. \quad (2.143)$$

This expansion is valid in a regime  $e^{-1/|\delta(\bar{h})|} < |1-z| < e^{1/|\delta(\bar{h})|}$ , which is near the double-lightcone limit for small anomalous dimensions. Now, the dependence on  $z$  — which controls the discontinuity in the inversion formula — can be factored out of the  $\bar{h}$  sum. Recall that the anomalous dimensions  $\delta(\bar{h})$  are themselves analytic functions of  $\bar{h}$ , and they can be computed perturbatively in a large- $\bar{h}$  expansion [13–17, 20, 23]. For example, the anomalous dimensions of a family  $[\phi\phi]_0$  can be expanded at large  $\bar{h}$ , and include terms such as

$$\delta(\bar{h}) \supset \sum_{\mathcal{O} \in \phi \times \phi} \frac{\delta(\mathcal{O})}{\bar{h}^{2h_{\mathcal{O}}}}. \quad (2.144)$$

<sup>35</sup>For  $h_e$  and  $h_f$ , the indices  $e$  and  $f$  stand for “external” and “family.” For the two-point function of two identical scalars  $\phi$ ,  $h_e = \Delta_\phi$ .

How can we compute the sums over  $\bar{h}$ ? With a more general treatment in mind, let's consider the sum

$$\sum_{\bar{h}=\bar{h}_0+\ell+\delta(\bar{h})} \frac{d\bar{h}}{d\ell} f(\bar{h})(1-\bar{z})^{\bar{h}-h_e}, \quad (2.145)$$

with a summand  $f(\bar{h})$  which grows at most as a power law at large  $\bar{h}$ . The summands of interest for us are of the form<sup>36</sup>

$$f(\bar{h}) = \delta^m(\bar{h}) S_{c,\Delta}(\bar{h}). \quad (2.146)$$

If we tried to expand in small  $\bar{z}$  and compute the  $\bar{h}$  sum order by order in  $\bar{z}$ , we see that for large enough powers of  $\bar{z}$  we get divergent sums in  $\bar{h}$ . In fact, this is to be expected. By the existence of the inversion formula, we know that such sums must have asymptotic pieces that reproduce the singular terms  $\bar{z}^a$ , which could not possibly be obtained from expanding in  $\bar{z}$  first (which produces only integer powers of  $\bar{z}$ ). Thus, we expect the result of such a sum to be of the form

$$\sum_{\bar{h}} \frac{d\bar{h}}{d\ell} f(\bar{h})(1-\bar{z})^{\bar{h}-h_e} = \sum_{a \in A} c_a \bar{z}^a + \sum_{k=0}^{\infty} \alpha_k \bar{z}^k, \quad (2.147)$$

with  $A \subset \mathbb{R} \setminus \mathbb{Z}_{\geq 0}$  some set of numbers which are not non-negative integers that we have to determine. (We can also have  $\bar{z}^a \log^m \bar{z}$  terms that we will write as  $\frac{\partial^m}{\partial a^m} \bar{z}^a$ .) Our task is reduced to computing the coefficients  $c_a$  and  $\alpha_k$ . To do this, we will separate the sum into asymptotic parts, which reproduce the  $\bar{z}^a$  terms, and leftover regular parts that are convergent sums in  $\bar{h}$ , with which we can compute the  $\alpha_k$  coefficients.

First, we determine the large- $\bar{h}$  asymptotics of  $f(\bar{h})$  in terms of the known functions  $S_{a,\Delta}(\bar{h})$ ,

$$f(\bar{h}) \sim \sum_{a \in A} c_{a,\Delta}[f] S_{a,\Delta}(\bar{h}). \quad (2.148)$$

Note that the set  $A$  is determined by the asymptotics of  $f(\bar{h})$ , but the expansion can be written for any choice of  $\Delta$ . For summands of interest like in (2.146), the asymptotic expansion is determined algorithmically from the large- $\bar{h}$  expansions of  $S_{c,\Delta}(\bar{h})$  and of  $\delta(\bar{h})$  à la (2.144). Once the asymptotics in (2.148) are obtained, we

<sup>36</sup>We will also be interested in sums including derivatives  $\partial_c^m S_{c,\Delta}(\bar{h})$ , as we will discuss later.

can compute the singular terms from the tails of the sums over the asymptotics, by using the crucial identity of the integer-spaced sum

$$\begin{aligned} \sum_{\substack{\bar{h}=\bar{h}_0+\ell \\ \ell=0,1,\dots}} S_{c,\Delta}(\bar{h})(1-\bar{z})^{\bar{h}} &= (1-\bar{z})^{\bar{h}_0} S_{c,\Delta}(\bar{h}_0) {}_2F_1\left(\begin{matrix} 1, \bar{h}_0 - \Delta - c \\ \bar{h}_0 - \Delta + 1 \end{matrix}; 1-\bar{z}\right) \\ &= \bar{z}^c (1-\bar{z})^\Delta - S_{c-1,\Delta+1}(\bar{h}_0)(1-\bar{z})^{\bar{h}_0} {}_2F_1\left(\begin{matrix} 1, \bar{h}_0 - \Delta - c \\ -c + 1 \end{matrix}; \bar{z}\right). \end{aligned} \quad (2.149)$$

Note that the first term is singular and the second term, proportional to  ${}_2F_1(\dots, \bar{z})$  is regular.

We claim that the noninteger-spaced sum over  $S_{c,\Delta}(\bar{h})$  (with  $\bar{h}$  determined by the anomalous dimensions  $\delta(\bar{h})$ ) has the same singular piece as the integer-spaced sum,

$$\sum_{\bar{h}=\bar{h}_0+\ell+\delta(\bar{h})} \frac{d\bar{h}}{d\ell} S_{c,\Delta}(\bar{h})(1-\bar{z})^{\bar{h}} = \bar{z}^c (1-\bar{z})^\Delta + \text{regular}. \quad (2.150)$$

This can be verified by an argument due to [20] applied to the present case. We convert the sum to a contour integral via Cauchy's residue theorem,<sup>37</sup>

$$\sum_{\ell=0}^{\infty} \frac{d\bar{h}}{d\ell} S_{c,\Delta}(\bar{h})(1-\bar{z})^{\bar{h}} = - \oint_{\gamma} \frac{d\bar{h}}{2\pi i} \pi \cot(\pi(\bar{h} - \bar{h}_0 - \delta(\bar{h}))) S_{c,\Delta}(\bar{h})(1-\bar{z})^{\bar{h}}, \quad (2.151)$$

where  $\gamma$  is a contour along the real axis that picks up the desired poles. We can deform the contour to one that runs parallel to the imaginary axis, plus arcs at infinity. The singular terms come from the asymptotics of this integral. As long as  $\delta(\bar{h})$  grows slower than  $\bar{h}$  as  $\bar{h} \rightarrow \pm i\infty$ , the asymptotic region of the integral approaches a  $\delta(\bar{h})$ -independent constant exponentially quickly, since

$$\pi \cot(\pi(\bar{h} - \bar{h}_0 - \delta(\bar{h}))) \rightarrow \mp 1 + O(e^{\mp 2s}) \quad \text{as } \bar{h} \rightarrow \pm is. \quad (2.152)$$

Therefore, the singular pieces are independent of  $\delta(\bar{h})$ . To be even more concrete, we can subtract the contour integral versions of the noninteger- and integer-spaced sums, and notice that the asymptotics vanish, or that if we expand the difference in small  $\bar{z}$ , the integrals in  $\bar{h}$  are convergent term by term so the singular terms must have canceled. Thus, we see that

$$\sum_{\bar{h}} \frac{d\bar{h}}{d\ell} f(\bar{h})(1-\bar{z})^{\bar{h}-h_e} = \sum_{a \in A} c_{a,\Delta}[f] \bar{z}^a (1-\bar{z})^{\Delta-h_e} + \text{regular}. \quad (2.153)$$

---

<sup>37</sup>This is also known as the Sommerfeld-Watson transform.

Note that we can always choose  $\Delta = h_e$  in the asymptotic expansion in (2.148) to simplify the organization of the singular terms,

$$\sum_{\bar{h}} \frac{d\bar{h}}{d\ell} f(\bar{h})(1 - \bar{z})^{\bar{h} - h_e} = \sum_{a \in A} c_{a, h_e}[f] \bar{z}^a + \text{regular}. \quad (2.154)$$

We are left with computing the coefficients  $\alpha_k$  of the regular terms. Since we have extracted the asymptotics, we can write convergent expressions for  $\alpha_k$  by subtracting the asymptotics and expanding in small  $\bar{z}$ . This will be best done by once again converting the sum over  $\bar{h}$  into a contour integral in the complex  $\bar{h}$  plane, via Cauchy's theorem. We want to write a contour integral of the form

$$\begin{aligned} \sum_{\bar{h} = \bar{h}_0 + \ell + \delta(\bar{h})} \frac{d\bar{h}}{d\ell} f(\bar{h})(1 - \bar{z})^{\bar{h} - h_e} &= \sum_{\bar{h} = \bar{h}_0 + \ell + \delta(\bar{h})} \frac{d\bar{h}}{d\ell} f(\bar{h}) \sum_{k=0}^{\infty} \binom{\bar{h} - h_e}{k} (-1)^k \bar{z}^k \\ &= - \oint_{h_c - i\infty}^{h_c + i\infty} \frac{d\bar{h}}{2\pi i} \pi \cot(\pi(\bar{h} - \bar{h}_0 - \delta(\bar{h}))) f(\bar{h}) \sum_{k=0}^{\infty} \binom{\bar{h} - h_e}{k} (-1)^k \bar{z}^k, \end{aligned} \quad (2.155)$$

where  $h_c = \bar{h}_0 + \delta(\bar{h}_0) - \epsilon$ , for some small  $\epsilon > 0$ . This contour integral will equal the sum only if  $f(\bar{h})$  decays fast enough on the arcs at infinity so that we may drop them, and if  $f(\bar{h})$  does not have any simple poles for  $\text{Re } \bar{h} \geq h_c$ . The second condition is easily remedied in case  $f(\bar{h})$  does have poles, by simply removing the residues coming from those poles. The first condition is related to the more important issue that for large enough  $k$ , the  $\bar{h}$  growth is divergent, and the sum over  $k$  and the contour integral do not commute. However, we can regulate the integral by subtracting the divergent asymptotics in the form of the integer-spaced sum until we get a convergent integral (for which the arcs vanish as well), and add back the known result of the integer-spaced sum. This gives the following formula

$$\begin{aligned} \alpha_k[p, \delta, h_e](\bar{h}_0) &= - \oint_{h_c - i\infty}^{h_c + i\infty} \frac{d\bar{h}}{2\pi i} \binom{\bar{h} - h_e}{k} (-1)^k \pi \\ &\quad \times \left( \cot(\pi(\bar{h} - \bar{h}_0 - \delta(\bar{h}))) f(\bar{h}) - \cot(\pi(\bar{h} - \bar{h}_0)) \sum_{\substack{a \in A \\ a < K}} c_{a, \Delta} S_{a, \Delta}(\bar{h}) \right) \\ &\quad + \sum_{\substack{a \in A \\ a < K}} c_{a, \Delta} (r_k(a, \Delta, h_e, \bar{h}_0) + s_k(a, \Delta, h_e, \bar{h}_0)). \end{aligned} \quad (2.156)$$

Here,  $K$  should be at least  $k$ , but larger  $K$  gives a faster converging integral. In the last line, we have added back terms with  $r_k$ , which is the coefficient of  $\bar{z}^k$  for the

integer spaced sum in (2.149),

$$\begin{aligned} r_k(a, \Delta, h_e, \bar{h}_0) &= -S_{a-1, \Delta+1}(\bar{h}_0) (1 - \bar{z})^{\bar{h}_0 - h_e} {}_2F_1 \left( \begin{matrix} 1, \bar{h}_0 - \Delta - a \\ -a + 1 \end{matrix}; \bar{z} \right) \Big|_{\bar{z}^k} \\ &= -S_{a-1, \Delta+1}(\bar{h}_0) \sum_{m=0}^k (-1)^m \binom{\bar{h}_0 - h_e}{m} \frac{(\bar{h}_0 - \Delta - a)_{k-m}}{(-a + 1)_{k-m}} \end{aligned} \quad (2.157)$$

and  $s_k$ , which is the contribution of spurious poles (coming from the asymptotics  $S_{a, \Delta}(\bar{h})$  we subtracted) that are picked up by the contour when  $h_c - \Delta - a \leq 0$ ,

$$\begin{aligned} s_k(a, \Delta, h_e, \bar{h}_0) &= \sum_{n=0}^{\lfloor a + \Delta - h_c \rfloor} \operatorname{Res}_{\bar{h} = a + \Delta - n} \binom{\bar{h} - h_e}{k} (-1)^k \pi \cot(\pi(\bar{h} - \bar{h}_0)) S_{a, \Delta}(\bar{h}) \\ &= \sum_{n=0}^{\lfloor a + \Delta - h_c \rfloor} \binom{a + \Delta - n - h_e}{k} (-1)^k \pi \cot(\pi(a + \Delta - n - \bar{h}_0)) \frac{(-1)^n}{n! \Gamma(-a) \Gamma(a - n + 1)}. \end{aligned} \quad (2.158)$$

The contour integral can be integrated numerically in *Mathematica* to high precision.

Finally, to finish our discussion, let's consider the alternating sum,

$$\sum_{\bar{h}} (-1)^\ell f(\bar{h}) (1 - \bar{z})^{\bar{h} - h_e}. \quad (2.159)$$

This sum is convergent order by order in the  $\bar{z}$  expansion, so one does not need to subtract off asymptotics. This sum is given by

$$\sum_{\bar{h}} (-1)^\ell \frac{d\bar{h}}{d\ell} f(\bar{h}) (1 - \bar{z})^{\bar{h} - h_e} = \sum_k \alpha_k^- [f, \delta, h_e](\bar{h}_0) \bar{z}^k, \quad (2.160)$$

where the coefficients  $\alpha_k^-$  are given by the contour integral with the replacement  $\cot \rightarrow \csc$ ,

$$\alpha_k^- [f, \delta, h_e](\bar{h}_0) = - \oint_{h_c - i\infty}^{h_c + i\infty} \frac{d\bar{h}}{2\pi i} \binom{\bar{h} - h_e}{k} (-1)^k \pi \csc(\pi(\bar{h} - \bar{h}_0 - \delta(\bar{h}))) f(\bar{h}). \quad (2.161)$$

Collecting our calculations, the full sum over operators with even spin is given by

$$\begin{aligned} &\sum_{\bar{h} = \bar{h}_0 + \ell + \delta(\bar{h})} (1 + (-1)^\ell) \frac{d\bar{h}}{d\ell} f(\bar{h}) (1 - \bar{z})^{\bar{h} - h_e} \\ &= \sum_{a \in A} c_{a, \Delta} [f] \bar{z}^a (1 - \bar{z})^{\Delta - h_e} + \sum_{k=0}^{\infty} \alpha_k^{\text{even}} [f, \delta, h_e](\bar{h}_0) \bar{z}^k, \end{aligned} \quad (2.162)$$

where

$$\alpha_k^{\text{even}} [f, \delta, h_e](\bar{h}_0) = \alpha_k [f, \delta, h_e](\bar{h}_0) + \alpha_k^- [f, \delta, h_e](\bar{h}_0). \quad (2.163)$$



### 2.6.2.2 Corrections to one-point functions from double-twist families

Armed with the technology to compute the sums over double-twist families, we return to understanding their contributions to one-point functions of operators. Let's recall the  $t$ -channel sum over  $[\phi\phi]_0$  in (2.140), and expand it in  $\delta \log(1-z)$  as in (2.143),

$$\begin{aligned} \sum_{\mathcal{O}} \frac{a_{\mathcal{O}}}{4\pi K_{\ell_{\mathcal{O}}}} \sum_{\bar{h}} (1+(-1)^{\ell}) \frac{d\bar{h}}{d\ell} S_{h_{\mathcal{O}}-\Delta_{\phi}, \Delta_{\phi}}(\bar{h}) (1-\bar{z})^{\bar{h}-\Delta_{\phi}} \\ \times \sum_{m=0}^{\infty} \frac{\delta(\bar{h})^m}{m!} \log^m(1-z) (1-z)^{h_f-\Delta_{\phi}}. \end{aligned} \quad (2.164)$$

Here, the sum is over the operators  $[\phi\phi]_{0,\ell}$  with  $\bar{h} = \bar{h}_0 + \ell + \delta_{[\phi\phi]_0}(\bar{h})$ , where  $\bar{h}_0$  is the  $\bar{h}$  of the lowest spin member of the family where we started the sum. For each  $\mathcal{O}$ , summing over  $\bar{h}$  yields

$$\begin{aligned} \sum_{m=0}^{\infty} \left( \sum_a c_{a,\Delta_{\phi}} \left[ \frac{\delta^m}{m!} S_{h_{\mathcal{O}}-\Delta_{\phi}, \Delta_{\phi}} \right] \bar{z}^a + \sum_{k=0}^{\infty} \alpha_k^{\text{even}} \left[ \frac{\delta^m}{m!} S_{h_{\mathcal{O}}-\Delta_{\phi}, \Delta_{\phi}, \delta, \Delta_{\phi}} \right] (\bar{h}_0) \bar{z}^k \right) \\ \times \log^m(1-z) (1-z)^{h_f-\Delta_{\phi}}. \end{aligned} \quad (2.165)$$

For  $[\phi\phi]_0$ ,  $h_f = \Delta_{\phi}$ , but we've kept it general here to demonstrate the general structure. Now, let's invert this piece of the two-point function to the  $s$ -channel. The integer powers  $\bar{z}^k$  invert to poles for  $[\phi\phi]_n$ , giving contributions to the one-point functions of these families, including  $[\phi\phi]_0$  itself. The contributions are controlled by

$$\text{Disc}[\log^m(1-z)(1-z)^{h_f-\Delta_{\phi}}] = \partial_{h_f}^m \text{Disc}[(1-z)^{h_f-\Delta_{\phi}}], \quad (2.166)$$

which inverts to a term

$$S_{h_f-\Delta_{\phi}}^{(m)}(\bar{h}) = \partial_{h_f}^m S_{h_f-\Delta_{\phi}}(\bar{h}) \quad (2.167)$$

in the large- $\bar{h}$  expansion of thermal coefficients. For example, including the self-corrections of  $[\phi\phi]_0$  to leading order in large spin yields

$$\begin{aligned} a_{[\phi\phi]_0}(J) = (1+(-1)^J) K_J \frac{d\bar{h}}{dJ} \\ \times \sum_{\mathcal{O}} \frac{a_{\mathcal{O}}}{K_{\ell_{\mathcal{O}}}} \left( S_{h_{\mathcal{O}}-\Delta_{\phi}, \Delta_{\phi}}(\bar{h}) \right. \\ \left. + \sum_{m=0}^{\infty} \alpha_0^{\text{even}} \left[ \frac{\delta^m}{m!} S_{h_{\mathcal{O}}-\Delta_{\phi}, \Delta_{\phi}, \delta, \Delta_{\phi}} \right] (\bar{h}_0) S_{0,\Delta_{\phi}}^{(m)}(\bar{h}) \right). \end{aligned} \quad (2.168)$$

We should remember that if we started the sum at some high  $\bar{h}_0$ , we should individually add the contributions of the low-lying members of the family that were excluded from the sum.

Once we have computed the self-corrections as in (2.168), there is nothing that stops us from iterating this procedure and computing the self-corrections from the new, once-self-corrected one-point functions. Instead of iterating indefinitely, we can solve for the fixed point of these self-corrections with a little cleverness. We have provided a method for this in appendix A.5.

The singular terms  $\bar{z}^a$  in (2.165) give poles at  $h = \Delta_\phi + a + n$ . We expect that these poles correspond to other families of operators with the given naïve twist — we will soon explore which families. Let's denote these families by  $[\Delta + a]_n$  for now. We see that the  $[\phi\phi]_0$  family contributes

$$a_{[\Delta+a]_n}^{([\phi\phi]_0)}(J) = (1 + (-1)^J) K_J \frac{d\bar{h}}{dJ} \sum_{\mathcal{O}} \frac{a_{\mathcal{O}}}{K_{\ell_{\mathcal{O}}}} \sum_m c_{a,\Delta_\phi} \left[ \frac{\delta^m}{m!} S_{h_{\mathcal{O}} - \Delta_\phi, \Delta_\phi} \right] S_{0,\Delta_\phi}^{(m)}(\bar{h}) \quad (2.169)$$

to the one-point functions of the  $[\Delta + a]_n$  families. The sum is over  $m$  such that  $S_{a,\Delta_\phi}$  appears in the asymptotic expansion of  $\frac{\delta^m}{m!} S_{h_{\mathcal{O}} - \Delta_\phi, \Delta_\phi}$ . Of course, this is rather schematic, since for interacting CFTs, the spectrum of families of higher-twist operators is very complicated, with large anomalous dimensions and mixing among families. Regardless, these contributions are present asymptotically in large  $J$ .

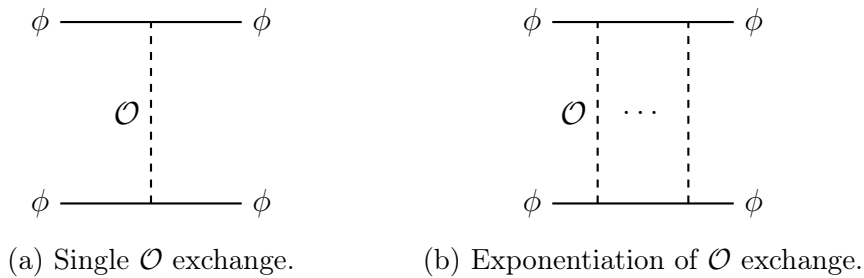


Figure 2.6: Large-spin diagrams illustrating the contribution to the anomalous dimensions of  $[\phi\phi]_n$  from the exchange of  $\mathcal{O}$ .

In general, can we say which other families of operators appear in the asymptotics of the sum of a given family, and therefore receive contributions via (2.165)? The large-spin expansion of the anomalous dimensions and OPE coefficients allows us to answer this question. Suppose  $\mathcal{O}$  is an operator in the  $\phi \times \phi$  OPE. Then,  $\mathcal{O}$  corrects the anomalous dimensions of the  $[\phi\phi]_0$  family, via the large-spin diagram in figure 2.6 [12, 20]. Consequently, there is a term in the asymptotic expansion of  $\delta_{[\phi\phi]_0}$  that goes

like

$$\delta_{[\phi\phi]_0}(\bar{h}) \sim \delta_{[\phi\phi]_0}^{(\mathcal{O})} \bar{h}^{-2h_{\mathcal{O}}} + \dots \quad (2.170)$$

where  $\delta_{[\phi\phi]_0}^{(\mathcal{O})}$  is some coefficient. Now, imagine the contribution of the identity operator to the  $[\phi\phi]_0$  thermal coefficients, which goes like  $S_{-\Delta_\phi, \Delta_\phi}(\bar{h})$  to leading order. Therefore, the sum over the  $[\phi\phi]_0$  family to first order in  $\delta_{[\phi\phi]_0}$  contains the asymptotic term

$$\delta_{[\phi\phi]_0}(\bar{h}) S_{-\Delta_\phi, \Delta_\phi}(\bar{h}) \sim \delta_{[\phi\phi]_0}^{(\mathcal{O})} S_{2h_{\mathcal{O}} - \Delta_\phi, \Delta_\phi}(\bar{h}) + \dots \quad (2.171)$$

This asymptotic piece corresponds to the diagram depicted in figure 2.7. In the  $t$ -channel sum over the  $[\phi\phi]_0$  family, this term produces the singular term  $\bar{z}^{2h_{\mathcal{O}} - \Delta_\phi}$ , which inverts to poles at  $h = 2h_{\mathcal{O}} + n$ , naïvely corresponding to the families  $[\mathcal{OO}]_n$ . For example, the residue for  $[\mathcal{OO}]_0$  from this contribution is

$$a_{[\mathcal{OO}]_0}^{([\phi\phi]_0)}(J) = (1 + (-1)^J) 4\pi K_J \frac{d\bar{h}}{dJ} \delta_{[\phi\phi]_0}^{(\mathcal{O})} S_{0, \Delta_\phi}^{(1)}(\bar{h}). \quad (2.172)$$

Thus, we see that the  $[\phi\phi]_0$  family contributes to the  $[\mathcal{OO}]_n$  families through its anomalous dimension! Similar arguments apply to the  $[\phi\phi]_n$  families. We could have guessed that we should obtain poles for the  $[\mathcal{OO}]_n$  families by crossing the diagram in figure 2.7 to the  $s$ -channel. As demonstrated in figure 2.8, the resulting  $s$ -channel process is proportional to  $b_{[\mathcal{OO}]_n}$ , so the inversion to the  $s$ -channel must have produced poles for  $[\mathcal{OO}]_n$ . We therefore see that the intuition from the diagrams agree with concrete calculations! One can also check that the expression for  $b_{[\mathcal{OO}]_0}$  obtained from the  $\langle\phi\phi\rangle_\beta$  correlator agrees with the expression obtained from the  $\langle\mathcal{OO}\rangle_\beta$  correlator to leading order in the large- $\bar{h}$  expansion.

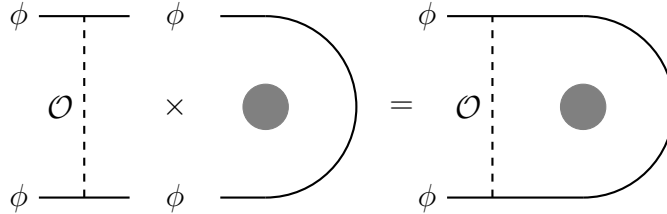


Figure 2.7: The diagram on the right can be thought of as the product of the two subdiagrams. Reading it from left to right, it is comprised of the contribution of  $\mathcal{O}$  to the anomalous dimensions of  $[\phi\phi]_n$ , and the thermal coefficients of the  $[\phi\phi]_n$  families proportional to  $b_1$ . Accordingly, it should be interpreted as the asymptotic piece with  $\delta_{[\phi\phi]_n}^{(\mathcal{O})}(\bar{h}) \times a_{[\phi\phi]_n}^{(1)}(\bar{h})$  in the sum over  $[\phi\phi]_0$ .

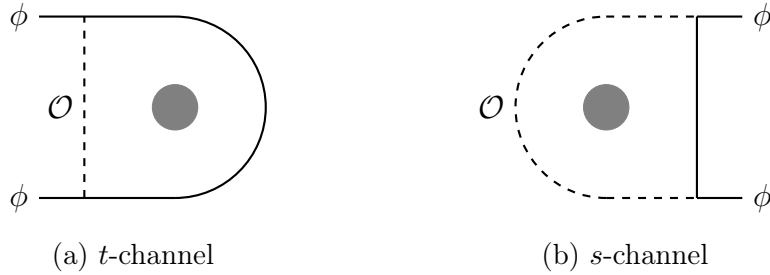


Figure 2.8: The  $t$ -channel sum over the asymptotic parts represented by the diagram on the left inverts to the  $s$ -channel process on the right. Accordingly, the inversion should produce poles for the  $[\mathcal{O}\mathcal{O}]_m$  families. The diagram on the right can itself be deciphered by reading it from right to left; first the external  $\phi$  operators form  $[\phi\phi]_n$ , which mixes with  $[\mathcal{O}\mathcal{O}]_m$  via exchange of a  $\phi$ , then the  $[\mathcal{O}\mathcal{O}]_m$  receive expectation values proportional to  $b_1$ .

In fact, the situation is much more general. For example, we can consider other terms in the asymptotic expansion of  $a_{[\phi\phi]_0}$ , such as  $S_{h_{\mathcal{O}'}-\Delta_\phi, \Delta_\phi}(\bar{h})$  coming from some other operator  $\mathcal{O}'$ . Then, the sum over  $[\phi\phi]_0$  to first order in  $\delta_{[\phi\phi]_0}$  produces the singular term  $\bar{z}^{2h_{\mathcal{O}'}+\Delta_\phi}$ , naively corresponding to multi-twist families  $[\mathcal{O}\mathcal{O}\mathcal{O}']$ . The diagrams for the sum over this asymptotic piece and the corresponding  $s$ -channel process are given in figure 2.9. We could also work to higher order in the anomalous dimensions, and obtain poles for multi-twist families, and so on.

However, we are unsure what the precise rules are for which diagrams are allowed, and how to interpret them in general. We will leave deriving these diagrams from physical arguments and further generalizing them to a future project.

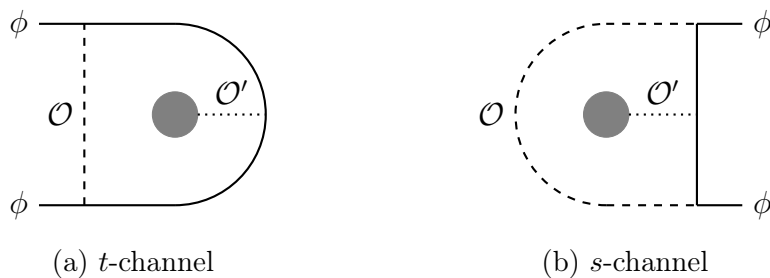


Figure 2.9: The  $t$ -channel diagram denotes a sum over the asymptotics  $\delta_{[\phi\phi]_n}^{(\mathcal{O})}(\bar{h}) \times a_{[\phi\phi]_n}^{(\mathcal{O}')}(\bar{h})$ . This inverts to poles for the  $[\mathcal{O}\mathcal{O}\mathcal{O}']_m$  families in the  $s$ -channel. When  $\mathcal{O}' = \mathbf{1}$ , we omit the line by convention and recover figure 2.8.

### 2.6.2.3 Corrections to pole locations

We are also in a position to address the issue of naïve versus true locations of poles of  $a(\Delta, J)$ , raised in section 2.6.1. Corrections to the locations of poles essentially arise from the asymptotics of the sums over the terms  $S_{c,\Delta}^{(m)}(\bar{h})$  with  $m > 0$ . By taking derivatives of the integer-spaced sum in (2.149),

$$\sum_{\substack{\bar{h}=\bar{h}_0+\ell \\ \ell=0,1,\dots}} S_{c,\Delta}^{(m)}(\bar{h})(1-\bar{z})^{\bar{h}} = \bar{z}^c(1-\bar{z})^\Delta \log^m \bar{z} + \text{regular}, \quad (2.173)$$

we see that sums over the asymptotics  $S_{c,\Delta}^{(m)}(\bar{h})$  produce  $\log^m \bar{z}$  terms. Such  $\log^m \bar{z}$  terms in  $g(z, \bar{z})$  in turn shift the location of the poles of  $a(\Delta, J)$  obtained from the  $\bar{z}$  integral in the inversion formula. For a nice way to see this, let's define the generating function

$$\tilde{g}_n(\bar{z}, \bar{h}) = \int_1^{z_{\max}} \frac{dz}{z} q_n(J) z^{\Delta_\phi - \bar{h} - n} \text{Disc}[g(z, \bar{z})]. \quad (2.174)$$

The thermal data  $a(\Delta, J)$  is obtained from  $\tilde{g}_n(\bar{z}, \bar{h})$  by doing the remaining  $\bar{z}$  integral in the inversion formula,

$$a(\Delta, J) = (1 + (-1)^J) K_J \int_0^1 \frac{d\bar{z}}{\bar{z}} \sum_{n=0}^{\infty} \bar{z}^{\Delta_\phi - h + n} \tilde{g}_n(\bar{z}, \bar{h}). \quad (2.175)$$

Now, consider the role of terms in  $\tilde{g}_n(\bar{z}, \bar{h})$  of the form

$$\sum_{m=0}^{\infty} f_m(\bar{h}) \bar{z}^c \log^m \bar{z}. \quad (2.176)$$

The claim is that such terms resum to  $f(\bar{h}) \bar{z}^{c+\delta(\bar{h})}$ , thus changing the location of poles as a function of  $\bar{h}$ , i.e. introducing anomalous dimensions!

Let's try to see this concretely. For example, how can we see the anomalous dimensions of  $[\phi\phi]_0$  arise? The anomalous dimensions must arise from sums of infinite families, yet which families? The anomalous dimension of  $[\phi\phi]_0$  contributes to other data in the theory, like in figures 2.8 and 2.9. What is the data in the theory that gives rise to the anomalous dimensions? Of course, there is nothing special about interpreting figures 2.8 and 2.9 as sums over  $[\phi\phi]_0$  in the  $t$ -channel, which invert to poles for the  $[\mathcal{O}\mathcal{O}]$  and  $[\mathcal{O}\mathcal{O}\mathcal{O}']$  families. Rather, these diagrams are supposed to be crossing symmetric! So, we can flip  $s$ - and  $t$ -channels in these diagrams, sum over the  $[\mathcal{O}\mathcal{O}]$  and  $[\mathcal{O}\mathcal{O}\mathcal{O}']$  families in the  $t$ -channel, and hopefully obtain the expected corrections to the  $[\phi\phi]$  anomalous dimensions when inverted to the  $s$ -channel.

Let's start with the simpler process in figure 2.8, but now with the  $[\mathcal{OO}]_0$  family running in the  $t$ -channel. Recall that the  $t$ -channel sum over the  $[\phi\phi]_0$  family inverted to poles for the  $[\mathcal{OO}]_0$  family (through the asymptotics in (2.171)) with residue  $a_{[\mathcal{OO}]_0}^{([\phi\phi]_0)}(J)$  given in (2.172). The  $t$ -channel sum over the  $[\mathcal{OO}]_0$  family looks like

$$\sum_{[\mathcal{OO}]_0} \frac{a_{[\mathcal{OO}]_0}(J)}{4\pi K_J} (1-z)^{h-\Delta_\phi} (1-\bar{z})^{\bar{h}-\Delta_\phi} \quad (2.177)$$

to leading order in  $(1-z)$ . Focusing on the term  $a_{[\mathcal{OO}]_0}^{([\phi\phi]_0)}(J)$  of  $a_{[\mathcal{OO}]_0}(J)$ , we have the sum

$$\sum_{[\mathcal{OO}]_0} (1+(-1)^J) \frac{d\bar{h}}{dJ} \delta_{[\phi\phi]_0}^{(\mathcal{O})} S_{0,\Delta_\phi}^{(1)}(\bar{h}) (1-z)^{h-\Delta_\phi} (1-\bar{z})^{\bar{h}-\Delta_\phi}. \quad (2.178)$$

Let's assume that  $\mathcal{O} \neq \phi$ , so  $\Delta_{\mathcal{O}} \neq \Delta_\phi$ . Then, expanding to leading (constant) order in  $\delta_{[\mathcal{OO}]_0}(\bar{h})$ , the sum becomes

$$\begin{aligned} \sum_{[\mathcal{OO}]_0} (1+(-1)^J) \frac{d\bar{h}}{dJ} \delta_{[\phi\phi]_0}^{(\mathcal{O})} S_{0,\Delta_\phi}^{(1)}(\bar{h}) (1-z)^{\Delta_{\mathcal{O}}-\Delta_\phi} (1-\bar{z})^{\bar{h}-\Delta_\phi} \\ = \delta_{[\phi\phi]_0}^{(\mathcal{O})} \log \bar{z} (1-z)^{\Delta_{\mathcal{O}}-\Delta_\phi} + \dots \end{aligned} \quad (2.179)$$

If  $\mathcal{O} = \phi$  is in the  $\phi \times \phi$  OPE, we should consider the sum over  $\delta_{[\phi\phi]_0}(\bar{h}) a_{[\phi\phi]_0}(J)$ ,

$$\begin{aligned} \sum_{[\phi\phi]_0} (1+(-1)^J) \frac{d\bar{h}}{dJ} \delta_{[\phi\phi]_0}^{(\phi)} \frac{1}{\bar{h}^{\Delta_\phi}} S_{-\Delta_\phi,\Delta_\phi}(\bar{h}) \log(1-z) (1-\bar{z})^{\bar{h}-\Delta_\phi} \\ = \sum_{[\phi\phi]_0} (1+(-1)^J) \frac{d\bar{h}}{dJ} \frac{-\delta_{[\phi\phi]_0}^{(\phi)}}{\Gamma(\Delta_\phi)} S_{0,\Delta_\phi}^{(1)}(\bar{h}) \log(1-z) (1-\bar{z})^{\bar{h}-\Delta_\phi} + \dots \\ = -\frac{\delta_{[\phi\phi]_0}^{(\phi)}}{\Gamma(\Delta_\phi)} \log \bar{z} \log(1-z) + \dots \end{aligned} \quad (2.180)$$

Note that we have we have used the asymptotic expansion

$$\frac{1}{\bar{h}^a} S_{-a,\Delta}(\bar{h}) = -\frac{1}{\Gamma(a)} S_{0,\Delta}^{(1)}(\bar{h}) + \dots \quad (2.181)$$

Doing the  $z$  integral and summing over  $\mathcal{O}$ , we obtain the contribution to  $\tilde{g}_0(\bar{z}, \bar{h})$

$$\sum_{\substack{\mathcal{O} \in \phi \times \phi \\ \mathcal{O} \neq \phi}} \delta_{[\phi\phi]_0}^{(\mathcal{O})} \log \bar{z} S_{\Delta_{\mathcal{O}}-\Delta_\phi,\Delta_\phi}(\bar{h}) - \frac{\delta_{[\phi\phi]_0}^{(\phi)}}{\Gamma(\Delta_\phi)} \log \bar{z} S_{0,\Delta_\phi}^{(1)}(\bar{h}). \quad (2.182)$$

Now, let's combine this with the contribution of the unit operator to  $\tilde{g}_0(\bar{z}, \bar{h})$ ,

$$\begin{aligned} \tilde{g}_0(\bar{z}, \bar{h}) &= S_{-\Delta_\phi, \Delta_\phi}(\bar{h}) + \log \bar{z} \left( \sum_{\substack{\mathcal{O} \in \phi \times \phi \\ \mathcal{O} \neq \phi}} \delta_{[\phi\phi]_0}^{(\mathcal{O})} S_{\Delta_{\mathcal{O}-\Delta_\phi, \Delta_\phi}}(\bar{h}) - \frac{\delta_{[\phi\phi]_0}^{(\phi)}}{\Gamma(\Delta_\phi)} S_{0, \Delta_\phi}^{(1)}(\bar{h}) \right) + \dots \\ &= S_{-\Delta_\phi, \Delta_\phi}(\bar{h}) \left( 1 + \log \bar{z} \sum_{\mathcal{O} \in \phi \times \phi} \delta_{[\phi\phi]_0}^{(\mathcal{O})} \frac{1}{\bar{h}^{\Delta_\phi}} + \dots \right) + \dots \end{aligned} \quad (2.183)$$

In the last step, we reverted the asymptotic expansion in (2.181) to separate the contribution to the pole location from the residue. This looks like the first few terms in the expansion of  $S_{-\Delta_\phi, \Delta_\phi}(\bar{h}) \bar{z}^{\delta_{[\phi\phi]_0}(\bar{h})}$  in small  $\delta_{[\phi\phi]_0}(\bar{h}) \log \bar{z}$  and in large  $\bar{h}$ . The higher powers of  $\log \bar{z}$  come from the exponentiation of the anomalous dimension, which arise from sums over multi-twist families, such as in the diagram depicted in figure 2.10. Essentially, any contribution to the anomalous dimension can be recovered by embedding the corresponding four-point function large-spin diagram and performing the thermal crossing operation. Thus, we see the beginnings of a self-consistent story of how the anomalous dimensions are incorporated into the large-spin perturbation theory of the thermal data. We can do the exact analysis with other asymptotics of  $a_{[\phi\phi]_0}(J)$ , by reversing the diagram in figure 2.9 and thinking of the sum over  $[\mathcal{O}\mathcal{O}']$ . Repeating our analysis above line by line, we'll start to recover the  $\mathcal{O}$  corrections to the anomalous dimensions for the poles proportional to  $a_{\mathcal{O}'}$ .

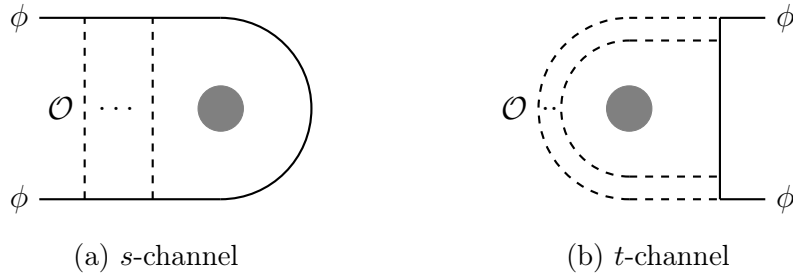


Figure 2.10: Higher order terms  $\delta_{[\phi\phi]}^m \log^m \bar{z}$  that sum up to shift the  $[\phi\phi]$  poles in  $a(\Delta, J)$  are produced by sums over multi-twist families in the  $t$ -channel.

We can also see how the anomalous dimensions of families other than  $[\phi\phi]_0$  arise as well. Let's consider a double-twist family  $[\mathcal{O}\mathcal{O}']$  for some  $\mathcal{O} \in \phi \times \phi$  with  $\mathcal{O} \neq \phi$ , and think about how their anomalous dimensions appear to correct their pole locations in  $a(\Delta, J)$ . Applying our thinking above, we can first find which families  $\delta_{[\mathcal{O}\mathcal{O}]}$  contribute to, and then reverse the process. This leads us to the process illustrated in figure 2.11. Let's see if the diagram indeed checks out. For simplicity, let's consider the  $[\mathcal{O}\mathcal{O}]_0$

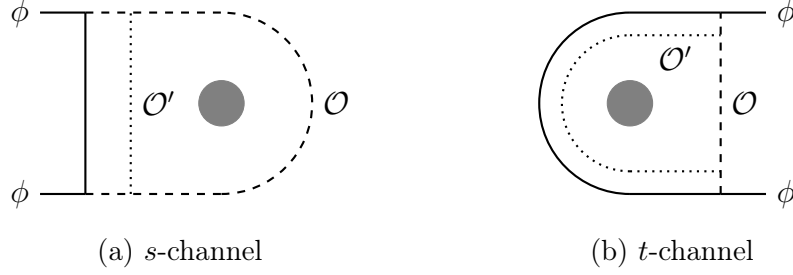


Figure 2.11: Poles in  $a(\Delta, J)$  for other double-twist families  $[\mathcal{O}\mathcal{O}]$  in  $\langle\phi\phi\rangle$  shift by anomalous dimensions through sums over multi-twist families  $[\phi\phi\mathcal{O}'\mathcal{O}']$  in the  $t$ -channel.

family, and suppose  $\mathcal{O}' \in \mathcal{O} \times \mathcal{O}$ , so

$$\delta_{[\mathcal{O}\mathcal{O}]_0}(\bar{h}) \supset \delta_{[\mathcal{O}\mathcal{O}]_0}^{(\mathcal{O}')} \frac{1}{\bar{h}^{2h_{\mathcal{O}'}}}. \quad (2.184)$$

Using the leading expression for  $a_{[\mathcal{O}\mathcal{O}]_0}$  computed in (2.172), we see that the  $t$ -channel sum over  $[\mathcal{O}\mathcal{O}]_0$  to first order in  $\delta_{[\mathcal{O}\mathcal{O}]_0}$  produces the singular term

$$\begin{aligned} \sum_{[\mathcal{O}\mathcal{O}]_0} (1 + (-1)^J) a_{[\mathcal{O}\mathcal{O}]_0}(J) \delta_{[\mathcal{O}\mathcal{O}]_0}(\bar{h}) (1-z)^{\Delta_{\mathcal{O}}-\Delta_{\phi}} \log(1-z) (1-\bar{z})^{\bar{h}-\Delta_{\phi}} \\ \supset -\Gamma(-2h_{\mathcal{O}'}) \delta_{[\phi\phi]_0}^{(\mathcal{O})} \delta_{[\mathcal{O}\mathcal{O}]_0}^{(\mathcal{O}')} \bar{z}^{2h_{\mathcal{O}'}} (1-z)^{\Delta_{\mathcal{O}}-\Delta_{\phi}} \log(1-z), \end{aligned} \quad (2.185)$$

where we have used the asymptotic expansion<sup>38</sup>

$$\frac{1}{\bar{h}^a} S_{0,\Delta}^{(1)}(\bar{h}) = -\Gamma(-a) S_{a,\Delta}(\bar{h}) + \dots, \quad (2.186)$$

which can be obtained from the asymptotic expansion in (2.181). Such a term inverts to poles for the multi-twist families  $[\phi\phi\mathcal{O}'\mathcal{O}']_n$ , as we expected from the diagram. The lowest-twist family has the leading residue

$$a_{[\phi\phi\mathcal{O}'\mathcal{O}']_0}(J) \supset (1 + (-1)^J) 4\pi K_J \frac{d\bar{h}}{dJ} \delta_{[\phi\phi]_0}^{(\mathcal{O})} (-\Gamma(-2h_{\mathcal{O}'})) \delta_{[\mathcal{O}\mathcal{O}]_0}^{(\mathcal{O}')} S_{\Delta_{\mathcal{O}}-\Delta_{\phi},\Delta_{\phi}}^{(1)}(\bar{h}). \quad (2.187)$$

Now, let's reverse the diagram, which tells us to sum over  $[\phi\phi\mathcal{O}'\mathcal{O}']_0$  in the  $t$ -channel to constant order in their anomalous dimensions. Performing this sum yields the singular terms

$$-\Gamma(-2h_{\mathcal{O}'}) \delta_{[\phi\phi]_0}^{(\mathcal{O})} \delta_{[\mathcal{O}\mathcal{O}]_0}^{(\mathcal{O}')} \bar{z}^{\Delta_{\mathcal{O}}-\Delta_{\phi}} \log \bar{z} (1-z)^{2h_{\mathcal{O}'}} + \dots \quad (2.188)$$

<sup>38</sup>For positive integer values of  $a$ , this asymptotic expansion is slightly modified, and one needs to be more careful with the analysis that follows.



which contribute the expected first-order shift to the  $[\mathcal{OO}]_0$  poles, since

$$\begin{aligned} \tilde{g}_0(\bar{z}, \bar{h}) &\supset \delta_{[\phi\phi]_0}^{(\mathcal{O})} \bar{z}^{\Delta_{\mathcal{O}} - \Delta_{\phi}} \left( S_{0, \Delta_{\phi}}^{(1)}(\bar{h}) - \log \bar{z} \sum_{\mathcal{O}' \in \mathcal{O} \times \mathcal{O}} \Gamma(-2h_{\mathcal{O}'}) \delta_{[\mathcal{OO}]_0}^{(\mathcal{O}')} S_{2h_{\mathcal{O}'}, \Delta_{\phi}}(\bar{h}) + \dots \right) \\ &= \delta_{[\phi\phi]_0}^{(\mathcal{O})} \bar{z}^{\Delta_{\mathcal{O}} - \Delta_{\phi}} S_{0, \Delta_{\phi}}^{(1)}(\bar{h}) \left( 1 + \log \bar{z} \sum_{\mathcal{O}' \in \mathcal{O} \times \mathcal{O}} \delta_{[\mathcal{OO}]_0}^{(\mathcal{O}')} \frac{1}{h^{2h_{\mathcal{O}'}}} + \dots \right). \end{aligned} \quad (2.189)$$

We see that we begin recovering the correct pole locations of the  $[\mathcal{OO}]_0$  family in the inversion of the  $\langle \phi\phi \rangle_{\beta}$  correlator. Once again, the higher-order corrections come from diagrams with exponentiated anomalous dimensions analogous to figure 2.10.

### 2.6.3 Case study: $\langle [\sigma\sigma]_0 \rangle_{\beta}$ in the 3d Ising model

Our primary example for applying the above technology is the 3d Ising CFT. At this point, much is known both analytically and numerically about the spectrum and OPE data of the 3d Ising CFT. This abundance of data makes the 3d Ising CFT a natural and ideal candidate for studying thermal correlators. In [20], the low-twist spectrum of the 3d Ising CFT has been computed via the lightcone four-point function bootstrap. Especially relevant to our analysis here is the analytic computation for the anomalous dimensions and OPE coefficients of the most important double-twist family,  $[\sigma\sigma]_0$ , which has the lowest twist trajectory. Taking the spectrum and OPE data as input, we will apply the thermal bootstrap to study the thermal coefficients of the  $[\sigma\sigma]_0$  family.

The most natural way to get a handle on the  $[\sigma\sigma]_0$  family is by studying the thermal correlator  $\langle \sigma\sigma \rangle_{\beta}$ . Let's remind ourselves about the relevant low-twist spectrum of the 3d Ising CFT. The first few lowest-twist primary operators in the  $\sigma \times \sigma$  OPE are

$$\sigma \times \sigma = \mathbf{1} + \epsilon + T + \sum_{\ell=4,6,\dots} [\sigma\sigma]_{0,\ell} + \dots \quad (2.190)$$

Our strategy will be to determine the thermal coefficients of  $[\sigma\sigma]_0$  in terms of  $b_{\epsilon}$  and  $b_T$ , which we treat as unknowns. In chapter 3, we will show how information about the low-twist families can be used in conjunction with the KMS condition in the Euclidean regime to “tie the knot” on the thermal bootstrap and estimate some thermal coefficients in the theory including  $b_{\epsilon}$  and  $b_T$ .

To numerically study the thermal coefficients in the  $[\sigma\sigma]_0$  family, we use the scaling dimensions of  $\sigma$  and  $\epsilon$ , obtained from the numerical bootstrap study [56]

$$\Delta_{\sigma} = .5181489(10), \quad \Delta_{\epsilon} = 1.412625(10). \quad (2.191)$$

Using our result (2.138), together with these numerical values, we compute the leading contributions to the  $[\sigma\sigma]_0$  one-point functions,

$$a_{[\sigma\sigma]_0}(J) = \sum_{\mathcal{O}=1,\epsilon,T} a_{\mathcal{O}}(1 + (-1)^J) \frac{K_J}{K_{\ell_{\mathcal{O}}}} \frac{\partial \bar{h}}{\partial J} S_{h_{\mathcal{O}} - \Delta_{\sigma}, \Delta_{\sigma}}(\bar{h}). \quad (2.192)$$

To emphasize the utility of this result, we can write the large-spin expansion of the thermal coefficients

$$\begin{aligned} a_{[\sigma\sigma]_0}(J) = (1 + (-1)^J) & \left[ \frac{1}{J^{\frac{1}{2} - \Delta_{\sigma}}} \left( 1.0354 + 0.000171 \frac{1}{J} + \mathcal{O}\left(\frac{1}{J^2}\right) \right) \right. \\ & + \frac{a_T}{J^{1 - \Delta_{\sigma}}} \left( 0.01218 + 0.001414 \frac{1}{J} + \mathcal{O}\left(\frac{1}{J^2}\right) \right) \\ & + \frac{a_{\epsilon}}{J^{\frac{1}{2} + \frac{\Delta_{\epsilon}}{2} - \Delta_{\sigma}}} \left( -0.28971 - 0.06859 \frac{1}{J} - \mathcal{O}\left(\frac{1}{J^2}\right) \right) \\ & \left. + \dots \right], \end{aligned} \quad (2.193)$$

where terms on each line come from the unit operator, the stress tensor and the  $\epsilon$  operator respectively. The final “...” include contributions of other operators that are either suppressed in the  $1/J$  expansion or with coefficients small enough that they can be neglected for reasonable values of the spin.

To go beyond asymptotically large spin and estimate thermal coefficients for operators with small spin, we should include higher-order corrections in  $1/J$ . The next contributions come from the  $[\sigma\sigma]_0$  family themselves. Thus, we need to sum over the  $[\sigma\sigma]_0$  family next. We use the leading expressions in the large-spin expansion (2.144) of the anomalous dimensions of  $[\sigma\sigma]_0$ , which were computed in [20] as

$$\delta_{[\sigma\sigma]_0}(\bar{h}) \sim -0.001422 \frac{1}{\bar{h}} - 0.04627 \frac{1}{\bar{h}^{\Delta_{\epsilon}}} + \dots \quad (2.194)$$

Upon first iteration, when considering the corrections from  $[\sigma\sigma]_0$  to itself only once, the corrected thermal coefficient is given by (2.168),

$$\begin{aligned} a_{[\sigma\sigma]_0}(J) = \sum_{\mathcal{O}=1,\epsilon,T} a_{\mathcal{O}}(1 + (-1)^J) & \frac{K_J}{K_{\ell_{\mathcal{O}}}} \frac{d\bar{h}}{dJ} \\ & \times \left( S_{h_{\mathcal{O}} - \Delta_{\sigma}, \Delta_{\sigma}}(\bar{h}) \right. \\ & \left. + \sum_{m=0}^{\infty} \alpha_0^{\text{even}} \left[ \frac{\delta_{[\sigma\sigma]_0}^m}{m!} S_{h_{\mathcal{O}} - \Delta_{\sigma}, \Delta_{\sigma}}, \delta_{[\sigma\sigma]_0}, \Delta_{\sigma} \right] (2h_{\sigma} + 4) S_{0, \Delta_{\sigma}}^{(m)}(\bar{h}) \right). \end{aligned} \quad (2.195)$$

We can compute the fixed point of the self corrections above using appendix A.5, with (3.28) as input. It turns out that the self-corrections of operators in the  $[\sigma\sigma]_0$  family is given by convergent sums over operators in the  $[\sigma\sigma]_0$  family, so one can also evaluate the sums numerically by choosing a large spin cut-off. By recursively repeating this numerical process the results converge to the fixed point determined analytically *à la* appendix A.5.<sup>39</sup>

To be concrete, the table below shows a few examples for the values of the thermal coefficients  $a_{[\sigma\sigma]_0,\ell}$  and for the thermal one-point functions  $b_{[\sigma\sigma]_0,\ell}$ :

| $\ell$ | $a_{[\sigma\sigma]_0,\ell}$             | $b_{[\sigma\sigma]_0,\ell}/\sqrt{c_{[\sigma\sigma]_0,\ell}}$ |
|--------|---|--|
| 4      | $2.1113 - 0.2163a_\epsilon + 0.0102a_T$ | $33.431 - 3.4255a_\epsilon + 0.16182a_T$                     |
| 6      | $2.1483 - 0.1724a_\epsilon + 0.0092a_T$ | $246.29 - 19.773a_\epsilon + 1.0500a_T$                      |
| 8      | $2.1628 - 0.1428a_\epsilon + 0.0083a_T$ | $1844.1 - 121.72a_\epsilon + 7.0586a_T$                      |
| 10     | $2.1714 - 0.1223a_\epsilon + 0.0076a_T$ | $1.3982 \times 10^4 - 787.68a_\epsilon + 48.839a_T$          |

Table 2.1: The thermal coefficients and one-point functions for operators in the  $[\sigma\sigma]_0$  family,  $a_{[\sigma\sigma]_0,\ell}$  and,  $b_{[\sigma\sigma]_0,\ell}/\sqrt{c_{[\sigma\sigma]_0,\ell}}$  respectively. Both coefficients are shown in terms of the unknown thermal coefficients  $a_\epsilon$  and  $a_T$  and include self-corrections from operators in the  $[\sigma\sigma]_0$  family and are shown in the normalization in which  $f_{\sigma\sigma[\sigma\sigma]_0,\ell}$  is positive. As explained in section 2.2.1.1, the Monte Carlo results in [74–76] lead to  $b_T = -0.459$ , or  $a_T = 2.105$ . This value is consistent with the estimate obtained in appendix A.1. We determine the thermal coefficients  $a_\epsilon$  and  $a_T$  using bootstrap methods in chapter 3.

## 2.7 Conclusions and future work

Modern advances in the conformal bootstrap have focused almost entirely on constraining OPE data using CFT correlation functions in flat space. Is there potential for more? A broader perspective on the bootstrap suggests future extensions toward probing dynamical questions in CFT, which are not obviously determined by OPE data in a tractable way.

As a step toward this end, we have developed an approach to bounding CFT observables at finite temperature. Treating the thermal two-point function on  $S^1_\beta \times \mathbb{R}^{d-1}$  in analogy with the flat-space four-point function, and the KMS condition as the analog of the crossing equations, one extracts constraints on the thermal one-point functions of local operators. A key intermediate tool (of independent interest) in realizing this approach was to derive a Lorentzian inversion formula (3.7) which, given a thermal

<sup>39</sup>We find that for small values of the spin the contribution of the stress-energy tensor is the most affected by self-corrections, with a 20% correction for  $J = 4$ .

two-point function, extracts thermal one-point coefficients and operator scaling dimensions. We applied this technique to the  $d = 3$  critical  $O(N)$  model, which yielded thermal one-point functions of higher-spin currents (2.106) and some scalar operators (2.115). More generally, we developed a large-spin perturbation theory, applicable to any CFT, in which thermal one-point functions are determined via an analytic expansion in inverse operator spin  $J$ . This included the universal contributions to thermal coefficients of double-twist operators,  $a_{[\phi\phi]_0,J}$ , from the presence of the unit operator and the stress tensor in the  $\phi \times \phi$  OPE (2.5). By summing over entire families of operators and plugging back into the large spin expansion, one can solve for CFT data to increasingly high accuracy. Together with the KMS crossing condition, this suggests an iterative algorithm, discussed further below, with which to “solve” the thermal sector of an abstract CFT.

There are many future directions to explore:

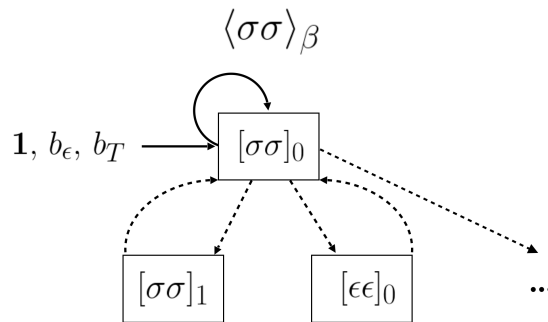
- In this work, we mostly consider a single thermal two-point function. However, the same one-point coefficients appear in the OPE decomposition of *every* two-point function in a theory (except when forbidden by symmetry). Thus, it might be very constraining to study larger systems of two-point functions simultaneously. We demonstrate the power of this observation when we consider a system of two correlators to study the 3d Ising CFT in chapter 3.
- A more straightforward generalization of our work would be to study thermal two-point functions of spinning operators. This is likely easier than studying spinning four-point functions on  $\mathbb{R}^d$ , due to the simplicity of the spinning thermal conformal blocks [71].
- Our Lorentzian inversion formula makes it straightforward to compute the perturbative expansion of thermal data to all orders in  $1/J$ , using the  $t$ -channel OPE for  $z < 2$ . However, there are also nonperturbative corrections that decay exponentially in  $J$ , coming from the region  $z > 2$  (outside the regime of validity of the  $t$ -channel OPE). How can we compute these corrections? Answering this question may require understanding the full analytic structure of thermal two-point functions better.
- It would be interesting to study more general compactifications. For example, one could study two-point functions on  $T^n \times \mathbb{R}^{d-n}$  for  $n \geq 2$ . On the other hand, there can also be multiple one-point structures on  $T^n$  for  $n \geq 2$ , so there

is more data to compute. For recent work on CFTs on spatial tori, see [105, 106].

- We derived thermal one-point functions of all single-trace operators in the critical  $O(N)$  model in  $d = 3$ . A clear target for the future is to generalize these results to other slightly broken higher-spin CFTs, such as the Chern-Simons-fundamental matter theories that are continuously connected to the  $O(N)$  model [107, 108]. The thermal mass and some current-current correlation functions at nonzero temperature have been computed in the large  $N$  limit of these theories, for arbitrary 't Hooft coupling  $\lambda$  [107, 109–111]. It would be satisfying if the thermal one-point functions  $b_{J_\ell}$  in these Chern-Simons-matter theories take the same form as in (2.106), with the appropriate thermal mass  $m_{\text{th}}(\lambda)$ . More generally, we would like to understand the constraints of slightly broken higher-spin symmetry on thermal correlations, in the spirit of [16, 65, 112, 113].
- Through the study of holographic CFTs, one can get a better intuition for the applicability of the inversion formula down to small values of the spin. Such a direction would entail studying the holographic thermal two-point function in the regimes discussed in section 2.3.5, in which  $|w| \rightarrow \infty$ . Besides offering better intuition for the applicability of the inversion formula, as discussed in section 2.5.2, the study of such a regime would also be illuminating for understanding the thermal properties of the stress-energy tensor as implied by black hole physics. It should also be possible to define geodesic Witten diagrams [114, 115] for black hole backgrounds in  $\text{AdS}_{d \geq 4}$ , which should define an effective two-point “thermal conformal block” for  $d \geq 3$  CFTs with large higher-spin gap.
- In section 2.6, it proved useful to use diagrams to organize terms in large-spin perturbation theory for thermal correlators. It would be nice to place these diagrams on firmer footing by giving a complete specification of the rules they satisfy and what terms they correspond to. This problem is already interesting in the context of large-spin perturbation theory for four-point functions [20, 116], where the diagrams have an interpretation in terms of physical processes in a special conformal frame [12].
- We have made predictions for thermal one-point functions in the 3d Ising CFT in terms of some unknowns, of which we expect  $b_T$  (computed via Monte Carlo in [74–76]) and  $b_\epsilon$  are the most important. It would be nice to compute  $b_\epsilon$ . To

our knowledge, it is not present in the literature, but should be straightforward to compute using e.g. using Monte Carlo simulation [117].<sup>40</sup> We will explore this in chapter 3.

- While in this paper we have made contact with the 3d Ising model by finding the large-spin expansion for the thermal one-point functions  $b_{[\sigma\sigma]_{0,J}}$ , one can imagine a more involved iterative strategy to solve the thermal bootstrap in the double-lightcone limit. This strategy can be summarized in the following diagram:



Following our study in section 2.6.3, we start by considering the OPE presentation of the thermal two-point function  $\langle\sigma\sigma\rangle_\beta$ , with the thermal one-point functions of a few low-twist operators as unknowns (in section 2.6.3, we consider  $b_\epsilon$  and  $b_T$  as unknowns). Then, we use the inversion formula on  $\langle\sigma\sigma\rangle_\beta$  in the double lightcone limit to determine the thermal coefficients of all remaining operators in the  $[\sigma\sigma]_0$  family as functions of the unknowns. Next, using the technology we developed in section 2.6.2, we sum over the  $[\sigma\sigma]_0$  family to determine the self-corrections to the thermal coefficients of the  $[\sigma\sigma]_0$  family, and also determine the thermal coefficients for the  $[\sigma\sigma]_1$  and  $[\epsilon\epsilon]_0$  families.

In principle, this process can be iterated further by summing over more and more families, and obtaining higher-order terms in the large-spin expansion. Also, by studying the thermal two-point functions of other operators, we get alternative handles on the thermal coefficients of families of operators. For instance, studying  $\langle\epsilon\epsilon\rangle_\beta$  yields more direct information about the  $[\epsilon\epsilon]_0$  family. Once the thermal coefficients of families of interest are determined to desired order, we have expressions for a large part of the low-twist spectrum, which still depend only on the unknown thermal one-point functions of the chosen low-twist operators ( $b_\epsilon$  and  $b_T$ ). Finally, these unknowns can be determined by

<sup>40</sup>See [32] where similar quantities were computed for the  $O(2)$  model.

moving away from the double lightcone limit and applying the KMS condition, thus determining the low-twist thermal one-point functions of the 3d Ising CFT. This procedure is the main subject of chapter 3.

- The eigenstate thermalization hypothesis (ETH) suggests that we can study thermal correlators as a limit of expectation values in a single eigenstate  $|\mathcal{O}\rangle$  with sufficiently large dimension. See [118] for a recent discussion of ETH in the context of CFTs. Assuming ETH, a thermal two-point function  $\langle\phi(x_1)\phi(x_2)\rangle_\beta$  is a limit of a family of four-point functions  $\langle\mathcal{O}(0)\phi(x_1)\phi(x_2)\mathcal{O}(\infty)\rangle$ , where we take  $\Delta_{\mathcal{O}} \rightarrow \infty$ ,  $x_{12} \rightarrow 0$  with the product  $\Delta_{\mathcal{O}}|x_{12}|$  held fixed.<sup>41</sup> It would be interesting to understand whether the ability to view thermal correlators as limits of pure correlators can bring new constraints to the thermal bootstrap. Note that certain properties of vacuum four-point functions may not survive the thermodynamic limit. For example, the analyticity structure changes, with the development of new “forbidden singularities” reflecting periodicity of the thermal circle [120].
- One big arena of physics at nonzero temperature that we have not even touched upon in this paper is transport. Quantities like the diffusivity, viscosity, electrical conductivity, and thermal conductivity are basic experimentally measurable quantities that provide a wealth of information about the low-energy excitations of a system. These transport coefficients have well-known expressions in terms of two-point functions of components of conserved currents or the stress-energy tensor [121–123]. The most interesting limit of the thermal two-point functions for transport phenomena is the low frequency limit, which translates to large separations in position space.

Apart from weak coupling expansions, transport has been exhaustively studied from a holographic perspective: For a recent review, see [124].

While the OPE of the thermal two-point function strongly constrains the short distance dynamics in the CFT, it does not directly constrain the long-distance behavior due to the absence of any OPE channel for  $|x| > \beta$ . It is easy to derive functional forms for correlators in the diffusive regime via hydrodynamics, which is the correct low-energy description [125]. Can bootstrap techniques allow us to derive this specific form of the diffusive correlator, and the value of the energy diffusion constant for the 3D Ising model? It would be very interesting to connect the OPE regime to the hydrodynamic regimes in a CFT.

---

<sup>41</sup>A similar thermodynamic limit was studied for large-charge correlators in [119].

## BOOTSTRAPPING THE 3D ISING MODEL AT FINITE TEMPERATURE

<sup>1</sup>L. Iliesiu, M. Kologlu, and D. Simmons-Duffin, “Bootstrapping the 3d Ising model at finite temperature”, (2018), [arXiv:1811.05451](https://arxiv.org/abs/1811.05451) [[hep-th](#)].

### 3.1 Introduction

In chapter 2, we initiated a study of conformal field theories at finite (i.e. nonzero) temperature in  $d > 2$  dimensions, using techniques from the conformal bootstrap. At finite temperature, the operator product expansion (OPE) can still be used to reduce  $n$ -point correlators to sums of  $n-1$ -point correlators. However, an important new ingredient at temperature  $T = 1/\beta$  is that non-unit operators can have nonzero one-point functions  $\langle \mathcal{O} \rangle_\beta$ . For example, the thermal one-point function of the stress tensor  $\langle T_{\mu\nu} \rangle_\beta$  encodes the free-energy density.

Thermal one-point functions are constrained by a type of “crossing-equation” first written down by El-Showk and Papadodimas [38]. They noted that the Kubo-Martin-Schwinger (KMS) condition for thermal two-point functions is not manifestly consistent with the OPE, and this leads to constraints on CFT data. An efficient way to study these constraints is to use the thermal Lorentzian inversion formula developed in chapter 2, which is an analog of Caron-Huot’s Lorentzian inversion formula for zero-temperature four-point functions [25, 26, 28].

In this work, we apply these ideas to estimate thermal one- and two-point functions in a strongly-coupled conformal field theory in  $d = 3$  dimensions: the 3d Ising CFT. Physically, this theory describes the 2+1-dimensional quantum transverse field Ising model at nonzero temperature, and the 3-dimensional statistical Ising model with a periodic direction of length  $\beta$  (both at criticality).<sup>1</sup> Besides its physical interest, an advantage of studying the 3d Ising CFT is that we can leverage a wealth of information about its zero-temperature OPE data from the conformal bootstrap [20, 41, 54–56]. The 3d Ising CFT is a case where Monte Carlo (MC) techniques are also very efficient for computing some finite-temperature observables [126]. However, we believe it is

---

<sup>1</sup>Note that the temperature we discuss in this work is not related to the “temperature” of the statistical Ising model that determines the spin-spin coupling. The latter quantity is set to its critical value.



worthwhile to develop bootstrap-based approaches. One might hope to eventually apply these approaches to theories that are more difficult to study with MC, like fermionic theories, or non-Lagrangian CFTs.

The thermal crossing equation of El-Showk and Papadodimas is difficult to study for two reasons. Firstly, it does not enjoy the positivity conditions that are important for rigorous numerical bootstrap techniques to work [11, 39, 40, 42, 43, 127]. Thus, we will not be able to compute rigorous bounds on thermal data and will have to content ourselves with estimates. Our rough strategy is to truncate the thermal crossing equation and approximate it by a finite set of linear equations for a finite set of variables. In spirit, this is similar to the “severe truncation” method initiated by Gliozzi [52, 128] and applied with some success in the boundary/defect bootstrap [44–51].

However, a second difficulty is that the thermal crossing equation converges more slowly than the crossing equation for flat-space four-point functions. Thus, naïve “severe truncation” is doomed to fail, and we need a more sophisticated approach. We will use the thermal Lorentzian inversion formula and large-spin perturbation theory to estimate the behavior of a few families of operators (specifically, the first few Regge trajectories) in terms of a small number of unknown parameters. This reduces the number of unknowns in the crossing equations and allows them to be solved approximately by a least-squares fit.

In section 3.2, we review the conformal bootstrap at finite temperature, following chapter 2, together with some features of the spectrum of the 3d Ising CFT [20] that play an important role in our calculation. In section 3.3, we outline our overall strategy and summarize the results. As a check, we perform an MC simulation of the 3d critical Ising model and find agreement with our determination of  $\langle\sigma\sigma\rangle_\beta$  to within statistical error, inside the regime of convergence of the OPE. Section 3.4 presents the details of our bootstrap-based calculation. The most complicated step is the estimation of thermal one-point coefficients for subleading Regge trajectories, which we perform by adapting the “twist-Hamiltonian” procedure of [20].

## 3.2 Review

### 3.2.1 The thermal bootstrap

A CFT at nonzero temperature  $T$  can equivalently be thought of as living on the space  $S^1_\beta \times \mathbb{R}^{d-1}$ , where  $\beta = 1/T$  is the length of the thermal circle. This space is conformally flat, so one can compute finite-temperature correlators using the OPE,

just as in flat space. However, an important difference compared to flat-space is that the thermal circle introduces a scale, and as a result operators can have nonzero one-point functions. Symmetries imply that the only operators with nonzero one-point functions are primary even-spin traceless symmetric tensors  $\mathcal{O}^{\mu_1 \dots \mu_J}$ . For such operators, we have

$$\langle \mathcal{O}^{\mu_1 \dots \mu_J}(x) \rangle_{S^1_\beta \times \mathbb{R}^{d-1}} = \frac{b_{\mathcal{O}}}{\beta^\Delta} (e^{\mu_1} \dots e^{\mu_J} - \text{traces}), \quad (3.1)$$

where  $\Delta$  is the dimension of  $\mathcal{O}$ ,  $e^\mu$  is a unit vector in the  $S^1$  direction, and  $b_{\mathcal{O}}$  is a dynamical constant.

Consider a two-point function of a real scalar primary  $\phi$  at finite temperature:

$$g(\tau, \mathbf{x}) = \langle \phi(\tau, \mathbf{x}) \phi(0) \rangle_{S^1_\beta \times \mathbb{R}^{d-1}}. \quad (3.2)$$

Here, we introduced coordinates  $x = (\tau, \mathbf{x})$ , where  $\tau \in [0, \beta)$  and  $\mathbf{x} \in \mathbb{R}^{d-1}$ . Assuming  $|x| = (\tau^2 + \mathbf{x}^2)^{1/2} < \beta$ , this two-point function can be evaluated using the OPE:

$$g(\tau, \mathbf{x}) = \sum_{\mathcal{O} \in \phi \times \phi} \frac{a_{\mathcal{O}}^{\langle \phi \phi \rangle}}{\beta^\Delta} C_J^{(\nu)} \left( \frac{x \cdot e}{|x|} \right) |x|^{\Delta - 2\Delta_\phi},$$

$$a_{\mathcal{O}}^{\langle \phi \phi \rangle} \equiv f_{\phi\phi\mathcal{O}} b_{\mathcal{O}} \frac{J!}{2^J (\nu)_J}. \quad (3.3)$$

Here,  $\mathcal{O}$  runs over primary operators appearing in the  $\phi \times \phi$  OPE, with OPE coefficients  $f_{\phi\phi\mathcal{O}}$ .  $\Delta$  is the scaling dimension of  $\mathcal{O}$ ,  $J$  is its spin, and  $\nu = (d-2)/2$ . We call each term in (3.3) a ‘‘thermal block.’’ The thermal one-point coefficient  $b_{\mathcal{O}}$  is defined in (3.1), and we have defined the thermal coefficients  $a_{\mathcal{O}}^{\langle \phi \phi \rangle}$  for later convenience.

For simplicity, we set  $\beta = 1$  in what follows. Let us use  $d-1$ -dimensional rotational invariance to set  $\mathbf{x} = (x, 0, \dots, 0) \in \mathbb{R}^{d-1}$  and introduce the coordinates

$$z = \tau + ix, \quad \bar{z} = \tau - ix. \quad (3.4)$$

Note that  $z, \bar{z}$  are complex conjugates in Euclidean signature.

The two-point function  $g(\tau, \mathbf{x})$  is invariant under  $\tau \rightarrow 1 - \tau$ . In the language of thermal physics, this is the KMS condition, and it is furthermore obvious from the geometry of  $S^1_\beta \times \mathbb{R}^{d-1}$ . However, the OPE expansion (3.3) is not manifestly invariant under  $\tau \rightarrow 1 - \tau$ . This leads to a nontrivial crossing equation that constrains thermal one-point functions  $b_{\mathcal{O}}$  in terms of scaling dimensions and OPE coefficients [38]. In terms of  $z$  and  $\bar{z}$ , the crossing equation/KMS condition is

$$g(z, \bar{z}) = g(1 - z, 1 - \bar{z}). \quad (3.5)$$

Here, we have also used that  $g$  is invariant under  $x \rightarrow -x$ .

The coefficients  $a_{\mathcal{O}}^{\langle\phi\phi\rangle}$  can be encoded in a function  $a^{\langle\phi\phi\rangle}(\Delta, J)$  that is meromorphic for  $\Delta$  in the right-half-plane, with residues of the form

$$a^{\langle\phi\phi\rangle}(\Delta, J) \sim -\frac{a_{\mathcal{O}}^{\langle\phi\phi\rangle}}{\Delta - \Delta_{\mathcal{O}}}. \quad (3.6)$$

In chapter 2, we showed that such a function can be obtained from a ‘‘thermal Lorentzian inversion formula’’

$$\begin{aligned} & a^{\langle\phi\phi\rangle}(\Delta, J) \\ &= (1 + (-1)^J) K_J \int_0^1 \frac{d\bar{z}}{\bar{z}} \int_1^{1/\bar{z}} \frac{dz}{z} (z\bar{z})^{\Delta_\phi - \frac{\Delta}{2} - \nu} (z - \bar{z})^{2\nu} F_J \left( \sqrt{\frac{\bar{z}}{z}} \right) \text{Disc}[g(z, \bar{z})] \\ & \quad + \theta(J_0 - J) a_{\text{arcs}}^{\langle\phi\phi\rangle}(\Delta, J). \end{aligned} \quad (3.7)$$

Here  $z, \bar{z}$  are treated as independent real variables, which means that the integral is over a Lorentzian regime  $x \rightarrow -ix_L$ . The first term contains the discontinuity

$$\text{Disc}[g(z, \bar{z})] \equiv \frac{1}{i} (g(z + i\epsilon, \bar{z}) - g(z - i\epsilon, \bar{z})), \quad (3.8)$$

and the functions  $K_J$  and  $F_J(w)$  are given by

$$K_J \equiv \frac{\Gamma(J+1)\Gamma(\nu)}{4\pi\Gamma(J+\nu)}, \quad (3.9)$$

$$F_J(w) = w^{J+d-2} {}_2F_1 \left( J+d-2, \frac{d}{2} - 1, J + \frac{d}{2}, w^2 \right). \quad (3.10)$$

The second line in (3.7) represents additional contributions that are present when  $J < J_0$ , where  $J_0$  controls the behavior of the two-point function in a Regge-like regime. We argued in chapter 2 that  $J_0 < 0$  for the 3d Ising CFT. In this work, we assume this is true and ignore these contributions.

### 3.2.1.1 Large-spin perturbation theory

The thermal inversion formula (3.7) becomes particularly powerful in conjunction with the KMS condition (3.5).

Let us call (3.3) the  $s$ -channel OPE, which in our new coordinates is an expansion around  $z = \bar{z} = 0$  and has the region of convergence

$$s\text{-channel OPE:} \quad |z|, |\bar{z}| < 1. \quad (3.11)$$

By the KMS condition, the two-point function admits another expansion around  $z = \bar{z} = 1$ , which we call the  $t$ -channel:

$$g(z, \bar{z}) = \sum_{\mathcal{O} \in \phi \times \phi} a_{\mathcal{O}}^{\langle \phi \phi \rangle} ((1-z)(1-\bar{z}))^{\frac{\Delta_{\mathcal{O}}}{2} - \Delta_{\phi}} C_{\ell_{\mathcal{O}}}^{(\nu)} \left( \frac{1}{2} \left( \sqrt{\frac{1-z}{1-\bar{z}}} + \sqrt{\frac{1-\bar{z}}{1-z}} \right) \right). \quad (3.12)$$

Its region of convergence is given by:

$$t\text{-channel OPE:} \quad |1-z|, |1-\bar{z}| < 1. \quad (3.13)$$

We can insert the  $t$ -channel OPE into the inversion formula (3.7) to find expressions for thermal coefficients in the  $s$ -channel. In this way, we uncover non-trivial relations between the thermal coefficients of different operators in the theory.

The integral in the inversion formula (3.7) is within the region of convergence of the  $t$ -channel OPE for  $1 \leq z < 2$ , but for  $z \geq 2$  it exits this region. Corrections to the residues of  $a(\Delta, J)$  coming from the region  $z \geq 2$  are exponentially suppressed in  $J$ . Thus, the  $t$ -channel OPE encodes the all-orders expansion in powers of  $1/J$  for thermal one-point coefficients.

Let us review how poles and residues of  $a(\Delta, J)$  arise from the thermal inversion formula. As an example, we study the poles and residues contributed by a single  $t$ -channel block. Individual  $t$ -channel blocks contribute poles at double-twist locations  $\Delta = 2\Delta_{\phi} + 2n + J$ , as shown in chapter 2. A similar phenomenon occurs in the flat-space lightcone bootstrap, where individual  $t$ -channel blocks again contribute to OPE data of double-twist operators. To obtain poles at other locations, one must sum infinite families of  $t$ -channel blocks before plugging them into the inversion formula. (We will see several examples below.) Nevertheless, individual  $t$ -channel blocks provide an important example that will be a building block for later calculations.

Poles in  $\Delta$  come from the region  $\bar{z} \sim 0$ . Therefore, when computing residues one can simply replace the upper bound of the  $z$  integral with  $1/\bar{z} \sim \infty$ . However, the range of the  $z$  integral must then be artificially restricted to  $z_{\max} = 2$  when plugging in the  $t$ -channel expansion, in order for the  $z$  integral to fully be within the region of OPE convergence. This restriction is essentially an approximation that discards corrections that die exponentially in  $J$ .

The residues are determined by a one-dimensional integral over  $z$ . To see this, we

first expand the function  $F_J\left(\sqrt{\bar{z}/z}\right)$  in  $\bar{z}$  in the inversion formula,

$$a^{\langle\phi\phi\rangle}(\Delta, J) = (1 + (-1)^J)K_J \int_0^1 \frac{d\bar{z}}{\bar{z}} \int_1^{1/\bar{z}} \frac{dz}{z} \sum_{r=0}^{\infty} q_r(J) z^{\Delta_\phi - \bar{h} - r} \bar{z}^{\Delta_\phi - h + r} \text{Disc}[g(z, \bar{z})], \quad (3.14)$$

where the coefficients  $q_r(J)$  are

$$q_r(J) \equiv (-1)^r \frac{(J + 2r)}{J} \frac{(J)_r (-r + \nu + 1)_r}{r!(J + \nu + 1)_r}, \quad (3.15)$$

and we have rewritten the inversion formula in terms of the quantum numbers

$$h = \frac{\Delta - J}{2}, \quad \bar{h} = \frac{\Delta + J}{2}. \quad (3.16)$$

The  $t$ -channel OPE can also be expanded in a power series in  $(1 - z)$  and  $(1 - \bar{z})$ ,

$$g(z, \bar{z}) = \sum_{\mathcal{O} \in \phi \times \phi} a_{\mathcal{O}}^{\langle\phi\phi\rangle} \sum_{s=0}^{\ell_{\mathcal{O}}} p_s(\ell_{\mathcal{O}}) (1 - z)^{h_{\mathcal{O}} - \Delta_\phi + s} (1 - \bar{z})^{\bar{h}_{\mathcal{O}} - \Delta_\phi - s}, \quad (3.17)$$

where

$$p_s(\ell) \equiv \frac{\Gamma(\ell - s + \nu)\Gamma(s + \nu)}{\Gamma(\ell - s + 1)\Gamma(s + 1)} \frac{1}{\Gamma(\nu)^2} = \frac{1}{4\pi K_\ell} \frac{(\ell + \nu)_{-s}}{(\ell + 1)_{-s}} \binom{\nu + s - 1}{s}. \quad (3.18)$$

The  $h_{\mathcal{O}}$  and  $\bar{h}_{\mathcal{O}}$  are the quantum numbers defined by (3.16) for each  $\mathcal{O}$  appearing in the OPE. Plugging in the term corresponding to an individual  $\mathcal{O}$  from the  $t$ -channel OPE into the inversion formula (3.7), we find<sup>2</sup>

$$\begin{aligned} a^{\langle\phi\phi\rangle, (\mathcal{O})}(\Delta, J) &\approx (1 + (-1)^J)K_J \int_0^1 \frac{d\bar{z}}{\bar{z}} \int_1^{z_{\max}} \frac{dz}{z} \sum_{r=0}^{\infty} q_r(J) z^{\Delta_\phi - \bar{h} - r} \bar{z}^{\Delta_\phi - h + r} \\ &\quad \times \text{Disc} \left[ a_{\mathcal{O}}^{\langle\phi\phi\rangle} \sum_{s=0}^{\ell_{\mathcal{O}}} p_s(\ell_{\mathcal{O}}) (1 - z)^{h_{\mathcal{O}} - \Delta_\phi + s} (1 - \bar{z})^{\bar{h}_{\mathcal{O}} - \Delta_\phi - s} \right] \\ &= a_{\mathcal{O}}^{\langle\phi\phi\rangle} (1 + (-1)^J)K_J \sum_{r=0}^{\infty} \sum_{s=0}^{\ell_{\mathcal{O}}} q_r(J) p_s(\ell_{\mathcal{O}}) \\ &\quad \times \frac{\Gamma(1 + \bar{h}_{\mathcal{O}} - \Delta_\phi - s)\Gamma(\Delta_\phi + r - h)}{\Gamma(\bar{h}_{\mathcal{O}} - h + 1 - s + r)} 2\pi S_{h_{\mathcal{O}} - \Delta_\phi + s, \Delta_\phi - r}(\bar{h}), \end{aligned} \quad (3.19)$$

<sup>2</sup>We assume that  $J$  is larger than  $J_0$ , so that the arcs do not contribute. As mentioned above, we expect  $J_0 < 0$  in the 3d Ising CFT, so the arcs don't contribute to the pole of any local operator.

Here, the superscripts  $a^{\langle\phi\phi\rangle,(\mathcal{O})}$  indicate that we are studying thermal coefficients for  $\langle\phi\phi\rangle$ , focusing on the contribution of the  $t$ -channel operator  $\mathcal{O}$ . To go from the first equation to the second equation above, we have performed the  $\bar{z}$  integral and defined the function  $S_{h_{\mathcal{O}}-\Delta_{\phi}+s,\Delta_{\phi}-r}(\bar{h})$  as

$$\begin{aligned} S_{c,\Delta}(\bar{h}) &= \frac{\sin(-\pi c)}{\pi} \int_1^{z_{\max}} \frac{dz}{z} z^{\Delta-\bar{h}} (z-1)^c \\ &= \frac{1}{\Gamma(-c)} \frac{\Gamma(\bar{h}-\Delta-c)}{\Gamma(\bar{h}-\Delta+1)} - \frac{1}{\Gamma(-c)\Gamma(1+c)} B_{1/z_{\max}}(\bar{h}-\Delta-c, 1+c). \end{aligned} \quad (3.20)$$

Here  $B_{1/z_{\max}}(\bar{h}-\Delta-c, 1+c)$  is the incomplete beta function, which decays as  $z_{\max}^{-\bar{h}} \sim z_{\max}^{-J}$  at large  $\bar{h}$ .

Note that in (3.19) the  $\bar{z}$ -integral has generated poles at double-twist locations  $\Delta = 2\Delta_{\phi} + 2n + J$ , coming from the factors  $\Gamma(\Delta_{\phi} + r - h)$ . Taking the residue of (3.19), we get the contribution of the operator  $\mathcal{O}$  to the  $[\phi\phi]_n$  families

$$\begin{aligned} a_{[\phi\phi]_n}^{\langle\phi\phi\rangle,(\mathcal{O})}(J) &= - \operatorname{Res}_{\Delta=2\Delta_{\phi}+2n+J} a^{\langle\phi\phi\rangle,(\mathcal{O})}(\Delta, J) \\ &= a_{\mathcal{O}}^{\langle\phi\phi\rangle} (1 + (-1)^J) 4\pi K_J \frac{d\bar{h}}{dJ} \sum_{r=0}^n \sum_{s=0}^{\ell_{\mathcal{O}}} q_r(J) p_s(\ell_{\mathcal{O}}) (-1)^{n-r} \\ &\quad \times \binom{\bar{h}_{\mathcal{O}} - \Delta_{\phi} - s}{n-r} S_{h_{\mathcal{O}}-\Delta_{\phi}+s,\Delta_{\phi}-r}(\bar{h}). \end{aligned} \quad (3.21)$$

For double-twist operators  $[\phi\phi]_n$ , we have  $\bar{h} = \Delta_{\phi} + n + J$ . The Jacobian factor  $\frac{d\bar{h}}{dJ}$  takes into account the leading correction to (3.21) when we additionally allow  $[\phi\phi]_n$  to have anomalous dimensions.

The function  $S_{h_{\mathcal{O}}-\Delta_{\phi}+s,\Delta_{\phi}-r}(\bar{h})$  can be expanded in large  $\bar{h}$  (equivalently large  $J$ ) as

$$S_{h_{\mathcal{O}}-\Delta_{\phi}+s,\Delta_{\phi}-r}(\bar{h}) = \frac{1}{\Gamma(-h_{\mathcal{O}} + \Delta_{\phi} - s)} \frac{1}{\bar{h}^{h_{\mathcal{O}}-\Delta_{\phi}+s+1}} + \mathcal{O}\left(\frac{1}{\bar{h}^{h_{\mathcal{O}}-\Delta_{\phi}+s+2}}\right). \quad (3.22)$$

Thus, we see that the contribution of the  $t$ -channel operator  $\mathcal{O}$  dies at large  $J$  at a rate controlled by the half-twist  $h_{\mathcal{O}} = \tau_{\mathcal{O}}/2$ . The unit operator has the lowest twist in any unitary theory, and thus gives the leading contribution at large  $J$ . A second important contribution comes from the stress tensor  $\mathcal{O} = T_{\mu\nu}$ , which gives a universal contribution proportional to the free energy density. In general, by including successively higher-twist contributions in the  $t$ -channel, we can build up a perturbative expansion for thermal coefficients in  $1/J$ . We will review this large-spin perturbation theory of the thermal coefficients and detail how we use it for the 3d Ising CFT in section 3.4.

| $\mathcal{O}$          | family               | $\mathbb{Z}_2$ | $\ell$ | $\Delta$               | $\tau = \Delta - \ell$ | $f_{\sigma\sigma\mathcal{O}}$   | $f_{\epsilon\epsilon\mathcal{O}}$ |
|------------------------|----------------------|----------------|--------|------------------------|------------------------|---------------------------------|-----------------------------------|
| $\epsilon$             | ?                    | +              | 0      | 1.412625( <b>10</b> )  | 1.412625( <b>10</b> )  | 1.0518537( <b>41</b> )          | 1.532435( <b>19</b> )             |
| $\epsilon'$            | $[\sigma\sigma]_1$   | +              | 0      | 3.82968(23)            | 3.82968(23)            | 0.053012(55)                    | 1.5360(16)                        |
| $T_{\mu\nu}$           | $[\sigma\sigma]_0$   | +              | 2      | 3                      | 1                      | 0.32613776(45)                  | 0.8891471(40)                     |
| $T'_{\mu\nu}$          | $[\sigma\sigma]_1$   | +              | 2      | 5.50915(44)            | 3.50915(44)            | 0.0105745(42)                   | 0.69023(49)                       |
| $C_{\mu\nu\rho\sigma}$ | $[\sigma\sigma]_0$   | +              | 4      | 5.022665(28)           | 1.022665(28)           | 0.069076(43)                    | 0.24792(20)                       |
| $\mathcal{O}$          | family               | $\mathbb{Z}_2$ | $\ell$ | $\Delta$               | $\tau = \Delta - \ell$ | $f_{\sigma\epsilon\mathcal{O}}$ | -                                 |
| $\sigma$               | ?                    | -              | 0      | 0.5181489( <b>10</b> ) | 0.5181489( <b>10</b> ) | 1.0518537( <b>41</b> )          |                                   |
| $\sigma'$              | ?                    | -              | 0      | 5.2906(11)             | 5.2906(11)             | 0.057235(20)                    |                                   |
|                        | $[\sigma\epsilon]_0$ | -              | 2      | 4.180305(18)           | 2.180305(18)           | 0.38915941(81)                  |                                   |

Table 3.1: A few low-dimension operators in the 3d Ising CFT, from [20]. The “?” are associated to scalars whose affiliation with a certain operator family is not fully established. Errors in bold are rigorous. All other errors are non-rigorous.

### 3.2.2 The 3d Ising CFT

In this work, we apply the thermal crossing equation and inversion formula to compute thermal one-point coefficients in the 3d Ising CFT. It will be crucial to incorporate as much information as possible about the known flat-space data (i.e. operator dimensions and OPE coefficients) of the theory. Indeed, our approach will be closely tailored to observed features of this data. We leave the question of how our approach can be generalized to arbitrary CFTs for future work. In this section, we review some features of the spectrum of the 3d Ising CFT that play an important role in what follows.

The low-dimension spectrum of the 3d Ising CFT is summarized in table 3.1. The lowest-dimension operator is a  $\mathbb{Z}_2$ -odd scalar  $\sigma$  with dimension  $\Delta_\sigma \approx 0.518$ . The lowest-dimension  $\mathbb{Z}_2$ -even scalar  $\epsilon$  has dimension  $\Delta_\epsilon \approx 1.412$ .

Some of the operators in table 3.1 are (conjecturally) identifiable as members of large-spin families — i.e. families of operators whose twists  $\tau = \Delta - \ell$  accumulate at large spin. This identification works as follows. At asymptotically large spin, it is known that there exist “multi-twist” operators  $[\mathcal{O}_1 \cdots \mathcal{O}_k]_{n,\ell}$  whose twists approach  $\tau_1 + \cdots + \tau_k + 2n$  as  $\ell \rightarrow \infty$ , where  $\tau_i = \Delta_{\mathcal{O}_i} - \ell_{\mathcal{O}_i}$  [20]. By analyticity in spin, all operators  $\mathcal{O}$  with spin above the Regge intercept  $\ell > \ell_0$  are expected to lie on curves  $\tau_i(\ell)$  that are analytic in  $\ell$  [25, 26]. Here,  $i$  labels the Regge trajectory of the operator. If the trajectory associated to  $\mathcal{O}$  approaches a multi-twist value  $\tau_1 + \cdots + \tau_k + 2n$  as  $\ell \rightarrow \infty$ , we say that  $\mathcal{O}$  is in the family  $[\mathcal{O}_1 \cdots \mathcal{O}_k]_n$ . In practice, to identify a particular family in numerics, one computes Regge trajectories using the lightcone bootstrap [13–17, 20, 23] or Lorentzian inversion formula [25, 26, 28] and observes

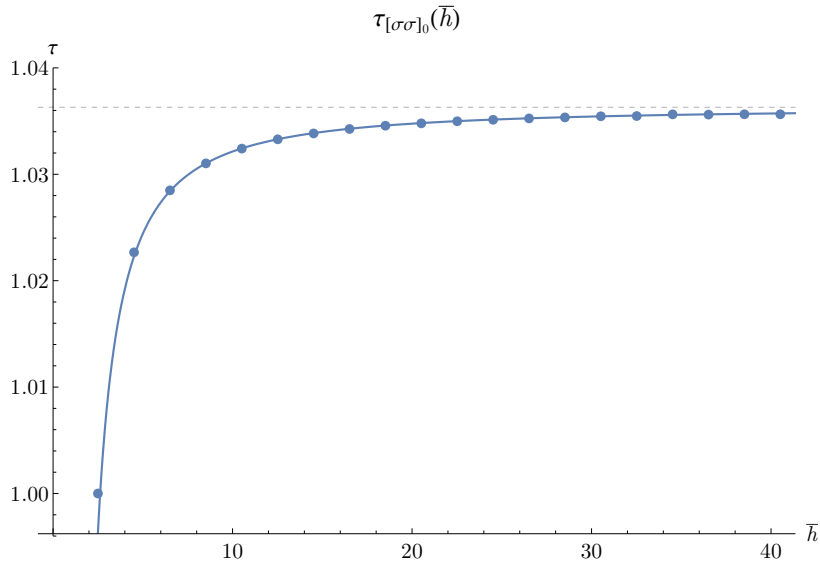


Figure 3.1: Twists of the double-twist family  $[\sigma\sigma]_0$ . Here, we plot  $\tau = \Delta - \ell$  versus  $\bar{h} = \frac{\Delta + \ell}{2}$ . The dots show estimates from [20] using the extremal functional method [41, 130, 131] and the numerical bootstrap. The curve shows the prediction of large-spin perturbation theory with only  $\Delta_\sigma, \Delta_\epsilon, f_{\sigma\sigma\epsilon}, c_T$  taken from the numerical bootstrap. Figure reproduced from [20].

which operators they pass through.<sup>3,4</sup>

Numerical bootstrap methods reveal large OPE coefficients in the  $\sigma \times \sigma$  and  $\epsilon \times \epsilon$  OPEs for operators in the families  $[\sigma\sigma]_0$ ,  $[\epsilon\epsilon]_0$ , and  $[\sigma\sigma]_1$ . Certain other trajectories with comparable twist are not described to high precision by numerics, including for example  $[\sigma\sigma\sigma]_0$ . Instead, numerics indicate that these other families have relatively small OPE coefficients in the  $\sigma \times \sigma$  and  $\epsilon \times \epsilon$  OPEs. In this work, we make the approximation that we can ignore large-spin families other than  $[\sigma\sigma]_0$ ,  $[\epsilon\epsilon]_0$ , and  $[\sigma\sigma]_1$ . It is difficult to quantify the error associated with this approximation, since other families could potentially possess large thermal one-point coefficients that do not play a role in flat-space correlators, but do contribute to thermal correlators. Nevertheless, we will find a mostly-consistent picture. However, we also see some indications that other families (in particular  $[\sigma\sigma\epsilon]_0$ ) could be important for more

<sup>3</sup>Operator mixing can make this procedure difficult in practice. Due to eigenvalue repulsion it may be difficult to track a trajectory out to infinite spin if it passes near other trajectories. It is also not known rigorously whether trajectories remain discrete in twist space when  $\ell$  is not an integer. See [20] for further discussion. None of these subtleties are visible in the first few orders of large-spin perturbation theory.

<sup>4</sup>The operators marked with “?” in table 3.1 are scalars. Whether scalar operators lie on Regge trajectories depends on the behavior of four-point functions in the Regge regime. It has been conjectured that scalars do lie on Regge trajectories in the 3d Ising CFT [129].



precise calculations (see section 3.4.4).

Let us discuss the families  $[\sigma\sigma]_0$ ,  $[\epsilon\epsilon]_0$ , and  $[\sigma\sigma]_1$  in more detail. The lowest-twist family  $[\sigma\sigma]_0$  has twists ranging from 1 at  $\ell = 2$  to  $2\Delta_\sigma = 1.036$  as  $\ell \rightarrow \infty$ . They are increasing and concave-down as a function of  $\ell$ , by Nachtmann's theorem [14, 98, 132]. The lowest-spin operator in the  $[\sigma\sigma]_0$  family is the spin-2 stress-tensor  $T_{\mu\nu}$ . The next operator  $C_{\mu\nu\rho\sigma}$  has spin-4 and controls the breaking of cubic symmetry when the Ising model is implemented on a cubic lattice [133]. The family  $[\sigma\sigma]_0$  is plotted up to spin 40 in figure 3.1. There we show both the numerical bootstrap predictions (dots) and the results of large-spin perturbation theory (curve), which agree to high precision [17, 20]. The curve  $\tau_{[\sigma\sigma]_0}(\bar{h})$  is well-approximated by  $2(2h_\sigma + \delta_{[\sigma\sigma]_0}(\bar{h}))$  where  $h_\sigma = \Delta_\sigma/2$  and

$$\begin{aligned} \delta_{[\sigma\sigma]_0}(\bar{h}) &= \frac{\sum_{\mathcal{O}=\epsilon,T} -f_{\sigma\sigma\mathcal{O}}^2 \frac{\Gamma(2\bar{h}_{\mathcal{O}})}{\Gamma(\bar{h}_{\mathcal{O}})^2} Q_{h_{\mathcal{O}}-\Delta_\sigma}(\bar{h})}{Q_{-\Delta_\sigma}(\bar{h}) - \sum_{\mathcal{O}=\epsilon,T} 2f_{\sigma\sigma\mathcal{O}}^2 (\psi^{(0)}(\bar{h}_{\mathcal{O}}) + \gamma) \frac{\Gamma(2\bar{h}_{\mathcal{O}})}{\Gamma(\bar{h}_{\mathcal{O}})^2} Q_{h_{\mathcal{O}}-\Delta_\sigma}(\bar{h})} \\ &= \frac{-0.000971264 \frac{\Gamma(\bar{h}-0.981851)}{\Gamma(\bar{h}+0.981851)} - 0.031588 \frac{\Gamma(\bar{h}-1.18816)}{\Gamma(\bar{h}+1.18816)}}{0.68256 \frac{\Gamma(\bar{h}-0.481851)}{\Gamma(\bar{h}+0.481851)} - 0.00248716 \frac{\Gamma(\bar{h}-0.981851)}{\Gamma(\bar{h}+0.981851)} + 0.0394879 \frac{\Gamma(\bar{h}-1.18816)}{\Gamma(\bar{h}+1.18816)}}, \end{aligned} \quad (3.23)$$

with  $Q_a(\bar{h}) = \frac{1}{\Gamma(-a)^2} \frac{\Gamma(\bar{h}-a-1)}{\Gamma(\bar{h}+a+1)}$ . The OPE coefficients of  $[\sigma\sigma]_0$  in the  $\sigma \times \sigma$  and  $\epsilon \times \epsilon$  OPEs can also be approximated in large-spin perturbation theory and are given in [20].

The families  $[\epsilon\epsilon]_0$  and  $[\sigma\sigma]_1$  are notable in that they experience large mixing with each other at small spins. For example, the operators  $[\sigma\sigma]_1$  have larger OPE coefficients than  $[\epsilon\epsilon]_0$  in the  $\epsilon \times \epsilon$  OPE for spins  $\ell \lesssim 25$ . This mixing can be described by supplementing large-spin perturbation theory with a procedure described in [20]. The resulting twists and OPE coefficients match well with estimates using the extremal functional method which is used in the numerical bootstrap to extract the spectrum of theories on the boundary of the allowed region [41]. We show the twists of the  $[\sigma\sigma]_1$  and  $[\epsilon\epsilon]_0$  families in figure 3.2.

### 3.3 Method and results

#### 3.3.1 Summary of method

The thermal bootstrap for the 3d Ising CFT consists of two parts. In the first part, we compute the thermal coefficients of a truncated (but infinite) subset of the spectrum in terms of the thermal coefficients of a few operators —  $\mathbf{1}$ ,  $\epsilon$ , and  $T$ , where  $a_\epsilon^{(\sigma\sigma)}$  and  $a_T^{(\sigma\sigma)}$

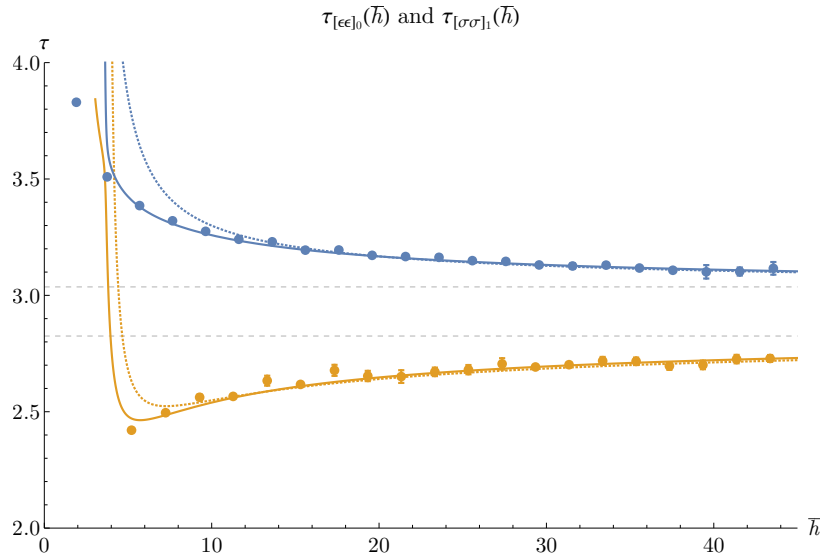


Figure 3.2: Twists of the double-twist families  $[\epsilon\epsilon]_0$  (orange) and  $[\sigma\sigma]_1$  (blue). Again, we plot  $\tau = \Delta - \ell$  versus  $\bar{h} = \frac{\Delta + \ell}{2}$ . The dots show estimates using the extremal functional method and the numerical bootstrap. The curves are estimates using large-spin perturbation theory and the mixing procedure described in [20] and reviewed in section 3.4.4. The dashed curves illustrate the effects of modifying the mixing procedure. Figure reproduced from [20].

are unknowns. Specifically, we use the thermal inversion formula to approximately determine the thermal coefficients of all operators in the  $[\sigma\sigma]_0$ ,  $[\sigma\sigma]_1$ , and  $[\epsilon\epsilon]_0$  families described in section 3.2.2. In the second part, we approximate  $\langle\sigma\sigma\rangle$  as a sum over the truncated spectrum with the thermal coefficients obtained in the first part. We determine the remaining unknowns by demanding that the KMS condition is satisfied in a region of the  $(z, \bar{z})$ -plane that is within the radius of converge of the s-channel OPE. The procedure is summarized graphically in figure 3.3. The initial steps are as follows:

1. Consider the thermal inversion formula for the  $\langle\sigma\sigma\rangle$  correlator.
2. Invert the low-twist operators  $\mathbf{1}$ ,  $\epsilon$ , and  $T$  in the  $t$ -channel OPE to compute  $a_{[\sigma\sigma]_0}^{\langle\sigma\sigma\rangle}(J)$  in terms of the unknowns  $a_{\epsilon, T}^{\langle\sigma\sigma\rangle}$ .
3. Sum over the  $[\sigma\sigma]_0$  family in the  $t$ -channel using the computed data. Invert the result to obtain self-corrections of the  $[\sigma\sigma]_0$  family.
4. Compute poles for higher-twist families up to twist 2 in the  $\langle\sigma\sigma\rangle$  and  $\langle\epsilon\epsilon\rangle$  correlators by summing the self-corrected thermal coefficients of the  $[\sigma\sigma]_0$  family

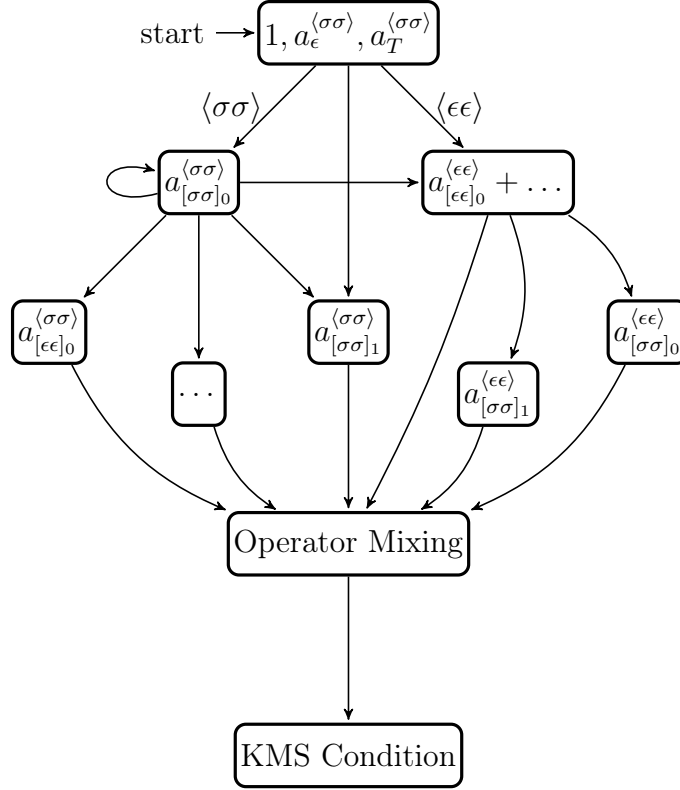


Figure 3.3: Diagram of the algorithm which is used to obtain the thermal coefficients in the 3d Ising CFT. Here, “...” represents contributions to the thermal coefficients of families other than  $[\sigma\sigma]_0$ ,  $[\sigma\sigma]_1$ , and  $[\epsilon\epsilon]_0$  that we account for when considering operator mixing.

together with  $\mathbf{1}$ ,  $\epsilon$ , and  $T$ .

5. Estimate the thermal coefficients of the  $[\sigma\sigma]_1$  and  $[\epsilon\epsilon]_0$  families at intermediate spin by “mixing” the residues according to the large anomalous dimensions.
6. Assuming the smoothness of the thermal coefficients in the  $[\sigma\sigma]_1$  family with  $\bar{h}$  up to  $J = 0$ , we interpolate the thermal coefficients of the  $[\sigma\sigma]_1$  family to estimate the thermal coefficients of  $\epsilon'$  and  $T'$ .
7. After these steps, we are almost ready to determine the unknowns. As a penultimate simplification, we use the fact that  $T$  is the spin-two member of the  $[\sigma\sigma]_0$  family. This requires that  $a_T^{(\sigma\sigma)}$  is equal to  $a_{[\sigma\sigma]_0}^{(\sigma\sigma)}$  ( $J = 2$ ), which we use to solve for  $a_T^{(\sigma\sigma)}$ . Thus, we are left with a single unknown,  $a_\epsilon^{(\sigma\sigma)}$ .

Finally, we approximate the  $\langle \sigma\sigma \rangle$  correlator by the truncated OPE including the scalars  $\mathbf{1}$  and  $\epsilon$ , and the low-twist families  $[\sigma\sigma]_0$ ,  $[\sigma\sigma]_1$ , and  $[\epsilon\epsilon]_0$ . We solve for the

final remaining unknown  $a_\epsilon^{\langle\sigma\sigma\rangle}$  by imposing that the KMS condition is close to being satisfied for a sampling of  $z$  and  $\bar{z}$  points in the interior of the square  $0 \leq z, \bar{z} \leq 1$ .

### 3.3.2 Results

In this section, before diving into the details of our computation, we summarize our results and compare to MC. To perform our computation, we must make some arbitrary choices and approximations. We enumerate them in section 3.3.2.3 and estimate the resulting errors. Overall, the results show robustness for a wide range of choices.

#### 3.3.2.1 One-point functions

After using the thermal inversion formula together with the KMS condition, we find that

$$a_\epsilon^{\langle\sigma\sigma\rangle} = 0.672(74), \quad a_T^{\langle\sigma\sigma\rangle} = 1.96(2), \quad b_\epsilon = 0.63(7), \quad b_T = -0.43(1). \quad (3.24)$$

The values and errors quoted capture the deviations seen over several runs of our algorithm with different parameter choices. For comparison the results obtained from MC are

$$b_\epsilon^{\text{MC}} = 0.667(3) [117], \quad b_T^{\text{MC}} = -0.459(3) [74, 134, 135]. \quad (3.25)$$

Note that the errors for the above two observables in MC are much smaller than for the bootstrap. This is due in part to the difficulty of using the thermal crossing equation, and also to the favorable behavior of finite-size effects when computing thermal correlators with MC, see appendix B.1. Improving the precision of thermal bootstrap results is clearly an important challenge for the future.

Our determinations for thermal coefficients in the three low-twist families,  $[\sigma\sigma]_0$ ,  $[\sigma\sigma]_1$  and  $[\epsilon\epsilon]_0$  are presented in figure 3.4.<sup>5</sup> Unfortunately, to our knowledge, there are no available MC results for the thermal one-point functions of such higher-spin operators. However, we can use the MC results for  $\epsilon$  and  $T$  in (3.25) together with the thermal inversion formula to compare to the results obtained in our computation. Note that due to the strong contribution of the unit operator in the inversion formula, the standard deviations in the thermal coefficient of all higher-spin operators in all three families are much smaller than that for  $a_\epsilon^{\langle\sigma\sigma\rangle}$  and  $a_T^{\langle\sigma\sigma\rangle}$ .

---

<sup>5</sup>We choose to present the thermal coefficients  $a_{\mathcal{O}}^{\langle\sigma\sigma\rangle}$  instead of the thermal one-point function due to the exponential increase of  $b_{\mathcal{O}}$  with the spin  $J$  (see definition (3.3)).

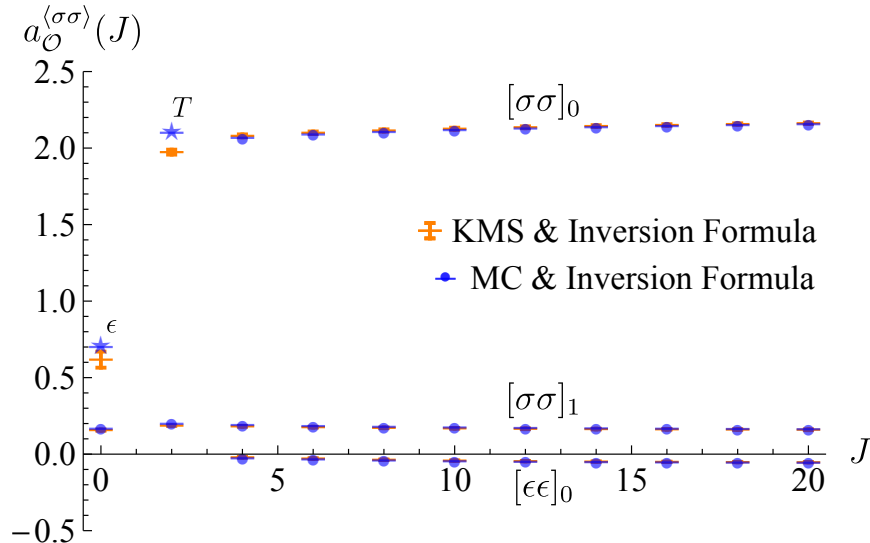


Figure 3.4: Thermal coefficients for the three families  $[\sigma\sigma]_0$ ,  $[\sigma\sigma]_1$ , and  $[\epsilon\epsilon]_0$ . The orange horizontal lines are obtained by using the KMS condition in combination with the thermal inversion formula and by averaging over several parameter choices. The spread given by the orange error bars is obtained by computing the operator mixing using different sets of  $\bar{z}$  values as explained in Section 3.4.4 and by imposing the KMS conditions in different regions on the thermal cylinder (see figure 3.13 for an example). The blue stars are MC estimates for  $a_\epsilon^{(\sigma\sigma), \text{MC}} = 0.711(3)$  [117] and  $a_T^{(\sigma\sigma), \text{MC}} = 2.092(13)$  [74, 134, 135]. The blue lines are the estimates for the thermal coefficients of all other operators in  $[\sigma\sigma]_0$ ,  $[\sigma\sigma]_1$  and  $[\epsilon\epsilon]_0$  families using these MC results together with the inversion formula. Note that the spread of the thermal coefficients of higher-spin operators estimated by the bootstrap are too small to be visible on this scale.

### 3.3.2.2 Two-point function of $\sigma$

In figure 3.5, we show the thermal two-point function  $\langle\sigma\sigma\rangle_\beta$  computed using our algorithm and compare it to a MC simulation that we performed. The details of our simulation are described in appendix B.1.

Overall, we find good agreement between the bootstrap prediction and MC inside the regime of convergence of the OPE. In part, this is due to the fact that the unit operator gives a large contribution in this region, and its contribution is known very precisely from the four-point function bootstrap. However, the thermal OPE also correctly recovers other features of the two-point function. For example, large-spin families sum up to correctly reproduce the  $t$ -channel singularity as  $\tau \rightarrow \pm 1$ .

We also observe decay of the two-point function in the spatial direction  $x$ . Exponential decay of thermal two-point functions in  $x$  can be established rigorously by expanding

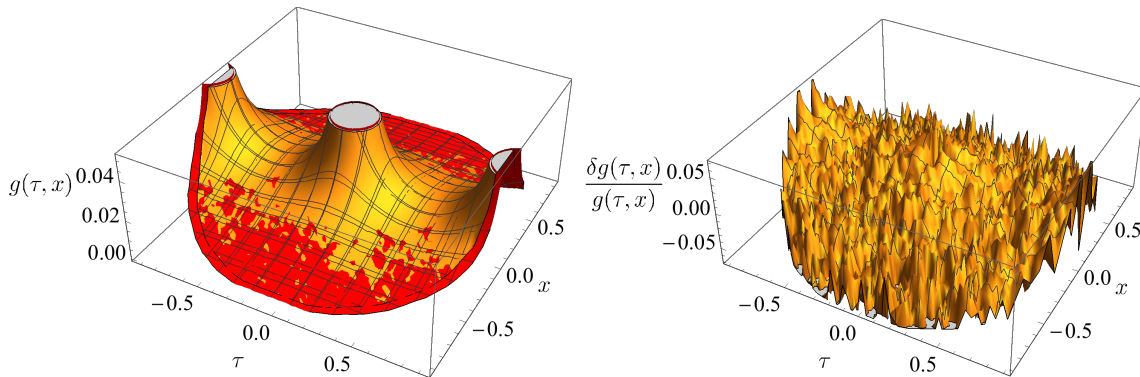


Figure 3.5: *Left*: The thermal two-point function obtained by applying the inversion formula and then solving the KMS condition (yellow) compared to that obtained from a MC simulation (red). Note that we restrict the plot to the region of OPE convergence around  $x = 0$  and  $\tau = 0$ . *Right*: Percentage difference between the two correlators, showing good agreement (within 5%) between the bootstrap and MC predictions. At small values of  $\sqrt{|x|^2 + \tau^2}$  we expect the MC results to be inaccurate due to lattice-size effects. As  $\sqrt{|x|^2 + \tau^2} \rightarrow \beta$ , we exit the region of OPE convergence, and we expect inaccuracies in the bootstrap calculation.

the correlator in states on  $\mathbb{R} \times S^1$ , as explained in [136, 137]. However, decay in  $x$  is not obvious from the OPE, where each term grows in magnitude in the  $x$  direction. The fact that we observe decay in  $x$  serves as a check on our calculation. At long distances, the correlator behaves as  $e^{-m_{\text{th}}x}$ , where  $m_{\text{th}}$  is the thermal mass. It would be interesting to understand how to determine or bound  $m_{\text{th}}$  using information in the OPE region.<sup>6</sup>

Finally, in figure 3.6 we test how close we are to satisfying the KMS condition within the region of OPE convergence. As emphasized in the figure, within an  $0.9\beta$  radius from the center of the OPE convergence the deviation from satisfying KMS is  $< 2\%$ .

### 3.3.2.3 Systematic errors

Our algorithm above involves a few choices of parameters. To check for robustness under different choices, we show the spread of results for the thermal coefficients in figure 3.4. Specifically, variations in our results are mainly due to the following choices:

- As we explain in section 3.4.4, the mixing of families requires a set of  $\bar{z}$  points. Figure 3.4 shows the results obtained when choosing different sets of  $\bar{z}$  values

<sup>6</sup>We thank Tom Hartman for discussions on this point.

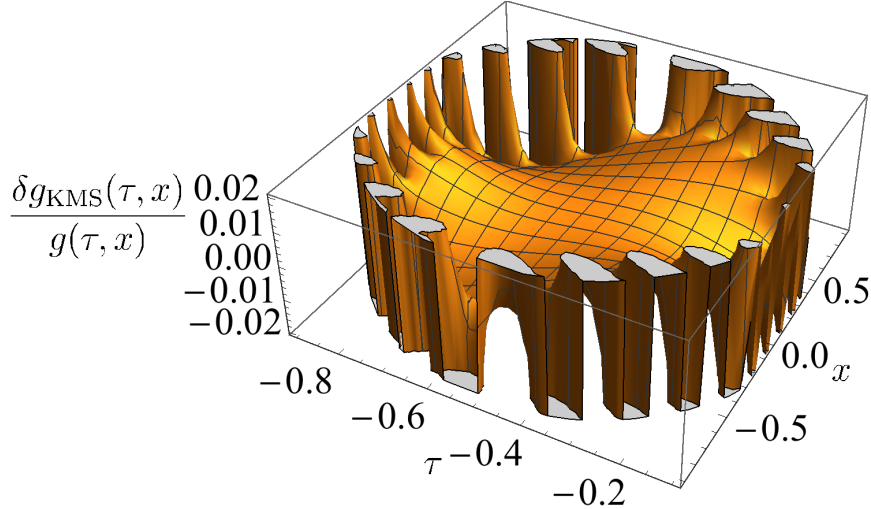


Figure 3.6: Evidence of how well the KMS condition is satisfied in the  $(\tau, x)$  plane in the region of OPE convergence. We plot the difference of the two-point function and its periodic image,  $\delta g_{\text{KMS}}(\tau, x) = g(1 + \tau, x) - g(\tau, x)$ , using the average thermal coefficients presented in figure 3.4. Note that towards the boundary of the region of OPE convergence, our estimates for the two-point function become worse and the KMS condition is further from being satisfied. For the range  $(\tau, x)$  shown above the deviation from satisfying KMS is  $< 2\%$ .

which span a full order of magnitude. When considering our results for  $a_\epsilon^{\langle\sigma\sigma\rangle}$ , the variation between the set with the lowest values of  $\bar{z}$  and those with the largest is at most  $\sim 10\%$ . As we will describe in section 3.4.4 and is already clear from figure 3.4, the error for higher spin thermal coefficients is significantly lower.

- In the final step of our algorithm, we choose a set of point in the  $(z, \bar{z})$ -plane, in the  $s$ -channel region of convergence, for which we require that the thermal two-point function satisfies the KMS condition approximately. When considering significantly different regions in the  $(z, \bar{z})$ -plane as exemplified in figure 3.13, the variation in  $a_\epsilon^{\langle\sigma\sigma\rangle}$  is only  $\sim 5\%$ . Once again, the error associated to this effect for operators with higher spins is significantly lower.

Besides the choices of parameters presented above, there are several other systematic errors:

- When requiring that the KMS condition is close to being satisfied at a wide variety of point in the  $(z, \bar{z})$ -plane, we truncate the OPE of the two-point function  $\langle\sigma\sigma\rangle$  to the three low-twist families  $\langle\sigma\sigma\rangle$ . For the ranges of points at which we

attempt to impose the KMS condition, corrections to the two-point function are dominated by the contribution of the next  $\mathbb{Z}_2$ -even operator  $\epsilon''$ .<sup>7</sup> Considering that the flat-space numerical bootstrap estimates the scaling dimension of this operator to be  $\Delta_{\epsilon''} \sim 6.9$ , we can compare the contribution of the thermal conformal block for this operator to the total contribution of all other operators in  $[\sigma\sigma]_0$ ,  $[\sigma\sigma]_1$ , and  $[\epsilon\epsilon]_0$  to  $\langle\sigma\sigma\rangle$ . This helps us estimate the error associated with neglecting this operator and higher twist operators to be  $\sim 4\%$ .

- The second largest systematic error which we expect comes from the fact that when using the inversion formula we truncate the range of integration to the t-channel region of convergence,  $z \leq 2$ . As discussed in section 3.2.1, we expect that the correction from the region  $z \geq 2$  to the thermal coefficient of an operator with spin  $J$  is exponentially suppressed in  $J$ . However, since we use the inversion formula for  $J \geq 4$ , one might worry that at small  $J$  this correction becomes large. To probe this we note that in the  $O(N)$ -model with  $N \rightarrow \infty$  the difference between the exact result and that extracted by inverting the OPE for an operator with  $J = 4$  is only  $\sim 2.8\%$ .<sup>8</sup>
- There are several systematic errors associated to the operator mixing procedure. The first is due to the truncation of the spectrum to operators of twist below a cut-off value. Since the contribution of operators with higher twist is visibly suppressed, such a truncation should only introduce a small error. The second is due to the fact that while multiple operator families serve as mixing inputs, we solely focus on  $[\sigma\sigma]_0$ ,  $[\sigma\sigma]_1$ , and  $[\epsilon\epsilon]_0$  as outputs. This assumes that, just like in the flat-space bootstrap, the thermal coefficients of these three double-twist families dominate over all other families with twists below the cut-off. While we have found this to be true for the thermal coefficients in the  $\langle\sigma\sigma\rangle$  correlator, there is one family — the multi-twist family  $[\sigma\sigma\epsilon]_0$  — which has a contribution comparable to that of  $[\epsilon\epsilon]_0$  in the  $\langle\epsilon\epsilon\rangle$  correlator. While we will discuss the contribution of this family extensively in section 3.4.3, here we note that neglecting its contribution in the mixing procedure leads to an overall difference of  $\sim 4\%$  in the mixing results. Finally, we note that after mixing we assume that the  $[\sigma\sigma]_1$  family is smooth in  $\bar{h}$  and we use a fit to estimate the

---

<sup>7</sup>We remind the reader that this operator is not part of any of the three double-twist families  $[\sigma\sigma]_0$ ,  $[\sigma\sigma]_1$  and  $[\epsilon\epsilon]_0$ .

<sup>8</sup>Specifically, the exact result found in chapter 2 predicts that as  $N \rightarrow \infty$ ,  $a_{[\sigma\sigma]_0, \ell=4}^{\text{exact}, \langle\sigma\sigma\rangle} = 0.964$ , while by restricting the inversion formula to the interval  $1 \leq z \leq 2$ , we find  $a_{[\sigma\sigma]_0, \ell=4}^{\text{OPE}, \langle\sigma\sigma\rangle} = 0.936$ .



thermal coefficients of the  $\epsilon'$  and  $T'$  operators. We find that by varying this fit, we introduce an overall error of  $\sim 3\%$  in the final results.

### 3.4 Details of the computation

In this section, we describe the details of the algorithm outlined in section 3.3.1. We will methodically iterate large-spin perturbation theory — working our way up in twist — to compute the thermal coefficients for the  $[\sigma\sigma]_0$ ,  $[\sigma\sigma]_1$ , and  $[\epsilon\epsilon]_0$  families.

In general, we will invert operators with  $h < 1$  from the  $t$ -channel, meaning we will work to order

$$S_{1-2h_\sigma, 2h_\sigma}(\bar{h}) \sim \frac{1}{\bar{h}^{2-2h_\sigma}} \quad (3.26)$$

for the thermal coefficients in the  $\langle\sigma\sigma\rangle$  correlator, dropping terms  $S_{c,\Delta}(\bar{h})$  with  $c > 1 - 2h_\sigma$ , and analogously for  $\langle\epsilon\epsilon\rangle$  with  $h_\sigma$  replaced with  $h_\epsilon$ .

#### 3.4.1 $[\sigma\sigma]_0$

We begin by solving for the lowest-twist family of operators in the theory,  $[\sigma\sigma]_0$ . The most direct way to study this family is through the  $\langle\sigma\sigma\rangle_\beta$  two-point function. Large-spin perturbation theory instructs us to start by inverting the lowest-twist operators in the  $t$ -channel. The first few low-twist primary operators in the  $\sigma \times \sigma$  OPE are

$$\sigma \times \sigma = \mathbf{1} + T + \sum_{\ell=4,6,\dots} [\sigma\sigma]_{0,\ell} + \epsilon + \dots \quad (3.27)$$

Note that  $[\sigma\sigma]_0$  operators are nearly killed by Disc and thus give smaller contributions than  $\mathbf{1}, T, \epsilon$ . Thus, we will initially neglect them, but we will add them in later. We have singled out  $T$  from the rest of the  $[\sigma\sigma]_0$  family because it has the largest anomalous dimension of the family and gives the least suppressed contribution. Inverting the operators  $\mathbf{1}, \epsilon$ , and  $T$ , we obtained a first approximation for  $a_{[\sigma\sigma]_0}^{(\sigma\sigma)}(J)$  chapter 2,

$$a_{[\sigma\sigma]_0}^{(\sigma\sigma)}(J) \supset \sum_{\mathcal{O}=\mathbf{1},\epsilon,T} a_{\mathcal{O}}^{(\sigma\sigma)} (1 + (-1)^J) \frac{K_J}{K_{\ell_{\mathcal{O}}}} \frac{\partial \bar{h}}{\partial J} S_{h_{\mathcal{O}} - \Delta_{\sigma}, \Delta_{\sigma}}(\bar{h}). \quad (3.28)$$

These contributions can be represented by the large-spin diagrams in figure 3.7.

The next most significant contribution comes from the  $[\sigma\sigma]_0$  family itself. To compute their contributions, one needs to sum over the family in the  $t$ -channel before inverting,



Figure 3.7: An illustration of how the inversion formula relates between  $s$ - and  $t$ -channels in the  $\langle \sigma\sigma \rangle_\beta$  correlator. A single term in the  $t$ -channel OPE  $\mathcal{O} \in \sigma \times \sigma$  represented in (a), inverts to a part of the sum over the  $[\sigma\sigma]_n$  families in the  $s$ -channel, which are represented in (b). Alternatively, the sum in (b) over  $a_{[\sigma\sigma]_n}^{\langle \sigma\sigma \rangle, (\mathcal{O})}$  reproduces the  $\mathcal{O}$  term in (a).

as discussed in chapter 2. The sum we need to do is<sup>9</sup>

$$\sum_{s=0}^{\infty} \sum_{\ell=\min(\ell_0, s)}^{\infty} p_s(\ell) a_{[\sigma\sigma]_0}^{\langle \sigma\sigma \rangle}(\bar{h}) (1-z)^{h(\bar{h})-2h_\sigma+s} (1-\bar{z})^{\bar{h}-2h_\sigma-s}, \quad (3.29)$$

where  $h(\bar{h}) = 2h_\sigma + \delta_{[\sigma\sigma]_0}(\bar{h})$  and  $\bar{h} = h(\bar{h}) + \ell$ . The sum is evaluated by expanding in small  $\delta(\bar{h}) \log(1-z)$ , and then regulating the asymptotic parts of the  $\bar{h}$  sum, as was explained in chapter 2. For the convenience of the reader, we reproduce the result here,

$$\begin{aligned} & \sum_{\ell=\ell_0}^{\infty} p_s(\ell) a_{[\sigma\sigma]_0}^{\langle \sigma\sigma \rangle}(\bar{h}) (1-z)^{2h_\sigma + \delta_{[\sigma\sigma]_0}(\bar{h}) - 2h_\sigma + s} (1-\bar{z})^{\bar{h} - 2h_\sigma - s} \\ &= \sum_{m=0}^{\infty} \left( \sum_{a \in A_m} c_a \left[ \frac{\delta_{[\sigma\sigma]_0}^m}{m!} p_s a_{[\sigma\sigma]_0}^{\langle \sigma\sigma \rangle} \right] \bar{z}^a + \sum_{k=0}^{\infty} \alpha_k \left[ \frac{\delta_{[\sigma\sigma]_0}^m}{m!} p_s a_{[\sigma\sigma]_0}^{\langle \sigma\sigma \rangle}, \delta_{[\sigma\sigma]_0}, 2h_\sigma + s \right] (\bar{h}_0) \bar{z}^k \right) \\ & \quad \times (1-z)^s \log^m(1-z), \end{aligned} \quad (3.30)$$

where  $\bar{h}_0 = 2h_\sigma + \ell_0$ . Here, the set  $A_m \subset \mathbb{R} \setminus \mathbb{Z}_{\geq 0}$  and the coefficients  $c_a[f]$  are determined by the large- $\bar{h}$  expansion of the summand  $f(\bar{h})$ , via (2.148).<sup>10</sup> The coefficients  $c_a[f]$  do not depend on the finite part of the sum. The coefficients  $\alpha_k$  are computed via the formula (2.156), and depend on the details of the sum. We call the terms  $\bar{z}^a$  (and  $\bar{z}^a \log^m \bar{z}$ ) ‘singular’ terms, and the  $\bar{z}^k$  ‘regular’ terms. The singular terms have are characterized by having nonzero  $s$ -channel discontinuity (near  $\bar{z} \sim 0$ ), while the regular terms have vanishing discontinuity.

<sup>9</sup>Note that terms with  $s > \ell$  are absent from the  $t$ -channel sum, so for sufficiently large  $s$ , we need to start the sum at higher  $\ell$ . We ensure this by letting the sum start at  $\ell = \min(\ell_0, s)$ .

<sup>10</sup>We note that the terms  $\bar{z}^a$  can also include terms of the form  $\bar{z}^a \log^m \bar{z}$  for  $m \in \mathbb{Z}_{\geq 0}$ .

The self-corrections of the  $[\sigma\sigma]_0$  family are determined by the  $k = 0$  term on the right hand side. We are only interested in the leading large- $\bar{h}$  contribution; recalling that the power of  $\bar{h}$  is controlled by the power of  $(1 - z)$ , we need only consider the term with  $s = 0$ . Taking the leading thermal coefficients in (3.28) and summing over the  $[\sigma\sigma]_0$  family starting at spin 4, and inverting, we obtain the first iteration of their self-correction;

$$a_{[\sigma\sigma]_0}^{(\sigma\sigma)}(J) \supset \sum_{\mathcal{O}=1,\epsilon,T} a_{\mathcal{O}}^{(\sigma\sigma)} (1 + (-1)^J) \frac{K_J}{K_{\ell_{\mathcal{O}}}} \frac{d\bar{h}}{dJ} \times \left( S_{h_{\mathcal{O}}-\Delta_{\sigma},\Delta_{\sigma}}(\bar{h}) + \sum_{m=0}^{\infty} \alpha_0^{\text{even}} \left[ \frac{\delta_{[\sigma\sigma]_0}^m}{m!} S_{h_{\mathcal{O}}-\Delta_{\sigma},\Delta_{\sigma}} \delta_{[\sigma\sigma]_0, \Delta_{\sigma}} \right] (2h_{\sigma} + 4) S_{0,\Delta_{\sigma}}^{(m)}(\bar{h}) \right). \quad (3.31)$$

Note that  $S_{0,\Delta}^{(0)}(\bar{h}) = 0$ , so self-corrections start at order  $\delta_{[\sigma\sigma]_0}$  and are suppressed by powers of the small anomalous dimensions. To evaluate the  $\alpha$ -sum above, we need the large-spin expansion of the  $[\sigma\sigma]_0$  anomalous dimensions reproduced in (3.23). Concretely, the first few terms in the large- $\bar{h}$  expansion are

$$\delta_{[\sigma\sigma]_0}(\bar{h}) \sim -0.001423 \frac{1}{\bar{h}} - 0.04628 \frac{1}{\bar{h}^{\Delta_{\epsilon}}} + \dots \quad (3.32)$$

In principle, we can iterate the self-correction indefinitely. The solution to this iteration is the fixed-point of the self-correction map. How to solve for this fixed-point was also explained in chapter 2. In practice, one needs to truncate to some order in the anomalous dimension expansion. Truncating to order  $\delta^2$ , the self-corrected thermal coefficients are

$$a_{[\sigma\sigma]_0}^{(\sigma\sigma)}(J) = (1 + (-1)^J) 4\pi K_J \frac{d\bar{h}}{dJ} \times \left( a_1^{(\sigma\sigma)} \left( S_{-\Delta_{\sigma},\Delta_{\sigma}}(\bar{h}) - 0.0119 S_{0,\Delta_{\sigma}}^{(1)}(\bar{h}) + 2.14 \times 10^{-5} S_{0,\Delta_{\sigma}}^{(2)}(\bar{h}) \right) + a_{\epsilon}^{(\sigma\sigma)} \left( S_{h_{\epsilon}-\Delta_{\sigma},\Delta_{\sigma}}(\bar{h}) + 0.0007999 S_{0,\Delta_{\sigma}}^{(1)}(\bar{h}) - 1.95 \times 10^{-6} S_{0,\Delta_{\sigma}}^{(2)}(\bar{h}) \right) + a_T^{(\sigma\sigma)} \frac{3}{8} \left( S_{h_T-\Delta_{\sigma},\Delta_{\sigma}}(\bar{h}) - 0.0001312 S_{0,\Delta_{\sigma}}^{(1)}(\bar{h}) + 3.01 \times 10^{-7} S_{0,\Delta_{\sigma}}^{(2)}(\bar{h}) \right) + \dots, \quad (3.33)$$

where the dots denote terms suppressed in large- $\bar{h}$  or in small  $\delta_{[\sigma\sigma]_0}$ . For convenience, plots of the three terms are given by the dashed curves in figure 3.12.

### 3.4.2 $[\sigma\sigma]_1$ and $[\epsilon\epsilon]_0$

The next families that we solve for require more care. First, we compute the leading contributions to their thermal coefficients in the large-spin limit. Afterwards, we discuss subtleties that arise when considering finite spin members of the two families.

#### 3.4.2.1 Tree level contributions

We start by computing the asymptotic contributions. Inverting the low-twist operators  $\mathbf{1}$ ,  $\epsilon$ ,  $T$ , and the  $[\sigma\sigma]_0$  family in the  $\langle\sigma\sigma\rangle$  correlator gives ‘tree-level’ contributions to the thermal coefficients of the  $[\sigma\sigma]_1$  family. We can compute the contributions of  $\mathbf{1}$ ,  $\epsilon$ , and  $T$  via (3.21) as

$$\begin{aligned}
& a_{[\sigma\sigma]_1}^{\langle\sigma\sigma\rangle,(\mathcal{O})}(J) \\
&= a_{\mathcal{O}}^{\langle\sigma\sigma\rangle}(1 + (-1)^J)4\pi K_J \frac{d\bar{h}}{dJ} \sum_{r=0}^1 \sum_{s=0}^{\ell_{\mathcal{O}}} q_r(J) p_s(\ell_{\mathcal{O}}) (-1)^{n-r} \binom{\bar{h}_{\mathcal{O}} - \Delta_{\sigma} - s}{n-r} S_{h_{\mathcal{O}} - \Delta_{\sigma} + s, \Delta_{\sigma} - r}(\bar{h}) \\
&= a_{\mathcal{O}}^{\langle\sigma\sigma\rangle}(1 + (-1)^J) \frac{K_J}{K_{\ell_{\mathcal{O}}}} \frac{d\bar{h}}{dJ} \left( -(\bar{h}_{\mathcal{O}} - \Delta_{\sigma}) S_{h_{\mathcal{O}} - \Delta_{\sigma}, \Delta_{\sigma}}(\bar{h}) - \frac{2+J}{3+2J} S_{h_{\mathcal{O}} - \Delta_{\sigma}, \Delta_{\sigma} - 1}(\bar{h}) \right) + \dots
\end{aligned} \tag{3.34}$$

where the dots denote higher order terms in  $1/\bar{h}$  that we will drop. We can also sum over the rest of the  $[\sigma\sigma]_0$  family and compute its contribution to the  $[\sigma\sigma]_1$  pole, similarly to how we computed the  $[\sigma\sigma]_0$  self-correction in (3.31). Their leading contribution is given by

$$\begin{aligned}
& a_{[\sigma\sigma]_1}^{\langle\sigma\sigma\rangle,([\sigma\sigma]_0)}(J) \\
&= (1 + (-1)^J)4\pi K_J \frac{d\bar{h}}{dJ} \sum_{r=0}^1 \sum_{m=0}^{\infty} q_r(J) \alpha_{n-r} \left[ \frac{\delta_{[\sigma\sigma]_0}^m}{m!} p_0 a_{[\sigma\sigma]_0}^{\langle\sigma\sigma\rangle}, \delta_{[\sigma\sigma]_0}, \Delta_{\sigma} \right] (2h_{\sigma} + 4) S_{0, \Delta_{\sigma} - r}^{(m)}(\bar{h}).
\end{aligned} \tag{3.35}$$

Thus, by adding terms from (3.34) with those from (3.35), we find that at large spin

$$a_{[\sigma\sigma]_1}^{\langle\sigma\sigma\rangle}(J) = \sum_{\mathcal{O}=\mathbf{1},\epsilon,T,[\sigma\sigma]_0} a_{[\sigma\sigma]_1}^{\langle\sigma\sigma\rangle,(\mathcal{O})}(J) + \dots \tag{3.36}$$

What about the  $[\epsilon\epsilon]_0$  family? The sum over the  $[\sigma\sigma]_0$  family inside the  $\langle\sigma\sigma\rangle$  correlator also contribute to the  $[\epsilon\epsilon]_0$  family. Concretely, the sum over the  $[\sigma\sigma]_0$  family contains asymptotics that sum to a ‘singular term’ that corresponds to a pole for the  $[\epsilon\epsilon]_0$  family. We can see this by the large spin diagrams in figure 3.8. This gives a

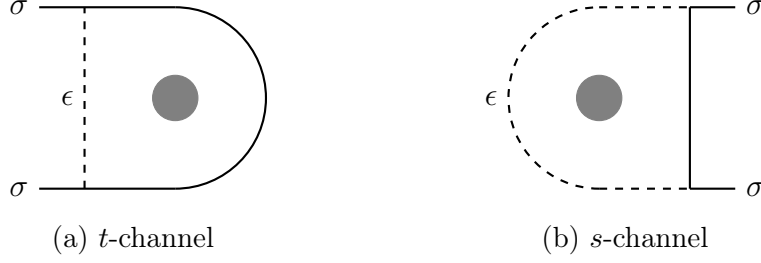


Figure 3.8: The asymptotic parts of the *t*-channel sum over  $[\sigma\sigma]_n$  represented by the diagram on the left inverts to the *s*-channel process on the right. Accordingly, their inversion should produce poles for the  $[\epsilon\epsilon]_m$  families. The diagram on the left is deciphered by reading it from left to right; first the external  $\sigma$  operators fuse into  $[\sigma\sigma]_n$  states, which exchange an  $\epsilon$  to correct their self-energy (anomalous dimension), then they receive expectation values proportional to  $b_{\mathbf{1}}$ . The diagram on the right can also be deciphered by reading it from right to left; first the external  $\sigma$  operators form  $[\epsilon\epsilon]_m$  via exchange of a  $\sigma$ , then the  $[\epsilon\epsilon]_m$  receive expectation values proportional to  $b_{\mathbf{1}}$ .

contribution

$$a_{[\epsilon\epsilon]_0}^{\langle\sigma\sigma\rangle}(J) \supset (1 + (-1)^J) 4\pi K_J a_{\mathbf{1}}^{\langle\sigma\sigma\rangle} \delta_{[\sigma\sigma]_0}^{(\epsilon)} \frac{\Gamma(\Delta_\sigma - \Delta_\epsilon)}{\Gamma(\Delta_\sigma)} S_{0,\Delta_\sigma}^{(1)}(\bar{h}). \quad (3.37)$$

Here, we have used the coefficient  $\delta_{[\sigma\sigma]_0}^{(\epsilon)}$  in the large- $\bar{h}$  expansion of the anomalous dimension,

$$\delta_{[\sigma\sigma]_0}(\bar{h}) = \sum_{\mathcal{O}} \delta_{[\sigma\sigma]_0}^{(\mathcal{O})} \frac{1}{\bar{h}^{2h_{\mathcal{O}}}}, \quad (3.38)$$

with the first few coefficients given in (3.23) and (3.32). Of course, this is only a naive approximation of the  $[\epsilon\epsilon]_0$  thermal coefficients which should only work for very large  $J$ . The  $[\epsilon\epsilon]_0$  family is more directly accessed in the  $\langle\epsilon\epsilon\rangle$  correlator, where inverting any single operator gives direct contribution to this family. For example, inverting the low-twist operators  $\mathbf{1}$ ,  $\epsilon$ , and  $T$  in the  $\langle\epsilon\epsilon\rangle$  correlator gives

$$a_{[\epsilon\epsilon]_0}^{\langle\epsilon\epsilon\rangle}(J) \supset \sum_{\mathcal{O}=\mathbf{1},\epsilon,T} a_{\mathcal{O}}^{\langle\epsilon\epsilon\rangle} (1 + (-1)^J) \frac{K_J}{K_{\ell_{\mathcal{O}}}} \frac{\partial \bar{h}}{\partial J} S_{h_{\mathcal{O}} - \Delta_{\epsilon}, \Delta_{\epsilon}}(\bar{h}). \quad (3.39)$$

Here, we labeled the thermal coefficients to indicate that they are the coefficients in the  $\langle\epsilon\epsilon\rangle$  correlator. The relation between the thermal coefficients in the two correlators is given by the ratio of the OPE coefficients,

$$a_{\mathcal{O}}^{\langle\sigma\sigma\rangle} = \frac{f_{\sigma\sigma\mathcal{O}}}{f_{\epsilon\epsilon\mathcal{O}}} a_{\mathcal{O}}^{\langle\epsilon\epsilon\rangle}. \quad (3.40)$$

Combining our result (3.33) for  $a_{[\sigma\sigma]_0}^{\langle\sigma\sigma\rangle}$  from  $\langle\sigma\sigma\rangle$  with the ratio of OPE coefficients  $f_{\sigma\sigma[\sigma\sigma]_0}/f_{\epsilon\epsilon[\sigma\sigma]_0}$  obtained from the analytic four-point function bootstrap, we can consider the contributions of the  $[\sigma\sigma]_0$  family in the  $\langle\epsilon\epsilon\rangle$  correlator. For example, their contribution to the  $[\epsilon\epsilon]_0$  thermal coefficients can be computed, correcting (3.39) as

$$\begin{aligned}
a_{[\epsilon\epsilon]_0}^{\langle\epsilon\epsilon\rangle}(J) \supset & \sum_{\mathcal{O}=1,\epsilon,T} a_{\mathcal{O}}^{\langle\epsilon\epsilon\rangle} (1 + (-1)^J) \frac{K_J}{K_{\ell_{\mathcal{O}}}} \frac{d\bar{h}}{dJ} S_{h_{\mathcal{O}}-\Delta_{\epsilon},\Delta_{\epsilon}}(\bar{h}) \\
& + (1 + (-1)^J) K_J \frac{d\bar{h}}{dJ} \sum_{m=0}^{\infty} \alpha_0 \left[ \frac{\delta_{[\sigma\sigma]_0}^m}{m!} \frac{f_{\epsilon\epsilon[\sigma\sigma]_0}}{f_{\sigma\sigma[\sigma\sigma]_0}} p_0 a_{[\sigma\sigma]_0}^{\langle\sigma\sigma\rangle}, \delta_{[\sigma\sigma]_0}, \Delta_{\sigma} \right] (2h_{\sigma} + 4) S_{\Delta_{\sigma}-\Delta_{\epsilon},\Delta_{\sigma}}^{(m)}(\bar{h}).
\end{aligned} \tag{3.41}$$

While at large  $\bar{h}$ , (3.36) and (3.41) provide good approximations for the thermal coefficients this will not be the case at small  $\bar{h}$ . In this regime, the two families  $[\sigma\sigma]_1$  and  $[\epsilon\epsilon]_0$  are very close together in twist, and have very large anomalous dimensions due to the operator mixing described in section 3.2.2. Naïvely, since the families are so close in twist, and strongly mix, we simply cannot be sure how the residues are distributed between the families. More systematically, the presence of large anomalous dimensions means that the poles for the families are actually quite far from the naïve locations at  $h = 2h_{\sigma} + 1$  and  $2h_{\epsilon}$  that were used to obtain (3.36) and (3.41). The effects that produce anomalous dimensions also produce corrections to the residues on a similar scale; since the anomalous dimensions are large at these intermediate  $\bar{h}$  values, the contributions to the residue must also be similarly large. Finally, there are altogether other poles for multi-twist families near the twists of these families, which the residues could further mix with.

We need to develop an approach to estimate the correct, mixed thermal coefficients. In order to estimate the correct, mixed thermal coefficients, we thus need to take into account all the corrections mentioned above. Towards that end, we now turn to developing some required technology.

### 3.4.3 The half-inverted correlator

Each individual  $t$ -channel block contributes only double-twist poles in the  $s$ -channel. However, the physical correlator has poles at non-double-twist locations. Consequently, the sum over  $t$ -channel blocks cannot commute with the inversion integral when  $\Delta$  is near the physical poles. To see why, consider a contour integral around the location of a physical pole in  $\Delta$ . This integral gives zero for every  $t$ -channel block, but is certainly nonzero for the full  $a(\Delta, J)$ . By contrast, the sum over  $t$ -channel blocks

does commute with the inversion integral when  $\Delta$  is imaginary. However, we would like to determine numerically what happens at real  $\Delta$ .

To get a better numerical handle on how poles can shift, we will work with a more convenient object than  $a(\Delta, J)$ . Let us imagine applying the inversion formula ‘halfway’, where we do the  $z$  integral to compute the residues, but leave the  $\bar{z}$  integral — which produces the poles — undone. We want to define a generating function of the form

$$(1 + (-1)^J)K_J \int_1^2 \frac{dz}{z} \sum_{r=0}^{\infty} q_r(J) z^{\Delta_\phi - \bar{h} - r} \bar{z}^{\Delta_\phi + r} \text{Disc}[g(z, \bar{z})]. \quad (3.42)$$

(Once again, we assume no contributions from the arcs of the inversion formula.) Now, instead of poles in  $h$ , we have powers  $\bar{z}^h$ . Furthermore, the anomalous dimension corrections to pole locations are of the form

$$\frac{\delta(\bar{h})^m}{m!} \bar{z}^h \log^m \bar{z}. \quad (3.43)$$

The idea is that (3.42) is almost the inverse Laplace transform in  $h$  of

$$a(h, \bar{h}) = a(\Delta = \bar{h} + h, J = \bar{h} - h) \quad (3.44)$$

— almost due to the pesky factor of  $K_J$ . The generating function we want should relate to  $a(h, \bar{h})$  along the lines of

$$\tilde{a}(\bar{z}, \bar{h}) = - \oint \frac{dh}{2\pi i} \bar{z}^h a(h, \bar{h}), \quad (3.45)$$

which is the inverse to

$$a(h, \bar{h}) = \int_0^1 \frac{d\bar{z}}{\bar{z}} \bar{z}^{-h} \tilde{a}(\bar{z}, \bar{h}). \quad (3.46)$$

The inverse Laplace transform (3.45) can be performed in a region of  $h$  where the inversion integral commutes with the sum over  $t$ -channel blocks, and thus we expect it to have a convergent expansion in  $t$ -channel blocks. The idea of defining a “half-inverted” correlator was discussed in the four-point function case in [20, 25].

The definitions (3.42) and (3.45) will agree if we make a few small modifications. Firstly, we should absorb the factor of  $K_J$  inside  $a(h, \bar{h})$ , so the contour integral in (3.45) does not pick up unwanted poles. (At small enough twist  $h$  such that we are away from poles in  $K_J$ , we can skip this step.) Secondly, we should reinterpret  $J$  in

$\tilde{a}(\bar{z}, \bar{h})$  as an appropriate differential operator,  $\hat{J}$ , as we will explain below. Thus, we define

$$\tilde{a}(\bar{z}, \bar{h}) = \frac{1}{4\pi} \int_1^2 \frac{dz}{z} \sum_{r=0}^{\infty} q_r(\hat{J}) z^{\Delta_\phi - \bar{h} - r} \bar{z}^{\Delta_\phi + r} \text{Disc}[g(z, \bar{z})], \quad (3.47)$$

which satisfies

$$a(h, \bar{h}) = (1 + (-1)^J) 4\pi K_J \int_0^1 \frac{d\bar{z}}{\bar{z}} \bar{z}^{-h} \tilde{a}(\bar{z}, \bar{h}). \quad (3.48)$$

We call  $\tilde{a}(\bar{z}, \bar{h})$  the half-inverted correlator.

Inside half-inverted correlators,  $J$  should be thought of as the linear operator

$$\hat{J} = \bar{h} - h = \bar{h} - \bar{z} \partial_{\bar{z}} \quad (3.49)$$

acting on the space of functions of the form  $\bar{z}^h \log^m \bar{z}$ . Note that  $\hat{J}$  appears in  $\tilde{a}(\bar{z}, \bar{h})$  inside  $q_r(\hat{J})$ , which are rational functions of  $\hat{J}$  for each integer  $r$ . Therefore, we will need to invert  $\hat{J}$  when acting on this space of functions. For brevity, let us denote

$$|h, m\rangle \equiv \bar{z}^h \log^m \bar{z}. \quad (3.50)$$

For our purposes,  $h > 0$  and  $m$  is a non-negative integer. For example, we have

$$\bar{z} \partial_{\bar{z}} |h, m\rangle = h |h, m\rangle + m |h, m-1\rangle. \quad (3.51)$$

Then, expressions such as

$$\frac{1}{c + d \hat{J}} = \frac{1}{c + d(\bar{h} - \bar{z} \partial_{\bar{z}})} \quad (3.52)$$

can be interpreted as the inverse of the appropriate linear operator acting on this space of functions. Inverting the operator  $\bar{z} \partial_{\bar{z}}$ , we have

$$(\bar{z} \partial_{\bar{z}})^{-1} |h, m\rangle = \frac{1}{h} \sum_{k=0}^m (-1)^k \frac{m!}{(m-k)!} \frac{1}{h^k} |h, m-k\rangle. \quad (3.53)$$

Similarly,

$$\frac{1}{c + d \hat{J}} |h, m\rangle = \frac{1}{c + d(\bar{h} - h)} \sum_{k=0}^m (-1)^k \frac{m!}{(m-k)!} \frac{1}{(c + d(\bar{h} - h))^k} |h, m-k\rangle. \quad (3.54)$$

With this interpretation, we can substitute  $\hat{J}$  for  $J$  as we did in (3.47), and define the half-inverted correlator as an honest function of  $\bar{z}$  and  $\bar{h}$  satisfying (3.48).



### 3.4.3.1 Contributions to the half-inverted correlators $\langle \widetilde{\sigma\sigma} \rangle$ and $\langle \widetilde{\epsilon\epsilon} \rangle$

Returning to the Ising model, by half-inverting our low-twist operators  $\mathbf{1}$ ,  $\epsilon$ ,  $T$ , and the  $[\sigma\sigma]_0$  family in the  $\langle \sigma\sigma \rangle$  and  $\langle \epsilon\epsilon \rangle$  correlators, we obtain leading-order-in-large- $\bar{h}$  approximations to the respective half-inverted correlators  $\langle \widetilde{\sigma\sigma} \rangle(\bar{z}, \bar{h})$  and  $\langle \widetilde{\epsilon\epsilon} \rangle(\bar{z}, \bar{h})$ . The terms we compute include those that give the naïve  $[\sigma\sigma]_1$  and  $[\epsilon\epsilon]_0$  thermal coefficients (3.36) and (3.41), but also include many other terms coming from the sum over the  $[\sigma\sigma]_0$  family.

We are not just limited to inverting the operators  $\mathbf{1}$ ,  $\epsilon$ ,  $T$ , and the  $[\sigma\sigma]_0$  family. While we do not know enough about any of the other families in the theory to compute all of their contributions, there are a special set of contributions that we can compute. In particular, while the regular terms  $\alpha_k$  depend on such particulars of the family as anomalous dimensions and an exact sum over the thermal coefficients, the singular terms do not. The singular terms only depend on the asymptotic expansions. Furthermore, the leading contributions to the singular terms are to constant order in the anomalous dimensions, thus we can compute them without any knowledge of the anomalous dimensions. Therefore, we can essentially take a half-inverted correlator, and attempt to partially solve it in the large- $\bar{h}$  regime. Suppose that the sum over  $[\sigma\sigma]_0$  produced a term

$$p(\bar{h})\bar{z}^{h_f} \subset \langle \widetilde{\sigma\sigma} \rangle \quad (3.55)$$

where  $h_f$  is the asymptotic half-twist of a multitwist family  $f$ . We can safely say that  $p(\bar{h})$  is a part of the large- $\bar{h}$  asymptotics of the thermal coefficient of the family  $f$ . Now, the sum over the family  $f$  in the  $t$ -channel includes a term

$$\begin{aligned} \sum_{\mathcal{O} \in f} (1 + (-1)^\ell) p(\bar{h}) (1 - \bar{z})^{\bar{h} - 2h_\sigma} (1 - z)^{h_f + \delta_f(\bar{h}) - 2h_\sigma} \supset \sum_{a \in A} c_a[p] \bar{z}^a (1 - z)^{h_f - 2h_\sigma} \\ + \mathcal{O}(\delta_f) + \text{regular}. \end{aligned} \quad (3.56)$$

Note that we can determine the singular term  $c_a[p(\bar{h})]$  without having to know about the small- $\bar{h}$  behavior of the thermal coefficients of the family  $f$ , or the anomalous dimensions  $\delta_f$ ! This is unlike the regular terms, which depend on knowing the small- $\bar{h}$  behavior of the thermal coefficients as well as the anomalous dimensions. Inverting the singular term in (3.56), we obtain a contribution to the half inverted correlator

$$\langle \widetilde{\sigma\sigma} \rangle \supset c_a[p] S_{h_f - 2h_\sigma, 2h_\sigma}(\bar{h}) \bar{z}^{2h_\sigma + a}. \quad (3.57)$$

So, we take the half-inverted correlators  $\langle \widetilde{\sigma\sigma} \rangle$  and  $\langle \widetilde{\epsilon\epsilon} \rangle$  computed from the contributions of  $\mathbf{1}$ ,  $\epsilon$ ,  $T$ , and  $[\sigma\sigma]_0$ , and augment them with the singular terms (3.57) coming from all the asymptotics of thermal coefficients of other families that appear in them.

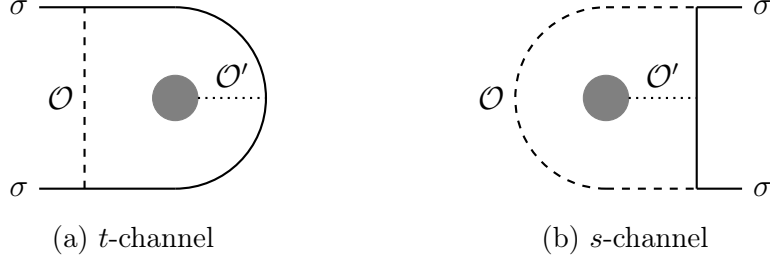


Figure 3.9: The  $t$ -channel diagram denotes a sum over the asymptotics  $\delta_{[\sigma\sigma]_n}^{(\mathcal{O})}(\bar{h}) \times a_{[\sigma\sigma]_n}^{(\sigma\sigma)(\mathcal{O}')}(\bar{h})$ . This inverts to poles for the  $[\mathcal{O}\mathcal{O}\mathcal{O}']_m$  families in the  $s$ -channel. Conversely, swapping the  $s$ - and  $t$ -channels, and summing over the  $[\mathcal{O}\mathcal{O}\mathcal{O}']_m$  family in the  $t$ -channel reproduces the anomalous dimensions of the  $[\sigma\sigma]_n$  family in the terms proportional to  $a_{\mathcal{O}'}$ .

In fact, these singular terms are crucial, and augmenting by them is a natural thing to do. For example, in order to reproduce known anomalous dimensions from the thermal inversion formula — such as those of the  $[\sigma\sigma]_0$  family — one needs to sum over multi-twist families in the  $t$ -channel chapter 2. The prototypical example of this process is illustrated in the thermal large-spin diagram in figure 3.9. Also, recovering the thermal coefficients of  $[\sigma\sigma]_0$  in  $\langle\epsilon\epsilon\rangle$  requires summing over generically multitwist families that are generated in  $\langle\epsilon\epsilon\rangle$  by the sum over  $[\sigma\sigma]_0$ , as illustrated in figure 3.10. We will now briefly review these relevant processes.

### 3.4.3.2 Generating anomalous dimensions in $\langle\sigma\sigma\rangle$

Let us illustrate how anomalous dimensions are generated for the half-inverted correlator  $\langle\widetilde{\sigma\sigma}\rangle$  by an example. We saw in (3.37) that the sum over  $[\sigma\sigma]_0$  in  $\langle\sigma\sigma\rangle$  produced a pole for the  $[\epsilon\epsilon]_0$  family. In particular, this means that the sum over  $[\sigma\sigma]_0$  contributes a term

$$\langle\widetilde{\sigma\sigma}\rangle(\bar{z}, \bar{h}) \supset \bar{z}^{2h_\epsilon} a_{\mathbf{1}}^{(\sigma\sigma)} \delta_{[\sigma\sigma]_0}^{(\epsilon)} \frac{\Gamma(\Delta_\sigma - \Delta_\epsilon)}{\Gamma(\Delta_\sigma)} S_{0, \Delta_\sigma}^{(1)}(\bar{h}) \quad (3.58)$$

to the half-inverted correlator  $\langle\widetilde{\sigma\sigma}\rangle(\bar{z}, \bar{h})$ . This implies that there is a term, given in (3.37), in the large- $\bar{h}$  expansion of  $a_{[\epsilon\epsilon]_0}^{(\sigma\sigma)}(\bar{h})$ . Now, we would be wrong to say that this is a good approximation to the thermal coefficients at small  $\bar{h}$ , but at large  $\bar{h}$ , we know such a term is there. By crossing symmetry of figure 3.8, this term is responsible for generating the  $\delta_{[\sigma\sigma]_0}^{(\epsilon)}$  correction to the anomalous dimensions of  $[\sigma\sigma]_0$  in  $\langle\widetilde{\sigma\sigma}\rangle$ .

Let us consider the contributions of  $[\epsilon\epsilon]_0$  to the thermal coefficients in  $\langle\sigma\sigma\rangle$ . To evaluate them, we need to analyze the  $t$ -channel sum over the family. This sum has

the same form as the sum (3.30) over the  $[\sigma\sigma]_0$  family,

$$\begin{aligned} & \sum_{\ell=\ell_0}^{\infty} p_0(\ell) a_{[\epsilon\epsilon]_0}^{\langle\sigma\sigma\rangle}(\bar{h}) (1-z)^{2h_\epsilon+\delta_{[\epsilon\epsilon]_0}(\bar{h})-2h_\sigma} (1-\bar{z})^{\bar{h}-2h_\epsilon} \\ &= \sum_{m=0}^{\infty} \left( \sum_{a \in A_m} c_a \left[ \frac{\delta_{[\epsilon\epsilon]_0}^m}{m!} p_0 a_{[\epsilon\epsilon]_0}^{\langle\sigma\sigma\rangle} \right] \bar{z}^a + \sum_{k=0}^{\infty} \alpha_k \left[ \frac{\delta_{[\epsilon\epsilon]_0}^m}{m!} p_0 a_{[\epsilon\epsilon]_0}^{\langle\sigma\sigma\rangle}, \delta_{[\epsilon\epsilon]_0}, 2h_\sigma \right] (\bar{h}_0) \bar{z}^k \right) \\ & \quad \times (1-z)^{2h_\epsilon-2h_\sigma} \log^m(1-z), \end{aligned} \quad (3.59)$$

where  $\bar{h} = 2h_\epsilon + \ell + \delta_{[\epsilon\epsilon]_0}(\bar{h})$  and  $\bar{h}_0 = 2h_\epsilon + \ell_0$ . One important difference is that since  $2h_\epsilon - 2h_\sigma \notin \mathbb{Z}_{\geq 0}$ , the terms with  $m = 0$  have nonzero discontinuity and contribute to the inversion formula. So, we can consider the leading term  $m = 0$  in the anomalous dimension expansion. Now, without knowledge of small- $\bar{h}$  values of  $a_{[\epsilon\epsilon]_0}^{\langle\sigma\sigma\rangle}(\bar{h})$ , we cannot reliably evaluate the  $\alpha_k$  coefficients. However, the coefficients  $c_a[p]$  only depend on the asymptotic expansion of  $p(\bar{h})$ , and are insensitive to small- $\bar{h}$  behavior. So, using the term of  $a_{[\epsilon\epsilon]_0}^{\langle\sigma\sigma\rangle}$  in (3.58), we can compute the leading singular term  $c_a \left[ p_0 a_{[\epsilon\epsilon]_0}^{\langle\sigma\sigma\rangle} \right] \bar{z}^a$ ,

$$\sum_{a \in A_0} c_a \left[ p_0 a_{[\epsilon\epsilon]_0}^{\langle\sigma\sigma\rangle} \right] \bar{z}^a \supset a_{\mathbf{1}}^{\langle\sigma\sigma\rangle} \delta_{[\sigma\sigma]_0}^{(\epsilon)} \frac{\Gamma(\Delta_\sigma - \Delta_\epsilon)}{\Gamma(\Delta_\sigma)} \log \bar{z}. \quad (3.60)$$

Half-inverting this term, we obtain the corresponding contribution

$$\langle \widetilde{\sigma\sigma} \rangle(\bar{z}, \bar{h}) \supset a_{\mathbf{1}}^{\langle\sigma\sigma\rangle} \delta_{[\sigma\sigma]_0}^{(\epsilon)} \frac{\Gamma(\Delta_\sigma - \Delta_\epsilon)}{\Gamma(\Delta_\sigma)} \bar{z}^{2h_\sigma} \log \bar{z} S_{2h_\epsilon-2h_\sigma, 2h_\sigma}(\bar{h}) + \dots \quad (3.61)$$

This is a correction to the anomalous dimension (pole location)  $\delta_{[\sigma\sigma]_0}$  of the  $[\sigma\sigma]_0$  family. As expected, this is exactly the term in large-spin perturbation theory that produces the contribution of  $\epsilon$  to the anomalous dimension through the crossing-symmetric process illustrated in figure 3.8. Other contributions arise from similar sums over other, potentially multi-twist families, as illustrated in figure 3.9.

One important point to highlight is that the contribution (3.61) above does not only produce the expected anomalous dimension, it also contributes to higher poles. The half-inversion of the term in (3.60) produces another term, contributing to the anomalous dimensions at the naïve location of the  $[\sigma\sigma]_1$  family,

$$\langle \widetilde{\sigma\sigma} \rangle(\bar{z}, \bar{h}) \supset a_{\mathbf{1}}^{\langle\sigma\sigma\rangle} \delta_{[\sigma\sigma]_0}^{(\epsilon)} \frac{\Gamma(\Delta_\sigma - \Delta_\epsilon)}{\Gamma(\Delta_\sigma)} \bar{z}^{2h_\sigma+1} \log \bar{z} q_1(\widehat{J}) S_{2h_\epsilon-2h_\sigma, 2h_\sigma-1}(\bar{h}). \quad (3.62)$$

In principle, this is an important contribution when considering the  $[\sigma\sigma]_1$  family, and through mixing, the  $[\epsilon\epsilon]_0$  family. The moral is that we should systematically generate

these terms by iterating  $t$ -channel sums and subsequent half-inversions, rather than by putting the anomalous dimensions in by hand whenever they are known, as we will also generate other contributions. In summary, we put in the anomalous dimensions of  $[\sigma\sigma]_0$  and recover them, but also generate some additional terms for  $[\sigma\sigma]_n$ .

### 3.4.3.3 Generating $[\sigma\sigma]_0$ in $\langle\tilde{\epsilon}\tilde{\epsilon}\rangle$

Another important phenomenon is the generation of the  $[\sigma\sigma]_0$  thermal coefficients in  $\langle\tilde{\epsilon}\tilde{\epsilon}\rangle$ . Using  $\langle\sigma\sigma\rangle$ , we already computed an expression for the  $[\sigma\sigma]_0$  thermal coefficients, which we believe to be accurate. One might be tempted to input them into  $\langle\tilde{\epsilon}\tilde{\epsilon}\rangle$  by hand. As with the anomalous dimensions above, it's worthwhile to generate the  $[\sigma\sigma]_0$  thermal coefficients in  $\langle\tilde{\epsilon}\tilde{\epsilon}\rangle$  systematically; similarly, contributions to the  $[\sigma\sigma]_1$  thermal coefficients in  $\langle\tilde{\epsilon}\tilde{\epsilon}\rangle$  are also generated.

The process with which the  $[\sigma\sigma]_0$  thermal coefficients are generated in  $\langle\tilde{\epsilon}\tilde{\epsilon}\rangle$  is depicted in figure 3.10. Our task boils down to looking at the singular terms arising from the sum over  $[\sigma\sigma]_0$  in  $\langle\epsilon\epsilon\rangle$ ,

$$\begin{aligned} & \sum_{\ell} p_0(\ell) \frac{f_{\epsilon\epsilon[\sigma\sigma]_0}(\bar{h})}{f_{\sigma\sigma[\sigma\sigma]_0}(\bar{h})} a_{[\sigma\sigma]_0}^{\langle\sigma\sigma\rangle}(\bar{h}) (1-z)^{2h_\sigma + \delta_{[\sigma\sigma]_0}(\bar{h}) - 2h_\epsilon} (1-\bar{z})^{\bar{h} - 2h_\sigma} \\ & \supset (1-z)^{2h_\sigma - 2h_\epsilon} \sum_{m=0}^{\infty} \log^m(1-z) \sum_{a \in A_m} c_a \left[ \frac{\delta_{[\sigma\sigma]_0}^m}{m!} p_0 \frac{f_{\epsilon\epsilon[\sigma\sigma]_0}}{f_{\sigma\sigma[\sigma\sigma]_0}} a_{[\sigma\sigma]_0}^{\langle\sigma\sigma\rangle} \right] \bar{z}^a, \end{aligned} \quad (3.63)$$

and then considering the sum over the families appearing there. The singular terms of the sums over those families (to constant order in their anomalous dimensions) reproduce the  $[\sigma\sigma]_0$  thermal coefficients we seek. As before, inverting anything that contributes to a pole for  $[\sigma\sigma]_0$  at  $h = 2h_\sigma$  also contributes to higher poles at  $h = 2h_\sigma + n$ , and in particular to  $[\sigma\sigma]_1$ .

### 3.4.4 Mixing between families

The combination of our effort so far allows us to compute good approximations for the half-inverted correlators  $\langle\tilde{\sigma}\tilde{\sigma}\rangle(\bar{z}, \bar{h})$  and  $\langle\tilde{\epsilon}\tilde{\epsilon}\rangle(\bar{z}, \bar{h})$ . To summarize our steps so far, our approximations are obtained first by half-inverting  $\mathbf{1}$ ,  $\epsilon$ ,  $T$ , and the  $[\sigma\sigma]_0$  family, and then further refined by augmenting by the singular terms coming from sums over other families (that appear in  $\langle\tilde{\sigma}\tilde{\sigma}\rangle(\bar{z}, \bar{h})$  and  $\langle\tilde{\epsilon}\tilde{\epsilon}\rangle(\bar{z}, \bar{h})$  from the asymptotics of the sum over the  $[\sigma\sigma]_0$  family). Let  $\tilde{g}^c(\bar{z}, \bar{h})$  denote the vector of half-inverted correlators

$$\tilde{g}(\bar{z}, \bar{h}) = (\langle\tilde{\sigma}\tilde{\sigma}\rangle(\bar{z}, \bar{h}), \langle\tilde{\epsilon}\tilde{\epsilon}\rangle(\bar{z}, \bar{h})), \quad (3.64)$$

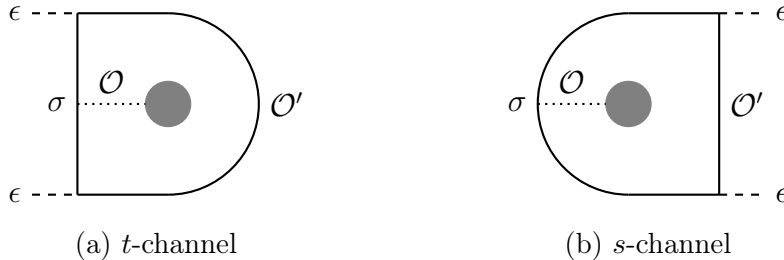


Figure 3.10: To obtain the  $[\sigma\sigma]$  thermal coefficients proportional to  $a_{\mathcal{O}}^{\langle\epsilon\epsilon\rangle}$  in the  $s$ -channel of  $\langle\epsilon\epsilon\rangle$ , one must invert sums over  $[\mathcal{O}\mathcal{O}'\mathcal{O}']$  in the  $t$ -channel. Of course, the diagrams are crossing symmetric, so the required  $t$ -channel terms are obtained from inverting the sum over  $[\sigma\sigma]$  in the first place.

where  $c$  labels the correlator. Our computations for the half-inverted correlators produce approximations of the form

$$\tilde{g}_{\text{naive}}^c(\bar{z}, \bar{h}) = \sum_f (a_f^c)^{\text{naive}}(\bar{h}) \bar{z}^{h_f^{\text{naive}}} (1 + \delta_f(\bar{h}) \log \bar{z} + O(\log^2 \bar{z})) \quad (3.65)$$

for each of the two correlators,  $c$ . Here, the sum is over several of the low-twist families  $f$ , such as  $[\sigma\sigma]_0$ ,  $[\sigma\sigma]_1$ ,  $[\epsilon\epsilon]_0$ , and a few others appearing as singular terms from the sum over  $[\sigma\sigma]_0$ . At sufficiently high  $\bar{h}$ , the  $\log \bar{z}$  terms, like those found in (3.61), correctly approximates the anomalous dimensions for some of these families.<sup>11</sup> However, at small  $\bar{h}$ , the thermal coefficients of families that are close in twist — and thus have similar powers of  $\bar{z}$  in the expansion (3.65) — prove difficult to disentangle. As reviewed in 3.2.2, in the case of the 3D Ising CFT, the contributions of  $[\sigma\sigma]_1$  and  $[\epsilon\epsilon]_0$  are difficult to disentangle as  $h_{[\sigma\sigma]_1}^{\text{naive}} = \Delta_\sigma + 1 = 1.518$ , while  $h_{[\epsilon\epsilon]_0}^{\text{naive}} = \Delta_\epsilon = 1.412$ . For this reason, we cannot simply identify the one point functions and anomalous dimensions of each family from the expansion (3.65). We will instead use the augmented half-inverted correlators from  $\tilde{g}_{\text{naive}}$  to implement a mixing procedure that disentangles the contributions of the three most important double-twist families in the 3D Ising CFT:  $[\sigma\sigma]_0$ ,  $[\sigma\sigma]_1$ , and  $[\epsilon\epsilon]_0$ .

Using the ingredients in section 3.4.3, we can now explain the mixing procedure. We expect a given half-inverted correlator to have the exact form

$$\tilde{g}^c(\bar{z}, \bar{h}) = \sum_f a_f^c(\bar{h}) \bar{z}^{h_f(\bar{h})}, \quad (3.66)$$

where the sum is over families  $f$  once again, with the thermal coefficients in each family given by  $a_f^c(\bar{h})$  and the exact half-twist given by  $h_f(\bar{h})$ . In the 3d Ising CFT

<sup>11</sup>Note that our approach does not lead to the expected  $\log \bar{z}$  terms for every family  $f$ . This is one reason for which considering mixing proves important.

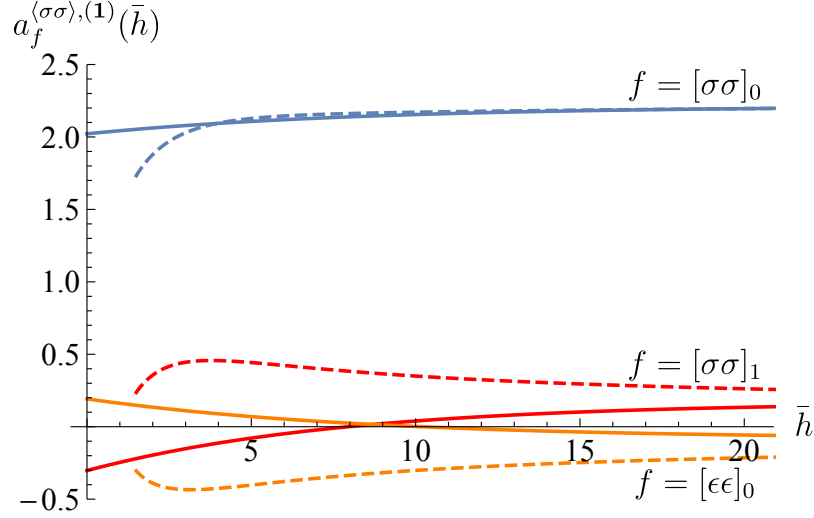


Figure 3.11: The effect of operator mixing for the thermal coefficients in the  $[\sigma\sigma]_0$ ,  $[\sigma\sigma]_1$ , and  $[\epsilon\epsilon]_0$  families. As an example we show the coefficient of  $a_1^{(\sigma\sigma)}$  in the thermal coefficients of each family. The dashed curves represent the predictions made by the inversion formula before implementing operator mixing, while the solid curves represent the post-mixing predictions, with the mixing region  $\mathcal{P}_{\text{mix}} = \{0.05, 0.1, \dots, 0.3\}$ .

we would like to truncate the sum of families to  $f \in \mathcal{F} = \{[\sigma\sigma]_0, [\sigma\sigma]_1, [\epsilon\epsilon]_0\}$ , which, due to their low twist, have the greatest contribution to the two correlators  $\langle\sigma\sigma\rangle$  and  $\langle\epsilon\epsilon\rangle$  in the light-cone limit. We will denote these truncations  $g_{\mathcal{F}}^c(\bar{z}, \bar{h})$ . At small  $\bar{z}$ ,  $g^c(\bar{z}, \bar{h})$  is dominated by the families  $f \in \mathcal{F}$ , and therefore well approximated by  $g_{\mathcal{F}}^c(\bar{z}, \bar{h})$ .

We do not include multi-twist families such as  $[\sigma\sigma\epsilon]$  and  $[\sigma\sigma\sigma\sigma]$  in the sum over  $f$  for two reasons. The first is that they give a small numerical contribution to the flat-space four-point functions  $\langle\sigma\sigma\sigma\sigma\rangle$ ,  $\langle\sigma\sigma\epsilon\epsilon\rangle$ ,  $\langle\epsilon\epsilon\epsilon\epsilon\rangle$ , so it is reasonable to guess that their contribution to thermal two-point functions is also small. The other reason is that we know much less about their anomalous dimensions and OPE coefficients, and thus would not be able to write a suitable ansatz. It will be important to better understand multi-twist operators to improve our techniques in the future.

The thermal coefficients appearing in different correlators are related by ratios of OPE coefficients. For each family, let us pick a thermal coefficient  $a^u(\bar{h})$  from a certain correlator that we would like to parametrize the thermal data of that family by. Given our choice of  $a^u(\bar{h})$ , we can form the matrix  $\lambda_u^c(\bar{z}, \bar{h})$  comprised of appropriate ratios of OPE coefficients such that

$$\tilde{g}_{\mathcal{F}}^c(\bar{z}, \bar{h}) = \lambda_u^c(\bar{z}, \bar{h}) a^u(\bar{h}). \quad (3.67)$$

Specifically, the exact contribution of the families  $[\sigma\sigma]_0$ ,  $[\sigma\sigma]_1$ , and  $[\epsilon\epsilon]_0$  to the half-inverted correlator can be written using,

$$a^u(\bar{h}) = \begin{pmatrix} a_{[\sigma\sigma]_0}^{\langle\sigma\sigma\rangle}(\bar{h}) \\ a_{[\sigma\sigma]_1}^{\langle\sigma\sigma\rangle}(\bar{h}) \\ a_{[\epsilon\epsilon]_0}^{\langle\epsilon\epsilon\rangle}(\bar{h}) \end{pmatrix}. \quad (3.68)$$

Accordingly, we have

$$\lambda_u^c = \begin{pmatrix} \bar{z}^{h_{[\sigma\sigma]_0}(\bar{h})} & \bar{z}^{h_{[\sigma\sigma]_1}(\bar{h})} & \frac{f_{\sigma\sigma[\epsilon\epsilon]_0}(\bar{h})}{f_{\epsilon\epsilon[\epsilon\epsilon]_0}(\bar{h})} \bar{z}^{h_{[\epsilon\epsilon]_0}(\bar{h})} \\ \frac{f_{\epsilon\epsilon[\sigma\sigma]_0}(\bar{h})}{f_{\sigma\sigma[\sigma\sigma]_0}(\bar{h})} \bar{z}^{h_{[\sigma\sigma]_0}(\bar{h})} & \frac{f_{\epsilon\epsilon[\sigma\sigma]_1}(\bar{h})}{f_{\sigma\sigma[\sigma\sigma]_1}(\bar{h})} \bar{z}^{h_{[\sigma\sigma]_1}(\bar{h})} & \bar{z}^{h_{[\epsilon\epsilon]_0}(\bar{h})} \end{pmatrix}. \quad (3.69)$$

We can now understand Eq. (3.65) as an approximation to the contribution of the families correlator,

$$\tilde{g}_{\text{naive}}^c(\bar{z}, \bar{h}) \approx \tilde{g}_{\mathcal{F}}^c(\bar{z}, \bar{h}). \quad (3.70)$$

Note that at large  $\bar{h}$ , due to the decrease in the anomalous dimensions for all three families in  $\mathcal{F}$ , the terms  $(a_f^c)^{\text{naive}}(\bar{h})$  appearing in (3.65) are close to the correct thermal coefficients appearing in (3.67). However, at small values of  $\bar{h}$ , as has been described in section 3.2.2, the anomalous dimensions of operators in the  $[\sigma\sigma]_1$  and  $[\epsilon\epsilon]_0$  become large and thus there is a large  $\bar{z}$ -power mismatch between the terms which  $(a_f^c)^{\text{naive}}(\bar{h})$  in (3.65) and those that include  $a_f^c(\bar{h})$  in (3.66). Thus, all the terms in the naive expansion (3.65) will mix and contribute to the accurate thermal coefficients for all three families in  $\mathcal{F}$ . As previously mentioned, this effect is especially noticeable on families such as  $[\sigma\sigma]_1$  and  $[\epsilon\epsilon]_0$  whose twists are close and whose naive contribution in (3.65) are difficult to distinguish at small  $\bar{h}$ . For this reason, we will refer to (3.70) as the mixing equation.

In solving for the mixed coefficients  $a^u(\bar{h})$  we have conveniently written (3.70) in matrix form. Thus, for each value of  $\bar{h}$  that we are interested in, we can treat the mixing equation as an over-determined linear system. Concretely, we can impose that (3.70) be satisfied for several values of  $\bar{z}$  from some set of values  $\mathcal{P}_{\text{mix}}$ . Of course, due to the truncation of the expansion (3.65), we get an overdetermined system of equations and it is impossible to satisfy the mixing equation for all values of  $\bar{z}$ . However, as one can see from figure 3.4, when choosing,

$$\mathcal{P}_{\text{mix}} = \{0.05, 0.1, \dots, \bar{z}_{\text{max}}\}, \quad \text{with } \bar{z}_{\text{max}} \in \{0.15, 0.2, \dots, 0.6\}. \quad (3.71)$$

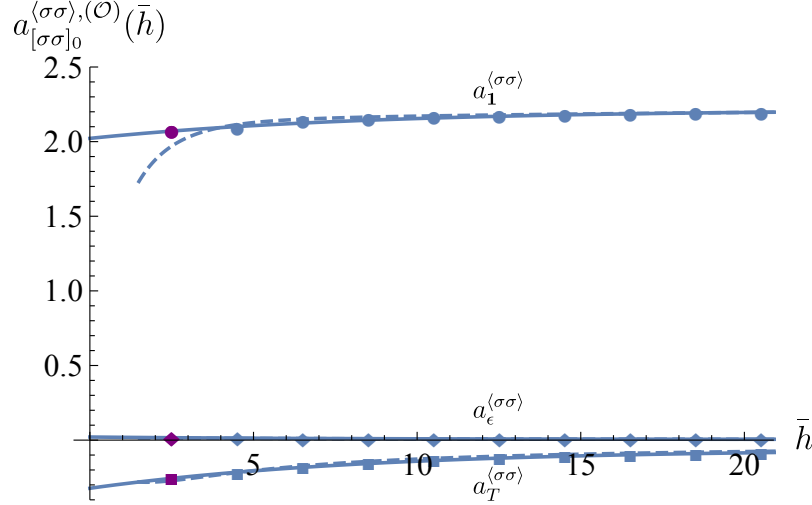


Figure 3.12: Estimates for the terms multiplying  $a_1^{(\sigma\sigma)}$ ,  $a_\epsilon^{(\sigma\sigma)}$ , and  $a_T^{(\sigma\sigma)}$  in the thermal coefficients  $a_{[\sigma\sigma]_0}^{(\sigma\sigma),(\mathcal{O})}(\bar{h})$ . The dashed blue curves are the predictions from the inversion formula before performing operator mixing while the solid curves are the predictions after accounting for operator mixing. The blue dots represent the post-mixing predictions for each local operator with  $J \geq 4$  in the  $[\sigma\sigma]_0$  family. The purple dots are the extrapolation of the thermal coefficient to the stress-energy tensor.

our results are robust under different choices of  $\mathcal{P}_{\text{mix}}$  (see figure 3.4).<sup>12</sup> Thus, we solve for each term proportional to each unknown  $a_{1,\epsilon,T}^c$  in  $a^u(\bar{h})$  using the method of least squares for each value of  $\bar{h}$ .<sup>13</sup> To exemplify our procedure, in figure 3.11, we show how the coefficients multiplying  $a_1^{(\sigma\sigma)}$  are affected by mixing.

We now use the estimates obtained from mixing to understand the thermal coefficients of operators with small spin. Since  $T$  is a member of the  $[\sigma\sigma]_0$  family, we can use our calculation of  $a_{[\sigma\sigma]_0}^{(\sigma\sigma)}$  to constrain  $a_T^{(\sigma\sigma)}$ . We thus extrapolate our results for the thermal coefficients of the  $[\sigma\sigma]_0$  family down to  $J = 2$  (see figure 3.12). After mixing, the thermal coefficient of  $T$  is computed in terms of the unknowns as

$$a_{[\sigma\sigma]_0}^{(\sigma\sigma)}(\bar{h} = 2.5) = \left( \frac{d\bar{h}}{dJ} \right) \Big|_{\bar{h}=2.5} \left( 2.07a_1^{(\sigma\sigma)} + 0.0163a_T^{(\sigma\sigma)} - 0.257a_\epsilon^{(\sigma\sigma)} \right). \quad (3.72)$$

Using the known anomalous dimensions for the  $[\sigma\sigma]_0$  family, we can compute  $d\bar{h}/dJ$ .<sup>14</sup>

<sup>12</sup>This remains true as long as  $\bar{z} \gg O(1)e^{-1/\delta_{\mathcal{O}}}$ , where  $\delta_{\mathcal{O}}$  is the average anomalous dimension at a certain value of  $\bar{h}$  for the three operator families that we are considering.

<sup>13</sup>We give an equal weight to each value of  $\bar{z}$  in the least square fit.

<sup>14</sup>Since [20] provides accurate values for the anomalous dimensions of all operators in  $[\sigma\sigma]_0$ ,  $[\sigma\sigma]_1$ , and  $[\epsilon\epsilon]_0$ , we can use a fit to the numerical results to accurately obtain  $d\bar{h}/dJ$ . At the  $\bar{h}$  values of local operators, the fit strongly agrees with the analytical predictions for the anomalous dimensions.



Of course, (3.72) should be equal to  $a_T^{\langle\sigma\sigma\rangle}$  itself! Solving for  $a_T^{\langle\sigma\sigma\rangle}$ , we have

$$a_T^{\langle\sigma\sigma\rangle} = 2.136a_1^{\langle\sigma\sigma\rangle} - 0.265a_\epsilon^{\langle\sigma\sigma\rangle}. \quad (3.73)$$

Recall that we can normalize all the thermal coefficients by that of the unit operator, thus setting  $a_1^{\langle\sigma\sigma\rangle} = 1$ . Therefore, we have only a single unknown left:  $a_\epsilon^{\langle\sigma\sigma\rangle}$ . We have successfully approximated the thermal coefficients of all operators in the three low-twist families of interest in terms of a single unknown!

A similar issue presents itself when one considers low-spin operators in the higher-twist families  $[\sigma\sigma]_1$  and  $[\epsilon\epsilon]_0$ . At spin 0 and 2, there are only the two operators  $\epsilon'$  and  $T'$ ; both belong to the  $[\sigma\sigma]_1$  family, whereas the  $[\epsilon\epsilon]_0$  family has no such operators [20]. Therefore, our mixing procedure does not work for these operators. However, it is crucial to estimate the thermal coefficients of  $\epsilon'$  and  $T'$  for solving the KMS condition. We have found it best to extract the thermal coefficients of the low-spin members of the  $[\sigma\sigma]_1$  family by extrapolating the mixed thermal coefficients down to small  $\bar{h}$  by a simple fit. This is motivated by results from the flat-space data where the OPE coefficients and anomalous dimensions of these two operators appear to lie on smooth curves with all other members of the  $[\sigma\sigma]_1$  family. The estimates for  $a_{\epsilon'}^{\langle\sigma\sigma\rangle}$  and  $a_{T'}^{\langle\sigma\sigma\rangle}$  obtained by performing such a fit can be extrapolated using figure 3.11.

### 3.4.5 Solving for $b_{\mathcal{O}}$

Finally, we will input the thermal coefficients we've obtained for the three families  $[\sigma\sigma]_0$ ,  $[\sigma\sigma]_1$ , and  $[\epsilon\epsilon]_0$  into the  $\langle\sigma\sigma\rangle$  correlator, and impose the KMS condition to determine the last unknown  $a_\epsilon^{\langle\sigma\sigma\rangle}$ . We do this via the following steps. We first evaluate the correlator minus its image under crossing in various regions of the  $(z, \bar{z})$  plane,  $\mathcal{P}_{\text{KMS}}$ . To determine  $a_\epsilon^{\langle\sigma\sigma\rangle}$ , we attempt to minimize:

$$\Lambda_{\text{KMS}}(a_\epsilon^{\langle\sigma\sigma\rangle}) = \sum_{(z, \bar{z}) \in \mathcal{P}_{\text{KMS}}} (g(z, \bar{z}) - g(1 - z, 1 - \bar{z}))^2. \quad (3.74)$$

By setting  $\partial\Lambda_{\text{KMS}}(a_\epsilon^{\langle\sigma\sigma\rangle})/\partial a_\epsilon^{\langle\sigma\sigma\rangle} = 0$  we can determine the results obtained in (3.24).

The thermal inversion formula guarantees that the KMS condition is satisfied in the proximity of the point  $(z, \bar{z}) = (0, 1)$ . Thus, if one tries to approximately impose KMS solely in that region, there would be an almost flat direction associated to the unknown  $a_\epsilon^{\langle\sigma\sigma\rangle}$  and, consequently, our numerical estimates would be inaccurate. However, if one imposes KMS in a region where the OPE does not converge well the results would once again be inaccurate. Thus, we try to impose that KMS is approximately satisfied in an intermediate region and check for robustness under changes of  $\mathcal{P}_{\text{KMS}}$  within this

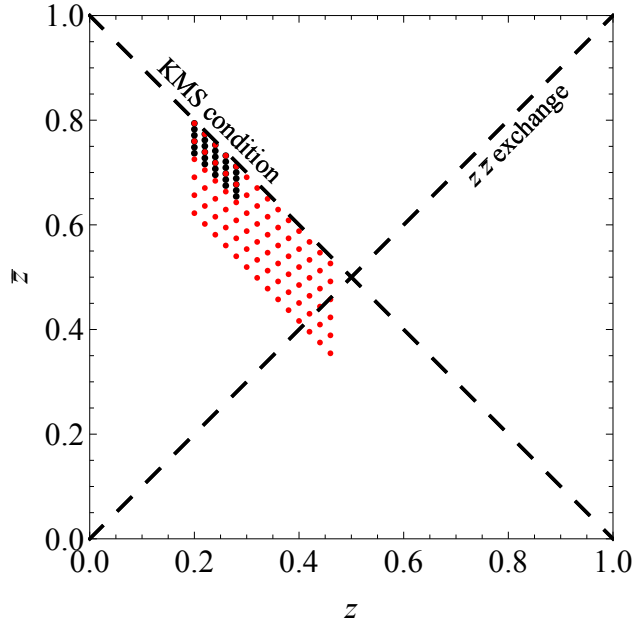


Figure 3.13: Example of the smallest (black) and largest (red) regions in  $(z, \bar{z})$  where we minimize the square of the difference of the two-point function and its periodic image, as in (3.74).

intermediate regime. We find that our results are indeed robust for various choices of the  $(z, \bar{z})$  region  $\mathcal{P}_{\text{KMS}}$  and, as mentioned before, for the choice of  $\bar{z}$  values  $\mathcal{P}_{\text{mix}}$  which are used to perform the mixing of the three families. To emphasize this, in figure 3.4, we show a spread of the thermal coefficients obtained by minimizing (3.74) for the values of  $\mathcal{P}_{\text{mix}}$  in (3.71) and for values of  $\mathcal{P}_{\text{KMS}}$  ranging between the two regions showed in (3.13). While the value of  $a_\epsilon^{(\sigma\sigma)}$  varies by at most  $\sim 10\%$  between any two choices of  $\mathcal{P}_{\text{mix}}$  and  $\mathcal{P}_{\text{KMS}}$ , the thermal coefficients for all other operators exhibit a much lower variance.<sup>15</sup> For instance, the stress energy tensor thermal coefficient varies by  $\sim 5\%$ , while the thermal coefficient of the spin-4 operator  $[\sigma\sigma]_{0,\ell=4}$  varies by  $\sim 1\%$ . To test how well the crossing equation is satisfied on the Euclidean thermal cylinder we plot the difference

$$\delta g_{\text{KMS}}(\tau, x) = g(x, 1 + \tau) - g(x, \tau), \quad (3.75)$$

in figure 3.6. The KMS condition is very close to being satisfied in the regime in which both the points  $(x, \tau)$  and  $(x, 1 + \tau)$  are close to the origin of the s-channel OPE,  $(0, 0)$ . For instance, we find that  $\delta g_{\text{KMS}}(-1/4, 1/4)/g(-1/4, 1/4) = 0.0037$ . This shows the great extent through which one could use the thermal inversion formula to

<sup>15</sup>This is partly due to the fact that the contribution of the unit operator dominates the thermal coefficients of higher spin operators.

systematically solve the KMS condition or, equivalently, solve the “crossing-equation” of El-Showk and Papadodimas [38].

### **Acknowledgements**

We thank Raghu Mahajan and Eric Perlmutter for collaboration in the early stages of this project and many stimulating discussions on finite-temperature physics. We also thank M. Hasenbusch for providing useful references and for sharing unpublished Monte-Carlo results through private correspondence. We additionally thank Tom Hartman and Douglas Stanford for discussions. DSD and MK are supported by Simons Foundation grant 488657 (Simons Collaboration on the Nonperturbative Bootstrap), a Sloan Research Fellowship, and a DOE Early Career Award under grant No. DE-SC0019085. LVI is supported by Simons Foundation grant 488653.

## SHOCKS, SUPERCONVERGENCE, AND A STRINGY EQUIVALENCE PRINCIPLE

<sup>1</sup>M. Kolođlu, P. Kravchuk, D. Simmons-Duffin, and A. Zhiboedov, “Shocks, Superconvergence, and a Stringy Equivalence Principle”, (2019), [arXiv:1904.05905](https://arxiv.org/abs/1904.05905) [[hep-th](#)].

### 4.1 Introduction

In General Relativity (GR), particles follow geodesics regardless of their polarizations or internal composition. This is sometimes called the “strong equivalence principle” [138]. However, in the presence of non-minimal (higher-derivative) couplings, this principle is no longer true — the path of a particle can depend on its polarization and is not given by a geodesic. Such modifications of GR are known to be in tension with causality and unitarity.<sup>1</sup>

A simple example is the propagation of a probe particle through a gravitational shock (gravitational field of a highly-boosted particle). In GR, propagation through a shock leads to a velocity kick and a Shapiro time delay. By contrast, in theories with non-minimal gravitational couplings, there can be gravitational birefringence: depending on the polarization of the probe particle, the effect of the shock can be different. Moreover, for certain polarizations, the probe particle can experience a time advance [96]. By arranging many shocks one after the other, one can accumulate the time advances and produce macroscopic violations of asymptotic causality. The restoration of causality requires an infinite set of massive higher-spin particles. It was argued in [96] that the masses of these higher-spin particles must be related to the scale that

---

<sup>1</sup>In quantum field theory, causality is a statement about commutativity of local operators at spacelike-separated points. In gravitational theories, we do not have local operators but the asymptotic structure of the gravitational field is weakly coupled and relatively simple. We can therefore introduce gravitational field operators at the asymptotic boundary of spacetime and impose their commutativity at spacelike separations. This leads to a notion of asymptotic causality [139]. In AdS/CFT, this becomes a familiar statement about commutativity of local CFT operators at spacelike-separated points on the boundary of AdS. In flat space, it is related to the rate of growth of the amplitude in the forward limit [96].

enters the modified gravitational coupling<sup>2</sup>

$$\alpha_{GB} \lesssim \frac{1}{m_{gap}^2}. \quad (4.1)$$

Indeed, this is what happens in string theory, where the higher-spin particles are string excitations. Similar bounds on three-point couplings were derived in [96–99, 140, 141]. A common feature of these arguments is the lack of a sharp equality relating the non-minimal couplings to the extra degrees of freedom required for causality.

In this work, we provide such an equality between  $\alpha_{GB}$  and contributions of massive states in a general gravitational theory. We note that non-minimal gravitational couplings introduce another feature that is absent in GR, namely non-commutativity of coincident gravitational shocks.<sup>3</sup> This is another violation of the strong equivalence principle. Indeed, as we review below, geodesics are insensitive to the ordering of gravitational shocks. On the other hand, for theories with non-minimal gravitational couplings, the effect of propagation through multiple shocks depends on the ordering of the shocks. What is less trivial is that this effect can be traced to pathological behavior of the scattering amplitude in the Regge limit. We find that the converse is also true: in any UV-complete gravitational theory, soft Regge behavior guarantees that coincident gravitational shocks must commute. This can be readily checked in tree-level string theory.

Therefore, we suggest that a weaker “stringy” equivalence principle does hold in general UV-complete gravitational theories: coincident gravitational shocks commute. In contrast to the causality discussion above, commutativity of coincident shocks leads to quantitative sum rules that equate the size of non-minimal couplings to the extra degrees of freedom that are present in the theory.

In section 4.2, we explain how commutativity of coincident shocks is equivalent to boundedness of amplitudes  $\mathcal{A}(s, t)$  in the Regge limit ( $t \rightarrow \infty$  with fixed  $s$ ). Specifically, shocks with spins  $J_1$  and  $J_2$  commute if and only if the Regge intercept of the theory  $J_0$  satisfies<sup>4</sup>

$$J_1 + J_2 > J_0 + 1. \quad (4.2)$$

---

<sup>2</sup>The subscript GB stands for the common Gauss-Bonnet modification of GR, but we mean it more generally as a statement about any non-minimal gravitational coupling.

<sup>3</sup>A shock is a region of curvature localized on a null surface. We say that two shocks become coincident in the limit that their null surfaces coincide.

<sup>4</sup>The Regge intercept depends on the value of the Mandelstam variable  $s$ , but we suppress that dependence here for simplicity.

For example, gravitational (spin-2) shocks commute if  $J_0 < 3$ . It has been argued that consistent weakly-coupled gravity theories in flat space actually obey  $J_0 \leq 2$  [96], so gravitational shocks certainly commute in this case (as do higher-spin shocks).

In section 4.2.2, we show that commutativity of coincident shocks is equivalent to certain dispersion relations called “superconvergence” sum rules [142, 143]. When applied to gravitational amplitudes, these sum rules express (squares of) non-minimal couplings in terms of three-point couplings of massive states. This shows that non-minimal couplings cannot exist without additional massive states, recovering a result from [96] in a different way. In subsequent sections, we study superconvergence sum rules in several examples, showing explicitly how they are obeyed in GR (section 4.2.3), disobeyed in higher-derivative gravity theories (section 4.2.4), but obeyed in string theories (sections 4.2.5 and 4.2.6). Indeed, the failure of superconvergence sum rules in higher-derivative theories like Gauss-Bonnet gravity gives an efficient way to show that they violate the Regge boundedness condition  $J_0 < 3$  without computing full amplitudes in those theories.

In AdS, commutativity of coincident shocks translates into a statement that can be proven nonperturbatively using CFT techniques. As we review in section 4.3, we can create shocks by integrating local operators along null lines on the boundary of AdS. It is most natural to study propagation through AdS shocks using observables called “event shapes” [31, 144–147], which we review in sections 4.3.2 and 4.3.3. Commutativity of coincident shocks becomes the statement that two null-integrated operators commute when placed on the same null plane:

$$\left[ \int_{-\infty}^{\infty} dv_1 \mathcal{O}_{1;v\dots v}(u=0, v_1, \vec{y}_1), \int_{-\infty}^{\infty} dv_2 \mathcal{O}_{2;v\dots v}(u=0, v_2, \vec{y}_2) \right] \stackrel{?}{=} 0. \quad (4.3)$$

Here, we use lightcone coordinates  $ds^2 = -du dv + d\vec{y}^2$ . The CFT operators lie on the same plane  $u = 0$  but at different transverse positions  $\vec{y}_1, \vec{y}_2 \in \mathbb{R}^{d-2}$ . Furthermore, their vector indices are aligned with the direction of integration (the  $v$ -direction). For example, when  $\mathcal{O}_1$  and  $\mathcal{O}_2$  are both the stress-tensor  $T_{\mu\nu}$ , (4.3) becomes a commutator of average null energy operators. An average null energy operator on the boundary creates a gravitational shock in the bulk.

The commutativity statement (4.3) might seem obvious, since  $\mathcal{O}_1$  and  $\mathcal{O}_2$  are spacelike-separated everywhere along their integration contours. However, the spacelike separation argument is too quick, and is actually *wrong* in some examples (see appendix C.2). The problem is that the positions of  $\mathcal{O}_1$  and  $\mathcal{O}_2$  coincide at the endpoints

of their integration contours (in an appropriate conformal frame), and one must be careful to analyze what happens there.

We perform a careful analysis of the commutator (4.3) in section 4.4, explaining the circumstances when it is well-defined (but not necessarily zero), and the additional conditions required for it to vanish. A necessary condition for vanishing is

$$J_1 + J_2 > J_0 + 1, \quad (4.4)$$

where  $J_1$  and  $J_2$  are the spins of  $\mathcal{O}_1$  and  $\mathcal{O}_2$ , and  $J_0$  is the Regge intercept of the CFT [25, 28, 148–150]. In chapter 5, we also show that a non-vanishing commutator necessarily leads to a Regge pole at  $J = J_1 + J_2 - 1$ .

In section 4.4.2.4, we prove that  $J_0 \leq 1$  in nonperturbative CFTs (generalizing arguments of [25, 151] to spinning correlators). This establishes commutativity of average null energy operators in nonperturbative theories<sup>5</sup>

$$\left[ \int_{-\infty}^{\infty} dv_1 T_{vv}(u=0, v_1, \vec{y}_1), \int_{-\infty}^{\infty} dv_2 T_{vv}(u=0, v_2, \vec{y}_2) \right] = 0, \quad (4.5)$$

for  $\vec{y}_1 \neq \vec{y}_2$ . For large- $N$  theories in the planar limit, the bound on chaos [84] implies that  $J_0 \leq 2$ . Thus, average null energy operators commute in planar theories as well. However, commutativity can be lost at higher orders in large- $N$  perturbation theory (and only recovered nonperturbatively).

The condition (4.4) is in direct analogy to the condition (4.2) in flat space. When it holds, one can derive analogous superconvergence sum rules for CFTs by evaluating event shapes of (4.3). In section 4.5, we show how to compute these event shapes using the conformal block decomposition, expressing them as sums over intermediate CFT states.<sup>6</sup> The relevant conformal blocks can be computed explicitly in any spacetime dimension. The blocks for stress tensors agree perfectly with our bulk calculations from section 4.3. The result is an infinite set of superconvergence sum rules for CFT data.

Of course, the usual crossing symmetry equations [9, 10] are also an infinite set of sum rules for CFT data. However, CFT superconvergence sum rules have some

---

<sup>5</sup>Commutativity of average null energy (ANEC) operators is important for understanding information-theoretic aspects of CFTs [152, 153], and plays a central role in the recently proposed BMS symmetry in CFT [154]. As far as we are aware, it is usually argued for using the fact that the stress tensors are spacelike separated. Our analysis closes a loophole in this argument.

<sup>6</sup>The conformal blocks we study in this work are for the “lightray-local  $\rightarrow$  lightray-local” channel. This is the conventional OPE. By contrast, in chapter 5 we develop a new type of OPE that allows one to describe the “lightray-lightray  $\rightarrow$  local-local” channel.

nice properties. In large- $N$  theories in the planar limit, they get contributions only from single-trace operators and non-minimal three-point structures (i.e. three-point structures that do not arise from GR in AdS). Thus, one obtains expressions for non-minimal three-point coefficients in terms of massive “stringy” states, analogous to superconvergence sum rules in flat space.

As an example, in 4d CFTs, we find the superconvergence sum rules

$$\begin{aligned} (t_4 + 2t_2)^2 &= \sum_{\phi} |\lambda_{TT\phi}|^2 \frac{15 \cdot 2^4 \pi^4 \Gamma(\Delta_{\phi} - 1) \Gamma(\Delta_{\phi})}{C_T \Gamma(4 - \frac{\Delta_{\phi}}{2})^2 \Gamma(2 + \frac{\Delta_{\phi}}{2})^6} + \text{non-scalar}, \\ (t_4 + 2t_2)^2 &= - \sum_{\phi} |\lambda_{TT\phi}|^2 \frac{360^2 \pi^4 \Gamma(\Delta_{\phi} - 1) \Gamma(\Delta_{\phi})}{7 C_T \Gamma(4 - \frac{\Delta_{\phi}}{2})^2 \Gamma(2 + \frac{\Delta_{\phi}}{2})^6} + \text{non-scalar}, \end{aligned} \quad (4.6)$$

along with an infinite number of others. Here,  $t_2$  and  $t_4$  are coefficients of non-Einstein three-point structures in the correlator  $\langle TTT \rangle$ , see [31]. For example, in 4d  $\mathcal{N} = 1$  theories, we have  $t_2 = \frac{6(c-a)}{c}$  and  $t_4 = 0$ . The sums in (4.6) run over scalar operators  $\phi$  with dimensions  $\Delta_{\phi}$  and OPE coefficients  $\lambda_{TT\phi}$  in the  $T \times T$  OPE. The term “non-scalar” refers to contributions of operators with spin  $J \geq 2$ , not including the stress-tensor (whose contribution is on the left-hand side of (4.6)). For simplicity, we have written only the sum rules that get contributions from scalar operators. Other sum rules give expressions for other combinations of  $t_2$  and  $t_4$ , but involve exclusively non-scalars. The factors  $\Gamma(4 - \frac{\Delta_{\phi}}{2})^{-2}$  in (4.6) ensure that contributions of double-trace operators are suppressed by  $O(1/N^4)$  in the large- $N$  limit. This is a generic feature of superconvergence sum rules and it stems from the fact that they can be written in terms of a double-discontinuity [25]. In particular, one can see explicitly that if no single-trace operators are present other than the stress tensor, then  $t_2$  and  $t_4$  must vanish in the planar limit.<sup>7,8</sup>

In [156], it was conjectured that for any CFT with a large gap  $\Delta_{\text{gap}}$  in the spectrum of spin  $J \geq 3$  single-trace operators (“stringy states”), non-minimal couplings in the effective bulk Lagrangian should be suppressed by powers of  $1/\Delta_{\text{gap}}$ . In section 4.6.1, we argue (non-rigorously) that the contributions of stringy states to superconvergence sum rules are suppressed by powers of  $1/\Delta_{\text{gap}}$ , and this establishes the conjecture of [156] (in the case of three-point couplings) in a way different from the arguments of [96–99, 140, 141]. We conclude in section 4.6.2.

<sup>7</sup>Strictly speaking the above equations only fix  $t_4 + 2t_2$ , but there are also linearly independent constraints from other components of the sum rule.

<sup>8</sup>Our methods for computing event shapes may be also useful for investigating positivity conditions. In [155] it was shown that positivity of multi-point energy correlators also leads to vanishing non-minimal couplings, e.g.  $t_2, t_4 = 0$  for  $\langle TTT \rangle$ , in theories with only gravitons and photons in the bulk.



In appendix C.1, we give more details about superconvergence sum rules in flat space. In appendix C.2, we give an example of the phenomenon of “detector cross-talk,” where naïvely spacelike light-ray operators can fail to commute. In the remaining appendices we provide details about sum rules in CFT.

**Note added:** After this work had been largely completed, we became aware of [157] which has some overlap with this paper.

## 4.2 Shocks and superconvergence in flat space

In General Relativity (GR), test bodies follow geodesics, and it follows that the effects of coincident shocks are commutative. To see this, consider a shockwave in flat space [158, 159]

$$ds^2 = -du dv + \frac{4\Gamma(\frac{D-4}{2})}{\pi^{\frac{D-4}{2}}} \frac{Gp^v}{|\vec{y}|^{D-4}} \delta(u) du^2 + d\vec{y}^2, \quad (4.7)$$

and let us study null geodesics in this geometry.<sup>9</sup>

A shockwave is a gravitational field created by a relativistic source. The Aichelburg-Sexl geometry (4.7) is an exact solution of Einstein’s equations with a stress-energy source  $T_{uu}(u, \vec{y}) = p^v \delta(u) \delta^{(D-2)}(\vec{y})$  localized on a null geodesic. The only non-trivial metric component  $h_{uu}(u, \vec{y}) = \frac{4\Gamma(\frac{D-4}{2})}{\pi^{\frac{D-4}{2}}} \frac{Gp^v}{|\vec{y}|^{D-4}} \delta(u)$  is a solution of the Laplace equation in the transverse plane parametrized by  $\vec{y}$  with a non-trivial source

$$\square_{\vec{y}} h_{uu}(u, \vec{y}) = -16\pi G T_{uu}(u, \vec{y}). \quad (4.8)$$

Famously, (4.7) continues to be an exact solution in any higher derivative theory of gravity as well [161]. Higher derivative interactions, however, lead to nontrivial corrections to the propagation of probe particles on the shockwave backgrounds.

Consider a probe particle on the shockwave background that follows a null geodesic. We can parameterize the null geodesic by  $u$ . Suppose the geodesic approaches the shock at impact parameter  $\vec{y}(u=0) = \vec{b}$ . Crossing the shock causes both a Shapiro time delay

$$v_{\text{after}} - v_{\text{before}} = \frac{4\Gamma(\frac{D-4}{2})}{\pi^{\frac{D-4}{2}}} \frac{Gp^v}{|\vec{b}|^{D-4}}, \quad (4.9)$$

---

<sup>9</sup>Obtaining such solutions from a smooth Cauchy data (or limits thereof) in gravitational theories can be subtle and was discussed for example in [160]. For us, the solution (4.7) is a convenient way to think about the high energy limit of gravitational scattering and per se does not play any role.

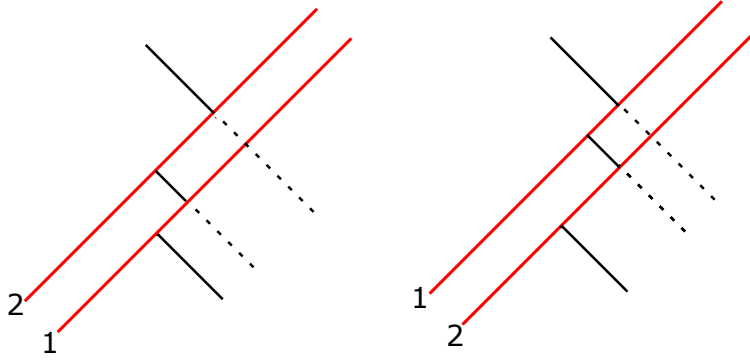


Figure 4.1: The probe geodesic is denoted by a black line and shock waves by red lines. Dashed lines mark time delay associated to each shock. In General Relativity propagation through a pair of closely situated shockwaves is commutative, namely the overall effect does not depend on the order of the shocks. This is no longer true in theories with higher derivative corrections. We argue that commutativity must hold in any UV complete theory.

and a velocity kick in the transverse plane due to gravitational attraction

$$\dot{\vec{y}}_{\text{after}} - \dot{\vec{y}}_{\text{before}} = -\frac{4\Gamma(\frac{D-2}{2})}{\pi^{\frac{D-4}{2}}} Gp^v \frac{\vec{b}}{|\vec{b}|^{D-2}}. \quad (4.10)$$

The same result can be obtained by analyzing wave equations on the shockwave backgrounds or using scattering amplitudes (as we review in detail below). In General Relativity the effect of a shockwave on a probe particle does not depend on the polarization of the particle. This is no longer true in higher-derivative theories of gravity. This can lead to Shapiro time advances and violations of asymptotic causality [96].

We can also consider a more complicated geometry constructed by a superposition of relativistic sources localized at different retarded times  $u_i$  and transverse positions  $\vec{b}_i$ . The exact gravitational field created by such a superposition is simply a sum of the shockwaves (4.7).

If a probe particle follows a geodesic, then propagation through a series of closely situated shocks leads to an additive effect. In particular, the result does not depend on the ordering of shocks and is commutative (figure 4.1). This is no longer true in theories with higher derivative corrections. In this case, the result of the propagation through a pair of closely situated shocks will generically depend on their ordering.

In this section, we show that commutativity of shockwaves is directly related to the Regge limit. In particular, we argue that in any UV complete theory (gravitational or not) the shock waves must commute. Therefore, any non-commutativity of shocks

present in the low energy effective theory should be exactly canceled by the extra degrees of freedom. The mathematical expression of this fact is encapsulated in the superconvergence sum rules which we describe in detail below.

### 4.2.1 Shockwave amplitudes

It will be instructive for our purposes to restate the discussion of the previous section in terms of scattering amplitudes. This has been done in [96], whose setup we review momentarily. In the simplest case of a propagation through a single shock, we consider an absorption of a virtual graviton by a probe particle

$$g^* X \rightarrow X', \quad (4.11)$$

where  $X$  and  $X'$  describe a particle in an initial and final state (these could be different) and  $g^*$  stands for a virtual graviton that is emitted from some extra source that we do not write down explicitly.<sup>10</sup> We denote the corresponding scattering amplitude  $\mathcal{A}_{g^* X \rightarrow X'}$ .

To discuss causality, we consider the high-energy behavior of the scattering amplitude in the forward direction, see [96]. A convenient choice of momenta and polarization for the process (4.11) is

$$\begin{aligned} p_X &= \left( p^u, \frac{\vec{q}^2}{4p^u}, -\frac{\vec{q}}{2} \right), & p_{X'} &= \left( -p^u, -\frac{\vec{q}^2}{4p^u}, -\frac{\vec{q}}{2} \right), \\ p_{g^*} &= (0, 0, \vec{q}), & \epsilon_{g^*} &= (0, -2, 0). \end{aligned} \quad (4.12)$$

Here, we use lightcone coordinates  $(u, v, \vec{y})$  with metric

$$ds^2 = -du dv + d\vec{y}^2, \quad \vec{y} \in \mathbb{R}^{D-2}. \quad (4.13)$$

The virtuality of the graviton is  $\vec{q}^2$ .

An interesting phenomenon occurs when studying this process in impact parameter space. In this case, the virtual graviton emitted by a source comes with the following wavefunction

$$\int d^{d-2} \vec{q} \frac{e^{i\vec{b} \cdot \vec{q}}}{\vec{q}^2} \mathcal{A}_{g^* X \rightarrow X'}(p^u, \vec{q}). \quad (4.14)$$

The remarkable property of this integral is that it can be evaluated by taking the residue at  $\vec{q}^2 = 0$ , so that the virtual graviton becomes on-shell! The on-shell condition

---

<sup>10</sup>In other words, the full description of (4.11) is in terms of a four-point amplitude.

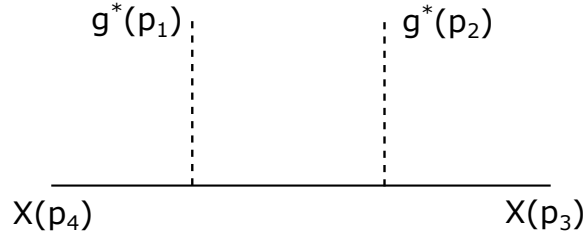


Figure 4.2: An elastic scattering of a probe particle and an on-shell shock state graviton. We will argue that the Regge behavior of this amplitude in consistent theories of gravity is such that gravitational shockwaves always commute. We adopt a CFT correlator-like prescription where the time in the diagram goes from right to left.

$\vec{q}^2 = 0$  requires that  $\vec{q}$  becomes complex. The result is that the physical phase shift  $\delta(p^v, \vec{b})$  is computed by a scattering amplitude in spacetime with mixed signature (making  $\vec{q}$  complex corresponds to a second Wick rotation). More precisely, we get

$$\delta(p^v, \vec{b}) \propto \mathcal{A}_{g^*X \rightarrow X'}(p^u, -i\partial_{\vec{b}}) \frac{1}{|\vec{b}|^{D-4}}, \quad (4.15)$$

where  $\mathcal{A}_{gX \rightarrow X'}$  is now a usual on-shell amplitude, albeit evaluated in slightly unusual kinematics. Note that the on-shell condition  $\vec{q}^2 = 0$  is reflected in (4.15) by the fact that  $\frac{1}{|\vec{b}|^{D-4}}$  is a harmonic function, so it is killed by  $(-i\partial_{\vec{b}})^2$ . The causality discussion of [96] then focuses on the properties of the on-shell amplitude  $\mathcal{A}_{g^*X \rightarrow X'}$ , and shows that in gravitational theories with higher derivative corrections it can lead to causality violations unless new degrees of freedom are added.

We would like to emphasize that the whole discussion can be formulated in terms of on-shell amplitudes with shockwave gravitons  $g^*$  and their properties. This is particularly useful in a gravitational theory, where there is no clear definition of off-shell observables. Therefore it is desirable to formulate the problem purely in terms of on-shell observables. This is the path we follow below.

In this paper we will be interested in elastic scattering of a probe  $X$  and two shockwave gravitons  $g^*$

$$g^*(p_2)X(p_3) \rightarrow g^*(p_1)X(p_4), \quad (4.16)$$

see figure 4.2. We choose the final state of the probe to be  $X$  for simplicity, but the whole discussion goes through intact for any other one-particle state  $X'$ .

A convenient choice of momenta is

$$\begin{aligned} p_1 &= (0, -p^v, \vec{q}_1), & p_2 &= (0, p^v, \vec{q}_2), \\ p_3 &= (p^u, 0, -\vec{q}_2), & p_4 &= (-p^u, 0, -\vec{q}_1), \end{aligned} \quad (4.17)$$

and again the shockwave gravitons have polarizations  $\epsilon_{g^*} = (0, -2, 0)$  as in (4.7). As above, we can think of each shockwave graviton as originating from a pair of particles that we have not written explicitly. In this way,  $\mathcal{A}_{g^*X \rightarrow g^*X}$  can be thought of as an economical description of the relevant part of the six-point amplitude. An on-shell condition is  $\vec{q}_1^2 = \vec{q}_2^2 = 0$ . As before this naturally arises in the impact parameter transform

$$\int d^{d-2} \vec{q}_1 \int d^{d-2} \vec{q}_2 e^{i\vec{q}_1 \cdot \vec{b}_1} e^{i\vec{q}_2 \cdot \vec{b}_2} \frac{1}{\vec{q}_1^2} \frac{1}{\vec{q}_2^2} \mathcal{A}_{g^*X \rightarrow g^*X}. \quad (4.18)$$

Below, we simply study the on-shell amplitude  $\mathcal{A}_{g^*X \rightarrow g^*X}$  as an object on its own, without referring to impact parameter space.<sup>11</sup>

One new feature of (4.17) compared to (4.12) is that the shockwave graviton transfers to the probe a large longitudinal momentum  $p^v$ . In [96] the shockwaves were carefully separated in the  $u$  direction such that  $p^v$  is effectively set to 0 and the amplitude  $\mathcal{A}_{g^*X \rightarrow g^*X}$  reduces to a product of a one-shock interactions  $\mathcal{A}_{g^*X \rightarrow X'} \mathcal{A}_{g^*X' \rightarrow X}$ . Our regime of interest is the opposite, namely we would like to put the shockwaves on top of each other. This effectively leads to studying  $\mathcal{A}_{g^*X \rightarrow g^*X}$  at arbitrarily large values of  $p^v$ .

### 4.2.2 Shock commutativity and the Regge limit

An important class of shockwave amplitudes arises when the shockwaves are localized on null planes. Such objects provide a natural translation into the language

<sup>11</sup>In a gravitational theory when trying to separate a probe from the rest of the system we should check that the joint system does not form a black hole. In particular, we would like the impact parameter  $b$  in the discussion above to be larger than the Schwarzschild radius of the system  $r_S^{D-3} = \sqrt{p^u p^v} G_N$ . In momentum space this implies that  $\frac{r_S^2}{b^2} < 1$ , where  $\vec{q}_1, \vec{q}_2 \sim \frac{1}{b}$ . This implies that for given  $\vec{q}_1, \vec{q}_2$  we can only consider  $\frac{p^u p^v}{m_{P_i}^2} < (m_{P_i}^2 b^2)^{D-3}$ . For energies  $\frac{p^u p^v}{m_{P_i}^2} > (m_{P_i}^2 b^2)^{D-3}$  the picture of a probe propagating through a shockwave is not the correct description of physics. This does not present a problem in a tree-level gravitational theory when we work to leading order in  $G_N$  and thus can make it arbitrarily small (or, similarly, if we consider gravitational deep inelastic scattering in a gapped QFT, see section 4.2.8). At finite  $G_N$ , we can still formally define the amplitude  $\mathcal{A}_{g^*X \rightarrow g^*X}$  in kinematics (4.17) with complex null transverse momenta, but its physical interpretation at arbitrarily high energies is less clear. We ignore this subtlety below and only consider tree-level examples in flat space, though we believe everything we say holds at finite  $G_N$  as well. This problem does not appear in our CFT discussion where  $g^*$  corresponds to a light-ray operator insertion in a boundary CFT and has, thus, a clear definition in a finite  $N$  CFT.

of on-shell amplitudes of propagation through classical shock backgrounds like (4.7). For simplicity, we consider  $2 \rightarrow 2$  scattering amplitudes of massless scalars in this section, where particles 1 and 2 play the role of shocks. We generalize to the case of gravitational (or spinning) shocks in the next section.

A shock wavefunction localized at  $u = u_0$  is given by

$$4\pi\delta(u - u_0)e^{i\vec{q}\cdot\vec{y}} = \int_{-\infty}^{\infty} dp^v e^{i(-\frac{1}{2}p^v(u-u_0)+\vec{q}\cdot\vec{y})} = \int_{-\infty}^{\infty} dp^v e^{\frac{i}{2}p^vu_0} e^{ip\cdot y},$$

$$p^\mu = (0, p^v, \vec{q}), \quad (4.19)$$

where  $\vec{q} \in \mathbb{C}^{D-2}$  is null. In order for  $p^\mu$  to be on-shell,  $\vec{q}$  must be complex. Note also that  $p^v$  is integrated over both positive and negative values. As explained in the previous section, such wavefunctions do not represent physical incoming or outgoing particles, but rather can be thought of as arising from poles of higher-point amplitudes.

Let shocks 1 and 2 be localized at  $u_1$  and  $u_2$ . We take particles 3 and 4 to be momentum eigenstates. Overall, the momenta in “all-incoming” conventions are given by (4.17), where we must integrate over  $p^v$  to create the delta-function localized shocks. Let us define the Mandelstam variables  $s = -(p_1 + p_2)^2 = -(\vec{q}_1 + \vec{q}_2)^2$  and  $t = -(p_2 + p_3)^2 = p^u p^v$ .<sup>12</sup>

Denote the scattering amplitude for particles 1, 2, 3, and 4 in momentum space by  $i\mathcal{A}(s, t)$ . Plugging in shock-wavefunctions (4.19) for particles 1 and 2, and applying momentum conservation  $p_1^v = -p_2^v = -p^v$ , we find that the amplitude for particles 3 and 4 scattering with shocks 1 and 2 is

$$\begin{aligned} \mathcal{Q}(u_1 - u_2) &\equiv i \int_{-\infty}^{\infty} dp^v \exp\left(-\frac{i}{2}p^v(u_1 - u_2)\right) \mathcal{A}(s = -(\vec{q}_1 + \vec{q}_2)^2, t = p^v p^u) \\ &= \frac{i}{p^u} \int_{-\infty}^{\infty} dt \exp\left(-\frac{i}{2}\frac{t}{p^u}(u_1 - u_2)\right) \mathcal{A}(s, t). \end{aligned} \quad (4.20)$$

The amplitude  $\mathcal{A}(s, t)$  may have singularities on the real  $t$ -axis. As usual, the correct prescription is to approach these singularities from above for positive  $t$  and below for negative  $t$ . The corresponding integration contour is shown in figure 4.3.

When the shocks are separated in the  $u$  direction, the amplitude should factorize into a product of  $S$ -matrix elements describing successive interactions with each shock.

---

<sup>12</sup>This labeling is chosen for consistency with our CFT conventions in section 4.5. Note that the roles of  $t$  and  $s$  are swapped relative to usual discussions of high energy scattering.

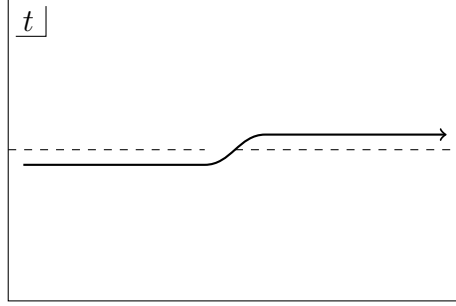


Figure 4.3: Integration contour for computing the shock amplitude. The integral is along the real axis, rotated by a small positive angle. The dashed lines represent  $t$ - and  $u$ -channel cuts. We assume that  $s < 0$ .

This comes about as follows. Note that the factor

$$\exp\left(-\frac{i}{2} \frac{t}{p^u} \Delta u\right) \quad (4.21)$$

causes the integrand in (4.20) to be exponentially damped in  $t$  in either the upper or lower half-plane, depending on the sign of  $\Delta u$ . For example, suppose  $\Delta u > 0$ . The integrand is damped for  $\text{Im } t < 0$ , so we can wrap the  $t$ -contour around the cut on the positive  $t$ -axis, giving a discontinuity (figure 4.4a)

$$\mathcal{Q}(\Delta u) = \frac{2\pi}{p^u} \int_0^\infty dt \exp\left(-\frac{i}{2} \frac{t}{p^u} \Delta u\right) \text{Disc}_t \mathcal{A}(s, t) \quad (\Delta u > 0), \quad (4.22)$$

where

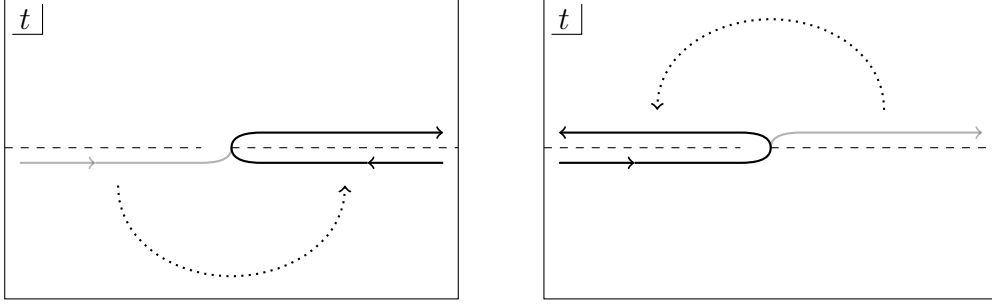
$$\text{Disc}_t f(t) \equiv \frac{i}{2\pi} (f(t + i\epsilon) - f(t - i\epsilon)), \quad (4.23)$$

so that  $\text{Disc}_t \frac{1}{t - m_X^2} = \delta(t - m_X^2)$ .

The formula (4.22) is true as long as  $\mathcal{A}(s, t)$  grows sub-exponentially in  $t$ . The discontinuity factors into products of on-shell amplitudes in the  $t$ -channel

$$\text{Disc}_t \mathcal{A}(s, t) = - \sum_X \delta(t - m_X^2) \mathcal{A}(23, -X) \mathcal{A}(X, 14) \quad (t > 0). \quad (4.24)$$

Here, we use all-incoming notation, so  $-X$  indicates the state  $X$  with momentum and helicities flipped. Plugging this into (4.22), we get an expression for the shock amplitude as a sum over intermediate states  $X$ . The physical interpretation is that particle 3 propagates through shock 2, creating an intermediate state  $X$ . The intermediate state  $X$  propagates through shock 1 to become particle 4.



(a) When  $\Delta u > 0$ , we can wrap the contour around the positive  $t$ -axis.

(b) When  $\Delta u < 0$ , we can wrap the contour around the negative  $t$ -axis.

Figure 4.4: Depending on whether the integrand decays exponentially in the upper or lower half-plane, we can deform the contour in different ways. In both cases, the old contour is shown in gray and the new contour in black. The direction of deforming the contour is indicated with a dotted arrow.

Next, suppose  $\Delta u < 0$ , so that shock 1 occurs before shock 2. In this case, we can fold the  $t$ -contour to wrap around the  $u$ -channel cut (figure 4.4b),

$$\mathcal{Q}(\Delta u) = -\frac{2\pi}{p^u} \int_{-\infty}^0 dt \exp\left(-\frac{i}{2} \frac{t}{p^u} \Delta u\right) \text{Disc}_t \mathcal{A}(s, t) \quad (\Delta u < 0). \quad (4.25)$$

The discontinuity now factorizes into a product of on-shell amplitudes in the  $u$ -channel

$$-\text{Disc}_t \mathcal{A}(s, t) = -\sum_X \delta(-t - s - m_X^2) \mathcal{A}(13, -X) \mathcal{A}(X, 24) \quad (t < 0). \quad (4.26)$$

Let us take a limit where the shocks become coincident,  $\Delta u \rightarrow 0^\pm$ . We find

$$\begin{aligned} \mathcal{Q}(0^+) &= \frac{2\pi}{p^u} \int_0^\infty dt \text{Disc}_t \mathcal{A}(s, t), \\ \mathcal{Q}(0^-) &= -\frac{2\pi}{p^u} \int_{-\infty}^0 dt \text{Disc}_t \mathcal{A}(s, t). \end{aligned} \quad (4.27)$$

For these quantities to be well-defined, the discontinuities should die faster than  $|t|^{-1}$  along the real  $t$ -axis. Let us assume this is the case. The commutator of coincident shocks is

$$\mathcal{Q}(0^+) - \mathcal{Q}(0^-) = \frac{2\pi}{p^u} \int_{-\infty}^\infty dt \text{Disc}_t \mathcal{A}(s, t) \quad (4.28)$$

$$= -\frac{2\pi}{p^u} \sum_X [\mathcal{A}(23, -X) \mathcal{A}(X, 14) - \mathcal{A}(13, -X) \mathcal{A}(X, 24)]. \quad (4.29)$$

It is not immediately obvious what the sum (4.29) should be. However, if  $\mathcal{A}(s, t)$  decays faster than  $t^{-1}$  in the limit of large complex  $t$  with fixed  $s$  (the Regge limit),



then we can close the integration contour in (4.28) by including arcs at infinity and shrink it to zero. Thus, coincident shocks commute if and only if the amplitude is sufficiently soft in the Regge limit.

When the amplitude decays faster than  $t^{-1}$  for fixed  $s$ , then we obtain the condition

$$\int_{-\infty}^{\infty} dt \text{Disc}_t \mathcal{A}(s, t) = 0 \quad (4.30)$$

which is an example of a ‘‘superconvergence’’ sum rule [142, 143]. In general, if the amplitude dies faster than  $t^{-N-1}$  in the Regge limit, we can integrate its discontinuity against  $t^n$  for  $0 \leq n < N$  to obtain additional superconvergence sum rules. Note that we obtain a different sum rule for each  $s$ . Superconvergence sum rules have been used, for example, to bootstrap the Veneziano amplitude [162].

#### 4.2.2.1 Spinning shocks

While scalar shock amplitudes must decay faster than  $t^{-1}$  to have a superconvergence sum rule, this condition gets relaxed for spinning shocks. Consider a massless spin- $J$  particle described by a traceless symmetric tensor field  $h_{\mu_1 \dots \mu_J}(x)$ . It is convenient to define a symmetric  $J$ -differential  $h_J(x, dx) = h_{\mu_1 \dots \mu_J}(x) dx^{\mu_1} \dots dx^{\mu_J}$ .

States are labeled by a momentum  $p^\mu$  and a transverse traceless-symmetric polarization tensor  $\epsilon_{\mu_1 \dots \mu_J}$ , modulo gauge redundancy. Let us parameterize the polarization tensor as a product of vectors  $\epsilon_{\mu_1 \dots \mu_J} = \epsilon_{\mu_1} \dots \epsilon_{\mu_J}$ , where  $\epsilon_\mu$  is transverse and null.<sup>13</sup> Thus, we can label momentum eigenstates by  $|p, \epsilon\rangle$  where  $p^\mu$  and  $\epsilon^\mu$  are vectors, and the state is a homogeneous polynomial of degree- $J$  in  $\epsilon$ .

A momentum eigenstate has wavefunction

$$\langle \Omega | h_J(x, dx) | p, \epsilon \rangle = (\epsilon \cdot dx)^J e^{ip \cdot x}. \quad (4.31)$$

We are interested in shock-wavefunctions of the form

$$\langle \Omega | h_J(x, dx) | \text{shock} \rangle = 4\pi \delta(u) (du)^J e^{i\vec{q} \cdot \vec{y}}. \quad (4.32)$$

For example, when  $J = 2$ ,  $h_J(x, dx) = h_{\mu\nu} dx^\mu dx^\nu$  has an interpretation as a metric perturbation. In this case, (4.32) is the perturbation in the Aichelburg-Sexl shockwave metric (Fourier-transformed in the transverse space) [158]. Comparing to (4.31), we

<sup>13</sup>Monomials of this form span the space of transverse traceless symmetric tensors, so this parameterization is without loss of generality.

see that

$$|\text{shock}\rangle = \int_{-\infty}^{\infty} dp^v |p^\mu = (0, p^v, \vec{q}), \epsilon^\mu = \eta^{\mu u} = (0, -2, 0)\rangle. \quad (4.33)$$

The computation of the shock amplitude and its commutator goes through essentially unchanged from the scalar case. To understand how the spinning amplitude should behave at large  $t$ , it is useful to tie the Mandelstam variable  $t$  to a symmetry generator. Consider a boost parameterized by  $z \in \mathbb{C}$ ,

$$\Lambda(z) : (u, v, \vec{y}) \rightarrow \left(\frac{u}{z}, zv, \vec{y}\right). \quad (4.34)$$

The boost acts on the momenta  $p_1, p_2$  by rescaling  $p^v \rightarrow zp^v$ , which also rescales  $t \rightarrow zt$ .<sup>14</sup> Thus, the shock commutator can be written

$$\mathcal{Q}(0^+) - \mathcal{Q}(0^-) = \frac{2\pi t}{p^u} \int_{-\infty}^{\infty} dz \text{Disc}_t \mathcal{A}(\epsilon_1, \epsilon_2, \epsilon_3, \epsilon_4; s, zt), \quad (4.35)$$

where

$$\epsilon_1 = \epsilon_2 = (0, -2, 0) \quad (4.36)$$

are the polarizations of the shocks, and  $\epsilon_3, \epsilon_4$  are the polarization vectors of the other particles.

Let us define a boosted amplitude  $\mathcal{A}(z)$  by acting with  $\Lambda(z)$  on particles 1 and 2, keeping particles 3 and 4 fixed. Note that the boost acts nontrivially on the polarization vectors (4.36):

$$\Lambda(z) : \epsilon_{1,2} \rightarrow z\epsilon_{1,2}. \quad (4.37)$$

Thus,

$$\mathcal{A}(z) = \mathcal{A}(z\epsilon_1, z\epsilon_2, \epsilon_3, \epsilon_4; s, zt) = z^{J_1+J_2} \mathcal{A}(\epsilon_1, \epsilon_2, \epsilon_3, \epsilon_4; s, zt). \quad (4.38)$$

In terms of the boosted amplitude, the shock commutator becomes

$$\mathcal{Q}(0^+) - \mathcal{Q}(0^-) = \frac{2\pi t}{p^u} \int_{-\infty}^{\infty} dz \frac{\text{Disc}_t \mathcal{A}(z)}{z^{J_1+J_2}}. \quad (4.39)$$

Suppose that  $\mathcal{A}(z)$  grows like  $z^{J_0}$  at large  $z$ , where  $J_0$  is a theory-dependent Regge intercept. (The Regge intercept may be  $s$ -dependent, but we are suppressing that dependence for now.) We see that the shock commutator vanishes if and only if

$$J_1 + J_2 > J_0 + 1. \quad (4.40)$$

---

<sup>14</sup>The action of the boost (4.34) is closely related to a BCFW deformation [163].

In the particular case where particles 1 and 2 are gravitons, the shock commutator vanishes if  $J_0 < 3$ . It was argued in [96] that — for physical  $s$  —  $J_0 > 2$  leads to a violation of causality.<sup>15</sup> Assuming this argument, it follows that coincident gravitational shocks commute and the superconvergence sum rule (4.30) holds in any causal theory. Furthermore, a failure of commutativity signals a violation of causality. It is instructive to see how (4.30) is obeyed (or not) in various examples.

We can also consider higher-point scattering amplitudes, where momenta  $p_3^\mu$  and  $p_4^\mu$  in the argument above stand for a sum of momenta of many particles. Assuming that the same bound on the Regge behavior holds for higher-point amplitudes, we get higher-point analogs of the superconvergence relation (4.30), where the integral is taken over the discontinuity with respect to  $t$  of higher-point amplitudes. We expect that commutativity of shocks should be true as “an operator equation,” in other words, for any scattering amplitude. This is what we find in AdS, where commutativity of shocks is dual to an operator equation in CFT. It would be interesting to explore this possibility further.

### 4.2.3 Shock commutativity in General Relativity

Let us re-derive commutativity of shocks in General Relativity using scattering amplitudes and equation (4.28). The on-shell condition for the intermediate particle implies that  $p^v = 0$  and  $p_X = (p_X^u, 0, \vec{q}_X)$ , where  $\vec{q}$  depends on the order of shocks. We choose the polarization of the intermediate particle to be  $\epsilon_X = (0, -2\frac{(\vec{e}_X \cdot \vec{q})}{p^u}, \vec{e}_X)$  so that the sum over intermediate states  $\sum_X \epsilon_X^\mu (\epsilon_X^*)^\nu$  acts as an identity matrix in the transverse space,  $\sum_X e_X^i (e_X^*)^j = \delta^{ij}$ . We write all amplitudes below in all-incoming notation.

#### 4.2.3.1 Minimally-coupled scalar

As the simplest example, consider a massless scalar field minimally coupled to gravity. The relevant scalar-scalar-graviton three-point amplitude takes the form

$$\mathcal{A}_{\phi_3\phi_X g_1} = \epsilon_1 \cdot p_3 \epsilon_1 \cdot p_X = -(p^u)^2, \quad (4.41)$$

where  $\epsilon_1 = (0, -2, 0)$  is the polarization of the graviton and we evaluated the amplitude in the kinematics of the previous section, in particular  $p_X = (-p^u, 0, \vec{q}_2 - \vec{q}_1)$ . Note that the three-point amplitude does not depend on the transverse momentum

<sup>15</sup>Note that kinematics [96] leads to amplitudes that grow with  $t$  and thus do not admit superconvergence sum rules that we consider here. We illustrate this in appendix (C.1.2).

of the shock  $\vec{q}_i$  and therefore the shock commutator vanishes. We find

$$\mathcal{Q}_{\text{scalar}}(0^\pm) = -\frac{2\pi}{p^u} \mathcal{A}_{\phi_3 \phi_X g_1} \mathcal{A}_{\phi_4 \phi_X g_2} = -2\pi(p^u)^3. \quad (4.42)$$

Finally, we can reach the same conclusion by considering a scalar field propagating on a shockwave background

$$\begin{aligned} ds^2 &= -du dv + \delta(u)h(u, \vec{y})du^2 + d\vec{y}^2, \\ h(u, \vec{y}) &= 4\pi(\epsilon_1 e^{i\vec{y}\cdot\vec{q}_1} + \epsilon_2 e^{i\vec{y}\cdot\vec{q}_2}), \end{aligned} \quad (4.43)$$

where  $\vec{q}_1^2 = \vec{q}_2^2 = 0$ . The wave equation  $\nabla^2 \phi = 0$  takes the form

$$\partial_u \partial_v \phi + \delta(u)h(u, \vec{y})\partial_v^2 \phi - \frac{1}{4}\partial_i^2 \phi = 0. \quad (4.44)$$

We solve across the locus  $u = 0$  as

$$\phi_{\text{after}} = e^{-h(0, \vec{y})\partial_v} \phi_{\text{before}}. \quad (4.45)$$

Choosing the initial state  $\phi_{\text{before}} = e^{-i\frac{1}{2}vp^u} e^{-i\vec{y}\vec{q}_2}$  as in the amplitude computation, and focusing on the term linear in  $\epsilon_1 \epsilon_2$ , we get

$$\phi_{\text{after}} = \delta_{\text{PS}} e^{-i\frac{1}{2}vp^u} e^{i\vec{y}\vec{q}_1}, \quad (4.46)$$

$$\delta_{\text{PS}} = -2\pi^2(p^u)^2, \quad (4.47)$$

where  $\delta_{\text{PS}}$  is the phase shift acquired by crossing a shock.

To compare with the amplitude computation, we must compute

$$\langle a_{p_4^u, \vec{q}_4} | \phi_{\text{after}} \rangle = 2p^u (2\pi)^{D-1} \delta(p_4^u + p^u) \delta^{(D-2)}(\vec{q}_4 + \vec{q}_1) \delta_{\text{PS}}, \quad (4.48)$$

which leads to

$$\mathcal{Q} = \frac{p^u \delta_{\text{PS}}}{\pi}, \quad (4.49)$$

in complete agreement with the amplitude computation. Note also that in this way, we can compute the effect of propagation of a probe through an arbitrary number of shocks. Again, we see that the order of shocks does not matter in this case.

### 4.2.3.2 Minimally-coupled photon

Next, let us consider particles with spin. It is convenient to choose external polarizations as follows

$$\epsilon_3 = \left( 0, -2 \frac{\vec{q}_2 \cdot \vec{e}_3}{p^u}, \vec{e}_3 \right), \quad (4.50)$$

$$\epsilon_4 = \left( 0, 2 \frac{\vec{q}_1 \cdot \vec{e}_4}{p^u}, \vec{e}_4 \right). \quad (4.51)$$

In Einstein-Maxwell theory, the three-point amplitude is given by

$$\begin{aligned} \mathcal{A}_{\gamma_3 \gamma_X g_1}^{F^2} &= \epsilon_1 \cdot p_3 \epsilon_1 \cdot p_X \epsilon_3 \cdot \epsilon_X - \epsilon_1 \cdot \epsilon_3 \epsilon_1 \cdot p_X \epsilon_X \cdot p_3 - \epsilon_1 \cdot \epsilon_X \epsilon_1 \cdot p_3 \epsilon_3 \cdot p_X \\ &= -(p^u)^2 \vec{e}_3 \cdot \vec{e}_X, \end{aligned} \quad (4.52)$$

where  $\epsilon_X = (0, -2 \frac{(\vec{e}_X \cdot \vec{q}_2 - \vec{q}_1)}{p^u}, \vec{e}_X)$  and we used that  $\epsilon_1 \cdot \epsilon_3 = \epsilon_1 \cdot \epsilon_X = 0$ .

Summing over intermediate states as in (4.28) trivially gives

$$\mathcal{Q}_{\text{photon}}(0^+) = -\frac{2\pi}{p^u} \sum_X \mathcal{A}_{\gamma_3 \gamma_X g_1}^{F^2} \mathcal{A}_{\gamma_4 \gamma_X g_2}^{F^2} = -2\pi (p^u)^3 \vec{e}_3 \cdot \vec{e}_4, \quad (4.53)$$

which obviously does not depend on the order of the shocks:

$$\sum_X \left( \mathcal{A}_{\gamma_3 \gamma_X g_1}^{F^2} \mathcal{A}_{\gamma_4 \gamma_X g_2}^{F^2} - \mathcal{A}_{\gamma_3 \gamma_X g_2}^{F^2} \mathcal{A}_{\gamma_4 \gamma_X g_1}^{F^2} \right) = 0. \quad (4.54)$$

Again, we can reproduce this result using the Einstein-Maxwell equations of motion on a shockwave background [96]

$$\partial_u F_{vi} + \delta(u) h \partial_v F_{vi} = 0. \quad (4.55)$$

Taking our initial state to be a plane wave, let us focus on the transverse polarizations  $\vec{A}_{\text{before}} = \vec{e}_3 e^{-i\frac{1}{2}vp^u} e^{-i\vec{y}\vec{q}_2}$ . After crossing the shock, we have

$$\vec{A}_{\text{after}} = e^{-h(0, \vec{y}) \partial_v} \vec{A}_{\text{before}}. \quad (4.56)$$

Again, computing the overlap we recover (4.53).

### 4.2.3.3 Gravitons

Finally, the three-point function of gravitons in General Relativity takes the form

$$\mathcal{A}_{g_3 g_X g_1}^R = (\epsilon_1 \cdot \epsilon_X \epsilon_3 \cdot p_1 + \epsilon_1 \cdot \epsilon_3 \epsilon_X \cdot p_3 + \epsilon_X \cdot \epsilon_3 \epsilon_1 \cdot p_X)^2 = (p^u)^2 (\vec{e}_3 \cdot \vec{e}_X)^2. \quad (4.57)$$

Summing over intermediate states, we find

$$\sum_X \mathcal{A}_{g_1 g_3 g_X}^R \mathcal{A}_{g_2 g_4 g_X}^R = (p^u)^4 (\vec{e}_3 \cdot \vec{e}_4)^2. \quad (4.58)$$

The result is independent of the shock ordering. This result can be reproduced via computing the propagation of a graviton through a shockwave background as above.

To summarize, minimally-coupled matter and gravitons lead to commuting gravitational shocks (at tree level). This can be verified by studying shock amplitudes, or by studying wave equations on a shockwave background.

## 4.2.4 Non-minimal couplings

### 4.2.4.1 Non-minimally coupled photons

Let us now demonstrate that commutativity of shocks can be lost in theories with non-minimal couplings to gravity. As a first example, consider a non-minimal coupling of photons to gravity of the schematic form  $\alpha_2 RFF$ . The relevant three-point amplitude takes the form

$$\mathcal{A}_{\gamma_3 \gamma_X g_1}^{RFF} = \epsilon_1 \cdot p_3 \epsilon_1 \cdot p_X \epsilon_3 \cdot p_X \epsilon_X \cdot p_3 = -(p^u)^2 \vec{e}_3 \cdot \vec{q}_1 \vec{e}_X \cdot \vec{q}_1, \quad (4.59)$$

where we used that  $\epsilon_X \cdot p_3 = -\vec{e}_X \cdot \vec{q}_1$ .

Summing over intermediate states, we can compute the commutator (4.28)

$$\begin{aligned} & \frac{1}{(p^u)^4} \sum_X \left( \mathcal{A}_{\gamma_3 \gamma_X g_1}^{F^2 + \alpha_2 RFF} \mathcal{A}_{\gamma_4 \gamma_X g_2}^{F^2 + \alpha_2 RFF} - \mathcal{A}_{\gamma_3 \gamma_X g_2}^{F^2 + \alpha_2 RFF} \mathcal{A}_{\gamma_4 \gamma_X g_1}^{F^2 + \alpha_2 RFF} \right) \\ &= \alpha_2^2 (\vec{e}_3 \cdot \vec{q}_1 \vec{e}_4 \cdot \vec{q}_2 - \vec{e}_3 \cdot \vec{q}_2 \vec{e}_4 \cdot \vec{q}_1) \vec{q}_1 \cdot \vec{q}_2, \end{aligned} \quad (4.60)$$

which is clearly nonvanishing. Let us reproduce the same result using equations of motion. In the presence of the  $RFF$  coupling, the equation of motion (4.55) gets modified to

$$\partial_u F_{vi} + \delta(u) (\delta_{ij} h + \alpha_2 \partial_i \partial_j h) \partial_v F_{vj} = 0. \quad (4.61)$$

The solution takes the same form as (4.56), except now the transfer matrix that describes how polarizations change when propagating through a shock is not diagonal. Instead it takes the form  $\delta_{ij} h + \alpha_2 \partial_i \partial_j h$ , which for a given shock is

$$M_{ij}(\vec{q}) = \delta_{ij} - \alpha_2 q_i q_j. \quad (4.62)$$

Different orderings of shocks now lead to different results. The commutator (4.60) becomes  $e_4^i [M(\vec{q}_1), M(\vec{q}_2)]_{ij} e_3^j$ . More generally, given multiple shocks ordered according to  $u_1 > u_2 > \dots > u_k$ , the amplitude is given by a corresponding product of (noncommuting) shockwave transfer matrices

$$\mathcal{Q} = \frac{p^u}{\pi} (4\pi)^k \left( \frac{ip^u}{2} \right)^k \vec{e}_4 \cdot M(\vec{q}_1) \cdots M(\vec{q}_k) \cdot \vec{e}_3. \quad (4.63)$$

#### 4.2.4.2 Higher derivative gravity

In higher-derivative gravity, there are two additional graviton three-point amplitudes:

$$\begin{aligned} \mathcal{A}_{g_3 g_X g_1}^{R^2} &= (\epsilon_1 \cdot \epsilon_X \epsilon_3 \cdot p_1 + \epsilon_1 \cdot \epsilon_3 \epsilon_X \cdot p_3 + \epsilon_X \cdot \epsilon_3 \epsilon_1 \cdot p_X) \epsilon_1 \cdot p_X \epsilon_X \cdot p_3 \epsilon_3 \cdot p_1 \\ &= -(p^u)^2 \vec{e}_3 \cdot \vec{e}_X \vec{e}_3 \cdot \vec{q}_1 \vec{e}_X \cdot \vec{q}_1, \\ \mathcal{A}_{g_3 g_X g_1}^{R^3} &= (\epsilon_1 \cdot p_X \epsilon_X \cdot p_3 \epsilon_3 \cdot p_1)^2 \\ &= (p^u)^2 (\vec{e}_3 \cdot \vec{q}_1)^2 (\vec{e}_X \cdot \vec{q}_1)^2. \end{aligned} \quad (4.64)$$

Together with  $\mathcal{A}^R$  given in (4.57), these form a complete list of three-point structures allowed by Lorentz invariance. To contract the three point amplitudes, we substitute

$$\sum_X (e_X^i e_X^j) (e_X^k e_X^l)^* \rightarrow \Pi^{ij,kl} \equiv \frac{1}{2} (\delta^{ik} \delta^{jl} + \delta^{il} \delta^{jk}) - \frac{1}{D-2} \delta^{ij} \delta^{kl}. \quad (4.65)$$

For a general linear combination  $R + \alpha_2 R^2 + \alpha_4 R^3$ , the shock commutator is

$$\begin{aligned} & \frac{1}{(p^u)^4} \sum_X \left( \mathcal{A}_{g_3 g_X g_1}^{R+\alpha_2 R^2+\alpha_4 R^3} \mathcal{A}_{g_4 g_X g_2}^{R+\alpha_2 R^2+\alpha_4 R^3} - \mathcal{A}_{g_3 g_X g_2}^{R+\alpha_2 R^2+\alpha_4 R^3} \mathcal{A}_{g_4 g_X g_1}^{R+\alpha_2 R^2+\alpha_4 R^3} \right) \\ &= \frac{1}{2} \alpha_2^2 \vec{e}_3 \cdot \vec{e}_4 \vec{q}_1 \cdot \vec{q}_2 (\vec{e}_3 \cdot \vec{q}_1 \vec{e}_4 \cdot \vec{q}_2 - \vec{e}_3 \cdot \vec{q}_2 \vec{e}_4 \cdot \vec{q}_1) \\ & \quad - \alpha_2 \alpha_4 \vec{q}_1 \cdot \vec{q}_2 (\vec{e}_3 \cdot \vec{q}_1 \vec{e}_4 \cdot \vec{q}_2 - \vec{e}_3 \cdot \vec{q}_2 \vec{e}_4 \cdot \vec{q}_1) (\vec{e}_3 \cdot \vec{q}_1 \vec{e}_4 \cdot \vec{q}_1 + \vec{e}_3 \cdot \vec{q}_2 \vec{e}_4 \cdot \vec{q}_2) \\ & \quad + \left( \alpha_4^2 (\vec{q}_1 \cdot \vec{q}_2)^2 - \frac{\alpha_2^2}{D-2} \right) [(\vec{e}_3 \cdot \vec{q}_1)^2 (\vec{e}_4 \cdot \vec{q}_2)^2 - (\vec{e}_3 \cdot \vec{q}_2)^2 (\vec{e}_4 \cdot \vec{q}_1)^2]. \end{aligned} \quad (4.66)$$

It is easy to check that this vanishes if and only if  $\alpha_2 = \alpha_4 = 0$ .

Again the same result can be obtained using the classical equations of motions as above, see [96]. The difference compared to General Relativity is that the shockwave transfer matrix is polarization-dependent, which leads to non-commutativity or violations of superconvergence relations in theories with non-minimal coupling to gravity.

Explicitly, the transfer matrix is

$$\begin{aligned}
M_{ij,kl}(\vec{q}) &= \Pi_{ij,kl} + \frac{\alpha_2}{4} \left( \delta_{ik}P_{jl} + \delta_{il}P_{jk} + \delta_{jl}P_{ik} + \delta_{jk}P_{il} - 4 \frac{\delta_{ij}P_{kl} + \delta_{kl}P_{ij}}{D-2} \right) + \alpha_4 P_{ijkl}, \\
P_{ij} &= q_i q_j, \\
P_{ijkl} &= q_i q_j q_k q_l.
\end{aligned} \tag{4.67}$$

To compute the transfer through  $n$  shocks, we simply multiply the corresponding transfer matrices, as in (4.63).

Non-minimal couplings of gravitons to matter also contribute to noncommutativity. For example, consider an interaction of the schematic form  $\phi R^2$  where  $\phi$  is a (possibly massive) scalar. The only possible three-point structure is

$$\mathcal{A}_{g_3 \phi_X g_1}^{\phi R^2} = ((\epsilon_1 \cdot \epsilon_3)(p_1 \cdot p_3) - (\epsilon_1 \cdot p_3)(\epsilon_3 \cdot p_1))^2 = (p^u)^2 (\vec{q}_1 \cdot \vec{e}_3)^2. \tag{4.68}$$

The  $\phi R^2$  coupling allows  $\phi$  to appear as an intermediate state when a graviton propagates through two shocks. The corresponding contribution to the shock commutator is

$$\sum_X \left( \mathcal{A}_{g_3 \phi_X g_1}^{\phi R^2} \mathcal{A}_{g_4 \phi_X g_2}^{\phi R^2} - \mathcal{A}_{g_3 \phi_X g_2}^{\phi R^2} \mathcal{A}_{g_4 \phi_X g_1}^{\phi R^2} \right) = (p^u)^4 ((\vec{q}_1 \cdot \vec{e}_3)^2 (\vec{q}_2 \cdot \vec{e}_4)^2 - (\vec{q}_2 \cdot \vec{e}_3)^2 (\vec{q}_1 \cdot \vec{e}_4)^2). \tag{4.69}$$

#### 4.2.5 Graviton scattering in string theory

Non-minimal couplings generically lead to non-commuting coincident shocks (at tree level). In any theory with Regge intercept  $J_0 < 3$ , the contributions from non-minimal couplings to the shock commutator must be cancelled by high-energy states or loop effects.

As a concrete example, consider graviton scattering in tree-level string theory. The amplitude takes the form [164, 165]

$$\begin{aligned}
\mathcal{A}_{gg \rightarrow gg}^{(i,j)} &= (K_{\mu_1 \mu_2 \mu_3 \mu_4}^{(i)} \epsilon_1^{\mu_1} \epsilon_2^{\mu_2} \epsilon_3^{\mu_3} \epsilon_4^{\mu_4}) (K_{\mu_1 \mu_2 \mu_3 \mu_4}^{(j)} \epsilon_1^{\mu_1} \epsilon_2^{\mu_2} \epsilon_3^{\mu_3} \epsilon_4^{\mu_4}) \\
&\quad \times (-\pi^2 \kappa^2) \frac{\Gamma(-s/2) \Gamma(-t/2) \Gamma(-u/2)}{\Gamma(s/2+1) \Gamma(t/2+1) \Gamma(u/2+1)} \quad (i, j \in \{b, ss\}),
\end{aligned} \tag{4.70}$$

in units where  $\alpha' = 2$ . (Recall that we have parametrized the graviton polarizations as  $\epsilon^{\mu\nu} = \epsilon^\mu \epsilon^\nu$ .)



There are two basic tensors  $K^{(i)}$  that can appear in the amplitude:  $K^{(b)}$ , which occurs in the open bosonic string, and  $K^{(ss)}$ , which appears in the open superstring. Accordingly, the four-point amplitude of closed strings has three possible tensor structures, corresponding to bosonic strings  $K^{(b)}K^{(b)}$ , heterotic strings  $K^{(b)}K^{(ss)}$ , and superstrings  $K^{(ss)}K^{(ss)}$ .

Plugging in the momenta (4.17) and polarization vectors (4.36) and (4.50), we find

$$\begin{aligned} K_{\mu_1\mu_2\mu_3\mu_4}^{(ss)} \epsilon_1^{\mu_1} \epsilon_2^{\mu_2} \epsilon_3^{\mu_3} \epsilon_4^{\mu_4} &= (p^u)^2 s \vec{e}_3 \cdot \vec{e}_4, \\ K_{\mu_1\mu_2\mu_3\mu_4}^{(b)} \epsilon_1^{\mu_1} \epsilon_2^{\mu_2} \epsilon_3^{\mu_3} \epsilon_4^{\mu_4} &= (p^u)^2 s \left( \vec{e}_3 \cdot \vec{e}_4 - \vec{e}_3 \cdot \vec{q}_1 \vec{e}_4 \cdot \vec{q}_1 - \vec{e}_3 \cdot \vec{q}_2 \vec{e}_4 \cdot \vec{q}_2 \right. \\ &\quad \left. + \frac{t}{2+u} \vec{e}_3 \cdot \vec{q}_2 \vec{e}_4 \cdot \vec{q}_1 + \frac{u}{2+t} \vec{e}_3 \cdot \vec{q}_1 \vec{e}_4 \cdot \vec{q}_2 \right). \end{aligned} \quad (4.71)$$

Including only the contribution from graviton exchange, the last two terms in (4.71) give a nontrivial shock commutator. However, if we boost the energy  $t \rightarrow zt$ , the gamma functions in (4.70) ensure that the amplitude dies as  $z^{-2+s}$ . Thus, upon integrating the full discontinuity, we must find that the graviton contribution is cancelled by heavy modes. For example, in the heterotic string, we find the sum rule

$$\int dt \text{Disc}_t \mathcal{A} = (p^u)^4 s \vec{e}_3 \cdot \vec{e}_4 (\vec{e}_3 \cdot \vec{q}_1 \vec{e}_4 \cdot \vec{q}_2 - \vec{e}_3 \cdot \vec{q}_2 \vec{e}_4 \cdot \vec{q}_1) \left( 1 + \sum_{n=1}^{\infty} r_n(s) \right) = 0, \quad (4.72)$$

where

$$r_n(s) = \frac{(s-2)(s+4n)}{s(n+1)(s+2n-2)} \frac{(s/2)_n^2}{n!^2}, \quad (4.73)$$

with  $(a)_n = \frac{\Gamma(a+n)}{\Gamma(a)}$  the Pochhammer symbol. In equation (4.72), 1 represents the graviton multiplet contribution and the sum over  $n \geq 1$  is the contribution of heavy modes. It is possible to decouple almost all the heavy modes by setting  $s = 0$ , in which case one finds

$$1 + r_1(0) = 0. \quad (4.74)$$

In general, the sum over heavy modes converges like  $\sum_n n^{s-3}$ .

#### 4.2.6 Shock $S$ -matrix in string theory

In addition to studying four-point amplitudes, we can equivalently analyze the equation of motion for a string on a shockwave background, analogous to our discussions of equations of motion for scalars, photons, and gravitons. Propagation of strings on

shockwave backgrounds was discussed in [161, 166–172]. This leads to an understanding of shock commutativity in terms of the string  $S$ -matrix for propagation through a shock.

Let us follow the conventions of [166]. Recall that the string mode operators obey

$$[\alpha_n^i, \alpha_m^j] = n\delta_{n+m,0}\delta^{ij}, \quad (4.75)$$

where negative modes  $n < 0$  create string excitations, while positive modes  $n > 0$  annihilate the vacuum

$$\alpha_{n>0}|0\rangle = 0. \quad (4.76)$$

We choose the conformal gauge for the worldsheet metric  $h^{\alpha\beta} = \eta^{\alpha\beta}$ , and fix the light-cone gauge

$$u(\sigma, \tau) = P^u\tau. \quad (4.77)$$

The closed string mode expansion takes the form

$$X^i(\sigma, \tau) = x^i + p^i\tau + \frac{i}{2}\sqrt{\alpha'} \sum_{n \neq 0} [\tilde{\alpha}_n^i e^{-2in\tau} - \alpha_n^{i\dagger} e^{2in\tau}] e^{-2in\sigma}, \quad (i = 2, \dots, D-1), \quad (4.78)$$

where  $\alpha_n^{i\dagger} = \alpha_{-n}^i$ .

Before and after a shock, the string propagates freely. If the shock geometry has the metric

$$ds^2 = -dudv + \delta(u)f(\vec{x})du^2 + d\vec{x}^2, \quad (4.79)$$

the transition through the shock is described by the  $S$ -matrix [166],

$$S_{\text{shock}} = e^{\frac{i}{2\pi}P^u \int_0^\pi f(\vec{X}(\sigma,0))d\sigma}. \quad (4.80)$$

As an example, consider a shock created by a fast-moving particle at position  $\vec{x}_a$ ,

$$f_a(\vec{X}(\sigma,0)) = \frac{\Gamma(\frac{D-4}{2})}{4\pi^{\frac{D-2}{2}}} \frac{1}{((\vec{X}(\sigma,0) - \vec{x}_a)^2)^{\frac{D-4}{2}}} = \int \frac{d^{D-2}\vec{q}}{q^2} e^{i\vec{q}\cdot(\vec{X}(\sigma,0) - \vec{x}_a)}. \quad (4.81)$$

In writing  $f_a$  above, there is an ambiguity in the ordering of operators  $X^i(\sigma,0)$ . However, this ambiguity is proportional to  $\vec{q}_1^2$  and is localized at zero impact parameter upon doing the Fourier transform. It is therefore irrelevant for our purposes.

Note that the operator  $\mathcal{S}_{\text{shock}}$  is diagonal in the position basis  $X^i(\sigma, 0)$  for the transverse oscillators. Thus, it instantaneously changes the momenta of the oscillators without affecting their positions. Overall, the effect of the shock on the string is the same as in the geodesic calculation (4.10): the center of mass of the string moves in the  $v$  direction (Shapiro time delay), and the transverse modes receive an instantaneous kick that depends on the profile  $f_a(\vec{X})$ . Essentially, each part of the string individually follows a geodesic through the shock. Thus, coincident shocks commute because they commute for geodesics.

To see this in more detail, consider the matrix element for propagation through two shocks

$$\langle \Psi | \left( \frac{i}{2\pi} P^u \right)^2 \int_0^\pi d\sigma f_1(\vec{X}(\sigma, 0)) \int_0^\pi d\sigma' f_2(\vec{X}(\sigma', 0)) | \Psi \rangle. \quad (4.82)$$

We are interested in states  $|\Psi\rangle$  that are eigenstates of  $\vec{x}$  (fixed center of mass position in the transverse plane), with a finite number of oscillator excitations above the vacuum. As in the previous section, let us choose  $\vec{x}|\psi_{\text{cm}}\rangle = \vec{0}$ . The relevant correlator takes the form

$$\int \frac{d^{D-2}\vec{q}_1}{\vec{q}_1^2} e^{-i\vec{q}_1 \cdot \vec{x}_1} \int \frac{d^{D-2}\vec{q}_2}{\vec{q}_2^2} e^{-i\vec{q}_2 \cdot \vec{x}_2} \int_0^\pi d\sigma \int_0^\pi d\sigma' \langle \psi_{\text{osc}} | e^{i\vec{q}_1 \cdot \vec{X}_{\text{osc}}(\sigma, 0)} e^{i\vec{q}_2 \cdot \vec{X}_{\text{osc}}(\sigma', 0)} | \psi_{\text{osc}} \rangle. \quad (4.83)$$

The same formula is valid for superstrings as well [166].

Let us first compute the correlator in the oscillator vacuum. We have

$$\langle 0_{\text{osc}} | e^{i\vec{q}_1 \cdot \vec{X}_{\text{osc}}(\sigma, 0)} e^{i\vec{q}_2 \cdot \vec{X}_{\text{osc}}(\sigma', 0)} | 0_{\text{osc}} \rangle = |2 \sin(\sigma - \sigma')|^{\frac{1}{2}\alpha' \vec{q}_1 \cdot \vec{q}_2}. \quad (4.84)$$

The integral over the worldsheet coordinate gives [31]

$$\int_0^{2\pi} \frac{d\sigma}{2\pi} \left| 2 \sin \frac{\sigma}{2} \right|^{\alpha' \vec{q}_1 \cdot \vec{q}_2} = \frac{2^{\alpha' \vec{q}_1 \cdot \vec{q}_2} \Gamma(\frac{1}{2} + \frac{\alpha' \vec{q}_1 \cdot \vec{q}_2}{2})}{\sqrt{\pi} \Gamma(1 + \frac{\alpha' \vec{q}_1 \cdot \vec{q}_2}{2})}. \quad (4.85)$$

Expanding at small  $\alpha'$  and plugging back into (4.83) reproduces the result from [31].

In general states, we can use the formula

$$: e^{i\vec{q}_1 \cdot \vec{X}_{\text{osc}}(\sigma, 0)} :: e^{i\vec{q}_2 \cdot \vec{X}_{\text{osc}}(\sigma', 0)} := |2 \sin(\sigma - \sigma')|^{\frac{1}{2}\alpha' \vec{q}_1 \cdot \vec{q}_2} : e^{i\vec{q}_1 \cdot \vec{X}_{\text{osc}}(\sigma, 0) + i\vec{q}_2 \cdot \vec{X}_{\text{osc}}(\sigma', 0)} : \quad (4.86)$$

and then Taylor expand inside the normal ordering. In this way, commutativity is manifest.

Let us now understand how commutativity is achieved in more detail. For concreteness, consider bosonic string theory and take a graviton as the external state

$$|\psi_{\text{osc}}\rangle = \tilde{\alpha}_{-1}^a \alpha_{-1}^b |0\rangle. \quad (4.87)$$

It is sufficient to keep only the leading  $\alpha'$  correction to see the effect:

$$\int_0^\pi \frac{d\sigma}{\pi} e^{i\vec{q} \cdot \vec{X}_{\text{osc}}(\sigma,0)} \sim 1 + \frac{\alpha'}{4} q_i q_j T^{ij}, \quad (4.88)$$

where

$$T^{ij} = \sum_{n>0} (\tilde{\alpha}_{-n}^{(i} - \alpha_n^{(i})(\tilde{\alpha}_n^{j)} - \alpha_{-n}^{j)}), \quad (4.89)$$

where  $(ij)$  stands for symmetrization. It is easy to check that  $[T^{ij}, T^{kl}] = 0$ .

Let us act with the operator (4.88) on a graviton state

$$\left(1 + \frac{\alpha'}{4} q_i q_j T^{ij}\right) \tilde{\alpha}_{-1}^a \alpha_{-1}^b |0\rangle. \quad (4.90)$$

Inside the operator  $T^{ij}$ , there are two types of terms. Firstly, the terms  $\tilde{\alpha}_{-1}^{(i} \tilde{\alpha}_1^{j)} + \alpha_{-1}^{(i} \alpha_1^{j)}$  shuffle massless modes among each other. These by themselves lead to non-commutative shocks. However, crucially there are also terms  $-\tilde{\alpha}_n^{(i} \alpha_n^{j)} - \alpha_{-n}^{(i} \tilde{\alpha}_{-n}^{j)}$  which move the state across the string levels. In particular, the first term leads to mixing with the tachyon, whereas the second term produces higher level states. For example, the  $n = 1$  term leads to mixing between the graviton and a spin-4 particle. As expected, the extra states restore commutativity.

#### 4.2.7 A stringy equivalence principle

We have seen that in string theory, extra states restore commutativity of coincident shocks and satisfy the corresponding superconvergence sum rule. This phenomenon should occur in any gravitational theory with  $J_0 < 3$ , where  $J_0$  is the Regge intercept. We give more details on the corresponding superconvergence sum rule in a generic tree-level theory of gravity in appendix C.1.3. In a non-tree-level theory with  $J_0 < 3$ , the superconvergence sum rule can receive contributions from loops or nonperturbative effects.

Reference [96] argued using causality that a tree-level theory of gravity should have  $J_0 \leq 2$ . Their argument applies for scattering at nonzero impact parameter. As far

as we are aware, there is currently no flat-space argument that the same should be true away from tree level, or at zero impact parameter.<sup>16</sup>

However, as we will see in the next section, shock commutativity in AdS can be proved rigorously, nonperturbatively, and for all values of the impact parameter. This leads us to conjecture that the same is true in flat space and dS as well. More precisely, we propose:

**Conjecture** (Stringy equivalence principle). *Coincident gravitational shocks commute in any nonperturbative theory of gravity in AdS, dS, or Minkowski spacetime.*

We use the term “equivalence principle” because this is a modified version of the statement that all particles follow geodesics. The word “stringy” comes from the fact that mixing with stringy states can restore shock commutativity that would otherwise be lost.

#### 4.2.8 Gravitational DIS and ANEC commutativity

We can easily repeat the same discussion in the context of a gapped QFT (or, more generally, a QFT that is free in the IR), where it becomes the statement about commutativity of the ANEC operators when evaluated in one-particle states. The virtual graviton  $g^*$  of the previous sections couples to the QFT stress-energy tensor as  $h_{\mu\nu}T^{\mu\nu}$ , and therefore the scattering process  $g^*X \rightarrow g^*X$  is described by the following matrix element

$$\mathcal{A}(s, t) = \langle p_4 | T(T_{vv}(p_1)T_{vv}(p_2)) | p_3 \rangle, \quad (4.91)$$

where as usual (4.91) describes the nontrivial part that multiplies  $\delta^{(D)}(\sum_i p_i)$ .<sup>17</sup> Unlike gravitational theories, there is no problem in defining off-shell observables in QFT and decoupling the probe that creates  $g^*$  from the rest of the system (by considering the  $G_N \rightarrow 0$  limit). One consequence of that is that we can formulate the problem using real momenta and keep  $g^*$  off-shell. As before, we will be interested in the

---

<sup>16</sup>It was proven in the 60’s that scattering amplitudes in gapped QFTs satisfy dispersion relations with at most two subtractions for  $|t| < R$  [173], where  $R$  depends on the mass of the lightest particle in the spectrum. A similar statement holds for scattering of particles with spin [174, 175]. The corresponding superconvergence sum rules for spinning particles were studied in [174]. It would be interesting to understand the relation between their work and the commutativity of gravitational shocks discussed here.

<sup>17</sup>For a related discussion see [14, 31, 176].

following kinematics:

$$\begin{aligned} p_1 &= (0, -p^v + \frac{\vec{q}_1^2}{p^u}, \vec{q}_1), & p_2 &= (0, p^v - \frac{\vec{q}_2^2}{p^u}, \vec{q}_2), \\ p_3 &= (p^u, \frac{\vec{q}_2^2}{p^u}, -\vec{q}_2), & p_4 &= (-p^u, -\frac{\vec{q}_1^2}{p^u}, -\vec{q}_1), \end{aligned} \quad (4.92)$$

where  $\vec{q}_1^2$  and  $\vec{q}_2^2$  are non-zero. We chose the probe particle to be massless, but it does not have to be the case. Mandelstam invariants take the form  $s = -(p_1 + p_2)^2 = (\vec{q}_1 + \vec{q}_2)^2$  and  $t = -(p_2 + p_3)^2 = p^u p^v$ . The matrix element that describes  $g^* X \rightarrow g^* X$  is time-ordered as in the usual description of deep inelastic scattering. The discontinuities of the time-ordered matrix element  $\mathcal{A}(s, t)$  are computed by the corresponding Wightman functions

$$\begin{aligned} \text{Disc}_{t>0} \mathcal{A}(s, t) &= \langle p_4 | T_{vv}(p_1) T_{vv}(p_2) | p_3 \rangle, \\ -\text{Disc}_{t<0} \mathcal{A}(s, t) &= \langle p_4 | T_{vv}(p_2) T_{vv}(p_1) | p_3 \rangle. \end{aligned} \quad (4.93)$$

Integrating the discontinuity over  $t$ , we get

$$\frac{1}{p^u} \int_{-\infty}^{\infty} dt \text{Disc}_t \mathcal{A}(s, t) = \int d^{d-2} \vec{y}_1 e^{i\vec{q}_1 \cdot \vec{y}_1} \langle p_4 | \left[ \int dv T_{vv}(u=0, v, \vec{y}_1), T_{vv}(0) \right] | p_3 \rangle, \quad (4.94)$$

where we used momentum conservation to rewrite the result in position space. We see that the integral over the discontinuity of  $\mathcal{A}(s, t)$  is related to the commutator of ANEC operators inserted at the same time  $u=0$ .

As in the scattering amplitude considerations of the previous section, causality considerations apply to the matrix element (4.91). In particular, for physical  $s$  we expect  $\mathcal{A}(s, t)$  to obey

$$|\mathcal{A}(s, t)| < \frac{1}{|t|}, \quad |t| \rightarrow \infty. \quad (4.95)$$

The Regge boundedness condition (4.95) together with the usual assumptions about the analyticity of  $\mathcal{A}(s, t)$  implies commutativity of ANECs in a gapped QFT via the superconvergence relations

$$0 = \oint \frac{dt}{2\pi i} \mathcal{A}(s, t) = \int_{-\infty}^{\infty} dt \text{Disc}_t \mathcal{A}(s, t) + \oint_{c_\infty} \frac{dt}{2\pi i} \mathcal{A}(s, t) = \int_{-\infty}^{\infty} dt \text{Disc}_t \mathcal{A}(s, t). \quad (4.96)$$

We conclude that for every  $\vec{q}_1$ , the commutator

$$\int d^{d-2} \vec{y}_1 e^{i\vec{q}_1 \cdot \vec{y}_1} \langle p_4 | \left[ \int dv T_{vv}(u=0, v, \vec{y}_1), T_{vv}(0) \right] | p_3 \rangle \quad (4.97)$$

vanishes. This implies that coincident ANEC operators commute inside one-particle states.

### 4.3 Event shapes in CFT and shocks in AdS

In this section, we study shock commutativity and superconvergence sum rules in AdS, interpreting them in CFT language. We focus on shocks created by integrating a local CFT operator along a null line on the boundary of AdS.<sup>18</sup> The simplest example is a gravitational shock created by the average null energy (ANEC) operator  $\mathcal{E} = \int dv T_{vv}$  [31]. We will argue that ANEC operators on the same null plane commute, and this leads to nontrivial superconvergence sum rules that must be satisfied by CFT data. One of the nice properties of such superconvergence sum rules is that in large- $N$  theories, they get contributions only from single-trace operators and non-minimal bulk couplings.

We start by introducing null integrals (“light-transforms”) of local operators in section 4.3.1. In section 4.3.2, we review “event shapes,” which are certain matrix elements of light-transformed operators. In section 4.3.3, we compute some simple event shapes in AdS, emphasizing the similarities to our shock amplitude calculations in section 4.2.

#### 4.3.1 Review: the light transform

We will be interested in integrals of a local CFT operator along a null line on the boundary of AdS. For example, let  $\mathcal{O}^{\mu_1 \dots \mu_J}$  be a traceless symmetric tensor, and consider the integral

$$\int_{-\infty}^{\infty} dv \mathcal{O}_{v \dots v}(u = 0, v, \vec{y}). \quad (4.98)$$

Here, we use lightcone coordinates (4.13), except we are now in  $d = D - 1$  dimensions (so that  $\vec{y} \in \mathbb{R}^{d-2}$ ). In holographic theories, such operators create shocks in the bulk. An example is the average null energy (ANEC) operator

$$\int_{-\infty}^{\infty} dv T_{vv}(u = 0, v, \vec{y}). \quad (4.99)$$

The ANEC operator on the boundary creates a gravitational shock in the bulk of the form described by the AdS-Aichelburg-Sexl metric.

In the examples (4.98) and (4.99), the integration contour starts at the point  $(u, v, \vec{y}) = (0, -\infty, \vec{y}) \in \mathcal{I}^-$  at past null infinity and ends at the point  $(u, v, \vec{y}) = (0, \infty, \vec{y}) \in \mathcal{I}^+$  at future null infinity. More generally, we can perform a conformal transformation to

---

<sup>18</sup>These backgrounds will already be rich enough to develop an analogy to the flat-space story. It would be interesting to study other types of shock backgrounds [177] in the future.

bring the initial point of the null integral to some generic point  $x$ . The result is an integral transform called the light-transform [28],

$$\mathbf{L}[\mathcal{O}](x, z) = \int_{-\infty}^{\infty} d\alpha (-\alpha)^{-\Delta-J} \mathcal{O}\left(x - \frac{z}{\alpha}, z\right). \quad (4.100)$$

Here,  $z \in \mathbb{R}^{1,d-1}$  is a null vector,  $\Delta$  and  $J$  are the dimension and spin of  $\mathcal{O}$ , and we use index-free notation

$$\mathcal{O}(x, z) = \mathcal{O}^{\mu_1 \cdots \mu_J}(x) z_{\mu_1} \cdots z_{\mu_J}. \quad (4.101)$$

The light-transformed operator depends on an initial point  $x$  and a null direction  $z$ . The integration contour runs from  $x$ , along the  $z$ -direction, to the point in the next Poincare patch on the Lorentzian cylinder with the same Minkowski coordinates as  $x$ .

An advantage of this language is that it makes the conformal transformation properties of null-integrated operators manifest.  $\mathbf{L}$  is a conformally-invariant integral transform that changes the quantum numbers as follows:

$$\mathbf{L} : (\Delta, J) \rightarrow (1 - J, 1 - \Delta). \quad (4.102)$$

In other words,  $\mathbf{L}[\mathcal{O}](x, z)$  transforms like a primary operator at  $x$  with dimension  $1 - J$  and (non-integer) spin  $1 - \Delta$ . As we will see, this simplifies several computations involving these operators. We see from (4.100) that the light-transform is well-defined whenever  $\Delta + J > 1$ . An important property is that  $\mathbf{L}[\mathcal{O}]$  annihilates the vacuum whenever it's defined. This can be established formally using the conformal transformation properties of  $\mathbf{L}[\mathcal{O}]$ , or by deforming the  $\alpha$  contour inside a correlation function involving  $\mathbf{L}[\mathcal{O}]$  [28].

### 4.3.2 Review: event shapes

We will be interested in matrix-elements of light-transformed operators called “event shapes.” First, consider a three-point function

$$\langle \Omega | \phi_1(x_1) \mathbf{L}[\mathcal{O}](x, z) \phi_2(x_2) | \Omega \rangle, \quad (4.103)$$

where we take  $\phi_1, \phi_2$  to be primary scalars for simplicity. This transforms like a three-point function of primary operators, which is fixed by conformal invariance up to an overall constant. Without loss of generality, we can place  $x$  at spatial infinity  $x \rightarrow \infty$  so that the light-transform contour runs along  $\mathcal{I}^+$ ,

$$\begin{aligned} \langle \Omega | \phi_1(x_1) \mathbf{L}[\mathcal{O}](\infty, z) \phi_2(x_2) | \Omega \rangle &\equiv \lim_{x \rightarrow \infty} x^{2(1-J)} \langle \Omega | \phi_1(x_1) \mathbf{L}[\mathcal{O}](x, I(x)z) \phi_2(x_2) | \Omega \rangle \\ &= \mathcal{M}(x_1 - x_2). \end{aligned} \quad (4.104)$$



The factor  $x^{2(1-J)}$  ensures a finite result as  $x \rightarrow \infty$ . (Recall that  $\mathbf{L}[\mathcal{O}]$  transforms like a primary with dimension  $1 - J$ .) We must act on the polarization vector  $z$  with the inversion matrix  $I^\mu{}_\nu(x) = \delta^\mu{}_\nu - \frac{2x^\mu x_\nu}{x^2}$ , so that  $x_1, x_2$  and  $z$  transform in the same way under Lorentz transformations.

The operator  $\mathbf{L}[\mathcal{O}](\infty, z)$  transforms like a primary inserted at spatial-infinity, which means it is annihilated by momentum generators

$$[P^\mu, \mathbf{L}[\mathcal{O}](\infty, z)] = 0. \quad (4.105)$$

Hence, the matrix element (4.104) is translationally-invariant, which is why we have written  $\mathcal{M}(x_1 - x_2)$  in (4.104). Recall that  $\phi_1, \phi_2$  are operator-valued distributions, so  $\mathcal{M}(x_1 - x_2)$  is really a translationally-invariant integral kernel that can be paired with test functions  $f_1(x_1), f_2(x_2)$ . This kernel can be diagonalized by going to momentum space. Let us define the Fourier-transformed states

$$|\phi(p)\rangle = \int d^d x e^{ip \cdot x} \phi(x) |\Omega\rangle. \quad (4.106)$$

Positivity of energy implies that  $|\phi(p)\rangle$  is nonvanishing only if  $p$  is inside the forward lightcone. The event shape is

$$\langle \phi_1(q) | \mathbf{L}[\mathcal{O}](\infty, z) | \phi_2(p) \rangle = (2\pi)^d \delta^d(p - q) \widetilde{\mathcal{M}}(p). \quad (4.107)$$

We often abuse notation and write

$$\widetilde{\mathcal{M}}(p) = \langle \phi_1(p) | \mathbf{L}[\mathcal{O}](\infty, z) | \phi_2(p) \rangle, \quad (4.108)$$

where it is understood that we have stripped off the momentum-conserving  $\delta$ -function.

The physical interpretation of  $\widetilde{\mathcal{M}}(p)$  is that the state  $|\phi_2(p)\rangle$  acts like a source in Minkowski space. Excitations from the source fly out to  $\mathcal{I}^+$ , where they hit the “detector”  $\mathbf{L}[\mathcal{O}](\infty, z)$ . Here,  $z$  specifies a particular direction on the celestial sphere  $S^{d-2}$  where the detector sits. Finally, we take the overlap of the resulting state with the sink  $\langle \phi_1(p) |$ . The correlator (5.49) is called a one-point “event shape” because it involves a single detector.

More generally, we can consider an expectation value of multiple detectors at  $\mathcal{I}^+$ , i.e. a multi-point event shape

$$\langle \phi_1(p) | \mathbf{L}[\mathcal{O}_1](\infty, z_1) \cdots \mathbf{L}[\mathcal{O}_n](\infty, z_n) | \phi_2(p) \rangle. \quad (4.109)$$

Multi-point event shapes involve a limit where the initial and final points of the light-transform contours become coincident. Specifically, all detector integration contours

start at spatial infinity and end at future infinity. We discuss the conditions under which this limit is well-defined in section 4.4.

Future null infinity  $\mathcal{I}^+$  is conformally equivalent to a null plane. For example, by performing a null inversion, we can bring  $\mathcal{I}^+$  to the plane  $u = 0$  in the  $(u, v, \vec{y})$  coordinates

$$(u, v, \vec{y}) = \left( -\frac{1}{x^-}, x^+ - \frac{\vec{x}^2}{x^-}, -\frac{\vec{x}}{x^-} \right). \quad (4.110)$$

In these coordinates, the event shape takes the form

$$\langle \phi_1(p) | \frac{1}{(1 + n_1^{d-1})^{\Delta_1 - 1}} \int dv_1 \mathcal{O}_{1v\dots v}(0, v_1, \vec{y}_1) \cdots \frac{1}{(1 + n_n^{d-1})^{\Delta_n - 1}} \int dv_n \mathcal{O}_{nv\dots v}(0, v_n, \vec{y}_n) | \phi_2(p) \rangle. \quad (4.111)$$

Note that the sink and source states are still defined via a Fourier transform with respect to  $x$ . The transverse position of the detectors  $\vec{y}_i$  are related to the null vectors  $z_i$  by stereographic projection,

$$z = (1, \vec{n}), \quad \vec{n} = (\vec{n}_\perp, n^{d-1}) = \left( \frac{2\vec{y}}{1 + \vec{y}^2}, \frac{1 - \vec{y}^2}{1 + \vec{y}^2} \right) \in S^{d-2}. \quad (4.112)$$

A consequence of writing the event shape in the form (4.111) is that it makes clear that the operators  $\mathcal{O}_i$  remain spacelike-separated along their integration contours. This ostensibly implies that detectors should commute. However, this argument ignores the fact that the operators become coincident at the ends of their integration contours. The question of commutativity of detectors is more subtle, and is related to singularities of four-point functions as we discuss in section 4.4.

### 4.3.3 Computing event shapes in the bulk

To understand the connection between event shapes and flat-space shock amplitudes, let us review how event shapes are computed in theories with a gravity dual [31, 178–180].<sup>19</sup> For simplicity, we focus on energy detectors. A multi-point event shape for ANEC operators  $\mathcal{E}$  is called an “energy correlator.” We will see that commutativity of energy detectors is essentially equivalent to the coincident shock commutativity discussed in section 4.2.

To begin, let us separate the detectors in the  $u$  direction, so that  $\mathbf{L}[\mathcal{O}_i]$  is at position  $u_i$  with the ordering  $u_1 > u_2 > \cdots > u_k$ . The insertion of an integrated stress tensor

<sup>19</sup>We thank Xián Camanho, Jose Edelman, Diego Hofman and Juan Maldacena for discussions on this topic.

$\sum_i \lambda_i \int_{-\infty}^{\infty} dv T_{vv}(u_i, v, \vec{y}_i)$  in a CFT is dual to the shockwave geometry

$$ds^2 = \frac{-du dv + \sum_{i=1}^{d-2} d\vec{y}^2 + dz^2 + \sum_i \delta(u - u_i) h_i(\vec{y}, z) (du)^2}{z^2}, \quad (4.113)$$

$$h_i(\vec{y}, z) = \lambda_i \frac{2^{d-1}}{\text{vol } S^{d-2}} \frac{z^d}{(z^2 + |\vec{y} - \vec{y}_i|^2)^{d-1}}. \quad (4.114)$$

To derive the proportionality constant in (4.114), recall that according to the standard AdS/CFT dictionary, the source for the stress tensor is encoded in the  $\frac{1}{z^2}$  deformation of the metric as  $z \rightarrow 0$ . One can check that (4.114) corresponds to a source  $\lambda_i \delta(u - u_i) \delta^{(d-2)}(\vec{y} - \vec{y}_i)$  for  $T_{vv}(y)$ .

A remarkable property of the metric (4.113) (or any superposition of such shock waves) is that it is an exact solution of Einstein's equations, even when arbitrary higher derivative corrections are included [181]. Here, we used the  $y = (u, v, \vec{y})$  coordinate system, which is related to the coordinate  $x$  by null inversion (4.110). The locus  $u = 0$  is the Poincare horizon of the original Poincare patch in  $x$ . We define energy detectors as

$$\mathcal{E}(\vec{n}) \equiv 2L[T](\infty, (1, \vec{n})), \quad \vec{n} \in S^{d-2}. \quad (4.115)$$

In the  $\vec{y}$  conformal frame, this is

$$\mathcal{E}(\vec{n}) = \frac{2}{(1 + n^{d-1})^{d-1}} \int_{-\infty}^{\infty} dv T_{vv}(u_i, v, \vec{y}_i), \quad (4.116)$$

where  $\vec{y} = \frac{\vec{n}_\perp}{1+n^{d-1}}$  and  $\vec{n} = (\vec{n}_\perp, n^{d-1})$ .

To compute energy correlators, we need to compute an overlap between states before and after propagation through a series of shocks

$$\mathcal{A}(\lambda_i) = \langle \Psi | \Psi' \rangle, \quad (4.117)$$

where  $|\Psi'\rangle$  represents the state after propagation through shocks. We compute the amplitude with shocks at locations  $u_1 > u_2 > \dots > u_k$ , and then subsequently take  $u_i \rightarrow 0$ . The energy correlator is given by

$$\langle \Psi | \mathcal{E}(\vec{n}_1) \cdots \mathcal{E}(\vec{n}_k) | \Psi \rangle = \prod_{i=1}^k \frac{2}{(1 + n_i^{d-1})^{d-1}} (-i\partial_{\lambda_1}) \cdots (-i\partial_{\lambda_k}) \mathcal{A}(\lambda_i) \Big|_{\lambda_i=0}. \quad (4.118)$$

We are interested in states dual to a single-trace operator insertion with momentum  $q$ :

$$|\Psi\rangle = \int dx e^{iqx} \mathcal{O}(x) |\Omega\rangle. \quad (4.119)$$

This corresponds to a single-particle state in the bulk. When the particle crosses a shock, it could lead to particle production. However, particle-production is suppressed to leading order in  $1/c_T$ . Instead, the leading-order effect is mixing with other single-particle states.

Mixing is captured by one-point energy correlators  $\langle \Psi_2 | \mathcal{E}(\vec{n}_1) | \Psi_1 \rangle$ . To understand these, let us study in more detail the propagation of fields on a shockwave background. This problem was considered in [31]. Consider a shock located at  $u = 0$ . Without loss of generality, we can set  $q = (q^0, 0, \dots, 0)$ . Using the bulk-to-boundary propagator, we can compute the wave-function of the particle in the bulk. In the vicinity of  $u = 0$ , it takes the form

$$\phi(u, v, \vec{y}, z) \sim e^{-i\frac{q^0}{2}v} \delta(z-1) \delta^{(d-2)}(\vec{y}). \quad (4.120)$$

In other words, the particle crosses  $u = 0$  at a fixed transverse location. In (4.120), we used the AdS  $y$ -coordinates, see formula (3.3) in [31]. The location of the probe particle in the radial direction is related to its momentum. For  $\vec{q} = 0$  we get  $z = 1$ .

Before and after the shockwave, the scalar field propagates freely. At the location of the shock, however, it changes discontinuously. The change is dictated by the equations of motions, which for the minimally coupled scalar field  $\phi$  become

$$\partial_u \partial_v \phi + \delta(u) h(\vec{y}, z) \partial_v^2 \phi + \dots = 0. \quad (4.121)$$

where we only kept the terms that contribute to the  $\delta(u)$  discontinuity. The matching condition for the field across the shock is obtained by integrating (4.121) over a small interval  $u \in [-\epsilon, \epsilon]$ , with the result

$$\phi_{\text{after}}(0, v, \vec{y}, z) = e^{-h\partial_v} \phi_{\text{before}}(0, v, \vec{y}, z). \quad (4.122)$$

Plugging in the wavefunction (4.120), we see that (4.122) becomes multiplication by a phase

$$\phi_{\text{after}}(0, v, \vec{y}, z) \sim e^{i\frac{q^0}{2}h(\vec{y}=\vec{0}, z=1)} \phi_{\text{before}}(0, v, \vec{y}, z). \quad (4.123)$$

Finally, using (4.118) and the expression (4.114) for  $h$ , we obtain

$$\langle \mathcal{E}(\vec{n}) \rangle_{\mathcal{O}(q)} \equiv \frac{\langle \Psi | \mathcal{E}(\vec{n}) | \Psi \rangle}{\langle \Psi | \Psi \rangle} = \frac{q^0}{\text{vol } S^{d-2}}. \quad (4.124)$$

This calculation is almost identical to our calculation of the amplitude for a minimally-coupled scalar to cross a shock in flat-space in section 4.2.3.1.

To compute a  $k$ -point energy correlator, we can imagine propagating the particle through a series of shocks at  $u_1 > u_2 > \dots > u_k$ , and then taking the limit  $u_i \rightarrow 0$ . Alternatively, we can simply multiply a series of one-point correlators (4.124). Either way, the result is

$$\langle \mathcal{E}(\vec{n}_1) \cdots \mathcal{E}(\vec{n}_k) \rangle_{\mathcal{O}(q)} \equiv \frac{\langle \Psi | \mathcal{E}(\vec{n}_1) \cdots \mathcal{E}(\vec{n}_k) | \Psi \rangle}{\langle \Psi | \Psi \rangle} = \left( \frac{q^0}{\text{vol } S^{d-2}} \right)^k. \quad (4.125)$$

The situation becomes more interesting if we include higher derivative corrections or mixing between fields. For example, consider a massless vector field  $A_\mu$ . As discussed in [96], the most general equation of motion for  $A_\mu$  takes the form

$$\nabla^\mu F_{\mu\nu} - \frac{a_2}{d(d-1)} \widehat{R}_\nu^{\mu\alpha\beta} \nabla_\mu F_{\alpha\beta} = 0, \quad (4.126)$$

where  $a_2$  is a non-minimal coupling constant, and following [181], we introduced the effective shockwave Riemann tensor  $\widehat{R}_\nu^{\mu\alpha\beta}$  via

$$R_{\mu\nu\rho\sigma} = -g_{\mu\rho}g_{\nu\sigma} + g_{\nu\rho}g_{\mu\sigma} + \widehat{R}_{\mu\nu\rho\sigma}. \quad (4.127)$$

The shockwave Riemann tensor is given by

$$\widehat{R}_{\mu\nu\rho\sigma} = l_{[\mu} K_{\nu][\rho} l_{\sigma]}, \quad (4.128)$$

where  $l_\mu = \partial_\mu u$  and  $K_{\mu\nu}$  is symmetric, satisfies  $K_{\mu\nu} l^\mu = 0$ , and takes the form

$$\begin{aligned} K_{zz} &= \frac{1}{2} (z^{-2} \partial_z^2 h - z^{-3} \partial_z h), \\ K_{zi} &= \frac{1}{2} \frac{\partial_i \partial_z h}{z^2}, \\ K_{ij} &= \frac{1}{2} (z^{-2} \partial_i \partial_j h - \delta_{ij} z^{-3} \partial_z h). \end{aligned} \quad (4.129)$$

For us, the relevant component of  $\widehat{R}_{\mu\nu\rho\sigma}$  is

$$\widehat{R}_{+ij+}|_{\vec{y}=0, z=1} = \frac{d(d-1)}{2} \left( \frac{1+n^{d-1}}{2} \right)^{d-1} \left( n_i n_j - \frac{\delta_{ij}}{d-1} \right). \quad (4.130)$$

Note that the indices  $i$  and  $j$  above go from  $i, j = 1, \dots, d-2$ , whereas the problem naturally has  $\text{SO}(d-1)$  symmetry. It is easy to make this symmetry manifest by going from planar coordinates to the coordinates of [181].

Consider now a perturbation to the transverse components of  $A_\mu$ ,

$$A_i(u, v, \vec{y}, z) \sim \epsilon_i e^{-i\frac{q_0 v}{2}} \delta^{d-2}(\vec{y}) \delta(z-1), \quad (4.131)$$

where  $\epsilon_i$  are components of a polarization vector  $\epsilon_\mu$ . The equations of motion become

$$\partial_u \partial_v A_i + \delta(u) \widehat{H}_{ij} \partial_v^2 A_j + \dots = 0, \quad (4.132)$$

$$\widehat{H}_{ij} = \sum_{a=1}^k \frac{\lambda_a}{\Omega_{S^{d-2}}} (1 + n_a^{d-1})^{d-1} (\widehat{H}_a)_{ij}, \quad (4.133)$$

$$(H_a)^{ij} \equiv \left[ \delta^{ij} + a_2 \left( n_a^i n_a^j - \frac{\delta^{ij}}{d-1} \right) \right]. \quad (4.134)$$

The solution is simply

$$A_i^{\text{after}} = \left[ e^{-\widehat{H} \partial_v} A^{\text{before}} \right]_i. \quad (4.135)$$

The formulas above are sufficient to compute a one-point energy correlator for the transverse components of  $A_\mu$ . However, note that the full problem additionally involves the component  $A_z$ , which also gets excited by crossing the shock. As we remarked above, its behavior is fixed by  $\text{SO}(d-1)$  symmetry. The effect of including  $A_z$  should be to enlarge the transfer matrix  $H_{ij}$  to include the  $(d-1)$ 'th component of  $n^\mu$ . The same formula (4.134) applies, except now the indices  $ij$  run from 1 to  $d-1$ .

We can now compute the energy correlator (4.118). As before, let us order the shocks such that  $u_1 > u_2 > \dots > u_k$  and then take the limit  $u_i \rightarrow 0$ . This introduces a corresponding ordering of the transfer matrices (4.134) that govern propagation through each shock. The result becomes

$$\langle \mathcal{E}(\vec{n}_1) \cdots \mathcal{E}(\vec{n}_k) \rangle_{\epsilon, J(q)} = \left( \frac{q^0}{\text{vol } S^{d-2}} \right)^k \frac{\epsilon^\dagger H_1 \cdots H_k \epsilon}{\epsilon^\dagger \epsilon}, \quad (4.136)$$

where the subscript on the left-hand side indicates that we compute the event shape in the state created by  $\epsilon \cdot J^\mu$ , where  $J^\mu$  is a current. A commutator  $[\mathcal{E}(n_1), \mathcal{E}(n_2)]$  is simply related to a commutator of transfer matrices  $[H_1, H_2]$ .

Let us next consider the case of gravity. As discussed in [96], the most general equation of motion for a gravitational perturbation takes the form

$$\delta R_{\mu\nu} + \alpha_2 \widehat{R}_{(\mu}{}^{\rho\alpha\beta} \delta R_{\nu)\rho\alpha\beta} + \alpha_4 \left[ \nabla_{(\mu} \nabla_{\nu)} \widehat{R}^{\alpha\beta\rho\sigma} \right] \delta R_{\alpha\beta\rho\sigma} = 0. \quad (4.137)$$

As before, it is enough to consider transverse perturbations  $h_{ij}$  and keep only the dependence on  $u$  and  $v$  (the rest is fixed by symmetries). Our equation becomes

$$\partial_u \partial_v h_{ij} + \delta(u) \widehat{H}_{ij, mn} \partial_v^2 h_{mn} + \dots = 0. \quad (4.138)$$

The form of the shockwave matrix  $\widehat{H}_{ij,mn}$  is fixed by the symmetries of the problem to be<sup>20</sup>

$$\begin{aligned}\widehat{H}_{ij,mn} &= \sum_{a=1}^k \frac{\lambda_a}{\Omega_{S^{d-2}}} (1 + n_a^{d-1})^{d-1} (H_a)_{ij,mn}, \\ H_{ij,kl}(\vec{n}) &\equiv \frac{1}{2} (\delta_{ik}\delta_{jl} + \delta_{il}\delta_{jk}) - \frac{1}{d-1} \delta_{ij}\delta_{kl} + \frac{t_2}{4} (\delta_{ik}P_{jl} + \delta_{il}P_{jk} + \delta_{jl}P_{ik} + \delta_{jk}P_{il}) \\ &\quad + t_4 P_{ijkl} - \frac{t_2 + t_4}{d-1} (\delta_{ij}P_{kl} + \delta_{kl}P_{ij}),\end{aligned}\tag{4.139}$$

where  $H_a = H(\vec{n}_a)$  and we have introduced

$$\begin{aligned}P_{ij} &= n_i n_j - \frac{\delta_{ij}}{d-1}, \\ P_{ijkl} &= n_i n_j n_k n_l - \frac{\delta_{ij}\delta_{kl} + \delta_{ik}\delta_{jl} + \delta_{il}\delta_{jk}}{(d+1)(d-1)},\end{aligned}\tag{4.140}$$

and used the known result for the one-point energy correlator.

The solution of (4.138) is

$$h_{ij}^{\text{after}} = \left[ e^{-\widehat{H}\partial_v} h^{\text{before}} \right]_{ij}.\tag{4.141}$$

The energy correlator (4.118) again depends on the ordering of the shocks. We get

$$\langle \mathcal{E}(\vec{n}_1) \cdots \mathcal{E}(\vec{n}_k) \rangle_{\epsilon, T(q^0)} = \left( \frac{q^0}{\Omega_{S^{d-2}}} \right)^k \frac{\epsilon^\dagger H_1 \cdots H_k \epsilon}{\epsilon^\dagger \epsilon}.\tag{4.142}$$

In these calculations, it was crucial to compute the propagation amplitude through separated shocks  $u_1 > u_2 > \cdots > u_k$ , and afterwards take the limit  $u_i \rightarrow 0$ . This is guaranteed to produce the ordering of operators  $\mathcal{E}(\vec{n}_1) \cdots \mathcal{E}(\vec{n}_k)$ . By comparing different orderings, we can obtain interesting consistency conditions on the theory. A different procedure is to first set  $u_i = 0$ , compute the propagation through a shock background  $h(\vec{y}, z) = \sum_i h_i(\vec{y}, z)$ , and then take derivatives with respect to  $\lambda_i$ . Instead of producing an ordered product of transfer matrices, this latter procedure produces a symmetrized product

$$\epsilon^\dagger H_1 H_2 \cdots H_k \epsilon.\tag{4.143}$$

If we only have access to this object, we cannot study commutativity. However, one can study positivity of energy correlators [155].

<sup>20</sup>The precise relation between  $\alpha_2$  and  $\alpha_4$  that appear in (4.137) and more familiar three-point structures  $t_2$  and  $t_4$  can be found in section 5 of [96].

#### 4.4 Products of light-ray operators and commutativity

In this section, we discuss in detail the question of when light-transformed operators on the same null plane commute. We find that commutativity requires nontrivial conditions on the OPE limit, lightcone limit, and Regge limit of CFT four-point functions, all of which we verify in the case of ANEC operators in a nonperturbative CFT. In the Regge limit, we find that  $J_0 < 3$  is a sufficient condition for commutativity of ANEC operators. One can argue using the light-ray OPE that it is also necessary, see chapter 5. Thus, superconvergence sum rules hold also in planar theories which do not satisfy nonperturbative bounds on the Regge limit, but do satisfy the bound on chaos  $J_0 \leq 2$  [84].

##### 4.4.1 Existence vs. commutativity

Our goal is to answer two related questions:

- Is a product of light-transforms at coincident points  $\mathbf{L}[\mathcal{O}_1](x, z_1)\mathbf{L}[\mathcal{O}_2](x, z_2)$  well-defined?
- Do light-transforms at coincident points commute,

$$[\mathbf{L}[\mathcal{O}_1](x, z_1), \mathbf{L}[\mathcal{O}_2](x, z_2)] = 0? \quad (4.144)$$

In event shapes, we set  $x = \infty$ , but the answer is the same for any  $x$ , by conformal invariance. We take  $z_1 \neq z_2$ , so that the integration contours for  $\mathbf{L}[\mathcal{O}_1]$  and  $\mathbf{L}[\mathcal{O}_2]$  are not identical.

The coincident limit of light-transformed operators is defined by

$$\lim_{y \rightarrow x} \mathbf{L}[\mathcal{O}_1](x, z_1)\mathbf{L}[\mathcal{O}_2](y, z_2). \quad (4.145)$$

That is, we first perform the light-transforms starting from distinct  $x$  and  $y$  and then take the limit where the initial points  $x$  and  $y$  coincide. To determine when the operator (4.145) exists, let us study a matrix element between states created by operators  $\mathcal{O}_3$  and  $\mathcal{O}_4$ <sup>21</sup>

$$\begin{aligned} & \lim_{y \rightarrow x} \langle \Omega | \mathcal{O}_4 \mathbf{L}[\mathcal{O}_1](x, z_1) \mathbf{L}[\mathcal{O}_2](y, z_2) \mathcal{O}_3 | \Omega \rangle \\ &= \lim_{y \rightarrow x} \int_{-\infty}^{\infty} d\alpha_1 d\alpha_2 (-\alpha_1)^{-\Delta_1 - J_1} (-\alpha_2)^{-\Delta_2 - J_2} \\ & \quad \times \langle \Omega | \mathcal{O}_4 \mathcal{O}_1(x - z_1/\alpha_1, z_1) \mathcal{O}_2(y - z_2/\alpha_2, z_2) \mathcal{O}_3 | \Omega \rangle. \end{aligned} \quad (4.146)$$

---

<sup>21</sup>The positions of  $\mathcal{O}_3, \mathcal{O}_4$  can be smeared to create normalizable states, though that will not be important in our analysis.



If the above integral converges absolutely in the limit  $y \rightarrow x$ , then we can commute the limit and the integral to obtain

$$= \int_{-\infty}^{\infty} d\alpha_1 d\alpha_2 (-\alpha_1)^{-\Delta_1 - J_1} (-\alpha_2)^{-\Delta_2 - J_2} \langle \Omega | \mathcal{O}_4 \mathcal{O}_1(x - z_1/\alpha_1, z_1) \mathcal{O}_2(x - z_2/\alpha_2, z_2) \mathcal{O}_3 | \Omega \rangle. \quad (4.147)$$

When (4.147) converges, commutativity is manifest because  $\mathcal{O}_1$  and  $\mathcal{O}_2$  remain spacelike-separated everywhere in the region of integration. In the next subsection, we analyze in detail when (4.147) converges.

However, it can happen that the integral (4.147) is not absolutely convergent. This does not necessarily mean that the product of operators (4.145) is ill-defined, but it does mean that commutativity can be lost. To understand how this works, let us start with the first line of (4.146) and use the fact that  $\mathbf{L}[\mathcal{O}_1]$  and  $\mathbf{L}[\mathcal{O}_2]$  annihilate the vacuum to rewrite the correlator in terms of a double-commutator:

$$\begin{aligned} & \lim_{y \rightarrow x} \langle \Omega | [\mathcal{O}_4, \mathbf{L}[\mathcal{O}_1](x, z_1)] [\mathbf{L}[\mathcal{O}_2](y, z_2), \mathcal{O}_3] | \Omega \rangle \\ &= \lim_{y \rightarrow x} \int_{-\infty}^{\infty} d\alpha_1 d\alpha_2 (-\alpha_1)^{-\Delta_1 - J_1} (-\alpha_2)^{-\Delta_2 - J_2} \\ & \quad \times \langle \Omega | [\mathcal{O}_4, \mathcal{O}_1(x - z_1/\alpha_1, z_1)] [\mathcal{O}_2(y - z_2/\alpha_2, z_2), \mathcal{O}_3] | \Omega \rangle. \end{aligned} \quad (4.148)$$

If this integral is absolutely convergent in the limit  $y \rightarrow x$ , then we can commute the limit and integration to obtain

$$\begin{aligned} &= \int_{-\infty}^{\infty} d\alpha_1 d\alpha_2 (-\alpha_1)^{-\Delta_1 - J_1} (-\alpha_2)^{-\Delta_2 - J_2} \\ & \quad \times \langle \Omega | [\mathcal{O}_4, \mathcal{O}_1(x - z_1/\alpha_1, z_1)] [\mathcal{O}_2(x - z_2/\alpha_2, z_2), \mathcal{O}_3] | \Omega \rangle, \end{aligned} \quad (4.149)$$

which differs from (4.147) only in that the Wightman function has been replaced by a double-commutator. The key point is that (4.149) might converge in a wider variety of situations than (4.147). This is because the double-commutator might be better behaved than the Wightman function in singular limits. Thus, the integral (4.149) gives a more general way to define matrix elements of the product (4.145), but it does not manifest commutativity. The fact that coincident light-transformed operators sometimes fail to commute has been noticed previously and is sometimes called “detector cross-talk” [147, 182]. We give an example of this phenomenon in appendix C.2.

To summarize,

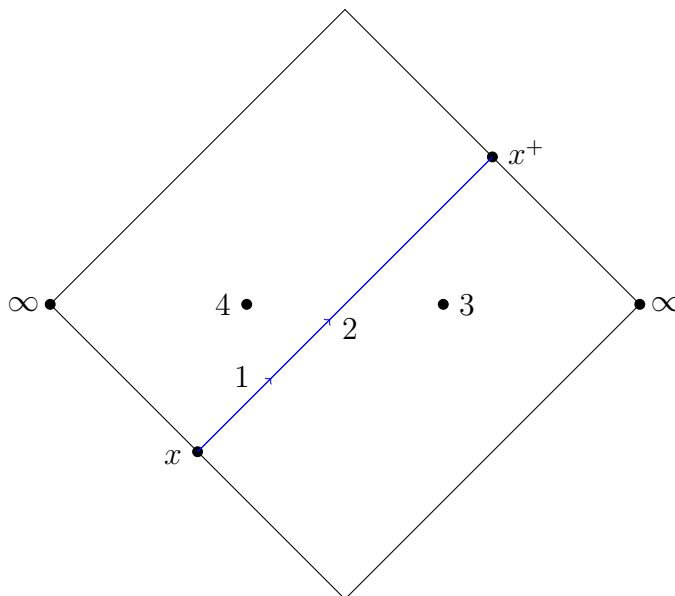


Figure 4.5: We consider the causal configuration where  $4 > x$  and  $3 < x^+$  with 3 and 4 spacelike from each other. The points 1 and 2 are integrated over parallel null lines in the same null plane, with nonzero transverse separation. Here, we have suppressed the transverse direction, so the null plane appears as a single diagonal line (blue) from  $x$  to  $x^+$ . (The conformal completion of the null plane also includes the left-moving diagonal line from  $x$  to  $\infty$  on the left, and then from  $\infty$  to  $x^+$  on the right.)

- Absolute convergence of the double commutator integral (4.149) is a sufficient condition for the existence of  $\mathbf{L}[\mathcal{O}_1](x, z_1)\mathbf{L}[\mathcal{O}_2](x, z_2)$ .
- Absolute convergence of the Wightman function integral (4.147) is a sufficient condition for the existence of  $\mathbf{L}[\mathcal{O}_1](x, z_1)\mathbf{L}[\mathcal{O}_2](x, z_2)$  and commutativity  $[\mathbf{L}[\mathcal{O}_1](x, z_1), \mathbf{L}[\mathcal{O}_2](x, z_2)] = 0$ .

Note that when the integrals do not converge absolutely, it may be still possible to prescribe values to them, but these values may suffer from ambiguities in how the integral is computed. In the following sections, we discuss in detail when the above conditions hold.

#### 4.4.2 Convergence of the Wightman function integral

Let us analyze in detail the conditions under which the Wightman function integral (4.147) is absolutely convergent. For now, we consider the causal configuration  $4 > x$ ,  $x^+ > 3$ , with 4 spacelike from 3, see figure 4.5. We comment on other configurations in section 4.4.4. The region of integration is shown in figure 4.6. Let us describe some of its important features.

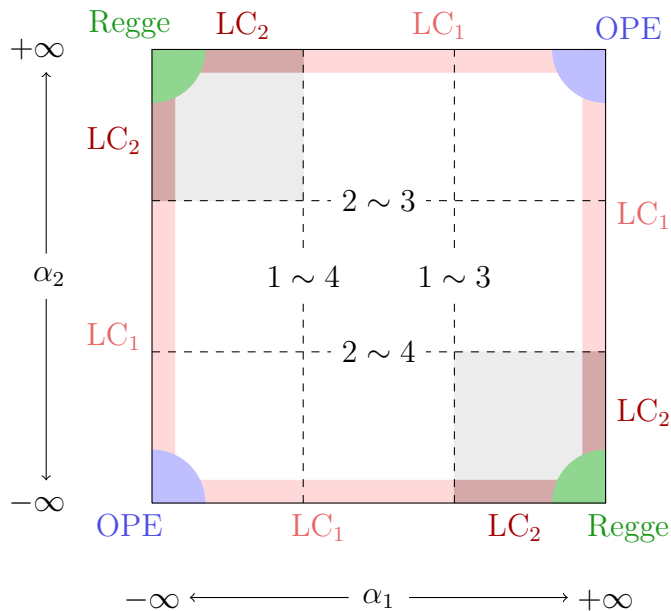


Figure 4.6: Integration region for the double light-transform of a Wightman function (4.147). The  $1 \times 2$  OPE converges in the white region (the “first sheet”), but it does not necessarily converge in the gray-shaded region (the “second sheet”). The OPE limit is indicated in blue, the Regge limit in green, the lightcone limit on the first sheet ( $LC_1$ ) in light red, and the lightcone limit on the second sheet ( $LC_2$ ) in dark red.

The dashed lines indicate when 1 and 2 become lightlike-separated from 3 and 4. When 1, 2 are spacelike from 4, or 1, 2 are spacelike from 3, we can rearrange the operators in the Wightman function so that 1 and 2 both act on the vacuum. The  $1 \times 2$  OPE is guaranteed to converge in this case [183, 184]. We refer to this region as the “first sheet” because the conformal cross-ratios need not move around branch points to get there.

Meanwhile, when  $4 > 1$  and  $2 > 3$ , or  $4 > 2$  and  $1 > 3$ , the  $1 \times 2$  OPE is not guaranteed to converge. (Other OPEs do converge in these regions.) We call these regions the “second sheet” (shaded gray in figure 4.6) because the cross ratios must move around branch points to get there.

We only need to analyze the convergence of the integral near the boundary of the integration region. Indeed, in the bulk of the integration region the only singularities are due to 1 or 2 becoming lightlike from 3 or 4. These singularities are removed by the  $i\epsilon$  prescriptions for operators  $\mathcal{O}_3$  and  $\mathcal{O}_4$ . After this, we can split the integral into the near-boundary region and the bulk region. The bulk region is compact and free of singularities, so the convergence of the integral there is straightforward.

On the boundary of the region of integration, there are several types of singularities.

- Firstly, when  $\alpha_1, \alpha_2 \rightarrow \pm\infty$  simultaneously, operators 1 and 2 become close on the first sheet. This singularity is described by the OPE.
- When  $\alpha_1 \rightarrow +\infty, \alpha_2 \rightarrow -\infty$  simultaneously or  $\alpha_1 \rightarrow -\infty, \alpha_2 \rightarrow +\infty$  simultaneously, this is the Regge limit, which lies on the second sheet. This singularity is described by conformal Regge theory [28, 149, 150].
- Another type of singularity occurs when either  $\alpha_1$  or  $\alpha_2$  approach  $\pm\infty$ , with the other variable held fixed. This is the lightcone limit, where 1 and 2 become lightlike separated. The lightcone limit on the first sheet is described by the  $1 \times 2$  OPE, while the lightcone limit on the second sheet is not necessarily described by the  $1 \times 2$  OPE.<sup>22</sup>

Our strategy will be to first analyze the singularities on the first sheet. Then we will use Rindler positivity and the Cauchy-Schwarz inequality to bound singularities on the second sheet in terms of singularities on the first.

#### 4.4.2.1 OPE limit on the first sheet

Let us begin by studying the OPE singularity on the first sheet. Without loss of generality, we take  $\alpha_1, \alpha_2 \rightarrow -\infty$ . We can choose a conformal frame where  $\mathcal{O}_1$  and  $\mathcal{O}_2$  are both approaching the origin. For simplicity, consider a traceless symmetric tensor  $\mathcal{O}_0 \in \mathcal{O}_1 \times \mathcal{O}_2$  with dimension  $\Delta_0$  and spin  $J_0$ . The contribution of  $\mathcal{O}_0$  in the OPE takes the form

$$\begin{aligned} & \mathcal{O}_1 \left( x_1 = -\frac{z_1}{\alpha_1}, z_1 \right) \mathcal{O}_2 \left( x_2 = -\frac{z_2}{\alpha_2}, z_2 \right) \\ & \supset \sum_{m,n,k} c_{mnk} (x_{12}^2)^{\frac{\Delta_0 - \Delta_1 - \Delta_2}{2}} (z_1 \cdot \hat{x}_{12})^{J_1 - n} (z_2 \cdot \hat{x}_{12})^{J_2 - k} \\ & \quad \times (\hat{x}_{12})_{\mu_1} \cdots (\hat{x}_{12})_{\mu_m} z_{1\nu_1} \cdots z_{1\nu_n} z_{2\rho_1} \cdots z_{2\rho_k} \mathcal{O}_0^{\mu_1 \cdots \mu_m \nu_1 \cdots \nu_n \rho_1 \cdots \rho_k}(0), \end{aligned} \quad (4.150)$$

where  $m+n+k = J_0$  and  $\hat{x}_{12} = x_{12}/(x_{12}^2)^{1/2}$ . The factors of  $x_{12}^2$  come from dimensional analysis. The factors of  $z_i \cdot \hat{x}_{12}$  come from demanding the correct homogeneity in  $z_i$ .

Let us make the change of variables

$$-\frac{1}{\alpha_1} = r\sigma, \quad -\frac{1}{\alpha_2} = r(1 - \sigma). \quad (4.151)$$

<sup>22</sup>The lightcone limit on the second sheet has been conjectured to have an asymptotic expansion in terms of  $1 \times 2$  OPE data [151]. We comment on the implications of this conjecture in section 4.4.2.6.

Supplying the appropriate factors  $(-\alpha_i)^{-\Delta_i - J_i}$ , the double light-transform of a single term above becomes

$$\begin{aligned} & \int \frac{dr}{r^3} \int_0^1 \frac{d\sigma}{\sigma^2(1-\sigma)^2} r^{\Delta_1 + J_1 + \Delta_2 + J_2} \sigma^{\Delta_1 + J_1} (1-\sigma)^{\Delta_2 + J_2} \\ & \times r^{\Delta_0 - \Delta_1 - \Delta_2} (\sigma(1-\sigma))^{\frac{\Delta_0 - \Delta_1 - \Delta_2}{2}} \left(\frac{1-\sigma}{\sigma}\right)^{\frac{J_1 - n}{2}} \left(\frac{\sigma}{1-\sigma}\right)^{\frac{J_2 - k}{2}} \\ & \times \left(\frac{\sigma z_1 - (1-\sigma)z_2}{\sqrt{-2z_1 \cdot z_2 \sigma(1-\sigma)}}\right)^m \times \dots, \end{aligned} \quad (4.152)$$

where “...” indicates quantities independent of  $r$  and  $\sigma$ . We have also written  $(\widehat{x}_{12})_{\mu_1} \cdots (\widehat{x}_{12})_{\mu_m}$  schematically as  $(\widehat{x}_{12})^m$ .

Requiring that the  $r$ -integral converge near  $r = 0$  gives the condition

$$J_1 + J_2 > 2 - \Delta_0. \quad (4.153)$$

This is a consequence of dimensional analysis. To derive it more succinctly, recall that  $\mathbf{L}[\mathcal{O}_i]$  has dimension  $\Delta_i^L \equiv 1 - J_i$ . If  $\mathcal{O}_0$  appears in the OPE, then the coincident limit of  $\mathbf{L}[\mathcal{O}_1]$  and  $\mathbf{L}[\mathcal{O}_2]$  can only be finite if  $\Delta_0 > \Delta_1^L + \Delta_2^L$ , which is equivalent to (4.153). In particular, this shows that (4.153) must hold even if  $\mathcal{O}_0$  is not a traceless symmetric tensor.

Requiring that the  $\sigma$ -integral converge near  $\sigma = 0, 1$  gives the conditions

$$\begin{aligned} J_1 + J_2 + \Delta_1 - \Delta_2 &> 2 - \tau_0 - 2n, \\ J_1 + J_2 + \Delta_2 - \Delta_1 &> 2 - \tau_0 - 2k, \end{aligned} \quad (4.154)$$

where  $\tau_0 \equiv \Delta_0 - J_0$  is the twist of  $\mathcal{O}_0$ . These conditions are strongest when  $n = k = 0$ , in which case they together become

$$J_1 + J_2 - |\Delta_1 - \Delta_2| > 2 - \tau_0. \quad (4.155)$$

The conditions (4.153) and (4.155) can be weakened slightly using the special kinematics of the light transform. Because the polarization vectors  $z_i$  are aligned with the positions  $x_i = -z_i/\alpha_i$ , the two-point function  $\langle \mathcal{O}_1 \mathcal{O}_2 \rangle$  vanishes except when  $\mathcal{O}_1$  and  $\mathcal{O}_2$  are scalars. Consequently, the unit operator does not appear in the  $\mathcal{O}_1 \times \mathcal{O}_2$  OPE, and we can write

$$\begin{aligned} J_1 + J_2 &> 2 - \Delta'_0 && (J_1 > 0 \text{ or } J_2 > 0), \\ J_1 + J_2 - |\Delta_1 - \Delta_2| &> 2 - \tau'_0 && (J_1 > 0 \text{ or } J_2 > 0), \end{aligned} \quad (4.156)$$

where  $\Delta'_0$  and  $\tau'_0$  are the smallest nonzero dimension and twist, respectively, appearing in the  $1 \times 2$  OPE.

If the conditions (4.156) are satisfied, then the integral of each term in the OPE expansion over the region  $r < r_0$  (for some sufficiently small  $r_0$ , indicated by the quarter-disc in the lower-left or upper-right corner of figure 4.6) converges, including the boundaries where it probes the light-cone regime. Furthermore, the OPE expansion converges absolutely and exponentially in this region, and integrating each term does not change this — the convergence rate only improves as we approach the OPE or light-cone boundary. In other words, the sum of integrals of absolute values converges. The Fubini-Tonelli theorem then establishes absolute convergence of the Wightman function integral over the OPE corners in figure 4.6 under conditions (4.156).

#### 4.4.2.2 Lightcone limit on the first sheet

We do not need to do additional work to analyze the lightcone limit on the first sheet. Studying the lightcone limit is equivalent to studying convergence of (4.152) when  $\sigma \rightarrow 0, 1$ , with  $r$  held fixed. Because the  $r$ -dependence of the integrand (4.152) factors out from the  $\sigma$ -dependence, this again gives (4.155). We do not have to worry about the null-cone singularities when 1 or 2 become light-like from 3 or 4, because these are avoided by  $i\epsilon$ -prescriptions for the operators 3 and 4.

In this section we will re-derive (4.155) in a way that works when  $\mathcal{O}_0$  is not a traceless symmetric tensor. This approach will also be helpful for the discussion of the lightcone limit on the second sheet.

Consider the product

$$\mathcal{O}_1(-z_1/\alpha_1, z_1)\mathcal{O}_2(-z_2/\alpha_2, z_2) = \sum_k f_k(\alpha_1)\mathcal{O}_k(0), \quad (4.157)$$

in the limit  $\alpha_1 \rightarrow -\infty$  with fixed  $\alpha_2$ . There exists a boost generator  $M$  such that  $e^{\lambda M} z_1 = e^{-\lambda} z_1$  and  $e^{\lambda M} z_2 = e^{\lambda} z_2$ . Let us define  $V(\lambda) = e^{-\lambda D} e^{\lambda M}$ , where  $D$  is the dilatation generator. Acting on the left-hand side of (4.157), we have

$$\begin{aligned} & V(\lambda)\mathcal{O}_1(-z_1/\alpha_1, z_1)\mathcal{O}_2(-z_2/\alpha_2, z_2)V(\lambda)^{-1} \\ &= e^{-\lambda(\Delta_1+\Delta_2-J_2+J_1)}\mathcal{O}_1(-e^{-2\lambda}z_1/\alpha_1, z_1)\mathcal{O}_2(-z_2/\alpha_2, z_2). \end{aligned} \quad (4.158)$$

Acting on a single term on the right-hand side, we have

$$V(\lambda)f_0(\alpha_1)\mathcal{O}_0(0)V(\lambda)^{-1} = e^{-\lambda\tau_0}f_0(\alpha_1)\mathcal{O}_0(0), \quad (4.159)$$

where  $\mathcal{O}_0$  has eigenvalue  $\tau_0$  under  $D - M$ . Comparing both sides gives

$$f_0(\alpha_1) \propto (-\alpha_1)^{\frac{-\tau_0 + \Delta_1 + \Delta_2 - J_2 + J_1}{2}}. \quad (4.160)$$

Requiring that  $\int d\alpha_1 (-\alpha_1)^{-\Delta_1 - J_1} f_0(\alpha_1)$  converges gives the condition

$$J_1 + J_2 + \Delta_1 - \Delta_2 > 2 - \tau_0. \quad (4.161)$$

From a similar analysis with  $1 \leftrightarrow 2$ , we recover (4.155).

We will also need a simple generalization of this result. Consider the same OPE (4.157), but with more general polarization vectors, i.e.

$$\mathcal{O}_1(-z_1/\alpha_1, z'_1) \mathcal{O}_2(-z_2/\alpha_2, z'_2) = \sum_k f_k(\alpha_1) \mathcal{O}_k(0). \quad (4.162)$$

For generic values of  $z'_i$ , both operators will not be eigenstates of  $M$ , but instead contain a mixture of different eigenstates. Suppose we isolate eigenstates with eigenvalues  $m_1$  and  $m_2$ . The corresponding piece of  $f_0(\alpha_1)$  will be then, by a straightforward generalization of the above argument

$$f_0(\alpha_1) \propto (-\alpha_1)^{\frac{-\tau_0 + \Delta_1 + \Delta_2 - m_1 - m_2}{2}}. \quad (4.163)$$

When  $z'_i = z_i$  as above, we have  $m_1 = -J_1$  and  $m_2 = J_2$ , recovering (4.160). For generic  $z'_i$  the dominant contribution to (4.162) will be determined by  $m_1 = -J_1$  and  $m_2 = -J_2$ , i.e.

$$f_0(\alpha_1) \propto (-\alpha_1)^{\frac{-\tau_0 + \Delta_1 + \Delta_2 + J_1 + J_2}{2}}. \quad (4.164)$$

On the other hand, in order for the stronger result (4.160) to be true it suffices to have  $z'_1 = z_1$ ,  $(z_2 \cdot z'_2) = O(\alpha_1^{-1})$  and  $z'_2$  has finite limit as  $\alpha_1 \rightarrow -\infty$ . In other words, we can allow  $z'_2$  to vary with  $\alpha_1$ . The condition on  $z'_1$  implies  $m_1 = -J_1$ , and is as good as generic  $z'_1$ . To understand the condition on  $z'_2$ , assume without any loss of generality that  $z_2 = (0, 1, \vec{0})$  in  $(u, v, \vec{y})$  coordinates. This implies that

$$z'_2 = ((-\alpha_1)^{-1} u_z(\alpha_1), u_z^{-1}(\alpha_1) y_z^2(\alpha_1), (-\alpha_1)^{\frac{1}{2}} \vec{y}_z(\alpha_1)), \quad (4.165)$$

where  $u_z(\alpha_1)$  and  $\vec{y}_z(\alpha_1)$  are  $O(1)$  as  $\alpha_1 \rightarrow -\infty$ . We have then

$$\begin{aligned} & \mathcal{O}_2(-z_2/\alpha_2, z'_2) \\ &= \sum_{n+k+l=J_2} (-\alpha_1)^{-n-l/2} u_z(\alpha_1)^{n-k} y_z^{2k}(\alpha_1) y_z^{i_1}(\alpha_1) \cdots y_z^{i_l}(\alpha_1) \mathcal{O}_{2, u \dots uv \dots v i_1 \dots i_l}(-z_2/\alpha_2) \end{aligned} \quad (4.166)$$

where  $\mathcal{O}_{2,u\dots uv\dots vi_1\dots i_l}$  has  $n$   $u$ -indices and  $k$   $v$ -indices. If we were contracting with  $z_2$ , we would only get  $v$ -indices, and  $m_2 = J_2$ . Thus,  $v$ -indices carry positive charge under  $M$ , and we have  $m_2 = k - n = J_2 - l - 2n$ . We thus see that for non-zero  $n$  or  $l$  we depart from the optimal eigenvalue  $m_2 = J_2$ . However, such terms are additionally suppressed by  $(-\alpha_1)^{-n-l/2}$ . Combining these two effects with the help of (4.163), we see that all terms contribute as (4.160).

#### 4.4.2.3 Rindler positivity

Rindler positivity enables us to bound second-sheet correlators in terms of first-sheet correlators. Its implications are simple for four-point functions of scalar primaries, and this case has been analyzed previously in [25, 151]. However, its implications are more subtle for spinning correlators, so let us discuss them in more detail.

Any CFT has an anti-unitary symmetry  $J = \text{CRT}$  satisfying  $J^2 = 1$ . This symmetry acts on local operators as

$$J\mathcal{O}(x, s)J^{-1} = i^F[\mathcal{O}(\bar{x}, e^{-\pi M_E^{01}} s)]^\dagger, \quad (4.167)$$

where  $\bar{x} = e^{-\pi M_E^{01}} x = (-x^0, -x^1, x^2, \dots)$ ,  $s$  is a polarization variable appropriate for the Lorentz irrep of  $\mathcal{O}$ , and  $M_E^{01} = iM^{01}$  is the Euclidean rotation in plane 01 which rotates positive  $x^1$  into positive  $ix^0$ . Fermion number is  $F = 0$  for bosonic  $\mathcal{O}$  and  $F = 1$  for fermionic  $\mathcal{O}$ . In this paper, we will only study its action on traceless-symmetric operators, which reduces to

$$J\mathcal{O}(x, z)J^{-1} = \mathcal{O}^\dagger(\bar{x}, \bar{z}), \quad (4.168)$$

where  $\bar{z} = (-z^0, -z^1, z^2, \dots)$ .

The statement of Rindler positivity is [185]

$$i^{-F}\langle\mathcal{O}|J\mathcal{O}_1\cdots\mathcal{O}_nJ\mathcal{O}_1\cdots\mathcal{O}_n|\mathcal{O}\rangle \geq 0, \quad (4.169)$$

where all operators  $\mathcal{O}_i$  lie in the right Rindler wedge  $x^1 > |x^0|$ , and  $F$  is 1 if the number of fermions among  $\mathcal{O}_1\cdots\mathcal{O}_n$  is odd and 0 otherwise.<sup>23</sup> This is a bit of an oversimplification; the general statement is that the operators  $\mathcal{O}_i$  should be smeared

<sup>23</sup>For  $F = 1$  this form of Rindler positivity was proven in [185] only under an additional assumption of “wedge ordering” of the coordinates of  $\mathcal{O}_i$ . The version without this assumption was proven using Tomita-Takesaki modular theory and assuming  $F = 0$ . While we have not proven this, we expect that the general version also holds for  $F = 1$ . This can probably be checked explicitly in CFT using conformal block expansions. We thank Nima Lashkari for discussions on this point.



with test functions, and one can take arbitrary linear combinations of such smeared products. When the correlation function is well-defined as a number (rather than just as a distribution), the smearing is not necessary.

Now let  $a$  and  $b$  be sums of products of (possibly smeared) operators contained in the right Rindler wedge, and define

$$(a, b) = i^{-F(a)} \langle \mathcal{O} | J a J b | \mathcal{O} \rangle, \quad (4.170)$$

where  $F(a) \in \{0, 1\}$  is defined as above. Then we have

$$(a, b)^* = (-i)^{-F(a)} \langle \mathcal{O} | a J b J | \mathcal{O} \rangle = i^{-F(a)} \langle \mathcal{O} | J b J a | \mathcal{O} \rangle = (b, a), \quad (4.171)$$

where we used anti-unitarity of  $J$ ,  $J|\mathcal{O}\rangle = |\mathcal{O}\rangle$ , and the fact that  $JbJ$  and  $a$  are space-like separated. Rindler positivity implies  $(a, a) > 0$ . Thus,  $(\cdot, \cdot)$  is a Hermitian inner product and we have the Cauchy-Schwarz inequality

$$|(a, b)|^2 \leq (a, a)(b, b). \quad (4.172)$$

Let us develop more conformally-invariant versions of these statements. The geometry that defines  $J$  is given by the codimension-1 planes  $x^0 \pm x^1 = 0$ . These planes can be described more invariantly as the past null cones of points  $A$  and  $B$  at future null infinity. Given these points, the right Rindler wedge is given by  $B > x > A^-$  and the left is given by  $A > x > B^-$ .<sup>24</sup> In general, for any spacelike-separated pair of points  $A$  and  $B$ , there exists an anti-unitary Rindler conjugation  $J_{AB}$  that depends on these two points and exchanges the two wedges. A positive-definite Hermitian inner product analogous to (4.170) can be defined for each  $J_{AB}$ .

It is convenient to describe the action of  $J_{AB}$  using the embedding formalism. Let  $X_A$  and  $X_B$  be the embedding space coordinates of  $A$  and  $B$ . Then  $J_{AB}$  acts on spacetime as a Euclidean rotation by  $\pi$  in the plane spanned by  $X_A$  and  $X_B$ . It can be written as<sup>25</sup>

$$J_{AB}(X) = X - 2 \frac{(X \cdot X_A)}{(X_A \cdot X_B)} X_B - 2 \frac{(X \cdot X_B)}{(X_A \cdot X_B)} X_A. \quad (4.173)$$

The action of  $J_{AB}$  on local operators is then

$$J_{AB} \mathcal{O}(X, Z) J_{AB}^{-1} = \mathcal{O}^\dagger(J_{AB}(X), J_{AB}(Z)). \quad (4.174)$$

<sup>24</sup>Here,  $A^-$  ( $B^-$ ) represents the point obtained by sending lightrays in all past directions from  $A$  ( $B$ ) and finding the point where they converge. See, e.g. [28] for details.

<sup>25</sup>We abuse notation and write  $J_{AB}$  for both the anti-unitary operator on Hilbert space and a linear transformation in the embedding space.

Consider now a configuration of points 1, 2, 3, 4 with the causal relationships  $4 > 1$  and  $2 > 3$ , where all other pairs of points are spacelike-separated. We can find a conformal transformation that brings these points into a configuration where the pair 1, 2 and the pair 3, 4 are each symmetric with respect to the standard Rindler reflection  $J$ . Thus, there must exist  $A, B$  such that  $J_{AB}$  maps  $1 \leftrightarrow 2$  and  $3 \leftrightarrow 4$ . In embedding-space language,

$$J_{AB}(X_1) = \lambda_{12}X_2, \quad J_{AB}(X_3) = \lambda_{34}X_4, \quad (4.175)$$

where we must introduce scaling factors  $\lambda_{ij}$  because the  $X$ 's are projective coordinates. Here,  $X_A, X_B$  and the coefficients  $\lambda_{12}, \lambda_{34}$  are all functions of  $X_1, \dots, X_4$ . These functions are somewhat complicated in general, but we will only need them in certain limits.

In our configuration, the Wightman correlator

$$\langle \mathcal{O} | \mathcal{O}_4 \mathcal{O}_1 \mathcal{O}_2 \mathcal{O}_3 | \mathcal{O} \rangle \quad (4.176)$$

is on the second sheet. However, we can write

$$\langle \mathcal{O} | \mathcal{O}_4 \mathcal{O}_1 \mathcal{O}_2 \mathcal{O}_3 | \mathcal{O} \rangle = (J_{AB}^{-1} \mathcal{O}_4 \mathcal{O}_1 J_{AB}, \mathcal{O}_2 \mathcal{O}_3), \quad (4.177)$$

and use the Rindler Cauchy-Schwarz inequality to write

$$|\langle \mathcal{O} | \mathcal{O}_4 \mathcal{O}_1 \mathcal{O}_2 \mathcal{O}_3 | \mathcal{O} \rangle|^2 \leq (\mathcal{O}_2 \mathcal{O}_3, \mathcal{O}_2 \mathcal{O}_3) (J_{AB}^{-1} \mathcal{O}_4 \mathcal{O}_1 J_{AB}, J_{AB}^{-1} \mathcal{O}_4 \mathcal{O}_1 J_{AB}). \quad (4.178)$$

Let us focus on the first factor (the second can be treated equivalently)

$$(\mathcal{O}_2 \mathcal{O}_3, \mathcal{O}_2 \mathcal{O}_3) = \langle \mathcal{O} | \overline{\mathcal{O}}_2 \overline{\mathcal{O}}_3 \mathcal{O}_2 \mathcal{O}_3 | \mathcal{O} \rangle \quad (4.179)$$

Here we use the notation  $\overline{\mathcal{O}} = J_{AB} \mathcal{O} J_{AB}^{-1}$ . Note that  $\overline{\mathcal{O}}_2$  is inserted at  $X_1$  and  $\overline{\mathcal{O}}_3$  is inserted at  $X_4$ . Both of these points are in the opposite Rindler wedge from  $X_2$  and  $X_3$ . This implies that  $\overline{\mathcal{O}}_3$  and  $\mathcal{O}_2$  commute, so we can reorder the operators to obtain

$$= \langle \mathcal{O} | \overline{\mathcal{O}}_2 \mathcal{O}_2 \overline{\mathcal{O}}_3 \mathcal{O}_3 | \mathcal{O} \rangle. \quad (4.180)$$

The operators  $\overline{\mathcal{O}}_2$  at  $X_1$  and  $\mathcal{O}_2$  at  $X_2$  now act on the vacuum. By the results of [183, 184], the correlator (4.180) is on the first sheet and we can use the OPE to control its behavior, and hence bound the left-hand side of (4.178). It is convenient that the correlators in the right hand side of (4.178) have the same insertion points  $X_i$  as the correlator in the left hand side, and hence the same cross-ratios.

Let us briefly mention how one can determine the points  $X_A$  and  $X_B$  as functions of  $X_i$ . To do this, we must solve the equations (4.175), together with the conditions

$$X_A^2 = X_B^2 = 0. \quad (4.181)$$

Using (4.173), we can see that  $X_A$  and  $X_B$  must have the form

$$\begin{aligned} X_A &= c_{A1}(X_1 - \lambda_{12}X_2) + c_{A3}(X_3 - \lambda_{34}X_4), \\ X_B &= c_{B1}(X_1 - \lambda_{12}X_2) + c_{B3}(X_3 - \lambda_{34}X_4), \end{aligned} \quad (4.182)$$

for some coefficients  $c_{ai}$ . We have 2 scalar equations coming from each equation in (4.175), by projecting on  $X_1 - \lambda_{12}X_2$  or  $X_3 - \lambda_{34}X_4$ . We also have 2 scalar equations (4.181), which adds up to 6 equations for 6 unknowns  $c_{ai}, \lambda_{ij}$ .

It is easy to solve these equations by making use of the conformal symmetry. For this, recall that all coordinates  $X$  are projective, and hence our unknowns  $c_{ai}$  and  $\lambda_{ij}$  have non-trivial projective weights as well. We can construct combinations such as

$$c_{A1} \frac{(X_1 \cdot X_2)}{(X_A \cdot X_2)}, \quad (4.183)$$

which are projective invariants. Projective invariants are the same as conformal invariants, and thus must be expressible in terms of cross-ratios, i.e.

$$c_{A1} \frac{(X_1 \cdot X_2)}{(X_A \cdot X_2)} = f_{A1}(z, \bar{z}). \quad (4.184)$$

The function  $f_{A1}(z, \bar{z})$  can be computed by using the expressions for  $X_i, X_A, X_B$  for the standard Rindler reflection  $J$ . As soon as we know the function  $f_{A1}(z, \bar{z})$ , we can find

$$c_{A1} = f_{A1}(z, \bar{z}) \frac{(X_A \cdot X_2)}{(X_1 \cdot X_2)}. \quad (4.185)$$

Note that the expression in the right-hand side depends on  $X_A$  but only through an overall coefficient  $(X_A \cdot X_2)$ . The same coefficient can be factored out from  $c_{A3}$ , and thus  $X_A$  is determined up to an overall rescaling, which is irrelevant. For example, we can simply set  $(X_A \cdot X_2) = 1$  to get a concrete solution. All the other coefficients  $c_{ai}$  and  $\lambda_{ij}$  can be determined in the same way. We will not need the complete solution, but it is helpful for explicitly checking our arguments.

#### 4.4.2.4 Regge limit

In the previous section, we saw that Rindler positivity implies a bound on the correlator of the form

$$\begin{aligned} |\langle \mathcal{O} | \mathcal{O}_4 \mathcal{O}_1 \mathcal{O}_2 \mathcal{O}_3 | \mathcal{O} \rangle|^2 &\leq \langle \mathcal{O} | \bar{\mathcal{O}}_2 \bar{\mathcal{O}}_3 \mathcal{O}_2 \mathcal{O}_3 | \mathcal{O} \rangle \langle \mathcal{O} | \mathcal{O}_4 \mathcal{O}_1 \bar{\mathcal{O}}_4 \bar{\mathcal{O}}_1 | \mathcal{O} \rangle \\ &= \langle \mathcal{O} | \bar{\mathcal{O}}_2 \mathcal{O}_2 \bar{\mathcal{O}}_3 \mathcal{O}_3 | \mathcal{O} \rangle \langle \mathcal{O} | \mathcal{O}_4 \bar{\mathcal{O}}_4 \mathcal{O}_1 \bar{\mathcal{O}}_1 | \mathcal{O} \rangle. \end{aligned} \quad (4.186)$$

We can now use the first-sheet bounds from sections 4.4.2.1 and 4.4.2.2 to bound the correlators in the right hand side. Before doing so, let us write out these correlators a bit more carefully. For example,

$$\langle \mathcal{O} | \bar{\mathcal{O}}_2 \mathcal{O}_2 \bar{\mathcal{O}}_3 \mathcal{O}_3 | \mathcal{O} \rangle = \langle \mathcal{O} | \mathcal{O}_2^\dagger(\lambda_{12}^{-1} X_1, \tilde{Z}_2) \mathcal{O}_2(X_2, Z_2) \mathcal{O}_3^\dagger(\lambda_{34} X_4, \tilde{Z}_3) \mathcal{O}_3(X_3, Z_3) | \mathcal{O} \rangle, \quad (4.187)$$

where

$$\tilde{Z}_i \equiv J_{AB}(Z_i). \quad (4.188)$$

Writing this in terms of real space operators, we find

$$\langle \mathcal{O} | \bar{\mathcal{O}}_2 \mathcal{O}_2 \bar{\mathcal{O}}_3 \mathcal{O}_3 | \mathcal{O} \rangle = \lambda_{12}^{\Delta_2} \lambda_{34}^{-\Delta_3} \langle \mathcal{O} | \mathcal{O}_2^\dagger(x_1, \tilde{z}_2) \mathcal{O}_2(x_2, z_2) \mathcal{O}_3^\dagger(x_4, \tilde{z}_3) \mathcal{O}_3(x_3, z_3) | \mathcal{O} \rangle. \quad (4.189)$$

Let us focus on the Regge limit when  $\alpha_1 \rightarrow +\infty$  and  $\alpha_2 \rightarrow -\infty$ . Similarly to section 4.4.2.1 it is convenient to work in the frame in which  $x_2$  is approaching the origin,

$$x_2 = -\frac{z_2}{\alpha_2}. \quad (4.190)$$

In this frame point  $x_1$  is in the next Poincare patch, so it is convenient to work with  $x_1^-$ , which is the image of  $x_1$  in the Poincare patch of  $x_2$ ,

$$x_1^- = -\frac{z_1}{\alpha_1}. \quad (4.191)$$

In fact, since  $\mathcal{O}(x_1)$  acts on future vacuum, the correlator (4.189) changes only by a constant phase upon replacement  $x_1 \rightarrow x_1^-$ , so the analysis is very similar to section 4.4.2.1. If the coefficients  $\lambda_{ij}$  and polarization vectors  $\tilde{z}_2$  and  $\tilde{z}_3$  were constant, we could simply reuse the results of that section.

Instead, since  $\lambda_{ij}$  and  $\tilde{z}_2, \tilde{z}_3$  depend on the  $x_i$  (and thus  $\alpha_1, \alpha_2$ ), we need to analyze their behavior in the limit  $\alpha_1 \rightarrow +\infty$  and  $\alpha_2 \rightarrow -\infty$ . Let us parameterize, similarly to (4.151)

$$\frac{1}{\alpha_1} = r\sigma, \quad -\frac{1}{\alpha_2} = r(1 - \sigma). \quad (4.192)$$

We have checked that in the limit  $r \rightarrow 0$  the coefficients  $\lambda_{12}, \lambda_{34}$  stay finite and

$$\tilde{z}_2 \rightarrow z_2, \quad \tilde{z}_3 \rightarrow z'_3, \quad (4.193)$$

where  $z'_3$  is finite and depends on  $z_3$  and relative positions of  $0, x_3, x_4$ . This means that in Regge limit at fixed  $\sigma$  (4.189) is bounded in absolute value by

$$C \left| \langle \mathcal{O} | \mathcal{O}_2^\dagger \left( x_1 = -\frac{z_1}{\alpha_1}, z_2 \right) \mathcal{O}_2 \left( x_2 = -\frac{z_2}{\alpha_2}, z_2 \right) \mathcal{O}_3^\dagger(x_4, z'_3) \mathcal{O}_3(x_3, z_3) | \mathcal{O} \rangle \right|, \quad (4.194)$$

for some constant  $C > 0$ . The same analysis applies to the second correlator in (4.186).

We can now reuse the arguments of section 4.4.2.1 to conclude that the Wightman function integral converges near the Regge limit, at fixed  $\sigma$ , provided that

$$J_1 + J_2 > 2 - \Delta_{\text{vac}}, \quad (4.195)$$

where  $\Delta_{\text{vac}}$  is the smallest scaling dimension appearing in the  $\mathcal{O}_2 \times \mathcal{O}_2^\dagger$  (or  $\mathcal{O}_1 \times \mathcal{O}_1^\dagger$ ) OPE. Since  $\mathcal{O}_2 \times \mathcal{O}_2^\dagger$  always contains the identity operator,  $\Delta_{\text{vac}} = 0$ . Note that the polarizations of both  $\mathcal{O}_2$  and  $\mathcal{O}_2^\dagger$  are  $z_2$ , so we cannot exclude the identity contribution using kinematics as we did in section 4.4.2.1. So we finally obtain the sufficient condition

$$J_1 + J_2 > 2. \quad (4.196)$$

Note that we have only shown that this is sufficient for convergence of the integral at fixed  $\sigma$ . We will discuss the case of  $\sigma$  approaching the light-cone boundaries, and thus of the two-variable integral, in the next section.

This latter condition is sufficient, but may turn out to be not necessary, since we cannot prove that the Cauchy-Schwartz bound (4.186) is tight. To allow for this possibility, let us introduce a parameter  $J_0$  which is defined as the smallest real number such that

$$\frac{\langle \mathcal{O} | \mathcal{O}_4 \mathcal{O}_1 \mathcal{O}_2 \mathcal{O}_3 | \mathcal{O} \rangle}{\sqrt{\langle \mathcal{O}_3(x_3) \mathcal{O}_3^\dagger(x_4) \rangle \langle \mathcal{O}_4(x_4) \mathcal{O}_4^\dagger(x_3) \rangle \langle \mathcal{O}_1(x_1) \mathcal{O}_1^\dagger(x_2) \rangle \langle \mathcal{O}_2(x_2) \mathcal{O}_2^\dagger(x_1) \rangle}} \in O(r^{1-J_0}), \quad (4.197)$$

where all polarization vectors in denominator are generic. Then the Wightman function integral converges in the Regge limit if

$$J_1 + J_2 > J_0 + 1. \quad (4.198)$$

The result of this section can in turn be summarized by saying that

$$J_0 \leq 1. \quad (4.199)$$

#### 4.4.2.5 Lightcone limit on the second sheet

Consider now the lightcone limit on the second sheet. The situation is very similar to the Regge regime, and we can use the same frame as above to analyze it. The only difference is that now we consider either  $\alpha_1 \rightarrow +\infty$  or  $\alpha_2 \rightarrow -\infty$ , corresponding to the right or the lower boundary in figure 4.6 respectively. The other two boundaries can be treated in the same way. For concreteness, let us focus on the limit  $\alpha_2 \rightarrow -\infty$ .

For simplicity, we will assume that  $x_1$  is in the same Poincare patch as  $x_2$ , and write

$$x_1 = -\frac{z_1}{\alpha_1}, \quad x_2 = -\frac{z_2}{\alpha_2}. \quad (4.200)$$

This time, we will have to discuss both correlators in the bound (4.186). Modulo factors of  $\lambda_{ij}$  in (4.189) and their analogues for the second correlator in (4.186), we are essentially interested in the behavior of the OPEs

$$\begin{aligned} \overline{\mathcal{O}}_2 \mathcal{O}_2 &\sim \mathcal{O}_2^\dagger(x_1, \tilde{z}_2) \mathcal{O}_2(x_2, z_2) \\ \mathcal{O}_1 \overline{\mathcal{O}}_1 &\sim \mathcal{O}_1(x_1, z_1) \mathcal{O}_1^\dagger(x_2, \tilde{z}_1). \end{aligned} \quad (4.201)$$

The  $\lambda$ -factors and polarizations entering  $\overline{\mathcal{O}}_3$  and  $\overline{\mathcal{O}}_4$ , similarly to Regge limit, can be ignored because they all tend to some generic finite limits.<sup>26</sup>

It is easy to determine the direction of  $\tilde{z}_1$  in the strict lightcone limit  $\alpha_2 = -\infty$ . In this limit, we find  $x_2 = 0$ , and  $z_1$  lies along the unique null ray which connects  $x_1$  and  $x_2$ . This is a conformally-invariant statement, and so it should hold after we apply  $J_{AB}$ . Applying  $J_{AB}$  sends  $x_1$  to  $x_2$ ,  $x_2$  to  $x_1$ , and  $z_1$  to  $\tilde{z}_1$ . Therefore, we find that  $\tilde{z}_1$  should also lie along the unique null ray connecting  $x_1$  and  $x_2$ , and thus it is proportional to  $z_1$ . In other words,

$$\tilde{z}_1 \rightarrow cz_1, \quad (4.202)$$

for some finite  $c$ . This implies that

$$(z_1 \cdot \tilde{z}_1) = O(\alpha_2^{-1}). \quad (4.203)$$

Using the results of section 4.4.2.2 (after swapping  $\alpha_1$  and  $\alpha_2$ ), we find that

$$\mathcal{O}_1(x_1, z_1) \mathcal{O}_1^\dagger(x_2, \tilde{z}_1) \sim (-\alpha_2)^{\frac{2\Delta_1 - 2J_1 - \tau_0}{2}}. \quad (4.204)$$

Here  $\tau_0$  is the smallest twist that appears in  $\mathcal{O}_1^\dagger \mathcal{O}_1$  OPE.

---

<sup>26</sup>This is true as long as we stay in the interior of the second sheet. These coefficients may diverge as we approach  $1 \sim 3$  lightcone limit. We comment on this subtlety below.

There is nothing special we can say about  $\tilde{z}_2$ , and it simply tends to some generic finite value in the limit. This and results of section 4.4.2.2 imply that

$$\mathcal{O}_2^\dagger(x_1, \tilde{z}_2)\mathcal{O}_2(x_2, z_2) \sim (-\alpha_2)^{\frac{2\Delta_2+2J_2-\tau_0}{2}}. \quad (4.205)$$

Combining these results we find that

$$|\langle \mathcal{O}|\mathcal{O}_4\mathcal{O}_1\mathcal{O}_2\mathcal{O}_3|\mathcal{O} \rangle| \leq C'(-\alpha_2)^{\frac{-\tau_0+\Delta_1+\Delta_2-J_1+J_2}{2}} \quad (4.206)$$

near the second sheet null-cone limit  $\alpha_2 \rightarrow -\infty$ . This bound is uniform away from the boundary between first and second sheets 1  $\sim$  3. Including the light-transform weight  $(-\alpha_2)^{-\Delta_2-J_2}$ , we conclude that the Wightman function integral converges absolutely in this region provided

$$J_1 + J_2 - \Delta_1 + \Delta_2 + \tau_0 > 2. \quad (4.207)$$

Combining this with the condition from  $\alpha_1 \rightarrow \pm\infty$  we find the sufficient condition

$$J_1 + J_2 > 2 + |\Delta_1 - \Delta_2| - \tau_0. \quad (4.208)$$

Similarly to the Regge limit, we cannot exclude the identity operator from  $\mathcal{O}_1^\dagger\mathcal{O}_1$  (or  $\mathcal{O}_2^\dagger\mathcal{O}_2$ ) OPE, and so we must set  $\tau_0 = 0$ , resulting in the final condition

$$J_1 + J_2 > 2 + |\Delta_1 - \Delta_2|. \quad (4.209)$$

There are two subtleties which we still need to address. One is the convergence of the two-variable integral near Regge limit – we have established the convergence of the radial integral in the previous section and of the angular integral in this section, but we have not yet proved that the double integral converges. To see that it does, note that we have succeeded in bounding both the Regge limit and the second-sheet lightcone limit by using Rindler positivity. A closer look at our arguments shows that for  $r < r_0$  and all  $\sigma$  the second-sheet correlator is bounded in absolute value by the product of first-sheet correlators times a uniform constant  $C''$ , where  $r_0$  is sufficiently small. Convergence of the double-integral of the product of first-sheet correlators can be established by the same methods as in section 4.4.2.4, and then the convergence of the integral on the second sheet follows immediately.

The second subtlety is that near the lightcone limit, either on the first or on the second sheet, we have only established the convergence of the integral provided we exclude a region near the boundary between the first and the second sheets. We now turn to a discussion of this subtlety.

#### 4.4.2.6 Asymptotic lighthcone expansion

The discussion of previous sections provides us with rigorous bounds on the growth of the Wightman function on the first and the second sheets. The situation is, however, qualitatively different for the two sheets.

On the first sheet, we have a tight bound on the growth in OPE and lightcone limits – we can use the convergent OPE expansion to see that the Wightman function actually does saturate the bound. This means that unless the conditions of sections 4.4.2.1 and 4.4.2.2 are satisfied, the Wightman function integral diverges (in absolute value sense).

On the second sheet, we have a potentially non-optimal bound on the growth in the Regge and lightcone limits, which we derived from the Cauchy-Schwarz inequality for Rindler reflection positivity. We have already pointed out that the growth in the Regge limit may be weaker than the bound, and we parametrized the true growth by an exponent  $J_0$ . Similarly, there is no a-priori reason to believe that the lightcone bound is tight.

In fact, there is a reason to believe that the growth of the correlator on the second sheet is the same as on the first sheet. Indeed, it is natural to expect that the lightcone OPE expansion, even though not convergent on the second sheet, is still valid asymptotically [151]. Schematically,

$$\mathcal{O}_1(x_1)\mathcal{O}_2(x_2) = \sum_{\tau_{\mathcal{O}} \leq \tau} (x_{12}^2)^{\frac{\tau_{\mathcal{O}} - \Delta_1 + m_1 - \Delta_2 + m_2}{2}} \mathcal{O}(x_2) + o\left((x_{12}^2)^{\frac{\tau - \Delta_1 + m_1 - \Delta_2 + m_2}{2}}\right), \quad (4.210)$$

where  $m_i$  is the boost eigenvalue of  $\mathcal{O}_i$  (similarly to section 4.4.2.2), and the sum on the right-hand side is over spin components of primaries and descendants. Such an asymptotic expansion is sufficient to establish the growth rate of the Wightman function near the second sheet lightcone limit, and gives the same results as on the first sheet. In particular, the contribution of the identity operator to (4.210) is excluded in the same way as on the first sheet, and we do not have to set  $\tau_0 = 0$  in (4.208) anymore.

By using the asymptotic expansion (4.210), we can also prove that the Wightman function integral converges in the lighthcone limit near the boundary between the first and the second sheets (with  $i\epsilon$  prescription employed for  $\mathcal{O}_3, \mathcal{O}_4$ ), closing the loophole in our arguments.

While (4.210) is a natural expectation, we do not have a general proof that it holds. An argument was given in [151] for the case of scalar  $\mathcal{O}_1 = \mathcal{O}_2$  and  $\mathcal{O}_3 = \mathcal{O}_4$ , with real



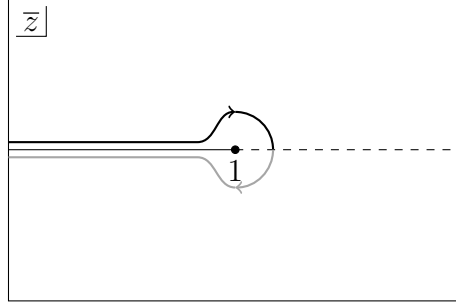


Figure 4.7: Trajectory of  $\bar{z}$  near the boundary between the first and the second sheets.

coordinates. In their argument, one splits the  $t$ -channel ( $\mathcal{O}_1 \times \mathcal{O}_4$  OPE) expansion of the Wightman function into two parts. The first part  $\mathcal{I}_1$  consists roughly of double-traces  $[\mathcal{O}_1 \mathcal{O}_2]_{n,\ell}$ , and is responsible for reproducing a finite number of terms in (4.210) in the  $s$ -channel. The second part  $\mathcal{I}_2$  contains all other contributions. By going sufficiently far into the  $s$ -channel lightcone regime, one can make sure that  $\mathcal{I}_1$  completely dominates over  $\mathcal{I}_2$ . Continuation of  $\mathcal{I}_1$  to the second sheet is straightforward, since it is simply equal to a finite number of terms in (4.210). The expansion (4.210) then follows if we can show that the second part  $\mathcal{I}_2$  remains subleading on the second sheet. In the setup of [151] this is easy to show, since all the terms in the  $t$ -channel channel expansion (and hence in  $\mathcal{I}_2$ ) are positive, and continuation to the second sheet merely adds some phases, which cannot increase the total sum.

This last step is problematic in more general setups. The positivity of  $t$ -channel contributions is due to the fact that the Wightman function considered in [151] is Rindler-reflection positive on the first sheet. As soon as we consider non-identical operators or operators with spin, the Rindler-reflection positivity ceases to be generic, and the argument cannot be applied. Still, the fact that (4.210) is valid at least for scalar  $\mathcal{O}_1 = \mathcal{O}_2$ , in some states, strongly suggests that it can be valid more generally. For the argument of [151] to fail in the general setup, it must be that the phases in  $\mathcal{I}_2$  on the first sheet conspire to give an abnormally small result for all values of  $\bar{z}$ , which seems rather unlikely.

In view of this discussion, we will assume that the asymptotic expansion (4.210) holds.

#### 4.4.3 Convergence of the double commutator integral

We now consider the convergence of the double commutator integral (4.149). The first observation is that the double-commutator vanishes when  $1 \approx 4$  or  $3 \approx 2$ . Our integration region is therefore restricted to  $1 < 4$  and  $2 > 3$ . This corresponds to the upper left shaded square in figure 4.6. Note, however, that it is now meaningless to

say that in this square the correlator is on the second sheet. The double-commutator consists of four Wightman correlators, and it is not guaranteed that they all have cross-ratios on the same sheet. In fact, by using the causal relations between the points and microcausality, we can write in this region

$$\begin{aligned} \langle \mathcal{O} | [\mathcal{O}_4, \mathcal{O}_1] [\mathcal{O}_2, \mathcal{O}_3] | \mathcal{O} \rangle &= \langle \mathcal{O} | \mathcal{O}_4 \mathcal{O}_1 \mathcal{O}_2 \mathcal{O}_3 | \mathcal{O} \rangle + \langle \mathcal{O} | \mathcal{O}_3 \mathcal{O}_1 \mathcal{O}_2 \mathcal{O}_4 | \mathcal{O} \rangle \\ &\quad - \langle \mathcal{O} | \mathcal{O}_1 \mathcal{O}_2 \mathcal{O}_3 \mathcal{O}_4 | \mathcal{O} \rangle - \langle \mathcal{O} | \mathcal{O}_3 \mathcal{O}_4 \mathcal{O}_1 \mathcal{O}_2 | \mathcal{O} \rangle. \end{aligned} \quad (4.211)$$

The first two Wightman functions are of the same type as studied in the previous subsection, and are on the second sheet. In the last two Wightman functions, the operators  $\mathcal{O}_1$  and  $\mathcal{O}_2$  act on the vacuum, and so they are on the first sheet.

When analyzing the convergence of the double commutator integral (4.149), once again we only need to consider the convergence near the boundaries of the integration region. Furthermore, we do not have to worry about the boundaries where  $2 \sim 3$  or  $1 \sim 4$ . Near these boundaries the integral is defined by  $i\epsilon$  prescriptions. More precisely, the double-commutator is obtained by folding integration contours in the Wightman function integral (4.147). Due to this folding, near these boundaries the four terms above pair up and form integration contours similar to figure 4.7. Overall, the double-commutator integral is an integral of a single Wightman function over a folded complex integration cycle in cross-ratio space. Everywhere away from the  $2 \sim 3$  or  $1 \sim 4$  boundaries this integration cycle can be split into four layers, and each layer can be interpreted as an integral of a Wightman function from (4.211). Near these boundaries the layers merge, wrapping around branch cuts and providing a canonical regularization of the integral.

We will continue to refer to the remaining two boundaries as the lightcone limits, and to the corner where they meet as the Regge limit. We can use the methods of the previous subsections to bound the growth of each Wightman function in (4.211) in these limits and find that the same conditions as we derived for (4.147) are also sufficient for convergence of the double-commutator integral.<sup>27</sup>

It is easy to see that weaker conditions are in fact sufficient for convergence of the double-commutator integral. Let us consider the lightcone limits first. The asymptotic expansion (4.210) essentially implies that we can approximate the double-commutator near these limits by replacing the Wightman functions in (4.211) by a finite number of  $s$ -channel conformal blocks for the leading twist operators, analytically continued to the desired Wightman orderings. However, it is known [25] that

<sup>27</sup>With the same caveat about the boundary between the first and second sheets as before.

$s$ -channel conformal blocks cancel in the combination (4.211). This means that the asymptotic expansion (4.210) does not contribute to the double-commutator. If this expansion were valid for any  $\tau$ , then we would conclude that the double-commutator decays faster than any power of  $\alpha_1$  or  $\alpha_2$  near the lightcone limits.

However, it is well-known that the spectrum of primaries in any OPE has accumulation points in twist [13, 14]. Let us denote the first twist accumulation point in  $\mathcal{O}_1 \times \mathcal{O}_2$  OPE by  $\tau_*$ . We can only trust (4.210) for  $\tau < \tau_*$ , since for  $\tau \geq \tau_*$  we would have to include infinitely many terms in the sum. Therefore, we can only conclude that the double-commutator grows in the lightcone regime no faster than at the rate determined by  $\tau_*$ . This leads to the following sufficient condition,

$$J_1 + J_2 - |\Delta_1 - \Delta_2| > 2 - \tau_*. \quad (4.212)$$

For the Regge limit, we do not have an analogue of (4.210), and we will simply introduce a growth exponent  $J_0^{\text{dDisc}}$  for the double-commutator in complete analogy with (4.197). The condition for absolute convergence of the double-commutator integral near the Regge limit is then

$$J_1 + J_2 > 1 + J_0^{\text{dDisc}}. \quad (4.213)$$

Similarly to  $J_0$ , Rindler positivity bounds imply

$$J_0^{\text{dDisc}} \leq 1. \quad (4.214)$$

#### 4.4.4 Summary of non-perturbative convergence conditions

Let us summarize the various conditions we have obtained thus far. Assuming the asymptotic light-cone expansion (4.210), we have shown that the Wightman function integral (4.147) converges absolutely if and only if the conditions

$$J_1 + J_2 > \max(2 - \Delta'_0, 1 + J_0), \quad (4.215)$$

$$J_1 + J_2 > 2 - \tau'_0 + |\Delta_1 - \Delta_2| \quad (4.216)$$

are satisfied. Here  $\tau'_0 \geq \frac{d-2}{2}$  and  $\Delta'_0 \geq \frac{d-2}{2}$  are the smallest non-zero twist and dimension that appear in the  $\mathcal{O}_1 \times \mathcal{O}_2$  OPE,<sup>28</sup>  $J_0$  is the growth exponent in the Regge limit, defined by (4.197). Using Rindler positivity, we have shown that

$$J_0 \leq 1. \quad (4.217)$$

---

<sup>28</sup>When  $J_1 = J_2 = 0$ , then we cannot exclude unit operator contributions in the OPE and lightcone limits and  $\Delta'_0$  and  $\tau'_0$  should be the lowest dimension and twist in their respective OPEs. In other words, they do not have to be nonzero in that case.

We have also shown that the above conditions with  $\tau'_0 = 0$  are sufficient even if we do not assume the asymptotic expansion (4.210), but simply use bounds from Rindler positivity.<sup>29</sup>

For the double-commutator integral (4.149), we have shown that the sufficient conditions for its convergence are

$$J_1 + J_2 > 1 + J_0^{\text{dDisc}}, \quad (4.218)$$

$$J_1 + J_2 > 2 - \tau_* + |\Delta_1 - \Delta_2|, \quad (4.219)$$

where  $\tau_* \geq d - 2$  is the first twist accumulation point in the  $\mathcal{O}_1 \times \mathcal{O}_2$  OPE, and  $J_0^{\text{dDisc}}$  parameterizes the Regge growth of the double-commutator in the same way that  $J_0$  parametrizes growth of the Wightman function through (4.197). Note that we have

$$\begin{aligned} \Delta'_0 &\geq \tau'_0 \geq \frac{d-2}{2}, \\ \tau_* &\geq \tau'_0 \geq \frac{d-2}{2}. \end{aligned} \quad (4.220)$$

Let us briefly discuss the values of  $J_0$  and  $J_0^{\text{dDisc}}$ . First of all, from the expansion (4.211) it follows that

$$J_0^{\text{dDisc}} \leq \max(1 - \Delta'_0, J_0). \quad (4.221)$$

Both  $J_0$  and  $J_0^{\text{dDisc}}$  can be studied using conformal Regge theory [25, 28, 149, 150]. Conformal Regge theory implies that the Regge limit of the four-point function behaves as  $1 + r^{1-j(0)}$ , where  $j(0)$  is the spin of the leading Regge trajectory at dimension  $\Delta = d/2$ . Here, the 1 comes from the identity operator in the  $\mathcal{O}_1 \times \mathcal{O}_2$  OPE. However, we are considering special kinematics where the unit operator does not contribute unless  $\mathcal{O}_1$  and  $\mathcal{O}_2$  are identical scalars. In these special kinematics, the four-point function behaves as  $r^{1-j(0)}$ . The double-discontinuity also does not get a contribution from the unit operator, so it also behaves as  $r^{1-j(0)}$ . Thus, we expect

$$\begin{aligned} J_0 = 1 \text{ and } J_0^{\text{dDisc}} = j(0) \leq 1 &\quad \text{if } \mathcal{O}_1 = \mathcal{O}_2 \text{ are identical scalars,} \\ J_0 = J_0^{\text{dDisc}} = j(0) \leq 1 &\quad \text{if } \mathcal{O}_1, \mathcal{O}_2 \text{ are not identical scalars.} \end{aligned} \quad (4.222)$$

Let us consider the case where  $\mathcal{O}_1, \mathcal{O}_2$  are not identical scalars. Note that if  $J_0$  is the intercept of the stress-tensor trajectory, then  $1 \geq J_0 \geq 2 - \frac{d}{2}$  by Nachtmann's theorem [14, 98, 132]. Furthermore, by unitarity  $1 - \Delta'_0 \leq 1 - \tau'_0 \leq 2 - \frac{d}{2}$ , so the condition

<sup>29</sup>This argument has a small loophole discussed, e.g., in section 4.4.2.6.

$J_1 + J_2 > 2 - \Delta'_0$  in (4.215) is redundant with  $J_1 + J_2 > 1 + J_0$ . If  $\Delta_1 = \Delta_2$ , then the conditions (4.216) and (4.219) are redundant as well.

As an example, consider the case where  $\mathcal{O}_1 = \mathcal{O}_2 = T$  (the stress tensor). By the above reasoning, a product of ANEC operators on the same null plane is well-defined and commutative if

$$3 > J_0 = J_0^{\text{dDisc}}. \quad (4.223)$$

In our analysis so far, we have considered the causal configuration  $4 > x$  and  $x^+ > 3$  with 3 and 4 spacelike. One can use  $\mathcal{O}_3, \mathcal{O}_4$  to generate a dense subspace of the Hilbert space while staying in this causal configuration. Thus, our analysis establishes well-definedness and commutativity (when applicable) acting on this dense subspace. However, this subspace does not include important states like momentum eigenstates, so we might hope to establish commutativity on a larger dense subspace.

Some different causal configurations can be reached by acting on  $\mathcal{O}_3$  and  $\mathcal{O}_4$  with the operator  $\mathcal{T}$  that translates operators to image points in other Poincare patches (see [28] for details). This operation simply introduces a phase, leaving our analysis unchanged. However, there exist other causal configurations that cannot be reached in this way: for example, if  $4 > x$  and  $x^+ > 3$  but 3 and 4 are timelike. In this case, one cannot use Rindler positivity and we have not found a way to rigorously bound the behavior of the correlator. We can argue non-rigorously as follows. To establish convergence of the Wightman or double-discontinuity integrals in the lightcone limit, we can invoke the asymptotic lightcone assumption of [151] described in section 4.4.2.6. Under this assumption, the analysis of the lightcone limit between 1 and 2 is independent of the positions of points 3 and 4, and thus identical to what we have already done. To establish convergence in the Regge limit, we can assume that the leading Regge behavior  $r^{1-J_0}$  predicted by conformal Regge theory continues to hold in this different causal configuration. It is possible that conformal Regge theory can be used to rigorously establish both of these assumptions. We leave this problem for future work.

In chapter 5, we establish a connection between commutativity and the Regge limit in a different way. We show that the commutator  $[\mathbf{L}[\mathcal{O}_1], \mathbf{L}[\mathcal{O}_2]]$  is nonvanishing if and only if the four-point function  $\langle \mathcal{O}_4 \mathcal{O}_1 \mathcal{O}_2 \mathcal{O}_3 \rangle$  has a Regge pole at  $J = J_1 + J_2 - 1$ . This again shows that the commutator vanishes if  $J_1 + J_2 > J_0 + 1$ , where  $J_0$  is the position of the rightmost Regge pole.

#### 4.4.5 Convergence in perturbation theory

Although we have shown that  $J_0 \leq 1$  in a nonperturbative theory, this bound can be violated at a fixed order in perturbation theory (e.g. either weak coupling or large- $N$ ). In large- $N$  perturbation theory, the bound on chaos [84] implies that

$$J_0^{\text{planar}} \leq 2, \quad (4.224)$$

where  $J_0^{\text{planar}}$  characterizes the Regge growth of the leading nontrivial term in  $1/N$ . This bound is saturated in holographic theories with a large gap, where  $J_0^{\text{planar}} = 2$  comes from tree-level graviton exchange in the bulk. At one-loop in the bulk, we get contributions from two graviton exchange, and hence we expect  $J_0^{1\text{-loop}} = 3$  in such theories.

From our discussion above, it follows that in these theories, products of ANEC operators on the same null plane should be well-defined and the ANEC operators should commute at planar level, since  $J_0^{\text{planar}} < 3$ . However, a product of ANEC operators on the same null plane is not well-defined at 1-loop order in the bulk, since  $J_0^{1\text{-loop}} \geq 3$ . To recover a well-defined observable, one would have to appropriately re-sum  $1/N$  effects.

Note that there is no contradiction with the product of ANEC operators being defined nonperturbatively. The four-point function has an expansion in powers of  $1/N$  at fixed values of cross-ratios, but this expansion does not commute with taking the Regge limit. Since the ANEC integrals probe the Regge limit, we find that these integrals do not commute with  $1/N$  expansion. Let us consider a (not necessarily physical) toy model of such a situation,

$$I_N = \int_1^\infty ds s^{-3} f_N(s), \quad f_N(s) = \frac{1}{1 + s/N^2}. \quad (4.225)$$

Here the  $I_N$  is the analogue of the energy-energy correlator, and  $f_N(s)$  is the analogue of the correlation function, where  $s \rightarrow +\infty$  is the Regge limit. The integral for  $I_N$  converges if  $f_N(s)$  grows as  $s^{j-1}$  with  $j < 3$ . This is true for  $N^0$  and  $N^{-2}$  terms in large- $N$  expansion of  $f_N(s)$ , which predict

$$I_N = \frac{1}{2} - N^{-2} + \dots. \quad (4.226)$$

The exact answer is

$$I_N = \frac{1}{2} - N^{-2} + \frac{\log(N^2 + 1)}{N^4}. \quad (4.227)$$

We see that term-wise integration is reliable for the orders at which it converges, but at higher orders  $I_N$  may cease to have a simple  $1/N$  expansion. We expect that something similar happens in energy-energy correlators, i.e.

$$\langle \mathcal{E}(n_1)\mathcal{E}(n_2) \rangle_{\epsilon T} = f^{\text{planar}}(n_1, n_2) + f_N^{\text{rest}}(n_1, n_2), \quad (4.228)$$

where  $f^{\text{planar}}(n_1, n_2)$  is computed from the planar part of the four-point function, and

$$\lim_{N \rightarrow \infty} f_N^{\text{rest}}(n_1, n_2) = 0, \quad (4.229)$$

but  $f_N^{\text{rest}}(n_1, n_2)$  does not admit an expansion in integer powers of  $1/N^2$ . In  $\mathcal{N} = 4$  SYM, at finite 't Hooft coupling  $J_0$  will be less than 2 and (4.228) may have more  $1/N$  terms in it.

#### 4.4.6 Other types of null-integrated operators

The works [153, 154] have considered other examples of operators integrated over null rays. For example, the authors of [153] introduced

$$L^n(\vec{y}) \equiv \int_{-\infty}^{\infty} dv v^{n+1} T_{vv}(u=0, v, \vec{y}). \quad (4.230)$$

They studied the algebra of such operators (under the assumption that products can be suitably renormalized) and found that it resembles a separate Virasoro algebra for each transverse point  $\vec{y}$ . The work [154] did a similar analysis of other null integrated operators and found that they generate a BMS algebra.

A first comment about the expression (4.230) is that it is generically divergent in any correlation function when  $n \geq d$ . A definition of  $L^n(\vec{y})$  which is not divergent is in terms of descendants of  $\mathbf{L}[T]$ , as we explain below.

Let us make two additional comments about such operators. Firstly, the additional insertions of  $v^{n+1}$  in the integrand make it more difficult to argue that products are well-defined and commutative, even at nonzero transverse separation  $\vec{y}_{12}$ . The required analysis is similar to the previous subsections. For example, suppose we would like to establish that  $\langle \mathcal{O}_4 | [L^n(\vec{y}_1), L^m(\vec{y}_2)] | \mathcal{O}_3 \rangle = 0$ , for nonzero  $\vec{y}_{12}$ . The integral of the Wightman function  $\langle \Omega | \mathcal{O}_4 T T \mathcal{O}_3 | \Omega \rangle$  is absolutely convergent in the Regge limit if

$$J_1 + J_2 > J_0 + 3 + n + m, \quad (4.231)$$

where  $J_1 = J_2 = 2$ . If  $0 < J_0 < 1$  (as expected for the 3d Ising model), we can only prove commutativity at nonzero  $\vec{y}_{12}$  for the cases  $n + m \leq 0$ . If  $J_0 = 1$  (as expected

in a gauge theory), we can only prove commutativity at nonzero  $\vec{y}_{12}$  for  $n + m < 0$ . One should also consider constraints coming from the lightcone limit. A full analysis of well-definedness and commutativity of more general light-ray operators is outside the scope of this work.

If Wightman function integrals are not absolutely convergent, then it may still be possible to renormalize products  $L^n(\vec{y}_1)L^m(\vec{y}_2)$ , but the renormalized product may not be commutative at nonzero  $\vec{y}_{12}$ .

This discussion assumes that the Regge limit is always dominated by a fixed Regge intercept  $J_0$ . More generally, the Regge limit of a four-point function is related to an integral over the leading Regge trajectory  $J_0(\nu)$  where  $\Delta = \frac{d}{2} + i\nu$  and  $\nu$  ranges from  $-\infty$  to  $\infty$  [149, 150]. The  $J_0$  we have discussed so far is shorthand for the maximum value of  $J_0(\nu)$  along this trajectory. However, it is possible to isolate different values of  $\nu$  by performing an integral transform in the transverse positions  $\vec{y}$ . Thus, perhaps by passing to  $\nu$  space and choosing a  $\nu$  such that  $J_0(\nu)$  is sufficiently small, one could alleviate the problems with defining products  $L^n(\vec{y}_1)L^m(\vec{y}_2)$ . We briefly discuss this possibility again in section 4.6.2.2.

Finally, let us explain how operators like  $L^n(\vec{y})$  and those in [154] can be described using light transforms. The significance of  $\mathbf{L}[T](x, z)$  is that it transforms like a conformal primary. By contrast, the operators  $L^n(\vec{y})$  can be understood as descendants of  $\mathbf{L}[T](x, z)$  — i.e. derivatives with respect to  $x$  and/or  $z$ . As usual in conformal field theory, correlators of descendants are determined by correlators of primaries.

Let us understand how this works for the case of

$$L^0(\vec{y}) = \int_{-\infty}^{\infty} dv v T_{vv}(u = 0, v, \vec{y}). \quad (4.232)$$

This expression looks like a light-transform, except that the object  $vT_{vv}$  in the integrand is not a conformal primary. To understand its conformal transformation properties, it is helpful to think of  $vT_{vv}$  as a component of a larger object

$$X^m T(X, Z), \quad (4.233)$$

where

$$X^m = (X^+, X^-, X^\mu) = (1, x^2, x^\rho) \in \mathbb{R}^{d,2} \quad (4.234)$$

is an embedding-space vector. Here,  $T(X, Z)$  is the embedding-space lift of  $T_{\mu\nu}(x)$ , which we describe in more detail in section 4.5.1.3. We recover  $vT_{vv}$  by setting  $m = v$  and  $Z = (0, 0, z)$  with  $z \cdot x = v$ .



The product  $X^m T(X, Z)$  is an example of acting on  $T(X, Z)$  with a weight-shifting operator [186]. Weight-shifting operators are conformally-covariant differential operators that shift the conformal weights of the objects they act on, in addition to introducing a free index for a finite-dimensional representation  $W$  of the conformal group. In this case,  $X^m$  is a 0-th order differential operator (since it does not involve any derivatives  $\frac{\partial}{\partial X}$  or  $\frac{\partial}{\partial Z}$ ). It transforms in the vector representation  $W = \square$  of  $\text{SO}(d, 2)$ , and shifts weights by  $(\Delta, J) \rightarrow (\Delta - 1, J)$ .

Some weight-shifting operators for  $W = \square$  are

$$\begin{aligned} \mathcal{D}_m^{-0} &= X_m, \\ \mathcal{D}_m^{0+} &= (J + \Delta)Z_m + X_m Z \cdot \frac{\partial}{\partial X}. \end{aligned} \quad (4.235)$$

Here  $m = +, -, 0, \dots, d - 1$  is a vector index for  $\text{SO}(d, 2)$ . The superscripts indicate how the operators shift dimension and spin, respectively:

$$\mathcal{D}_m^{\alpha\beta} : (\Delta, J) \rightarrow (\Delta + \alpha, J + \beta). \quad (4.236)$$

The representation  $W = \square$  possesses other weight-shifting operators that will not be important for our discussion.

Weight-shifting operators and conformally-invariant integral transforms satisfy a natural algebra. We can guess the form of this algebra simply by inspecting quantum numbers. For example, because  $\mathbf{L} : (\Delta, J) \rightarrow (1 - J, 1 - \Delta)$ , we must have<sup>30</sup>

$$\mathbf{L} \mathcal{D}_m^{\alpha,\beta} \propto \mathcal{D}_m^{-\beta, -\alpha} \mathbf{L}. \quad (4.237)$$

In particular,

$$\begin{aligned} \mathbf{L}[X_m T(X, Z)] &= \mathbf{L}[\mathcal{D}_m^{-0} T(X, Z)] \\ &\propto \mathcal{D}_m^{0+} \mathbf{L}[T](X, Z) \\ &= \left( -d Z_m + X_m Z \cdot \frac{\partial}{\partial X} \right) \mathbf{L}[T](X, Z). \end{aligned} \quad (4.238)$$

The operator  $L^0(\vec{y})$  can be obtained by appropriately specializing  $X, Z$  above:

$$L^0(\vec{y}) \propto \left( -d Z_m + X_m Z \cdot \frac{\partial}{\partial X} \right) \mathbf{L}[T](X, Z) \Big|_{\substack{X_0 = -(0, 0, \frac{1}{2}, \frac{1}{2}, \vec{0}) \\ Z_0 = (1, \vec{y}^2, 0, 0, \vec{y})}}. \quad (4.239)$$

<sup>30</sup>In general, a conformally-invariant integral transform  $\mathbf{I}_r$  is associated to a Weyl reflection  $r$  of  $\text{SO}(d, 2)$  [28, 187, 188]. When we commute a weight-shifting operator  $D^w$  with weight  $w$  past the integral transform, the weight gets reflected,  $\mathbf{I}_r D^w = D^{r(w)} \mathbf{I}_r$ .

## 4.5 Computing event shapes using the OPE

In this section, we discuss how event shapes can be computed using the OPE of the boundary CFT. Simple examples of event shapes have been computed before, for example in [31]. Our goal here is to provide tools for the calculation of  $n$ -point event shapes with general intermediate and external operators. For the purposes of this paper, this will allow us to match the results of section 4.3 and to express the commutativity of shocks as an exact constraint on the CFT data. We will also compute in closed form all conformal blocks which appear in scalar two-point event shapes, which may be useful in other contexts.

Let us give a brief overview of this section. We start by introducing the appropriate conformal blocks in section 4.5.1. After describing their general structure, we explain in detail how they can be computed in subsections 4.5.1.2-4.5.1.4. We then use these results in section 4.5.2 to match the bulk results of section 4.3, and in section 4.5.3 to describe the constraints that shock commutativity implies for the CFT data. Finally, in section 4.5.4 we give a closed-form expression for a general conformal block appearing in a scalar event shape, and demonstrate how the expansion works in a simple generalized free theory example.

### 4.5.1 $t$ -channel blocks

Let us consider a general two-point event shape<sup>31</sup>

$$\langle \mathcal{O}_4(p) | \mathbf{L}[\mathcal{O}_1](\infty, z_1) \mathbf{L}[\mathcal{O}_2](\infty, z_2) | \mathcal{O}_3(p) \rangle. \quad (4.240)$$

We can rewrite it by inserting a complete set of states between the two light transforms

$$\sum_{\Psi} \langle \mathcal{O}_4(p) | \mathbf{L}[\mathcal{O}_1](\infty, z_1) | \Psi \rangle \langle \Psi | \mathbf{L}[\mathcal{O}_2](\infty, z_2) | \mathcal{O}_3(p) \rangle. \quad (4.241)$$

By the operator-state correspondence, the Hilbert space is spanned by states created by a single insertion of a local operator, and thus the above sum can be interpreted as an OPE expansion of  $\mathcal{O}_4 \mathbf{L}[\mathcal{O}_1]$  or  $\mathbf{L}[\mathcal{O}_2] \mathcal{O}_3$  in terms of local operators. However, since the states  $\langle \mathcal{O} | \mathcal{O}_4 \mathbf{L}[\mathcal{O}_1]$  and  $\mathbf{L}[\mathcal{O}_2] \mathcal{O}_3 | \mathcal{O} \rangle$  are not, strictly speaking, of finite norm, it is not obvious that this expansion converges. In this paper, we will assume that it does, modulo some remarks that we defer to section 4.5.1.1. We also discuss there some informal arguments in favor of convergence.

To compute the expansion (4.241), we first reorganize it into conformal families

$$\sum_{\mathcal{O}} \sum_{\Psi_{\mathcal{O}}} \langle \mathcal{O}_4(p) | \mathbf{L}[\mathcal{O}_1](\infty, z_1) | \Psi_{\mathcal{O}} \rangle \langle \Psi_{\mathcal{O}} | \mathbf{L}[\mathcal{O}_2](\infty, z_2) | \mathcal{O}_3(p) \rangle, \quad (4.242)$$

---

<sup>31</sup>We are suppressing possible Lorentz indices for  $\mathcal{O}_3$  and  $\mathcal{O}_4$ .

where we sum over primary operators  $\mathcal{O}$ , and  $\Psi_{\mathcal{O}}$  run over an orthonormal basis of descendants of  $\mathcal{O}$ . Let us focus on the contribution of a single primary operator  $\mathcal{O}$ . To simplify the discussion, assume for the moment that  $\mathcal{O}$  is a scalar.

Normally, the sum over the descendants  $\Psi_{\mathcal{O}}$  is rather complicated, since in order to perform it one needs to find an orthonormal basis in the conformal multiplet of  $\mathcal{O}$ . A simple, although a bit unorthodox, way to perform such orthogonalization is to consider the momentum eigenstates

$$|\mathcal{O}(p)\rangle \equiv \int d^d x e^{ipx} \mathcal{O}(x) |\mathcal{O}\rangle. \quad (4.243)$$

Since we are in Lorentzian signature, these states are perfectly well-defined (as distributions in  $p$ ). They also form an orthogonal set thanks to momentum conservation,

$$\langle \mathcal{O}(q) | \mathcal{O}(p) \rangle = \mathcal{A}(\Delta) (2\pi)^d \delta^d(p - q) (-p^2)^{\Delta - \frac{d}{2}} \theta(p), \quad (4.244)$$

where the right hand side is completely fixed by momentum conservation, Lorentz and scale invariance, and energy positivity, up to an overall factor  $\mathcal{A}(\Delta)$ . Here,  $\Delta$  is the scaling dimension of  $\mathcal{O}$ . Moreover, these states are complete in the conformal multiplet of  $\mathcal{O}$ , which follows from completeness of the states

$$\int d^d x f(x) \mathcal{O}(x) |\mathcal{O}\rangle, \quad (4.245)$$

where  $f$  ranges over Schwartz test functions [27]. Using this basis, we can write<sup>32</sup>

$$\sum_{\Psi_{\mathcal{O}}} |\Psi_{\mathcal{O}}\rangle \langle \Psi_{\mathcal{O}}| = \mathcal{A}(\Delta)^{-1} \int_{p>0} \frac{d^d p}{(2\pi)^d} (-p^2)^{\frac{d}{2} - \Delta} |\mathcal{O}(p)\rangle \langle \mathcal{O}(p)|, \quad (4.246)$$

This expression is morally equivalent to the shadow integral approach to conformal blocks (see, e.g. [190]). An important difference is, however, that (4.246) is a rigorous identity in the Hilbert space, and does not require subtraction of any analogs of shadow contributions.

Expression (4.246) turns out to be perfectly suited for our needs. Indeed, in (4.242) we are taking an inner product of  $\langle \Psi_{\mathcal{O}}|$  with momentum eigenstates,<sup>33</sup> and this localizes the  $p$  integral in (4.246). Using this observation, we find the following expression for the contribution of  $\mathcal{O}$  to the event shape (4.240)

$$\begin{aligned} & \mathcal{A}(\Delta)^{-1} \int_{q>0} \frac{d^d q}{(2\pi)^d} (-q^2)^{\frac{d}{2} - \Delta} \langle \mathcal{O}_4(p) | \mathbf{L}[\mathcal{O}_1](\infty, z_1) | \mathcal{O}(q) \rangle \langle \mathcal{O}(q) | \mathbf{L}[\mathcal{O}_2](\infty, z_2) | \mathcal{O}_3(p) \rangle \\ & = \mathcal{A}(\Delta)^{-1} (-p^2)^{\frac{d}{2} - \Delta} \langle \mathcal{O}_4(p) | \mathbf{L}[\mathcal{O}_1](\infty, z_1) | \mathcal{O}(p) \rangle \langle \mathcal{O}(p) | \mathbf{L}[\mathcal{O}_2](\infty, z_2) | \mathcal{O}_3(p) \rangle \end{aligned} \quad (4.247)$$

<sup>32</sup>A version of (4.246) with spin was recently used in [189]. We will use a slightly different generalization to spin.

<sup>33</sup>Recall that  $\mathbf{L}[\mathcal{O}_i]$  is inserted at infinity and is thus translationally-invariant

Above, we used momentum conservation to go to the last line, and as usual abused the notation by implicitly removing the momentum-conserving  $\delta$ -functions in the final three-point functions.

Let us immediately note an important feature of this expansion. Since the light transform  $\mathbf{L}[\mathcal{O}_2]$  annihilates the vacuum, we can write

$$\langle \mathcal{O}(p) | \mathbf{L}[\mathcal{O}_2](\infty, z_2) | \mathcal{O}_3(p) \rangle = \langle \mathcal{O}(p) | [\mathbf{L}[\mathcal{O}_2](\infty, z_2), \mathcal{O}_3(p)] | \mathcal{O} \rangle, \quad (4.248)$$

which, analogously to the situation with  $t$ -channel conformal blocks in the Lorentzian inversion formula [25], implies that the contribution of  $\mathcal{O}$  vanishes if it is a double-trace of  $\mathcal{O}_2\mathcal{O}_3$ .<sup>34</sup>

In (4.247), we have essentially computed (in the case of scalar  $\mathcal{O}$ ) what we will call the  $t$ -channel conformal blocks for the event shape (4.240). We use the name  $t$ -channel block, because we would like to reserve  $s$ -channel to mean the OPE of  $\mathbf{L}[\mathcal{O}_1]\mathbf{L}[\mathcal{O}_2]$ , which we discuss in chapter 5. More precisely, the conformal block corresponding to (4.247) is given by stripping off the OPE coefficients,

$$\begin{aligned} & G_{\Delta,0}^{t,ab}(p, z_1, z_2) \\ &= \mathcal{A}(\Delta)^{-1} (-p^2)^{\frac{d}{2}-\Delta} \langle \mathcal{O}_4(p) | \mathbf{L}[\mathcal{O}_1](\infty, z_1) | \mathcal{O}(p) \rangle^{(a)} \langle \mathcal{O}(p) | \mathbf{L}[\mathcal{O}_2](\infty, z_2) | \mathcal{O}_3(p) \rangle^{(b)}, \end{aligned} \quad (4.249)$$

where we used a superscript <sup>(a)</sup> to indicate that we are working not with a physical three-point function, but with a standard conformally-invariant three-point tensor structure with label  $a$ . We will denote the conformal block for exchange of  $\mathcal{O}$  in a general Lorentz representation  $\rho_{\mathcal{O}}$  by

$$G_{\Delta_{\mathcal{O}},\rho_{\mathcal{O}}}^{t,ab}(p, z_1, z_2). \quad (4.250)$$

Again, the indices of operators  $\mathcal{O}_3$  and  $\mathcal{O}_4$  are implicit in this notation. The analog of (4.249) for these more general blocks is a bit more involved, owing to the spin indices of  $\mathcal{O}$ , and we defer its discussion to section 4.5.1.2.

With this notation, the event shape can be written as

$$\langle \mathcal{O}_4(p) | \mathbf{L}[\mathcal{O}_1](\infty, z_1) \mathbf{L}[\mathcal{O}_2](\infty, z_2) | \mathcal{O}_3(p) \rangle = \sum_{\mathcal{O},a,b} \lambda_{14\mathcal{O},a} \lambda_{23\mathcal{O},b} G_{\Delta_{\mathcal{O}},\rho_{\mathcal{O}}}^{t,ab}(p, z_1, z_2), \quad (4.251)$$

---

<sup>34</sup>The reason is that in this case the commutator vanishes, as can be checked from explicit expressions for the three-point tensor structures.

where  $\rho_{\mathcal{O}}$  is the Lorentz representation of  $\mathcal{O}$ , and  $\lambda$  are the OPE coefficients dual to the chosen basis of three-point tensor structures.

In principle, the  $t$ -channel event shape conformal blocks can be computed from the usual conformal blocks by applying the light- and Fourier transforms. However, the kinematics of event shapes are very special, and it is easier to directly use (4.249). In particular, as we will soon see, any  $t$ -channel event shape block can be written in terms of simple functions, which is not true for general conformal blocks.

To conclude this section, let us note that the above discussion can be straightforwardly generalized to multi-point event shapes such as

$$\langle \mathcal{O}'_1(p) | \mathbf{L}[\mathcal{O}_1](\infty, z_1) \cdots \mathbf{L}[\mathcal{O}_n](\infty, z_n) | \mathcal{O}'_{n+1}(p) \rangle. \quad (4.252)$$

We can insert a complete set of states in between each consecutive pair of light transforms.<sup>35</sup> The conformal block is obtained by restricting the sums over states to conformal multiplets of some primary operators  $\mathcal{O}'_i$ ,

$$\sum_{\Psi_{\mathcal{O}'_i}} \langle \mathcal{O}'_1(p) | \mathbf{L}[\mathcal{O}_1](\infty, z_1) | \Psi_{\mathcal{O}'_2} \rangle \langle \Psi_{\mathcal{O}'_2} | \cdots | \Psi_{\mathcal{O}'_n} \rangle \langle \Psi_{\mathcal{O}'_n} | \mathbf{L}[\mathcal{O}_n](\infty, z_n) | \mathcal{O}'_{n+1}(p) \rangle. \quad (4.253)$$

Assuming again that all operators  $\mathcal{O}'_2, \dots, \mathcal{O}'_n$  are scalars, and repeating the arguments leading to (4.249), we obtain the expression for the conformal block

$$\begin{aligned} G_{\Delta,0}^{t,a_2 \cdots a_n}(p, z_1, \dots, z_n) = \\ \mathcal{A}(\Delta_{n+1})(-p^2)^{-\frac{d}{2} + \Delta_{n+1}} \prod_{i=1}^n \mathcal{A}(\Delta_{i+1})^{-1} (-p^2)^{\frac{d}{2} - \Delta_{i+1}} \langle \mathcal{O}'_i(p) | \mathbf{L}[\mathcal{O}_i](\infty, z_i) | \mathcal{O}'_{i+1}(p) \rangle^{(a_i)}. \end{aligned} \quad (4.254)$$

Again, the generalization to  $\mathcal{O}'_i$  of non-trivial spin is straightforward.

#### 4.5.1.1 Convergence of $t$ -channel expansion

In this section, we discuss in more detail the convergence of the expansion (4.241). On general grounds, (4.241) converges absolutely if the states  $\mathbf{L}[\mathcal{O}_2](\infty, z_2) \mathcal{O}_3 | \mathcal{O}$  and  $\mathbf{L}[\mathcal{O}_1^\dagger](\infty, z_1) \mathcal{O}_4^\dagger | \mathcal{O}$  have finite norm. This is certainly not the case since we have, for example,

$$\| \mathbf{L}[\mathcal{O}_2](\infty, z_2) | \mathcal{O}_3(p) \rangle \|^2 = \langle \mathcal{O} | [\mathcal{O}_3(p)]^\dagger \mathbf{L}[\mathcal{O}_2^\dagger](\infty, z_2) \mathbf{L}[\mathcal{O}_2](\infty, z_2) \mathcal{O}_3(p) | \mathcal{O} \rangle, \quad (4.255)$$

---

<sup>35</sup>Multi-point conformal blocks of this topology are sometimes called “comb-channel” blocks.

which is in general divergent because of the momentum-conserving delta-function and the fact that polarizations of the two detectors are the same. We can try to avoid both problems by considering the smeared ket state

$$\int D^{d-2} z_2 d^d p f(z_2, p) \mathbf{L}[\mathcal{O}_2](\infty, z_2) |\mathcal{O}_3(p)\rangle, \quad (4.256)$$

and similarly for the bra. If we only had  $\mathcal{O}_3$  and not the light-transform  $\mathbf{L}[\mathcal{O}_2]$ , this state would be finite-norm by the usual Wightman axioms. In order to have a finite-norm state with the insertion of  $\mathcal{O}_2$ , we would like to also have smearing over the coordinates of  $\mathcal{O}_2$  with an appropriate test function. Smearing over  $z_2$  is in principle equivalent to smearing of  $\mathcal{O}_2$ , but the effective smearing function is not a test function – it only has support on future null infinity, which is codimension 1. Whether this smearing yields a finite-norm state is not obvious. One instance in which it does is given by uniform smearing of  $z_2$  over the celestial sphere and  $\mathcal{O}_2 = T$ . In this case we get

$$\begin{aligned} & \int D^{d-2} z_2 d^d p f(z_2, p) \mathbf{L}[T](\infty, z_2) |\mathcal{O}_3(p)\rangle \\ & \propto \int d^d p f(p) H |\mathcal{O}_3(p)\rangle = \int d^d p p^0 f(p) |\mathcal{O}_3(p)\rangle, \end{aligned} \quad (4.257)$$

which is finite-norm. There are several other smearing functions which give different components of momentum generator  $P^\mu$ .<sup>36</sup> More generally, we can also smear the coordinate  $x_2$  of  $\mathbf{L}[\mathcal{O}_2](x_2, z_2)$ , which yields a finite-norm state and thus a convergent expansion (4.241), and take the limit of localized  $x_2 = \infty$ . If the event shape is well-defined in the first place (c.f. discussion in section 4.4), then one can expect this limit to commute with the expansion (4.241), thus showing that smearing in polarization vectors is sufficient.<sup>37</sup>

In chapter 5, we will relate the event shape (4.240) to the Lorentzian OPE inversion formula at spin  $J_1 + J_2 - 1$ , with  $\Delta = \frac{d}{2} + i\nu$  on the principal series. In particular, the coefficient function  $C(\Delta = \frac{d}{2} + i\nu, J = J_1 + J_2 - 1)$  appearing in the inversion formula is equal to a smearing of the two-point event shape with a particular test function that depends on  $\nu$ . In  $\nu$ -space, the question of convergence of the OPE expansion (4.241) is thus equivalent to the question of convergence of the conventional  $t$ -channel conformal

<sup>36</sup>For  $\mathcal{O}_2 = T$  a general smearing over  $z_2$  can be interpreted as a difference of modular Hamiltonians for two particular spatial regions [153]. It is unclear whether  $\int d^d p f(p) |\mathcal{O}_3(p)\rangle$  is in the domain of this difference. We thank Nima Lashkari for discussion on this point.

<sup>37</sup>Additional smearing in  $p$  should not be important since the dependence of event shape on  $p$  is essentially fixed by Lorentz invariance.

block expansion, when inserted into the Lorentzian inversion formula. Thus, the  $t$ -channel expansion for the event shape converges in  $\nu$ -space if  $J_1 + J_2 - 1 > J_0$  [25, 26]. This is equivalent to the condition for the event shape to make sense in the first place.

In what follows we will mostly be interested in event shapes in the space of spherical harmonics, as opposed to  $\nu$ -space. We will study in section 4.5.4.4 a simple example in which (4.241) converges after smearing with a test function, provided this test function vanishes sufficiently quickly near the collinear limit  $z_1 \propto z_2$ . Smearing with spherical harmonics does not have this property, but it can be achieved by taking appropriate finite linear combinations. The number of such “subtractions” in the example of section 4.5.4.4 depends on the scaling dimensions of  $\mathcal{O}_1$  and  $\mathcal{O}_2$ . We will take it as an assumption that this is the general picture. Furthermore, we will assume that no subtractions are necessary if  $\mathcal{O}_1 = \mathcal{O}_2 = T$ , and smearing polarizations  $z_1$  and  $z_2$  against spherical harmonics already leads to a convergent expansion (4.241).<sup>38</sup> It would be interesting to examine this question more rigorously.

Let us finally comment on a related subtlety. In the preceding discussion we showed that the ANEC operators commute in the sense

$$[\mathbf{L}[T](\infty, z_1), \mathbf{L}[T](\infty, z_2)] = 0 \tag{4.258}$$

for non-collinear  $z_1$  and  $z_2$ . In principle, we have not excluded the possibility of contact terms at  $z_1 \propto z_2$  in the right-hand side. Since we only study the  $t$ -channel expansion after smearing with test functions, we might worry that the smeared commutators do not vanish because of these potential contact terms. It was argued in [154] that under natural assumptions there are no contact terms in this commutator, and we will work under this assumption. Even if there are contact terms, one can still perform the same subtractions as above to avoid them.

#### 4.5.1.2 Fourier transform of Wightman two-point function

In this section we discuss the generalization of (4.246) to  $\mathcal{O}$  with non-trivial spin, and compute the coefficients  $\mathcal{A}(\Delta)$  and their generalizations in the case of traceless-symmetric  $\mathcal{O}$ .

---

<sup>38</sup>If this turns out not to be the case, our results can be straightforwardly modified to account for the subtractions. Note that the discussion of convergence is irrelevant for applications to planar theories with a finite number of single-trace exchanges, since the sum over  $\mathcal{O}$  in (4.242) is finite in such theories.

The identity (4.246) is essentially dual to the two-point function in momentum space (4.244). Thus, in order to find its generalization to  $\mathcal{O}$  with spin, we should study the general Wightman two-point function in momentum space.

The two-point function is constrained by scale, translation, Lorentz, and special conformal invariance. Let us set special conformal invariance aside for the moment and consider the implications of the other symmetries. First of all, scale and translation invariance imply

$$\langle \mathcal{O}^\alpha(p) | \mathcal{O}^\beta(q) \rangle = (2\pi)^d \delta^d(p - q) (-p^2)^{\Delta - \frac{d}{2}} \theta(p) F^{\alpha\beta}(p/|p|) \quad (4.259)$$

for some function  $F$ . Lorentz invariance further constrains the form of  $F$ . Suppose we have defined

$$F^{\alpha\beta}(\widehat{e}_0), \quad (4.260)$$

where  $\widehat{e}_0$  is the unit vector along the time direction. Then Lorentz invariance allows us to determine  $F^{\alpha\beta}(v)$  for any unit-normalized timelike  $v$ , and thus also the complete two-point function. The value of (4.260) is only constrained by invariance under  $\text{SO}(d - 1)$  rotations. In other words, the allowed values of (4.260) are in one-to-one correspondence with

$$(\rho_{\mathcal{O}}^\dagger \otimes \rho_{\mathcal{O}})^{\text{SO}(d-1)}. \quad (4.261)$$

Under reduction to  $\text{SO}(d - 1)$ , any Lorentz irrep  $\rho_{\mathcal{O}}$  decomposes into  $\text{SO}(d - 1)$  irreducible components without multiplicities. The complex conjugate irrep  $\rho_{\mathcal{O}}^\dagger$  decomposes into dual  $\text{SO}(d - 1)$  irreps. This implies that a natural basis of invariants is given by

$$\Pi_\lambda^{\alpha\beta}(v) \quad (4.262)$$

where  $\lambda$  is an  $\text{SO}(d - 1)$  irrep which appears in the decomposition of  $\rho_{\mathcal{O}}$ . These invariants are defined, up to a constant multiple, by the following property:  $\Pi_\lambda^{\alpha\beta}(\widehat{e}_0)$  is the  $\text{SO}(d - 1)$  invariant which has non-zero components only along the irrep  $\lambda$  in index  $\beta$  and  $\lambda^*$  in index  $\alpha$ . We will see explicit examples of such invariants below. Using this basis, we can write

$$F^{\alpha\beta}(v) = \sum_{\lambda \in \rho_{\mathcal{O}}} \mathcal{A}_\lambda(\Delta, \rho_{\mathcal{O}}) \Pi_\lambda^{\alpha\beta}(v), \quad (4.263)$$

for some coefficients  $\mathcal{A}_\lambda$  and thus [27]

$$\langle \mathcal{O}^\alpha(p) | \mathcal{O}^\beta(q) \rangle = (2\pi)^d \delta^d(p - q) (-p^2)^{\Delta - \frac{d}{2}} \theta(p) \sum_{\lambda \in \rho_{\mathcal{O}}} \mathcal{A}_\lambda(\Delta, \rho) \Pi_\lambda^{\alpha\beta}(p/|p|). \quad (4.264)$$



Invariance under special conformal transformations now fixes the relation between coefficients  $\mathcal{A}_\lambda$  with different  $\lambda$  [27], yielding a unique solution for the momentum-space two-point function. We will determine these coefficients for traceless-symmetric  $\mathcal{O}$  below.

To proceed, we will need the dual invariants  $\Pi_{\alpha\beta,\lambda}(v)$ , defined by the completeness relation

$$\sum_{\lambda \in \rho_{\mathcal{O}}} \Pi_{\alpha\beta,\lambda}(v) \Pi_{\lambda}^{\beta\sigma}(v) = \delta_{\alpha}^{\sigma}. \quad (4.265)$$

It is an easy exercise to establish the existence of  $\Pi_{\alpha\beta,\lambda}(v)$  from basic representation-theoretic arguments. Using these invariants, we can write the general form of (4.246) as<sup>39</sup>

$$\sum_{\Psi_{\mathcal{O}}} |\Psi_{\mathcal{O}}\rangle \langle \Psi_{\mathcal{O}}| = \sum_{\lambda \in \rho_{\mathcal{O}}} \mathcal{A}_{\lambda}(\Delta, \rho)^{-1} \int_{p>0} \frac{d^d p}{(2\pi)^d} (-p^2)^{\frac{d}{2}-\Delta} \Pi_{\alpha\beta,\lambda}(p) |\mathcal{O}^{\alpha}(p)\rangle \langle \mathcal{O}^{\beta}(p)|. \quad (4.266)$$

The general  $t$ -channel conformal block is then given by

$$\begin{aligned} G_{\Delta,\rho}^{t,ab}(p, z_1, z_2) &= \sum_{\lambda \in \rho_{\mathcal{O}}} \mathcal{A}_{\lambda}(\Delta, \rho)^{-1} (-p^2)^{\frac{d}{2}-\Delta} \langle \mathcal{O}_4(p) | \mathbf{L}[\mathcal{O}_1](\infty, z_1) | \mathcal{O}^{\alpha}(p) \rangle^{(a)} \\ &\quad \times \Pi_{\alpha\beta,\lambda}(p) \langle \mathcal{O}^{\beta}(p) | \mathbf{L}[\mathcal{O}_2](\infty, z_2) | \mathcal{O}_3(p) \rangle^{(b)}. \end{aligned} \quad (4.267)$$

The simplest ingredients which enter into (4.267) are the coefficients  $\mathcal{A}_{\lambda}(\Delta, \rho)$  and the invariants  $\Pi_{\alpha\beta,\lambda}(p)$ . In the case when  $\rho_{\mathcal{O}}$  is traceless-symmetric tensor,  $\lambda$  is a traceless-symmetric tensor of spin  $s = 0, 1, \dots, J$ . The invariant  $\Pi_s(p)$  has two sets of traceless-symmetric indices,

$$\Pi_s^{\mu_1 \dots \mu_J; \nu_1 \dots \nu_J}(p). \quad (4.268)$$

We can view  $\Pi_s(p)$  as a linear operator on traceless-symmetric spin- $J$  tensors, and define  $\Pi_s(p)$  as the orthogonal projectors onto the spin- $s$   $\text{SO}(d-1)$  irrep inside the spin- $J$  traceless-symmetric irrep of  $\text{SO}(d-1, 1)$ . Note that  $\Pi_s(p)$  have to be proportional to these projectors; requiring them to be equal to the projectors gives a convenient normalization with which  $\Pi_{\alpha\beta,\lambda}$  and  $\Pi_{\lambda}^{\alpha\beta}$  are equal. In particular, equation (4.265) follows from, in operator notation,

$$\sum_{s=0}^J \Pi_s(p) \Pi_s(p) = \sum_{s=0}^J \Pi_s(p) = 1, \quad (4.269)$$

---

<sup>39</sup>Here and below we abuse the notation by writing  $\Pi(p)$  instead of  $\Pi(p/|p|)$ . In other words, we assume that  $\Pi(p) = \Pi(p/|p|)$ , i.e.  $\Pi$  is a scale-invariant function. This is consistent because we have only defined  $\Pi(v)$  for  $v^2 = -1$ .

where we have used the standard properties of projectors.

It is convenient to contract the indices with null polarization vectors  $z_1$  and  $z_2$  to define

$$\Pi_{J,s}(p; z_1, z_2) \equiv z_{1,\mu_1} \cdots z_{1,\mu_J} \Pi_s^{\mu_1 \cdots \mu_J; \nu_1 \cdots \nu_J}(p) z_{2,\nu_1} \cdots z_{2,\nu_J}. \quad (4.270)$$

We have included an explicit  $J$  label to keep track of the Lorentz irrep when working in index-free formalism. By Lorentz invariance and the homogeneity properties of  $\Pi_s(p)$ , we must have

$$\Pi_{J,s}(p; z_1, z_2) \equiv (-p^2)^{-J} (-z_1 \cdot p)^J (-z_2 \cdot p)^J \Pi_{J,s}(\eta), \quad (4.271)$$

where  $\Pi_{J,s}(\eta)$  is a polynomial of degree at most  $J$  and

$$1 - \eta = \frac{p^2(z_1 \cdot z_2)}{(z_1 \cdot p)(z_2 \cdot p)}. \quad (4.272)$$

In particular, if we set  $p = (1, 0, \dots, 0)$  and  $z_1 = (1, n_i)$ , where  $n_i$  are unit vectors in  $\mathbb{R}^{D-1}$ , then  $\eta = (n_1 \cdot n_2)$ . Since  $\Pi_{J,s}$  is projecting the spin- $J$   $\text{SO}(d)$  irrep onto the spin- $s$   $\text{SO}(d-1)$  irrep, we should have

$$\Pi_{J,s}(\eta) \propto C_s^{\binom{d-3}{2}}(\eta), \quad (4.273)$$

where  $C_s^{\binom{d-3}{2}}$  is a Gegenbauer polynomial.<sup>40</sup> We can fix the coefficients by requiring, as a linear operator,

$$\sum_{s=0}^J \Pi_{J,s}(p) = 1, \quad (4.274)$$

or in other words

$$\sum_{s=0}^J \Pi_{J,s}(\eta) = (z_1 \cdot z_2)^J = (\eta - 1)^J. \quad (4.275)$$

This leads to

$$\Pi_{J,s}(\eta) = \frac{2^{-J} J! (d+J-2)_J (d-2)_J (-1)^{s+J} (d+2s-3)}{\binom{d-1}{2}_J (J-s)! (d-3)_{J+s+1}} C_s^{\binom{d-3}{2}}(\eta). \quad (4.276)$$

We will normalize the time-ordered two-point function for spacelike separation by

$$\langle \mathcal{O}(x_1, z_1) \mathcal{O}(x_2, z_2) \rangle = \frac{(z_1 \cdot I(x_{12}) \cdot z_2)^J}{x_{12}^{2\Delta}}, \quad (4.277)$$

---

<sup>40</sup>This follows, for example, from the quadratic Casimir equation for  $\text{SO}(d-1)$ .

where

$$I_{\mu\nu}(x) = h_{\mu\nu} - 2\frac{x_\mu x_\nu}{x^2}. \quad (4.278)$$

With this normalization, one can compute [82]

$$\begin{aligned} & \langle \mathcal{O}(p, z_1) | \mathcal{O}(p, z_2) \rangle \\ &= \frac{2^{d-2\Delta} 2\pi^{\frac{d+2}{2}} \Gamma(\Delta + 2 - d)}{\Gamma(\Delta - \frac{d-2}{2}) \Gamma(\Delta + J) \Gamma(\Delta + 2 - d - J)} \\ & \quad \times \sum_{s=0}^J \frac{(-1)^s (\Delta - 1)_s}{(d - \Delta - 1)_s} (-1)^{J+s} \Pi_{J,s}(p; z_1, z_2) (-p^2)^{\Delta - \frac{d}{2}} \theta(p). \end{aligned} \quad (4.279)$$

We reproduce the calculation in appendix C.3. We then read off

$$\mathcal{A}_s(\Delta, J) = \frac{2^{d-2\Delta} 2\pi^{\frac{d+2}{2}} \Gamma(\Delta + 2 - d)}{\Gamma(\Delta - \frac{d-2}{2}) \Gamma(\Delta + J) \Gamma(\Delta + 2 - d - J)} \frac{(-1)^s (\Delta - 1)_s}{(d - \Delta - 1)_s} (-1)^{J+s}. \quad (4.280)$$

An interesting application of (4.279) is that it proves sufficiency of the usual unitarity bounds. One can check that when these bounds are satisfied, the combination  $(-1)^{J+s} \Pi_{J,s}(p; z_1, z_2)$  corresponds to a positive-definite bilinear form,  $(-1)^{J+s} \mathcal{A}_s(\Delta, J)$  is positive, and that (4.279) is locally integrable. This is sufficient to show that

$$\int \frac{d^d p}{(2\pi)^d} f_{\mu_1 \dots \mu_J}(p) | \mathcal{O}^{\mu_1 \dots \mu_J}(p) \rangle \quad (4.281)$$

has non-negative norm for any test function  $f$ .

Let us look at some simple cases which are relevant for the examples that we discuss below. First of all, if  $J = 0$ , we can only have  $s = 0$  and

$$\mathcal{A}_0(\Delta, 0) = \frac{2^{d-2\Delta} 2\pi^{\frac{d+2}{2}}}{\Gamma(\Delta - \frac{d-2}{2}) \Gamma(\Delta)}. \quad (4.282)$$

This is positive for  $\Delta > \frac{d-2}{2}$ , in accord with the unitarity bound. As  $\Delta \rightarrow \frac{d-2}{2}$ ,  $\mathcal{A}_0(\Delta, 0)$  goes to 0. Combined with the factor  $(-p^2)^{\Delta - \frac{d}{2}}$  we find that for  $\Delta = \frac{d-2}{2}$  the two-point function is proportional to  $\delta(p^2)$ , as is expected for the theory of free scalars.<sup>41</sup>

Suppose now  $J = 1$ . We have

$$\mathcal{A}_0(\Delta, 1) = -\frac{2^{d-2\Delta} 2\pi^{\frac{d+2}{2}} (\Delta - d + 1)}{\Gamma(\Delta - \frac{d-2}{2}) \Gamma(\Delta + 1)}, \quad (4.283)$$

$$\mathcal{A}_1(\Delta, 1) = \frac{2^{d-2\Delta} 2\pi^{\frac{d+2}{2}} (\Delta - 1)}{\Gamma(\Delta - \frac{d-2}{2}) \Gamma(\Delta + 1)}. \quad (4.284)$$

---

<sup>41</sup>Recall that  $\frac{\epsilon}{x^{1-\epsilon}} \rightarrow \delta(x)$ .

This has the positivity properties mentioned above for  $\Delta > d - 1$ , and for  $\Delta = d - 1$  we find

$$\mathcal{A}_0(\Delta, 1) = 0, \quad (4.285)$$

$$\mathcal{A}_1(\Delta, 1) = \frac{2^{3-d} \pi^{\frac{d+2}{2}} (d-2)}{\Gamma(\frac{d}{2}) \Gamma(d)}. \quad (4.286)$$

This is consistent with the fact that spin-1 operators with  $\Delta = d - 1$  are conserved currents, i.e. they transform in a short multiplet. The condition  $\mathcal{A}_0(\Delta, 1) = 0$  simply says that the scalar  $s = 0$  component vanishes,

$$p_\mu \mathcal{O}^\mu(p) = 0. \quad (4.287)$$

In position space this is just the conservation equation

$$\partial_\mu \mathcal{O}^\mu(x) = 0. \quad (4.288)$$

This pattern persists for higher-spin operators: at the unitarity bound  $\Delta = J + d - 2$  only the  $s = J$  component of the operator survives, i.e. only  $\mathcal{A}_J(\Delta, J)$  is non-zero. This is the CFT analog of the statement that massless particles transform in irreducible representations of the little group  $\text{SO}(d - 1)$  rather than  $\text{SO}(d)$  (here one should think about QFT in  $d + 1$  dimensions, i.e. the flat space limit of  $\text{AdS}_{d+1}/\text{CFT}_d$  correspondence), see, e.g. [191].

#### 4.5.1.3 Light transform of a general three-point function

We now turn to the calculation of the three-point functions which enter (4.267). We will first apply the light-transform and then the Fourier transform.

In this section we heavily utilize the embedding formalism [192, 193]. Let us briefly review the basic features of this formalism. The space-time points in  $\mathbb{R}^{d-1,1}$  are put in one-to-one correspondence with null rays in  $\mathbb{R}^{d,2}$ . The conformal group  $\text{SO}(d, 2)$  acts linearly in this space. The points in  $\mathbb{R}^{d,2}$  are denoted by  $X$  and null rays can be described by  $X$  subject to  $X^2 = 0$  and identification  $X \sim \lambda X$  for  $\lambda > 0$ . If we introduce the components  $X^\pm, X^\mu$  (where  $\mu$  runs over indices of  $\mathbb{R}^{d-1,1}$ ) such that

$$X^2 = -X^+ X^- + X^\mu X_\mu, \quad (4.289)$$

then  $x^\mu \in \mathbb{R}^{d-1,1}$  can be embedded as

$$(X^+, X^-, X^\mu) = (1, x^2, x^\mu). \quad (4.290)$$

Here we used  $X \sim \lambda X$  to set  $X^+ = 1$ .<sup>42</sup> Local operators can be described by functions  $\mathcal{O}(X)$ , defined for  $X^2 = 0$ , which are homogeneous

$$\mathcal{O}(\lambda X) = \lambda^{-\Delta} \mathcal{O}(X). \quad (4.291)$$

Traceless-symmetric spin- $J$  representations are described by adding dependence on a polarization vector  $Z$ , subject to  $Z^2 = X \cdot Z = 0$ , and

$$\mathcal{O}(X, \lambda Z + \alpha X) = \lambda^J \mathcal{O}(X, Z). \quad (4.292)$$

In terms of the  $\mathbb{R}^{d-1,1}$  polarization vector  $z$  and coordinate  $x$ , we can identify

$$(Z^+, Z^-, Z^\mu) = (0, 2(x \cdot z), z^\mu). \quad (4.293)$$

Here, we used the equivalence  $Z \sim Z + \alpha X$  to set  $Z^+ = 0$ .

We will use the embedding formalism to compute the action of the light transform (4.100) on correlation functions of local operators. For this, we need its form in embedding space [28],

$$\mathbf{L}[\mathcal{O}](X, Z) = \int_{-\infty}^{+\infty} d\alpha \mathcal{O}(Z - \alpha X, -X). \quad (4.294)$$

Note that the arguments  $X$  and  $Z$  are effectively swapped in the right hand side compared to the Minkowski coordinates  $x$  and  $z$  entering in (4.100).

As shown in [192], a general parity-even three-point function of traceless-symmetric primary operators can be built out of two basic objects  $V_{i,jk}$  and  $H_{ij}$ , defined as

$$\begin{aligned} H_{ij} &= -2(Z_i \cdot Z_j)(X_i \cdot X_j) + 2(Z_i \cdot X_j)(Z_j \cdot X_i) = -4Z_i^{[m} X_i^{n]} Z_{j,[m} X_{j,n]}, \\ V_{i,jk} &= \frac{(Z_i \cdot X_j)(X_i \cdot X_k) - (Z_i \cdot X_k)(X_i \cdot X_j)}{(X_j \cdot X_k)} = 2 \frac{Z_i^{[m} X_i^{n]} X_{j,m} X_{k,n}}{(X_j \cdot X_k)}. \end{aligned} \quad (4.295)$$

Note that due to the condition (4.292),  $Z_i$  only enters these expressions in the combination  $Z_i^{[m} X_i^{n]}$ . Moreover, this is also the combination in which  $X_i$  enters into those invariants above which contain  $Z_i$ .

This fact greatly simplifies the computation of the light transform (4.294) of three-point structures. Indeed, the definition instructs us to replace  $X \rightarrow Z - \alpha X$ ,  $Z \rightarrow -X$ , and integrate over  $\alpha$ . The combination  $Z_i^{[m} X_i^{n]}$  is invariant under this replacement and thus factors out of the integral. For example, this implies that

$$\mathbf{L}_i[V_{i,jk} F(Z_i, X_i, \dots)] = V_{i,jk} \mathbf{L}_i[F(Z_i, X_i, \dots)], \quad (4.296)$$

---

<sup>42</sup>The points with  $X^+ = -1$  correspond to a different Poincare patch of the Lorentzian cylinder. For details see, e.g., [28].

where notation  $\mathbf{L}_i$  means that the light transform is applied to point  $i$ . Similarly, we can factor out all  $H_{jk}$  from under  $\mathbf{L}_i$ .<sup>43</sup>

Therefore, if we start with a three-point tensor structure

$$\langle \mathcal{O}_1 \mathcal{O}_2 \mathcal{O}_3 \rangle = \frac{g(V_{1,23}, H_{12}, H_{13}, H_{23}) V_{2,31}^{m_2} V_{3,12}^{m_3}}{X_{12}^{\frac{\bar{\tau}_1 + \bar{\tau}_2 - \bar{\tau}_3}{2}} X_{13}^{\frac{\bar{\tau}_1 + \bar{\tau}_3 - \bar{\tau}_2}{2}} X_{23}^{\frac{\bar{\tau}_2 + \bar{\tau}_3 - \bar{\tau}_1}{2}}}, \quad (4.297)$$

where  $g$  is an arbitrary function with appropriate homogeneity, and  $\bar{\tau}_i = \Delta_i + J_i$ , we find that

$$\langle 0 | \mathcal{O}_2 \mathbf{L}[\mathcal{O}_1] \mathcal{O}_3 | 0 \rangle = g(V_{1,23}, H_{12}, H_{13}, H_{23}) \langle 0 | \mathcal{O}'_2 \mathbf{L}[\phi_1] \mathcal{O}'_3 | 0 \rangle. \quad (4.298)$$

Here we defined the three-point tensor structure

$$\langle \phi_1 \mathcal{O}'_2 \mathcal{O}'_3 \rangle = \frac{V_{2,31}^{m_2} V_{3,12}^{m_3}}{X_{12}^{\frac{\bar{\tau}_1 + \bar{\tau}_2 - \bar{\tau}_3}{2}} X_{13}^{\frac{\bar{\tau}_1 + \bar{\tau}_3 - \bar{\tau}_2}{2}} X_{23}^{\frac{\bar{\tau}_2 + \bar{\tau}_3 - \bar{\tau}_1}{2}}}, \quad (4.299)$$

where new formal operators  $\mathcal{O}'_i$  have spin  $J'_i = m_i$  and dimension  $\Delta'_i = \Delta_i + J_i - m_i$ . The scalar  $\phi_1$  has dimension  $\Delta_\phi = \bar{\tau}_1$ . Thus, the light-transform of a general three-point tensor structure is reduced to light-transforms of a special class of three-point tensor structures, where the light-transformed operator is a scalar.

On general grounds, we must have

$$\langle 0 | \mathcal{O}'_2 \mathbf{L}[\phi_1] \mathcal{O}'_3 | 0 \rangle \propto \frac{V_{1,23}^{1-\Delta_\phi} V_{2,31}^{J'_2} V_{3,12}^{J'_3} f\left(\frac{H_{12}}{V_{1,23} V_{2,31}}, \frac{H_{13}}{V_{1,23} V_{3,12}}\right)}{X_{12}^{\frac{\bar{\tau}'_1 + \bar{\tau}'_2 - \bar{\tau}'_3}{2}} X_{13}^{\frac{\bar{\tau}'_1 + \bar{\tau}'_3 - \bar{\tau}'_2}{2}} X_{23}^{\frac{\bar{\tau}'_2 + \bar{\tau}'_3 - \bar{\tau}'_1}{2}}}, \quad (4.300)$$

where  $f(x, y) = 1 + O(x, y)$  is a polynomial of degree at most  $m_2$  in  $x$  and at most  $m_3$  in  $y$ , and we defined  $J'_1 = 1 - \Delta_\phi$  and  $\Delta'_1 = 1$ . We did not allow any factors of  $H_{23}$  because they contain inner products ( $z_2 \cdot z_3$ ) and it is easy to see that the light-transform integral cannot produce them.

To further constrain the form of the function  $f$  it is useful to step back and discuss some general properties of the light-transform. The light-transform in general acts on continuous-spin operators and yields new continuous spin operators. Here “continuous-spin” doesn’t necessarily mean  $J \notin \mathbb{Z}_{\geq 0}$ , but rather that the operator is

<sup>43</sup>An alternative way to phrase this observation is to say that  $Z^{[m]X^n}$  is a weight-shifting operator [186] that commutes with the action of the light-transform. Indeed, it is the only weight-shifting operator in the adjoint representation which shifts  $(\Delta, J)$  by  $(-1, 1)$ , and this shift is invariant under the Weyl reflection associated with  $\mathbf{L}$ . The only non-differential weight-shifting operators which enjoy this property are the powers of  $Z^{[m]X^n}$ .

not polynomial in its polarization vector  $z$  (or  $Z$  in embedding space notation). In this sense, the  $J = 0$  operator  $\phi_1$  in (4.299) is special in that it is polynomial in  $Z_1$ .<sup>44</sup> We will refer only to the operators which satisfy this requirement as “integer-spin.”

The structure (4.299) is the only three-point tensor structure that is free of  $(z_2 \cdot z_3)$  and also consistent with all three operators being of integer spin. Similarly, the structure (4.300) can be singled out as the only structure which is free of  $(z_2 \cdot z_3)$  and corresponds to two integer-spin operators and the *light-transform of an integer-spin operator*  $\phi_1$ .

The fact that  $\phi_1$  is an integer-spin operator can be expressed as

$$D_m \phi_1 = \left( \left( \frac{d}{2} - 2 \right) \frac{\partial}{\partial Z^m} - \frac{1}{2} Z_m \frac{\partial^2}{\partial Z \cdot \partial Z} \right) \phi_1 = 0, \quad (4.301)$$

where  $D_m$  is the Todorov/Thomas operator [192].<sup>45</sup> This should be thought of as a shortening condition for  $\phi_1$ . It is natural to expect that there exists a differential operator  $D_m^L$  which provides a dual shortening condition for  $\mathbf{L}[\phi_1]$ , i.e.

$$D_m \phi_1 = 0 \implies D_m^L \mathbf{L}[\phi_1] = 0. \quad (4.302)$$

It is easy to guess the quantum numbers of  $D_m^L \mathbf{L}[\phi_1]$  by assuming that they are just those of  $\mathbf{L}[D_m \phi_1]$ . A simple exercise shows that it has  $\Delta = 2$ ,  $J = 1 - \Delta_\phi$ , and the index  $m$  should be thought of as being in the second row of the Young diagram (the first row is accounted for by  $Z$ ). This allows us to write an ansatz for  $D_m^L$  and fix the coefficients by requiring consistency with various embedding space constraints. We find that

$$W^m D_m^L = (\Delta_\phi - 1) \left( W \cdot \frac{\partial}{\partial X} \right) + \left( Z \cdot \frac{\partial}{\partial X} \right) \left( W \cdot \frac{\partial}{\partial Z} \right) \quad (4.303)$$

satisfies all the required properties, including (4.302). Here  $W$  is a polarization vector for the second-row indices, and satisfies  $W^2 = W \cdot X = W \cdot Z = 0$  and  $W \sim W + \alpha Z + \beta X$ .<sup>46</sup>

We can therefore constrain the function  $f$  by requiring that

$$\langle 0 | \mathcal{O}'_2 (D_m^L \mathbf{L}[\phi_1]) \mathcal{O}'_3 | 0 \rangle = 0. \quad (4.304)$$

<sup>44</sup>In this case it simply means that it is independent of  $Z_1$ .

<sup>45</sup>This rather involved form of  $D_m$  is required to make sure it is consistent with the fact that  $\phi$  is only defined for  $Z^2 = X^2 = Z \cdot X = 0$ . Because of this, a single derivative  $\partial/\partial Z$  is not good enough.

<sup>46</sup>We discuss/review the embedding formalism for general Young diagrams in chapter 5.

By expanding this equation into appropriate conformally-invariant tensor structures, we find the following constraints for  $f$ ,

$$\begin{aligned} [x(x+2)\partial_x^2 - y(y+2)\partial_x\partial_y + ((1+x)(\Delta_\phi - J'_2) + (1+y)J'_3 + \Delta'_{23})\partial_x - J'_2(\Delta_\phi - 1)]f(x, y) &= 0, \\ [y(y+2)\partial_y^2 - x(x+2)\partial_x\partial_y + ((1+y)(\Delta_\phi - J'_3) + (1+x)J'_2 - \Delta'_{23})\partial_y - J'_3(\Delta_\phi - 1)]f(x, y) &= 0. \end{aligned} \quad (4.305)$$

The solution to these equations with  $f(x, y) = 1 + O(x, y)$  is given by

$$f(x, y) = F_2(-J'_1; -J'_2, -J'_3; \frac{1}{2}(\tau'_1 + \tau'_2 - \tau'_3), \frac{1}{2}(\tau'_1 - \tau'_2 + \tau'_3); -\frac{1}{2}x, -\frac{1}{2}y), \quad (4.306)$$

where as before  $J'_1 = 1 - \Delta_\phi$ ,  $\Delta'_1 = 1$ , and  $\tau'_i = \Delta'_i - J'_i$ , while  $F_2$  is the Appell  $F_2$  hypergeometric function

$$F_2(\alpha; \beta, \beta'; \gamma, \gamma'; x, y) \equiv \sum_{m=0}^{\infty} \sum_{n=0}^{\infty} \frac{(\alpha)_{m+n}(\beta)_m(\beta')_n}{m!n!(\gamma)_m(\gamma')_n} x^m y^n. \quad (4.307)$$

Note that the coefficients of the Taylor expansion of  $F_2$  in either variable are given by  ${}_2F_1$  hypergeometric functions in the other variable.

Since we have uniquely fixed the form of the function  $f(x, y)$ , it only remains to fix the overall coefficient in (4.300). This can be done by choosing a degenerate kinematic configuration which simplifies the integrals. We do this in appendix C.4. Here we just quote the result,

$$\begin{aligned} \langle 0 | \mathcal{O}'_2 \mathbf{L}[\phi_1] \mathcal{O}'_3 | 0 \rangle &= -2\pi i \frac{e^{i\pi\bar{\tau}'_2} 2^{J'_1} \Gamma(-J'_1)}{\Gamma(\frac{\tau'_1 + \tau'_2 - \tau'_3}{2}) \Gamma(\frac{\tau'_1 - \tau'_2 + \tau'_3}{2})} \frac{(-V_{1,23})^{J'_1} (-V_{2,31})^{J'_2} (-V_{3,12})^{J'_3}}{X_{12}^{\frac{\bar{\tau}'_1 + \bar{\tau}'_2 - \bar{\tau}'_3}{2}} X_{13}^{\frac{\bar{\tau}'_1 + \bar{\tau}'_3 - \bar{\tau}'_2}{2}} (-X_{23})^{\frac{\bar{\tau}'_2 + \bar{\tau}'_3 - \bar{\tau}'_1}{2}}} \\ &\times f\left(\frac{H_{12}}{V_{1,23}V_{2,31}}, \frac{H_{13}}{V_{1,23}V_{3,12}}\right) \quad ((3 > 2) \approx 1). \end{aligned} \quad (4.308)$$

which holds for causal relations  $(3 > 2) \approx 1$ . In other words, 3 is in the future of 2 and both are spacelike from 1.

Let us apply the results of this section to an example which will be useful below, namely to the three-point function  $\langle TJJ \rangle$ , where  $T$  is the stress-tensor and  $J$  is a spin-1 current. We have the general form for the three-point function

$$\langle T_1 J_2 J_3 \rangle = \frac{aV_1^2 V_2 V_3 + bV_1 H_{12} V_3 + cV_1 H_{13} V_2 + hV_1^2 H_{23} + kH_{12} H_{13}}{X_{12}^{\frac{\bar{\tau}_1 + \bar{\tau}_2 - \bar{\tau}_3}{2}} X_{13}^{\frac{\bar{\tau}_1 + \bar{\tau}_3 - \bar{\tau}_2}{2}} X_{23}^{\frac{\bar{\tau}_2 + \bar{\tau}_3 - \bar{\tau}_1}{2}}}, \quad (4.309)$$

where  $\tau_1 = d + 2$ ,  $\tau_2 = \tau_3 = d$ , and we have added subscripts to the operators to indicate at which point they are inserted. Furthermore, we used the standard notation



$V_1 = V_{1,23}$ ,  $V_2 = V_{2,31}$  and  $V_3 = V_{3,12}$ . The coefficients  $a, b, c, h, k$  are constrained by the conservation conditions for  $T$  and  $J$ , by permutation symmetry in the two  $J$ s, and by the Ward identity for stress-tensor. These imply

$$b = c, \quad (d+2)h - db - a = 0, \quad (d-2)k - 2h + 2b = 0, \quad (4.310)$$

and

$$C_J = \frac{(k-b)S_d}{d}, \quad S_d = \text{vol } S^{d-1} = \frac{2\pi^{d/2}}{\Gamma(\frac{d}{2})}, \quad (4.311)$$

where  $C_J$  is defined as

$$\langle J_2 J_3 \rangle = C_J \frac{H_{23}}{X_{23}^{\frac{d}{2}}}. \quad (4.312)$$

In this section, however, it is more convenient to treat the structures that are multiplied by  $a, b, c, h, k$  independently. Let us focus on the structure with coefficient  $a$  in (4.309). Using the results above, we find that

$$\langle J_2 \mathbf{L}[T_1] J_3 \rangle = V_1^2 \mathbf{L}_1 \left[ \frac{V_2 V_3}{X_{12}^{\frac{d+2}{2}} X_{13}^{\frac{d+2}{2}} X_{23}^{\frac{d-2}{2}}} \right], \quad (4.313)$$

where the light transform is applied to the correlation function with

$$J'_1 = -d - 1, \quad \Delta'_1 = 1, \quad (4.314)$$

$$J'_2 = J'_3 = 1, \quad \Delta'_2 = \Delta'_3 = d - 1. \quad (4.315)$$

We can now use equations (4.308) and (4.306) to write (for  $(3 > 2) \approx 1$ ),

$$\mathbf{L}_1 \left[ \frac{V_2 V_3}{X_{12}^{\frac{d+2}{2}} X_{13}^{\frac{d+2}{2}} X_{23}^{\frac{d-2}{2}}} \right] = 2\pi i \frac{2^{-d-1} \Gamma(d+1)}{\Gamma(\frac{d+2}{2})^2} \frac{V_1^{-d-1} V_2 V_3}{X_{12}^{-\frac{d}{2}} X_{13}^{-\frac{d}{2}} (-X_{23})^{\frac{3d}{2}}} f \left( \frac{H_{12}}{V_1 V_2}, \frac{H_{13}}{V_1 V_3} \right), \quad (4.316)$$

where

$$\begin{aligned} f(x, y) &= F_2(-J'_1; -1, -1; \frac{1}{2}(d+2), \frac{1}{2}(d+2); -\frac{1}{2}x, -\frac{1}{2}y) \\ &= 1 + \frac{d+1}{d+2}(x+y) + \frac{d+1}{d+2}xy. \end{aligned} \quad (4.317)$$

Therefore, in this case

$$\begin{aligned} &\langle J_2 \mathbf{L}[T_1] J_3 \rangle \\ &= 2\pi i \frac{2^{-d-1} \Gamma(d+1)}{\Gamma(\frac{d+2}{2})^2} \frac{V_1^{-d+1} V_2 V_3 + \frac{d+1}{d+2} (V_1^{-d} V_3 H_{12} + V_1^{-d} V_2 H_{13} + V_1^{-d-1} H_{12} H_{13})}{X_{12}^{-\frac{d}{2}} X_{13}^{-\frac{d}{2}} (-X_{23})^{\frac{3d}{2}}}. \end{aligned} \quad (4.318)$$

Calculation of the light transforms for other structures, corresponding to coefficients  $b, c, h, k$ , is completely analogous. The complete result is

$$\begin{aligned} & \langle J_2 \mathbf{L}[T_1] J_3 \rangle \\ &= 2\pi i \frac{2^{-d-1} \Gamma(d+1)}{\Gamma(\frac{d+2}{2})^2} V_1^{-d-1} \frac{a' V_1^2 V_2 V_3 + b' V_1 H_{12} V_3 + c' V_1 H_{13} V_2 + h' V_1^2 H_{23} + k' H_{12} H_{13}}{X_{12}^{-\frac{d}{2}} X_{13}^{-\frac{d}{2}} (-X_{23})^{\frac{3d}{2}}}, \end{aligned} \quad (4.319)$$

where

$$\begin{aligned} a' &= a, \quad b' = -\frac{d}{d+2}b + \frac{d+1}{d+2}a, \quad c' = -\frac{d}{d+2}c + \frac{d+1}{d+2}a, \\ k' &= k + \frac{d+1}{d+2}(a - b - c). \end{aligned} \quad (4.320)$$

Note that the algorithm for computing the light transform is much simpler than in the case of the shadow transform [194].

#### 4.5.1.4 Fourier transform of three-point functions

Above, we have described how to compute the light transform

$$\langle 0 | \mathcal{O}_2(x_2, z_2) \mathbf{L}[\mathcal{O}_1](x_1, z_1) \mathcal{O}_3(x_3, z_3) | 0 \rangle \quad (4.321)$$

for a general three-point structure. We now need to set  $x_1 = \infty$  and Fourier-transform  $\mathcal{O}_2$  and  $\mathcal{O}_3$ . Since after setting  $x_1 = \infty$  the three-point function becomes translation-invariant in  $x_2$  and  $x_3$ , it suffices to only Fourier-transform  $\mathcal{O}_3$ . Therefore, we want to compute the Fourier transforms

$$\langle \mathcal{O}_2(p, z_2) | \mathbf{L}[\mathcal{O}_1](\infty, z_1) | \mathcal{O}_3(p, z_2) \rangle = \int d^d x e^{ipx} \langle 0 | \mathcal{O}_2(0, z_2) \mathbf{L}[\mathcal{O}_1](\infty, z_1) \mathcal{O}_3(x, z_3) | 0 \rangle. \quad (4.322)$$

The configuration in the integrand corresponds to

$$\begin{aligned} X_1 &= (0, 1, \vec{0}), & X_2 &= (1, 0, \vec{0}), & X_3 &= (1, x^2, x), \\ Z_1 &= (0, 0, z_1), & Z_2 &= (0, 0, z_2), & Z_3 &= (0, 2(x \cdot z_3), z_3). \end{aligned} \quad (4.323)$$

Under this substitution we have

$$\begin{aligned} V_{1,23} &= -x^{-2}(x \cdot z_1), & V_{2,31} &= (x \cdot z_2), & V_{3,12} &= (x \cdot z_3), \\ H_{12} &= (z_1 \cdot z_2), & H_{23} &= x^2(z_2 \cdot I(x) \cdot z_3), & H_{31} &= (z_1 \cdot z_3). \end{aligned} \quad (4.324)$$

Using these identities, the three-point function under the integral in (4.322) can be reduced to a linear combination of terms of the form

$$(z_1 \cdot z_2)^{n_{12}} (z_2 \cdot z_3)^{n_{23}} (z_3 \cdot z_1)^{n_{31}} (-x \cdot z_2)^{m_2} (-x \cdot z_3)^{m_3} (-x \cdot z_1)^{1-\Delta_1-n_{12}-n_{31}} (-x^2)^{\lambda/2} \quad (4.325)$$

where

$$\begin{aligned} \lambda &= (1 - J_1) - \Delta_2 - \Delta_3 - m_2 - m_3 - (1 - \Delta_1 - n_{12} - n_{31}), \\ J_2 &= n_{23} + n_{12} + m_2, \\ J_3 &= n_{31} + n_{23} + m_3, \end{aligned} \quad (4.326)$$

and  $m_2, m_3, n_{12}, n_{23}, n_{31}$  are non-negative integers.

In the simplest case when  $J_2 = J_3 = 0$ , there is only one structure

$$\frac{(-x \cdot z_1)^{1-\Delta_1}}{(-x^2)^{\frac{\Delta_2+\Delta_3-(1-J_1)+(1-\Delta_1)}{2}}}. \quad (4.327)$$

It is straightforward to compute the Fourier transform

$$\begin{aligned} &\int d^d x e^{ipx} \frac{(-x \cdot z_1)^{1-\Delta_1}}{(-x^2)^{\frac{\Delta_2+\Delta_3-(1-J_1)+(1-\Delta_1)}{2}}} \\ &= \widehat{\mathcal{F}}_{\Delta_2+\Delta_3-(1-J_1), 1-\Delta_1}(-p \cdot z_1)^{1-\Delta_1} (-p^2)^{\frac{\Delta_2+\Delta_3-(1-J_1)-(1-\Delta_1)-d}{2}} \theta(p), \end{aligned} \quad (4.328)$$

where the  $i\epsilon$  prescription  $x^0 \rightarrow x^0 + i\epsilon$  has to be used, and the coefficient  $\widehat{\mathcal{F}}_{\Delta, J}$  is given by

$$\widehat{\mathcal{F}}_{\Delta, J} = 2\pi \frac{e^{-i\pi\Delta/2} 2^{d-\Delta} \pi^{\frac{d}{2}}}{\Gamma(\frac{\Delta+J}{2}) \Gamma(\frac{\Delta+2-d-J}{2})}. \quad (4.329)$$

We can reuse this result for general  $J_2$  and  $J_3$ . Note that exactly the same calculation as above works for structures with  $m_2 = m_3 = 0$ . To obtain the result for non-zero  $m_2$  and  $m_3$ , we can introduce the following auxiliary basis,

$$\begin{aligned} &\{z_1^{J_1} z_2^{J_2} z_3^{J_3} | x^{-\Delta}\}_{n_{12} n_{23} n_{31}} \\ &\equiv (-x^2)^{\frac{-\Delta-m_1-m_2-m_3}{2}} (z_1 \cdot z_2)^{n_{12}} (z_2 \cdot z_3)^{n_{23}} (z_3 \cdot z_1)^{n_{31}} (z_2 \cdot D_{z_1})^{m_2} (z_3 \cdot D_{z_1})^{m_3} (-x \cdot z_1)^{m_1+m_2+m_3}, \end{aligned} \quad (4.330)$$

where  $m_2$  and  $m_3$  are given by (4.326),  $m_1 = J_1 - n_{12} - n_{31}$ , and  $D_z$  is the Thomas/Todorov operator [192]. Acting with, for example,  $(z_2 \cdot D_{z_1})$  on  $(-x \cdot z_1)^\alpha$  produces terms of

two types. One contains  $(x \cdot z_2)$ , which is the desired term. If we had only this term, then (4.330) would be proportional to (4.325). However, there is a second term, proportional to  $(z_1 \cdot z_2)$ . Nevertheless, it is clear that this term leads to contributions to (4.330) which have fewer powers of  $(x \cdot z_i)$  than (4.325). This means that the relationship between the structures (4.330) and (4.325) is given by a triangular matrix, and thus can be straightforwardly inverted. In particular (4.325) and (4.330) span the same space of structures.

The advantage of using (4.330) is that, obviously,

$$\int d^d x e^{ipx} \{z_1^{J_1} z_2^{J_2} z_3^{J_3} |x^{-\Delta}\}_{n_1 n_2 n_3} = \widehat{\mathcal{F}}_{\Delta, J_1+J_2+J_3-2n_1-2n_2-2n_3} \{z_1^{J_1} z_2^{J_2} z_3^{J_3} |p^{\Delta-d}\}_{n_1 n_2 n_3} \theta(p). \quad (4.331)$$

Therefore, the Fourier transform (4.322) can be computed by expanding the integrand in the basis (4.330) and applying (4.331).

This method works well in practice if  $J_2$  and  $J_3$  are some concrete integers which are not very large. For example, let us use it to compute the example we studied above, namely

$$\langle J(p, z_2) | \mathbf{L}[T](\infty, z_1) | J(p, z_3) \rangle. \quad (4.332)$$

which corresponds to  $J_2 = J_3 = 1$ . We have to look at five structures,

$$\begin{aligned} \langle J(0, z_2) | \mathbf{L}[T](\infty, z_1) | J(x, z_3) \rangle = \\ \tilde{a} \{z_1^{1-d} z_2 z_3 |x^{-2d+1}\}_{000} + \tilde{b} \{z_1^{1-d} z_2 z_3 |x^{-2d+1}\}_{100} + \tilde{c} \{z_1^{1-d} z_2 z_3 |x^{-2d+1}\}_{010} \\ + \tilde{h} \{z_1^{1-d} z_2 z_3 |x^{-2d+1}\}_{001} + \tilde{k} \{z_1^{1-d} z_2 z_3 |x^{-2d+1}\}_{110}. \end{aligned} \quad (4.333)$$

For example,

$$\begin{aligned} & \{z_1^{1-d} z_2 z_3 |x^{-2d+1}\}_{000} \\ &= \frac{(d-3)_4 (-x \cdot z_1)^{-1-d}}{4(-x^2)^{\frac{d+2}{2}}} \left( \frac{d-2}{d-1} (x \cdot z_1)^2 (x \cdot z_2)(x \cdot z_3) - x^2 (x \cdot z_1)(z_1 \cdot z_2)(x \cdot z_3) \right. \\ & \quad \left. - x^2 (x \cdot z_1)(x \cdot z_2)(z_1 \cdot z_3) + x^4 (z_1 \cdot z_2)(z_1 \cdot z_3) \right. \\ & \quad \left. + \frac{1}{d-1} x^2 (x \cdot z_1)^2 (z_2 \cdot z_3) \right). \end{aligned} \quad (4.334)$$

After computing the other structures, it is straightforward to plug (4.324) into (4.319) to find the coefficients  $\tilde{a}, \tilde{b}, \tilde{c}, \tilde{h}, \tilde{k}$  and then use (4.331). These intermediate steps get somewhat messy and we do not reproduce them explicitly here.

To write down the final result, it is convenient to apply a Lorentz transformation and a dilatation so that  $p = (1, \vec{0})$ . We can then choose  $z_i = (1, n_i)$ , where  $n_i$  are unit vectors. In this frame the Fourier transform becomes

$$\begin{aligned} & \langle J_2(p, z_2) | \mathbf{L}[T](\infty, z_1) | J_3(p, z_3) \rangle \\ &= C_J S_d^2 \frac{2^{1-2d} \pi^{2-d} (d-2)}{d-1} \left( (n_2 \cdot n_3) + a_2 \left( (n_1 \cdot n_2)(n_1 \cdot n_3) - \frac{(n_2 \cdot n_3)}{d-1} \right) \right), \end{aligned} \quad (4.335)$$

where  $C_J$  and  $a_2$  define  $b$  by

$$b = \frac{C_J (d-2) d (a_2 + d(d-1))}{S_d (d-1)^3}. \quad (4.336)$$

The other constants  $a, c, h, k$  are determined by  $b$  and  $C_J$  through equations (4.310) and (4.311).

Notice that this method of computing Fourier transforms quickly gets out of hand if, say,  $J_3$  is large, or if we want to keep it as a free parameter. The latter is important if we want to compute all the conformal blocks for a particular event shape. In section 4.5.4.1, we describe the calculation of Fourier transforms relevant for scalar event shapes at generic  $J_3$ . This can be used as a seed for calculation of Fourier transforms for more complicated event shapes at generic  $J_3$ , although we will not pursue this direction.

### 4.5.2 Holographic multi-point event shapes

In section 4.3.3 we have computed the following  $n$ -point even shapes in the bulk theory,

$$\langle \mathcal{E}(n_1) \cdots \mathcal{E}(n_k) \rangle_\phi, \quad \langle \mathcal{E}(n_1) \cdots \mathcal{E}(n_k) \rangle_{\epsilon, J}, \quad \langle \mathcal{E}(n_1) \cdots \mathcal{E}(n_k) \rangle_{\epsilon, T}. \quad (4.337)$$

From the boundary  $t$ -channel point of view, this calculation corresponds to keeping only the “comb”  $t$ -channel  $k$ -point blocks which exchange, respectively,  $\phi$ ,  $J$ , or  $T$  in all intermediate channels. We discussed the computation of such  $t$ -channel  $k$ -point blocks in section 4.5.1; here we would like to see how they reproduce the bulk calculations.

In this section we write all event shapes in the configuration  $p = (1, \vec{0})$ ,  $z_i = (1, n_i)$ . In the simplest scalar case, we have

$$\begin{aligned} \langle \phi(p) | \mathcal{E}(n_1) \cdots \mathcal{E}(n_k) | \phi(p) \rangle &= \langle \phi(p) | \mathcal{E}(n_1) | \phi(p) \rangle \frac{1}{\mathcal{A}(\Delta)} \langle \phi(p) | \mathcal{E}(n_2) | \phi(p) \rangle \cdots \\ &\quad \times \frac{1}{\mathcal{A}(\Delta)} \langle \phi(p) | \mathcal{E}(n_k) | \phi(p) \rangle \end{aligned} \quad (4.338)$$

while

$$\langle \phi(p) | \phi(p) \rangle = \mathcal{A}(\Delta), \quad (4.339)$$

where we again use notation where the momentum conserving delta-functions  $(2\pi)^d \delta^d(0)$  are implicitly removed. Combining these expressions together, we find that

$$\begin{aligned} \langle \mathcal{E}(n_1) \cdots \mathcal{E}(n_k) \rangle_\phi &= \frac{\langle \phi(p) | \mathcal{E}(n_1) \cdots \mathcal{E}(n_k) | \phi(p) \rangle}{\langle \phi(p) | \phi(p) \rangle} \\ &= \left( \frac{\langle \phi(p) | \mathcal{E}(n_1) | \phi(p) \rangle}{\mathcal{A}(\Delta)} \right)^k = \left( \frac{1}{\text{vol } S^{d-2}} \right)^k. \end{aligned} \quad (4.340)$$

The last equality follows from the Ward identity

$$\int_{S^{d-2}} d^{d-2}n \langle \phi(p) | \mathcal{E}(n) | \phi(p) \rangle = p^0 \langle \phi(p) | \phi(p) \rangle, \quad (4.341)$$

together with the fact that because of Lorentz invariance,  $\langle \phi(p) | \mathcal{E}(n) | \phi(p) \rangle$  is independent of  $n$ . Of course, we can also explicitly compute  $\langle \phi(p) | \mathcal{E}(n) | \phi(p) \rangle$  using the algorithm described in the previous subsection, with the same result. Clearly, given our choice of  $p$ , (4.340) is equivalent to (4.125).

This straightforwardly generalizes to the event shapes in  $\epsilon \cdot J$  and  $\epsilon \cdot T$  states. When spinning operators are exchanged, according to (4.267), we need to glue the three-point functions using  $\text{SO}(d-1)$  projectors while summing over different  $\text{SO}(d-1)$  components. However, when we are working with  $J$  or  $T$ , the three-point functions only have a single  $\text{SO}(d-1)$  component — of spin-1 or spin-2, respectively — because of the shortening conditions. Thus, the projectors act trivially. For example, in the case of an  $\epsilon \cdot J$  event shape, we have

$$\begin{aligned} &\langle \epsilon \cdot J(p) | \mathcal{E}(n_1) \cdots \mathcal{E}(n_k) | \epsilon \cdot J(p) \rangle \\ &= \langle \epsilon \cdot J(p) | \mathcal{E}(n_1) | J_i(p) \rangle \frac{1}{C_J \mathcal{A}_1(\Delta, 1)} \langle J_i(p) | \mathcal{E}(n_2) | J_j(p) \rangle \cdots \\ &\quad \times \frac{1}{C_J \mathcal{A}_1(\Delta, 1)} \langle J_l(p) | \mathcal{E}(n_k) | \epsilon \cdot J(p) \rangle, \end{aligned} \quad (4.342)$$

while

$$\langle \epsilon \cdot J(p) | \epsilon \cdot J(p) \rangle = C_J \mathcal{A}_1(\Delta, 1) \epsilon^\dagger \cdot \epsilon. \quad (4.343)$$

Notice that we only sum over spatial indices above. This is because for  $p = (1, \vec{0})$ ,  $|J_0(p)\rangle = 0$ . We thus match the bulk result (4.136) if

$$\frac{\langle J_i(p) | \mathcal{E}(n) | J_j(p) \rangle}{C_J \mathcal{A}_1(\Delta, 1)} = \frac{H_{ij}(n)}{\text{vol } S^{d-2}}. \quad (4.344)$$

Using (4.335), (4.285), and recalling that  $\mathcal{E} = 2\mathbf{L}[T]$ , we can see that this is indeed true if the parameters  $a_2$  in (4.335) and (4.134) are identified. Effectively, we are saying that if one-point event shapes match, so do the higher-point event shapes (in the setting where only on single-trace operator is exchanged). In the case of one-point event shapes this matching is well-known.

Similarly, for the stress-tensor we need to check

$$\frac{\langle T_{ij}(p)|\mathcal{E}(n)|T_{kl}(p)\rangle}{C_T \mathcal{A}_2(\Delta, 2)} = \frac{H_{ij,kl}(n)}{\text{vol } S^{d-2}}. \quad (4.345)$$

This is also well-known to be true, given appropriate identifications of OPE coefficients. This result is also easily reproduced using our algorithm.

Let us finally consider an example of a non-minimal coupling of scalars to gravity analogous to the one considered in the end of section 4.2.4.2. That is, we consider the contribution of a scalar primary  $\phi$  to

$$\langle T(p, z_4)|\mathcal{E}(n_1)\mathcal{E}(n_2)|T(p, z_3)\rangle. \quad (4.346)$$

This contribution is given by

$$\frac{\langle T(p, z_4)|\mathcal{E}(n_1)|\phi(p)\rangle \langle \phi(p)|\mathcal{E}(n_2)|T(p, z_3)\rangle}{\langle \phi(p)|\phi(p)\rangle}. \quad (4.347)$$

Conservation and tracelessness of  $T$  imply that

$$\langle T(p, z_4)|\mathcal{E}(n_1)|\phi(p)\rangle \propto n_4^a n_4^b \left( n_1^a n_1^b - \frac{\delta^{ab} n_1 \cdot n_1}{d-1} \right) = (n_1 \cdot n_4)^2 - \frac{1}{d-1}. \quad (4.348)$$

Explicit calculation shows that if

$$\langle T_1 T_2 \phi \rangle = \lambda_{TT\phi} \frac{V_{1,23}^2 V_{2,31}^2 + \dots}{X_{12}^{\frac{\bar{\tau}_1 + \bar{\tau}_2 - \bar{\tau}_3}{2}} X_{13}^{\frac{\bar{\tau}_1 + \bar{\tau}_3 - \bar{\tau}_2}{2}} X_{23}^{\frac{\bar{\tau}_2 + \bar{\tau}_3 - \bar{\tau}_1}{2}}}, \quad (4.349)$$

where  $\dots$  contain contributions from  $H_{12}^2$  and  $V_{1,23} V_{2,31} H_{12}$  which are fixed by conservation of  $T$ , then

$$\begin{aligned} & \langle T(p, z_4)|\mathcal{E}(n_1)|\phi(p)\rangle \\ &= \lambda_{TT\phi} \frac{2^{1-d-\Delta} \pi^{2+\frac{d}{2}} e^{\frac{i\pi}{2}(d-\Delta)} (d-1)\Gamma(d+1)}{(d-2)\Gamma(d-\frac{\Delta}{2})\Gamma(2+\frac{\Delta}{2})^2\Gamma(\frac{d+\Delta}{2})} \left( (n_1 \cdot n_4)^2 - \frac{1}{d-1} \right). \end{aligned} \quad (4.350)$$

We see that this is non-zero unless  $\Delta = 2d + 2n$ , i.e. unless  $\phi$  has the dimension of a double-trace  $[TT]_{0,n}$ . This means that the contribution of a generic single-trace  $\phi$  to (4.346) is non-zero and proportional to

$$\left( (n_1 \cdot n_4)^2 - \frac{1}{d-1} \right) \left( (n_2 \cdot n_3)^2 - \frac{1}{d-1} \right). \quad (4.351)$$

Computing the commutator  $[\mathcal{E}(n_1), \mathcal{E}(n_2)]$  is equivalent to antisymmetrizing in  $n_1$  and  $n_2$ , which clearly gives a non-zero result when applied to the above expression. We therefore see that, similarly to flat space case, a non-minimally coupled scalar ( $\lambda_{TT\phi} \neq 0$ ) leads to a non-zero shock commutator, and must therefore be accompanied by non-minimal couplings to other fields.

### 4.5.3 Structure of the general sum rule

In this section we describe the general properties of the sum rule which expresses the commutativity of shocks,

$$\langle \mathcal{O}_4(p, z_4) | [\mathbf{L}[\mathcal{O}_1](\infty, z_1), \mathbf{L}[\mathcal{O}_2](\infty, z_2)] | \mathcal{O}_3(p, z_3) \rangle = 0. \quad (4.352)$$

Particularly, we would like to understand some natural components in which this equation can be decomposed, and how various operators in the  $t$ -channel contribute to these components.

The sum rule is obtained by writing (4.352) as

$$\langle \mathcal{O}_4 | \mathbf{L}[\mathcal{O}_1] \mathbf{L}[\mathcal{O}_2] | \mathcal{O}_3 \rangle - \langle \mathcal{O}_4 | \mathbf{L}[\mathcal{O}_2] \mathbf{L}[\mathcal{O}_1] | \mathcal{O}_3 \rangle = 0, \quad (4.353)$$

and expanding both event shapes in  $t$ -channel conformal blocks. While this is meaningful in any CFT, it is especially interesting to consider this sum rule in a large- $N$  theory.

Let us assume that  $\mathcal{O}_i$  are single-trace. At leading order in  $1/N$ , the four-point function  $\langle \mathcal{O}_4 \mathcal{O}_1 \mathcal{O}_2 \mathcal{O}_3 \rangle$  is given by the disconnected part. The disconnected part, if at all non-zero, receives contributions from the identity and the double-trace operators only. However, as noted in section 4.5.1, double-trace operators do not contribute to the event shapes in (4.353), and thus to the sum rule. The same is true for the identity operator, since  $\mathbf{L}[\mathcal{O}_i] | \mathcal{O} \rangle = 0$ . The story here is analogous to that of the Lorentzian inversion formula, since each term in (4.353) can be written as a double commutator.

Therefore, the leading contribution to the sum rule is given by the single-trace operators.<sup>47</sup> As we have seen in the examples above and in section 4.3.3, there exist special, minimal couplings of single trace operators, with which they do not contribute to the sum rule. The sum rule is therefore satisfied if all single trace operators have minimal three-point functions. However, if some single trace operator has a non-minimal

---

<sup>47</sup>Note that it does not make much sense to go to higher  $1/N$  orders, since for example in the case  $\mathcal{O}_1 = \mathcal{O}_2 = T$  the event shapes are ill-defined beyond the planar order, c.f. section 4.4.5.



coupling, its contribution must be canceled by non-minimal couplings of some other operators.

In the rest of this section we will study the symmetries of the sum rule, and the constraints that these symmetries impose on the potential cancellation of non-minimal couplings.

#### 4.5.3.1 Tensor structures

First, let us discuss the symmetries of equation (4.352). It contains the momentum  $p$ , which we are free to set to any value. We can choose  $p = (1, \vec{0})$ . After this, the only symmetry remaining is the  $\text{SO}(d-1)$  of spatial rotations transverse to  $p$ . It is therefore convenient to decompose the spin degrees of freedom of all four operators under this subgroup.

For the integer-spin operators  $\mathcal{O}_4$  and  $\mathcal{O}_3$ , the decomposition is simple and is described, for example, in [71, 195]. In the simplest case of a  $\text{SO}(1, d-1)$  traceless-symmetric tensor of spin  $J$ , upon reduction to  $\text{SO}(d-1)$  we get traceless-symmetric tensors of spins  $s = 0, \dots, J$ . If the operator is conserved, then only  $s = J$  survives. In general, let us denote by  $\rho_i$  the  $\text{SO}(1, d-1)$  irreps of these operators, and by  $\lambda_i \in \rho_i$  their  $\text{SO}(d-1)$  components.

Decomposition of continuous-spin operators  $\mathbf{L}[\mathcal{O}_1]$  and  $\mathbf{L}[\mathcal{O}_2]$  is a bit more non-trivial. Let us explain how it works in the case when the original  $\mathcal{O}_1$  and  $\mathcal{O}_2$  are traceless-symmetric, so that  $\mathbf{L}[\mathcal{O}_i]$  are as well. In this case, all that we know about  $\mathbf{L}[\mathcal{O}_1](\infty, z_1)$  as a function of  $z_1$  is that it is homogeneous. This homogeneity allows us to completely encode this function by its values for  $z_1 = (1, n_1)$ , and these values are completely unconstrained. We therefore conclude that  $\mathbf{L}[\mathcal{O}_1](\infty, z_1)$  is equivalent to a scalar function on  $S^{d-2}$  parametrized by  $n_1$ . As is well-known, under the action of  $\text{SO}(d-1)$ , the space of such functions decomposes into all possible traceless-symmetric representations

$$\{\text{functions on } S^{d-2}\} \simeq \bigoplus_{j=0}^{\infty} j, \quad (4.354)$$

where  $j$  denotes a traceless-symmetric irrep of  $\text{SO}(d-1)$  of spin  $j$ . Alternatively, we can say that we are allowed to smear  $\mathbf{L}[\mathcal{O}_1](\infty, z_1)$  with a spherical harmonic of  $n_1$ , and such smeared operators transform nicely under  $\text{SO}(d-1)$ . Furthermore, any smearing function can be decomposed into spherical harmonics.

The left-hand side of (4.352) is an  $\text{SO}(d-1)$  invariant of the four operators, i.e. an element of

$$\left( \bigoplus_{j_1, j_2=0}^{\infty} \bigoplus_{\substack{\lambda_3 \in \rho_3 \\ \lambda_4 \in \rho_4}} j_1 \otimes j_2 \otimes \lambda_3 \otimes \lambda_4 \right)^{\text{SO}(d-1)}. \quad (4.355)$$

Such invariants can be conveniently labeled by

$$\{j_1, j_2 | \lambda | \lambda_3, \lambda_4\}_s, \quad (4.356)$$

where  $\lambda \in j_1 \otimes j_2$  and  $\lambda^* \in \lambda_3 \otimes \lambda_4$ , and  $s$  stands for  $s$ -channel. This invariant is obtained by restricting to a particular term in the direct sums above, and by selecting a particular irrep in  $j_1 \otimes j_2$ .<sup>48,49</sup> The left hand side of the sum rule can then be expanded

$$\langle \mathcal{O}_4 | [\mathbf{L}[\mathcal{O}_1], \mathbf{L}[\mathcal{O}_2]] | \mathcal{O}_3 \rangle = \sum_{j_1, j_2=0}^{\infty} \sum_{\substack{\lambda_3 \in \rho_3 \\ \lambda_4 \in \rho_4}} \sum_{\substack{\lambda \in j_1 \otimes j_2 \\ \lambda^* \in \lambda_3 \otimes \lambda_4}} c_{j_1, j_2 | \lambda | \lambda_3, \lambda_4} \{j_1, j_2 | \lambda | \lambda_3, \lambda_4\}_s. \quad (4.357)$$

The sum rule can be written in components as

$$c_{j_1, j_2 | \lambda | \lambda_3, \lambda_4} = 0. \quad (4.358)$$

Note that these are scalar equations, i.e. they contain no cross-ratios.

We would now like to understand which  $t$ -channel operators these components receive contributions from. First, note that the  $t$ -channel computes not the commutator, but the individual event shapes (note the arguments in the second event shape),

$$\langle \mathcal{O}_4 | \mathbf{L}[\mathcal{O}_1](n_1) \mathbf{L}[\mathcal{O}_2](n_2) | \mathcal{O}_3 \rangle = \sum E_{j_1, j_2 | \lambda | \lambda_3, \lambda_4}^{12} \{j_1, j_2 | \lambda | \lambda_3, \lambda_4\}_s \quad (4.359)$$

$$\langle \mathcal{O}_4 | \mathbf{L}[\mathcal{O}_2](n_1) \mathbf{L}[\mathcal{O}_1](n_2) | \mathcal{O}_3 \rangle = \sum E_{j_1, j_2 | \lambda | \lambda_3, \lambda_4}^{21} \{j_1, j_2 | \lambda | \lambda_3, \lambda_4\}_s. \quad (4.360)$$

The coefficients in the sum rule are given by<sup>50</sup>

$$c_{j_1, j_2 | \lambda | \lambda_3, \lambda_4} = E_{j_1, j_2 | \lambda | \lambda_3, \lambda_4}^{12} - E_{j_2, j_1 | \lambda | \lambda_3, \lambda_4}^{21}, \quad (4.361)$$

<sup>48</sup>It may be the case that  $\lambda^*$  appears in  $\lambda_3 \otimes \lambda_4$  with multiplicity. In this case, we need to add an extra label.

<sup>49</sup>In the case  $\mathcal{O}_1 = \mathcal{O}_2$ , the sum rule is explicitly antisymmetric in  $n_1$  and  $n_2$ . This is reflected in a restriction  $j_1 \leq j_2$  and a selection rule on  $\lambda$  for  $j_1 = j_2$ . Also, the definition of the invariant for  $j_1 < j_2$  must be altered slightly.

<sup>50</sup>There might be an additional relative coefficient between the two terms which depends on the convention for Clebsch-Gordan coefficients and normalization of the invariants. Note that in case  $j_1 = j_2$  the operation of permuting  $j_1$  and  $j_2$  has a definite eigenvalue  $\pm 1$  depending on  $\lambda$ . In the case  $\mathcal{O}_1 = \mathcal{O}_2$  the two terms either cancel or add up, depending on the sign. This corresponds to the selection rule on  $\lambda$  mentioned above.

so it is sufficient to understand how  $t$ -channel operators contribute to  $E^{12}$  and  $E^{21}$ .

The structures defined above are natural from the point of view of computing the commutator, but for the  $t$ -channel expansion the more natural structures are

$$\{\lambda_4, j_1 | \lambda | j_2, \lambda_3\}_t, \quad (4.362)$$

which are obtained similarly to  $\{\dots\}_s$  structures, but with

$$\lambda \in \otimes j_1 \otimes \lambda_4, \quad \lambda^* \in j_2 \otimes \lambda_3. \quad (4.363)$$

The usefulness of these structures comes from the fact that  $\lambda$  here is exactly the same as the one summed over in (4.267). In other words, an operator  $\mathcal{O}$  only contributes to (4.362) with  $\lambda \in \rho_{\mathcal{O}}$ , where  $\rho_{\mathcal{O}}$  is the  $\text{SO}(d-1, 1)$  irrep of  $\mathcal{O}$ . Since there are finitely many choices for  $\lambda_3$  and  $\lambda_4$  (for a given event shape), this implies that given an  $\mathcal{O}$ , there is a selection rule on possible  $j_1$  and  $j_2$ .

For example, let us consider the sum rule for

$$\langle T | [\mathcal{E}, \mathcal{E}] | T \rangle = 0. \quad (4.364)$$

In this case, we have only one choice for  $\lambda_3$  and  $\lambda_4$  because of the conservation of  $T$ , i.e.  $\lambda_3 = \lambda_4 = 2$  — the spin-two traceless-symmetric irrep. Let us, for simplicity, consider contributions to the sum rule of traceless-symmetric operators. For an operator of spin  $J$ , the allowed contributions are  $\lambda = 0, \dots, J$ . The condition  $\lambda \in \lambda_4 \otimes j_1$  then implies  $j_1 \in \{\lambda - 2, \lambda, \lambda + 2\}$ , and similarly for  $j_2$ . We then conclude that an operator of spin  $J$  contributes only to the structures (either  $\{\dots\}_t$  or  $\{\dots\}_s$ ) with  $j_1, j_2 \in \{0, \dots, J + 2\}$ .

This is already non-trivial, since it tells us that contributions to the sum rule from operators of bounded spin live in a finite-dimensional space. This also implies, for example, that in the sum rule, a generic contribution of a spin-6 operator cannot be canceled by a spin-0 operator. It is less obvious whether a spin- $J$  operator can be completely canceled by spin- $J$  operators. In principle, we can have lots of spin- $J$  operators all contributing to the same finitely many components of the sum rule, so it might seem that there are enough free parameters to cancel out all components. However, in a unitary theory, due to the reality properties of OPE coefficients, the contributions of operators have fixed signs, and it might be that it is impossible to satisfy the sum rule by non-minimal couplings of operators of a single spin  $J$ . It might even be true that no finite set of spins is sufficient. We leave the investigation of this question to future work.

### 4.5.3.2 $\langle T|\mathcal{E}\mathcal{E}|T\rangle$ example

Here, let us consider two simple contributions to (4.364), from the exchange of a stress-tensor itself and from a massive scalar. We will only consider the structures to which the scalar contributes non-trivially. According to the above discussion, before taking the commutator the scalar only contributes to

$$\{2, 2|0|2, 2\}_t, \quad (4.365)$$

which, after taking the commutator, becomes a combination of

$$\{2, 2|\lambda|2, 2\}_t \quad (4.366)$$

with all allowed  $\lambda$ , i.e.  $\lambda = 0, 2, 4, (3, 1), (2, 2), (1, 1)$ , where  $(\ell_1, \ell_2)$  denotes a Young diagram with two rows  $\ell_1 \geq \ell_2$ . As we explained above, for the commutator it is more natural to look at the  $\{2, 2|\lambda|2, 2\}_s$  structures. From the point of view of the  $\{2, 2|\lambda|2, 2\}_s$  structures, the commutator only contributes to  $\lambda$  which are in the antisymmetric product  $2 \otimes 2$ , i.e. to  $\lambda = (3, 1)$  and  $\lambda = (1, 1)$ . This means that we will only get 2 equations involving scalar contributions.

In fact, we can compute that under taking the commutator

$$\begin{aligned} \{2, 2|0|2, 2\}_t &\rightarrow \frac{d^2 - d - 4}{(d+1)(d-2)} \{2, 2|0|2, 2\}_t - \frac{d-1}{(d+3)(d-3)} \{2, 2|2|2, 2\}_t - \frac{1}{36} \{2, 2|4|2, 2\}_t \\ &\quad - \frac{1}{12} \{2, 2|(2, 2)|2, 2\}_t + \frac{1}{d+1} \{2, 2|(1, 1)|2, 2\}_t + \frac{1}{8} \{2, 2|(3, 1)|2, 2\}_t \\ &= \frac{1}{4} \{2, 2|(3, 1)|2, 2\}_s + \frac{2}{d+1} \{2, 2|(1, 1)|2, 2\}_s, \end{aligned} \quad (4.367)$$

where the explicit expressions for structures  $\{\dots\}_t$  and  $\{\dots\}_s$  are given in appendix C.5.

On the other hand, stress-tensor contribution to  $j_1 = j_2 = 2$  is only through

$$\{2, 2|2|2, 2\}_t \quad (4.368)$$

because  $T$  has only a spin-2  $\text{SO}(d-1)$  component. Under taking the commutator, it

goes to

$$\begin{aligned}
\{2, 2|2|2, 2\}_t &\rightarrow -\frac{2(d-3)(d+3)}{(d+1)(d-1)(d-2)}\{2, 2|0|2, 2\}_t + \frac{d^2 - 2d + 9}{2(d+3)(d-3)}\{2, 2|2|2, 2\}_t \\
&\quad - \frac{d-3}{18(d-1)}\{2, 2|4|2, 2\}_t + \frac{d+3}{12(d-1)}\{2, 2|(2, 2)|2, 2\}_t \\
&\quad + \frac{(d-3)(d+3)}{2(d-1)(d+1)}\{2, 2|(1, 1)|2, 2\}_t - \frac{1}{2(d-1)}\{2, 2|(3, 1)|2, 2\}_t \\
&= -\frac{1}{d-1}\{2, 2|(3, 1)|2, 2\}_s + \frac{(d-3)(d+3)}{(d-1)(d+1)}\{2, 2|(1, 1)|2, 2\}_s.
\end{aligned} \tag{4.369}$$

Scalar exchange of dimension  $\Delta$  contributes, according to the result of section 4.5.2,

$$\begin{aligned}
\langle T(n_4)|\mathcal{E}(n_1)\mathcal{E}(n_2)|T(n_3)\rangle &\ni |\lambda_{TT\phi}|^2 q(\Delta) \left( (n_1 \cdot n_4)^2 - \frac{1}{d-1} \right) \left( (n_2 \cdot n_3)^2 - \frac{1}{d-1} \right) \\
&= |\lambda_{TT\phi}|^2 q(\Delta) \{2, 2|0|2, 2\}_t,
\end{aligned} \tag{4.370}$$

where

$$q(\Delta) = \frac{2^{1-3d}\pi^{3+\frac{d}{2}}(d-1)^2\Gamma(d+1)^2}{(d-2)^2\Gamma(d-\frac{\Delta}{2})^2\Gamma(2+\frac{\Delta}{2})^4\Gamma(\frac{d+\Delta}{2})^2}\Gamma(\Delta)\Gamma(\Delta+1-\frac{d}{2}) \geq 0 \tag{4.371}$$

is a non-negative function. The stress-tensor exchange contribution to  $j_1 = j_2 = 2$  is given by

$$\langle T(n_4)|\mathcal{E}(n_1)\mathcal{E}(n_2)|T(n_3)\rangle \ni \frac{C_T 2^{-1-3d}\pi^{3-\frac{d}{2}}((4+d)t_2 + 4t_4)^2\Gamma(d+3)}{(d-1)d(d+1)^2(d+4)\Gamma(3+\frac{d}{2})\Gamma(\frac{d}{2})^2}\{2, 2|2|2, 2\}_t. \tag{4.372}$$

We therefore get two sum rules in which scalars participate, corresponding to the structures  $\{2, 2|(3, 1)|2, 2\}_s$  and  $\{2, 2|(1, 1)|2, 2\}_s$ ,

$$\begin{aligned}
&-\frac{C_T 2^{-1-3d}\pi^{3-\frac{d}{2}}((4+d)t_2 + 4t_4)^2\Gamma(d+3)}{(d-1)^2d(d+1)^2(d+4)\Gamma(3+\frac{d}{2})\Gamma(\frac{d}{2})^2} + \frac{1}{4} \sum_{\phi} |\lambda_{TT\phi}|^2 q(\Delta_{\phi}) + \text{non-scalar} = 0, \\
&\frac{C_T 2^{-1-3d}(d^2-9)\pi^{3-\frac{d}{2}}((4+d)t_2 + 4t_4)^2\Gamma(d+3)}{(d-1)^2d(d+1)^3(d+4)\Gamma(3+\frac{d}{2})\Gamma(\frac{d}{2})^2} + \frac{2}{d+2} \sum_{\phi} |\lambda_{TT\phi}|^2 q(\Delta_{\phi}) + \text{non-scalar} = 0.
\end{aligned} \tag{4.373}$$

For example, in  $d = 4$  this reduces to

$$\begin{aligned}
&-\frac{C_T \pi (t_4 + 2t_2)^2}{15 \cdot 2^{13}} + \frac{1}{4} \sum_{\phi} |\lambda_{TT\phi}|^2 q(\Delta_{\phi}) + \text{non-scalar} = 0, \\
&\frac{7C_T \pi (t_4 + 2t_2)^2}{75 \cdot 2^{13}} + \frac{1}{3} \sum_{\phi} |\lambda_{TT\phi}|^2 q(\Delta_{\phi}) + \text{non-scalar} = 0,
\end{aligned} \tag{4.374}$$

which we quoted in (4.6) in the introduction. Here “non-scalar” represents contributions of higher-spin operators, starting from massive spin-2. We see explicitly that there can be no cancellation between massive scalars. Furthermore, there is a component of the contribution of scalars which cannot be canceled by the stress-tensor exchange. (The reverse is obvious since the stress-tensor contributes also to components other than  $j_1 = j_2 = 2$ .) One can also take appropriate linear combinations of these equations to obtain separate sum rules for  $(t_4 + 2t_2)^2$  and scalar contributions.

#### 4.5.4 General $t$ -channel blocks for scalar event shapes

In this section, we derive a closed form expression for all  $t$ -channel conformal blocks appearing in

$$\langle \phi_4 | \mathbf{L}[\phi_1] \mathbf{L}[\phi_2] | \phi_3 \rangle, \quad (4.375)$$

where  $\phi_i$  are all scalars. The only essential difference from the algorithm of section 4.5.1 is that we perform Fourier transform in a slightly different way, and we keep the intermediate spin as a free parameter.

##### 4.5.4.1 Fourier transform for scalar event shapes

We start with the three-point tensor structure

$$\langle \phi_1 \phi_2 \mathcal{O}_3 \rangle = \frac{V_{3,12}^{J_3}}{X_{12}^{\frac{\Delta_1 + \Delta_2 - \Delta_3 - J_3}{2}} X_{13}^{\frac{\Delta_1 + \Delta_3 - \Delta_2 + J_3}{2}} X_{23}^{\frac{\Delta_2 + \Delta_3 - \Delta_1 + J_3}{2}}}. \quad (4.376)$$

Using results of section 4.5.1, we find for  $1 \approx (3 > 2)$

$$\begin{aligned} & \langle 0 | \phi_2 \mathbf{L}[\phi_1] \mathcal{O}_3 | 0 \rangle \\ &= -2\pi i \frac{e^{i\pi\Delta_2} 2^{1-\Delta_1} \Gamma(\Delta_1 - 1)}{\Gamma(\frac{\Delta_1 + \Delta_2 - \Delta_3 + J_3}{2}) \Gamma(\frac{\Delta_1 - \Delta_2 + \Delta_3 - J_3}{2})} \\ & \quad \times \frac{(-V_{1,32})^{1-\Delta_1} (-V_{3,12})^{J_3}}{X_{12}^{\frac{2-\Delta_1 + \Delta_2 - \Delta_3 - J_3}{2}} X_{13}^{\frac{2-\Delta_1 + \Delta_3 - \Delta_2 + J_3}{2}} (-X_{23})^{\frac{\Delta_2 + \Delta_3 - 2 + \Delta_1 + J_3}{2}}} \\ & \quad \times {}_2F_1 \left( \Delta_1 - 1, -J_3; \frac{1}{2}(\Delta_1 + \Delta_2 - \Delta_3 + J_3); -\frac{1}{2} \frac{H_{13}}{V_{1,23} V_{3,12}} \right). \end{aligned} \quad (4.377)$$

We now want to find the Fourier transform (4.322), so we have to specialize to configuration (4.323). Using (4.324), we find

$$\begin{aligned} & \langle 0 | \phi_2(0) \mathbf{L}[\phi_1](\infty, z_1) \mathcal{O}_3(x, z_3) | 0 \rangle \\ &= -2\pi i \frac{e^{i\pi\Delta_2} 2^{1-\Delta_1} \Gamma(\Delta_1 - 1)}{\Gamma(\frac{\Delta_1 + \Delta_2 - \Delta_3 + J_3}{2}) \Gamma(\frac{\Delta_1 - \Delta_2 + \Delta_3 - J_3}{2})} \frac{(-x \cdot z_1)^{1-\Delta_1} (-x \cdot z_3)^{J_3}}{(-x^2)^{\frac{\Delta_2 + \Delta_3 - \Delta_1 + J_3}{2}}} \\ & \quad \times {}_2F_1\left(\Delta_1 - 1, -J_3; \frac{1}{2}(\Delta_1 - \Delta_2 + \Delta_3 - J_3); \frac{1}{2} \frac{x^2(z_1 \cdot z_3)}{(x \cdot z_1)(x \cdot z_3)}\right). \end{aligned} \quad (4.378)$$

In (4.378), we have a rather non-trivial function of  $x$ , and it is not obvious whether it should have a simple Fourier transform. Let us define functions

$$[z_1^{m_1} z_2^{m_2} | x] \equiv (-z_1 \cdot x)^{m_1} (-z_2 \cdot x)^{m_2} {}_2F_1(-m_1, -m_2; 1 - \nu - m_1 - m_2; \frac{x^2(z_1 \cdot z_2)}{2(x \cdot z_1)(x \cdot z_2)}). \quad (4.379)$$

These functions are homogeneous in  $x$  and satisfy

$$\partial_x^2 [z_1^{m_1} z_2^{m_2} | x] = 0. \quad (4.380)$$

This means that

$$[z_1^{m_1} z_2^{m_2} | x] = \mathbb{Q}_{\mu_1 \dots \mu_{m_1+m_2}}^{m_1, m_2}(z_1, z_2) (x^{\mu_1} \dots x^{\mu_{m_1+m_2}} - \text{traces}) \quad (4.381)$$

for some function  $\mathbb{Q}$ . Therefore, for the purposes of computing the Fourier transform, we can treat these functions as  $(z \cdot x)^{m_1+m_2}$ , where  $z$  is a null vector. In other words,

$$\int d^d x e^{ipx} [z_1^{m_1} z_2^{m_2} | x] (-x^2)^{-\frac{\Delta+m_1+m_2}{2}} = \widehat{\mathcal{F}}_{\Delta, m_1+m_2} [z_1^{m_1} z_2^{m_2} | p] (-p^2)^{\frac{\Delta-m_1-m_2-d}{2}} \theta(p). \quad (4.382)$$

We can find the decomposition

$$\begin{aligned} & (-x \cdot z_1)^{1-\Delta_1} (-x \cdot z_3)^{J_3} {}_2F_1(\Delta_1 - 1, -J_3; \frac{1}{2}(\Delta_1 - \Delta_2 + \Delta_3 - J_3); \frac{x^2(z_1 \cdot z_3)}{2(x \cdot z_1)(x \cdot z_3)}) \\ &= \sum_{k=0}^{J_3} \alpha_k (-z_1 \cdot z_3)^k (-x^2)^k [z_1^{1-\Delta_1-k} z_3^{J_3-k} | x]. \end{aligned} \quad (4.383)$$

where

$$\alpha_k = 2^k \frac{(\Delta_1 - 1)_k (-J_3)_k (\frac{2-d+\Delta_1+\Delta_2-\Delta_3-J_3}{2})_k}{k! (-\frac{d}{2} + \Delta_1 - J_3 + k)_k (\frac{\Delta_1 - \Delta_2 + \Delta_3 - J_3}{2})_k}. \quad (4.384)$$

This yields the following Fourier transform

$$\begin{aligned} \langle \phi_2(p) | \mathbf{L}[\phi_1](\infty, z_1) | \mathcal{O}(p, z_3) \rangle &= -2\pi i \frac{e^{i\pi\Delta_2} 2^{1-\Delta_1} \Gamma(\Delta_1 - 1)}{\Gamma\left(\frac{\Delta_1 + \Delta_2 - \Delta_3 + J_3}{2}\right) \Gamma\left(\frac{\Delta_1 - \Delta_2 + \Delta_3 - J_3}{2}\right)} \\ &\times \sum_{k=0}^{J_3} \alpha_k \widehat{\mathcal{F}}_{\Delta_2 + \Delta_3 - 1, 1 - \Delta_1 + J_3 - 2k}(-z_1 \cdot z_3)^k [z_1^{1-\Delta_1-k} z_3^{J_3-k} |p] (-p^2)^{\frac{\Delta_2 + \Delta_3 + \Delta_1 - J_3 + 2k - 2 - d}{2}} \theta(p). \end{aligned} \quad (4.385)$$

Surprisingly, this sum reassembles into another hypergeometric function,

$$\begin{aligned} &\langle \phi_2(p) | \mathbf{L}[\phi_1](\infty, z_1) | \mathcal{O}(p, z_3) \rangle \\ &= -2\pi i \frac{e^{i\pi\Delta_2} 2^{1-\Delta_1} \Gamma(\Delta_1 - 1)}{\Gamma\left(\frac{\Delta_1 + \Delta_2 - \Delta_3 + J_3}{2}\right) \Gamma\left(\frac{\Delta_1 - \Delta_2 + \Delta_3 - J_3}{2}\right)} \widehat{\mathcal{F}}_{\Delta_2 + \Delta_3 - 1, 1 - \Delta_1 + J_3}(-p^2)^{\frac{\Delta_2 + \Delta_3 + \Delta_1 - J_3 - 2 - d}{2}} \theta(p) \\ &\quad \times (-p \cdot z_1)^{1-\Delta_1} (-p \cdot z_3)^{J_3} \\ &\quad \times {}_3F_2(\Delta_1 - 1, -J_3, \Delta_3 - 1; \frac{\Delta_1 + \Delta_2 + \Delta_3 - d - J_3}{2}, \frac{\Delta_1 - \Delta_2 + \Delta_3 - J_3}{2}; \frac{p^2(z_1 \cdot z_3)}{2(p \cdot z_1)(p \cdot z_3)}). \end{aligned} \quad (4.386)$$

It would be interesting to understand whether one can arrive at this expression in a more direct way, which generalizes to more complicated three-point functions.

Note that one can in principle use this result as a “seed” to compute more complicated objects, such as

$$\langle T(p, z_2) | \mathbf{L}[T](\infty, z_1) | \mathcal{O}_3(p, z_3) \rangle \quad (4.387)$$

by using weight-shifting operators [186, 193]. We can always choose the weight-shifting operator acting on the point at infinity to be powers of  $Z_1^m X_1^n$ , which evaluates to something  $x$ -independent. Weight-shifting operators acting on points 2 and 3 can be rewritten as differential operators in momentum space, since any weight-shifting operator is polynomial in both coordinates and derivatives [186]. This suggests that an expression in terms of linear combinations of  ${}_3F_2$  functions can always be found for this type of objects.

#### 4.5.4.2 Decomposition into $\text{SO}(d-1)$ components

The last step in the computation of  $t$ -channel event-shape conformal blocks is to compute the  $\text{SO}(d-1)$ -invariant contraction

$$\langle \mathcal{O}_4(p) | \mathbf{L}[\mathcal{O}_1](\infty, z_1) | \mathcal{O}^\alpha(p) \rangle^{(a)} \Pi_{\alpha\beta,\lambda}(p) \langle \mathcal{O}^\beta(p) | \mathbf{L}[\mathcal{O}_2](\infty, z_2) | \mathcal{O}_3(p) \rangle^{(b)}. \quad (4.388)$$

For this, it is convenient to decompose the spin degrees of freedom of  $\mathcal{O}^\alpha(p)$  in each three-point function into irreducible components under the  $\text{SO}(d-1)$ .



Take the scalar structure

$$f(z_3) = \langle \phi_2(p) | \mathbf{L}[\phi_1](\infty, z_1) | \mathcal{O}_3(p, z_3) \rangle. \quad (4.389)$$

For the moment, we are considering it just as a function of  $z_3$ . We can write

$$f(z_3) = f_{\mu_1 \dots \mu_{J_3}} z_3^{\mu_1} \dots z_3^{\mu_{J_3}} = \sum_{s=0}^{J_3} f_{\mu_1 \dots \mu_{J_3}} \Pi_{J_3, s}^{\mu_1 \dots \mu_{J_3}}{}_{\nu_1 \dots \nu_{J_3}}(p) z_3^{\nu_1} \dots z_3^{\nu_{J_3}} \quad (4.390)$$

The indices of the traceless-symmetric  $f_{\mu_1} \dots f_{\mu_J}$  have to be provided by  $p$  and  $z_1$ .<sup>51</sup> It may appear that there are several choices of how many indices to fill with  $p$ , but in fact all possibilities are exhausted by using no  $p$  at all. The reason is that there is only one way to obtain a given  $\text{SO}(d-1)$  irrep from a given  $\text{SO}(d-1, 1)$ , and in this case we are trying to extract spin- $s$  irrep from  $\mathbf{L}[\phi_1]$ . We thus find that

$$\begin{aligned} & \langle \phi_2(p) | \mathbf{L}[\phi_1](\infty, z_1) | \mathcal{O}_3(p, z_3) \rangle \\ &= \sum_{s=0}^{J_3} \langle \phi_2 | \mathbf{L}[\phi_1] | \mathcal{O}_3^{(s)} \rangle (-p \cdot z_1)^{1-\Delta_1-J_3} \Pi_{J_3, s}(p; z_1, z_3) (-p^2)^{\frac{\Delta_2+\Delta_3-2+\Delta_1+J_3-d}{2}} \theta(p) \end{aligned} \quad (4.391)$$

for some numbers  $\langle \phi_2 | \mathbf{L}[\phi_1] | \mathcal{O}_3^{(s)} \rangle$ .

Another way of arriving at this conclusion is to specialize to kinematics  $p = (1, \vec{0})$  and  $z_i = (1, n_i)$ . In this kinematics, the three-point function (4.389) is necessarily a function of  $(n_1 \cdot n_2)$ , where  $n_i$  live on the unit sphere. The question of decomposing into  $\text{SO}(d-1)$  representations is then equivalent to decomposition of this function into spherical harmonics of  $n_2$ , which are proportional to  $\Pi_{J_3, s}(n_1 \cdot n_2)$  since the latter is essentially a Gegenbauer polynomial.

To perform the decomposition explicitly, we rewrite the result (4.386) in the special kinematics,

$$\begin{aligned} & \langle \phi_2(p) | \mathbf{L}[\phi_1](\infty, z_1) | \mathcal{O}(p, z_3) \rangle \\ &= -2\pi \frac{e^{i\pi\Delta_2} 2^{1-\Delta_1} \Gamma(\Delta_1 - 1)}{\Gamma(\frac{\Delta_1+\Delta_2-\Delta_3+J_3}{2}) \Gamma(\frac{\Delta_1-\Delta_2+\Delta_3-J_3}{2})} \widehat{\mathcal{F}}_{\Delta_2+\Delta_3-1, 1-\Delta_1+J_3} \\ & \quad \times {}_3F_2(\Delta_1 - 1, -J_3, \Delta_3 - 1; \frac{\Delta_1+\Delta_2+\Delta_3-d-J_3}{2}, \frac{\Delta_1-\Delta_2+\Delta_3-J_3}{2}; \frac{1-\eta}{2}), \end{aligned} \quad (4.392)$$

where  $\eta = (n_1 \cdot n_2)$ . The hypergeometric function truncates to a polynomial in  $\eta$  thanks to the argument  $-J_3$ , making the decomposition straightforward for each

<sup>51</sup>The contribution of  $h^{\mu\nu}$  is fixed by tracelessness condition and in any case vanishes after contracting with traceless symmetric projector.

given  $J_3$ . Interestingly, we can find a closed-form expression for the coefficients,

$$\begin{aligned} & {}_3F_2(\Delta_1 - 1, -J_3, \Delta_3 - 1; \frac{\Delta_1 + \Delta_2 + \Delta_3 - d - J_3}{2}, \frac{\Delta_1 - \Delta_2 + \Delta_3 - J_3}{2}; \frac{1-\eta}{2}) \\ &= \sum_{s=0}^{J_3} \gamma_s(\Delta_1, \Delta_2, \Delta_3, J_3) \Pi_{J_3, s}(\eta), \end{aligned} \quad (4.393)$$

where

$$\begin{aligned} & \gamma_s(\Delta_1, \Delta_2, \Delta_3, J_3) \\ &= \frac{(-1)^{J_3-s} 2^{3-d-J_3-2s} \sqrt{\pi} \Gamma(J_3 + s + d - 2) (\Delta_1 - 1)_s (\Delta_3 - 1)_s}{\Gamma(J_3 + \frac{d-2}{2}) \Gamma(s + \frac{d-1}{2}) (\frac{1}{2}(\Delta_1 - \Delta_2 + \Delta_3 - J_3))_s (\frac{1}{2}(\Delta_1 + \Delta_2 + \Delta_3 - d - J_3))_s} \\ & \times {}_4F_3 \left( \begin{matrix} s + \frac{d}{2} - 1, -J_3 + s, \Delta_1 + s - 1, \Delta_3 + s - 1 \\ 2s + d - 2, \frac{\Delta_1 - \Delta_2 + \Delta_3 - J_3 + 2s}{2}, \frac{\Delta_1 + \Delta_2 + \Delta_3 - d - J_3 + 2s}{2} \end{matrix}; 1 \right). \end{aligned} \quad (4.394)$$

We thus conclude that

$$\begin{aligned} & \langle \phi_2 | \mathbf{L}[\phi_1] | \mathcal{O}_3^{(s)} \rangle \\ &= -2\pi i \frac{e^{i\pi\Delta_2} 2^{1-\Delta_1} \Gamma(\Delta_1 - 1)}{\Gamma(\frac{\Delta_1 + \Delta_2 - \Delta_3 + J_3}{2}) \Gamma(\frac{\Delta_1 - \Delta_2 + \Delta_3 - J_3}{2})} \widehat{\mathcal{F}}_{\Delta_2 + \Delta_3 - 1, 1 - \Delta_1 + J_3} \gamma_s(\Delta_1, \Delta_2, \Delta_3, J_3), \end{aligned} \quad (4.395)$$

where  $\widehat{\mathcal{F}}$  is given by (4.329).

#### 4.5.4.3 Complete scalar event shape blocks

We have found that

$$\begin{aligned} & \langle \phi_2(p) | \mathbf{L}[\phi_1](\infty, z_1) | \mathcal{O}_3(p, z_3) \rangle \\ &= \sum_{s=0}^{J_3} \langle \phi_2 | \mathbf{L}[\phi_1] | \mathcal{O}_3^{(s)} \rangle (-p \cdot z_1)^{1-\Delta_1 - J_3} \Pi_{J_3, s}(p; z_1, z_3) (-p^2)^{\frac{\Delta_2 + \Delta_3 - 2 + \Delta_1 + J_3 - d}{2}} \theta(p), \end{aligned} \quad (4.396)$$

where the coefficients  $\langle \phi_2 | \mathbf{L}[\phi_1] | \mathcal{O}_3^{(s)} \rangle$  are given in (4.395). By applying Hermitian conjugation, we find

$$\begin{aligned} & \langle \mathcal{O}_3(p, z_3) | \mathbf{L}[\phi_1](\infty, z_1) | \phi_2(p) \rangle \\ &= \sum_{s=0}^{J_3} \langle \mathcal{O}_3^{(s)} | \mathbf{L}[\phi_1] | \phi_2 \rangle (-p \cdot z_1)^{1-\Delta_1 - J_3} \Pi_{J_3, s}(p; z_1, z_3) (-p^2)^{\frac{\Delta_2 + \Delta_3 - 2 + \Delta_1 + J_3 - d}{2}} \theta(p), \end{aligned} \quad (4.397)$$

where

$$\langle \mathcal{O}_3^{(s)} | \mathbf{L}[\phi_1] | \phi_2 \rangle \equiv \langle \phi_2 | \mathbf{L}[\phi_1] | \mathcal{O}_3^{(s)} \rangle^*. \quad (4.398)$$

Using (4.267), we then find the scalar event shape t-channel conformal block

$$\begin{aligned} G_{\Delta,J}^t(p; z_1, z_2) &= \sum_{s=0}^J \langle \phi_4 | \mathbf{L}[\phi_1] | \mathcal{O}^{(s)} \rangle \mathcal{A}_s(\Delta, J)^{-1} \langle \mathcal{O}^{(s)} | \mathbf{L}[\phi_2] | \phi_3 \rangle \Pi_{J,s}(p; z_1, z_2) \\ &\quad \times (-p^2)^{\frac{\Delta_3 + \Delta_4 - 4 + \Delta_1 + \Delta_2 + 2J - d}{2}} (-p \cdot z_1)^{1 - \Delta_1 - J} (-p \cdot z_2)^{1 - \Delta_2 - J}. \end{aligned} \quad (4.399)$$

To find the above expression, we used the identity  $\Pi_{J,s} \Pi_{J,s'} = \delta_{ss'} \Pi_{J,s}$ .

As we discussed above, in order for the  $t$ -channel expansion to converge, we should smear the event shape over the polarizations of detectors

$$\int D^{d-2} z_1 D^{d-2} z_2 f(z_1, z_2) \langle \phi_4(p) | \mathbf{L}[\phi_1](\infty, z_1) \mathbf{L}[\phi_2](\infty, z_2) | \phi_3(p) \rangle. \quad (4.400)$$

It is convenient to use the following smearing functions

$$f_s(z_1, z_2) \propto (-p \cdot z_1)^{\Delta_1 + 1 - d} (-p \cdot z_2)^{\Delta_2 + 1 - d} C_s^{\left(\frac{d-3}{2}\right)}(\eta), \quad (4.401)$$

so that the result simply picks out the coefficient of the Gegenbauer polynomial  $C_s^{\left(\frac{d-3}{2}\right)}(\eta)$  in the event shape. We can define the corresponding blocks  $G_{\Delta,J}^t(s)$  by the identity, for  $p = (1, \vec{0})$ ,

$$\langle \phi_4(p) | \mathbf{L}[\phi_1](\infty, z_1) \mathbf{L}[\phi_2](\infty, z_2) | \phi_3(p) \rangle = \sum_s \sum_{\mathcal{O}} \lambda_{14\mathcal{O}} \lambda_{23\mathcal{O}}^* G_{\Delta_{\mathcal{O}}, J_{\mathcal{O}}}^t(s) C_s^{\left(\frac{d-3}{2}\right)}(\eta). \quad (4.402)$$

Using (4.399) and (4.276), we find

$$G_{\Delta,J}^t(s) = \frac{2^{-J} J! (d+J-2)_J (d-2)_J (-1)^{s+J} (d+2s-3)}{\left(\frac{d-1}{2}\right)_J (J-s)! (d-3)_{J+s+1}} \frac{\langle \phi_4 | \mathbf{L}[\phi_1] | \mathcal{O}^{(s)} \rangle \langle \mathcal{O}^{(s)} | \mathbf{L}[\phi_2] | \phi_3 \rangle}{\mathcal{A}_s(\Delta, J)}. \quad (4.403)$$

Here, the reduced three-point functions  $\langle \phi_4 | \mathbf{L}[\phi_1] | \mathcal{O}^{(s)} \rangle$  are given by (4.395) and (4.398) (with appropriate permutation of indices), while the coefficients  $\mathcal{A}_s(\Delta, J)$  are given by (4.280). In interpreting this result, it is also important to note our normalizations of two- and three-point tensor structures (4.277) and (4.376).

#### 4.5.4.4 Example: scalar event shape in (generalized) free scalar CFT

In this section, we will consider an example of the  $t$ -channel decomposition of the scalar event shape

$$\langle \mathcal{O} | \phi_4 \mathbf{L}[\phi_1] \mathbf{L}[\phi_2] \phi_3 | \mathcal{O} \rangle \quad (4.404)$$

for the four-point function of scalars of dimension  $\Delta = 2$  in 4d,

$$\langle \phi_1 \phi_2 \phi_3 \phi_4 \rangle = \frac{1}{x_{14}^2 x_{23}^2 x_{13}^2 x_{24}^2} + \text{disconnected}. \quad (4.405)$$

This four-point function is given by a box Wick contraction, and the disconnected part is any sum of products of two-point functions, such as  $\langle \phi_1 \phi_2 \rangle \langle \phi_3 \phi_4 \rangle$ . The scalars  $\phi_i$  are not necessarily identical. For example, we can think about  $\phi_i$  as being double-trace operators  $\phi_1 = \rho^2, \phi_2 = \sigma^2, \phi_3 = \phi_4 = \rho\sigma$ , where  $\rho$  and  $\sigma$  are fundamental free scalars. In this case, we are looking at a state with one  $\rho$  and one  $\sigma$  particle, and  $\mathbf{L}[\phi_1]$  detects  $\rho$  while  $\mathbf{L}[\phi_2]$  detects  $\sigma$ .

First, we observe that the disconnected part does not contribute to (5.182), since  $\mathbf{L}[\phi_i]$  annihilates the vacuum state. We then note that

$$\langle \phi_1 \phi_2 \phi_3 \phi_4 \rangle = \langle \phi_1 \phi'_3 \phi'_4 \rangle \langle \phi_2 \phi'_3 \phi'_4 \rangle, \quad (4.406)$$

where  $\phi'_i$  are fictitious scalars of scaling dimension  $\Delta/2 = 1$ . This allows us to compute (5.182) by reusing the results of section 4.5.1.3. We find

$$\begin{aligned} \langle 0 | \phi'_4 \mathbf{L}[\phi_1] \phi'_3 | 0 \rangle &= -2\pi i \frac{e^{i\pi\Delta/2} 2^{1-\Delta} \Gamma(\Delta-1)}{\Gamma(\frac{\Delta}{2})^2} \frac{(-V_{1,43})^{1-\Delta}}{(x_{14}^2)^{\frac{2-\Delta}{2}} (x_{13}^2)^{\frac{2-\Delta}{2}} (-x_{43}^2)^{\frac{2\Delta-2}{2}}} \\ &= i\pi \frac{(-V_{1,43})^{-1}}{-x_{43}^2}, \quad ((3 > 4) \approx 1) \end{aligned} \quad (4.407)$$

and similarly for  $\langle 0 | \phi'_4 \mathbf{L}[\phi_2] \phi'_3 | 0 \rangle$ . Sending 1 and 2 to infinity, 4 to 0, and 3 to  $x > 0$ , we find

$$\langle 0 | \phi'_4 \mathbf{L}[\phi_1] \phi'_3 | 0 \rangle = i\pi (-(x \cdot z_1))^{-1}, \quad (4.408)$$

and multiplying by  $\langle 0 | \phi'_4 \mathbf{L}[\phi_2] \phi'_3 | 0 \rangle$ , we get

$$\langle 0 | \phi_4 \mathbf{L}[\phi_1] \mathbf{L}[\phi_2] \phi_3 | 0 \rangle = -\pi^2 (-(x \cdot z_1))^{-1} (-(x \cdot z_2))^{-1}. \quad (4.409)$$

Now, we need to compute the Fourier transform of the above expression with the  $i\epsilon$ -prescription  $x^0 \rightarrow x^0 + i\epsilon$ . For this, it is convenient to use Lorentz invariance

to set  $z_1 = (1, 1, 0, 0)$  and  $z_2 = (1, -1, 0, 0)$ . Introducing the lightcone coordinates  $x^\pm = x^0 \pm x^1$ , we find

$$\int d^4x e^{ipx} (-x \cdot z_1)^{-1} (-x \cdot z_2)^{-1} = \frac{1}{2} (2\pi)^2 \delta^2(\vec{p}) f(p^+) f(p^-), \quad (4.410)$$

where  $\vec{p} = (p^2, p^3)$  and

$$f(p) = \int dx e^{-\frac{i}{2}px} (x + i\epsilon)^{1-\Delta} = 2^{3-\Delta} \pi \frac{e^{\frac{i\pi}{2}(1-\Delta)}}{\Gamma(\Delta-1)} p^{\Delta-2} \theta(p) = -2\pi i \theta(p). \quad (4.411)$$

We thus find

$$\langle \phi_4(p) | \mathbf{L}[\phi_1] \mathbf{L}[\phi_2] | \phi_3(p) \rangle = 8\pi^6 \theta(p) \delta^2(\vec{p}). \quad (4.412)$$

It is easy to find the covariant form

$$\langle \phi_4(p) | \mathbf{L}[\phi_1] \mathbf{L}[\phi_2] | \phi_3(p) \rangle = 8\pi^6 \theta(p) \delta^2(\vec{p}) (-p^2) (-z_1 \cdot p)^{-1} (-z_2 \cdot p)^{-1}, \quad (4.413)$$

where

$$\delta^2(\vec{p}) = \frac{1}{\pi} \delta(\vec{p}^2) = \frac{1}{\pi} \delta \left( p^2 - 2 \frac{(z_1 \cdot p)(z_2 \cdot p)}{(z_1 \cdot z_2)} \right). \quad (4.414)$$

Now, setting  $p = (1, \vec{0})$  and  $z_i = (1, n_i)$ , we get

$$\langle \phi_4(p) | \mathbf{L}[\phi_1] \mathbf{L}[\phi_2] | \phi_3(p) \rangle = 16\pi^5 \delta((n_1 \cdot n_2) + 1). \quad (4.415)$$

The delta-function forces  $n_1$  and  $n_2$  to point in opposite directions. This corresponds simply to the fact that  $\phi_3 = \rho\sigma$  creates a pair of particles, and by momentum conservation they must fly off in opposite directions, since we have set the spatial component of  $p$  to 0.

We would like to compute this event shape using the  $t$ -channel OPE. We will first expand the four-point function (4.405) in the  $14 \rightarrow 23$  channel and then use the resulting expansion to sum the event shape conformal blocks.

The disconnected piece of (4.405) only contains the contributions of the identity and double-trace operators. The double-trace operators do not contribute to the event shape, as seen in the discussion below (4.248). The identity operator also doesn't contribute, as its contribution is

$$\langle \phi_4(p) | \mathbf{L}[\phi_1] | \mathcal{O} \rangle \langle \mathcal{O} | \mathbf{L}[\phi_2] | \phi_3(p) \rangle = 0, \quad (4.416)$$

since light-transforms annihilate the vacuum state [28].

The connected contribution can be rewritten as

$$\langle \phi_1(x_1)\phi_2(x_2)\phi_3(x_3)\phi_4(x_4) \rangle = \frac{1}{x_{14}^2 x_{23}^2} \langle \phi'_2(x_4)\phi'_1(x_1)\phi'_2(x_2)\phi'_1(x_3) \rangle, \quad (4.417)$$

where  $\phi'_1$  and  $\phi'_2$  are fictitious canonically normalized free scalars of dimension  $\Delta/2 = 1$ . The prefactor  $\frac{1}{x_{14}^2 x_{23}^2}$  simply plays the role of shifting the external dimensions of conformal blocks, and so we have the identity

$$\lambda_{14\mathcal{O}}\lambda_{23\mathcal{O}} = \lambda_{12\mathcal{O}}\lambda_{21\mathcal{O}} \quad (4.418)$$

where in the right hand side we mean the OPE coefficients which enter into the decomposition of the function  $\langle \phi'_2(x_4)\phi'_1(x_1)\phi'_2(x_2)\phi'_1(x_3) \rangle$ . Since this is a four-point function of free fields, only a single family of higher-spin currents  $\mathcal{O}$  with  $\Delta = J + 2$  contribute to its OPE. In our conventions, we have [196]

$$\lambda_{12\mathcal{O}}\lambda_{21\mathcal{O}} = (-1)^J \lambda_{12\mathcal{O}}^2 = (-1)^J \frac{2^J \Gamma(J+1)^2}{\Gamma(2J+1)}. \quad (4.419)$$

Setting  $\Delta_1 = \Delta_2 = \Delta_3 = \Delta_4 = 2$ , we find

$$G_{J+2,J}^t(s) = \frac{2^{J+4} \pi^{\frac{9}{2}} \Gamma(J + \frac{3}{2})}{\Gamma(J+1)} \delta_{J,s}. \quad (4.420)$$

The reason only  $s = J$  is allowed is because  $\Delta = J + 2$  corresponds to conserved higher-spin currents, which only have one  $\text{SO}(d-1)$  component. Using (4.402), we find

$$\begin{aligned} & \langle \phi_4(p) | \mathbf{L}[\phi_1](\infty, z_1) \mathbf{L}[\phi_2](\infty, z_2) | \phi_3(p) \rangle = \\ & = \sum_s \sum_{\mathcal{O}} \lambda_{14\mathcal{O}} \lambda_{23\mathcal{O}}^* G_{\Delta_{\mathcal{O}}, J_{\mathcal{O}}}^t(s) C_s^{(\frac{d-3}{2})}(\eta) = \sum_{J=0}^{\infty} (-1)^J \frac{2^J \Gamma(J+1)^2}{\Gamma(2J+1)} \frac{2^{J+4} \pi^{\frac{9}{2}} \Gamma(J + \frac{3}{2})}{\Gamma(J+1)} P_J(\eta) \\ & = 8\pi^5 \sum_{J=0}^{\infty} (-1)^J (2J+1) P_J(\eta) = 16\pi^5 \delta(\eta+1). \end{aligned} \quad (4.421)$$

The last equality follows from the completeness relation for Legendre polynomials and  $P_J(-1) = (-1)^J$ . This result indeed agrees with (4.415). Note that the convergence here is only in a distributional sense, i.e. we have to smear the event shape with some test function in  $\eta$  before computing the sum.

A more nontrivial check is to repeat the same calculation in a generalized free theory (GFT). The event shape is the same up to a coefficient,

$$\langle \phi_4(p) | \mathbf{L}[\phi_1] \mathbf{L}[\phi_2] | \phi_3(p) \rangle = \frac{16^{3-2\Delta_f} \pi^5}{\Gamma(\Delta_f)^4} \delta((n_1 \cdot n_2) + 1), \quad (4.422)$$

where  $\Delta_f$  is the dimension of the fundamental fields  $\rho$  and  $\sigma$  ( $\Delta_f = 1$  for the free scalar case considered above). We can use the same logic to obtain the relevant OPE coefficients from the known GFT ones [87, 156]. The main difference is that each Legendre polynomial  $P_s(\eta)$  receives contribution from infinitely many operators  $[\rho\sigma]_{n,J}$  with  $J \geq s$  and  $n \geq 0$ .<sup>52</sup> The sum is now much more non-trivial and we cannot tackle it analytically. We have focused on the coefficients in front of  $P_0(\eta)$  and  $P_1(\eta)$ , and found numerically that the sum over  $n$  converges rather quickly. However, the sum over  $J$  appears to behave as

$$\sim \sum_J (-1)^J J^{2\Delta_f-3}, \quad (4.423)$$

and so it diverges for  $\Delta_f > 3/2$  and converges for  $\Delta_f < 3/2$ . In the latter case, convergence can be improved by an Euler transform,<sup>53</sup> which allows us to check for a few sample values of  $\Delta_f$  with  $1 < \Delta_f < 3/2$  that the  $t$ -channel sum agrees to high precision with

$$\frac{16^{3-2\Delta_f}\pi^5}{2\Gamma(\Delta_f)^4}P_0(\eta) - 3\frac{16^{3-2\Delta_f}\pi^5}{2\Gamma(\Delta_f)^4}P_1(\eta) + \dots, \quad (4.425)$$

which is the expansion of (4.422).<sup>54</sup>

Based on intuition from  $\nu$ -space described in chapter 5, we expect that the divergence for  $\Delta_f \geq 3/2$  is due to the behavior of our test functions near the collinear limit  $\eta = 1$ . Recall that if

$$\langle \phi_4(p) | \mathbf{L}[\phi_1] \mathbf{L}[\phi_2] | \phi_3(p) \rangle = \sum_s a_s P_s(\eta), \quad (4.426)$$

then the coefficients  $a_s$  are given by smearing the event shape with the test functions

$$f_s(\eta) = \frac{1}{2}(2s+1)P_s(\eta). \quad (4.427)$$

To moderate the contribution of  $\eta = 1$ , we can smear with linear combinations of functions  $f_s$  which vanish at  $\eta = 1$  as  $(\eta - 1)^k$  for sufficiently high  $k$ . Suppose that

<sup>52</sup>Note that these operators are not double-traces of  $\rho\sigma$  and  $\rho^2$  or  $\sigma^2$ , so they do contribute to the OPE.

<sup>53</sup>For series  $\sum_{n=0}^{\infty} (-1)^n a_n$  the Euler transform is

$$\sum_{n=0}^{\infty} (-1)^n a_n = \sum_{n=0}^{\infty} \frac{(-1)^n b_n}{2^{n+1}}, \quad (4.424)$$

where  $b_n = \sum_{k=0}^n (-1)^k \binom{n}{k} a_k$ . It generally tends to improve the rate of convergence of slowly-converging series.

<sup>54</sup>In fact, Euler transform makes the sum over  $J$  convergent for all values of  $\Delta_f$ .

$\sum_s \alpha_s f_s(\eta)$  is one such combination for a fixed  $k$ . We are then led to consider the expansion

$$\sum_{\mathcal{O}} \lambda_{14\mathcal{O}} \lambda_{23\mathcal{O}}^* \sum_s \alpha_s G_{\Delta_{\mathcal{O}}, J_{\mathcal{O}}}^t(s) C_s^{\binom{d-3}{2}}(\eta). \quad (4.428)$$

Numerically, we find that the sum over primary operators with different spin behaves as

$$\sum_J (-1)^J J^{\omega_k}, \quad (4.429)$$

where  $w_k$  is monotonically non-increasing function of  $k$ . Specifically, for any choice of  $\Delta_f$ , we find that  $w_k$  starts at  $w_0 = 2\Delta_f - 3$  as described above, and then decreases monotonically with  $k$  until it saturates at some value  $w_* < 0$ .<sup>55</sup> This means that for any value of  $\Delta_f$  the expansion converges for test functions which vanish sufficiently quickly at  $\eta = 1$ .

## 4.6 Discussion

### 4.6.1 Bounds on heavy contributions to non-minimal couplings

A quantitative understanding of the superconvergence sum rule requires some extra analysis which we postpone for future work. Here, we sketch its qualitative implications. For simplicity, we consider a toy model for a gravitational scattering amplitude, but the argument for the CFT correlator is essentially the same. In our discussion, the rough correspondence between amplitudes and CFT correlators is

| amplitude        | four-point function        |
|------------------|----------------------------|
| $t$              | $(z\bar{z})^{-1/2}$        |
| $s$              | $(\Delta - \frac{d}{2})^2$ |
| $J$              | $J$                        |
| $a_J^\pm(s)$     | $C^\pm(\Delta, J)$         |
| Disc             | dDisc                      |
| Froissart-Gribov | Lorentzian inversion       |

The basic idea was explained in [25] and goes as follows. Let us imagine a theory with a large gap  $\Delta_{\text{gap}} \gg 1$  in the spectrum of particles (or operators). We would like to bound the contribution of heavy, or stringy, modes to the superconvergence sum

<sup>55</sup>Typically  $w_k \approx w_{k-1} - 2$ , but we have not studied this in sufficient detail either numerically or analytically.



rule and therefore determine the maximal allowed value of non-minimal three-point graviton couplings. To do so, recall that given a polynomially bounded “amplitude”  $\mathcal{A}(s, t)$  with “partial wave” expansion

$$\mathcal{A}(s, t) = \sum_J a_J(s) \nu^J, \quad \nu = \frac{t - u}{2}, \quad (4.430)$$

we can write a “Froissart-Gribov inversion formula” which takes the following form

$$a_J^\pm(s) = \int_0^\infty \frac{d\nu}{\nu} \nu^{-J} \text{Disc}_t \mathcal{A}(s, \nu) \pm \int_{-\infty}^0 \frac{d\nu}{-\nu} (-\nu)^{-J} \text{Disc}_u \mathcal{A}(s, \nu). \quad (4.431)$$

where  $\text{Disc}_u = -\text{Disc}_t$ . Convergence properties of the integral (4.431) depend on the behavior of the amplitude at large  $t$  and fixed  $s$ . In a consistent theory, the integral converges for  $J > 1$ . In particular, we can evaluate (4.431) at  $J = 2$ , for which the integral (4.431) must reproduce the graviton pole at  $s = 0$ ,

$$a_{J=2}^+(s) \sim \frac{1}{c_T} \frac{1}{s}. \quad (4.432)$$

More generally, away from the graviton pole, the integral over the discontinuity should correctly reproduce the Pomeron pole

$$a_J^+(s) \sim \frac{C_{\phi\phi P}^2(s)}{J - J(s)}. \quad (4.433)$$

We expect that  $a_J^+(s)$  is suppressed by  $1/c_T$  for small  $s$ . This suppression does not follow from our knowledge of the three-point coefficients  $C_{\phi\phi P}^2(s)$ . Indeed, the value of the residue in (4.433) solely reflects the asymptotic behavior of the discontinuity in (4.431),

$$\text{Disc}_t \mathcal{A}(s, \nu) \sim C_{\phi\phi P}^2(s) \nu^{J(s)} \quad \text{at large } \nu. \quad (4.434)$$

Demanding that the asymptotic behavior reproduces the graviton pole (4.432) via the inversion formula (4.431) suggests that  $C_{\phi\phi P}^2(s)$  is suppressed by  $1/c_T$ . However, we can imagine an isolated “outlier state” at some intermediate scale  $\nu^*$  that contributes to  $\text{Disc}_t \mathcal{A}(s, \nu) \sim C_{\phi\phi P^*}^2(s) \delta(\nu - \nu^*)$  with a large coefficient  $C_{\phi\phi P^*}^2(s)$ . Through (4.431), such an outlier state would invalidate the estimate  $a_J^+(s) \sim \frac{1}{c_T}$  away from the pole. In what follows, we assume that there are no outliers. The same assumption was made in [25].

In a large-gap theory we expect  $J(s) = 2 + \frac{s}{\Delta_{\text{gap}}^2}$ . Correctly reproducing the  $\frac{1}{c_T}$  residue of the graviton pole (4.432) from (4.433) thus requires that  $C_{\phi\phi P}^2(s) \sim \frac{1}{c_T} \frac{1}{\Delta_{\text{gap}}^2}$ . Note

also that by plugging  $\text{Disc}_t \mathcal{A}(s, \nu) \sim C_{\phi\phi P}^2(s) \nu^{J(s)}$  for  $\nu > \Delta_{\text{gap}}^2$  into (4.431) (and thus assuming no outliers), we get

$$a_J^+(s) \sim \frac{1}{c_T} \frac{1}{\Delta_{\text{gap}}^2} \frac{1}{J - J(s)} (\Delta_{\text{gap}}^2)^{J(s)-J}. \quad (4.435)$$

The superconvergence sum rule is the statement that  $a_{J=3}^-(s) = 0$ . Note that only the square of the non-minimal three-point coupling contributes to  $a_{J=3}^-(s)$ , see e.g. (4.66). We can write it as follows

$$\alpha_{\text{GB}}^2(s) + \int_{\Delta_{\text{gap}}^2}^{\infty} \frac{d\nu}{\nu} \nu^{-3} \text{Disc}_t \mathcal{A}(s, \nu) - \int_{-\infty}^{-\Delta_{\text{gap}}^2} \frac{d\nu}{-\nu} (-\nu)^{-3} \text{Disc}_u \mathcal{A}(s, \nu) = 0, \quad (4.436)$$

where we separated the contribution from the graviton pole  $\alpha_{\text{GB}}(s)$  from the rest (“GB” stands for Gauss-Bonnet — a particular type of nonminimal coupling that contributes to  $\alpha_{\text{GB}}$ ).

Next, we would like to bound the contribution of heavy states in (4.436). The estimate goes as follows

$$\begin{aligned} |\alpha_{\text{GB}}^2(s)| &= \left| \int_{\Delta_{\text{gap}}^2}^{\infty} \frac{d\nu}{\nu} \nu^{-3} \text{Disc}_t \mathcal{A}(s, \nu) - \int_{-\infty}^{-\Delta_{\text{gap}}^2} \frac{d\nu}{-\nu} (-\nu)^{-3} \text{Disc}_u \mathcal{A}(s, \nu) \right| \\ &\leq a_{J=3}^+(s) \sim \frac{1}{\Delta_{\text{gap}}^4} \frac{1}{c_T} \quad (s \ll \Delta_{\text{gap}}^2) \end{aligned} \quad (4.437)$$

where we used the positivity of  $\text{Disc}_t \mathcal{A}(s, \nu)$  and  $\text{Disc}_u \mathcal{A}(s, \nu)$ , which follow from unitarity in an appropriate kinematical region. We see that what follows is the same qualitative conclusion as was obtained in [96]. This time, however, we have a precise sum rule that must be satisfied. We will show in chapter 5 that the superconvergence sum rule in CFT can be written as

$$C^-(\Delta = \frac{d}{2} + i\nu, J = 3) = 0, \quad (4.438)$$

where  $C^\pm(\Delta, J)$  is the quantity computed by the Lorentzian inversion formula, so the argument in the CFT case proceeds analogously to the one here.

#### 4.6.2 Conclusions and future directions

In this work, we found connections between commutativity of coincident shocks, superconvergence sum rules, and boundedness in the Regge and lightcone limits. These connections hold both in flat space and in AdS.

In flat space, we defined “shock amplitudes” as amplitudes with special external wavefunctions. We showed that boundedness of amplitudes in the Regge limit is a sufficient condition for commutativity of coincident shocks. Furthermore, when coincident shocks commute, one obtains superconvergence sum rules that constrain the matter content and three-point couplings of the theory. It was argued in [96] that causal theories of gravity should have Regge intercept  $J_0 \leq 2$ . Assuming this, it follows that coincident gravitational shocks commute. The associated superconvergence sum rules relate non-minimal gravitational couplings to three-point couplings of stringy states.

In AdS, commutativity of coincident shocks is dual to the question of commutativity of certain null-integrated operators (e.g. ANEC operators) in a CFT. This question can be studied on its own using CFT techniques. In particular, we show using CFT methods that ANEC operators on the same null plane commute. (This result holds both nonperturbatively and in the planar limit, but it can be violated at fixed loop order in bulk perturbation theory.) This establishes commutativity of coincident gravitational shocks in AdS. We conjecture that coincident gravitational shocks commute in UV-complete gravitational theories in flat space, AdS, dS, and possibly beyond, dubbing this a “stringy equivalence principle.”

The CFT version of superconvergence sum rules can be obtained by inserting complete sets of states between the null-integrated operators. In large- $N$  theories, such sum rules relate non-minimal bulk couplings to the massive single-trace spectrum. However, the resulting sum rules are completely general, independent from holography, and interesting on their own.

Let us discuss some open questions and future directions.

#### 4.6.2.1 Constraints on UV-complete gravitational theories

Higher derivative gravitational couplings are inconsistent with commutativity of coincident shocks, unless their effects are cancelled in the superconvergence sum rule. This cancellation can occur in different ways. In weakly-coupled (tree-level) gravity theories, the cancellation must involve massive (stringy) states. More generally, the cancellation could involve loop effects. An important problem is to compute independent bounds on non-graviton contributions to the superconvergence sum rules. This would give quantitative bounds on the size of non-minimal gravitational couplings. A toy version of this argument was presented in the previous section. However, it will be important to make it precise.

Another interesting question is the extent to which the low-energy matter content of the Standard Model is consistent with commutativity of coincident gravitational shocks. If one could compute the Standard Model contribution to superconvergence sum rules (including loop effects) and find that it is nonzero, that would establish the necessity of additional massive states, and possibly hint at their properties.

To incorporate loop effects (e.g. loops in the Standard Model or  $1/N$  effects in CFT), it may be necessary to use eikonal techniques to re-sum gravitational exchanges. The reason is that  $n$ -graviton exchange on its own leads to Regge growth with spin  $J_0 = 1 + n$ , which would invalidate superconvergence sum rules.

#### 4.6.2.2 Bootstrapping amplitudes and four-point functions

In the context of flat-space amplitudes, superconvergence sum rules have been used to bootstrap the Veneziano amplitude [162]. This result relies on assuming linear Regge trajectories. The assumption of linear trajectories has two nice effects. Firstly, it removes the necessity of bootstrapping masses — one can focus only on three-point couplings. Secondly, because Regge trajectories behave as  $J(s) = \text{const.} + \alpha' s$ , one can make  $J(s)$  arbitrarily negative by making  $s$  arbitrarily negative. When  $J(s) \leq -k$ , for integer  $k$ , one obtains a new superconvergence sum rule obtained by inserting  $t^k$  into a dispersion relation.

It would be interesting to perform an analogous exercise in CFT, with the goal of using superconvergence sum rules to bootstrap a planar four-point function in AdS with finite  $\alpha'$ . In CFT, we do not have linear Regge trajectories. However, perhaps one could take the known single-trace spectrum computed from integrability [197–199] as input and try to bootstrap the three-point couplings. In  $\mathcal{N} = 4$  SYM theory, the analog of  $J(s) = \text{const.} + \alpha' s$  is [148]

$$J(\nu) = 2 - \frac{\Delta(4 - \Delta)}{2\sqrt{\lambda}} + \dots = 2 - \frac{\nu^2 + 4}{2\sqrt{\lambda}} + \dots, \quad (4.439)$$

where  $\lambda$  is the 't Hooft coupling,  $\Delta = 2 + i\nu$ , and “...” represents subleading corrections in  $1/\lambda$ . Here,  $-\nu^2/(2\sqrt{\lambda})$  is analogous to  $\alpha' s$ . In the flat space limit,  $\lambda \rightarrow \infty$  with  $\nu^2/\sqrt{\lambda}$  held fixed, it is possible to make  $J(\nu)$  arbitrarily negative by making  $\nu^2/(2\sqrt{\lambda})$  large [149].<sup>56</sup> It would be interesting to know whether this is true more generally (e.g. at finite  $\lambda$ ): can  $J(\nu)$  always be made arbitrarily negative by going to large  $\nu$ ?

---

<sup>56</sup>We thank David Meltzer for discussions on this point.

If so, one should be able to obtain additional superconvergence sum rules beyond the ones we have discussed at sufficiently large  $\nu^2$ . We expect such sum rules should come from commutativity of the operators  $L^n(\vec{y})$  defined in [153] and other descendants of  $\mathbf{L}[T](x, z)$ , such as those studied in [154]. Note that these operators only need to commute when transformed to  $\nu$  space and placed at sufficiently large  $\nu$ . To transform to  $\nu$ -space, one must smear the operators in the transverse positions  $\vec{y}$  against an appropriate  $d-2$ -dimensional three-point structure, see chapter 5.

It would be interesting to understand how our flat space analysis is embedded into the corresponding limit of the AdS/CFT duality. Indeed, in theories with sub-AdS locality there is no problem in localizing both the shocks and the probes in the region of spacetime much less than  $L_{AdS}$  [200]. Therefore the flat space analysis should apply in this limit. Shockwaves that are well-localized in the AdS interior were analyzed for example in [177]. The same idea should apply to high energy scattering in non-trivial backgrounds, e.g. in the vicinity of a black hole horizon [201]. Presumably, the commutativity of shocks in this case is related to the consistency conditions on the spinning scramblon couplings [202]. More generally, the statement that gravitational shocks commute locally at every point in AdS should constrain spinning couplings to the “modulon” [203], a mode that saturates the modular bound on chaos and captures local high energy gravitational scattering in the bulk. It seems plausible that saturation of the modular chaos bound together with the corresponding superconvergence conditions uniquely select Einstein gravity in AdS as the dual theory.<sup>57</sup>

### 4.6.2.3 Generalizations

Although we have focused mostly on superconvergence sum rules coming from commutativity of ANEC operators, one additionally gets sum rules from studying  $[\mathbf{L}[\mathcal{O}_1], \mathbf{L}[\mathcal{O}_2]]$  for any pair of operators  $\mathcal{O}_1, \mathcal{O}_2$  with sufficiently large  $J_1 + J_2$ . A further generalization could come from studying commutativity of more general continuous-spin light-ray operators defined in [28]. Can one show that such general light-ray operators commute on the same null plane as well,  $[\mathcal{O}_1, \mathcal{O}_2] = 0$ ? As we show in chapter 5, one way to obtain such light-ray operators is from OPEs of more traditional null integrals,  $\mathbf{L}[\mathcal{O}_1]\mathbf{L}[\mathcal{O}_2] \sim \sum_k \mathcal{O}_k$ . In this case, commutativity of  $\mathcal{O}_k$  would follow from commutativity of null-integrated operators. However, the general construction of continuous-spin light-ray operators is more complicated.

---

<sup>57</sup>We thank Tom Faulkner for discussions on this point.

In addition to introducing continuous-spin light-ray operators in the CFT context, it is interesting to ask whether they can be introduced in the amplitudes context as well. In CFT, null integrated operators  $\mathbf{L}[\mathcal{O}_{i,J}]$  can be analytically continued in spin to obtain more general light-ray operators  $\mathbb{O}_{i,J}^{\pm}$ , where  $i$  labels Regge trajectories. It is natural to guess that the shock amplitudes defined in section 4.2.1 can be analytically continued in the spin of the shocks. This would provide a vast generalization of the amplitudes usually considered. It would be interesting to investigate such analytically continued amplitudes in string theory.

#### 4.6.2.4 Further applications

In the main text we discussed a set of extra consistency conditions (superconvergence relations) on the CFT spectrum which follow from commutativity of average null energy operators. Together with ANEC, commutativity also implies that products of multiple average null energy operators are positive-semidefinite. Therefore, we can further require that

$$\langle \Psi | \mathbf{L}[T] \cdots \mathbf{L}[T] | \Psi \rangle \geq 0. \quad (4.440)$$

Using the results of section 5, this leads to extra conditions on the OPE data of the theory. In numerical bootstrap calculations, boundedness of the Regge limit is manifest, and therefore superconvergence relations are automatically true. On the other hand, from the point of view of four-point functions, the positivity conditions (4.440) are extra nontrivial conditions. For example, positivity of two-point energy correlators follows from unitarity of six-point functions, and thus is not manifest from the conformal block expansion of a four-point function. It would be interesting to include these positivity constraints in the numerical bootstrap. In particular, it will be interesting to see how they affect the stress-tensor bootstrap results [204].

It will be interesting to apply the  $t$ -channel OPE formulas to QCD-like theories, say  $\mathcal{N} = 4$  SYM. An appealing feature of the  $t$ -channel OPE is that in the planar limit the contribution of double-trace operators is suppressed by an extra power of  $\frac{1}{N^2}$ . Therefore, to leading order only the single trace data is needed. We hope that one day these will be computed at finite  $\lambda$  using integrability techniques, see e.g. [198, 205, 206]. It will be also interesting to use the  $t$ -channel OPE to reproduce the known weak coupling results [182, 207], and try to extend the  $t$ -channel analysis to actual QCD, where the state of the art is the NLO analytic result [208]. Note that in the case of  $\mathcal{N} = 4$  SYM, due to superconformal symmetry energy-energy correlation can

be computed using the four-point function of scalars to which (4.403) can be directly applied.

### **Acknowledgements**

We thank Alex Belin, Xián Camanho, Cliff Cheung, Simon Caron-Huot, Thomas Dumitrescu, Tom Faulkner, Nima Lashkari, Raghu Mahajan, Juan Maldacena, David Meltzer, Shiraz Minwalla, Eric Perlmutter, Douglas Stanford, and Eduardo Teste for discussions. DSD thanks the KITP and the organizers of the “Chaos and Order” workshop for hospitality during some of this work. DSD is supported by Simons Foundation grant 488657 (Simons Collaboration on the Nonperturbative Bootstrap), a Sloan Research Fellowship, and a DOE Early Career Award under grant No. DE-SC0019085. PK is supported by DOE grant No. DE-SC0009988. This research was supported in part by the National Science Foundation under Grant No. NSF PHY-1748958, as well as by the U.S. Department of Energy, Office of Science, Office of High Energy Physics, under Award Number DE-SC0011632.

## THE LIGHT-RAY OPE AND CONFORMAL COLLIDERS

<sup>1</sup>M. Kolođlu, P. Kravchuk, D. Simmons-Duffin, and A. Zhiboedov, “The light-ray OPE and conformal colliders”, (2019), [arXiv:1905.01311](https://arxiv.org/abs/1905.01311) [[hep-th](#)].

### 5.1 Introduction

In this work, we study a product of null-integrated operators on the same null plane in a conformal field theory (CFT) in  $d > 2$  dimensions (figure 5.1):

$$\int_{-\infty}^{\infty} dv_1 \mathcal{O}_{1;v\dots v}(u=0, v_1, \vec{y}_1) \int_{-\infty}^{\infty} dv_2 \mathcal{O}_{2;v\dots v}(u=0, v_2, \vec{y}_2). \quad (5.1)$$

Here, we use lightcone coordinates

$$ds^2 = -du dv + \vec{y}^2, \quad \vec{y} \in \mathbb{R}^{d-2}. \quad (5.2)$$

The operators are located at different transverse positions  $\vec{y}_1, \vec{y}_2 \in \mathbb{R}^{d-2}$ , and their spin indices are aligned with the direction of integration (the  $v$  direction). As an example, when  $\mathcal{O}_1$  and  $\mathcal{O}_2$  are stress-tensors, (5.1) is a product of average null energy (ANEC) operators. In chapter 4, we established sufficient conditions for the existence of the product (5.1).

Such null-integrated operators arise naturally in “event shape” observables in collider physics [31, 144–147]. They also appear in shape variations of information-theoretic quantities in quantum field theory [152, 153, 209], as generators of asymptotic symmetry groups [154], and in studies of positivity and causality [101, 140, 157, 210–214]. We review event shapes and null-integrated operators in section 5.2.

Each null-integrated operator is pointlike in the transverse plane  $\mathbb{R}^{d-2}$ , so it is natural to ask whether there exists an operator product expansion (OPE) describing the behavior of the product (5.1) at small  $|\vec{y}_{12}|$ :

$$\int_{-\infty}^{\infty} dv_1 \mathcal{O}_{1;v\dots v}(u=0, v_1, \vec{y}_1) \int_{-\infty}^{\infty} dv_2 \mathcal{O}_{2;v\dots v}(u=0, v_2, \vec{y}_2) \stackrel{?}{=} \sum_i |\vec{y}_{12}|^{\delta_i - (\Delta_1 - 1) - (\Delta_2 - 1)} \mathbb{O}_i. \quad (5.3)$$

Here, the objects  $\mathbb{O}_i$  have dimensions  $\delta_i$  and the powers of  $|\vec{y}_{12}|$  are fixed by dimensional analysis.



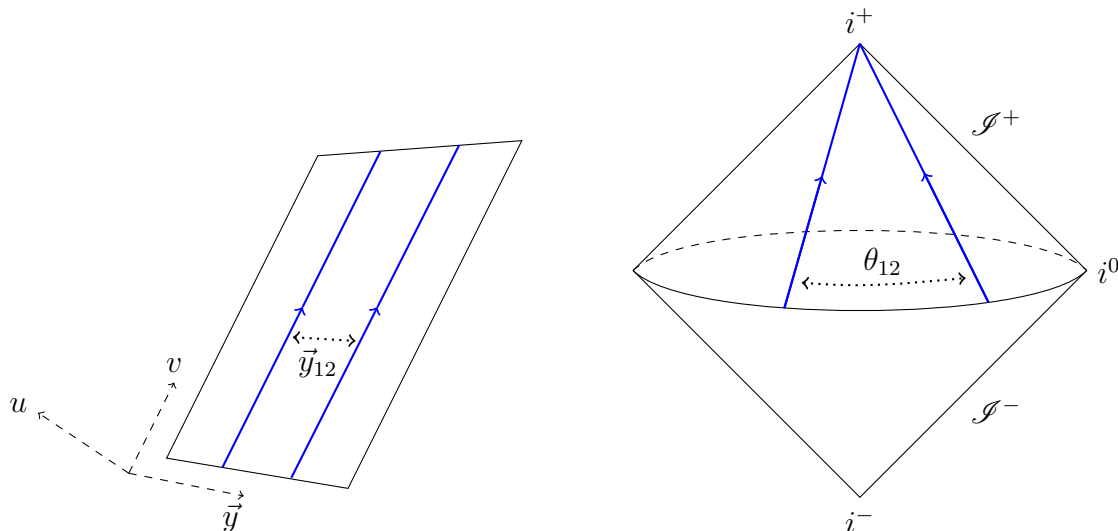


Figure 5.1: The local operators  $\mathcal{O}_1$  and  $\mathcal{O}_2$  are integrated along parallel null lines (blue) on the same null plane. On the left, we show a conformal frame where the null plane is  $u = 0$ , and the operators are at different transverse positions  $\vec{y}_1, \vec{y}_2 \in \mathbb{R}^{d-2}$ . On the right, we show a conformal frame where the null plane is future null infinity  $\mathcal{I}^+$  and the null-integrated operators are separated by an angle  $\theta_{12}$  on the celestial sphere. We give the relationship between  $\theta_{12}$  and  $\vec{y}_{12}$  in (5.10). Note that the entire circle at spatial infinity is really a single point  $i^0$ . Thus, the operators become coincident at the beginnings and ends of their integration contours.

The OPE for *local* operators is a powerful tool in CFT. It allows one to compute correlation functions and to formulate the bootstrap equations [9, 10]. A similar OPE for null-integrated operators (5.1) could have myriad applications. Thus, we would like to ask whether (5.3) exists, whether it is convergent or asymptotic, and what the objects  $\mathbb{O}_i$  are.

Hofman and Maldacena analyzed this question in  $\mathcal{N} = 4$  SYM and found the leading terms in the small- $|\vec{y}_{12}|$  expansion where  $\mathcal{O}_1, \mathcal{O}_2$  are stress tensors and currents [31]. At weak-coupling, the leading objects are certain integrated Wilson-line operators. At strong coupling, the leading objects can be described using string theory in AdS: they are certain stringy shockwave backgrounds. What is the analog of these results in a general nonperturbative CFT? Can we extend the leading terms to a systematic convergent expansion?

There is a simple and beautiful argument for the existence of an OPE of *local* operators in a nonperturbative CFT (see e.g. [215]): Consider a pair of local operators  $\mathcal{O}_1, \mathcal{O}_2$  in Euclidean signature. We surround the operators with a sphere  $S^{d-1}$  (assuming all other operator insertions are outside the sphere) and perform the path integral inside

the sphere. This produces a state  $|\Psi\rangle$  on the sphere. In a scale-invariant theory,  $|\Psi\rangle$  can be expanded in dilatation eigenstates

$$\mathcal{O}_1\mathcal{O}_2|0\rangle = |\Psi\rangle = \sum_i |\mathcal{O}_i\rangle. \quad (5.4)$$

By the state-operator correspondence, these eigenstates are equivalent to insertions of local operators at the origin  $|\mathcal{O}_i\rangle = \mathcal{O}_i(0)|0\rangle$ . Thus (5.4) is the desired OPE.

Unfortunately, this argument does not work for the product (5.1). There is no obvious way to surround the null-integrated operators with an  $S^{d-1}$  such that other operators are outside the sphere. The structure of (5.3) suggests that perhaps we should surround the null-integrated operators with an  $S^{d-3}$  in the transverse space  $\mathbb{R}^{d-2}$ . However there is no obvious Hilbert space of states associated with such an  $S^{d-3}$ .<sup>1</sup>

Nevertheless, using different technology, we will show that a convergent OPE (5.3) for null-integrated operators does exist in a general nonperturbative CFT. The objects appearing on the right-hand side are the light-ray operators  $\mathbb{O}_{i,J}^\pm$  defined in [28] with a particular spin  $J = J_1 + J_2 - 1$ . Each  $\mathbb{O}_{i,J}^\pm$  is obtained by smearing a pair of local operators in a special way in the neighborhood of a light-ray. We review this construction in section 5.3.2. The matrix elements of  $\mathbb{O}_{i,J}^\pm$  can be computed via a generalization of Caron-Huot's Lorentzian inversion formula [25, 28]. The spectrum of operators  $\mathbb{O}_{i,J}^\pm$  is related to the spectrum of local operators by analytic continuation in spin  $J$ ;  $i$  labels different Regge trajectories. For example, if  $\mathcal{O}_1 = \mathcal{O}_2 = T$ , then  $J = 3$  and we obtain an OPE in terms of  $\mathbb{O}_{i,3}^+$ , see figure 5.2.

Our strategy to establish the OPE (5.3) is as follows. First, in section 5.3.3, we decompose the left-hand side of (5.3) into conformal irreps by smearing the transverse coordinates  $\vec{y}_1, \vec{y}_2$ , using harmonic analysis for the transverse conformal group  $\text{SO}(d-1, 1)$ . In section 5.3.4, we focus on a single irrep and compute its matrix elements. Such matrix elements can be written in terms of an integral of a double commutator. After some manipulation, we express this integral as a linear combination of the generalized Lorentzian inversion formula of [28], i.e. as a sum of matrix elements of  $\mathbb{O}_{i,J}^\pm$ 's. Thus, the original product of operators is a sum of  $\mathbb{O}_{i,J}^\pm$ 's.

---

<sup>1</sup>An older argument for the existence of the OPE exists due to Mack [183], relying on very different methods. Mack shows that a product of operators acting on the vacuum  $\mathcal{O}_1\mathcal{O}_2|\Omega\rangle$  can be expanded in a sum of single operators acting on the vacuum  $\sum_i \mathcal{O}_i|\Omega\rangle$ . However, this result is insufficient for our purposes. One reason is that acting with (5.1) on the vacuum immediately gives zero (as we will review shortly). Instead, we would like to act on nontrivial states, and then the theorem of [183] does not apply.

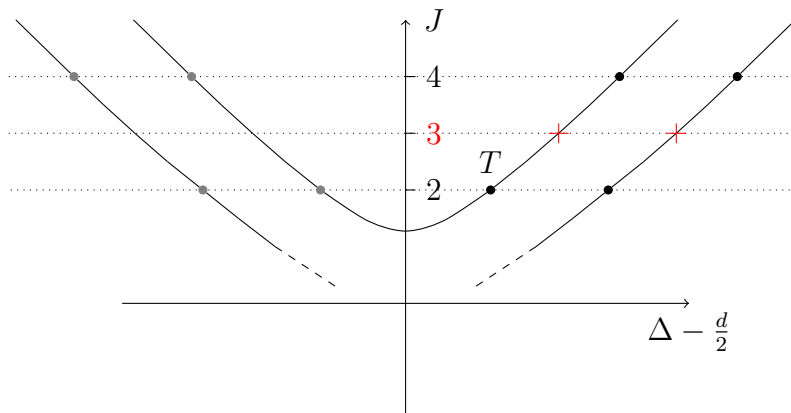


Figure 5.2: Chew-Frautschi plot of neutral even-spin operators. Local operators are denoted by black dots, gray dots denote shadow operators. Solid lines represent Regge trajectories. The OPE  $\int dv T_{vv} \times \int dv T_{vv}$  contains spin-3 light-ray operators on even-spin Regge trajectories, shown here by red crosses.

The light-ray OPE (5.3) and the construction of light-ray operators in [28] give two different ways of creating light-ray operators, and it is not obvious a priori that they should be related. For example, the light-ray operators of [28] involve smearing a pair of local operators in a region *off the null plane* orthogonal to the light-ray. By contrast, in the light-ray OPE, we move operators in the  $\vec{y}$  directions, keeping them *on the null plane*. Even though the smearing kernels are very different, the resulting operators turn out to be related, essentially due to analyticity properties of conformal correlators. The fact that the light-ray operators of [28] can be obtained in two very different ways suggests that they may represent some kind of complete set of observables associated to a light ray, in the same sense that local operators represent a complete set of observables associated to a point.

As an example, consider the case where  $\mathcal{O}_1 = \phi_1$  and  $\mathcal{O}_2 = \phi_2$  are scalars, so that  $J_1 + J_2 - 1 = -1$ .<sup>2</sup> Following the procedure above, we find the OPE<sup>3</sup>

$$\int_{-\infty}^{\infty} dv_1 \phi_1(0, v_1, \vec{y}_1) \int_{-\infty}^{\infty} dv_2 \phi_2(0, v_2, \vec{y}_2) = \pi i \sum_i \mathcal{C}_{\Delta_i - 1}(\vec{y}_{12}, \partial_{\vec{y}_2}) \left( \mathbb{O}_{i,-1}^+(\vec{y}_2) + \mathbb{O}_{i,-1}^-(\vec{y}_2) \right). \quad (5.5)$$

Here,  $\mathcal{C}_\delta(\vec{y}, \partial_{\vec{y}})$  is the same differential operator that appears in an OPE of local

<sup>2</sup>According to the analysis of chapter 4, a product of null-integrated scalars is only well-defined in theories with Regge intercept  $J_0 < -1$ . Here, we assume this is the case.

<sup>3</sup>A more precise expression involves an integral over  $\Delta$  instead of a sum over Regge trajectories. The  $\Delta$  contour can be deformed to pick up singularities in the  $\Delta$  plane. When these singularities are isolated poles, we arrive at the sum of Regge trajectories (5.5). We discuss these points in section 5.5.2.

primary scalars in  $d - 2$  dimensions. It has an expansion

$$\mathcal{C}_\delta(\vec{y}, \partial_{\vec{y}}) = |\vec{y}|^{\delta - (\Delta_1 - 1) - (\Delta_2 - 1)} \left( 1 + \frac{\Delta_1 - \Delta_2 + \delta}{2\delta} \vec{y} \cdot \partial_{\vec{y}} + \dots \right), \quad (5.6)$$

where the coefficients are fixed by  $(d-2)$ -dimensional conformal invariance. The objects  $\mathbb{O}_{i,-1}^\pm$  are light-ray operators associated to the  $i$ -th Regge trajectory, evaluated at spin  $J = -1$ . The superscript  $\pm$  is called the “signature” and it indicates the transformation properties of the light-ray operator under a combination of CRT and Hermitian conjugation.

In section 5.3.4.4, we generalize (5.5) to arbitrary Lorentz representations for  $\mathcal{O}_1, \mathcal{O}_2$ . The light-ray operators on the right-hand side have spin  $J = J_1 + J_2 - 1$ , where  $J_1, J_2$  are the spins of  $\mathcal{O}_1, \mathcal{O}_2$ .<sup>4</sup> For example, when  $\mathcal{O}_1, \mathcal{O}_2$  are the stress tensor, we have a sum of spin-3 light-ray operators

$$\int dv_1 T_{vv}(0, v_1, \vec{y}_1) \int dv_2 T_{vv}(0, v_2, \vec{y}_2) = \pi i \sum_{s=\pm} \sum_{\lambda, a} \sum_i \mathcal{D}_{\Delta_i-1, \lambda}^{(a), s}(\vec{y}_{12}, \partial_{\vec{y}_2}) \mathbb{O}_{i, J=3, \lambda, (a)}^s(\vec{y}_2). \quad (5.7)$$

Here,  $\lambda$  is an  $\text{SO}(d-2)$  representation encoding spin in the transverse plane,  $s = \pm$  is a signature,  $(a)$  labels conformally-invariant three-point structures, and  $\mathcal{D}_{\delta, \lambda}^{(a), s}$  is a differential operator that generalizes  $\mathcal{C}_\delta$ .

In section 5.6 we find that the light-ray OPE also carries information about contact terms in the  $\vec{y}_1 \rightarrow \vec{y}_2$  limit. These contact terms are important in at least two aspects. First they are a part of the physical information present in event shape observables. Second, they arise in commutators of null-integrated operators [154], leading to an interesting algebra.

An interesting property of the light-ray OPE is that the transverse spins that appear are bounded. Specifically, the possible  $\text{SO}(d-2)$  representations appearing in  $\int dv_1 \mathcal{O}_1 \int dv_2 \mathcal{O}_2$  are given by listing all  $\text{SO}(d-1, 1)$  representations in the local OPE  $\mathcal{O}_1 \times \mathcal{O}_2$ , and removing the first rows of their Young diagrams. (We give a simpler version of this rule in (5.150).) For example, in the OPE of null-integrated scalars (5.5), the maximal transverse spin is zero (since only traceless symmetric tensors appear in  $\phi_1 \times \phi_2$ ). In the OPE of ANEC operators (5.7), the possible transverse representations are  $\bullet, \square, \square\square, \square\square\square, \square\square\square\square, \begin{smallmatrix} \square & \square \\ \square & \square \end{smallmatrix}, \begin{smallmatrix} \square & \square & \square \\ \square & \square & \square \end{smallmatrix}$ . This is very different from the naïve expectation that an OPE of point-like objects can contain objects with arbitrarily high spin. Ultimately, it is a consequence of the same analyticity properties that relate different smearings of local operators.

<sup>4</sup>For the definition of  $J$  in general representations, see appendix D.2.

### 5.1.1 Commutators and superconvergence

Our analysis does not assume or require that null-integrated operators commute. Indeed, we can write an expression for a commutator of null-integrated operators using the OPE. For example, the commutator of ANEC operators is given by the odd-signature terms in (5.7),

$$\left[ \int dv_1 T_{vv}(0, v_1, \vec{y}_1), \int dv_2 T_{vv}(0, v_2, \vec{y}_2) \right] = \pi i \sum_{\lambda, a} \sum_i \mathcal{D}_{\Delta_i-1, \lambda}^{(a), -}(\vec{y}_{12}, \partial_{\vec{y}_2}) \mathbb{O}_{i, J=3, \lambda, (a)}^-(\vec{y}_2). \quad (5.8)$$

In chapter 4, we showed that a commutator of ANEC operators vanishes if  $J_0 < 3$ , where  $J_0$  is the Regge intercept of the theory, and furthermore  $J_0 \leq 1$  in unitary CFTs. It is interesting to understand how vanishing occurs on the right-hand side of (5.8). Note that the operators on the right-hand side are light-ray operators with spin 3 and odd signature. We show in section 5.4.1 that if  $J_0 < 3$ , such operators must be null integrals of local spin-3 operators.<sup>5</sup> However, local spin-3 operators are not allowed in the  $T \times T$  OPE by conservation conditions and Ward identities [191]. Thus, the commutator vanishes.

As we explain in section 5.4.1, this argument generalizes to establish vanishing of a commutator of null-integrated operators whenever  $J_1 + J_2 > J_0 + 1$ . It turns out that even if local operators with signature  $(-1)^{J_1+J_2-1}$  and spin  $J_1 + J_2 - 1$  do appear in the local  $\mathcal{O}_1 \times \mathcal{O}_2$  OPE, they do not survive in the light-ray OPE. This provides another (somewhat circuitous) way to derive the commutativity conditions of chapter 4. An exception can occur at vanishing transverse separation  $\vec{y}_{12} = 0$ . In that case, the commutator may contain contact terms, which can be computed by our light-ray OPE formula. As an example, in section 5.6.1, we describe how to compute contact terms in a commutator of null-integrated nonabelian currents (assuming  $J_0 < 1$ ), reproducing results of [154].

Vanishing of the commutator of ANEC operators means that the odd-signature terms in (5.7) disappear, and the OPE of ANEC operators can be simplified to a sum of even-signature light-ray operators with spin 3. This generalizes the results of [31].

Despite the fact that local spin-3 operators are not allowed in the  $T \times T$  OPE, we can try to compute their OPE data with the Lorentzian inversion formula. This is equivalent to evaluating matrix elements of the right-hand side of (5.8). The result must be zero. However, if we plug the OPE in a different channel (the “ $t$ -channel”)

<sup>5</sup>This justifies an assumption made in [154].

into the inversion formula, we obtain sums that are not zero term by term. The conditions that these sums vanish are precisely the “superconvergence” sum rules of chapter 4. As we explain in section 5.4.3, in this language it is simple to argue that (suitably-smearred) superconvergence sum rules have a convergent expansion in  $t$ -channel blocks.

### 5.1.2 Celestial blocks and event shapes

An important application of the light-ray OPE is to event shapes [31, 144–147]. For example, to compute a two-point event shape, we place a pair of null-integrated operators (“detectors”) along future null infinity (right half of figure 5.1) and evaluate a matrix element in a momentum eigenstate  $|\mathcal{O}(p)\rangle$ . By applying the OPE (5.5), we obtain a sum of matrix elements of individual light-ray operators  $\mathbb{O}_{i,J}^\pm$  in momentum eigenstates  $|\mathcal{O}(p)\rangle$ ,

$$\mathcal{C}_{\Delta_i-1}(\vec{y}_{12}, \partial_{\vec{y}_2}) \langle \mathcal{O}(p) | \mathbb{O}_{i,J}^\pm(\vec{y}_2) | \mathcal{O}(p) \rangle. \quad (5.9)$$

The quantity (5.9) is fixed by conformal symmetry up to a constant. It plays a role for event shapes analogous to the role that conformal blocks play in the usual OPE expansion of local 4-point functions. It is proportional to a function of a single cross-ratio

$$\zeta = \frac{1 - \cos \theta_{12}}{2} = \frac{\vec{y}_{12}^2}{(1 + \vec{y}_1^2)(1 + \vec{y}_2^2)} \in [0, 1], \quad (5.10)$$

where  $\theta_{12}$  is the angle between detectors on the celestial sphere. We have also written  $\zeta$  in terms of the transverse positions  $\vec{y}_1, \vec{y}_2$  in the conventions of [31]. In an event shape,  $\zeta \rightarrow 0$  is the collinear limit, while  $\zeta \rightarrow 1$  corresponds to back-to-back detectors. We call (5.9) a “celestial block.”

In section 5.5, we compute celestial blocks by solving an appropriate conformal Casimir equation. For example, when  $\mathcal{O}$  is a scalar, the result is<sup>6</sup>

$$f_{\Delta}^{\Delta_1, \Delta_2}(\zeta) = \zeta^{\frac{\Delta - \Delta_1 - \Delta_2 + 1}{2}} {}_2F_1 \left( \frac{\Delta - 1 + \Delta_1 - \Delta_2}{2}, \frac{\Delta - 1 - \Delta_1 + \Delta_2}{2}, \Delta + 1 - \frac{d}{2}, \zeta \right). \quad (5.11)$$

Note that  $f_{\Delta}^{\Delta_1, \Delta_2}$  becomes a pure power  $\zeta^{\frac{\Delta - \Delta_1 - \Delta_2 + 1}{2}}$  in the collinear limit  $\zeta \rightarrow 0$ .

<sup>6</sup>Celestial blocks are an analytic continuation of the boundary conformal blocks studied in [44, 216].

The light-ray OPE thus yields an expansion for two-point event shapes in celestial blocks. For example, using (5.5) and superconformal symmetry [217, 218], an energy-energy correlator (EEC) in  $\mathcal{N} = 4$  SYM can be written as

$$\langle \mathcal{E}(\vec{n}_1) \mathcal{E}(\vec{n}_2) \rangle_{\psi(p)} = \frac{(p^0)^2}{8\pi^2} \mathcal{F}_{\mathcal{E}}(\zeta),$$

$$\mathcal{F}_{\mathcal{E}}(\zeta) = \sum_i p_{\Delta_i} \frac{4\pi^4 \Gamma(\Delta_i - 2)}{\Gamma(\frac{\Delta_i - 1}{2})^3 \Gamma(\frac{3 - \Delta_i}{2})} f_{\Delta_i}^{4,4}(\zeta) + \frac{1}{4} (2\delta(\zeta) - \delta'(\zeta)), \quad (5.12)$$

where  $\Delta_i$  runs over dimensions of Regge trajectories at spin  $J = -1$ , and  $p_{\Delta_i}$  are squared OPE coefficients of operators in the **105** representation of  $\text{SO}(6)$  in the  $\mathcal{O}_{20'} \times \mathcal{O}_{20'}$  OPE, analytically continued to spin  $J = -1$ . The state  $\psi(p)$  carries momentum  $p = (p^0, 0, 0, 0)$  and is created by acting with an  $\mathcal{O}_{20'}$  operator on the vacuum. The angle between energy detectors is  $\cos \theta = \vec{n}_1 \cdot \vec{n}_2$ , and  $\zeta$  is defined by (5.10). The coupling-independent contact terms  $\frac{1}{4}(2\delta(\zeta) - \delta'(\zeta))$  are related to the contribution of protected operators to the EEC.

Thus, (5.12) expresses the EEC in  $\mathcal{N} = 4$  SYM in terms of OPE data. This formula holds nonperturbatively in both the size of the gauge group  $N_c$  and the 't Hooft coupling  $\lambda$ . In section 5.7, we check it against previous results at weak and strong coupling and find perfect agreement. Using known results for leading-twist OPE data in  $\mathcal{N} = 4$  SYM, we use (5.12) to make new predictions for the small-angle limit of  $\mathcal{N} = 4$  energy-energy correlators through 4 loops (NNNLO).

We conclude in section 5.8 with discussion and future directions. In appendix D.1 we summarize our notation, in appendix D.2 we review general representations of orthogonal groups, and in appendix D.3 we clarify some points about analytic continuation in spin. Appendices D.4, D.5 and D.6 contain details of the calculations described in the main text.

**Note added:** During the last stages of this work we learned about [219] and [220] which have some overlap with our analysis. Let us briefly describe the results of [219] and [220] in relation to our work.

In [219] the EEC in  $\mathcal{N} = 4$  SYM was analyzed using the Mellin space approach of [147]. We analyze  $\mathcal{N} = 4$  SYM in section 5.7. It was shown in [219] how the back-to-back  $\zeta \rightarrow 1$  limit of the EEC is captured by the double light-cone limit of the correlation function studied in [221]. It led to the derivation of (D.85) and identification of the coefficient function  $H(a)$  with a certain spin-independent part of the three-point functions of large spin twist-2 operators. We do not analyze  $\zeta \rightarrow 1$

limit of the EEC in a generic CFT in the present paper. Similarly, a leading small angle asymptotic of the EEC in  $\mathcal{N} = 4$  SYM, the small  $\zeta$  limit of (5.313), was rederived in [219].<sup>7</sup> Based on (5.313), the four-loop small angle asymptotic was worked out in [219], we do it in section 5.7.7. This represents the leading small-angle asymptotic of our complete, non-perturbative OPE formula (5.12).

In [220] a factorization formula describing the small  $\zeta \rightarrow 0$  limit for the EEC was derived in a generic massless QFT, conformal or asymptotically free, in terms of the time-like data of the theory. The authors [220] applied their results to QCD,  $\mathcal{N} = 1$ , and  $\mathcal{N} = 4$  SYM, in particular they analyzed the effects of a non-zero  $\beta$ -function which goes beyond our considerations in the present paper. In the conformal case of  $\mathcal{N} = 4$  SYM which is relevant to our analysis, the leading small-angle asymptotic was derived in [220] through three loops.

In addition, both [219, 220] emphasized the importance of contact terms in the EEC (we compute these using the OPE in section 5.6.2), the way to compute them from the small angle and back-to-back limits, see appendix D.6, and their importance to the Ward identities (5.233, 5.234). In particular, [219, 220] checked that the  $\mathcal{N} = 4$  SYM NLO result [182] satisfies Ward identities, we do this in section 5.7.5.4. In [219] it was also checked that the NNLO result [207] satisfies Ward identities, which we do in section 5.7.6.

## 5.2 Kinematics of light-ray operators and event shapes

### 5.2.1 Null integrals and symmetries

Let us begin by examining the symmetries of a product of light-ray operators (5.1). This analysis will already give a hint why the objects  $\mathbb{O}_{i,J}^\pm$  appear in the OPE.

Firstly, consider a boost

$$(u, v, \vec{y}) \rightarrow (\lambda^{-1}u, \lambda v, \vec{y}), \quad \lambda \in \mathbb{R}^+. \quad (5.13)$$

Each null-integrated operator  $\int dv_i \mathcal{O}_{i;v\dots v}$  has boost eigenvalue  $1 - J_i$ , where 1 comes from the measure  $dv_i$  and  $-J_i$  comes from the lowered  $v$ -indices. Thus, the product (5.1) has boost eigenvalue  $(1 - J_1) + (1 - J_2) = 1 - (J_1 + J_2 - 1)$ . In other words, it transforms like the null integral of an operator with spin  $J_1 + J_2 - 1$  [31].

Another important symmetry is CRT, which is an anti-unitary symmetry taking

$$(u, v, \vec{y}) \rightarrow (-u, -v, \vec{y}). \quad (5.14)$$

---

<sup>7</sup>We reported (5.313) to G.Korchensky in September 2018.



Combining CRT with Hermitian conjugation, we obtain a linear map on the space of operators. It is easy to check that

$$\left( (\text{CRT}) \int_{-\infty}^{\infty} dv \mathcal{O}_{i;v\dots v}(0, v, \vec{y}) (\text{CRT})^{-1} \right)^\dagger = (-1)^{J_i} \int_{-\infty}^{\infty} dv \mathcal{O}_{i;v\dots v}(0, v, \vec{y}). \quad (5.15)$$

We call the eigenvalue with respect to the combination of CRT and Hermitian conjugation the “signature” of the operator. Applying CRT and Hermitian conjugation to (5.1), we find

$$\left[ \int_{-\infty}^{\infty} dv_1 \mathcal{O}_{1;v\dots v}(0, v_1, \vec{y}_1), \int_{-\infty}^{\infty} dv_2 \mathcal{O}_{2;v\dots v}(0, v_2, \vec{y}_2) \right] \quad \text{has signature } (-1)^{J_1+J_2-1} \quad (5.16)$$

$$\left\{ \int_{-\infty}^{\infty} dv_1 \mathcal{O}_{1;v\dots v}(0, v_1, \vec{y}_1), \int_{-\infty}^{\infty} dv_2 \mathcal{O}_{2;v\dots v}(0, v_2, \vec{y}_2) \right\} \quad \text{has signature } (-1)^{J_1+J_2}, \quad (5.17)$$

where  $[ , ]$  and  $\{ , \}$  denote a commutator and anticommutator, respectively. The extra minus sign in the commutator appears because Hermitian conjugation reverses operator ordering.

It often happens (under circumstances described in chapter 4 and discussed in section 5.4.1) that the commutator (5.16) vanishes. For example, a commutator of ANEC operators on the same null plane vanishes. For simplicity, suppose that the commutator vanishes. In this case, the product (5.1) is the same as the anticommutator (5.17). Thus, (5.1) transforms like the null-integral of an operator with spin  $J_1 + J_2 - 1$  and signature  $(-1)^{J_1+J_2}$ . An integrated local operator can never have these quantum numbers. This shows that the OPE (5.3) cannot be computed by simply performing the usual OPE between  $\mathcal{O}_1$  and  $\mathcal{O}_2$  inside the integral.

### 5.2.2 Review: embedding formalism and the Lorentzian cylinder

It is instructive to re-derive the selection rule  $J = J_1 + J_2 - 1$  in a different way, using conformal transformation properties of null-integrated operators. These properties are easiest to understand in the embedding formalism [9, 192, 222–227].

In the embedding formalism, Minkowski space is realized as a subset of the projective null cone in  $\mathbb{R}^{d,2}$ . Let us choose coordinates  $X = (X^+, X^-, X^\mu) = (X^+, X^-, X^0, \dots, X^{d-1})$  on  $\mathbb{R}^{d,2}$ , with metric

$$X \cdot X = -X^+ X^- - (X^0)^2 + (X^1)^2 + \dots + (X^{d-1})^2. \quad (5.18)$$

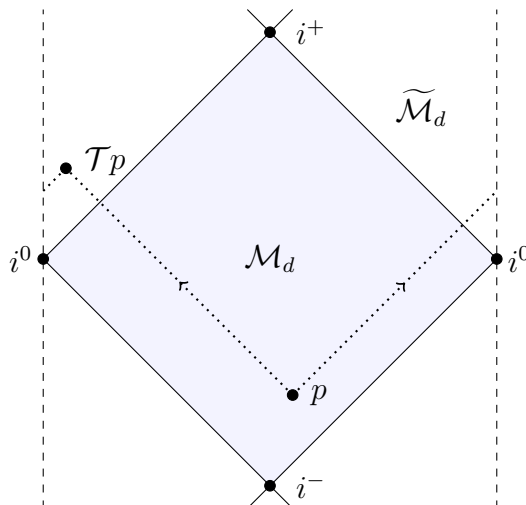


Figure 5.3: Minkowski patch  $\mathcal{M}_d$  (blue, shaded) inside the Lorentzian cylinder  $\widetilde{\mathcal{M}}_d$  in the case of 2 dimensions. Spacelike infinity of  $\mathcal{M}_d$  is marked by  $i^0$  and future/past infinity are marked by  $i^\pm$ . The dashed lines should be identified. The point  $\mathcal{T}p$  is obtained from  $p$  by shooting light-rays in all possible future directions (dotted lines) and finding the first point where they converge.

The projective null cone is the locus  $X \cdot X = 0$ , modulo positive rescalings  $X \sim \lambda X$  ( $\lambda \in \mathbb{R}_+$ ). This space is topologically  $S^1 \times S^{d-1}$ . Lorentzian CFTs live on the universal cover of the projective null cone  $\widetilde{\mathcal{M}}_d$ , which is topologically  $\mathbb{R} \times S^{d-1}$  — sometimes called the Lorentzian cylinder. The conformal group  $\widetilde{\text{SO}}(d, 2)$  is the universal cover of  $\text{SO}(d, 2)$ .

Minkowski space corresponds to the locus  $X = (X^+, X^-, X^\mu) = (1, x^2, x^\mu) \in \mathbb{R}^{d,2}$ , where  $x \in \mathbb{R}^{d-1,1}$ . Spatial infinity  $i^0$  is obtained by taking  $x \rightarrow \infty$  in a spacelike direction and rescaling  $X$  so it remains finite, yielding  $X_{i^0} = (0, 1, 0)$ . Timelike infinity  $i^\pm$  corresponds to  $X_{i^\pm} = (0, -1, 0)$ . (Note that future and past infinity  $i^\pm$  correspond to the same embedding-space vector, but they are distinguished on the universal cover of the projective null cone.) Finally, null infinity corresponds to the points  $X_{\mathcal{I}^\pm}(\sigma, z) = (0, -2\sigma, z)$ ,  $z = (\pm 1, \vec{n})$ , where  $\vec{n} \in S^{d-2}$  is a point on the celestial sphere and  $\sigma$  is retarded time.

The Lorentzian cylinder  $\widetilde{\mathcal{M}}_d$  is tiled by Minkowski “patches” (figure 5.3). To every point  $p \in \widetilde{\mathcal{M}}_d$ , there is an associated point  $\mathcal{T}p$  obtained by shooting light rays in all future directions from  $p$  and finding the point where they converge in the next patch. In embedding coordinates,  $\mathcal{T}$  takes  $X \rightarrow -X$ . For example,  $\mathcal{T}$  takes spatial infinity  $i^0$  to future infinity  $i^+$ . We sometimes write  $p^+ \equiv \mathcal{T}p$  and  $p^- \equiv \mathcal{T}^{-1}p$ .

To describe operators with spin, it is helpful to introduce index-free notation. Given

a traceless symmetric tensor  $\mathcal{O}^{\mu_1 \cdots \mu_J}(x)$ , we can contract its indices with a future-pointing null polarization vector  $z_\mu$  to form

$$\mathcal{O}(x, z) \equiv \mathcal{O}^{\mu_1 \cdots \mu_J}(x) z_{\mu_1} \cdots z_{\mu_J}. \quad (5.19)$$

When  $\mathcal{O}^{\mu_1 \cdots \mu_J}(x)$  is an integer-spin local operator,  $\mathcal{O}(x, z)$  is a homogeneous polynomial of degree  $J$ .

In the embedding formalism, the operator  $\mathcal{O}(x, z)$  gets lifted to a homogeneous function  $\mathcal{O}(X, Z)$  of coordinates  $X, Z \in \mathbb{R}^{d,2}$ , subject to the relations  $X^2 = X \cdot Z = Z^2 = 0$  [192]. It is defined by

$$\mathcal{O}(X, Z) = (X^+)^{-\Delta} \mathcal{O} \left( x = \frac{X}{X^+}, z = Z - \frac{Z^+}{X^+} X \right), \quad (5.20)$$

where  $\Delta$  is the dimension of  $\mathcal{O}$ . The advantage of  $\mathcal{O}(X, Z)$  is that conformal transformations act linearly on the coordinates  $X, Z$ . Note that  $\mathcal{O}(X, Z)$  has gauge invariance

$$\mathcal{O}(X, Z) = \mathcal{O}(X, Z + \beta X), \quad (5.21)$$

and homogeneity

$$\mathcal{O}(\lambda X, \alpha Z) = \lambda^{-\Delta} \alpha^J \mathcal{O}(X, Z). \quad (5.22)$$

The operator  $\mathcal{O}(x, z)$  on  $\mathbb{R}^{d-1,1}$  can be recovered by the dictionary

$$\mathcal{O}(x, z) = \mathcal{O} \left( X = (1, x^2, x), Z = (0, 2x \cdot z, z) \right). \quad (5.23)$$

Index-free notation and the procedure of lifting operators to the embedding space can be generalized to arbitrary representations of the Lorentz group. We describe this construction in appendix D.2.

### 5.2.3 Review: the light transform

Null-integrated operators like those in (5.1) can be understood in terms of a conformally-invariant integral transform called the ‘‘light-transform’’ [28]. In embedding-space language, the light-transform is defined by

$$\mathbf{L}[\mathcal{O}](X, Z) \equiv \int_{-\infty}^{\infty} d\alpha \mathcal{O}(Z - \alpha X, -X). \quad (5.24)$$

This transform is invariant under  $\widetilde{\text{SO}}(d, 2)$  because (5.24) only depends on the embedding-space vectors  $X, Z$ . It respects the gauge redundancy (5.21) because a shift  $Z \rightarrow$

$Z + \beta X$  can be compensated by shifting  $\alpha \rightarrow \alpha + \beta$  in the integral. The initial point of the integration contour in (5.24) is  $X$ , since  $Z - (-\infty)X$  is projectively equivalent to  $X$ . Furthermore, if  $\mathcal{O}(X, Z)$  has homogeneity (5.22), then its light-transform has homogeneity

$$\mathbf{L}[\mathcal{O}](\lambda X, \alpha Z) = \lambda^{-(1-J)} \alpha^{1-\Delta} \mathbf{L}[\mathcal{O}](X, Z). \quad (5.25)$$

Thus,  $\mathbf{L}[\mathcal{O}]$  transforms like a primary at  $X$  with dimension  $1 - J$  and spin  $1 - \Delta$ :

$$\mathbf{L} : (\Delta, J) \rightarrow (1 - J, 1 - \Delta). \quad (5.26)$$

Note that the light-transform naturally gives rise to operators with non-integer spin.

In Minkowski coordinates,  $\mathbf{L}$  becomes

$$\begin{aligned} \mathbf{L}[\mathcal{O}](x, z) &= \int_{-\infty}^{\infty} d\alpha \mathcal{O}(Z - \alpha X, -X) \Big|_{\substack{X=(1, x^2, x) \\ Z=(0, 2x \cdot z, z)}} \\ &= \int_{-\infty}^{\infty} d\alpha (-\alpha)^{-\Delta-J} \mathcal{O}\left(X - \frac{Z}{\alpha}, Z\right) \Big|_{\substack{X=(1, x^2, x) \\ Z=(0, 2x \cdot z, z)}} \\ &= \int_{-\infty}^{\infty} d\alpha (-\alpha)^{-\Delta-J} \mathcal{O}\left(x - \frac{z}{\alpha}, z\right). \end{aligned} \quad (5.27)$$

In the second line above, we used gauge invariance (5.21) to shift  $-X \rightarrow -X - (Z - \alpha X)/\alpha = -Z/\alpha$  and then homogeneity (5.22) to pull out factors of  $(-\alpha)$ . In the third line, we used (5.23). The integration contour in (5.27) starts at  $x$  when  $\alpha = -\infty$  and reaches the boundary of Minkowski space when  $\alpha = 0$ . The correct prescription there is to continue the contour into the next Poincare patch to the point  $\mathcal{T}x \in \widetilde{\mathcal{M}}_d$ . The expression (5.27) makes it clear that  $\mathbf{L}[\mathcal{O}]$  converges whenever  $\Delta + J > 1$ , as long as there are no other operators at  $x$  or  $\mathcal{T}x$ .<sup>8</sup> Note that  $\mathbf{L}[\mathcal{O}](x, z)$  is not a polynomial in  $z$  and thus cannot be written in terms of an underlying tensor with  $1 - \Delta$  indices.

For any local operator  $\mathcal{O}$  satisfying  $\Delta + J > 1$ , the light-transform  $\mathbf{L}[\mathcal{O}]$  annihilates the vacuum  $|\Omega\rangle$ . The reason is that if  $\mathbf{L}[\mathcal{O}]|\Omega\rangle$  did not vanish, then it would be a primary state with spin  $1 - \Delta \notin \mathbb{Z}_{\geq 0}$ , which is not allowed in a unitary CFT [27]. One can also verify that  $\mathbf{L}[\mathcal{O}]|\Omega\rangle = 0$  by deforming the  $\alpha$  contour in the complex plane inside a Wightman correlation function [28].

<sup>8</sup>More precisely,  $\mathbf{L}[\mathcal{O}]$  converges as an operator-valued tempered distribution when  $\Delta + J > 1$ . To define  $\mathbf{L}[\mathcal{O}](x, z)$  as a distribution, we must show how to smear it against a test function,  $\int d^d x f(x) \mathbf{L}[\mathcal{O}](x, z)$ . We do so by integrating the light-transform by parts  $\int d^d x (\mathcal{T}^{-1} \mathbf{L}[f])(x, z) \mathcal{O}(x, z)$ . This makes it clear that  $\mathbf{L}[\mathcal{O}]$  converges whenever  $\mathbf{L}[f]$  converges for any test function  $f$ . This again leads to the condition  $\Delta + J > 1$ .

Let us now return to the boost selection rule  $J = J_1 + J_2 - 1$  from section 5.2.1. To recover the setup of that section, we can set

$$\begin{aligned} X_0 &= -(0, 0, \frac{1}{2}, \frac{1}{2}, \vec{0}) \in \mathcal{I}^-, \\ Z_0 &= (1, \vec{y}^2, 0, 0, \vec{y}), \end{aligned} \quad (5.28)$$

where  $\vec{0}, \vec{y} \in \mathbb{R}^{d-2}$ . Note that these satisfy the conditions  $X_0^2 = X_0 \cdot Z_0 = Z_0^2 = 0$ . The light-transform becomes

$$\mathbf{L}[\mathcal{O}](X_0, Z_0) = \int_{-\infty}^{\infty} d\alpha \mathcal{O}_{v\dots v}(u=0, v=\alpha, \vec{y}), \quad (5.29)$$

Thus, we should think of  $\int dv \mathcal{O}_{v\dots v}$  as a primary operator associated to the point  $X_0$  at past null infinity.

Consider now a product of null-integrated operators

$$\mathbf{L}[\mathcal{O}_1](X_0, Z_0) \mathbf{L}[\mathcal{O}_2](X_0, Z'_0) = \int_{-\infty}^{\infty} dv_1 \mathcal{O}_{1;v\dots v}(0, v_1, \vec{y}_1) \int_{-\infty}^{\infty} dv_2 \mathcal{O}_{2;v\dots v}(0, v_2, \vec{y}_2). \quad (5.30)$$

This is a product of primaries associated to the *same* point  $X_0$  at past null infinity (with different polarization vectors  $Z_0, Z'_0$ ). Thus, the dimension of the product (assuming it is well-defined) is the sum of the dimensions:  $(1 - J_1) + (1 - J_2) = 1 - (J_1 + J_2 - 1)$ .<sup>9</sup> This is the same as the dimension of the light-transform of an operator with spin  $J_1 + J_2 - 1$ . Hence, we have recovered the selection rule from section 5.2.1.

The relationship between this argument and the one in section 5.2.1 is that the dilatation generator that measures dimension around the point  $X_0$  is the same as the boost generator discussed in section 5.2.1.

An important observation is that the product (5.30) transforms like a primary operator at the point  $X_0$ . This is because both factors  $\mathbf{L}[\mathcal{O}_1](X_0, Z_0)$  and  $\mathbf{L}[\mathcal{O}_2](X_0, Z'_0)$  are killed by the special conformal generators that fix  $X_0$ . (Alternatively, we can simply

---

<sup>9</sup>Ordinarily in CFT, we do not consider a product of operators at coincident points. Instead, we place them at separated points and study the singularity as they approach each other, for example

$$\phi_1(x)\phi_2(0) \sim \sum_k x^{\Delta_k - \Delta_1 - \Delta_2} \phi_k(0). \quad (5.31)$$

The dimensionful factor  $x^{\Delta_k - \Delta_1 - \Delta_2}$  allows the scaling dimension  $\Delta_k$  to be different from  $\Delta_1 + \Delta_2$ . However, if the coincident limit  $x \rightarrow 0$  is nonsingular, the only operators that survive the limit must obey the selection rule  $\Delta_k = \Delta_1 + \Delta_2$ .

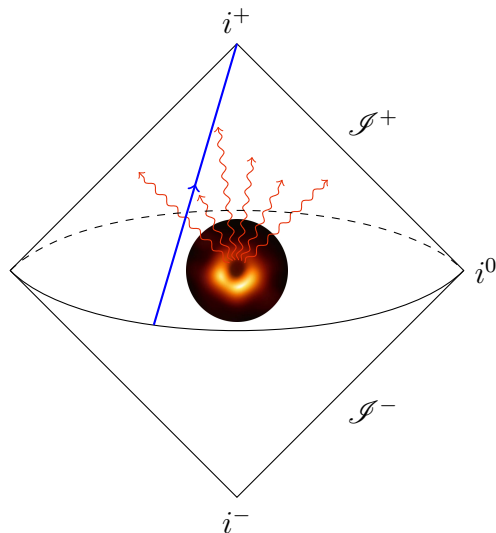


Figure 5.4: A one-point event shape [228]. The detector  $\mathcal{O} = \mathcal{O}_{\text{EHT}}$  is integrated along a null line (blue) along future null infinity, starting at spatial infinity  $i^0$  and ending at future timelike infinity  $i^+$ . (Note that the circle at spatial infinity is really a single point.) The red wavy lines indicate energy propagating from the interior of Minkowski space out to null infinity, created by the insertion of the source  $\phi_1(p)$ .

observe that (5.30) is a homogeneous function of  $X_0$  on the null cone in the embedding space, which again implies that it transforms like a primary.) Thus, when we consider the OPE expansion of (5.30) in the limit  $Z_0 \rightarrow Z'_0$ , the only terms appearing will be other primary operators at the point  $X_0$ .

#### 5.2.4 Review: event shapes and the celestial sphere

The symmetries of light-ray operators on a null plane are easiest to understand when we take the null plane to be  $\mathcal{S}^+$ . This corresponds to choosing the embedding-space coordinates

$$\begin{aligned} X_\infty &= (0, 1, 0), \\ Z_\infty(z) &= (0, 0, z), \end{aligned} \tag{5.32}$$

where  $z \in \mathbb{R}^{d-1,1}$  is a future-pointing null vector. The integration contour for the light-transform now lies inside  $\mathcal{S}^+$ , running from  $i^0$  to  $i^+$  along the  $z$  direction (figure 5.4).

The operator  $\mathbf{L}[\mathcal{O}](\infty, z) \equiv \mathbf{L}[\mathcal{O}](X_\infty, Z_\infty(z))$  transforms like a primary inserted at spatial infinity, which means it is killed by momentum generators

$$[P^\mu, \mathbf{L}[\mathcal{O}](\infty, z)] = 0. \tag{5.33}$$

Consequently, its matrix elements with other operators are translationally-invariant, for example

$$\langle \Omega | \phi_2(x_2) \mathbf{L}[\mathcal{O}](\infty, z) \phi_1(x_1) | \Omega \rangle = f(x_1 - x_2). \quad (5.34)$$

(Throughout this work, we use  $\phi$  to denote scalar operators and  $\mathcal{O}$  to denote operators in general Lorentz representations.) Thus, it is natural to go to momentum space,

$$\langle \phi_2(q) | \mathbf{L}[\mathcal{O}](\infty, z) | \phi_1(p) \rangle = (2\pi)^d \delta^d(p - q) \tilde{f}(p), \quad (5.35)$$

where

$$|\phi_i(p)\rangle \equiv \int d^d x e^{ip \cdot x} \phi_i(x) |\Omega\rangle. \quad (5.36)$$

Note that  $|\phi_i(p)\rangle$  vanishes unless  $p$  is inside the forward lightcone  $p > 0$ , by positivity of energy.<sup>10</sup> We often abuse notation by writing

$$\langle \phi_2(p) | \mathbf{L}[\mathcal{O}](\infty, z) | \phi_1(p) \rangle = \tilde{f}(p), \quad (5.37)$$

where it is understood that we have stripped off the momentum-conserving factor  $(2\pi)^d \delta^d(p + q)$ .

More generally, we can consider a product of light-transforms along  $\mathcal{S}^+$ , inserted between momentum eigenstates

$$\langle \phi_2(p) | \mathbf{L}[\mathcal{O}_1](\infty, z_1) \cdots \mathbf{L}[\mathcal{O}_n](\infty, z_n) | \phi_1(p) \rangle. \quad (5.38)$$

Following [229], we call such matrix elements “event shapes.” This terminology comes from interpreting (5.38) as the expectation value of a product of “detectors”  $\mathcal{O}_1, \dots, \mathcal{O}_n$  in a “source” state  $|\phi_1(p)\rangle$  and “sink” state  $\langle \phi_2(p)|$ . The detectors sit at points on the celestial sphere and are integrated over retarded time to capture signals that propagate to null infinity.

In addition to being translationally-invariant,  $\mathbf{L}[\mathcal{O}](\infty, z)$  transforms in a simple way under  $d$ -dimensional Lorentz transformations  $\text{SO}(d - 1, 1)$ : they act linearly on the polarization vector  $z$ . The Lorentz group in  $d$ -dimensions is the same as the Euclidean conformal group on the  $(d - 2)$ -dimensional celestial sphere. Indeed, we can

---

<sup>10</sup>It is sometimes hard to keep track of signs in Lorentzian signature, so let us explain this point. Ignoring position-dependence for simplicity, we have  $\phi(t) = e^{iHt} \phi(0) e^{-iHt}$ . The minus sign is in the right-hand exponential  $e^{-iHt}$  because that operator generates Schrodinger time-evolution. Acting on the vacuum, we obtain  $e^{iHt} \phi(0) |\Omega\rangle$ , which is a sum of positive-imaginary exponentials  $e^{iEt}$ . To get a nonzero result under the Fourier transform, we must multiply by  $e^{-iEt}$ , which is contained in the factor  $e^{ip \cdot x}$ .

think of  $z \in \mathbb{R}^{d-1,1}$  as an embedding-space coordinate for the celestial sphere  $S^{d-2}$ . Furthermore,  $\mathbf{L}[\mathcal{O}](\infty, z)$  is homogeneous of degree  $1 - \Delta$  in  $z$ , due to (5.25). Thus,  $\mathbf{L}[\mathcal{O}](\infty, z)$  transforms like a primary operator on the celestial sphere with dimension  $\delta = \Delta - 1$ .

In the previous coordinates (5.28), the group  $\text{SO}(d-1, 1)$  acted by conformal transformations on the transverse direction  $\vec{y}$ . The coordinates  $\vec{y}$  are stereographic coordinates on  $S^{d-2}$ . Thus, we have proven the claim from section 5.2.1 that  $\int dv \mathcal{O}_{v\dots v}$  transforms as a primary in the transverse space.

The event shape (5.38) is similar to a correlator of operators with dimensions  $\delta_i = \Delta_i - 1$  in a Euclidean  $(d-2)$ -dimensional CFT. However, the presence of a timelike momentum  $p$  breaks the Lorentz group further to  $\text{SO}(d-1)$ . In the language of  $(d-2)$ -dimensional CFT, this is similar to the symmetry-breaking pattern that occurs in the presence of a spherical codimension-1 boundary or defect [44, 216]. This fact will play an important role in section 5.5. We can choose a center-of-mass frame  $p = (p^0, 0, \dots, 0)$  and write  $z_i = (1, \vec{n}_i)$  with  $\vec{n}_i \in S^{d-2}$ . The dependence on  $p^0$  is fixed by dimensional analysis, so we can additionally set  $p^0 = 1$ . The event shape then becomes a nontrivial function of dot-products  $\vec{n}_i \cdot \vec{n}_j$ .

In addition to respecting symmetries, event shapes are useful for studying positivity conditions. For example, consider the average null energy operator  $\mathcal{E} = 2\mathbf{L}[T]$ , where  $T_{\mu\nu}$  is the stress tensor.  $\mathcal{E}$  is positive-semidefinite [31, 152, 210]. To test this, we could compute the expectation value of  $\mathcal{E}$  in several different states (primaries and descendants at different points, etc.) and then aggregate the resulting positivity conditions. However, it is sufficient to study event shapes  $\langle \mathcal{O}_i(p) | \mathcal{E} | \mathcal{O}_j(p) \rangle$  for the following reason. The Hilbert space of a CFT is densely spanned by states of the form

$$\sum_i \int d^d x f_i(x) \mathcal{O}_i(x) | \Omega \rangle, \quad (5.39)$$

where  $\mathcal{O}_i$  are primary operators and  $f_i(x)$  are test functions. Positivity of  $\mathcal{E}$  is thus equivalent to the statement that for any collection of test functions  $f_i(x)$ ,

$$\sum_{i,j} \int d^d x_1 d^d x_2 f_i^*(x_1) f_j(x_2) K_{ij}(x_1 - x_2) \geq 0, \quad (5.40)$$

where

$$K_{ij}(x_1 - x_2) \equiv \langle \Omega | \mathcal{O}_i(x_1) \mathcal{E}(\infty, z) \mathcal{O}_j(x_2) | \Omega \rangle. \quad (5.41)$$



This is the same as saying that  $K_{ij}(x_1 - x_2)$  is a positive-semidefinite integral kernel. To determine whether a kernel is positive-semidefinite, we should compute its eigenvalues and check that they are positive. Because  $K_{ij}(x_1 - x_2)$  is translation-invariant, it can be partially diagonalized by going to Fourier space. Thus,  $\mathcal{E}$  is positive-semidefinite if and only if its one-point event shapes are positive-semidefinite.

### 5.2.4.1 1-point event shapes

As an example, let us compute a one-point event shape  $\langle \phi_2 | \mathbf{L}[\mathcal{O}] | \phi_1 \rangle$ , where  $\mathcal{O}$  has dimension  $\Delta$  and spin  $J$ , and  $\phi_1, \phi_2$  are scalars. We start from the Wightman function<sup>11</sup>

$$\begin{aligned} & \langle 0 | \phi_2(x_2) \mathcal{O}(x_3, z_3) \phi_1(x_1) | 0 \rangle \\ &= \frac{(2V_{3,12})^J}{(x_{12}^2 + i\epsilon x_{21}^0)^{\frac{\Delta_1 + \Delta_2 - \Delta - J}{2}} (x_{13}^2 + i\epsilon x_{31}^0)^{\frac{\Delta_1 - \Delta_2 + \Delta + J}{2}} (x_{32}^2 + i\epsilon x_{23}^0)^{\frac{\Delta_2 - \Delta_1 + \Delta + J}{2}}}, \end{aligned} \quad (5.42)$$

where

$$V_{3,12} \equiv \frac{z_3 \cdot x_{13} x_{23}^2 - z_3 \cdot x_{23} x_{13}^2}{x_{12}^2}. \quad (5.43)$$

In (5.42), we have written the  $i\epsilon$  prescription appropriate for the given operator ordering. This is obtained by introducing small imaginary parts  $x_i^0 \rightarrow x_i^0 - i\epsilon_i$  with  $\epsilon_2 > \epsilon_3 > \epsilon_1$  in the same order as the operators appearing in the Wightman function. We often omit explicit  $i\epsilon$ 's, restoring them only when necessary during a computation. In these cases, the  $i\epsilon$  prescription should be inferred from the ordering of the operators in the correlator.

The light-transform of (5.42) is [28]

$$\begin{aligned} & \langle 0 | \phi_2(x_2) \mathbf{L}[\mathcal{O}](x_3, z_3) \phi_1(x_1) | 0 \rangle \\ &= \frac{L(\phi_1 \phi_2[\mathcal{O}])(2V_{3,12})^{1-\Delta}}{(x_{12}^2)^{\frac{\Delta_1 + \Delta_2 - (1-J) - (1-\Delta)}{2}} (x_{13}^2)^{\frac{\Delta_1 - \Delta_2 + (1-J) + (1-\Delta)}{2}} (-x_{23}^2)^{\frac{\Delta_2 - \Delta_1 + (1-J) + (1-\Delta)}{2}}} \quad (2 > 3 > 1^-), \end{aligned} \quad (5.44)$$

where

$$L(\phi_1 \phi_2[\mathcal{O}]) \equiv -2\pi i \frac{\Gamma(\Delta + J - 1)}{\Gamma(\frac{\Delta + \Delta_1 - \Delta_2 + J}{2}) \Gamma(\frac{\Delta - \Delta_1 + \Delta_2 + J}{2})}. \quad (5.45)$$

<sup>11</sup>We use the same conventions for two- and three-point structures as [28]. These include some extra factors of  $2^J$  that ensure that three-point structures glue together into a conventionally-normalized conformal block. These conventions are convenient when discussing inversion formulas. We also use correlators  $\langle 0 | \dots | 0 \rangle$  in the fictitious state  $|0\rangle$  to indicate functions whose form is fixed by conformal invariance (as opposed to correlators in a physical theory). See appendix D.1 for a summary of our notation.

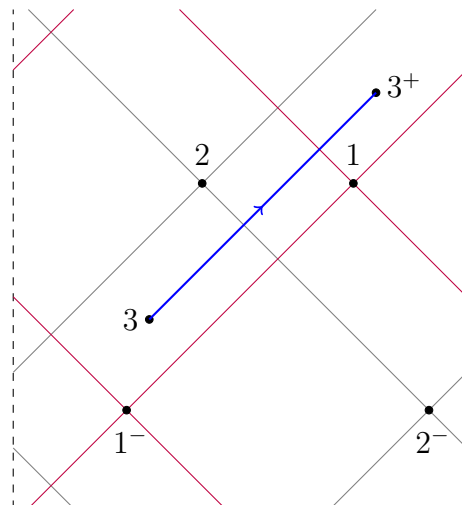


Figure 5.5: The causal relationship between points  $2 > 3 > 1^-$  used in (5.44). The lightcone of 2 is drawn in gray and the lightcone of 1 in purple.

This indeed has the form of a conformally-invariant three-point function with an operator with dimension  $1 - J$  and spin  $1 - \Delta$ . The notation  $i > j$  means “ $x_i$  is inside the future lightcone of  $x_j$ .” Below, we will also use the notation  $i \approx j$  to indicate that  $x_i$  is spacelike from  $x_j$ . We have written (5.44) in the kinematics  $2 > 3 > 1^-$  (figure 5.5), where all the quantities in parentheses are positive. This time, we have left the  $i\epsilon$  prescription implicit.

We should now take  $x_3$  to spatial infinity. Keeping track of  $i\epsilon$  prescriptions, we find

$$\langle 0 | \phi_2(x_2) \mathbf{L}[\mathcal{O}](\infty, z) \phi_1(x_1) | 0 \rangle = L(\phi_1 \phi_2[\mathcal{O}]) \frac{e^{i\pi\Delta_2} (-2z \cdot x_{12} + i\epsilon)^{1-\Delta}}{(-x_{12}^2 + i\epsilon x_{12}^0)^{\frac{\Delta_1 + \Delta_2 - (1-J) + (1-\Delta)}{2}}}. \quad (5.46)$$

This is indeed translation-invariant. It is straightforward to compute the Fourier transform

$$\begin{aligned} & \int d^d x e^{ipx} \frac{(-2x \cdot z + i\epsilon)^{1-\Delta}}{(-x^2 + i\epsilon x^0)^{\frac{\Delta_1 + \Delta_2 - (1-J) + (1-\Delta)}{2}}} \\ &= \widehat{\mathcal{F}}_{\Delta_1 + \Delta_2 - (1-J), 1-\Delta} (-2p \cdot z)^{1-\Delta} (-p^2)^{\frac{\Delta_1 + \Delta_2 - (1-J) - (1-\Delta) - d}{2}} \theta(p), \end{aligned} \quad (5.47)$$

where

$$\widehat{\mathcal{F}}_{\Delta, J} \equiv \frac{e^{-i\pi\frac{\Delta}{2}} 2^{d+1-\Delta} \pi^{\frac{d+2}{2}}}{\Gamma(\frac{\Delta+J}{2}) \Gamma(\frac{\Delta+2-d-J}{2})}. \quad (5.48)$$

The theta function  $\theta(p) \equiv \theta(-p^2)\theta(p^0)$  restricts  $p$  to lie in the forward lightcone.

Overall, the one-point event shape is given by

$$\begin{aligned} & \int d^d x e^{ip \cdot x} \langle 0 | \phi_2(0) \mathbf{L}[\mathcal{O}](\infty, z) \phi_1(x) | 0 \rangle \\ &= \frac{2^{d-\Delta_1-\Delta_2-J+3} \pi^{\frac{d}{2}+2} e^{i\pi \frac{\Delta_2-\Delta_1-J}{2}} \Gamma(J+\Delta-1) (-2p \cdot z)^{1-\Delta} (-p^2)^{\frac{\Delta_1+\Delta_2+\Delta+J-2-d}{2}} \theta(p)}{\Gamma(\frac{J+\Delta+\Delta_1-\Delta_2}{2}) \Gamma(\frac{J+\Delta-\Delta_1+\Delta_2}{2}) \Gamma(\frac{J-\Delta+\Delta_1+\Delta_2}{2}) \Gamma(\frac{J+\Delta+\Delta_1+\Delta_2-d}{2})} \theta(p). \end{aligned} \quad (5.49)$$

Note that this is consistent with dimensional analysis in  $p$ , homogeneity in  $z$ , and Lorentz invariance. In chapter 4, we describe an algorithm for computing more general one-point event shapes.

### 5.2.4.2 2-point event shapes

A two-point event shape is constrained by dimensional analysis, homogeneity, and Lorentz invariance to take the form

$$\langle \phi_4(p) | \mathbf{L}[\mathcal{O}_1](\infty, z_1) \mathbf{L}[\mathcal{O}_2](\infty, z_2) | \phi_3(p) \rangle = \frac{(-p^2)^{\frac{\Delta_1+\Delta_2+\Delta_3+\Delta_4-4-d}{2}} \theta(p)}{(-2z_1 \cdot p)^{\Delta_1-1} (-2z_2 \cdot p)^{\Delta_2-1}} \mathcal{G}_{\mathcal{O}_1 \mathcal{O}_2}(\zeta), \quad (5.50)$$

where  $\mathcal{G}_{\mathcal{O}_1 \mathcal{O}_2}(\zeta)$  is a function of the cross-ratio

$$\zeta \equiv \frac{(-2z_1 \cdot z_2)(-p^2)}{(-2p \cdot z_1)(-2p \cdot z_2)} = \frac{1 - \vec{n}_1 \cdot \vec{n}_2}{2}. \quad (5.51)$$

$\zeta$  takes values between 0 and 1. In the last step of (5.51) we evaluated  $\zeta$  in a center-of-mass frame where  $p = (p^0, \vec{0})$  and  $z_i = (1, \vec{n}_i)$ . The limit  $\zeta \rightarrow 0$  corresponds to the detector directions  $z_1$  and  $z_2$  becoming parallel, which is described by the light-ray-light-ray OPE discussed in section 5.3. The limit  $\zeta \rightarrow 1$  corresponds to the detectors becoming back-to-back in the frame of  $p$ .

## 5.3 The light-ray-light-ray OPE

### 5.3.1 Summary of computation

In this section, we compute an expansion for

$$\mathbf{L}[\mathcal{O}_1](x, z_1) \mathbf{L}[\mathcal{O}_2](x, z_2) \quad (5.52)$$

as  $z_1 \rightarrow z_2$ . Here, we summarize the key steps of the computation. Our summary will be schematic. We omit details and illustrate calculations using diagrams (which do not capture some subtleties).

The first step is to decompose (5.52) into irreducible representations of the conformal group. As discussed in section 5.2.3, (5.52) transforms like a primary at the point  $x$  with scaling dimension  $(1 - J_1) + (1 - J_2)$ . However, it does not transform irreducibly under the Lorentz group  $\text{SO}(d - 1, 1)$  that fixes  $x$ . The appropriate set of irreducible representations are principal series representations labeled by  $\delta \in \frac{d-2}{2} + i\mathbb{R}$ . To obtain such a representation, we smear the polarizations  $z_1, z_2$  against a kernel  $t_\delta$ <sup>12</sup>

$$\begin{aligned} \mathbb{W}_\delta(x, z_0) &\propto \int Dz_1 Dz_2 \mathbf{L}[\mathcal{O}_1](x, z_1) \mathbf{L}[\mathcal{O}_2](x, z_2) t_\delta(z_1, z_2, z_0) \\ &= \int dx_1 dx_2 Dz_1 Dz_2 L_\delta(x_1, z_1, x_2, z_2; x, z_0) \mathcal{O}_1(x_1) \mathcal{O}_2(x_2), \end{aligned} \quad (5.53)$$

where  $Dz$  is a measure on the projective null cone defined in (5.87). We write  $t_\delta$  explicitly in (5.108).

On the second line of (5.53), we implicitly defined a kernel  $L_\delta$  that combines the light transforms with smearing in  $z_1, z_2$ . We can represent  $L_\delta$  pictorially by

$$1 \begin{array}{c} \nearrow \\ \searrow \end{array} \begin{array}{c} \circ \\ L_\delta \end{array} \begin{array}{c} \longrightarrow \\ \longrightarrow \end{array} \mathcal{O}^L = 1 \begin{array}{c} \longrightarrow \\ \longrightarrow \end{array} \begin{array}{c} \square \\ \mathbf{L} \end{array} \begin{array}{c} \longrightarrow \\ \longrightarrow \end{array} \begin{array}{c} \longrightarrow \\ \longrightarrow \end{array} \begin{array}{c} \longrightarrow \\ \longrightarrow \end{array} \begin{array}{c} \longrightarrow \\ \longrightarrow \end{array} \mathcal{O}^L. \quad (5.54)$$

The incoming arrows labeled 1 and 2 indicate that  $L_\delta$  acts on the representations of  $\mathcal{O}_1, \mathcal{O}_2$ . The outgoing arrow labeled  $\mathcal{O}^L$  indicates that  $L_\delta$  produces an object transforming with the quantum numbers of  $\mathbf{L}[\mathcal{O}]$ , i.e.  $(1 - J, 1 - \Delta)$  where  $\mathcal{O}$  has dimension and spin  $(\Delta, J) = (\delta + 1, J_1 + J_2 - 1)$ . On the right-hand side, the boxes labeled  $\mathbf{L}$  take the light-transform of  $\mathcal{O}_1$  and  $\mathcal{O}_2$ . Then, we split each representation into two lines; the solid blue line denotes the Minkowski position  $x_i$  of the representation, and the dashed red line denotes the null polarization  $z_i$  — equivalently, the position on the celestial sphere. The reason for this split is to accommodate for the next two operations, which act only on either Minkowski or celestial coordinates. The blue triangle represents making the points  $x_i$  coincident. The red three-point kernel represents smearing polarization vectors with  $t_\delta$ .

The next step is to compute matrix elements of  $\mathbb{W}_\delta$ . Because a light-transformed

<sup>12</sup>The actual kernel can also depend on a finite-dimensional representation  $\lambda$  of  $\text{SO}(d - 2)$ , but we suppress that detail here for simplicity.

operator kills the vacuum, we have

$$\begin{aligned} \langle \Omega | \mathcal{O}_4 \mathbb{W}_\delta \mathcal{O}_3 | \Omega \rangle &= \int dx_1 dx_2 D z_1 D z_2 L_\delta \langle \mathcal{O} | \mathcal{O}_4 \mathcal{O}_1 \mathcal{O}_2 \mathcal{O}_3 | \mathcal{O} \rangle \\ &= \int dx_1 dx_2 D z_1 D z_2 L_\delta \langle \mathcal{O} | [\mathcal{O}_4, \mathcal{O}_1] [\mathcal{O}_2, \mathcal{O}_3] | \mathcal{O} \rangle. \end{aligned} \quad (5.55)$$

The appearance of the double commutator suggests that we could relate the matrix elements of  $\mathbb{W}_\delta$  to the Lorentzian inversion formula. To see this relation, first note that by conformal invariance we have

$$\langle \Omega | \mathcal{O}_4 \mathbb{W}_\delta \mathcal{O}_3 | \Omega \rangle = A_b(\delta) \langle 0 | \mathcal{O}_4 \mathbf{L}[\mathcal{O}] \mathcal{O}_3 | 0 \rangle^{(b)}, \quad (5.56)$$

where  $\langle 0 | \mathcal{O}_4 \mathcal{O} \mathcal{O}_3 | 0 \rangle^{(b)}$  are conformally-invariant three-point structures for the given representations, and in (5.56) we have their light-transforms. The different structures have a label  $b$ , and summation over  $b$  is implicit. Diagrammatically, we can express (5.55) and (5.56) as

The diagrammatic equation (5.57) shows two structures. On the left, a circle labeled 'dDisc[g]' has two incoming lines from the left labeled '3' and '4', and two outgoing lines to the right labeled '1' and '2'. These lines connect to a circle labeled 'L\_\delta', which then has a single outgoing line labeled 'O^L'. This is followed by an equals sign and a multiplication sign. On the right, a circle labeled 'b' has two incoming lines from the left labeled '3' and '4', and a single outgoing line labeled 'O'. This line connects to a square labeled 'L', which then has a single outgoing line labeled 'O^L'. The entire right-hand side is enclosed in large parentheses with a comma and the label '(5.57)'.

where “dDisc” indicates the double-commutator.

The function  $A_b(\delta)$  contains the matrix elements we are interested in. To extract it, we pair with a dual structure (the pairing will be defined in (5.95))

$$A_b(\delta) = (\langle \Omega | \mathcal{O}_4 \mathbb{W}_\delta \mathcal{O}_3 | \Omega \rangle, (\langle 0 | \mathcal{O}_4 \mathbf{L}[\mathcal{O}] \mathcal{O}_3 | 0 \rangle^{(a)})^{-1}). \quad (5.58)$$

The dual structure  $(\langle 0 | \mathcal{O}_4 \mathbf{L}[\mathcal{O}] \mathcal{O}_3 | 0 \rangle^{(a)})^{-1}$  is the one that satisfies

The diagrammatic equation (5.59) shows two structures enclosed in large parentheses. The first structure is a circle labeled 'b' with two incoming lines from the left labeled '3' and '4', and a single outgoing line labeled 'O'. This line connects to a square labeled 'L', which then has a single outgoing line labeled 'O^L'. The second structure is identical to the first, but the circle is labeled 'a' and is enclosed in a dashed green circle with a '-1' superscript. The entire right-hand side is followed by an equals sign and the label 'delta\_a^b' with a superscript 'b' and a subscript 'a', and the label '(5.59)'.

We denote the operation of inverting a structure by an enclosing green circle,  $\text{green circle}^{-1}$ ,

suggestively labeled by a green inverse ( $^{-1}$ ). In pictorial language, (5.58) is

$$A_b(\delta) = \left( \begin{array}{c} \text{Diagram with } d\text{Disc}[g], L_\delta, \mathcal{L}, b \text{ and lines } 1, 2, 3, 4 \end{array} \right). \quad (5.60)$$

This is a four-point pairing between the double-commutator and a particular conformal block, as can be seen by cutting along the lines of the operators 1, 2, 3, and 4:

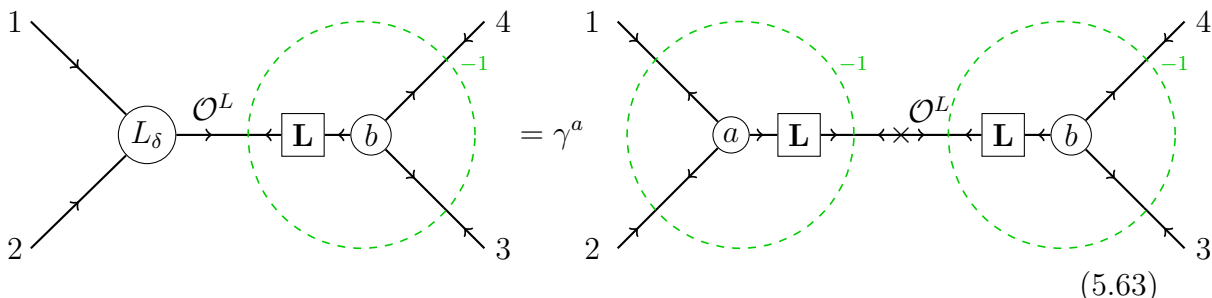
$$A_b(\delta) = \left( \begin{array}{c} \text{Diagram with } d\text{Disc}[g] \text{ and lines } 1, 2, 3, 4 \end{array}, \begin{array}{c} \text{Diagram with } L_\delta, \mathcal{L}, b \text{ and lines } 1, 2, 3, 4 \end{array} \right). \quad (5.61)$$

The generalized Lorentzian inversion formula [28] also has this form,

$$C_{ab}^+(\Delta, J) + C_{ab}^-(\Delta, J) = \left( \begin{array}{c} \text{Diagram with } d\text{Disc}[g] \text{ and lines } 1, 2, 3, 4 \end{array}, \begin{array}{c} \text{Diagram with } a, \mathcal{L}, \mathcal{L}, b \text{ and lines } 1, 2, 3, 4 \end{array} \right). \quad (5.62)$$

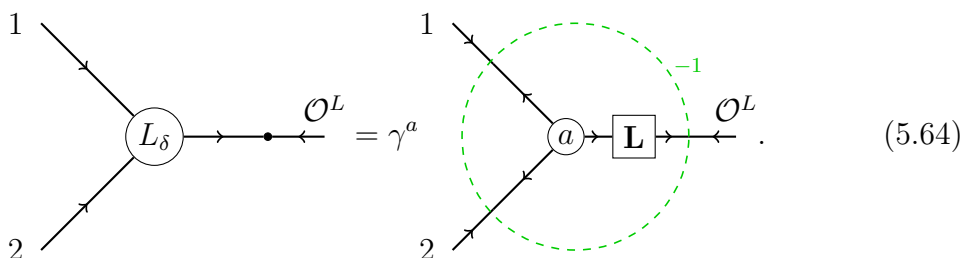
Here, the cross represents the formation of a conformal block from a pair of three-point structures by summing over descendent operators and dividing by their norms. The norms are computed using a two-point structure, which in this case is  $\langle \mathbf{L}[\mathcal{O}]\mathbf{L}[\mathcal{O}] \rangle^{-1}$ , defined in (5.96).

Therefore, we can relate  $A_b(\delta)$  to  $C_{ab}^\pm(\delta+1, J_1+J_2-1)$  by relating the two conformal blocks in (5.61) and (5.62),



$$(5.63)$$

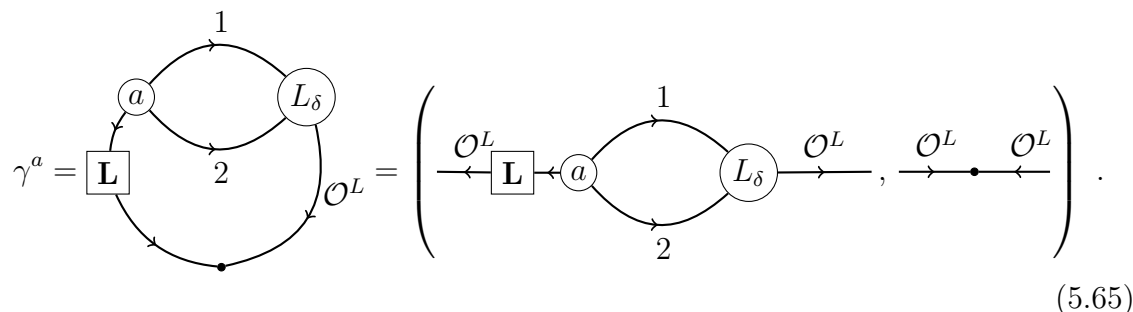
Both conformal blocks are obtained by gluing three-point structures. The structure appearing on the right is the same for both blocks, so we only need to relate the structures on the left,



$$(5.64)$$

The inverse of the cross on the right-hand side of (5.63) is integration against a two-point structure.<sup>13</sup> Here, the two-point structure is indicated by a dot on the left-hand side of (5.64). The operation of integrating against a two-point structure is a Lorentzian shadow transform, which changes the quantum numbers from  $(1-J, 1-\Delta)$  (labeled as  $\mathcal{O}^L$  with an outgoing arrow) to  $(J+d-1, \Delta-d+1)$  (labeled as  $\mathcal{O}^L$  with an ingoing arrow).

Thus, we can compute  $\gamma^a$  by pairing both sides of (5.64) with the structure  $\langle \mathcal{O}_4 \mathbf{L}[\mathcal{O}] \mathcal{O}_3 \rangle^{(a)}$ ,



$$(5.65)$$

Here, we rearranged our diagram into a pairing of two-point structures. Finally, we must compute the bubble diagram on the right-hand side. After substituting the

<sup>13</sup>The correct two-point structure is actually  $\langle \mathbf{L}[\mathcal{O}] \mathbf{L}[\mathcal{O}] \rangle^{-1}$ , but this detail is not reflected in the diagrams for the sake of simplicity.

definition of  $L_\delta$  (5.54), we obtain an expression involving a triple light transform of the three-point structure  $a$ ,

$$(5.66)$$

The superscripts  $\mathbf{L}^\pm$  are related to a subtlety not captured in the diagrams. The double-discontinuity produces additional  $\theta$ -functions in the expression for the block on the right-hand side of (5.61). On the left-hand side of (5.64), these theta functions modify the kernel  $L_\delta$  so that the light-transforms become “half light-transforms”  $\mathbf{L}^\pm$ , i.e. null integrals over semi-infinite lines. These are what appear in (5.66).<sup>14</sup>

It turns out that the result of (5.66), and therefore also  $\gamma^a$ , is remarkably simple. In section 5.3.4.4, we conjecture a formula for it in the case of an arbitrary three-point structure  $\langle 0|\mathcal{O}_1\mathcal{O}_2|0\rangle^{(a)}$  of operators in arbitrary representations. Putting everything together, we obtain

$$A_b(\delta) = \gamma^a(C_{ab}^+(\delta + 1, J_1 + J_2 - 1) + C_{ab}^-(\delta + 1, J_1 + J_2 - 1)), \quad (5.67)$$

which can be written

$$\langle \Omega|\mathcal{O}_4\mathbb{W}_\delta\mathcal{O}_3|\Omega\rangle = -\gamma^a\langle \Omega|\mathcal{O}_4\left(\mathbb{O}_{\delta+1, J_1+J_2-1(a)}^+ + \mathbb{O}_{\delta+1, J_1+J_2-1(a)}^-\right)\mathcal{O}_3|\Omega\rangle. \quad (5.68)$$

This expresses matrix elements of the smeared product  $\mathbb{W}_\delta$  in terms of matrix elements of light-ray operators. The smearing can be undone by suitably integrating over  $\delta$ ,

$$\langle \Omega|\mathcal{O}_4\mathbf{L}[\mathcal{O}_1](x, z_1)\mathbf{L}[\mathcal{O}_2](x, z_2)\mathcal{O}_3|\Omega\rangle = \int d\delta \mathcal{C}_\delta(z_1, z_2, \partial_z)\langle \Omega|\mathcal{O}_4\mathbb{W}_\delta(x, z)\mathcal{O}_3|\Omega\rangle, \quad (5.69)$$

where  $\mathcal{C}_\delta$  is a differential operator. Lifting this to an operator equation, we have

$$\begin{aligned} & \mathbf{L}[\mathcal{O}_1](x, z_1)\mathbf{L}[\mathcal{O}_2](x, z_2) \\ &= -\int d\delta \gamma^a \mathcal{C}_\delta(z_1, z_2, \partial_z) \left( \mathbb{O}_{\delta+1, J_1+J_2-1(a)}^+(x, z) + \mathbb{O}_{\delta+1, J_1+J_2-1(a)}^-(x, z) \right). \end{aligned} \quad (5.70)$$

Finally, the  $\delta$ -contour can be closed to the right, picking up a sum over light-ray operators, as discussed in section 5.5.2.

<sup>14</sup>If we took three full light-transforms of a time-ordered three-point structure in an appropriate causal configuration, we would get two pieces, one of which would be the object appearing in (5.66), and the other would differ by a permutation.



### 5.3.2 Review: light-ray operators and the Lorentzian inversion formula

Let us now proceed with the detailed computation. The objects that will ultimately appear in the OPE expansion of  $\mathbf{L}[\mathcal{O}_1](x, z_1)\mathbf{L}[\mathcal{O}_2](x, z_2)$  are light-ray operators [28]. In this section, we collect some facts about these operators that will be needed below.

For simplicity, consider first the case where  $\mathcal{O}_1 = \phi_1$  and  $\mathcal{O}_2 = \phi_2$  are scalars. Light-ray operators are defined by starting with a bi-local object that transforms as a primary under the conformal group  $\widetilde{\text{SO}}(d, 2)$ ,

$$\mathbb{O}_{\Delta, J}^{\pm}(x, z) = \int d^d x_1 d^d x_2 K_{\Delta, J}^{\pm}(x_1, x_2, x, z) \phi_1(x_1) \phi_2(x_2). \quad (5.71)$$

The object  $\mathbb{O}_{\Delta, J}^{\pm}$  has dimension  $1 - J$  and spin  $1 - \Delta$ , which are the quantum numbers of the light-transform of an operator with dimension  $\Delta$  and spin  $J$ . The  $\pm$  sign is the signature, which is the eigenvalue under a combination of CRT and Hermitian conjugation, as discussed in section 5.2.1.

The object  $\mathbb{O}_{\Delta, J}^{\pm}$  is meromorphic in  $\Delta$  and  $J$  and has poles of the form

$$\mathbb{O}_{\Delta, J}^{\pm}(x, z) \sim \frac{1}{\Delta - \Delta_i^{\pm}(J)} \mathbb{O}_{i, J}^{\pm}(x, z). \quad (5.72)$$

Its residues  $\mathbb{O}_{i, J}^{\pm}$  are light-ray operators. Light-ray operators are analytic continuations in spin of light-transforms of local operators. When  $J$  is a nonnegative integer, we have

$$\mathbb{O}_{i, J}^{(-1)^J} = f_{12\mathcal{O}_{i, J}} \mathbf{L}[\mathcal{O}_{i, J}], \quad J \in \mathbb{Z}_{\geq 0}. \quad (5.73)$$

Here,  $\mathcal{O}_{i, J}$  is a spin- $J$  operator appearing in the  $\phi_1 \times \phi_2$  OPE with coefficient  $f_{12\mathcal{O}_{i, J}}$ , and  $i$  labels different Regge trajectories. Note that the even-signature light-ray operators  $\mathbb{O}_{i, J}^+$  are analytic continuations in  $J$  of light-transformed even-spin operators, while  $\mathbb{O}_{i, J}^-$  are analytic continuations in  $J$  of light-transformed odd-spin operators.

Matrix elements of light-ray operators can be computed via a Lorentzian inversion formula. Let  $\phi_3, \phi_4$  be primary scalars for simplicity. A time-ordered correlator involving the object  $\mathbb{O}_{\Delta, J}^{\pm}$  is given by

$$\langle \phi_4 \mathbb{O}_{\Delta, J}^{\pm}(x, z) \phi_3 \rangle_{\Omega} = -C^{\pm}(\Delta, J) \langle 0 | \phi_4 \mathbf{L}[\mathcal{O}](x, z) \phi_3 | 0 \rangle. \quad (5.74)$$

We use the shorthand notation that  $\phi_i$  is at position  $x_i$  unless otherwise specified. We also use the notation from [28] where correlators in the state  $|\Omega\rangle$  are physical, while correlators in the state  $|0\rangle$  are conformally-invariant structures for the given

representations. The structure on the right-hand side of (5.74) is the light-transform of the standard three-point structure for two scalars and a spin- $J$  operator, analytically continued in  $J$ ,

$$\begin{aligned} & \langle 0 | \phi_4 \mathbf{L}[\mathcal{O}](x_0, z_0) \phi_3 | 0 \rangle \\ &= \frac{L(\phi_3 \phi_4[\mathcal{O}]) (2V_{0,34})^{1-\Delta}}{(x_{34}^2)^{\frac{\Delta_3+\Delta_4-(1-J)-(1-\Delta)}{2}} (x_{30}^2)^{\frac{\Delta_3+(1-J)-\Delta_4+(1-\Delta)}{2}} (-x_{40}^2)^{\frac{\Delta_4+(1-J)-\Delta_3+(1-\Delta)}{2}}}. \end{aligned} \tag{5.75}$$

The coefficient  $L(\phi_3 \phi_4[\mathcal{O}])$  is given in (5.45).

In (5.74), the time-ordering acts on  $\phi_1, \phi_2$  inside  $\mathbb{O}_{\Delta, J}^\pm$ . Thus the object  $\mathbb{O}_{\Delta, J}^\pm$  is not really an operator. However, its singularities as a function of  $\Delta$  come only from the region where  $\phi_4$  acts on the future vacuum and  $\phi_3$  acts on the past vacuum, so upon taking residues, we obtain a genuine operator

$$\begin{aligned} \langle \Omega | \phi_4 \mathbb{O}_{i, J}^\pm(x, z) \phi_3 | \Omega \rangle &= \text{Res}_{\Delta=\Delta_i^\pm(J)} \langle \phi_4 \mathbb{O}_{\Delta, J}^\pm(x, z) \phi_3 \rangle_\Omega \\ &= - \text{Res}_{\Delta=\Delta_i^\pm(J)} C^\pm(\Delta, J) \langle 0 | \phi_4 \mathbf{L}[\mathcal{O}](x, z) \phi_3 | 0 \rangle. \end{aligned} \tag{5.76}$$

The coefficient function  $C^\pm(\Delta, J)$  is given by Caron-Huot’s formula [25]

$$\begin{aligned} C^\pm(\Delta, J) &= \frac{\kappa_{\Delta+J}}{4} \left[ \int_0^1 \int_0^1 \frac{dz d\bar{z}}{z^2 \bar{z}^2} \left| \frac{\bar{z}-z}{z\bar{z}} \right|^{d-2} \text{dDisc}_t[g(z, \bar{z})] G_{J+d-1, \Delta-d+1}^{\tilde{\Delta}_i}(z, \bar{z}) \right. \\ &\quad \left. \pm \int_{-\infty}^0 \int_{-\infty}^0 \frac{dz d\bar{z}}{z^2 \bar{z}^2} \left| \frac{\bar{z}-z}{z\bar{z}} \right|^{d-2} \text{dDisc}_u[g(z, \bar{z})] \widehat{G}_{J+d-1, \Delta-d+1}^{\tilde{\Delta}_i}(z, \bar{z}) \right], \end{aligned} \tag{5.77}$$

where

$$\kappa_{\Delta+J} = \frac{\Gamma(\frac{\Delta+J+\Delta_1-\Delta_2}{2}) \Gamma(\frac{\Delta+J-\Delta_1+\Delta_2}{2}) \Gamma(\frac{\Delta+J+\Delta_3-\Delta_4}{2}) \Gamma(\frac{\Delta+J-\Delta_3+\Delta_4}{2})}{2\pi^2 \Gamma(\Delta+J) \Gamma(\Delta+J-1)}. \tag{5.78}$$

Here, we have defined a stripped four-point function  $g(z, \bar{z})$ , which is a function of conformal cross-ratios<sup>15</sup>

$$\begin{aligned} \langle \phi_1 \phi_2 \phi_3 \phi_4 \rangle_\Omega &= T^{\Delta_i}(x_i) g(z, \bar{z}) \\ T^{\Delta_i}(x_i) &\equiv \frac{1}{(x_{12}^2)^{\frac{\Delta_1+\Delta_2}{2}} (x_{34}^2)^{\frac{\Delta_3+\Delta_4}{2}}} \left( \frac{x_{14}^2}{x_{24}^2} \right)^{\frac{\Delta_2-\Delta_1}{2}} \left( \frac{x_{14}^2}{x_{13}^2} \right)^{\frac{\Delta_3-\Delta_4}{2}}. \end{aligned} \tag{5.79}$$

<sup>15</sup>We use the letter  $z$  both for future-pointing null vectors and for conformal cross-ratios. We hope that this does not cause confusion.

The  $t$ -channel double-discontinuity  $\text{dDisc}_t$  is defined by

$$\begin{aligned} -2\text{dDisc}_t[g](z, \bar{z}) &\equiv \frac{\langle \Omega | [\phi_4, \phi_1] [\phi_2, \phi_3] | \Omega \rangle}{|T^{\Delta_i}(x_i)|} \\ &= -2 \cos(\pi\phi) g(z, \bar{z}) + e^{i\pi\phi} g^\circ(z, \bar{z}) + e^{-i\pi\phi} g^\circ(z, \bar{z}), \\ \phi &= \frac{\Delta_2 - \Delta_1 + \Delta_3 - \Delta_4}{2}, \end{aligned} \quad (5.80)$$

where  $g^\circ$  or  $g^\circ$  indicates we should take  $\bar{z}$  around 1 in the direction shown, leaving  $z$  held fixed. Similarly,

$$\begin{aligned} -2\text{dDisc}_u[g](z, \bar{z}) &\equiv \frac{\langle \Omega | [\phi_4, \phi_2] [\phi_1, \phi_3] | \Omega \rangle}{|T^{\Delta_i}(x_i)|} \\ &= -2 \cos(\pi\phi') g(z, \bar{z}) + e^{i\pi\phi'} g^\circ(z, \bar{z}) + e^{-i\pi\phi'} g^\circ(z, \bar{z}), \\ \phi' &= \frac{\Delta_2 - \Delta_1 + \Delta_4 - \Delta_3}{2}. \end{aligned} \quad (5.81)$$

where now  $g^\circ$  or  $g^\circ$  indicates we should take  $\bar{z}$  around  $-\infty$  in the direction shown, leaving  $z$  held fixed.

Finally,  $G_{\Delta, J}^{\tilde{\Delta}_i}(z, \bar{z})$  denotes a conformal block for external scalars with dimensions  $\tilde{\Delta}_i \equiv d - \Delta_i$ , exchanging an operator with dimension  $\Delta$  and spin  $J$ . In our conventions, it behaves as  $z^{\frac{\Delta-J}{2}} \bar{z}^{\frac{\Delta+J}{2}}$  for positive cross-ratios satisfying  $z \ll \bar{z} \ll 1$ . Similarly,  $\widehat{G}_{\Delta, J}^{\tilde{\Delta}_i}(z, \bar{z})$  is a solution to the Casimir equation that behaves like  $(-z)^{\frac{\Delta-J}{2}} (-\bar{z})^{\frac{\Delta+J}{2}}$  for negative cross-ratios satisfying  $|z| \ll |\bar{z}| \ll 1$ . In Caron-Huot's formula (5.77),  $G$  and  $\widehat{G}$  appear with dimension and spin swapped according to  $(\Delta, J) \rightarrow (J+d-1, \Delta-d+1)$ .

### 5.3.2.1 More general representations

Before generalizing to non-scalar  $\mathcal{O}_1, \mathcal{O}_2$ , we must establish some notation for conformal representations. A primary operator  $\mathcal{O}$  is labeled by a dimension  $\Delta$  and a representation  $\rho$  of  $\text{SO}(d-1, 1)$ , which we can think of as a list of weights under the Cartan subalgebra of  $\text{SO}(d-1, 1)$ .

When  $\mathcal{O}$  is local,  $\rho$  is finite-dimensional. In this case, we define shadow and Hermitian conjugate representations to have weights

$$\begin{aligned} \tilde{\mathcal{O}} &: (d - \Delta, \rho^R), \\ \mathcal{O}^\dagger &: (\Delta, (\rho^R)^*), \end{aligned} \quad (5.82)$$

where  $\rho^R$  denotes the reflection of  $\rho$  and  $(\rho^R)^*$  is the dual of  $\rho^R$ . The conjugate shadow representation  $\tilde{\mathcal{O}}^\dagger$  has weights

$$\tilde{\mathcal{O}}^\dagger : (d - \Delta, \rho^*), \quad (5.83)$$

and thus admits a conformally-invariant pairing with  $\mathcal{O}$ :

$$\int d^d x \mathcal{O}(x) \tilde{\mathcal{O}}^\dagger(x), \quad (5.84)$$

where the  $\text{SO}(d-1, 1)$  indices of  $\mathcal{O}(x)$  and  $\tilde{\mathcal{O}}^\dagger(x)$  are implicitly contracted.

For continuous-spin operators,  $\rho$  is no longer finite-dimensional. It has weights  $\rho = (J, \lambda)$ , where  $J \in \mathbb{C}$  is spin and  $\lambda$  is a finite-dimensional representation of  $\text{SO}(d-2)$ . We can think of  $J$  as the length of the first row of the Young diagram of  $\rho$ , while  $\lambda$  encodes the remaining rows. Altogether, we specify the multiplet of  $\mathcal{O}$  by a triplet  $(\Delta, J, \lambda)$ .

Operators with non-integer  $J$  admit a different kind of conformally-invariant pairing

$$\int d^d x D^{d-2} z \mathcal{O}(x, z) \mathcal{O}^{S^\dagger}(x, z). \quad (5.85)$$

Here,  $\mathcal{O}^{S^\dagger}$  has weights

$$\mathcal{O}^{S^\dagger} : (d - \Delta, 2 - d - J, \lambda^*). \quad (5.86)$$

In (5.85), we implicitly contract the  $\text{SO}(d-2)$  indices in the representations  $\lambda$  and  $\lambda^*$ . The measure  $D^{d-2} z$  is defined by

$$D^{d-2} z \equiv \frac{d^d z \delta(z^2) \theta(z^0)}{\text{vol } \mathbb{R}_+}, \quad (5.87)$$

where  $\mathbb{R}_+$  acts by rescaling  $z$ . Note that  $D^{d-2} z \mathcal{O}(x, z) \mathcal{O}^{S^\dagger}(x, z)$  is homogeneous of degree 0 in  $z$ , so that the integral is well-defined. Using the pairings (5.84) for integer-spin operators and (5.85) for continuous-spin operators, we can construct conformally-invariant pairings between two- and three-point structures, as we will see below.

In the diagrams in section 5.3.1 and below, we use an outgoing arrow labeled  $\mathcal{O}$  to denote a representation  $\mathcal{O}$ , and an ingoing arrow labeled  $\mathcal{O}$  to denote the dual representation, either  $\tilde{\mathcal{O}}^\dagger$  or  $\mathcal{O}^{S^\dagger}$  as appropriate to  $\mathcal{O}$ . Joining lines represents the conformally-invariant pairing appropriate for the representations.

When  $\mathcal{O}_1, \mathcal{O}_2$  are not scalars, the OPE  $\mathcal{O}_1 \times \mathcal{O}_2$  can contain operators  $\mathcal{O}$  with weights  $(\Delta, J, \lambda)$ , where  $\lambda$  is nontrivial. In addition,  $\mathcal{O}$  can appear with multiple tensor structures. Physical three-point correlators are linear combinations of the possible structures, labeled by indices  $a, b$

$$\begin{aligned} \langle \mathcal{O}_1 \mathcal{O}_2 \mathcal{O}^\dagger \rangle_\Omega &= f_{12\mathcal{O}^\dagger(a)} \langle \mathcal{O}_1 \mathcal{O}_2 \mathcal{O}^\dagger \rangle^{(a)}, \\ \langle \mathcal{O}_3 \mathcal{O}_4 \mathcal{O} \rangle_\Omega &= f_{34\mathcal{O}(b)} \langle \mathcal{O}_3 \mathcal{O}_4 \mathcal{O} \rangle^{(b)}. \end{aligned} \quad (5.88)$$

(Sums over  $a, b$  are implicit.) Following the notation of [28] (see also appendix D.1), we use the subscript  $\Omega$  to distinguish physical correlators from conformally-invariant structures.

Thus, when  $\mathcal{O}_1, \mathcal{O}_2$  are not scalars,  $\mathbb{O}_{\Delta, J}^{\pm}$  gets generalized to have an additional  $\text{SO}(d-2)$  representation label  $\lambda$  and structure label  $a$ :  $\mathbb{O}_{\Delta, J, \lambda(a)}^{\pm}$ . It has residues

$$\mathbb{O}_{\Delta, J, \lambda(a)}^{\pm} \sim \frac{1}{\Delta - \Delta_i^{\pm}(J, \lambda)} \mathbb{O}_{i, J, \lambda(a)}, \quad (5.89)$$

which for integer  $J$  and signature  $\pm = (-1)^J$  become light-transforms of local operators:

$$\mathbb{O}_{i, J, \lambda(a)}^{(-1)^J} = f_{12} \mathcal{O}_{i, J, \lambda(a)}^{\dagger} \mathbf{L}[\mathcal{O}_{i, J, \lambda}], \quad J \in \mathbb{Z}_{\geq 0}. \quad (5.90)$$

Let  $\mathcal{O}_3, \mathcal{O}_4$  be primary operators (not necessarily scalars). Three-point functions containing  $\mathbb{O}_{i, J, \lambda(a)}^{\pm}$  are given by

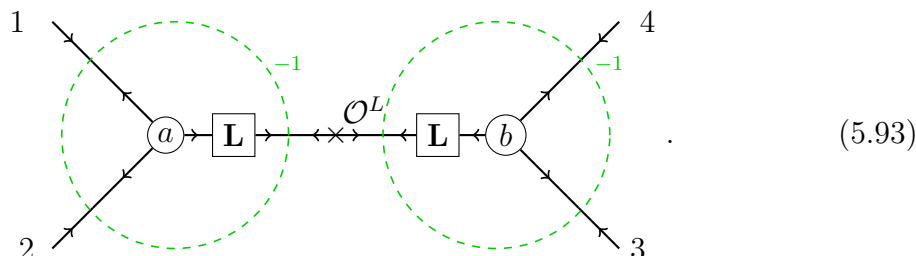
$$\begin{aligned} \langle \mathcal{O}_4 \mathbb{O}_{\Delta, J, \lambda(a)}^{\pm}(x, z) \mathcal{O}_3 \rangle_{\Omega} &= -C_{ab}^{\pm}(\Delta, J, \lambda) \langle 0 | \mathcal{O}_4 \mathbf{L}[\mathcal{O}](x, z) \mathcal{O}_3 | 0 \rangle^{(b)}, \\ \langle \Omega | \mathcal{O}_4 \mathbb{O}_{i, J, \lambda(a)}^{\pm}(x, z) \mathcal{O}_3 | \Omega \rangle &= - \text{Res}_{\Delta = \Delta_i^{\pm}(J, \lambda)} C_{ab}^{\pm}(\Delta, J, \lambda) \langle 0 | \mathcal{O}_4 \mathbf{L}[\mathcal{O}](x, z) \mathcal{O}_3 | 0 \rangle^{(b)}. \end{aligned} \quad (5.91)$$

(We suppress spin indices on  $\mathcal{O}_3, \mathcal{O}_4$  and only indicate the  $x, z$  dependence of  $\mathbb{O}$ .) The coefficients  $C_{ab}^{\pm}(\Delta, J, \lambda)$  are given by the generalized Lorentzian inversion formula

$$\begin{aligned} &C_{ab}^{\pm}(\Delta, J, \lambda) \\ &= \frac{-1}{2\pi i} \int_{\substack{4 > 1 \\ 2 > 3}} \frac{d^d x_1 \cdots d^d x_4}{\text{vol}(\widetilde{\text{SO}}(d, 2))} \langle \mathcal{O} | [\mathcal{O}_4, \mathcal{O}_1] [\mathcal{O}_2, \mathcal{O}_3] | \mathcal{O} \rangle \\ &\quad \times \mathcal{T}_2^{-1} \mathcal{T}_4^{-1} \frac{(\mathcal{T}_2 \langle 0 | \mathcal{O}_2 \mathbf{L}[\mathcal{O}^{\dagger}] \mathcal{O}_1 | 0 \rangle^{(a)})^{-1} (\mathcal{T}_4 \langle 0 | \mathcal{O}_4 \mathbf{L}[\mathcal{O}] \mathcal{O}_3 | 0 \rangle^{(b)})^{-1}}{\langle \mathbf{L}[\mathcal{O}] \mathbf{L}[\mathcal{O}^{\dagger}] \rangle^{-1}} \\ &\pm \frac{-1}{2\pi i} \int_{\substack{4 > 2 \\ 1 > 3}} \frac{d^d x_1 \cdots d^d x_4}{\text{vol}(\widetilde{\text{SO}}(d, 2))} \langle \mathcal{O} | [\mathcal{O}_4, \mathcal{O}_2] [\mathcal{O}_1, \mathcal{O}_3] | \mathcal{O} \rangle \\ &\quad \times \mathcal{T}_1^{-1} \mathcal{T}_4^{-1} \frac{(\mathcal{T}_1 \langle 0 | \overline{\mathcal{O}}_2^{\dagger} \mathbf{L}[\mathcal{O}^{\dagger}](\bar{x}, -\bar{z}) \overline{\mathcal{O}}_1^{\dagger} | 0 \rangle^{(a)})^{-1} (\mathcal{T}_4 \langle 0 | \mathcal{O}_4 \mathbf{L}[\mathcal{O}] \mathcal{O}_3 | 0 \rangle^{(b)})^{-1}}{\langle \mathbf{L}[\mathcal{O}] \mathbf{L}[\mathcal{O}^{\dagger}] \rangle^{-1}}. \end{aligned} \quad (5.92)$$

A cartoon diagram for the first integral on the right hand side is given in (5.62). Let us describe the ingredients in (5.92) in detail. Again, we use the shorthand notation that  $\mathcal{O}_i$  is at position  $x_i$ . The integral is over a Lorentzian configuration where  $4 > 1$ ,  $2 > 3$ , and all other pairs of points are spacelike separated. In terms of cross-ratios, this is the same as the integration region  $0 < z, \bar{z} < 1$  in (5.77).

The object in the second line of (5.92) is schematic notation for a conformal block obtained by merging the two three-point structures  $(\mathcal{T}_2\langle 0|\mathcal{O}_2\mathbf{L}[\mathcal{O}^\dagger]\mathcal{O}_1|0\rangle^{(a)})^{-1}$  and  $(\mathcal{T}_4\langle 0|\mathcal{O}_4\mathbf{L}[\mathcal{O}]\mathcal{O}_3|0\rangle^{(b)})^{-1}$ , using the two-point structure  $\langle \mathbf{L}[\mathcal{O}]\mathbf{L}[\mathcal{O}^\dagger]\rangle^{-1}$ . (It is not simply a ratio of three-point and two-point structures.) The precise merging procedure is described in [28] — it is essentially the usual procedure of summing over products of descendent three-point functions to obtain a conformal block, generalized to continuous spin. We will see some examples below. Pictorially, the block is



The three-point structures making up the conformal block are defined by

$$\begin{aligned} \left( (\mathcal{T}_2\langle 0|\mathcal{O}_2\mathbf{L}[\mathcal{O}^\dagger]\mathcal{O}_1|0\rangle^{(a)})^{-1}, \mathcal{T}_2\langle 0|\mathcal{O}_2\mathbf{L}[\mathcal{O}^\dagger]\mathcal{O}_1|0\rangle^{(c)} \right)_L &= \delta_a^c, \\ \left( (\mathcal{T}_4\langle 0|\mathcal{O}_4\mathbf{L}[\mathcal{O}]\mathcal{O}_3|0\rangle^{(b)})^{-1}, \mathcal{T}_4\langle 0|\mathcal{O}_4\mathbf{L}[\mathcal{O}]\mathcal{O}_3|0\rangle^{(d)} \right)_L &= \delta_b^d, \end{aligned} \quad (5.94)$$

where  $\mathcal{T}_i$  is translation to the next Minkowski patch discussed in section 5.2.2. Here,  $(\cdot, \cdot)_L$  is a conformally-invariant pairing defined by using (5.84) for  $\mathcal{O}_1, \mathcal{O}_2$  and (5.85) for  $\mathcal{O}$ :

$$\begin{aligned} & \left( \langle \mathcal{O}_1\mathcal{O}_2\mathcal{O} \rangle, \langle \tilde{\mathcal{O}}_1^\dagger\tilde{\mathcal{O}}_2^\dagger\mathcal{O}^{\text{St}} \rangle \right)_L \\ & \equiv \int_{\substack{2 < 1 \\ x \approx 1, 2}} \frac{d^d x_1 d^d x_2 d^d x D^{d-2} z}{\text{vol}(\widetilde{\text{SO}}(d, 2))} \langle \mathcal{O}_1(x_1)\mathcal{O}_2(x_2)\mathcal{O}(x, z) \rangle \langle \tilde{\mathcal{O}}_1^\dagger(x_1)\tilde{\mathcal{O}}_2^\dagger(x_2)\mathcal{O}^{\text{St}}(x, z) \rangle \\ & = \frac{1}{2^{2d-2} \text{vol}(\text{SO}(d-2))} \frac{\langle \mathcal{O}_1(e^0)\mathcal{O}_2(0)\mathcal{O}(\infty, z) \rangle \langle \tilde{\mathcal{O}}_1^\dagger(e^0)\tilde{\mathcal{O}}_2^\dagger(0)\mathcal{O}^{\text{St}}(\infty, z) \rangle}{(-2z \cdot e^0)^{2-d}}. \end{aligned} \quad (5.95)$$

The notation  $1/\text{vol}(\widetilde{\text{SO}}(d, 2))$ , means that the integral should be gauge-fixed using the Fadeev-Popov procedure. To obtain the last line, we used  $\widetilde{\text{SO}}(d, 2)$  transformations to gauge-fix  $x_2 = 0, x_1 = e^0, x = \infty$ , where  $e^0$  is a unit-vector in the time direction. Finite-dimensional Lorentz indices are implicitly contracted between the two three-point structures.

The two-point structure in the denominator of (5.92) is defined by

$$\left( \langle \mathbf{L}[\mathcal{O}]\mathbf{L}[\mathcal{O}^\dagger] \rangle^{-1}, \langle \mathbf{L}[\mathcal{O}]\mathbf{L}[\mathcal{O}^\dagger] \rangle \right)_L = 1. \quad (5.96)$$

Here,  $\langle \mathbf{L}[\mathcal{O}]\mathbf{L}[\mathcal{O}^\dagger] \rangle$  is the double light-transform of a time-ordered two-point structure. Even though the light-transform of an operator annihilates the vacuum, the light-transform of a time-ordered structure is delta-function supported. After light-transforming again, we obtain a two-point structure that is nonzero at separated points. These details are explained in [28]. The Lorentzian two-point pairing is given by

$$\begin{aligned}
& \frac{(\langle \mathcal{O}\mathcal{O}^\dagger \rangle, \langle \mathcal{O}^S\mathcal{O}^{S\dagger} \rangle)_L}{\text{vol}(\text{SO}(1,1))^2} \\
& \equiv \int_{x_1 \approx x_2} \frac{d^d x_1 d^d x_2 D^{d-2} z_1 D^{d-2} z_2}{\text{vol}(\widetilde{\text{SO}}(d,2))} \langle \mathcal{O}^a(x_1, z_1) \mathcal{O}^{b\dagger}(x_2, z_2) \rangle \langle \mathcal{O}_b^S(x_2, z_2) \mathcal{O}_a^{S\dagger}(x_1, z_1) \rangle, \\
& = \frac{\langle \mathcal{O}^a(0, z_1) \mathcal{O}^{b\dagger}(\infty, z_2) \rangle \langle \mathcal{O}_b^S(\infty, z_2) \mathcal{O}_a^{S\dagger}(0, z_1) \rangle}{2^{2d-2} \text{vol}(\text{SO}(d-2))} \frac{1}{(-2z_1 \cdot z_2)^{2-d}}. \tag{5.97}
\end{aligned}$$

In the last line, we gauge-fixed  $x_1 = 0, x_2 = \infty$ .

The last line of (5.92) includes a three-point structure that has been acted on by a combination of CRT and Hermitian conjugation,

$$\begin{aligned}
\overline{\mathcal{O}_i}^\dagger & \equiv ((\text{CRT})\mathcal{O}_i(\text{CRT}))^\dagger, \\
\bar{x} & = (-x^0, -x^1, x^2, \dots, x^{d-1}), \\
\bar{z} & = (-z^0, -z^1, z^2, \dots, z^{d-1}). \tag{5.98}
\end{aligned}$$

The role of this term is to ensure that  $\mathbb{O}^\pm$  has the correct signature  $\pm 1$ . We give more details on this term in appendix D.3.

### 5.3.3 Harmonic analysis on the celestial sphere

Consider a product of light-transforms of local operators, placed at the same space-time point

$$\mathbf{L}[\mathcal{O}_1](x, z_1) \mathbf{L}[\mathcal{O}_2](x, z_2). \tag{5.99}$$

For simplicity, we take  $\mathcal{O}_1, \mathcal{O}_2$  to be traceless symmetric tensors. Each light-transformed operator has dimension  $1 - J_i$ , and thus the product (5.99) transforms like an operator with dimension  $(1 - J_1) + (1 - J_2) = 1 - (J_1 + J_2 - 1)$  located at  $x$ .

We would like to additionally decompose (5.99) into irreducible representations of the Lorentz group that fixes  $x$ . To do so, we can use harmonic analysis [82] (or ‘‘conglomeration’’ [87]) for  $\text{SO}(d-1, 1)$ , treating it as a Euclidean conformal group in  $d-2$  dimensions. Harmonic analysis for  $\text{SO}(d+1, 1)$  was reviewed in [194]. In this section, we collect some of the needed ingredients from [194], replacing  $d \rightarrow d-2$ .

The  $\text{SO}(d-1, 1)$  representations that will appear are  $d-2$ -dimensional operator representations  $\mathcal{P}_{\delta,\lambda}$  with scaling dimension  $\delta$  and finite-dimensional  $\text{SO}(d-2)$ -representation  $\lambda$ . We write  $\mathcal{P}_\delta$  when  $\lambda$  is trivial. We can think of the null vectors  $z_i \in \mathbb{R}^{d-1,1}$  as embedding-space coordinates for the celestial sphere  $S^{d-2}$ . In this language, for example, we have a celestial three-point structure

$$\langle \mathcal{P}_{\delta_1}(z_1)\mathcal{P}_{\delta_2}(z_2)\mathcal{P}_{\delta_3}(z_3) \rangle = \frac{1}{z_{12}^{\frac{\delta_1+\delta_2-\delta_3}{2}} z_{23}^{\frac{\delta_2+\delta_3-\delta_1}{2}} z_{13}^{\frac{\delta_3+\delta_1-\delta_2}{2}}}, \quad z_{ij} \equiv -2z_i \cdot z_j. \tag{5.100}$$

Here,  $\mathcal{P}_\delta$  are not physical operators — they label representations of  $\text{SO}(d-1, 1)$ , and (5.100) denotes the unique three-point structure (up to normalization) for the given representations. We will also use the notation [28]

$$\tilde{\mathcal{P}}_{\delta,\lambda} \equiv \mathcal{P}_{2-d-\delta,\lambda^R}, \quad \tilde{\mathcal{P}}_{\delta,\lambda}^\dagger \equiv \mathcal{P}_{2-d-\delta,\lambda^*}, \tag{5.101}$$

where  $\lambda^R$  is the reflected representation and  $\lambda^*$  is the dual representation to  $\lambda$ .<sup>16</sup>

We will be particularly interested in principal series representations of  $\text{SO}(d-1, 1)$ , which have  $\delta \in \frac{d-2}{2} + i\mathbb{R}$ . Their significance is that they furnish a complete set of irreducible representations for decomposing objects that transform under  $\text{SO}(d-1, 1)$ .<sup>17</sup> For example, consider a function  $f(z_1, z_2)$  that transforms like a product of scalar operators with dimensions  $\delta_1, \delta_2$  on  $S^{d-2}$ . It can be decomposed into traceless-symmetric-tensor principal series representations, i.e. representations where  $\lambda$  is the spin- $j$  traceless symmetric tensor representation of  $\text{SO}(d-2)$ . We denote these by  $\mathcal{P}_{\delta,j}$ .

Let us define the “partial wave”

$$W_{\delta,j}(z) \equiv \alpha_{\delta,j} \int D^{d-2}z_1 D^{d-2}z_2 \langle \tilde{\mathcal{P}}_{\delta_1}^\dagger(z_1)\tilde{\mathcal{P}}_{\delta_2}^\dagger(z_2)\mathcal{P}_{\delta,j}(z) \rangle f(z_1, z_2) \tag{5.102}$$

$$= \begin{array}{c} \text{---} \mathcal{P}_{\delta,j} \text{---} \\ \text{---} \left( \text{---} t_{\delta,j} \text{---} \right) \text{---} \\ \text{---} \left( \text{---} f \text{---} \right) \text{---} \\ \text{---} \end{array}, \tag{5.103}$$

where

$$\alpha_{\delta,j} \equiv \frac{\mu^{(d-2)}(\delta, j) S_E^{(d-2)}(\mathcal{P}_{\delta_1}\mathcal{P}_{\delta_2}[\tilde{\mathcal{P}}_{\delta,j}^\dagger])}{\langle \mathcal{P}_{\delta_1}\mathcal{P}_{\delta_2}\tilde{\mathcal{P}}_{\delta,j}^\dagger \rangle, \langle \tilde{\mathcal{P}}_{\delta_1}^\dagger\tilde{\mathcal{P}}_{\delta_2}^\dagger\mathcal{P}_{\delta,j} \rangle} \tag{5.104}$$

<sup>16</sup>In odd dimensions,  $\lambda^R = \lambda$ . In even dimensions,  $\lambda^R$  is given by swapping the spinor Dynkin labels of  $\lambda$ .

<sup>17</sup>When  $d = 3$ , we can also have discrete-series representations appearing. We comment on the role of such representations in section 5.5.2.



and

$$t_{\delta,j}(z_1, z_2, z) = \alpha_{\delta,j} \langle \tilde{\mathcal{P}}_{\delta_1}^\dagger(z_1) \tilde{\mathcal{P}}_{\delta_2}^\dagger(z_2) \mathcal{P}_{\delta,j}(z) \rangle. \tag{5.105}$$

The integration measure in (5.102) is given by (5.87). The quantities in (5.104) are the Plancherel measure  $\mu^{(d-2)}(\delta, j)$  for  $\text{SO}(d-1, 1)$ , a shadow transform factor  $S_E^{(d-2)}(\mathcal{P}_{\delta_1} \mathcal{P}_{\delta_2} [\tilde{\mathcal{P}}_{\delta,j}^\dagger])$ , and a three-point pairing ( $\langle \mathcal{P}_{\delta_1} \mathcal{P}_{\delta_2} \tilde{\mathcal{P}}_{\delta,j}^\dagger \rangle, \langle \tilde{\mathcal{P}}_{\delta_1}^\dagger \tilde{\mathcal{P}}_{\delta_2}^\dagger \mathcal{P}_{\delta,j} \rangle$ ). Explicit definitions and formulas for all of these quantities are available in [194]. We will not need them here, since these factors will ultimately cancel. The only formula we will need is the ‘‘bubble’’ integral [194]

$$\text{Bubble diagram} = \mathcal{P}_{\delta,j} \mathcal{P}_{\delta,j}^\dagger \times \text{vol SO}(1, 1), \tag{5.106}$$

which is

$$\begin{aligned} \alpha_{\delta,j} \int D^{d-2} z_1 D^{d-2} z_2 \langle \tilde{\mathcal{P}}_{\delta_1}^\dagger(z_1) \tilde{\mathcal{P}}_{\delta_2}^\dagger(z_2) \mathcal{P}_{\delta,j}(z) \rangle \langle \mathcal{P}_{\delta_1}(z_1) \mathcal{P}_{\delta_2}(z_2) \mathcal{P}_{\delta,j}^\dagger(z') \rangle \\ = \langle \mathcal{P}_{\delta,j}(z) \mathcal{P}_{\delta,j}^\dagger(z') \rangle \text{vol SO}(1, 1). \end{aligned} \tag{5.107}$$

Here  $\langle \mathcal{P}_{\delta,j}(z) \mathcal{P}_{\delta,j}^\dagger(z') \rangle$  is a two-point structure on the celestial sphere.<sup>18</sup> The infinite factor  $\text{vol SO}(1, 1)$  will cancel in all calculations below. In the notation of section 5.3.1, we have

$$t_\delta(z_1, z_2, z) = t_{\delta,0}(z_1, z_2, z). \tag{5.108}$$

The function  $f(z_1, z_2)$  can be expanded in partial waves [82, 194]

$$f(z_1, z_2) = \sum_{j=0}^{\infty} \int_{\frac{d-2}{2}-i\infty}^{\frac{d-2}{2}+i\infty} \frac{d\delta}{2\pi i} \mathcal{C}_{\delta,j}(z_1, z_2, \partial_{z_2}) W_{\delta,j}(z_2). \tag{5.109}$$

The differential operator  $\mathcal{C}_{\delta,j}(z_1, z_2, \partial_z)$  is defined by

$$\mathcal{C}_{\delta,j}(z_1, z_2, \partial_{z_2}) \langle \mathcal{P}_{\delta,j}(z_2) \mathcal{P}_{\delta,j}^\dagger(z') \rangle = \langle \mathcal{P}_{\delta_1}(z_1) \mathcal{P}_{\delta_2}(z_2) \mathcal{P}_{\delta,j}^\dagger(z') \rangle, \tag{5.110}$$

This is simply the  $d-2$ -dimensional version of the usual differential operator appearing in an OPE of conformal primaries. Thus, (5.109) takes the form of an OPE in  $d-2$  dimensions, where we have a contour integral over the principal series  $\delta \in \frac{d-2}{2} + i\mathbb{R}$

<sup>18</sup>Specifically, it is the two-point structure used to obtain the shadow factor  $S_E^{(d-2)}$  in the definition of  $\alpha_{\delta,j}$ .

instead of a sum over  $\delta$ . The contour can sometimes be deformed to give a sum, as we will see below.

Several objects above carry indices, and we are leaving the contraction of indices between dual objects implicit. For example,  $\mathcal{P}_{\delta,j}(z)$  carries  $j$  traceless-symmetric indices for the tangent bundle of  $S^{d-2}$ , and consequently  $W_{\delta,j}(z)$  does too. The differential operator  $\mathcal{C}_{\delta,j}$  also carries these indices, and they are contracted in (5.109).

When  $f(z_1, z_2)$  transforms like a product of more general operators in representations  $\mathcal{P}_{\delta_1, \lambda_1}$  and  $\mathcal{P}_{\delta_2, \lambda_2}$ , then there can be multiple celestial three-point structures

$$\langle \widetilde{\mathcal{P}}_{\delta_1, \lambda_1}^\dagger(z_1) \widetilde{\mathcal{P}}_{\delta_2, \lambda_2}^\dagger(z_2) \mathcal{P}_{\delta, \lambda}(z) \rangle^{(\alpha)}, \quad (5.111)$$

labeled by an index  $\alpha$ . Consequently, the partial wave  $W_{\delta, \lambda}^{(\alpha)}(z)$  and differential operator  $\mathcal{C}_{\delta, \lambda, \alpha}$  carry additional structure labels, and we have a more general expansion

$$f(z_1, z_2) = \sum_{\lambda, \alpha} \int_{\frac{d-2}{2}-i\infty}^{\frac{d-2}{2}+i\infty} \frac{d\delta}{2\pi i} \mathcal{C}_{\delta, \lambda, \alpha}(z_1, z_2, \partial_{z_2}) W_{\delta, \lambda}^{(\alpha)}(z_2). \quad (5.112)$$

### 5.3.4 Light-ray OPE from the Lorentzian inversion formula

Applying (5.102) and (5.109) to the product (5.99), we have

$$\mathbf{L}[\mathcal{O}_1](x, z_1) \mathbf{L}[\mathcal{O}_2](x, z_2) = \sum_{j=0}^{\infty} \int_{\frac{d-2}{2}-i\infty}^{\frac{d-2}{2}+i\infty} \frac{d\delta}{2\pi i} \mathcal{C}_{\delta, j}(z_1, z_2, \partial_{z_2}) \mathbb{W}_{\delta, j}(x, z_2), \quad (5.113)$$

where the partial waves are given by

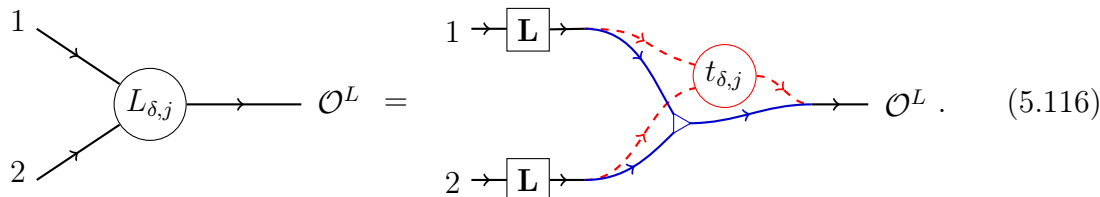
$$\begin{aligned} \mathbb{W}_{\delta, j}(x, z) &= \alpha_{\delta, j} \int D^{d-2} z_1 D^{d-2} z_2 \langle \widetilde{\mathcal{P}}_{\delta_1}^\dagger(z_1) \widetilde{\mathcal{P}}_{\delta_2}^\dagger(z_2) \mathcal{P}_{\delta, j}(z) \rangle \mathbf{L}[\mathcal{O}_1](x, z_1) \mathbf{L}[\mathcal{O}_2](x, z_2) \\ &= \int d^d x_1 d^d x_2 D^{d-2} z_1 D^{d-2} z_2 L_{\delta, j}(x_1, z_1, x_2, z_2; x, z) \mathcal{O}_1(x_1, z_1) \mathcal{O}_2(x_2, z_2), \end{aligned} \quad (5.114)$$

and the kernel  $L_{\delta, j}$  is given by

$$\begin{aligned} L_{\delta, j}(x_1, z_1, x_2, z_2; x, z) &\equiv \alpha_{\delta, j} \langle \widetilde{\mathcal{P}}_{\delta_1}^\dagger(z_1) \widetilde{\mathcal{P}}_{\delta_2}^\dagger(z_2) \mathcal{P}_{\delta, j}(z) \rangle \\ &\times \int_{-\infty}^{\infty} d\alpha_1 d\alpha_2 (-\alpha_1)^{-\delta_1 - J_1 - 1} (-\alpha_2)^{-\delta_2 - J_2 - 1} \delta^{(d)} \left( x - \frac{z_1}{\alpha_1} - x_1 \right) \delta^{(d)} \left( x - \frac{z_2}{\alpha_2} - x_2 \right). \end{aligned} \quad (5.115)$$

Here, we have defined  $\delta_i = \Delta_i - 1$ . We are taking  $\mathcal{O}_1, \mathcal{O}_2$  to be traceless symmetric tensors for simplicity, so that the partial wave expansion (5.113) only includes traceless

symmetric tensors of spin- $j$  on the celestial sphere. We remove this restriction in section 5.3.4.4. We can represent the kernel  $L_{\delta,j}$  pictorially as:



The blue solid and red dashed lines represent the Minkowski and celestial coordinates, respectively. We will not need to plug in the definition of  $L_{\delta,j}$  until the very end of our computation, accordingly we will omit the blue and red lines until necessary.

The object  $\mathbb{W}_{\delta,j}(x, z)$  is a bilocal integral that transforms like a primary of  $\text{SO}(d, 2)$  with weights  $(1 - J, 1 - \Delta, j)$ , where  $J = J_1 + J_2 - 1$  and  $\Delta = \delta + 1$ .  $\mathbb{O}_{\Delta, J, j(a)}^{\pm}(x, z)$  is another bilocal integral that transforms in the same way. However, the integration kernels that define  $\mathbb{W}_{\delta,j}$  and  $\mathbb{O}_{\Delta, J, j(a)}^{\pm}$  are very different, so it is not immediately clear what the relationship is between them. For example, the kernel  $L_{\delta,j}$  has  $\delta$ -function support when  $x_1, x_2$  lie on the future null cone of  $x$ . By contrast, the kernel used to define  $\mathbb{O}_{\Delta, J, j(a)}^{\pm}$  has support off the null cone of  $x$ .

Another puzzle is that  $L_{\delta,j}$  is nonvanishing for all  $j \in \mathbb{Z}_{\geq 0}$ . By contrast, the object  $\mathbb{O}_{\Delta, J, j(a)}^{\pm}(x, z)$  is only defined when  $j$  is such that operators with weights  $(\Delta, J, j)$  can appear in the  $\mathcal{O}_1 \times \mathcal{O}_2$  OPE. For fixed  $\mathcal{O}_1, \mathcal{O}_2$ , this condition restricts  $j$  to a finite set. For example, if  $\mathcal{O}_1, \mathcal{O}_2$  are scalars, then only operators with  $j = 0$  (i.e. traceless symmetric tensors of  $\text{SO}(d - 1, 1)$ ) can appear in  $\mathcal{O}_1 \times \mathcal{O}_2$ . See section 5.3.4.4 for the rule that determines the allowed values of  $j$ .

Despite these puzzles,  $\mathbb{W}_{\delta,j}$  will actually be a linear combination of  $\mathbb{O}_{\Delta, J, j(a)}^{\pm}$ 's. A necessary condition for this to be true is that exotic values of  $j$  (i.e. values that aren't allowed in the  $\mathcal{O}_1 \times \mathcal{O}_2$  OPE) lead to vanishing  $\mathbb{W}_{\delta,j}$ , even though  $L_{\delta,j}$  is nonzero. We will see that this is indeed true.

### 5.3.4.1 Matrix elements of $\mathbb{W}_{\delta,j}$

To determine  $\mathbb{W}_{\delta,j}(x, z)$ , it suffices to study its matrix elements in states created by local primary operators  $\mathcal{O}_3$  and  $\mathcal{O}_4$ :

$$\begin{aligned} & \langle \Omega | \mathcal{O}_4 \mathbb{W}_{\delta,j}(x, z) \mathcal{O}_3 | \Omega \rangle \\ &= \alpha_{\delta,j} \int D^{d-2} z_1 D^{d-2} z_2 \langle \tilde{\mathcal{P}}_{\delta_1}^\dagger(z_1) \tilde{\mathcal{P}}_{\delta_2}^\dagger(z_2) \mathcal{P}_{\delta,j}(z) \rangle \langle \Omega | \mathcal{O}_4 \mathbf{L}[\mathcal{O}_1](x, z_1) \mathbf{L}[\mathcal{O}_2](x, z_2) \mathcal{O}_3 | \Omega \rangle. \end{aligned} \quad (5.117)$$

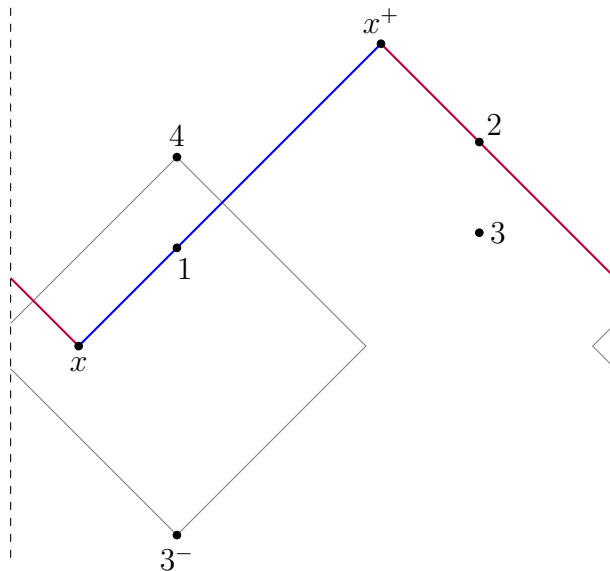


Figure 5.6: We study a configuration where  $4 > x > 3^-$ . Points 1 and 2 are integrated over distinct null lines from  $x$  to  $x^+$  (blue and purple). The diamond formed by the past null cone of 4 and future null cone of  $3^-$  is indicated in gray.

As usual,  $\mathcal{O}_i$  is at point  $x_i$  unless otherwise specified. Without loss of generality, let us assume the causal relationships  $4 > x > 3^-$  (figure 5.6). Other causal relationships can be obtained by analytic continuation in  $x, x_3, x_4$ .

Because  $\mathbf{L}[\mathcal{O}_i]$  annihilates the vacuum, we can write (5.117) as the integral of a double-commutator

$$\begin{aligned}
 &= \alpha_{\delta,j} \int D^{d-2} z_1 D^{d-2} z_2 \langle \tilde{\mathcal{P}}_{\delta_1}^\dagger(z_1) \tilde{\mathcal{P}}_{\delta_2}^\dagger(z_2) \mathcal{P}_{\delta,j}(z) \rangle \langle \Omega | [\mathcal{O}_4, \mathbf{L}[\mathcal{O}_1](x, z_1)] [\mathbf{L}[\mathcal{O}_2](x, z_2), \mathcal{O}_3] | \Omega \rangle \\
 &= \int d^d x_1 d^d x_2 D^{d-2} z_1 D^{d-2} z_2 L_{\delta,j}(x_1, z_1, x_2, z_2; x, z) \theta(4 > 1) \theta(2 > 3) \\
 &\quad \times \langle \Omega | [\mathcal{O}_4, \mathcal{O}_1(x_1, z_1)] [\mathcal{O}_2(x_2, z_2), \mathcal{O}_3] | \Omega \rangle. \tag{5.118}
 \end{aligned}$$

In the last line, we introduced  $\theta$ -functions  $\theta(4 > 1)\theta(2 > 3)$  that remove the regions where  $x_1$  is spacelike from  $x_4$  and  $x_2$  is spacelike from  $x_3$ . They are redundant because commutators vanish at spacelike separation. However, they will play an important role later, so we include them. Pictorially, we have

$$\tag{5.119}$$

To avoid visual clutter, we will omit theta functions in our diagrams.

The fact that (5.118) is the integral of a double commutator suggests that we should relate it to the Lorentzian inversion formula. In fact, the proof of the generalized Lorentzian inversion formula in [28] proceeds from an expression similar to (5.118). We now follow the steps of that derivation.

First note that conformal invariance implies

$$\langle \Omega | \mathcal{O}_4 \mathbb{W}_{\delta,j}(x, z) \mathcal{O}_3 | \Omega \rangle = A_b(\delta, j) \langle 0 | \mathcal{O}_4 \mathbf{L}[\mathcal{O}](x, z) \mathcal{O}_3 | 0 \rangle^{(b)}, \quad (5.120)$$

where  $\mathcal{O}$  has quantum numbers  $(\Delta, J, \lambda) = (\delta + 1, J_1 + J_2 - 1, j)$ ,  $\langle 0 | \mathcal{O}_4 \mathcal{O} \mathcal{O}_3 | 0 \rangle^{(b)}$  is a basis of structures for the given representations, and  $A_b(\delta, j)$  are coefficients we would like to determine. A sum over  $b$  is implicit. In terms of diagrams, that is

$$\text{Diagrammatic equation (5.121)} \quad (5.121)$$

Following [28], it is useful to act on both sides with  $\mathcal{T}_4$  (equivalently relabel  $x_4 \rightarrow \mathcal{T}_4 x_4 = x_4^+$ ), giving

$$\mathcal{T}_4 \langle \Omega | \mathcal{O}_4 \mathbb{W}_{\delta,j}(x, z) \mathcal{O}_3 | \Omega \rangle = A_b(\delta, j) \mathcal{T}_4 \langle 0 | \mathcal{O}_4 \mathbf{L}[\mathcal{O}](x, z) \mathcal{O}_3 | 0 \rangle^{(b)}. \quad (5.122)$$

Note that  $\mathcal{T}_4$  simply acts on three-point structures by multiplication by a phase. Nevertheless, it is useful to keep the abstract notation in (5.122). This relabeling turns the causal relationship  $4 > x > 3^-$  into  $3 > 4$  and  $3 \approx x$  and  $4 \approx x$  (see figure 5.7). Here  $i \approx j$  means  $x_i$  is spacelike from  $x_j$ , see appendix D.1. We write these relationships compactly as  $(3 > 4) \approx x$ . Our Lorentzian pairing (5.95) is defined for this type of causal relationship. Thus, to isolate  $A_b(\delta, j)$ , we can take the

Lorentzian pairing of both sides with a dual structure

$$A_b(\delta, j) = \quad (5.123)$$

This gives

$$\begin{aligned}
 A_b(\delta, j) &= \left( (\mathcal{T}_4 \langle 0 | \mathcal{O}_4 \mathbf{L}[\mathcal{O}](x, z) \mathcal{O}_3 | 0 \rangle^{(b)})^{-1}, \mathcal{T}_4 \langle \Omega | \mathcal{O}_4 \mathbb{W}_{\delta, j}(x, z) \mathcal{O}_3 | \Omega \rangle \right)_L \\
 &= \int_{\substack{4 > 1 \\ 2 > 3}} \frac{d^d x_1 d^d x_2 d^d x_3 d^d x_4 D^{d-2} z_1 D^{d-2} z_2}{\text{vol } \widetilde{\text{SO}}(d, 2)} \langle \Omega | [\mathcal{O}_4, \mathcal{O}_1(x_1, z_1)] [\mathcal{O}_2(x_2, z_2), \mathcal{O}_3] | \Omega \rangle \\
 &\quad \times \mathcal{T}_2^{-1} \mathcal{T}_4^{-1} \left[ \int d^d x D^{d-2} z (\mathcal{T}_4 \langle 0 | \mathcal{O}_4 \mathbf{L}[\mathcal{O}](x, z) \mathcal{O}_3 | 0 \rangle^{(b)})^{-1} \right. \\
 &\quad \left. \times (\mathcal{T}_2 L_{\delta, j})(x_1, z_1, x_2, z_2; x, z) \theta(4^+ > 1) \theta(2^+ > 3) \right]. \quad (5.124)
 \end{aligned}$$

Here, we have plugged in (5.95) and (5.118). We then changed variables  $x_4 \rightarrow x_4^-$ , acted with  $\mathcal{T}_2^{-1} \mathcal{T}_2$  in the last line, and used  $\mathcal{T}_2 \theta(2 > 3) = \theta(2^+ > 3)$ . Again, these relabelings are for the purposes of later applying the Lorentzian pairing (5.95).

The bracketed quantity in (5.124) is the object obtained by cutting the pairing (5.123) on the lines labeled 1, 2, 3, and 4. Because of the factors  $\mathcal{T}_2^{-1} \mathcal{T}_4^{-1}$  outside the brackets, the configuration of points inside the brackets (figure 5.7) is obtained from figure 5.6 by relabeling  $2 \rightarrow 2^+$  and  $4 \rightarrow 4^+$ . Note that the bracketed quantity is a conformally-invariant function of  $x_1, x_2, x_3, x_4$  that is an eigenfunction of the conformal Casimirs acting simultaneously on points 1, 2 (or equivalently 3, 4). Hence it is a linear combination of conformal blocks. To compute it, we can follow the computation in appendix H of [28]. The kernel  $\mathcal{T}_2 L_{\delta, j}$  forces  $x$  to lie on the past lightcone of  $x_1$  and the future lightcone of  $x_2$  (see figure 5.7). Thus, as  $x_1 \rightarrow x_2$  (equivalently  $x_3 \rightarrow x_4$ ) the integration point  $x$  is forced to stay away from  $x_3, x_4$ .

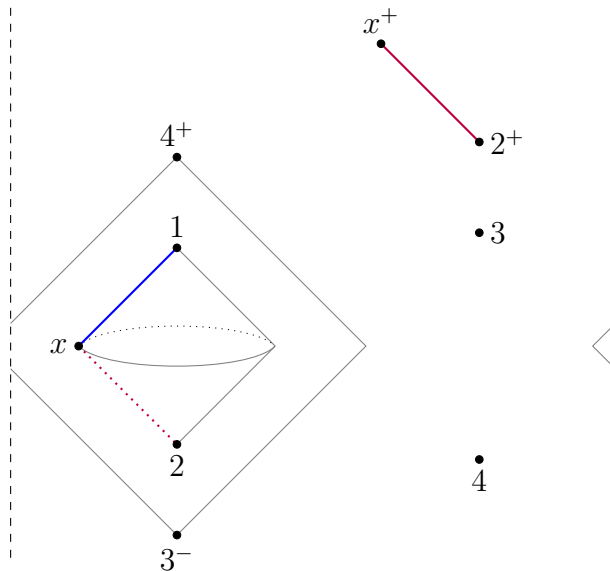


Figure 5.7: After relabeling  $2 \rightarrow 2^+$  and  $4 \rightarrow 4^+$ , we have  $4^+ > 1 \gtrsim x \gtrsim 2 > 3^-$ , where “ $i \gtrsim j$ ” means  $i$  is on the future null cone of  $j$ . Let us imagine that  $1, 2, 3, 4$  are fixed and ask where  $x$  can be. We see that  $x$  is spacelike from  $3, 4$  and  $3 > 4$ , equivalently  $(3 > 4) \approx x$ . Furthermore,  $x$  is constrained to lie on the  $S^{d-2}$  given by the intersection of the past lightcone of  $1$  and future lightcone of  $2$ . We show lightlike segments between  $x$  and  $1$  (solid blue) and between  $2^+$  and  $x^+$  (solid purple), which are subsets of the light-transform contours from figure 5.6. The image of the solid purple segment under  $\mathcal{T}^{-1}$  is shown in dotted purple.

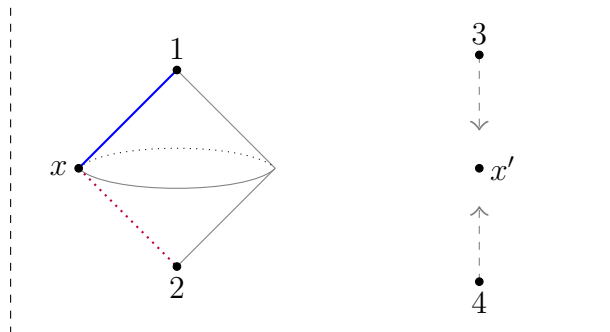


Figure 5.8: To compute the block appearing in (5.124), we take the limit  $3, 4 \rightarrow x'$  inside the integral over  $x, z$ . Note that we have  $(1 > 2) \approx x'$ .

This means we can compute the integral by taking an OPE-type limit  $x_3, x_4 \rightarrow x'$  inside the integrand (figure 5.8).

First, we write the  $34$  three-point structure as a linear operator  $B(x_3, x_4, \partial_{x'}, \partial_{z'})$

acting on a two-point function<sup>19</sup>

$$(\mathcal{T}_4 \langle 0 | \mathcal{O}_4 \mathbf{L}[\mathcal{O}] (x, z) \mathcal{O}_3 | 0 \rangle^{(b)})^{-1} = B(x_3, x_4, \partial_{x'}, \partial_{z'}) \langle \mathcal{O}^F(x', z') \mathcal{O}^{F\dagger}(x, z) \rangle. \quad (5.125)$$

Here,  $\mathcal{O}^{F\dagger}$  has the weights of something that can be paired with  $\mathbf{L}[\mathcal{O}]$ , namely  $(J + d - 1, \Delta - d + 1, j)$  where  $\Delta = \delta + 1$  and  $J = J_1 + J_2 - 1$ . We must also replace

$$\theta(4^+ > 1) \theta(2^+ > 3) \rightarrow \theta(x'^+ > 1) \theta(2^+ > x'), \quad (5.126)$$

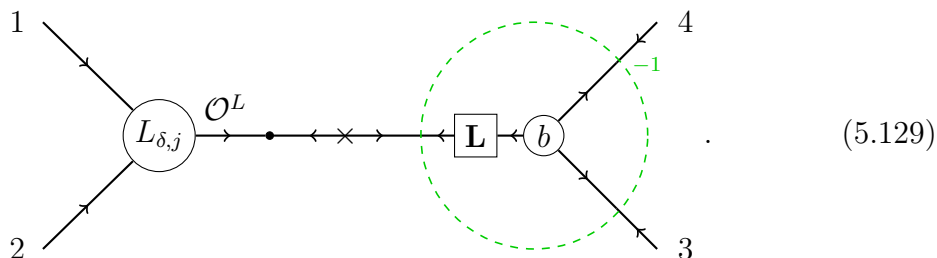
since we are taking the limit  $x_3, x_4 \rightarrow x'$ . Because of the restriction  $1 > 2$ , (5.126) is equivalent to  $\theta((1 > 2) \approx x')$ . The two-point function in (5.125) is then integrated against the 12 three-point structure, giving a Lorentzian shadow transform

$$\int_{x \approx x'} d^d x D^{d-2} z \langle \mathcal{O}^F(x', z') \mathcal{O}^{F\dagger}(x, z) \rangle \mathcal{T}_2 L_{\delta, j}(x_1, z_1, x_2, z_2; x, z) = \mathbf{S}[\mathcal{T}_2 L_{\delta, j}](x_1, z_1, x_2, z_2; x', z'). \quad (5.127)$$

The result is the conformal block

$$\begin{aligned} & B(x_3, x_4, \partial_{x'}, \partial_{z'}) \mathbf{S}[\mathcal{T}_2 L_{\delta, j}](x_1, z_1, x_2, z_2; x', z') \theta((1 > 2) \approx x') \\ &= \frac{(\mathbf{S}[\mathcal{T}_2 L_{\delta, j}] \theta((1 > 2) \approx x')) (\mathcal{T}_4 \langle 0 | \mathcal{O}_4 \mathbf{L}[\mathcal{O}] (x, z) \mathcal{O}_3 | 0 \rangle^{(b)})^{-1}}{\langle \mathcal{O}^F \mathcal{O}^{F\dagger} \rangle}. \end{aligned} \quad (5.128)$$

In the second line, we use the notation for a conformal block where the three-point structures in the numerator should be merged using the two-point function in the denominator. The precise meaning of this notation is the first line of (5.128). Pictorially, the block can be represented as



At this point, we can understand why  $A_b(\delta, j)$  vanishes for exotic  $j$  not allowed in the  $\mathcal{O}_1 \times \mathcal{O}_2$  OPE. Recall that  $L_{\delta, j}$  does not vanish for exotic  $j$ . This is possible essentially because  $L_{\delta, j}$  involves  $\delta$ -functions, and the presence of these  $\delta$ -functions changes the space of conformally-invariant three-point structures. However, the shadow-transformed structure  $\mathbf{S}[\mathcal{T}_2 L_{\delta, j}]$  does not contain any  $\delta$ -functions because

<sup>19</sup>Although we have written  $B$  as a differential operator in  $z'$ , it must actually be an integral operator when  $J$  is not an integer. See [28] for an explicit expression.



they are integrated over in (5.127). Thus, it is subject to the usual classification of conformally-invariant three-point structures. It transforms like a three-point function  $\langle \mathcal{O}_1 \mathcal{O}_2 \mathcal{O}^{\dagger} \rangle$ , where  $\mathcal{O}^{\dagger}$  has quantum numbers  $(J+d-1, \Delta-d+1, j)$ . The space of conformally-invariant three-point structures for  $\langle \mathcal{O}_1 \mathcal{O}_2 \mathcal{O}^{\dagger} \rangle$  is the same as the space of conformally-invariant three-point structures for  $\langle \mathcal{O}_1 \mathcal{O}_2 \mathcal{O}^{\dagger} \rangle$ . Thus,  $\mathbf{S}[\mathcal{T}_2 L_{\delta,j}]$  must vanish for exotic  $j$ .

### 5.3.4.2 Relating to the inversion formula

After writing the quantity in brackets in (5.124) as a conformal block, our formula for  $A_b(\delta, j)$  looks extremely similar to the Lorentzian inversion formula (5.92). There are two main differences. Firstly, our formula for  $A_b(\delta, j)$  contains the three-point structure  $\mathbf{S}[\mathcal{T}_2 L_{\delta,j}] \theta((1 > 2) \approx x')$  instead of  $(\mathcal{T}_2 \langle 0 | \mathcal{O}_2 \mathbf{L}[\mathcal{O}^{\dagger}] \mathcal{O}_1 | 0 \rangle^{(a)})^{-1}$ . We need to express the former as a linear combination of the latter, and this is achieved by pairing with  $\mathcal{T}_2 \langle 0 | \mathcal{O}_2 \mathbf{L}[\mathcal{O}^{\dagger}] \mathcal{O}_1 | 0 \rangle^{(a)}$ .

The second difference is that (5.124) involves an integral only over the double-commutator  $\langle \Omega[\mathcal{O}_4, \mathcal{O}_1][\mathcal{O}_2, \mathcal{O}_3] | \Omega \rangle$ , corresponding to the “ $t$ -channel” term in (5.92). It does not include a contribution from the “ $u$ -channel” term. This is accounted for by averaging over even and odd spins.

In summary, comparing (5.128) and (5.92), we find

$$\begin{aligned}
 A_b(\delta, j) &= -2\pi i \times \frac{1}{2} (C_{ab}^+(\delta+1, J_1+J_2-1, j) + C_{ab}^-(\delta+1, J_1+J_2-1, j)) \\
 &\quad \times \frac{\langle \mathbf{L}[\mathcal{O}] \mathbf{L}[\mathcal{O}^{\dagger}] \rangle^{-1}}{\langle \mathcal{O}^{\dagger} \mathcal{O}^{\dagger} \rangle} (\mathbf{S}[\mathcal{T}_2 L_{\delta,j}] \theta((1 > 2) \approx x'), \mathcal{T}_2 \langle 0 | \mathcal{O}_2 \mathbf{L}[\mathcal{O}^{\dagger}] \mathcal{O}_1 | 0 \rangle^{(a)})_L.
 \end{aligned}
 \tag{5.130}$$

Note that in this formula, the ratio of two-point structures  $\frac{\langle \mathbf{L}[\mathcal{O}] \mathbf{L}[\mathcal{O}^{\dagger}] \rangle^{-1}}{\langle \mathcal{O}^{\dagger} \mathcal{O}^{\dagger} \rangle}$  is simply a number — it does not refer to the formation of a conformal block. The three-point pairing can be simplified further by rewriting it as a two-point pairing:

$$\left( \begin{array}{c} \text{Circular diagram with vertices } \mathbf{L}, a, L_{\delta,j} \text{ and arcs } 1, 2, O^L \\ \text{Linear diagram with vertices } \mathbf{L}, a, L_{\delta,j}, \mathbf{L} \text{ and arrows } O^{L\dagger}, O^L, O^{L\dagger} \end{array} \right)_L.
 \tag{5.131}$$

In full detail, we have

$$\begin{aligned}
& (\mathbf{S}[\mathcal{T}_2 L_{\delta,j}] \theta((1 > 2) \approx x'), \mathcal{T}_2 \langle 0 | \mathcal{O}_2 \mathbf{L}[\mathcal{O}^\dagger] \mathcal{O}_1 | 0 \rangle^{(a)})_L \\
&= \int_{\substack{(1>2) \approx x' \\ x \approx x'}} \frac{d^d x_1 d^d x_2 d^d x' d^d x D^{d-2} z_1 D^{d-2} z_2 D^{d-2} z' D^{d-2} z}{\text{vol } \widetilde{\text{SO}}(d, 2)} \langle \mathcal{O}^{\text{F}}(x', z') \mathcal{O}^{\text{F}\dagger}(x, z) \rangle \\
&\quad \times \mathcal{T}_2 L_{\delta,j}(x_1, z_1, x_2, z_2; x, z) \mathcal{T}_2 \langle 0 | \mathcal{O}_2(x_2, z_2) \mathbf{L}[\mathcal{O}^\dagger](x', z') \mathcal{O}_1(x_1, z_1) | 0 \rangle^{(a)} \\
&= \frac{1}{\text{vol SO}(1, 1)^2} \left( \langle \mathcal{O}^{\text{F}} \mathcal{O}^{\text{F}\dagger} \rangle, \int_{\substack{1 \approx x' \\ 2 > x'}} d^d x_1 d^d x_2 D^{d-2} z_1 D^{d-2} z_2 L_{\delta,j}(x_1, z_1, x_2, z_2; x, z) \right. \\
&\quad \left. \times \langle 0 | \mathcal{O}_2(x_2, z_2) \mathbf{L}[\mathcal{O}^\dagger](x', z') \mathcal{O}_1(x_1, z_1) | 0 \rangle^{(a)} \right)_L. \tag{5.132}
\end{aligned}$$

In the last equality, we made the change of variables  $x_2 \rightarrow \mathcal{T}_2^{-1} x_2 = x_2^-$  and recognized the integrals over  $x, z, x', z'$  as a Lorentzian two-point pairing (5.97). The infinite factors  $\text{vol SO}(1, 1)^2$  will cancel shortly. Plugging in the definition of  $L_{\delta,j}$  (5.115), we have

$$\begin{aligned}
A_b(\delta, j) &= -\pi i (C_{ab}^+(\delta + 1, J_1 + J_2 - 1, j) + C_{ab}^-(\delta + 1, J_1 + J_2 - 1, j)) \\
&\quad \times \frac{(\langle \mathbf{L}[\mathcal{O}] \mathbf{L}[\mathcal{O}^\dagger] \rangle^{-1}, Q_{\delta,j}^{(a)})_L}{\text{vol SO}(1, 1)^2}, \tag{5.133}
\end{aligned}$$

where

$$\begin{aligned}
Q_{\delta,j}^{(a)}(x, z; x', z') &= \alpha_{\delta,j} \int D^{d-2} z_1 D^{d-2} z_2 \langle \widetilde{\mathcal{P}}_{\delta_1}^\dagger(z_1) \widetilde{\mathcal{P}}_{\delta_2}^\dagger(z_2) \mathcal{P}_{\delta,j}(z) \rangle \\
&\quad \times \langle 0 | \mathbf{L}^+[\mathcal{O}_2](x, z_2) \mathbf{L}[\mathcal{O}^\dagger](x', z') \mathbf{L}^-[\mathcal{O}_1](x, z_1) | 0 \rangle^{(a)}. \tag{5.134}
\end{aligned}$$

Here,  $\mathbf{L}^-[\mathcal{O}_1]$  indicates that the light-transform contour should be restricted to  $x_1$  spacelike from  $x'$ , and  $\mathbf{L}^+[\mathcal{O}_2]$  indicates that the light-transform contour should be restricted to  $x_2$  in the future of  $x'$  (figure 5.9).

Thus our task reduces to expressing  $Q_{\delta,j}$  as a multiple of  $\langle \mathbf{L}[\mathcal{O}] \mathbf{L}[\mathcal{O}^\dagger] \rangle$ . To do so, it suffices to set  $x = \infty$  and  $x' = 0$ . Lorentz invariance and homogeneity in  $z$ 's guarantee

$$\frac{\langle 0 | \mathbf{L}^+[\mathcal{O}_2](\infty, z_1) \mathbf{L}[\mathcal{O}^\dagger](0, z') \mathbf{L}^-[\mathcal{O}_1](\infty, z_2) | 0 \rangle^{(a)}}{\text{vol SO}(1, 1)} = q_{\delta,j}^{(a)} \langle \mathcal{P}_{\delta_1}(z_1) \mathcal{P}_{\delta_2}(z_2) \mathcal{P}_{\delta,j}^\dagger(z') \rangle, \tag{5.135}$$

for some constant  $q_{\delta,j}^{(a)}$ . With hindsight, we have included a factor  $\text{vol SO}(1, 1)^{-1}$  on the left-hand side so that  $q_{\delta,j}^{(a)}$  is finite. Applying the bubble formula (5.107), we find

$$\frac{1}{\text{vol SO}(1, 1)^2} Q_{\delta,j}^{(a)}(\infty, z, 0, z') = q_{\delta,j}^{(a)} \langle \mathcal{P}_{\delta,j}(z) \mathcal{P}_{\delta,j}^\dagger(z') \rangle. \tag{5.136}$$

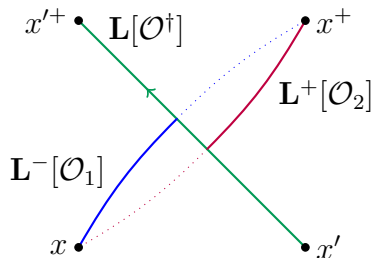


Figure 5.9: Integration contours for the triple light-transform  $\langle 0 | \mathbf{L}^+[\mathcal{O}_2] \mathbf{L}[\mathcal{O}^\dagger] \mathbf{L}^-[\mathcal{O}_1] | 0 \rangle$ .  $\mathcal{O}^\dagger$  is integrated along a complete null line from  $x'$  to  $x'^+$  (solid green).  $\mathcal{O}_1$  is integrated along a half null line spacelike from  $x'$  (solid blue), and  $\mathcal{O}_2$  is integrated along a half null line in the future of  $x'$  (solid purple).

Meanwhile, Lorentz invariance and homogeneity imply

$$\langle \mathbf{L}[\mathcal{O}](\infty, z) \mathbf{L}[\mathcal{O}^\dagger](0, z') \rangle = r_{\delta, j} \langle \mathcal{P}_{\delta, j}(z) \mathcal{P}_{\delta, j}^\dagger(z') \rangle. \quad (5.137)$$

So that

$$A_b(\delta, j) = -\pi i \left( C_{ab}^+(\delta + 1, J_1 + J_2 - 1, j) + C_{ab}^-(\delta + 1, J_1 + J_2 - 1, j) \right) \frac{q_{\delta, j}^{(a)}}{r_{\delta, j}}. \quad (5.138)$$

Finally, combining (5.113), (5.120), (5.91), and writing  $\delta = \Delta - 1$ , we have

$$\begin{aligned} & \mathbf{L}[\mathcal{O}_1](x, z_1) \mathbf{L}[\mathcal{O}_2](x, z_2) \\ &= \pi i \sum_{j=0}^{j_{\max}} \int_{\frac{d}{2}-i\infty}^{\frac{d}{2}+i\infty} \frac{q_{\Delta-1, j}^{(a)}}{r_{\Delta-1, j}} \mathcal{C}_{\delta, j}(z_1, z_2, \partial_{z_2}) \left( \mathbb{O}_{\Delta, J_1+J_2-1, j(a)}^+(x, z_2) + \mathbb{O}_{\Delta, J_1+J_2-1, j(a)}^-(x, z_2) \right). \end{aligned} \quad (5.139)$$

The differential operator  $\mathcal{C}_{\delta, j}$  is defined by (5.110). Here,  $j_{\max}$  is the maximum “non-exotic” value of  $j$  — specifically, the maximum length of the second row of the  $\text{SO}(d-1, 1)$  Young diagrams associated to operators appearing in the  $\mathcal{O}_1 \times \mathcal{O}_2$  OPE.

### 5.3.4.3 Example: scalar $\mathcal{O}_1, \mathcal{O}_2$

As an example, consider the case where  $\mathcal{O}_1 = \phi_1$  and  $\mathcal{O}_2 = \phi_2$  are scalars.<sup>20</sup> We have  $J = J_1 + J_2 - 1 = -1$ . Furthermore,  $j_{\max} = 0$  since only traceless symmetric tensors of  $\text{SO}(d-1, 1)$  can appear in the  $\phi_1 \times \phi_2$  OPE.

<sup>20</sup>As discussed in chapter 4, the product of light-transforms at coincident points may not be well-defined in this case. In this section, we ignore these issues and assume the product is well-defined.

Let us compute  $q_{\delta,0}$  and  $r_{\delta,0}$ . The unique Wightman structure for two scalars and a spin  $J = -1$  operator is

$$\langle 0|\phi_2(x_2)\mathcal{O}(x_0, z_0)\phi_1(x_1)|0\rangle = \frac{(2V_{0,12})^{-1}}{x_{12}^{\Delta_1+\Delta_2-\Delta+1}x_{20}^{\Delta_2+\Delta-\Delta_1-1}x_{01}^{\Delta+\Delta_1-\Delta_2-1}}, \quad (5.140)$$

The light-transform of  $\mathcal{O}$  is given by (5.44) with the relabeling  $(1, 2, 3) \rightarrow (2, 1, 0)$ , and  $J = -1$ . In embedding-space language, we find

$$\langle 0|\phi_2(X_2)\mathbf{L}[\mathcal{O}](X_0, Z_0)\phi_1(X_1)|0\rangle = \frac{L(\phi_1\phi_2[\mathcal{O}])(2V_{0,12})^{1-\Delta}}{(X_{12})^{\frac{\Delta_1+\Delta_2-3+\Delta}{2}}(X_{10})^{\frac{\Delta_1-\Delta_2+3-\Delta}{2}}(-X_{20})^{\frac{\Delta_2-\Delta_1+3-\Delta}{2}}}, \quad (5.141)$$

where

$$\begin{aligned} X_{ij} &\equiv -2X_i \cdot X_j, \\ V_{k,ij} &\equiv \frac{(Z_k \cdot X_i)(X_k \cdot X_j) - (Z_k \cdot X_j)(X_k \cdot X_i)}{X_i \cdot X_j}. \end{aligned} \quad (5.142)$$

We should now specialize  $X_0 = (1, 0, 0)$  and compute the remaining light transforms  $\mathbf{L}^-[\phi_1](X_\infty, Z_1)$  and  $\mathbf{L}^+[\phi_2](X_\infty, Z_2)$ . We set

$$\begin{aligned} X_1 &= Z_1 - \alpha_1 X_\infty = (0, 0, z_1) - \alpha_1(0, 1, 0), \\ X_2 &= Z_2 - \alpha_2 X_\infty = (0, 0, z_2) - \alpha_2(0, 1, 0), \\ X_0 &= (1, 0, 0), \\ Z_0 &= (0, 0, z_0), \end{aligned} \quad (5.143)$$

and integrate

$$\begin{aligned} &\frac{\langle 0|\mathbf{L}^+[\phi_2](X_\infty, Z_2)\mathbf{L}[\mathcal{O}](X_0, Z_0)\mathbf{L}^-[\phi_1](X_\infty, Z_1)|0\rangle}{\text{vol SO}(1, 1)} \\ &= \frac{L(\phi_1\phi_2[\mathcal{O}])}{\text{vol SO}(1, 1)} \int_0^\infty d\alpha_2 \int_{-\infty}^0 d\alpha_1 \frac{(-2\alpha_2 z_0 \cdot z_1 + 2\alpha_1 z_0 \cdot z_2)^{1-\Delta}}{(-2z_1 \cdot z_2)^{\frac{\Delta_1+\Delta_2-3+\Delta}{2}}(-\alpha_1)^{\frac{\Delta_1-\Delta_2+3-\Delta}{2}}\alpha_2^{\frac{\Delta_2-\Delta_1+3-\Delta}{2}}} \\ &= \frac{L(\phi_1\phi_2[\mathcal{O}])}{\text{vol SO}(1, 1)} \left( \int_0^\infty \frac{d\alpha_2}{\alpha_2} \right) \frac{\Gamma(\frac{\Delta-1+\Delta_1-\Delta_2}{2})\Gamma(\frac{\Delta-1+\Delta_2-\Delta_1}{2})}{\Gamma(\Delta-1)} \langle \mathcal{P}_{\delta_1}(z_1)\mathcal{P}_{\delta_2}(z_2)\mathcal{P}_\delta(z_0) \rangle \\ &= -\frac{2\pi i}{\Delta-2} \langle \mathcal{P}_{\delta_1}(z_1)\mathcal{P}_{\delta_2}(z_2)\mathcal{P}_\delta(z_0) \rangle, \end{aligned} \quad (5.144)$$

where  $\delta_i = \Delta_i - 1$ ,  $\delta = \Delta - 1$ , and the celestial three-point structure  $\langle \mathcal{P}_{\delta_1}(z_1)\mathcal{P}_{\delta_2}(z_2)\mathcal{P}_\delta(z_0) \rangle$  is defined in (5.100). To get the third line, we integrated over  $\alpha_1$ . The infinite factor  $\text{vol SO}(1, 1)$  cancels against the unbounded integral over  $\alpha_2$ . Alternatively, we could have used  $\text{SO}(1, 1)$ -gauge invariance to fix  $\alpha_2 = 1$ .

Thus, we find

$$q_{\Delta-1,0} = -\frac{2\pi i}{\Delta-2}. \quad (5.145)$$

Meanwhile, the quantity  $r_{\Delta-1,0}$  was computed in [28] to be

$$r_{\Delta-1,0} = -\frac{2\pi i}{\Delta+J-1} \Big|_{J=-1} = -\frac{2\pi i}{\Delta-2}. \quad (5.146)$$

The ratio  $q_{\Delta-1,0}/r_{\Delta-1,0}$  is simply 1! We find

$$\mathbf{L}[\phi_1](x, z_1) \mathbf{L}[\phi_2](x, z_2) = \pi i \int_{\frac{d}{2}-i\infty}^{\frac{d}{2}+i\infty} \frac{d\Delta}{2\pi i} \mathcal{C}_{\Delta-1,0}(z_1, z_2, \partial_{z_2}) \left( \mathbb{O}_{\Delta,-1}^+(x, z_2) + \mathbb{O}_{\Delta,-1}^-(x, z_2) \right). \quad (5.147)$$

#### 5.3.4.4 Generalization and map to celestial structures

Let us summarize our result so far in slightly different language. In addition, we will generalize to the case where  $\mathcal{O}_1, \mathcal{O}_2$  are not necessarily traceless symmetric tensors. Suppose  $\mathcal{O}_i$  have weights  $(\Delta_i, J_i, \lambda_i)$ , where the  $\lambda_i$  are  $\text{SO}(d-2)$  representations. The light-transforms  $\mathbf{L}[\mathcal{O}_i](\infty)$  transform as tensors in the representation  $\lambda_i$  on the celestial sphere. To describe them, we can use the notation of appendix D.2. We write  $\mathbf{L}[\mathcal{O}_i](\infty, z, \vec{w})$ , where  $\vec{w} = w_1, \dots, w_{n-1} \in \mathbb{C}^d$  is a collection of null polarization vectors orthogonal to  $z$ , encoding rows in the Young diagram of  $\lambda_i$ . The light-ray operators appearing in the OPE may also have nontrivial  $\lambda$ . In what follows,  $\mathcal{O}$  stands for the representation with weights  $(\Delta, J, \lambda) = (\delta+1, J_1+J_2-1, \lambda)$ .

Lorentz-invariance guarantees that there exists an  $\text{SO}(d-1, 1)$ -invariant differential operator  $\mathcal{D}_{\delta,\lambda}^{(a)}(z_1, \vec{w}_1, z_2, \vec{w}_2, \partial_{z_2}, \partial_{\vec{w}_2})$  on the celestial sphere such that

$$\begin{aligned} & \mathcal{D}_{\delta,\lambda}^{(a)}(z_1, \vec{w}_1, z_2, \vec{w}_2, \partial_{z_2}, \partial_{\vec{w}_2}) \langle \mathbf{L}[\mathcal{O}](\infty, z_2, \vec{w}_2) \mathbf{L}[\mathcal{O}^\dagger](0, z_0, \vec{w}_0) \rangle \\ &= \frac{\langle 0 | \mathbf{L}^+[\mathcal{O}_2](\infty, z_2, \vec{w}_2) \mathbf{L}[\mathcal{O}^\dagger](0, z_0, \vec{w}_0) \mathbf{L}^-[\mathcal{O}_1](\infty, z_1, \vec{w}_1) | 0 \rangle^{(a)}}{\text{vol SO}(1, 1)}. \end{aligned} \quad (5.148)$$

In the notation of section 5.3.4.2, when  $\lambda$  is the spin- $j$  representation of  $\text{SO}(d-2)$ , we have  $\mathcal{D}_{\delta,j}^{(a)} = (q_{\delta,j}^{(a)}/r_{\delta,j}) \mathcal{C}_{\delta,j}$ . The derivation of section 5.3.4.2 generalizes straightforwardly to give<sup>21</sup>

$$\begin{aligned} & \mathbf{L}[\mathcal{O}_1](x, z_1, \vec{w}_1) \mathbf{L}[\mathcal{O}_2](x, z_2, \vec{w}_2) \\ &= \pi i \sum_{\lambda} \int_{\frac{d}{2}-i\infty}^{\frac{d}{2}+i\infty} \frac{d\Delta}{2\pi i} \mathcal{D}_{\delta,\lambda}^{(a)}(z_1, \vec{w}_1, z_2, \vec{w}_2, \partial_{z_2}, \partial_{\vec{w}_2}) \\ & \quad \times \left( \mathbb{O}_{\Delta, J_1+J_2-1, \lambda(a)}^+(x, z_2, \vec{w}_2) + \mathbb{O}_{\Delta, J_1+J_2-1, \lambda(a)}^-(x, z_2, \vec{w}_2) \right). \end{aligned} \quad (5.149)$$

<sup>21</sup>As we discuss in section 5.4.1, only the term with signature  $(-1)^{J_1+J_2}$  contributes at  $z_1 \not\propto z_2$ .

Here,  $\lambda$  ranges over  $\text{SO}(d-2)$  representations that can appear in the  $\mathcal{O}_1 \times \mathcal{O}_2$  OPE.

A simple rule to determine the allowed  $\lambda$  is as follows. Let  $\rho_i = (J_i, \lambda_i)$  be the Lorentz irreps of  $\mathcal{O}_1$  and  $\mathcal{O}_2$ . The allowed  $\lambda$  are those satisfying

$$\lambda \subset \text{Res}_{\text{SO}(d-2)}^{\text{SO}(d-1,1)} \rho_1 \otimes \rho_2, \quad (5.150)$$

where  $\text{Res}_H^G$  denotes restriction of a representation of group  $G$  to its subgroup  $H$ . One can derive this rule by considering the three-point structure  $\langle \mathcal{O}_1(x_1) \mathcal{O}(x_0, z) \mathcal{O}_2(x_2) \rangle$  as a function of  $x_1, x_2, x_0$ , and  $z$ . It furthermore carries indices for  $\rho_1, \rho_2$  and  $\lambda$  which we have suppressed. Using conformal invariance, we can fix  $x_1, x_0, x_2$  to lie on a line in the time direction and  $z$  to be  $(1, 1, 0, \dots)$ . The stabilizer group of this configuration is  $\text{SO}(d-2)$ , and the correlator must be invariant under this stabilizer group. This leads to (5.150). The result is equivalent to the rule stated in the introduction, which implies that the  $\lambda$  that appear are exactly those for which a Lorentzian inversion formula exists.

Equation (5.148) essentially defines a map from a three-point structure  $\langle \mathcal{O}_1 \mathcal{O}_2 \mathcal{O}^\dagger \rangle^{(a)}$  in  $d$ -dimensions to a differential operator  $\mathcal{D}_{\delta, \lambda}^{(a)}$  in  $d-2$  dimensions. We saw in section (5.3.4.3) that when  $\mathcal{O}_1, \mathcal{O}_2$  are scalars, this map is surprisingly simple: it takes the standard Wightman structure (5.140) to the standard differential operator  $\mathcal{C}_{\delta, 0}$ . In fact, this map turns out to be simple in general. We claim that  $\mathcal{D}_{\delta, \lambda}^{(a)}$  is determined by

$$\begin{aligned} & \mathcal{D}_{\delta, \lambda}^{(a)}(z_1, \vec{w}_1, z_2, \vec{w}_2, \partial_{z_2}, \partial_{\vec{w}_2}) \left( (-2H_{20}) \langle \mathcal{O}(X_2, Z_2, \vec{W}_2) \mathcal{O}^\dagger(X_0, Z_0, \vec{W}_0) \rangle \Big|_{\text{celestial}} \right) \\ &= X_{12} (-2V_{0,21}) \langle 0 | \mathcal{O}_2(X_2, Z_2, \vec{W}_2) \mathcal{O}^\dagger(X_0, Z_0, \vec{W}_0) \mathcal{O}_1(X_1, Z_1, \vec{W}_1) | 0 \rangle^{(a)} \Big|_{\text{celestial}}. \end{aligned} \quad (5.151)$$

Here, we use embedding-space language, as explained in appendix D.2. The objects  $V_{i,jk}$  and  $H_{ij}$  are defined in appendix D.4, see also [192]. The two-point and three-point structures above are each specialized to the ‘‘celestial’’ locus

$$f(X_i, Z_i, \vec{W}_i) \Big|_{\text{celestial}} \equiv f(X_i, Z_i, \vec{W}_i) \Big|_{\substack{Z_0 = -(1,0,0) \\ Z_1 = -(0,1,0) \\ Z_2 = -(0,1,0) \\ X_i = (0,0,z_i) \\ W_{i,j} = (0,0,w_{i,j})}}. \quad (5.152)$$

This corresponds to placing all three operators on the celestial sphere given by the intersection of the future lightcone of the origin and the future lightcone of spatial infinity (figure 5.10). It is easy to check that the three-point function on the right-hand side of (5.151), after restricting to the celestial locus, has homogeneity  $-\delta_i = 1 - \Delta_i$  in

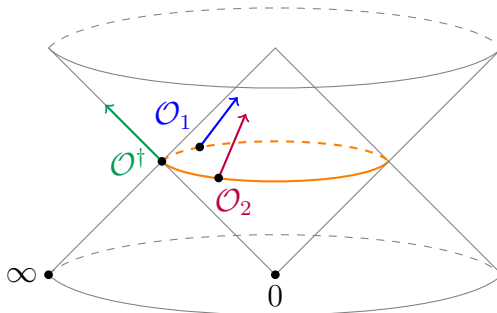


Figure 5.10: The celestial locus configuration appearing in (5.151) and (5.152). The operators  $\mathcal{O}_1$ ,  $\mathcal{O}_2$ , and  $\mathcal{O}^\dagger$  are placed on the celestial sphere (orange) that is the intersection of the future null cones of 0 and  $\infty$ . The arrows indicate the directions of the polarization vectors of each operator (which are inherited from their original light-transform contours).

$z_i$ , and hence transforms like a three-point function of operators with dimensions  $\delta_i$  in  $d - 2$  dimensions. Similarly, the two-point function on the left-hand side transforms correctly in  $d - 2$  dimensions.

For example, when  $\mathcal{O}_1 = \phi_1$ ,  $\mathcal{O}_2 = \phi_2$  are scalars and  $\mathcal{O}$  is a traceless symmetric tensor with dimension  $\Delta$ , one can check from (5.140) that

$$\begin{aligned} (-2H_{20})\langle\mathcal{O}(X_2, Z_2)\mathcal{O}^\dagger(X_0, Z_0)\rangle|_{\text{celestial}} &= \langle\mathcal{P}_\delta(z_2)\mathcal{P}_\delta(z_0)\rangle, \\ X_{12}(-2V_{0,21})\langle 0|\phi_2(X_2)\mathcal{O}^\dagger(X_0, Z_0)\phi_1(X_1)|0\rangle|_{\text{celestial}} &= \langle\mathcal{P}_{\delta_1}(z_1)\mathcal{P}_{\delta_2}(z_2)\mathcal{P}_\delta(z_0)\rangle, \end{aligned} \quad (5.153)$$

which easily gives  $\mathcal{D}_{\delta,0} = \mathcal{C}_{\delta,0}$ .

We have checked that (5.151) is equivalent to (5.148) for arbitrary traceless symmetric tensor representations by explicit calculation, see appendix D.4. It can also be justified by examining the limit as  $z_1 \rightarrow z_2$  in (5.148). It would be nice to prove (5.151) more directly.

One important caveat to this discussion is that it only applies for separated points, i.e. when  $z_1$  is not proportional to  $z_2$ . As we will see in section 5.6, this map has to be modified in some special cases if one wishes to study  $z_1 \propto z_2$  contact terms.

## 5.4 Commutativity

### 5.4.1 Light-ray OPE for the commutator

In chapter 4, we argued on general grounds that  $\mathbf{L}[\mathcal{O}_1](x, z_1, \vec{w}_1)$  and  $\mathbf{L}[\mathcal{O}_2](x, z_2, \vec{w}_2)$  commute, given certain conditions on  $J_1$  and  $J_2$ . Our derivation of the light-ray

OPE does not assume commutativity. In fact, even when commutativity holds, it is obscured in our derivation, since  $\mathbf{L}[\mathcal{O}_1]$  and  $\mathbf{L}[\mathcal{O}_2]$  are treated differently. For example, to obtain a double-commutator, we subtract the action of  $\mathbf{L}[\mathcal{O}_1]$  on the future vacuum and  $\mathbf{L}[\mathcal{O}_2]$  on the past vacuum.

It is instructive to see how commutativity appears from the point of view of the light-ray OPE. This will lead to nontrivial consistency conditions on the space of light-ray operators. In the remainder of this section, we assume the light-ray operators  $\mathbf{L}[\mathcal{O}_1]$  and  $\mathbf{L}[\mathcal{O}_2]$  are not coincident  $z_1 \not\propto z_2$ . We discuss how our arguments should be modified for coincident lightrays in section 5.6.

We derived an expression for  $\mathbf{L}[\mathcal{O}_1]\mathbf{L}[\mathcal{O}_2]$  in (5.149). We can obtain an expression for the reverse ordering  $\mathbf{L}[\mathcal{O}_2]\mathbf{L}[\mathcal{O}_1]$  by applying Rindler and Hermitian conjugation to both sides. Using (D.53) and (D.54), we find

$$\begin{aligned} & \mathbf{L}[\mathcal{O}_2](x, z_2, \vec{w}_2)\mathbf{L}[\mathcal{O}_1](x, z_1, \vec{w}_1) \\ &= \pi i \sum_{\lambda} \int_{\frac{d}{2}-i\infty}^{\frac{d}{2}+i\infty} \frac{d\Delta}{2\pi i} \mathcal{D}_{\delta,\lambda}^{(a)}(z_1, \vec{w}_1, z_2, \vec{w}_2, \partial_{z_2}, \partial_{\vec{w}_2}) \\ & \quad \times \left( (-1)^{J_1+J_2} \mathbb{O}_{\Delta, J_1+J_2-1, \lambda(a)}^+(x, z_2, \vec{w}_2) + (-1)^{J_1+J_2-1} \mathbb{O}_{\Delta, J_1+J_2-1, \lambda(a)}^-(x, z_2, \vec{w}_2) \right). \end{aligned} \quad (5.154)$$

Taking the difference with (5.149), we get the commutator

$$\begin{aligned} & [\mathbf{L}[\mathcal{O}_1](x, z_1, \vec{w}_1), \mathbf{L}[\mathcal{O}_2](x, z_2, \vec{w}_2)] \\ &= 2\pi i \sum_{\lambda} \int_{\frac{d}{2}-i\infty}^{\frac{d}{2}+i\infty} \frac{d\Delta}{2\pi i} \mathcal{D}_{\delta,\lambda}^{(a)}(z_1, \vec{w}_1, z_2, \vec{w}_2, \partial_{z_2}, \partial_{\vec{w}_2}) \mathbb{O}_{\Delta, J_1+J_2-1, \lambda(a)}^{(-1)^{J_1+J_2-1}}(x, z_2, \vec{w}_2) \\ &= -2\pi i \sum_i \mathcal{D}_{\delta_i, \lambda_i}^{(a)}(z_1, \vec{w}_1, z_2, \vec{w}_2, \partial_{z_2}, \partial_{\vec{w}_2}) \mathbb{O}_{i, J_1+J_2-1, \lambda(a)}^{(-1)^{J_1+J_2-1}}(x, z_2, \vec{w}_2). \end{aligned} \quad (5.155)$$

In the last line, we have assumed that the behavior of the integrand at large  $\Delta$  is such that we can deform the  $\Delta$ -contour to pick up poles on the positive real axis, obtaining a sum over Regge trajectories  $i$ . For more detail on deforming the  $\Delta$  contour, see section 5.5.2.

The operators on the right-hand side of (5.155) have spin  $J = J_1 + J_2 - 1$  and signature  $(-1)^J$ . For example, when  $J_1 \equiv J_2 \pmod{2}$ , the commutator is given by a sum of light-ray operators with odd  $J$  and odd signature. This is easy to understand from symmetries: the light-transforms  $\mathbf{L}[\mathcal{O}_i]$  have signature  $(-1)^{J_i}$ , and the commutator introduces an additional  $-1$ , since Hermitian conjugation reverses operator ordering.



These quantum numbers are exactly the ones needed for  $\mathbb{O}_{i, J_1+J_2-1, \lambda_i}^{(-1)^{J_1+J_2-1}}$  to be the light-transform of a local operator. Let us assume this is the case (we return to this assumption in section 5.4.2). Using (5.90), we have

$$\begin{aligned} & [\mathbf{L}[\mathcal{O}_1](x, z_1, \vec{w}_1), \mathbf{L}[\mathcal{O}_2](x, z_2, \vec{w}_2)] \\ &= -2\pi i \sum_i \mathcal{D}_{\delta_i, \lambda_i}^{(a)}(z_1, \vec{w}_1, z_2, \vec{w}_2, \partial_{z_2}, \partial_{\vec{w}_2}) f_{12\mathcal{O}_i^\dagger(a)} \mathbf{L}[\mathcal{O}_i](x, z_2, \vec{w}_2), \end{aligned} \quad (5.156)$$

where each  $\mathcal{O}_i$  has quantum numbers  $(\Delta, J, \lambda) = (\delta_i + 1, J_1 + J_2 - 1, \lambda_i)$ .

There are now two slightly different cases. In the first case, the local operators that would appear in the right hand side of (5.156) are not allowed to appear in the Euclidean OPE.<sup>22</sup> In other words,  $f_{12\mathcal{O}_i^\dagger(a)}$  are zero by selection rules. In this case we immediately find that the commutator is identically zero.

The second case is when  $f_{12\mathcal{O}_i^\dagger(a)}$  are not forbidden by Euclidean selection rules. To see that the commutator vanishes in this case, recall that the differential operator  $\mathcal{D}_{\delta, \lambda}^{(a)}$  is nonzero only if the three-point structure  $\langle \dots \rangle^{(a)}$  survives the map to celestial structures (5.151). However, the structure  $\langle \dots \rangle^{(a)}$  cannot survive this map if it also appears in a three-point function of local operators, modulo a small subtlety to be discussed below. The reason is that  $V_{0,21}|_{\text{celestial}} = 0$ , so the right-hand side of (5.151) vanishes unless  $\langle \dots \rangle^{(a)}$  contains a pole  $V_{0,21}^{-1}$  that can cancel this zero. Such poles are not allowed in three-point functions of local operators (which must be polynomial in polarization vectors  $z_i$ ). It follows that

$$f_{12\mathcal{O}_i^\dagger(a)} \mathcal{D}_{\delta_i, \lambda_i}^{(a)} = 0 \quad (5.157)$$

for any local operator  $\mathcal{O}_i$ . Hence, the commutator  $[\mathbf{L}[\mathcal{O}_1], \mathbf{L}[\mathcal{O}_2]]$  vanishes again.

There is a small subtlety in the above argument, which is due to the fact the statements about the map to celestial structures are correct for separated points only. As we will show in section 5.6, it does sometimes happen that tensor structures appearing in three-point functions of local operators map to contact terms on the celestial sphere.

The above argument was somewhat abstract, so let us give a concrete example. Consider the case  $\mathcal{O}_1 = \mathcal{O}_2 = T$ , where  $T$  is the stress tensor in a 3d CFT. The commutator  $[\mathbf{L}[T], \mathbf{L}[T]]$  is a sum of spin-3 light-ray operators on odd-signature Regge trajectories. By our assumption above, such operators are light-transforms of local

<sup>22</sup>This includes the cases when  $J_1 + J_2 - 1$  is negative, i.e.  $J_1 = J_2 = 0$ .

spin-3 operators. However, the  $T \times T$  OPE does not contain any spin-3 operators, due to selection rules and Ward identities [191, 204]. (Odd-spin operators appearing in  $T \times T$  have spins  $5, 7, \dots$ ) Thus, the commutator  $[\mathbf{L}[T], \mathbf{L}[T]]$  must vanish. No contact terms arise in this case.

### 5.4.2 Finishing the argument with conformal Regge theory

The key step in the above argument was the assumption that

$$\mathbb{O}_{i, J_1+J_2-1, \lambda(a)}^{(-1)^{J_1+J_2-1}} = f_{12\mathcal{O}_i^\dagger(a)} \mathbf{L}[\mathcal{O}_i], \quad (5.158)$$

where  $\mathcal{O}_i$  is a local operator of spin  $J_1 + J_2 - 1$ . As discussed in section 5.3.2.1, this is true by construction in the case when  $f_{12\mathcal{O}_i^\dagger(a)}$  is allowed to be non-zero by selection rules of the Euclidean OPE.<sup>23</sup> More precisely, this is true under the condition  $J_1 + J_2 - 1 > J_0$ , which comes from the fact that the Lorentzian inversion formula is only guaranteed to reproduce Euclidean OPE data for spins larger than  $J_0$ . We return to this condition later in this section.

We are also interested in the case where  $f_{12\mathcal{O}_i^\dagger(a)}$  is forbidden by the selection rules of the Euclidean OPE. In this case, there is nothing that we can write in the right-hand side of (5.158) and so we would like to argue that in this case

$$\mathbb{O}_{i, J_1+J_2-1, \lambda(a)}^{(-1)^{J_1+J_2-1}} = 0. \quad (5.159)$$

We can argue for (5.159) using conformal Regge theory and boundedness in the Regge limit. Let us first review some aspects of conformal Regge theory, using a four-point function of scalars for simplicity. We follow the presentation of [28]. One starts with a four-point function in a Euclidean partial wave expansion

$$\langle \phi_1 \phi_2 \phi_3 \phi_4 \rangle = \sum_{J=0}^{\infty} \oint \frac{d\Delta}{2\pi i} C(\Delta, J) (\mathcal{F}_{\Delta, J}(x_i) + \mathcal{H}_{\Delta, J}(x_i)). \quad (5.160)$$

Here, we've split each partial wave into a piece  $\mathcal{F}_{\Delta, J}(x_i)$  that dies at large positive  $J$  and a piece  $\mathcal{H}_{\Delta, J}(x_i)$  that dies at large negative  $J$ . For simplicity, we only keep track of  $\mathcal{F}_{\Delta, J}$ . The sum runs over nonnegative integer  $J$  because these are the allowed spins in the Euclidean OPE.

---

<sup>23</sup>Saying that  $f_{12\mathcal{O}_i^\dagger(a)} = 0$  even though it is allowed by Euclidean OPE amounts to saying that there is no corresponding pole in  $\mathbb{O}_{\Delta, J, \lambda(a)}^\pm$  and hence no  $\mathbb{O}_{i, J_1+J_2-1, \lambda(a)}^{(-1)^{J_1+J_2-1}}$  in the first place.

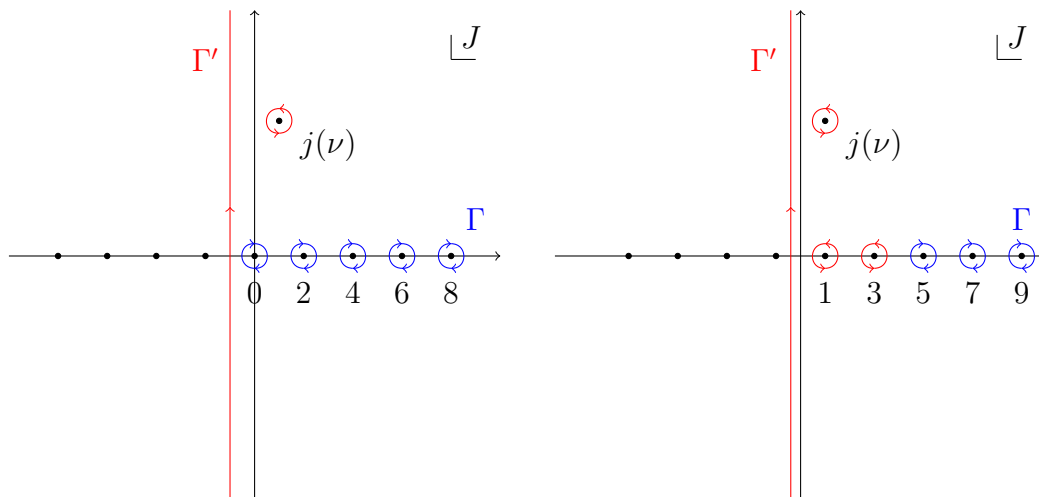


Figure 5.11: Deformation of Regge contour in Sommerfeld-Watson transform. Left: even spins in the case of scalar four-point function. Right: odd spins in the case of  $\langle TT\mathcal{O}_3\mathcal{O}_4\rangle$ .

The key step is the Sommerfeld-Watson transform: we rewrite the sum over  $J$  as a contour integral

$$\sum_{J=0}^{\infty} \oint \frac{d\Delta}{2\pi i} C(\Delta, J) \mathcal{F}_{\Delta, J}(x_i) = - \oint_{\Gamma} dJ \oint \frac{d\Delta}{2\pi i} \left( \frac{C^+(\Delta, J)}{1 - e^{-i\pi J}} + \frac{C^-(\Delta, J)}{1 + e^{-i\pi J}} \right) \mathcal{F}_{\Delta, J}(x_i), \quad (5.161)$$

where  $\Gamma$  encircles all nonnegative integers clockwise. We now deform the contour  $\Gamma \rightarrow \Gamma'$  towards the imaginary  $J$  axis (left panel of figure 5.11). When we do, we pick up any poles or branch cuts in the integrand that were not encircled by the original contour  $\Gamma$ . We refer to such singularities as ‘‘Regge poles.’’ In figure 5.11 we show a single Regge pole at  $J = j(\nu)$ . The behavior of the correlator in the Regge limit is determined by the Regge poles. If the Regge growth exponent is  $J_0$ , then all Regge poles must have real part less or equal to  $J_0$ .

Let us now consider what happens in spinning four-point functions when we have non-trivial selection rules. For concreteness, we will focus on the case  $\mathcal{O}_1 = \mathcal{O}_2 = T$  and study matrix elements of  $\mathbb{O}_{i, J_1+J_2-1, \lambda(a)}^{(-1)^{J_1+J_2-1}} = \mathbb{O}_{i, 3, (a)}^-$  (i.e.  $\lambda = 0$ ) between generic states created by  $\mathcal{O}_3$  and  $\mathcal{O}_4$ . These matrix elements show up as residues of the poles of the function  $C_{ab}^-(\Delta, J = 3, \lambda = 0)$  which appears in the partial wave expansion of  $\langle TT\mathcal{O}_3\mathcal{O}_4\rangle$ . Note that there are no local spin-3 (or spin-1) operators in  $T \times T$  OPE allowed by selection rules. In order to prove (5.159) we must show that this function does not have physical poles.

To see this, imagine applying conformal Regge theory to  $\langle TT\mathcal{O}_3\mathcal{O}_4\rangle$ . We will arrive at the generalization of (5.161), where the factor<sup>24</sup>

$$\frac{1}{1 + e^{-i\pi J}} \quad (5.162)$$

will create poles for all odd  $J$ , including  $J = 1$  and  $J = 3$ . However, since  $J = 1, 3$  are not allowed in the Euclidean OPE, the contour  $\Gamma$  must not circle these poles, see right panel of figure 5.11. This implies that these poles will be picked up by  $\Gamma'$ . If  $J_0 < 3$ , we must conclude that the residue of  $J = 3$  pole vanishes, and so

$$C_{ab}^-(\Delta, J = 3, \lambda = 0) = 0. \quad (5.163)$$

This straightforwardly generalizes to other situations, and we conclude that (5.158) holds provided  $J_1 + J_2 - 1 > J_0$ . If this condition is satisfied, the arguments in the previous section show that  $[\mathbf{L}[\mathcal{O}_1](x, z_1), \mathbf{L}[\mathcal{O}_2](x, z_2)]$  vanishes for  $z_1 \not\propto z_2$ . This is precisely the same result as obtained in chapter 4, where it was shown that  $J_1 + J_2 - 1 > J_0$  is a necessary condition for the product  $\mathbf{L}[\mathcal{O}_1](x, z_1)\mathbf{L}[\mathcal{O}_2](x, z_2)$  to be well-defined and commutative.

### 5.4.3 Superconvergence in $\nu$ -space

We have seen that when  $J_1 + J_2 - 1 > J_0$ , the commutator (5.155) vanishes. This follows from the analysis of chapter 4, or alternatively from the arguments of sections 5.4.1 and 5.4.2 using the light-ray OPE and conformal Regge theory.<sup>25</sup> From (5.155), commutativity is equivalent to the statement that

$$\langle \Omega | \mathcal{O}_4 \mathbb{O}_{\frac{d}{2} + i\nu, J_1 + J_2 - 1, \lambda(a)}^{(-1)^{J_1 + J_2 - 1}}(x, z_2, \vec{w}_2) \mathcal{O}_3 | \Omega \rangle = 0, \quad \text{if } J_1 + J_2 - 1 > J_0, \quad (5.164)$$

where we have written  $\Delta = \frac{d}{2} + i\nu$ , and the above conditions hold for all  $\nu \in \mathbb{R}$ . Using (5.91), we can also write this as

$$C_{ab}^{(-1)^{J_1 + J_2 - 1}} \left( \frac{d}{2} + i\nu, J_1 + J_2 - 1, \lambda \right) = 0, \quad \text{if } J_1 + J_2 - 1 > J_0. \quad (5.165)$$

What constraints do these conditions imply on CFT data?

<sup>24</sup>One might argue that in this case we should use a different factor in the Sommerfeld-Watson transform. However, the factor  $\frac{1}{1 + e^{-i\pi J}}$  is the unique factor which has the same residue at all sufficiently large odd  $J$  and an appropriate behavior at infinity in the complex plane.

<sup>25</sup>More precisely, those arguments applied to the case where the null directions  $z_1$  and  $z_2$  are not coincident  $z_1 \not\propto z_2$ . For coincident null directions, there can be contact terms. In that case, the discussion in this section would need to be modified by subtracting those contact terms before passing to  $\nu$ -space. In the case of ANEC operators, contact terms are absent.

For simplicity, let us specialize to the case where  $\mathcal{O}_1 = \mathcal{O}_2 = \mathcal{O}_3 = \mathcal{O}_4 = \phi$  are identical scalars (so that  $\lambda = \bullet$  and the labels  $a, b$  are trivial). Recall that  $C^\pm(\Delta, J)$  is computed by plugging the physical four-point function  $g(z, \bar{z})$  into the Lorentzian inversion formula (5.77) and performing the integral. The four-point function has an expansion in  $t$ -channel conformal blocks that converges exponentially inside the square  $z, \bar{z} \in (0, 1)$  [184]:

$$\begin{aligned} g(z, \bar{z}) &= \left( \frac{z\bar{z}}{(1-z)(1-\bar{z})} \right)^{\Delta_\phi} \sum_{\Delta', J'} p_{\Delta', J'} G_{\Delta', J'}(1-z, 1-\bar{z}). \\ \text{dDisc}_t[g](z, \bar{z}) &= \left( \frac{z\bar{z}}{(1-z)(1-\bar{z})} \right)^{\Delta_\phi} \sum_{\Delta', J'} 2 \sin^2 \left( \pi \frac{\Delta' - 2\Delta_\phi}{2} \right) p_{\Delta', J'} G_{\Delta', J'}(1-z, 1-\bar{z}). \end{aligned} \quad (5.166)$$

On the second line, we have written an expansion for  $\text{dDisc}[g]$ . Because  $\text{dDisc}$  inserts positive, bounded factors  $2 \sin^2 \left( \pi \frac{\Delta' - 2\Delta_\phi}{2} \right)$  into the  $t$ -channel block expansion, the  $t$ -channel block expansion for  $\text{dDisc}[g]$  converges exponentially inside the square as well.

Inserting (5.166) into the Lorentzian inversion formula, we obtain an expression for  $C^\pm(\Delta, J)$  as a sum

$$C^\pm(\Delta, J) = \sum_{\Delta', J'} p_{\Delta', J'} \mathcal{B}^\pm(\Delta, J; \Delta', J'), \quad (5.167)$$

where  $\mathcal{B}^\pm(\Delta, J; \Delta', J')$  is the Lorentzian inversion of a single  $t$ -channel block. The functions  $\mathcal{B}^\pm(\Delta, J; \Delta', J')$  were computed in  $d = 2$  and  $d = 4$  dimensions in [230]. We expect the sum (5.167) to converge whenever  $\Delta = \frac{d}{2} + i\nu$  is on the principal series and  $J > J_0$  is larger than the Regge intercept. We argue for this using the Fubini-Tonelli theorem in appendix D.5.

Plugging (5.167) into (5.165), we obtain an infinite set of sum rules<sup>26</sup>

$$0 = \sum_{\Delta', J'} p_{\Delta', J'} \mathcal{B}^- \left( \frac{d}{2} + i\nu, -1; \Delta', J' \right), \quad \text{if } J_0 < -1. \quad (5.168)$$

As we will see in section 5.5.4, these are precisely the superconvergence sum rules of chapter 4, written as a function of a different variable  $\nu$ . In  $\nu$ -space, we have a clear argument that the sum is convergent. More generally, for spinning light-ray

<sup>26</sup>We expect that  $J_0 < -1$  is not true in most interesting theories. Here, we have this condition because we specialized to scalar operators for simplicity.

operators, we find

$$\begin{aligned}
0 &= C_{ab}^{(-1)^{J_1+J_2-1}} \left( \frac{d}{2} + i\nu, J_1 + J_2 - 1, \lambda \right) \\
&= \sum_{\Delta', J', \lambda'} p_{\Delta', J', \lambda'}^{cd} \mathcal{B}_{ab;cd}^{(-1)^{J_1+J_2-1}} \left( \frac{d}{2} + i\nu, J_1 + J_2 - 1, \lambda; \Delta', J', \lambda' \right), \quad \text{if } J_1 + J_2 - 1 > J_0,
\end{aligned} \tag{5.169}$$

where  $\mathcal{B}_{ab;cd}^\pm$  is the spinning analog of  $\mathcal{B}^\pm$ , including three-point structure labels  $a, b, c, d$ . Equation (5.169) may be a good starting point for analyzing contributions of stringy states to superconvergence sum rules in holographic theories.

We give more details on the relationship between (5.169) and the sum rules from chapter 4 in section 5.5.4.

## 5.5 The celestial block expansion

### 5.5.1 Celestial blocks

For the purpose of computing event shapes, we would like to apply the light-ray OPE inside momentum eigenstates. Matrix elements of individual light-ray operators  $\mathbb{O}_{\Delta, J}$  in momentum eigenstates are proportional to the one-point event shape (5.49). To apply the OPE (5.139), we must understand how to apply the differential operator  $\mathcal{C}_{\delta, 0}(z_1, z_2, \partial_{z_2})$  to these matrix elements:

$$\mathcal{C}_{\delta, 0}(z_1, z_2, \partial_{z_2}) \langle \phi(p) | \mathbb{O}_{\Delta, J}(\infty, z_2) | \phi(p) \rangle \propto \mathcal{C}_{\delta, 0}(z_1, z_2, \partial_{z_2}) (-2z_2 \cdot p)^{-\delta}. \tag{5.170}$$

We call the resulting objects ‘‘celestial blocks’’ because they capture the full contribution of a light-ray operator and its  $z$ -derivatives to an event shape.

The right-hand side of (5.170) is fixed by Lorentz-invariance and homogeneity to have the form

$$\mathcal{C}_{\delta, 0}(z_1, z_2, \partial_{z_2}) (-2z_2 \cdot p)^{-\delta} = \frac{(-p^2)^{\frac{\delta_1 + \delta_2 - \delta}{2}}}{(-2z_1 \cdot p)^{\delta_1} (-2z_2 \cdot p)^{\delta_2}} f(\zeta), \tag{5.171}$$

where the cross-ratio  $\zeta$  is given by

$$\zeta = \frac{(-2z_1 \cdot z_2)(-p^2)}{(-2z_1 \cdot p)(-2z_2 \cdot p)}. \tag{5.172}$$

Furthermore, it is an eigenvector of the quadratic Casimir of the Lorentz group acting simultaneously on  $z_1, z_2$ , or equivalently acting on  $p$ . Specifically, it is killed by the differential operator

$$-\frac{1}{2} \left( p_\mu \frac{\partial}{\partial p^\nu} - p_\nu \frac{\partial}{\partial p^\mu} \right) \left( p^\mu \frac{\partial}{\partial p_\nu} - p^\nu \frac{\partial}{\partial p_\mu} \right) - \delta(\delta - d + 2). \tag{5.173}$$

This gives the Casimir differential equation

$$0 = 4(1 - \zeta)\zeta^2 f''(\zeta) - 2\zeta(2(\delta_1 + \delta_2 + 1)\zeta + d - 2(\delta_1 + \delta_2 + 2))f'(\zeta) + ((\delta - \delta_1 - \delta_2)(d - \delta - \delta_1 - \delta_2 - 2) - 4\delta_1\delta_2\zeta)f(\zeta). \quad (5.174)$$

Meanwhile, from the definition of  $\mathcal{C}_{\delta,0}$ , we see that

$$\mathcal{C}_{\delta,0}(z_1, z_2, \partial_{z_2})(-2z_2 \cdot p)^{-\delta} = (-2z_1 \cdot z_2)^{\frac{\delta - \delta_1 - \delta_2}{2}}(-2z_2 \cdot p)^{-\delta} + \dots, \quad (5.175)$$

where “...” represent higher-order terms in the separation between  $z_1$  and  $z_2$  on the celestial sphere. In terms of  $f(\zeta)$ , this becomes

$$f(\zeta) = \zeta^{\frac{\delta - \delta_1 - \delta_2}{2}}(1 + O(\zeta)). \quad (5.176)$$

The solution to the Casimir equation with boundary condition (5.176) is

$$f_{\Delta}^{\Delta_1, \Delta_2}(\zeta) = \zeta^{\frac{\Delta - \Delta_1 - \Delta_2 + 1}{2}} {}_2F_1\left(\frac{\Delta - 1 + \Delta_1 - \Delta_2}{2}, \frac{\Delta - 1 - \Delta_1 + \Delta_2}{2}, \Delta + 1 - \frac{d}{2}, \zeta\right), \quad (5.177)$$

where we have written  $\delta_i = \Delta_i - 1$  for future convenience.

Essentially the same function has appeared previously in the literature as the conformal block for a two-point function of local operators in the presence of a spherical codimension-1 boundary [44, 216]. The reason is that the momentum  $p$  breaks  $\text{SO}(d-1, 1)$  in a similar way to a boundary in a  $d-2$  dimensions. To see this, consider an embedding space coordinate  $X \in \mathbb{R}^{d-1,1}$  for a  $d-2$ -dimensional CFT. A spherical codimension-1 boundary is specified by  $P \cdot X = 0$ , for some spacelike  $P \in \mathbb{R}^{d-1,1}$  [48]. The vector  $P$  breaks the symmetry from  $\text{SO}(d-1, 1)$  to  $\text{SO}(d-2, 1)$ . In our case, we have a timelike vector  $p$  that breaks the symmetry from  $\text{SO}(d-1, 1)$  to  $\text{SO}(d-1)$ . However, the Casimir equation is the same in both cases, and the only difference is a minus sign in our definition of the cross-ratio  $\zeta$ .

Now, we can finally write the light-ray OPE for a two-point event shape. For simplicity, we consider the case where the sink, source, and detectors are all scalars. From the OPE (5.139), we have

$$\begin{aligned} & \langle \phi_4(p) | \mathbf{L}[\phi_1](\infty, z_1) \mathbf{L}[\phi_2](\infty, z_2) | \phi_3(p) \rangle \\ &= \pi i \int_{\frac{d}{2} - i\infty}^{\frac{d}{2} + i\infty} \frac{d\Delta}{2\pi i} \mathcal{C}_{\Delta-1,0}(z_1, z_2, \partial_{z_2}) \langle \phi_4(p) | \mathbb{O}_{\Delta,-1}^+(\infty, z_2) + \mathbb{O}_{\Delta,-1}^-(\infty, z_2) | \phi_3(p) \rangle \\ &= -\pi i \int_{\frac{d}{2} - i\infty}^{\frac{d}{2} + i\infty} \frac{d\Delta}{2\pi i} (C^+(\Delta, -1) + C^-(\Delta, -1)) \mathcal{C}_{\Delta-1,0}(z_1, z_2, \partial_{z_2}) \langle \phi_4(p) | \mathbf{L}[\mathcal{O}](\infty, z_2) | \phi_3(p) \rangle, \end{aligned} \quad (5.178)$$

where  $\langle 0|\phi_4\mathcal{O}\phi_3|0\rangle$  is the standard Wightman structure (5.140) with  $2 \rightarrow 4$  and  $1 \rightarrow 3$ . Plugging in the expression (5.49) for the light transform and Fourier transform (with appropriate relabelings), and using (5.171) we find

$$\langle \phi_4(p)|\mathbf{L}[\phi_1](\infty, z_1)\mathbf{L}[\phi_2](\infty, z_2)|\phi_3(p)\rangle = \frac{(-p^2)^{\frac{\Delta_1+\Delta_2+\Delta_3+\Delta_4-4-d}{2}}\theta(p)}{(-2z_1 \cdot p)^{\Delta_1-1}(-2z_2 \cdot p)^{\Delta_2-1}}\mathcal{G}_{\phi_1\phi_2}(\zeta), \quad (5.179)$$

where

$$\begin{aligned} \mathcal{G}_{\phi_1\phi_2}(\zeta) &= 2^{d+4-\Delta_3-\Delta_4}\pi^{\frac{d}{2}+3}e^{i\pi\frac{\Delta_4-\Delta_3}{2}} \\ &\times \int_{\frac{d}{2}-i\infty}^{\frac{d}{2}+i\infty} \frac{d\Delta}{2\pi i} \frac{\Gamma(\Delta-2)(C^+(\Delta, -1)+C^-(\Delta, -1))}{\Gamma(\frac{\Delta-1+\Delta_3-\Delta_4}{2})\Gamma(\frac{\Delta-1-\Delta_3+\Delta_4}{2})\Gamma(\frac{\Delta_3+\Delta_4-\Delta-1}{2})\Gamma(\frac{\Delta-1+\Delta_3+\Delta_4-d}{2})} f_{\Delta}^{\Delta_1, \Delta_2}(\zeta). \end{aligned} \quad (5.180)$$

In the special case where the sink and source are the same  $\phi_3 = \phi_4 = \phi$ , it is natural to define an expectation value by dividing by a zero-point event shape:

$$\langle \phi(p)|\phi(p)\rangle \equiv \int d^d x e^{ip \cdot x} \langle 0|\phi(0)\phi(x)|0\rangle = \frac{2^{d+1-2\Delta_\phi}\pi^{\frac{d+2}{2}}}{\Gamma(\Delta_\phi - \frac{d-2}{2})\Gamma(\Delta_\phi)} (-p^2)^{\frac{2\Delta_\phi-d}{2}} \theta(p). \quad (5.181)$$

We find

$$\frac{\langle \phi(p)|\mathbf{L}[\phi_1](\infty, z_1)\mathbf{L}[\phi_2](\infty, z_2)|\phi(p)\rangle}{\langle \phi(p)|\phi(p)\rangle} = \frac{\Gamma(\Delta_\phi - \frac{d-2}{2})\Gamma(\Delta_\phi)}{2^{d+1-2\Delta_\phi}\pi^{\frac{d+2}{2}}} \frac{(-p^2)^{\frac{\Delta_1+\Delta_2}{2}-2}\mathcal{G}_{\phi_1\phi_2}(\zeta)}{(-2z_1 \cdot p)^{\Delta_1-1}(-2z_2 \cdot p)^{\Delta_2-1}}. \quad (5.182)$$

### 5.5.2 Contour deformation in $\Delta$ and spurious poles

In (5.180), the celestial block expansion of  $\mathcal{G}_{\phi_1\phi_2}(\zeta)$  takes the form of an integral over the principal series  $\Delta \in \frac{d}{2} + i\mathbb{R}$ . When  $\zeta < 1$ , the celestial block  $f_{\Delta}^{\Delta_1, \Delta_2}(\zeta)$  is exponentially damped in the right-half  $\Delta$ -plane, so we can deform the contour into this region and pick up poles in the integrand.

The coefficient function  $C^\pm(\Delta, J)$  contains poles of the form

$$C^\pm(\Delta, J) \ni -\frac{p_i^\pm(J)}{\Delta - \Delta_i^\pm(J)}, \quad (5.183)$$

where  $p_i^\pm(J)$  are products of OPE coefficients analytically-continued in  $J$ , and  $\Delta_i^\pm(J)$  are dimensions analytically-continued in  $J$ .<sup>27</sup> When we deform the  $\Delta$ -contour, we

<sup>27</sup>We comment on the possibility of non-simple poles or branch-cuts in  $\Delta$  below.



pick up contributions from these poles. They are interpreted as light-ray operators in the light-ray OPE.

In general,  $C^\pm(\Delta, J)$  can also contain “spurious” poles at  $\Delta = d + J + n$  for integer  $n$ , originating from poles in the conformal block  $G_{J+d-1, \Delta-d+1}(z, \bar{z})$  in the Lorentzian inversion formula (5.77). In the usual conformal block expansion, these spurious poles cancel with poles in  $G_{\Delta, J}(z, \bar{z})$  that are encountered when deforming the  $\Delta$ -contour from the principal series to the positive real axis [25, 26, 82, 149]. However, the celestial block  $f_{\Delta}^{\Delta_1, \Delta_2}(\zeta)$  does not have poles in  $\Delta$  to the right of the principal series.<sup>28</sup> Thus, it is not clear how spurious poles in  $C^\pm(\Delta, J)$  could cancel.

Remarkably, it turns out that when we set  $J = -1$ , spurious poles in  $C^\pm(\Delta, J)$  are absent. This can be seen as follows. Note that the following combination of conformal blocks is free of poles to the right of  $\Delta = \frac{d}{2}$  [25]:

$$G_{J+d-1, \Delta-d+1}(z, \bar{z}) - r_{\Delta, J} G_{\Delta, J}(z, \bar{z}), \quad (5.184)$$

where

$$\begin{aligned} r_{\Delta, J} = & \frac{\Gamma(J + \frac{d-2}{2})\Gamma(J + \frac{d}{2})}{\Gamma(J+1)\Gamma(J+d-2)} \frac{\Gamma(\Delta-1)\Gamma(\Delta-d+2)}{\Gamma(\Delta - \frac{d}{2})\Gamma(\Delta - \frac{d-2}{2})} \\ & \times \frac{\Gamma(J - \Delta + d)\Gamma(\frac{-d-J+\Delta-\Delta_1+\Delta_2+2}{2})\Gamma(\frac{-d-J+\Delta+\Delta_3-\Delta_4+2}{2})}{\Gamma(\Delta - J - d + 2)\Gamma(\frac{d+J-\Delta-\Delta_1+\Delta_2}{2})\Gamma(\frac{d+J-\Delta+\Delta_3-\Delta_4}{2})}. \end{aligned} \quad (5.185)$$

Suppose first that  $d \neq 4$ . Setting  $J = -1$ , the factor  $\Gamma(J+1)^{-1}$  in (5.185) ensures that  $r_{\Delta, -1} = 0$ , so that  $G_{J+d-1, \Delta-d+1}|_{J=-1}$  is free of poles to the right of  $\Delta = \frac{d}{2}$ . In the special case  $d = 4$ , we have [231, 232]

$$G_{\Delta, -1} = \frac{z\bar{z}}{z - \bar{z}} (k_{\Delta-1}(z)k_{\Delta-1}(\bar{z}) - k_{\Delta-1}(z)k_{\Delta-1}(\bar{z})) = 0, \quad (5.186)$$

so that  $G_{J+d-1, \Delta-d+1}|_{J=-1}$  is again free of poles to the right of  $\Delta = \frac{d}{2}$ .<sup>29</sup>

Let us also comment on the case  $d = 3$ . There, the Lorentz group is  $\text{SL}(2, \mathbb{R})$ , whose harmonic analysis is slightly different than for the higher-dimensional Lorentz groups. In particular, the Plancherel measure for  $\text{SL}(2, \mathbb{R})$  has support on discrete series representations in addition to principal series representations. In this case, we expect the contribution of discrete series representations to be cancelled by poles in

<sup>28</sup>Assuming  $|\Delta_1 - \Delta_2|$  is not too large. See [28, 194] for examples of how to treat the case where  $|\Delta_1 - \Delta_2|$  is large.

<sup>29</sup>Note that the case  $d = 2$  is not relevant to our discussion, since there is no transverse space  $\mathbb{R}^{d-2}$  in which to consider the light-ray OPE.

$C^\pm(\Delta, J)$ , in the same way as occurs in the four-point function of fermions in the SYK model [233].

The end result is that spurious poles and discrete state contributions are absent in the celestial block expansion for all  $d > 2$ . Deforming the  $\Delta$ -contour, we obtain  $\mathcal{G}_{\phi_1\phi_2}(\zeta)$  as a sum of contributions from light-ray operators when  $\zeta < 1$

$$\begin{aligned} \mathcal{G}_{\phi_1\phi_2}(\zeta) &= 2^{d+4-\Delta_3-\Delta_4} \pi^{\frac{d}{2}+3} e^{i\pi \frac{\Delta_4-\Delta_3}{2}} \\ &\times \sum_i \frac{\Gamma(\Delta_i - 2) (p_{\Delta_i}^+ + p_{\Delta_i}^-)}{\Gamma(\frac{\Delta_i-1+\Delta_3-\Delta_4}{2}) \Gamma(\frac{\Delta_i-1-\Delta_3+\Delta_4}{2}) \Gamma(\frac{\Delta_3+\Delta_4-\Delta_i-1}{2}) \Gamma(\frac{\Delta_i-1+\Delta_3+\Delta_4-d}{2})} f_{\Delta_i}^{\Delta_1, \Delta_2}(\zeta) \\ &\text{(when } \zeta < 1\text{)}. \end{aligned} \quad (5.187)$$

Here,  $i$  labels Regge trajectories and we have abbreviated  $\Delta_i = \Delta_i(J = -1)$  and  $p_{\Delta_i}^\pm = p_i^\pm(J = -1)$ . When  $\zeta = 1$ , the celestial block  $f_{\Delta_i}^{\Delta_1, \Delta_2}(\zeta)$  is no longer exponentially damped at large positive  $\Delta$ , so (5.187) does not apply. We will see examples of how to treat the case  $\zeta = 1$  in section 5.7.3.

We expect that the above analysis extends to the more general light-ray OPE  $\mathbf{L}[\mathcal{O}_1]\mathbf{L}[\mathcal{O}_2]$ , where  $\mathcal{O}_1$  and  $\mathcal{O}_2$  have general spins  $J_1$  and  $J_2$ . In this case, the contour integral over  $\Delta$  in (5.149) should become (in schematic notation)

$$\mathbf{L}[\mathcal{O}_1]\mathbf{L}[\mathcal{O}_2] = -\pi i \sum_{i,\lambda} \mathcal{D}_{\Delta_i-1,\lambda}^{(a)} \left( \mathbb{O}_{i,J_1+J_2-1,\lambda(a)}^+ + \mathbb{O}_{i,J_1+J_2-1,\lambda(a)}^- \right). \quad (5.188)$$

Let us return to the assumption that  $C^\pm(\Delta, J)$  (more generally  $\mathbb{O}_{\Delta,J,\lambda(a)}^\pm$ ) has only simple poles in  $\Delta$ . This is known to be true when the signature and spin are such that  $C^\pm(\Delta, J)$  describes light-transforms of local operators, i.e. when  $J \in \mathbb{Z}_{\geq 0}$  and  $\pm 1 = (-1)^J$ . However, for more general values of  $J$ , the singularity structure of  $C^\pm(\Delta, J)$  as a function of  $\Delta$  is not known. In the presence of other types of singularities like higher poles and branch cuts, one can define light-ray operators  $\mathbb{O}_{i,J}^\pm$  in terms of discontinuities across those singularities, and then suitable generalizations of (5.187) and (5.188) apply.

### 5.5.3 No contribution from disconnected terms

Consider an event shape of identical scalars

$$\langle \phi(p) | \mathbf{L}[\phi] \mathbf{L}[\phi] | \phi(p) \rangle. \quad (5.189)$$

The four-point function of  $\phi$ 's can be split into connected and disconnected pieces

$$\begin{aligned} & \langle \phi(x_1)\phi(x_2)\phi(x_3)\phi(x_4) \rangle \\ &= \langle \phi(x_1)\phi(x_2)\phi(x_3)\phi(x_4) \rangle_c \\ & \quad + \langle \phi(x_1)\phi(x_2) \rangle \langle \phi(x_3)\phi(x_4) \rangle + \langle \phi(x_1)\phi(x_3) \rangle \langle \phi(x_2)\phi(x_4) \rangle + \langle \phi(x_1)\phi(x_4) \rangle \langle \phi(x_3)\phi(x_2) \rangle. \end{aligned} \quad (5.190)$$

After taking the light-transforms to compute (5.189), the disconnected terms in (5.190) must drop out. The reason is that the light-transform of a Wightman two-point function vanishes, since the light-transformed operator annihilates the vacuum.

Despite the simplicity of this argument, vanishing of disconnected contributions in the celestial block expansion is slightly nontrivial. The mechanism is similar to the vanishing of spurious poles discussed in section 5.5.2. Note that the contribution of disconnected terms to  $C^+(\Delta, J)$  is given by the OPE coefficient function of Mean Field Theory (MFT). This is [87, 194]

$$\begin{aligned} & C^{\text{MFT}}(\Delta, J) \\ &= \frac{2^{d+1-2\Delta} \Gamma(J + \frac{d}{2}) \Gamma(\frac{d+1+J-\Delta}{2}) \Gamma(\Delta - 1) \Gamma(\frac{\Delta+J}{2}) \Gamma(\frac{d}{2} - \Delta_\phi)^2 \Gamma(\frac{J-\Delta}{2} + \Delta_\phi) \Gamma(\frac{\Delta+J-d}{2} + \Delta_\phi)}{\Gamma(J+1) \Gamma(\frac{d+J-\Delta}{2}) \Gamma(\Delta - \frac{d}{2}) \Gamma(\frac{\Delta+J-1}{2}) \Gamma(\frac{2d+J-\Delta-2\Delta_\phi}{2}) \Gamma(\frac{d+J+\Delta-2\Delta_\phi}{2}) \Gamma(\Delta_\phi)^2}. \end{aligned} \quad (5.191)$$

Due to the factor  $\Gamma(J+1)^{-1}$ , this function vanishes at  $J = -1$ . Thus, we have

$$C^\pm(\Delta, J = -1) = C_c^\pm(\Delta, J = -1), \quad (5.192)$$

where the subscript  $c$  indicates the contribution of the connected term alone. Consequently, disconnected terms do not contribute to the celestial block expansion (5.180), as expected.

#### 5.5.4 Relationship to $t$ -channel blocks and superconvergence

In chapter 4, we introduced an alternative expansion for event shapes in terms of  $t$ -channel event-shape blocks  $G_{\Delta', J'}^t(p, z_1, z_2)$ . We computed  $G_{\Delta', J'}^t(p, z_1, z_2)$  by inserting a projector onto an individual conformal multiplet  $\mathcal{O}_{\Delta', J'}$  between  $\mathbf{L}[\mathcal{O}_1]$  and  $\mathbf{L}[\mathcal{O}_2]$ . An alternative way to obtain it is to first find the contribution of the  $t$ -channel four-point block  $G_{\Delta', J'}(1-z, 1-\bar{z})$  in the Lorentzian inversion formula and then plug this into the celestial block expansion (5.180).

For example, in the case of scalars  $\mathcal{O}_i = \phi_i$  with dimensions  $\Delta_i$ , we claim that

$$G_{\Delta', J'}^t(p, z_1, z_2) = \frac{(-p^2)^{\frac{\Delta_1 + \Delta_2 + \Delta_3 + \Delta_4 - 4 - d}{2}} \theta(p)}{(-2z_1 \cdot p)^{\Delta_1 - 1} (-2z_2 \cdot p)^{\Delta_2 - 1}} \mathcal{G}_{\Delta', J'}^t(\zeta), \quad (5.193)$$

where

$$\begin{aligned} \mathcal{G}_{\Delta', J'}^t(\zeta) &= 2^{d+4-\Delta_3-\Delta_4} \pi^{\frac{d}{2}+3} e^{i\pi \frac{\Delta_4-\Delta_3}{2}} \\ &\times \int_{\frac{d}{2}-i\infty}^{\frac{d}{2}+i\infty} \frac{d\Delta}{2\pi i} \frac{\Gamma(\Delta-2) (\mathcal{B}^+(\Delta, -1; \Delta', J') + \mathcal{B}^-(\Delta, -1; \Delta', J'))}{\Gamma(\frac{\Delta-1+\Delta_3-\Delta_4}{2}) \Gamma(\frac{\Delta-1-\Delta_3+\Delta_4}{2}) \Gamma(\frac{\Delta_3+\Delta_4-\Delta-1}{2}) \Gamma(\frac{\Delta-1+\Delta_3+\Delta_4-d}{2})} f_{\Delta}^{\Delta_1, \Delta_2}(\zeta). \end{aligned} \quad (5.194)$$

Here  $\mathcal{B}(\Delta, J; \Delta', J')$  is the Lorentzian inversion of a single  $t$ -channel block (defined near (5.167)) and  $G_{\Delta', J'}^t(p, z_1, z_2)$  are the functions defined in (4.399). We have verified this identity numerically for some special cases in  $d = 2$  and  $d = 4$  using formulas for  $\mathcal{B}^{\pm}$  from [230].

One property of event-shape  $t$ -channel blocks is that they are regular in the limit  $z_1 \rightarrow z_2$ . This is consistent with (5.194) because the Lorentzian inversion of a single  $t$ -channel block contains double and single poles at double-trace values of  $\Delta$ , and no other singularities in  $\Delta$  [25, 230]. Thus, when we deform the  $\Delta$ -contour in (5.194) to pick up poles, we obtain only double-trace celestial blocks, which are indeed regular near  $\zeta = 0$ .

Equation (5.194) lets us clarify the relationship between (5.169) and the superconvergence sum rules written in chapter 4. Equation (5.169) is a superconvergence sum rule written in  $\nu$ -space, obtained by decomposing the commutator (5.155) into celestial conformal partial waves. By contrast, the sum rules of chapter 4 are obtained by decomposing the commutator into  $t$ -channel conformal multiplets (each of which is a finite sum of spherical harmonics on the celestial sphere). To go from (5.169) to the formulas of chapter 4, we can integrate (5.169) against celestial blocks.

## 5.6 Contact terms

In addition to giving a convergent expansion for the product

$$\mathbf{L}[\mathcal{O}_1](x, z_1, \vec{w}_1) \mathbf{L}[\mathcal{O}_2](x, z_2, \vec{w}_1) \quad (5.195)$$

for  $z_1 \not\propto z_2$ , the OPE expansion (5.149) can also capture contact terms in the limit  $z_1 \rightarrow z_2$ , such as those studied in [154]. A complete description of possible contact terms is beyond the scope of this work. Instead, in this section, we will study two specific examples and explain how (5.149), suitably interpreted, can be used to determine contact terms at  $z_1 \propto z_2$ . The contact terms in both examples ultimately arise for the same reason: we must be careful about the distributional interpretation of the integrand in (5.149). In particular, we must ensure that this distribution is analytic in  $\Delta$ .

### 5.6.1 Charge detector commutator

Our first example concerns contact terms in the OPE of charge detectors,<sup>30</sup>

$$\mathbf{L}[J^a](x, z_1)\mathbf{L}[J^b](x, z_2), \quad (5.196)$$

where  $J^a$  is a current for a global symmetry group  $G$ , and  $a$  is an adjoint index for  $G$ . From [154], the commutator should contain a contact term

$$[\mathbf{L}[J^a](x, z_1), \mathbf{L}[J^b](x, z_2)] = if^{abc}\delta^{d-2}(z_1, z_2)\mathbf{L}[J^c](x, z_1), \quad (5.197)$$

where  $f^{abc}$  are the structure constants of  $G$ , and  $\delta^{d-2}(z_1, z_2)$  is a delta-function on the null cone. To see this, note that

$$\int D^{d-2}z \mathbf{L}[J^a](x, z) = Q^a, \quad (5.198)$$

and we should have

$$[Q^a, J^b(x, z)] = if^{abc}J^c(x, z). \quad (5.199)$$

Requiring that  $[\mathbf{L}[J^a](x, z_1), \mathbf{L}[J^b](x, z_2)]$  vanishes for  $z_1 \not\propto z_2$  we arrive at (5.197). Vanishing of this commutator for  $z_1 \not\propto z_2$  was justified in chapter 4 if  $J_0 < 1$ . This also follows from the arguments of section 5.4.1.

We would now like to argue for (5.197) using the light-ray OPE. Recall that the commutator is a sum of light-transforms of local operators with spin  $J_1 + J_2 - 1 = 1$ . Thus, we must understand three-point structures

$$\langle J^a(x_1, z_1)J^b(x_2, z_2)\mathcal{O}_\Delta^c(x_3, z_3) \rangle^{(a)} \quad (5.200)$$

where  $\mathcal{O}_\Delta^c$  is a local spin-1 operator in the adjoint representation of  $G$ , with dimension  $\Delta$ . There exist two tensor structures

$$\langle J(x_1, z_1)J(x_2, z_2)\mathcal{O}_\Delta(x_3, z_3) \rangle^{(1)} = \frac{V_1H_{23} + V_2H_{13} + (\Delta + d - 2)V_3H_{12} + (\Delta + 3)V_1V_2V_3}{X_{12}^{\frac{2d-\Delta-1}{2}} X_{13}^{\frac{\Delta+1}{2}} X_{23}^{\frac{\Delta+1}{2}}}, \quad (5.201)$$

$$\begin{aligned} &\langle J(x_1, z_1)J(x_2, z_2)\mathcal{O}_\Delta(x_3, z_3) \rangle^{(2)} = \\ &\frac{(\Delta - 2d + 3)((\Delta + 1)(V_1H_{23} + V_2H_{13}) - (\Delta - 2d + 1)V_3H_{12}) + (\Delta - d + 1)(\Delta + 3)V_3^{-1}H_{23}H_{13}}{X_{12}^{\frac{2d-\Delta-1}{2}} X_{13}^{\frac{\Delta+1}{2}} X_{23}^{\frac{\Delta+1}{2}}}. \end{aligned} \quad (5.202)$$

---

<sup>30</sup>Note that a sufficient condition for the charge-charge correlator to exist is  $J_0 < 1$ . Therefore, we expect that we encounter divergences in gauge theories both in the weak and strong coupling perturbative expansion. On the other hand, we expect that it exists in the critical  $O(N)$  model.

Here we used the convention  $V_1 = V_{1,23}$  and its cyclic permutations, and  $H_{ij}, V_{i,jk}, X_{ij}$  are defined in appendix D.4, see also [192]. The second structure cannot appear in the local three-point function (5.200) for generic  $\Delta$  because of the term involving  $V_3^{-1}$ . However, when  $\mathcal{O} = J$  and  $\Delta = d - 1$ , the term with  $V_3^{-1}$  vanishes, and this structure is allowed.<sup>31</sup> Moreover, at  $\Delta = d - 1$  Ward identities fix the coefficient  $\lambda_2$  of the second structure as

$$\lambda_2^{abc} = \frac{C_J f^{abc}}{(d^2 - 4) \text{vol } S^{d-1}}, \quad (5.203)$$

where  $C_J$  is defined by

$$\langle J^a(x_1, z_1) J^b(x_2, z_2) \rangle = C_J \frac{H_{12} \delta^{ab}}{X_{12}^d}. \quad (5.204)$$

We will now argue that the second structure survives the map to celestial structures even at  $\Delta = d - 1$  as a contact term.

According to the results of section 5.3.4.4, naïvely, when  $\Delta = d - 1$  the structure (5.202) does not survive the map to celestial structures because it does not contain factors of  $V_3^{-1}$ . However, this is only true for  $z_1 \not\propto z_2$ . When  $z_1 \propto z_2$ , this claim must be modified. It should be possible to see this directly by performing a more careful analysis of the map to celestial structures. However, we can also use the following indirect argument. According to the results of section 5.3.4.4, for generic  $\Delta$  the structure (5.202) gets mapped to the following OPE contribution

$$\mathbf{L}[J^a](x_0, \vec{y}_1) \mathbf{L}[J^b](x_0, \vec{y}_2) \ni i\pi \frac{(\Delta + 3)(\Delta - d + 1)\lambda_2^{abc}}{C_J} (|\vec{y}_{12}|^{(\Delta-1)-2(d-2)} + \dots) \mathbf{L}[\mathcal{O}^c](x_0, \vec{y}_2). \quad (5.205)$$

This result is obtained using (5.149) and (5.151). Here, we put  $x_0$  at past null infinity and used transverse coordinates  $\vec{y}_i$  to parametrize the detectors. The factor  $(\Delta - d + 1)$  appears because only the term with  $V_3^{-1}$  in (5.202) contributes. We can now take the limit  $\Delta \rightarrow d - 1$  in this expression, taking into account that

$$(\Delta - d + 1)|\vec{y}_{12}|^{(\Delta-1)-2(d-2)} \rightarrow (\text{vol } S^{d-3}) \delta^{d-2}(\vec{y}_1 - \vec{y}_2), \quad (5.206)$$

while the higher-order terms in the parenthesis in (5.205) are less singular and go to zero. We then find

$$\begin{aligned} \mathbf{L}[J^a](x_0, \vec{y}_1) \mathbf{L}[J^b](x_0, \vec{y}_2) &\ni i\pi \frac{(d+2)\lambda_2^{abc} \text{vol } S^{d-3}}{C_J} \delta^{d-2}(\vec{y}_1 - \vec{y}_2) \mathbf{L}[J^c](x_0, \vec{y}_2) \\ &= \frac{i f^{abc}}{2} \delta^{d-2}(\vec{y}_1 - \vec{y}_2) \mathbf{L}[J^c](x_0, \vec{y}_2). \end{aligned} \quad (5.207)$$

---

<sup>31</sup>We thank Simon Caron-Huot for pointing out this interpretation of the second structure at  $\Delta = d - 1$ .

It follows from the discussion in 5.4.1 that this is the only term that survives after taking the commutator,<sup>32</sup> and so we find

$$[\mathbf{L}[J^a](x_0, \vec{y}_1), \mathbf{L}[J^b](x_0, \vec{y}_2)] = i f^{abc} \delta^{d-2}(\vec{y}_1 - \vec{y}_2) \mathbf{L}[J^c](x_0, \vec{y}_2), \quad (5.208)$$

as expected.

We expect that it should be possible to generalize this discussion to other commutators considered in [154]. The main difficulty in this generalization is that the operators considered in [154] are descendants of light transforms chapter 4. We expect that the light-ray OPE can be generalized to OPE of these descendants; we briefly discuss this direction in section 5.8.

### 5.6.2 Contact terms in energy correlators in $\mathcal{N} = 4$ SYM

Our second example concerns the celestial block expansion (5.180). For simplicity, we will specialize to  $\Delta_i = 2$ , which is relevant for the case of energy-energy correlator in  $\mathcal{N} = 4$  SYM studied in the next section, see (5.227) and (5.228).

We will focus on the function

$$\begin{aligned} \widehat{f}_\Delta(\zeta) &= \frac{4\pi^4 \Gamma(\Delta - 2)}{\Gamma(\frac{\Delta-1}{2})^3 \Gamma(\frac{3-\Delta}{2})} f_\Delta^{4,4}(\zeta) \\ &= \frac{4\pi^4 \Gamma(\Delta - 2)}{\Gamma(\frac{\Delta-1}{2})^3 \Gamma(\frac{3-\Delta}{2})} \zeta^{\frac{\Delta-7}{2}} {}_2F_1\left(\frac{\Delta-1}{2}, \frac{\Delta-1}{2}, \Delta - 1, \zeta\right) \end{aligned} \quad (5.209)$$

that multiplies  $C^+(\Delta, -1)$  under the integral in (5.228). Naïvely, this function vanishes at  $\Delta = 3 + 2n$  due to the  $\Gamma$ -function in the denominator. However, at the same time the factor  $\zeta^{\frac{\Delta-7}{2}}$  becomes singular as  $\zeta^{n-2}$  if  $n = 0, 1$ . To interpret (5.228) in a distributional sense and simultaneously treat it as the integral of an analytic function, we must ensure that we make sense of  $\widehat{f}_\Delta(\zeta)$  as a distribution that is analytic in  $\Delta$ . This distribution must be defined for  $\zeta \in [0, 1]$ .

For  $\text{Re } \Delta > 5$ ,  $\widehat{f}_\Delta(z)$  is integrable near  $\zeta = 0$  and thus uniquely defines a distribution analytic in  $\Delta$ . Therefore, for all other  $\Delta$  the distribution  $\widehat{f}_\Delta(z)$  must be defined by analytic continuation in  $\Delta$ . For example,

$$\widehat{f}_5(\zeta) = \lim_{\Delta \rightarrow 5} \widehat{f}_\Delta(\zeta) = \lim_{\Delta \rightarrow 5} 8\pi^4 \frac{\Delta-5}{2} \zeta^{\frac{\Delta-7}{2}} = 8\pi^4 \delta(\zeta), \quad (5.210)$$

and similarly

$$\widehat{f}_3(\zeta) = 4\pi^4 \delta'(\zeta) - 2\pi^4 \delta(\zeta). \quad (5.211)$$

---

<sup>32</sup>This is assuming that the first structure (5.201) does not produce contact terms under the map to celestial structures.

The other values of  $\Delta$  that give negative integer powers of  $\zeta$  are  $\Delta = 1 - 2n$  for  $n \geq 0$ . In these cases, we find  $\widehat{f}_\Delta(\zeta) = 0$ , due to higher-order zeros coming from  $\Gamma(\frac{\Delta-1}{2})^3$  in the denominator. For other values of  $\Delta$ , the exponent of  $\zeta$ , even if large and negative, is non-integer, and analytic continuation in  $\Delta$  defines a distribution even though there is no zero coming from the  $\Gamma$ -functions.

As we will see in the next section, the function relevant for scalar event shapes in  $\mathcal{N} = 4$  SYM is  $\zeta^2 \widehat{f}_\Delta(\zeta)$ . Since we only found a delta function and its first derivative in  $\widehat{f}_\Delta(\zeta)$ , this means that there are no contact terms in the scalar event shapes. Alternatively, by repeating the above analysis for  $\zeta^2 \widehat{f}_\Delta(\zeta)$  we find that it stops being integrable at  $\Delta = 1$ , at which point the  $\Gamma(\frac{\Delta-1}{2})^3$  factor in denominator kicks in, and we do not get interesting distributions.

We will also need a slight refinement of the result for  $\widehat{f}_\Delta(\zeta)$  near  $\Delta = 5$ . Near this point, the only term non-integrable in  $\zeta$  comes from the leading term of the  ${}_2F_1$ , so we can write

$$\widehat{f}_\Delta(\zeta) \sim \frac{4\pi^4 \Gamma(\Delta - 2)}{\Gamma(\frac{\Delta-1}{2})^3 \Gamma(\frac{3-\Delta}{2})} \zeta^{\frac{\Delta-7}{2}}. \quad (5.212)$$

Furthermore,

$$\frac{4\pi^4 \Gamma(\Delta - 2)}{\Gamma(\frac{\Delta-1}{2})^3 \Gamma(\frac{3-\Delta}{2})} = 4\pi^4 (\Delta - 5) + 2\pi^4 (\Delta - 5)^2 - \pi^4 (\Delta - 5)^3 + O((\Delta - 5)^4), \quad (5.213)$$

and

$$\zeta^{\frac{\Delta-7}{2}} = \frac{2}{\Delta - 5} \delta(\zeta) + \left[ \frac{1}{\zeta} \right]_0 + \frac{\Delta - 5}{2} \left[ \frac{\log \zeta}{\zeta} \right]_0 + O((\Delta - 5)^2), \quad (5.214)$$

so

$$\begin{aligned} \widehat{f}_\Delta(\zeta) &\sim 8\pi^4 \delta(\zeta) + 4\pi^4 \left( \delta(\zeta) + \left[ \frac{1}{\zeta} \right]_0 \right) (\Delta - 5) \\ &\quad - 2\pi^4 \left( \delta(\zeta) - \left[ \frac{1}{\zeta} \right]_0 - \left[ \frac{\log \zeta}{\zeta} \right]_0 \right) (\Delta - 5)^2 + O((\Delta - 5)^3). \end{aligned} \quad (5.215)$$

Here the distribution  $[\zeta^{-1}]_0$  is in principle defined by the Laurent expansion in which it appears. Otherwise, one can define it as the unique distribution which agrees with  $\zeta^{-1}$  on test functions which vanish at  $\zeta = 0$  and for which

$$\int_0^1 d\zeta \left[ \frac{1}{\zeta} \right]_0 = 0. \quad (5.216)$$

Similar comments apply to  $[\zeta^{-1} \log \zeta]_0$ . It is straightforward to obtain subleading terms in (5.215). In section 5.7 we will see that the contact terms we just described are necessary to satisfy the Ward identities for the energy-energy correlator.



### 5.7 Event shapes in $\mathcal{N} = 4$ SYM

In this section, we apply the machinery derived above to scalar half-BPS operators in  $\mathcal{N} = 4$  SYM. We re-derive some previous results both at weak and strong coupling and make further predictions. The basic operators of interest are

$$\mathcal{O}^{IJ} = \text{Tr} \left( \Phi^I \Phi^J - \frac{1}{6} \delta^{IJ} \Phi^K \Phi^K \right), \quad (5.217)$$

which transform as traceless symmetric tensors of  $\text{SO}(6)$ , i.e. in the  $\mathbf{20}'$  representation. These operators are part of a supermultiplet that also contains R-symmetry conserved currents, supersymmetric currents, and the stress tensor, among other operators.

We will study a scalar event shape, where the detectors, source, and sink are all built from  $\mathcal{O}^{IJ}$ 's. Superconformal Ward identities relate the four-point function of  $\mathbf{20}'$  scalars to four-point functions of other operators in the stress tensor multiplet [234, 235]. These relations were explicitly worked out in [217, 218]. In particular they imply a simple relation between scalar event shapes and energy-energy correlators which we review below.

The structure of the section is as follows. We first review basic properties of the four-point function of  $\mathbf{20}'$  operators and define the scalar event shape of interest. We then explain its relation to the energy-energy correlator which is the main subject of our interest. In sections 5.7.3, 5.7.4, 5.7.5, we apply the light-ray OPE at weak coupling at tree-level, 1-loop, and 2-loops (at leading and subleading twist), finding agreement with previous results and completing them with contact term contributions. In section 5.7.7, we use known OPE data to make a new prediction for the the small-angle limit at 3 and 4-loops. In section 5.7.8, we apply the OPE at strong coupling, again finding agreement with previous results.

#### 5.7.1 Review: event shapes in $\mathcal{N} = 4$ SYM

The scalar event shape of interest is built from  $\mathcal{O}^{IJ}$ 's, where the  $R$ -symmetry indices are contracted with particular polarizations. Following the conventions of [147], we treat the in- and out-states differently from the detectors. For the in- and out-states, we contract  $\mathcal{O}^{IJ}$  with null polarization vectors  $Y_I \in \mathbb{C}^6$ ,

$$\mathcal{O}(x, Y) = \left( \frac{N_c^2 - 1}{2\pi^4} \right)^{-1/2} \mathcal{O}^{IJ}(x) Y_I Y_J. \quad (5.218)$$

The two-point function of  $\mathcal{O}(x, Y)$  is given by

$$\langle \mathcal{O}(x, \bar{Y}) \mathcal{O}(0, Y) \rangle = \left( \frac{N_c^2 - 1}{2\pi^4} \right)^{-1} \frac{N_c^2 - 1}{32\pi^4} \frac{(Y \cdot \bar{Y})^2}{x^4} = \frac{(Y \cdot \bar{Y})^2}{16x^4}. \quad (5.219)$$

For the detectors, we contract the  $R$ -symmetry indices of  $\mathcal{O}^{IJ}$  with traceless symmetric tensors  $S_{IJ}$ ,

$$\mathcal{O}(x, S) = 2\mathcal{O}^{IJ}(x)S_{IJ}. \quad (5.220)$$

Obviously,  $\mathcal{O}(x, Y)$  and  $\mathcal{O}(x, S)$  encode the same thing, with the  $R$ -symmetry indices treated slightly differently.

Let us denote  $\mathcal{O}(z) \equiv \frac{1}{2}\mathbf{L}[\mathcal{O}](\infty, z)$ , where  $z$  is a future-pointing null vector.<sup>33</sup> Our scalar event shape is defined by

$$\langle \mathcal{O}(z_1, S_1)\mathcal{O}(z_2, S_2) \rangle_{p, Y} \equiv \sigma_{\text{tot}}^{-1}(p, Y) \int d^d x e^{-ip \cdot x} \langle \Omega | \mathcal{O}(x, \bar{Y}) \mathcal{O}(z_1, S_1) \mathcal{O}(z_2, S_2) \mathcal{O}(0, Y) | \Omega \rangle, \quad (5.221)$$

$$\sigma_{\text{tot}}(p, Y) \equiv \int d^d x e^{-ip \cdot x} \langle \Omega | \mathcal{O}(x, \bar{Y}) \mathcal{O}(0, Y) | \Omega \rangle = 2\pi^3 \frac{(Y \cdot \bar{Y})^2}{16} \theta(p). \quad (5.222)$$

This event shape is sometimes called “scalar flow,” by analogy with energy flow observables that measure the flow of energy at null infinity.

Following [147], let us choose the  $R$ -symmetry structures

$$\begin{aligned} Y_0 &= (1, 0, 1, 0, i, i), \\ S_0 &= \text{diag}(1, -1, 0, 0, 0, 0), \\ S'_0 &= \text{diag}(0, 0, 1, -1, 0, 0). \end{aligned} \quad (5.223)$$

With this choice, we have  $\langle \mathcal{O}(x, \bar{Y}_0) \mathcal{O}(0, Y_0) \rangle = \frac{1}{x^4}$ . Moreover, only the **105** representation of  $\text{SO}(6)$  contributes to the  $\mathcal{O}(n_1, S) \times \mathcal{O}(n_2, S')$  OPE. Finally, superconformal Ward identities relate the event shape with these choices to energy correlators

$$\langle \mathcal{E}(z_1) \mathcal{E}(z_2) \rangle_{p, Y_0} = \frac{16(-p^2)^2}{(-2z_1 \cdot z_2)^2} \langle \mathcal{O}(z_1, S_0) \mathcal{O}(z_2, S'_0) \rangle_{p, Y_0} + \text{protected contact terms}. \quad (5.224)$$

(The energy correlators are independent of  $Y$ .) In [217], this relation was derived while ignoring contact terms at  $z_1 \propto z_2$ . We will find that consistency with the OPE requires correcting this relation by contact terms. We expect that these contact terms come from the protected part of the **20'** four-point function. We discuss them in more detail below.

---

<sup>33</sup>The factor of  $\frac{1}{2}$  is for consistency with the definitions of [147].

Using (5.182), the scalar event shape can be written

$$\langle \mathcal{O}(z_1, S_0) \mathcal{O}(z_2, S'_0) \rangle_{p, Y_0} = \left(\frac{1}{2}\right)^2 \frac{1}{2\pi^3} \frac{\mathcal{G}_{\mathcal{O}\mathcal{O}}(\zeta)}{(-2z_1 \cdot p)(-2z_2 \cdot p)}, \quad (5.225)$$

where the factor  $(\frac{1}{2})^2$  in (5.225) comes from  $\mathcal{O}(z) \equiv \frac{1}{2} \mathbf{L}[\mathcal{O}](\infty, z)$ . The function  $\mathcal{G}_{\mathcal{O}\mathcal{O}}(\zeta)$  has a celestial block expansion given by (5.180):

$$\mathcal{G}_{\mathcal{O}\mathcal{O}}(\zeta) = \int_{2-i\infty}^{2+i\infty} \frac{d\Delta}{2\pi i} C^+(\Delta, -1) \frac{16\pi^5 \Gamma(\Delta - 2)}{\Gamma(\frac{\Delta-1}{2})^3 \Gamma(\frac{3-\Delta}{2})} f_{\Delta}^{2,2}(\zeta). \quad (5.226)$$

Here,  $C^+(\Delta, -1)$  encodes the OPE data of the  $\langle \mathcal{O}\mathcal{O}\mathcal{O}\mathcal{O} \rangle$  four-point function, analytically continued to spin  $J = -1$ . We discuss this four-point function in section 5.7.2. Since the **105** representation appears in the symmetrized tensor square of the **20'** representation, the OPE contains only even spin operators. This is the reason for the absence of  $C^-(\Delta, -1)$  in (5.226).

The superconformal Ward identity (5.224) lets us obtain a celestial block expansion for the energy-energy correlator in terms of OPE data for the scalar four-point function. Let us define the function  $\mathcal{F}_{\mathcal{E}}(\zeta)$  by

$$\langle \mathcal{E}(z_1) \mathcal{E}(z_2) \rangle_{p, Y_0} = \frac{4 \text{vol } S^2}{2\pi^3} \frac{(-p^2)^4}{(-2z_1 \cdot p)^3 (-2z_2 \cdot p)^3} \mathcal{F}_{\mathcal{E}}(\zeta). \quad (5.227)$$

Here we include the factor  $4 \text{vol } S^2 = 16\pi$  because it simplifies the Ward identities discussed below. The relation (5.224) implies that  $\mathcal{F}_{\mathcal{E}}$  has the celestial block expansion

$$\mathcal{F}_{\mathcal{E}}(\zeta) = \int_{2-i\infty}^{2+i\infty} \frac{d\Delta}{2\pi i} C^+(\Delta, -1) \frac{4\pi^4 \Gamma(\Delta - 2)}{\Gamma(\frac{\Delta-1}{2})^3 \Gamma(\frac{3-\Delta}{2})} f_{\Delta}^{4,4}(\zeta) + \xi(\zeta), \quad (5.228)$$

where

$$f_{\Delta}^{4,4}(\zeta) = \zeta^{\frac{\Delta-7}{2}} {}_2F_1\left(\frac{\Delta-1}{2}, \frac{\Delta-1}{2}, \Delta-1, \zeta\right), \quad (5.229)$$

$$\xi(\zeta) \equiv \frac{1}{4}(2\delta(\zeta) - \delta'(\zeta)). \quad (5.230)$$

Here,  $C^+(\Delta, -1)$  is the same function that enters (5.226). The function  $\xi(\zeta)$  represents the protected coupling-independent contact terms mentioned in (5.224). Below, we fix  $\xi(\zeta)$  by requiring consistency with Ward identities and check that it is indeed independent of the coupling (at one and two loops, and at strong coupling). Its effect is to remove the contribution of short multiplets from  $C^+(\Delta, -1)$  in (5.228). It would be interesting to derive the presence of  $\xi(\zeta)$  from first principles along the lines of [217].

For  $0 < \zeta \leq 1$ , the superconformal Ward identity relating scalar flow and the energy-energy correlator takes the simple form

$$\mathcal{F}_{\mathcal{E}}(\zeta) = \frac{\mathcal{G}_{\mathcal{O}\mathcal{O}}(\zeta)}{4\pi\zeta^2}, \quad (0 < \zeta \leq 1). \quad (5.231)$$

However, the celestial block expansion (5.228) also captures contact terms at  $\zeta = 0$  that are not captured by (5.231).

When evaluating the celestial block expansion for  $\zeta < 1$ , we will find it convenient to close the  $\Delta$ -contour to the right as discussed in section 5.5.2 and write the event shape as a sum over Regge trajectories, see (5.187). For example, we have

$$\mathcal{F}_{\mathcal{E}}(\zeta) = \sum_i p_{\Delta_i} \frac{4\pi^4 \Gamma(\Delta_i - 2)}{\Gamma(\frac{\Delta_i - 1}{2})^3 \Gamma(\frac{3 - \Delta_i}{2})} f_{\Delta_i}^{4,4}(\zeta) + \xi(\zeta), \quad (\zeta < 1). \quad (5.232)$$

Before computing  $\mathcal{F}_{\mathcal{E}}(\zeta)$ , let us comment on some of its properties. First,  $\mathcal{F}_{\mathcal{E}}(\zeta)$  is constrained by Ward identities. By integrating  $\mathcal{E}(z_1)$  over the celestial sphere with the appropriate weight, we can produce different components of the translation generators  $P^\mu$ . In the energy correlator (5.227), these must evaluate to  $p^\mu$ , which leads to the Ward identities

$$\int_0^1 d\zeta \mathcal{F}_{\mathcal{E}}(\zeta) = \frac{1}{2}, \quad (5.233)$$

$$\int_0^1 d\zeta (2\zeta - 1) \mathcal{F}_{\mathcal{E}}(\zeta) = 0. \quad (5.234)$$

Since (5.233), (5.234) are sensitive to the values of  $\mathcal{F}_{\mathcal{E}}(\zeta)$  at arbitrary angle  $\zeta$  they can be used as a nontrivial consistency check on the computations of  $\mathcal{F}_{\mathcal{E}}(\zeta)$ .

Finally, note that  $\mathcal{F}_{\mathcal{E}}(\zeta)$  has a weak-coupling expansion

$$\mathcal{F}_{\mathcal{E}}(\zeta) = \mathcal{F}_{\mathcal{E}}^{(0)}(\zeta) + a \mathcal{F}_{\mathcal{E}}^{(1)}(\zeta) + \dots, \quad a \equiv \frac{g_{\text{YM}}^2 N_c}{4\pi^2}. \quad (5.235)$$

$\mathcal{F}_{\mathcal{E}}(\zeta)$  is explicitly known up to two-loop order [182], and as a two-fold integral at three loops [207].<sup>34</sup> It is also easily computable at strong coupling, reproducing the result of Hofman and Maldacena [31].

### 5.7.2 Review: four-point function of $20'$ operators

The main ingredient in computing  $\mathcal{F}_{\mathcal{E}}(\zeta)$  is the four-point function of  $20'$  operators that enters in the definition of the scalar event shape (5.221), specialized to the  $R$ -symmetry structures (5.223). This is

$$\langle \mathcal{O}(x_4, \bar{Y}_0) \mathcal{O}(x_1, S_0) \mathcal{O}(x_2, S'_0) \mathcal{O}(x_3, Y_0) \rangle = \frac{G^{(105)}(u, v)}{x_{12}^4 x_{34}^4}. \quad (5.236)$$

<sup>34</sup>The quantity  $\text{EEC}(\zeta)$  computed in [182, 207] is equal to our  $\mathcal{F}_{\mathcal{E}}(\zeta)$ .

It will be convenient to write  $G^{(105)}(u, v)$  in two different ways. Firstly, we have

$$G^{(105)}(u, v) = \frac{c}{2(2\pi)^4} \left( u^2 + \frac{u^2}{v^2} \right) + \frac{1}{(2\pi)^4} \frac{u^2}{v} \left( \frac{1}{2} + u\Phi(u, v) \right), \quad (5.237)$$

where the central charge  $c$  is given by

$$c = \frac{N_c^2 - 1}{4}. \quad (5.238)$$

Here, the function  $\Phi(u, v) = \Phi(v, u) = \frac{1}{v}\Phi\left(\frac{u}{v}, \frac{1}{v}\right)$  encodes the dependence of the correlator on the coupling  $a$  (it is zero for  $a = 0$ ). It is known explicitly up to three loops [236]. The integrand for  $G^{(105)}(u, v)$  is known up to ten loops in the planar limit [237, 238].

The other way of writing  $G^{(105)}(u, v)$  is to organize it into the contribution of short and long supermultiplets in the superconformal block expansion,

$$G^{(105)}(u, v) = \frac{c}{2(2\pi)^4} u^2 G^{(\text{short})}(u, v) + \mathcal{H}(u, v), \quad (5.239)$$

where  $G^{(\text{short})}(u, v)$  encodes the contribution from protected operators and was computed in [239].  $\mathcal{H}(u, v)$  encodes the contribution of long multiplets and can be written in terms of superconformal blocks as follows

$$\mathcal{H}(u, v) = \sum_{\Delta} \sum_{\text{even } J} a_{\Delta, J} g_{\Delta+4, J}(u, v) = \sum_{\Delta} \sum_{\text{even } J} p_{\Delta, J} g_{\Delta, J}(u, v) \quad (5.240)$$

where  $g_{\Delta, J}(u, v)$  are the usual conformal blocks and  $a_{\Delta, J}$  is the three-point coupling to a given superconformal primary, see e.g. [239].<sup>35</sup> We will use  $p_{\Delta, J}$  to denote the three-point coupling to a given conformal primary. Note that only even spin operators enter in the OPE decomposition of  $G^{(105)}(u, v)$ .

Because of the factor  $\Gamma\left(\frac{3-\Delta}{2}\right)^{-1}$  in (5.232), most protected operators from  $G^{(\text{short})}(u, v)$  will not contribute to  $\mathcal{F}_{\mathcal{E}}(\zeta)$ . However, operators with dimensions  $\Delta = 3$  and  $\Delta = 5$  can contribute contact terms at  $\zeta = 0$ , in accordance with the discussion in section 5.6.2.

### 5.7.3 Tree level

To get the tree-level correlator we set  $\Phi(u, v) = 0$  in (5.236). Recall from section 5.5.3 that

$$C^+(\Delta, J = -1) = C_c(\Delta, J = -1), \quad (5.241)$$

---

<sup>35</sup>Note that [62] used a different conformal block normalization.

where  $C_c(\Delta, -1)$  corresponds to the connected part of the four-point function. Written in terms of cross-ratios, the connected tree-level correlator takes the form

$$\langle \mathcal{O}(x_4, \bar{Y}_0) \mathcal{O}(x_1, S_0) \mathcal{O}(x_2, S'_0) \mathcal{O}(x_3, Y_0) \rangle_c^{\text{tree}} = \frac{1}{2(2\pi)^4} \frac{1}{x_{14}^2 x_{23}^2 x_{13}^2 x_{24}^2} = \frac{1}{x_{12}^4 x_{34}^4} \left( \frac{1}{2(2\pi)^4} \frac{u^2}{v} \right). \quad (5.242)$$

Plugging into the inversion formula, we have

$$C_c^{\text{tree}}(\Delta, J) = 2 \frac{\kappa_{\Delta+J}}{4} \int_0^1 \int_0^1 \frac{dz d\bar{z}}{z^2 \bar{z}^2} \frac{(z - \bar{z})^2}{(z\bar{z})^2} G_{J+3, \Delta-3}(z, \bar{z}) d\text{Disc} \left[ \frac{1}{2(2\pi)^4} \frac{(z\bar{z})^2}{(1-z)(1-\bar{z})} \right], \quad (5.243)$$

where the factor of 2 in front comes from the fact that the  $t$ - and  $u$ -channel terms in the inversion formula are equal.  $d\text{Disc}_{\frac{1}{1-\bar{z}}}$  is delta-function supported near  $\bar{z} = 1$ . To regulate it, we will replace

$$\frac{z\bar{z}}{(1-z)(1-\bar{z})} \rightarrow \frac{(z\bar{z})^{1+\delta}}{((1-z)(1-\bar{z}))^{1+\delta}}. \quad (5.244)$$

Recall that [231, 232]

$$G_{J+3, \Delta-3}(z, \bar{z}) = \frac{z\bar{z}}{z - \bar{z}} (k_{\Delta+J}(z) k_{4+J-\Delta}(\bar{z}) - k_{\Delta+J}(\bar{z}) k_{4+J-\Delta}(z)),$$

$$k_\beta(z) = z^{\beta/2} {}_2F_1 \left( \frac{\beta}{2}, \frac{\beta}{2}, \beta, z \right). \quad (5.245)$$

Doing the integral and removing the regulator  $\delta \rightarrow 0$  leads to the result

$$C_c^{\text{tree}}(\Delta, J) = \frac{\Gamma(\frac{\Delta+J}{2})^4}{\Gamma(\Delta+J-1)\Gamma(\Delta+J)} \frac{1}{2(2\pi)^4} \left( \frac{\Gamma(\Delta+J)}{\Gamma(\frac{\Delta+J}{2})^2} I_1(\frac{J+4-\Delta}{2}, -1) - I_1(\frac{\Delta+J}{2}, -1) \frac{\Gamma(J+4-\Delta)}{\Gamma(\frac{J+4-\Delta}{2})^2} \right), \quad (5.246)$$

where

$$I_\alpha(h, p) \equiv \int_0^1 \frac{dz}{z(1-z)} z^\alpha \left( \frac{z}{1-z} \right)^p k_{2h}(z)$$

$$= \frac{\Gamma(\alpha+p+h)\Gamma(-p)}{\Gamma(\alpha+h)} {}_3F_2(h, h, \alpha+p+h; 2h, \alpha+h; 1). \quad (5.247)$$

We can now compute the energy-energy correlator by plugging (5.246) at  $J = -1$  into (5.228). The result is

$$\begin{aligned}
C_c^{\text{tree}}(\Delta, -1) & \frac{4\pi^4\Gamma(\Delta-2)}{\Gamma(\frac{\Delta-1}{2})^3\Gamma(\frac{3-\Delta}{2})} \\
&= \frac{1}{8} \left( \frac{1}{\Gamma(\frac{\Delta-1}{2})} \frac{I_1(\frac{3-\Delta}{2}, -1)}{\Gamma(\frac{3-\Delta}{2})} - I_1(\frac{\Delta-1}{2}, -1) \frac{\Gamma(\frac{\Delta-1}{2})}{\Gamma(\Delta-1)} \frac{\Gamma(3-\Delta)}{\Gamma(\frac{3-\Delta}{2})^3} \right) \\
&= \frac{1}{8} \frac{\Gamma(\frac{\Delta-1}{2})}{\Gamma(\Delta-1)\Gamma(\frac{3-\Delta}{2})} \int_0^1 \frac{dz}{z} \left( \frac{\Gamma(\Delta-1)}{\Gamma(\frac{\Delta-1}{2})^2} k_{3-\Delta}(z) - \frac{\Gamma(3-\Delta)}{\Gamma(\frac{3-\Delta}{2})^2} k_{\Delta-1}(z) \right) \\
&= \frac{1}{8} \frac{\Gamma(\frac{\Delta-1}{2})^2}{\Gamma(\Delta-2)}. \tag{5.248}
\end{aligned}$$

This expression is free of poles to the right of the principal series, so by closing the contour in (5.228) to the right we conclude that  $\mathcal{F}_\mathcal{E}(\zeta) = 0$  for  $0 < \zeta < 1$ . This ignores the possibility of contact terms discussed in section 5.6.2, which we now address.

Let us start by studying contact terms at  $\zeta = 0$ . As explained in section 5.6.2, apart from the protected contact term  $\xi(\zeta)$  in (5.230), the energy correlator  $\mathcal{F}_\mathcal{E}(x)$  may receive contact terms from the integral (5.228). Indeed, when  $\zeta = 0$ , the distribution  $\widehat{f}_\Delta(\zeta)$  does not vanish at  $\Delta = 3, 5$ , and we in fact have

$$\begin{aligned}
\mathcal{F}_\mathcal{E}^{(0)}(\zeta) &= -(4\pi^4\delta'(\zeta) - 2\pi^4\delta(\zeta))\text{res}_{\Delta=3} C_c^{\text{tree}}(\Delta, -1) - 8\pi^4\delta(\zeta)\text{res}_{\Delta=5} C_c^{\text{tree}}(\Delta, -1) + \xi(\zeta) \\
&= \frac{1}{4}\delta(\zeta), \quad (\zeta < 1). \tag{5.249}
\end{aligned}$$

Let us now analyze contact terms at  $\zeta = 1$ . When  $\zeta = 1$ , we should worry about the convergence of the integral when closing the contour, since there is no suppression coming from  $\zeta^{\frac{\Delta-7}{2}}$  in the celestial block. To probe possible delta-function terms localized at  $\zeta = 1$  let us consider moments of the energy flow

$$\int_0^1 d\zeta \zeta^N \mathcal{F}_\mathcal{E}^{(0)}(\zeta) = \frac{\delta_{N,0}}{4} + \int_{C_0-i\infty}^{C_0+i\infty} \frac{d\Delta}{2\pi i} C_c^{\text{tree}}(\Delta, J = -1) \frac{4\pi^4\Gamma(\Delta-2)}{\Gamma(\frac{\Delta-1}{2})^3\Gamma(\frac{3-\Delta}{2})} \int_0^1 d\zeta \zeta^N f_\Delta^{4,4}(\zeta), \tag{5.250}$$

where we deformed the integration contour to  $\text{Re}[\Delta] = C_0 > 5$  so that the integral  $\int_0^1 d\zeta \zeta^N f_\Delta^{4,4}(\zeta)$  converges for  $N \geq 0$ . We find that at large  $|\Delta| \gg 1$  the integrand behaves as

$$\int_0^1 d\zeta \zeta^N \mathcal{F}_\mathcal{E}^{(0)}(\zeta) = \frac{\delta_{N,0}}{4} + \int_{2-i\infty}^{2+i\infty} \frac{d\Delta}{2\pi i} \frac{1}{2\Delta} = \frac{1 + \delta_{N,0}}{4}, \tag{5.251}$$

where we evaluated the  $\Delta$  integral using the principal value prescription. If we subtract off this leading behavior, then the contour deformation in  $\Delta$  becomes legitimate and we get 0 for the remainder. This implies that  $\mathcal{F}_{\mathcal{E}}^{(0)}(\zeta) \ni \frac{1}{4}\delta(1 - \zeta)$ , in agreement with the straightforward scattering amplitude evaluation, see e.g. [147]. More generally, we see that distributional terms supported at  $\zeta = 1$  are encoded in the large- $\Delta$  behavior of  $C^+(\Delta, J = -1)$ .

To summarize, the energy-energy correlator at tree-level is given by

$$\mathcal{F}_{\mathcal{E}}^{(0)}(\zeta) = \frac{1}{4}(\delta(\zeta) + \delta(1 - \zeta)). \quad (5.252)$$

Note that this is the unique expression with delta functions at  $\zeta = 0$  and  $\zeta = 1$  that satisfies both Ward identities (5.233) and (5.234).

#### 5.7.4 One loop

To study perturbative corrections, let us briefly discuss how they are encoded in  $C^+(\Delta, J)$ . Non-perturbatively, we have poles of the form

$$C^+(\Delta, J) \sim -\frac{a_i(a)}{\Delta - \Delta_i(a)}, \quad (5.253)$$

where  $a_i(a)$  and  $\Delta_i(a)$  are, respectively, the product of OPE coefficients and scaling dimension of an exchanged operator.

We furthermore have expansions

$$a_i(a) = a_i^{(0)} + a a_i^{(1)} + a^2 a_i^{(2)} + \dots, \quad (5.254)$$

$$\Delta_i(a) = \Delta_i^{(0)} + a \gamma_i^{(1)} + a^2 \gamma_i^{(2)} + \dots, \quad (5.255)$$

and thus

$$C^+(\Delta, J) \sim -\frac{a_i^{(0)}}{\Delta - \Delta_i^{(0)}} + a \left( -\frac{a_i^{(1)}}{\Delta - \Delta_i^{(0)}} - \frac{a_i^{(0)} \gamma_i^{(1)}}{(\Delta - \Delta_i^{(0)})^2} \right) + \dots. \quad (5.256)$$

Suppose now that there is a degeneracy at tree level, i.e.  $\Delta_i^{(0)} = \Delta_*^{(0)}$ . Then we have

$$\begin{aligned} C^+(\Delta, J) &\sim -\frac{\sum_i a_i^{(0)}}{\Delta - \Delta_*^{(0)}} + a \left( -\frac{\sum_i a_i^{(1)}}{\Delta - \Delta_*^{(0)}} - \frac{\sum_i a_i^{(0)} \gamma_i^{(1)}}{(\Delta - \Delta_*^{(0)})^2} \right) + \dots \\ &\sim -\frac{\langle a_*^{(0)} \rangle}{\Delta - \Delta_*^{(0)}} + a \left( -\frac{\langle a_*^{(1)} \rangle}{\Delta - \Delta_*^{(0)}} - \frac{\langle a_*^{(0)} \gamma_*^{(1)} \rangle}{(\Delta - \Delta_*^{(0)})^2} \right) + \dots, \end{aligned} \quad (5.257)$$

where we introduced the notation  $\langle \dots \rangle$  (used extensively below) representing the total contribution of operators that are degenerate at tree level. Below, the subscript



\* will be replaced by a label referring to the degenerate group of operators. The contribution of these poles to (5.228) now becomes

$$\begin{aligned} \mathcal{F}_{\mathcal{E}}^{(1)}(\zeta) \ni & \langle a_*^{(1)} \rangle \left[ \frac{4\pi^4 \Gamma(\Delta - 2)}{\Gamma(\frac{\Delta-1}{2})^3 \Gamma(\frac{3-\Delta}{2})} f_{\Delta}^{4,4}(\zeta) \right]_{\Delta=\Delta_*^{(0)}} \\ & + \langle a_*^{(0)} \gamma_*^{(1)} \rangle \left[ \partial_{\Delta} \frac{4\pi^4 \Gamma(\Delta - 2)}{\Gamma(\frac{\Delta-1}{2})^3 \Gamma(\frac{3-\Delta}{2})} f_{\Delta}^{4,4}(\zeta) \right]_{\Delta=\Delta_*^{(0)}} . \end{aligned} \quad (5.258)$$

In this section, we will not compute  $C^+(\Delta, -1)$ , but rather use the known OPE data  $\langle a_*^{(1)} \rangle$  and  $\langle a_*^{(0)} \gamma_*^{(1)} \rangle$ , analytically continued to  $J = -1$ . The complete OPE data for the one-loop correlator was written down in [240]. Recall from section 5.7.2 that the contribution of long multiplets, which are the ones that receive loop corrections, is given by

$$\mathcal{H}(u, v) = \frac{c}{2(2\pi)^4} u^2 \left( 1 + \frac{1}{v^2} - G^{(\text{short})}(u, v) \right) + \frac{1}{(2\pi)^4} \frac{u^2}{v} \left( \frac{1}{2} + u\Phi(u, v) \right). \quad (5.259)$$

At tree level, this can be decomposed into superconformal blocks (5.240) as follows, see (2.21) in [240],

$$\begin{aligned} \langle a_{\tau=2, J}^{(0)} \rangle &= \frac{1}{(2\pi)^4} \frac{\Gamma(J+3)^2}{\Gamma(2J+5)}, \\ \langle a_{\tau, J}^{(0)} \rangle &= \frac{c}{(2\pi)^4} \frac{\Gamma(\frac{\tau}{2}+1)^2 \Gamma(\frac{\tau}{2}+J+2)^2}{\Gamma(\tau+1)\Gamma(\tau+2J+3)} \left( (\tau+J+2)(J+1) + \frac{(-1)^{\tau/2}}{c} \right), \end{aligned} \quad (5.260)$$

where we used twist  $\tau = \Delta - J$  and even spin  $J \geq 0$  to label the operators, with  $\tau = 4, 6, 8, \dots$  in the second line.

Note that for  $\tau > 2$  there are degeneracies in the spectrum, so  $\langle \dots \rangle$  notation is necessary. One can check that (5.260) indeed correctly reproduces (5.259) upon setting  $\Phi(u, v)$  to zero.

In perturbation theory, we write

$$\Phi(u, v) = a \Phi^{(1)}(u, v) + a^2 \Phi^{(2)}(u, v) + \dots, \quad (5.261)$$

and similarly for  $\mathcal{H}(u, v)$ . At one loop we have

$$\begin{aligned} \mathcal{H}^{(1)}(u, v) &= \frac{1}{(2\pi)^4} \frac{u^3}{v} \Phi^{(1)}(u, v), \\ \Phi^{(1)}(u, v) &= -\frac{1}{4} \frac{1}{z - \bar{z}} \left( 2\text{Li}_2(z) - 2\text{Li}_2(\bar{z}) + \log z \bar{z} \log \frac{1-z}{1-\bar{z}} \right). \end{aligned} \quad (5.262)$$

Analogously to (5.258), the OPE data enters as

$$\delta\mathcal{H}(u, v) = \sum_{\tau=2,4,\dots; \text{ even } J}^{\infty} \left( \langle a_{\tau,J}^{(1)} \rangle G_{\tau+4+J,J} + \langle a_{\tau,J}^{(0)} \gamma_{\tau,J}^{(1)} \rangle \partial_{\tau} G_{\tau+4+J,J} \right), \quad (5.263)$$

where for convenience we labeled the superconformal primaries by twist  $\tau = \Delta - J$  instead of the dimension (as we did in (5.240)).

The result of the one-loop decomposition for anomalous dimensions is, see (A.24-A.25) in [240],

$$\begin{aligned} \langle \gamma_{2,J} \rangle &\equiv \frac{\langle a_{2,J}^{(0)} \gamma_{2,J}^{(1)} \rangle}{\langle a_{2,J}^{(0)} \rangle} = 2S_1(J+2), \\ \langle \gamma_{\tau,J} \rangle &\equiv \frac{\langle a_{\tau,J}^{(0)} \gamma_{\tau,J}^{(1)} \rangle}{\langle a_{\tau,J}^{(0)} \rangle} = -\frac{2[\eta+1]S_1(\frac{\tau}{2}) + [\eta-1]S_1(\frac{\tau}{2} + J + 1)}{c(\tau+J+2)(J+1) + \frac{\eta}{c}}, \end{aligned} \quad (5.264)$$

where following [240] we introduced  $\eta = (-1)^{\tau/2}$  and

$$S_k(N) = \sum_{i=1}^N \frac{1}{i^k}. \quad (5.265)$$

We can concisely write the OPE coefficients at one loop by defining

$$\langle a_{\tau,J}^{(1)} \rangle \equiv \langle \alpha_{\tau,J} \rangle \langle a_{\tau,J}^{(0)} \rangle + \frac{1}{2} \partial_J \langle a_{\tau,J}^{(0)} \gamma_{\tau,J}^{(1)} \rangle. \quad (5.266)$$

The coefficients  $\langle \alpha_{\tau,J} \rangle$  are

$$\begin{aligned} \langle \alpha_{2,J} \rangle &= -\zeta_2, \\ \langle \alpha_{\tau,J} \rangle &= -\frac{2}{c} \frac{1}{\left( (\tau+J+2)(L+1) + \frac{(-1)^{\tau/2}}{c} \right)} \left( \frac{1-\eta}{2} \zeta_2 + (1+\eta)S_1(\frac{\tau}{2})^2 - \frac{1+\eta}{2} S_2(\frac{\tau}{2}) \right. \\ &\quad \left. - (1+\eta)S_1(\frac{\tau}{2})S_1(\tau) + [(2\eta-1)S_1(\frac{\tau}{2}) + (1-\eta)S_1(\tau)]S_1(\frac{\tau}{2} + L + 1) \right), \end{aligned} \quad (5.267)$$

Note that for superconformal primaries of twist  $\tau$  and spin  $J$  we should set  $\Delta_*^{(0)} = 4 + \tau + J$  in (5.258). Here the shift by 4 is due to the form of the superconformal block in (5.240). This means that for twist  $\tau = 2n$ ,  $n \geq 1$ , and spin  $J = -1$  we have to use  $\Delta_*^{(0)} = 3 + 2n$ . In this case, the first term in (5.258) vanishes for  $\zeta \neq 0$  due to the

factor  $\Gamma(\frac{\Delta-3}{2})^{-1}$ . Thus, the only relevant term is the one proportional to  $\langle a_{\tau,-1}^{(0)} \gamma_{\tau,-1}^{(1)} \rangle$  for which we get

$$\langle a_{\tau,-1}^{(0)} \gamma_{\tau,-1}^{(1)} \rangle = (-1)^{\tau/2+1} \frac{\Gamma(1 + \frac{\tau}{2})^4 S_1(\frac{\tau}{2})}{4\pi^4 \Gamma(1 + \tau)^2}. \quad (5.268)$$

From this we conclude that for  $0 < \zeta < 1$

$$\begin{aligned} \mathcal{F}_{\mathcal{E}}^{(1)}(\zeta) &= 2\pi^4 \sum_{n=1}^{\infty} (-1)^{n+1} \langle a_{\tau=2n,-1}^{(0)} \gamma_{\tau=2n,-1}^{(1)} \rangle \frac{1}{r_{n+1}} f_{3+2n}^{4,4}(\zeta) \\ &= \sum_{n=1}^{\infty} \frac{(n!)^2}{2(2n)!} S_1(n) f_{3+2n}^{4,4}(z) = -\frac{1}{4} \frac{\log(1-\zeta)}{\zeta^2(1-\zeta)}, \end{aligned} \quad (5.269)$$

where

$$r_h = \frac{\Gamma(h)^2}{\Gamma(2h-1)}. \quad (5.270)$$

Again our results are in perfect agreement with the direct evaluation performed in [147].

Let us now analyze the contact terms at  $\zeta = 0$  and  $\zeta = 1$  in  $\mathcal{F}_{\mathcal{E}}(\zeta)$ . First, let us fix these contact terms using the result for  $0 < \zeta < 1$

$$\mathcal{F}_{\mathcal{E}}^{(1)}(\zeta) = -\frac{1}{4} \frac{\log(1-\zeta)}{\zeta^2(1-\zeta)} \quad (0 < \zeta < 1), \quad (5.271)$$

together with Ward identities. We will then check that we reproduce the same contact terms at  $\zeta = 0$  using the light-ray OPE. We can rewrite (5.271) as

$$\mathcal{F}_{\mathcal{E}}^{(1)}(\zeta) = \frac{1}{4\zeta} - \frac{1}{4} \frac{\log(1-\zeta)}{1-\zeta} + \mathcal{F}_{\mathcal{E}}^{(1),\text{reg}}(\zeta), \quad (5.272)$$

where  $\mathcal{F}_{\mathcal{E}}^{(1),\text{reg}}(\zeta)$  is integrable near 0 and 1, and so has an unambiguous distributional interpretation. We then only need to interpret the first two terms. The most general expression we can write is<sup>36</sup>

$$\mathcal{F}_{\mathcal{E}}^{(1)}(\zeta) = c_0^{(1)} \delta(\zeta) + c_1^{(1)} \delta(1-\zeta) + \frac{1}{4} \left[ \frac{1}{\zeta} \right]_0 - \frac{1}{4} \left[ \frac{\log(1-\zeta)}{1-\zeta} \right]_1 + \mathcal{F}_{\mathcal{E}}^{(1),\text{reg}}(\zeta), \quad (5.273)$$

where  $[\dots]_0$  is defined near (5.216), and the definition of  $[\dots]_1$  is analogous with  $\zeta \rightarrow 1-\zeta$ . Ward identities (5.233) and (5.234) require

$$\int_0^1 d\zeta \mathcal{F}_{\mathcal{E}}^{(1)}(\zeta) = \int_0^1 d\zeta (2\zeta-1) \mathcal{F}_{\mathcal{E}}^{(1)}(\zeta) = 0, \quad (5.274)$$

<sup>36</sup>We assume that there are no derivatives of delta-functions. We verify this at  $\zeta = 0$  using the OPE.

from which we find

$$c_0^{(1)} = -\frac{1}{4}, \quad c_1^{(1)} = -\frac{\zeta_2}{4}. \quad (5.275)$$

We would now like to reproduce the distributional piece near  $\zeta = 0$

$$\mathcal{F}_{\mathcal{E}}^{(1)}(\zeta) = -\frac{1}{4}\delta(\zeta) + \frac{1}{4}\left[\frac{1}{\zeta}\right]_0 + \text{regular} \quad (5.276)$$

from the OPE. From the discussion in section 5.6.2 together with (5.258), this piece is given by

$$\begin{aligned} \mathcal{F}_{\mathcal{E}}^{(1)}(\zeta) &\ni \langle a_{\tau=2,-1}^{(1)} \rangle \widehat{f}_5(\zeta) + \langle a_{\tau=2,-1}^{(0)} \gamma_{\tau=2,-1}^{(1)} \rangle \partial_{\Delta} \widehat{f}_{\Delta}(\zeta)|_{\Delta=5} \\ &= -\frac{1}{16\pi^4} \times 8\pi^4 \delta(\zeta) + \frac{1}{16\pi^4} \times 4\pi^4 \left( \delta(\zeta) + \left[\frac{1}{\zeta}\right]_0 \right) \\ &= -\frac{1}{4}\delta(\zeta) + \frac{1}{4}\left[\frac{1}{\zeta}\right]_0, \end{aligned} \quad (5.277)$$

where we used (5.215). This is precisely the expected result.

To summarize, the full one-loop energy-energy correlator takes the form

$$\mathcal{F}_{\mathcal{E}}^{(1)}(\zeta) = -\frac{1}{4}\delta(\zeta) - \frac{\zeta_2}{4}\delta(1-\zeta) + \frac{1}{4}\left[\frac{1}{\zeta}\right]_0 - \frac{1}{4}\left[\frac{\log(1-\zeta)}{1-\zeta}\right]_1 + \mathcal{F}_{\mathcal{E}}^{(1),\text{reg}}(\zeta), \quad (5.278)$$

where  $\mathcal{F}_{\mathcal{E}}^{(1),\text{reg}}(\zeta)$  is defined via (5.272). The distributional part at  $\zeta = 1$  is in agreement with the one obtained in [147]. We also derive this  $\zeta = 1$  contact term from a different point of view in appendix D.6.

### 5.7.5 Two loops

Next, we would like to perform a similar analysis for the two-loop result [241, 242]. In this case, we must expand both the three-point coefficients and the anomalous dimensions up to second order. We have

$$\begin{aligned} &\mathcal{H}^{(2)}(u, v) \\ &= \sum_{\tau=2,4,\dots; \text{ even } J}^{\infty} \left( \langle a_{\tau,J}^{(2)} \rangle G_{\tau+4,J} + \langle a_{\tau,J}^{(1)} \gamma_{\tau,J}^{(1)} + a_{\tau,J}^{(0)} \gamma_{\tau,J}^{(2)} \rangle \partial_{\tau} G_{\tau+4,J} + \frac{1}{2} \langle a_{\tau,J}^{(0)} (\gamma_{\tau,J}^{(1)})^2 \rangle \partial_{\tau}^2 G_{\tau+4,J} \right), \end{aligned} \quad (5.279)$$

and a similar extension of (5.258) for the celestial block expansion (5.232). The explicit expression for  $\mathcal{H}^{(2)}$  is [221]

$$\begin{aligned} \mathcal{H}^{(2)}(u, v) &= \frac{1}{(2\pi)^4} \frac{u^3}{v} \left( \frac{1}{2} (1 + u + v) [\Phi^{(1)}(u, v)]^2 \right. \\ &\quad \left. + 2 \left[ \Phi^{(2)}(u, v) + \Phi^{(2)}(v, u) + \frac{1}{v} \Phi^{(2)} \left( \frac{u}{v}, \frac{1}{v} \right) \right] \right), \\ \Phi^{(2)}(z, \bar{z}) &= \frac{1}{16} \frac{1}{z - \bar{z}} \left( 6(\text{Li}_4(z) - \text{Li}_4(\bar{z})) - 3 \log(z\bar{z})(\text{Li}_3(z) - \text{Li}_3(\bar{z})) \right. \\ &\quad \left. + \frac{1}{2} \log^2(z\bar{z})(\text{Li}_2(z) - \text{Li}_2(\bar{z})) \right). \end{aligned} \quad (5.280)$$

A complete OPE expansion of this result is not available in the literature (as far as we know). Otherwise, we could simply evaluate the OPE data at  $J = -1$ , plug into the celestial OPE formula, and read off the answer for the energy-energy correlator. Some parts of the OPE expansion were obtained in [243], whose results we use below. For simplicity we focus on the term that involves  $\langle a_{\tau, J}^{(1)} (\gamma_{\tau, J}^{(1)})^2 \rangle$ , which on the celestial sphere maps to terms containing  $\log^2 \zeta$ .

Below, it will be useful to explicitly write the small- $z$  expansion of  $\partial_\tau^2 G_{\tau+4, J}$ , which takes the form

$$\begin{aligned} \partial_\tau^2 G_{\tau+4, J} &= (z\bar{z})^{2+\frac{\tau}{2}} \log^2 z \left( \frac{1}{4} \tilde{g}_{\tau+4, J} + \frac{1}{4} (z\bar{z}) \tilde{g}_{\tau+4, J}^{\text{sub}} + \dots \right), \\ \tilde{g}_{\tau, J} &= g_{\tau/2, J} = \bar{z}^J {}_2F_1 \left( \frac{\tau}{2} + J, \frac{\tau}{2} + J, \tau + 2J, \bar{z} \right), \\ \tilde{g}_{\tau, J}^{\text{sub}}(\bar{z}) &= \tilde{g}_{\tau+4, J-2}(\bar{z}) + \frac{\tau-2}{4} \tilde{g}_{\tau+2, J-1}(\bar{z}) - \delta_{J,0} \tilde{g}_{\tau+2, -2}(\bar{z}), \end{aligned} \quad (5.281)$$

where we only kept the terms containing  $\log^2 z$ .

### 5.7.5.1 Leading twist

The leading-twist contribution to  $\mathcal{H}^{(2)}$  takes the form  $(z\bar{z})^3 \log^2 z f_3(\bar{z})$ , where

$$f_3(\bar{z}) = \frac{1}{16} \frac{1}{(2\pi)^4} \frac{1}{(1 - \bar{z})\bar{z}^2} \left( \log^2[1 - \bar{z}] + 2\bar{z} \text{Li}_2(\bar{z}) \right). \quad (5.282)$$

Since there is no tree-level degeneracy for twist-two operators, this is equal to

$$f_3(\bar{z}) = \frac{1}{2} \sum_{\text{even } J} a_{2, J}^{(0)} \left( \gamma_{2, J}^{(1)} \right)^2 \left[ \frac{1}{4} \tilde{g}_{6, J}(\bar{z}) \right]. \quad (5.283)$$

Indeed one can check that (5.283) reproduces (5.282).

### 5.7.5.2 Subleading twist

Knowing  $\langle a_{\tau,J}^{(1)}(\gamma_{\tau,J}^{(1)})^2 \rangle$  at  $\tau = 2$  allows us to compute the  $\zeta^2 \log \zeta$  piece in  $\mathcal{F}^{(2)}(\zeta)$ . A really nontrivial check would be to reproduce the  $\zeta^3 \log \zeta$  term. Indeed the two-loop result of [182] contains both rational and transcendental pieces ( $\pi^2$ ) at this order. The latter should come from the analytically continued  $\langle \gamma^2 \rangle \neq \langle \gamma \rangle^2$ , due to the degeneracy of twist 4 operators.

We can compute the required OPE data from the piece  $(z\bar{z})^4 \log^2 z f_4(\bar{z}) \in \mathcal{H}^{(2)}$ , where

$$\begin{aligned} f_4(\bar{z}) &= -\frac{1}{16} \frac{1}{(2\pi)^4} \frac{1}{(1-\bar{z})\bar{z}^4} (2\bar{z}^2 + \bar{z}(\bar{z}-2) \log[1-\bar{z}] - (2+\bar{z}^2) \log^2[1-\bar{z}] - 2\bar{z}(1+\bar{z})\text{Li}_2(\bar{z})). \end{aligned} \quad (5.284)$$

This receives contributions from descendants of twist-two operators as well as from the subleading twist-four Regge trajectory. The subleading trajectory has tree-level degeneracies that we have not resolved, and therefore we cannot simply compute the result using our one-loop analysis.

The function (5.284) has decomposition

$$f_4(\bar{z}) = \frac{1}{2} \sum_{\text{even } J} a_{2,J}^{(0)} \left( \gamma_{2,J}^{(1)} \right)^2 \left[ \frac{1}{4} \tilde{g}_{8,J}^{\text{sub}}(\bar{z}) \right] + \frac{1}{2} \sum_{\text{even } J} \langle a_{4,J}^{(0)} [\gamma_{4,J}^{(1)}]^2 \rangle \left[ \frac{1}{4} \tilde{g}_{8,J}(\bar{z}) \right]. \quad (5.285)$$

Using

$$\tilde{g}_{\tau,J}(\bar{z}) = \bar{z}^{-\frac{\tau}{2}} \tilde{g}_{0,\tau+J}(\bar{z}) \quad (5.286)$$

and (5.281) it is easy to compute the contribution of descendants of twist 2 operators. After that we are left with the contribution of twist-four primaries

$$\begin{aligned} \tilde{f}_4(\bar{z}) &= \frac{1}{2(2\pi)^4 \bar{z}^4} \left( -\frac{9}{2} - \frac{1}{4} \frac{\bar{z}^2}{1-\bar{z}} + \frac{(\bar{z}-2)(18 - \frac{\bar{z}^2}{1-\bar{z}})}{8\bar{z}} \log(1-\bar{z}) + \frac{1}{8} \left( 1 + \frac{\bar{z}^2}{1-\bar{z}} \right) \log^2(1-\bar{z}) \right), \end{aligned} \quad (5.287)$$

which admits the decomposition (5.285) with the second term only. From this, we find<sup>37</sup>

<sup>37</sup>To solve this decomposition problem, one can use the methods of [243].

$$\langle a_{4,J}^{(0)}[\gamma_{4,J}^{(1)}]^2 \rangle = \frac{1}{4\pi^4} \frac{2^{-8-2J}\sqrt{\pi}}{3\Gamma(J+7/2)} \left( -\frac{6(11+7J+J^2)\Gamma(3+J)}{4+J} - \Gamma(4+J) \left( \pi^2 + 6(1-2S_1(3+J))S_1(3+J) + 3S_2(2+\frac{J}{2}) - 3S_2(\frac{5+J}{2}) \right) \right). \quad (5.288)$$

Evaluating at  $J = -1$ , we finally get

$$\langle a_{4,-1}^{(0)}[\gamma_{4,-1}^{(1)}]^2 \rangle = -\frac{2}{9}(\pi^2 - 11) \frac{1}{2(2\pi)^4}. \quad (5.289)$$

Note the appearance of the transcendental quantity  $\pi^2$  which is absent for even integer  $J$ .

### 5.7.5.3 Two-loop energy correlator

Expanding (5.232) to the second order, we get

$$\mathcal{F}_{\mathcal{E}}^{(2)}(\zeta) = 2\pi^4 \sum_{n=1}^{\infty} \left( \left( \langle a_{\tau=2n,-1}^{(0)} \gamma_{\tau=2n,-1}^{(2)} \rangle + \langle a_{\tau=2n,-1}^{(1)} \gamma_{\tau=2n,-1}^{(1)} \rangle \right) \frac{(-1)^{n+1}}{r_{n+1}} f_{3+2n}^{4,4}(\zeta) + \langle a_{\tau=2n,-1}^{(0)} [\gamma_{\tau=2n,-1}^{(1)}]^2 \rangle (-1)^{n+1} \frac{1}{2} \partial_n \left[ \frac{f_{3+2n}^{4,4}(\zeta)}{r_{n+1}} \right] \right). \quad (5.290)$$

Here, we used the fact that corrections to three-point coefficients alone do not contribute to scalar flow, due to the vanishing of the prefactor in (5.232) at tree-level twists.

Since we do not have degeneracies at twist two, we can fully predict the  $n = 1$  term in (5.290). For  $n = 2$ , corresponding to twist-four operators, we only computed the term  $\langle a_{4,-1}^{(0)}[\gamma_{4,-1}^{(1)}]^2 \rangle$ . The only missing element in the twist two sector is the two-loop anomalous dimension. It takes the following form (see e.g. formula (5.29) in [243])

$$\gamma_{2,J}^{(2)} = 2S_{-2,1}(J+2) - 2S_1(J+2)(S_2(J+2) + S_{-2}(J+2)) - (S_3(J+2) + S_{-3}(J+2)), \quad (5.291)$$

where  $S_{-2,1}(N) = \sum_{n=1}^N \frac{(-1)^n}{n^2} S_1(n)$  is an example of a nested harmonic sum. The relevant analytic continuation from even spins to  $J = -1$  gives

$$\gamma_{2,-1}^{(2),+} = 2S_{-2,1}^+(1) + \frac{\pi^2}{3} - 6 + \frac{3}{2}\zeta_3 = -4 + \frac{\pi^2}{3} - \zeta_3, \quad (5.292)$$

where we used standard methods [244] to perform the analytic continuation.

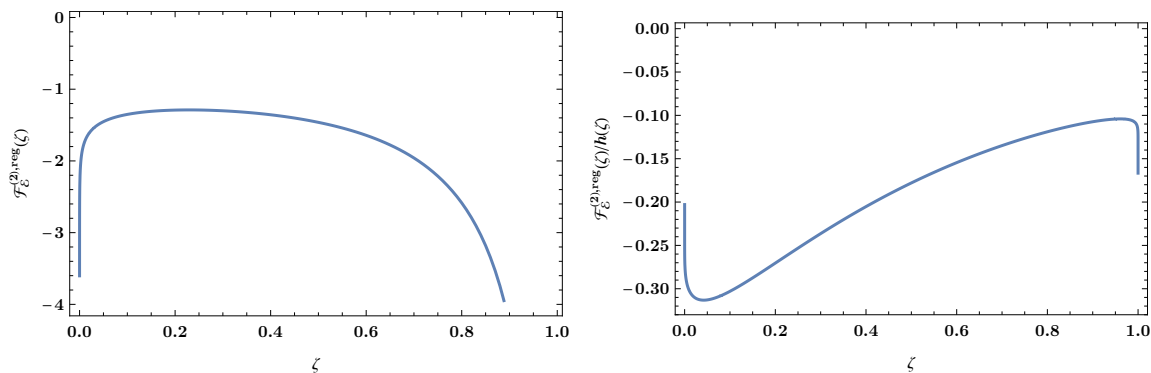


Figure 5.12: Integrable part  $\mathcal{F}_{\mathcal{E}}^{(2),\text{reg}}(\zeta)$  of the two-loop energy correlator. Left:  $\mathcal{F}_{\mathcal{E}}^{(2),\text{reg}}(\zeta)$  as a function of  $\zeta$ . Right:  $\mathcal{F}_{\mathcal{E}}^{(2),\text{reg}}(\zeta)/h(\zeta)$  as a function of  $\zeta$ , where  $h(\zeta) = (1 - \log \zeta)(1 - \log(1 - \zeta))^3$ .

Plugging everything back, we get the following prediction for the small-angle expansion of the scalar flow observable at two loops

$$\mathcal{F}_{\mathcal{E}}^{(2)}(\zeta) = \frac{1}{4\zeta} \left( 1 + \frac{\pi^2 - 5}{6}\zeta + \dots \right) \log \zeta + \frac{1}{4\zeta} \left( -\frac{1}{2}\zeta_3 + \frac{\pi^2}{6} - 3 \right) + \dots \quad (5.293)$$

This coincides with the expansion of the result in [182]. In principle, by performing the OPE decomposition of the small  $z$  expansion of the two-loop result (5.280) further and evaluating it at  $J = -1$ , we can predict higher order terms in the small-angle (small  $\zeta$ ) expansion of the scalar event shape.

#### 5.7.5.4 Contact terms

Let us also check that we reproduce the correct  $\zeta = 0$  contact terms in  $\mathcal{F}_{\mathcal{E}}^{(2)}(\zeta)$ . Firstly, as in the one-loop example, we can use the Ward identities to fix the contact terms in the two-loop result of [182]. We have

$$\begin{aligned} \mathcal{F}_{\mathcal{E}}^{(2)}(\zeta) = & \frac{1}{4\zeta} \left( \frac{\pi^2}{6} - \frac{1}{2}\zeta_3 - 3 \right) + \frac{1}{4} \frac{\log \zeta}{\zeta} + \frac{\zeta_3}{8} \frac{1}{1-\zeta} + \frac{\pi^2 \log(1-\zeta)}{16} \frac{1}{1-\zeta} + \frac{1}{8} \frac{\log^3(1-\zeta)}{1-\zeta} \\ & + \mathcal{F}_{\mathcal{E}}^{(2),\text{reg}}(\zeta), \end{aligned} \quad (5.294)$$

where  $\mathcal{F}_{\mathcal{E}}^{(2),\text{reg}}(\zeta)$  is integrable both at  $\zeta = 0$  and  $\zeta = 1$ . We show the plot of  $\mathcal{F}_{\mathcal{E}}^{(2),\text{reg}}(\zeta)$  in figure 5.12. It only has integrable  $\log^k$ -type singularities at the endpoints. To demonstrate this, we show also the ratio  $\mathcal{F}_{\mathcal{E}}^{(2),\text{reg}}(\zeta)/h(\zeta)$  with  $h(\zeta) = (1 - \log \zeta)(1 - \log(1 - \zeta))^3$ . This ratio is finite, but approaches its limits near  $\zeta = 0, 1$  in a non-analytic way due to  $1/\log^k$  type non-analyticities.



As before, we make an ansatz for the distribution by writing

$$\begin{aligned} \mathcal{F}_{\mathcal{E}}^{(2)}(\zeta) = & \frac{1}{4} \left[ \frac{1}{\zeta} \right]_0 \left( \frac{\pi^2}{6} - \frac{1}{2} \zeta_3 - 3 \right) + \frac{1}{4} \left[ \frac{\log \zeta}{\zeta} \right]_0 + \frac{\zeta_3}{8} \left[ \frac{1}{1-\zeta} \right]_1 + \frac{\pi^2}{16} \left[ \frac{\log(1-\zeta)}{1-\zeta} \right]_1 \\ & + \frac{1}{8} \left[ \frac{\log^3(1-\zeta)}{1-\zeta} \right]_1 + c_0^{(2)} \delta(\zeta) + c_1^{(2)} \delta(1-\zeta) + \mathcal{F}_{\mathcal{E}}^{(2),\text{reg}}(\zeta), \end{aligned} \quad (5.295)$$

where  $[\zeta^{-1} \log^k \zeta]_0$  is defined by the Taylor expansion of  $\zeta^{-1+\epsilon}$  in  $\epsilon$  to the appropriate order, and similarly for  $[(1-\zeta)^{-1} \log^k(1-\zeta)]_1$ . The Ward identities (5.233) and (5.234) require that

$$0 = c_0^{(2)} + c_1^{(2)} + \int_0^1 d\zeta \mathcal{F}_{\mathcal{E}}^{(2),\text{reg}}(\zeta), \quad (5.296)$$

$$0 = -c_0^{(2)} + c_1^{(2)} - \frac{1}{2}(\zeta_3 + 1) + \frac{5\pi^2}{24} + \int_0^1 d\zeta (2\zeta - 1) \mathcal{F}_{\mathcal{E}}^{(2),\text{reg}}(\zeta). \quad (5.297)$$

The explicit expression for  $\mathcal{F}_{\mathcal{E}}^{(2),\text{reg}}(\zeta)$  follows easily from the definition and the results of [182]. Due to its complexity, we computed the above integrals numerically,

$$\int_0^1 d\zeta \mathcal{F}_{\mathcal{E}}^{(2),\text{reg}}(\zeta) = -2.6133007151791604187079457 \dots, \quad (5.298)$$

$$\int_0^1 d\zeta (2\zeta - 1) \mathcal{F}_{\mathcal{E}}^{(2),\text{reg}}(\zeta) = -1.047646501079170962972713 \dots, \quad (5.299)$$

from which we can determine

$$\begin{aligned} c_0^{(2)} &= 1.26039667304023767931294 \dots, \\ c_1^{(2)} &= 1.35290404213892273939500 \dots \end{aligned} \quad (5.300)$$

Using Mathematica's `FindIntegerNullVector`, we found that to the available precision these numbers are given by

$$\begin{aligned} c_0^{(2)} &= \frac{11\pi^4}{1440} - \frac{\pi^2}{8} + \frac{7}{4}, \\ c_1^{(2)} &= \frac{\pi^4}{72}. \end{aligned} \quad (5.301)$$

To summarize, the distributional piece of  $\mathcal{F}_{\mathcal{E}}^{(2)}(\zeta)$  near  $\zeta = 0$  is

$$\mathcal{F}_{\mathcal{E}}^{(2)}(\zeta) = \left( \frac{11\pi^4}{1440} - \frac{\pi^2}{8} + \frac{7}{4} \right) \delta(z) + \frac{1}{4} \left[ \frac{1}{\zeta} \right]_0 \left( \frac{\pi^2}{6} - \frac{1}{2} \zeta_3 - 3 \right) + \frac{1}{4} \left[ \frac{\log \zeta}{\zeta} \right]_0 + \dots \quad (5.302)$$

As at one loop, from the OPE point of view these pieces are determined completely by twist-two OPE data. In particular, we have

$$\begin{aligned} \mathcal{F}_{\mathcal{E}}^{(2)}(\zeta) &= \langle a_{\tau=2,-1}^{(2)} \rangle \widehat{f}_5(\zeta) + \langle a_{\tau=2,-1}^{(1)} \gamma_{\tau=2,-1}^{(1)} + a_{\tau=2,-1}^{(0)} \gamma_{\tau=2,-1}^{(2)} \rangle \partial_{\Delta} \widehat{f}_{\Delta}(\zeta)|_{\Delta=5} \\ &\quad + \frac{1}{2} \langle a_{\tau=2,-1}^{(0)} (\gamma_{\tau=2,-1}^{(1)})^2 \rangle \partial_{\Delta}^2 \widehat{f}_{\Delta}(\zeta)|_{\Delta=5} + \dots \end{aligned} \quad (5.303)$$

All OPE data in this equation except for  $\langle a_{\tau=2,-1}^{(2)} \rangle$  has been described above. We give  $\langle a_{\tau=2,-1}^{(2)} \rangle$  in the next section in equation (5.315). Using these results and (5.215), we precisely reproduce (5.302). A calculation in appendix D.6 also reproduces the value of  $c_1^{(2)}$  in (5.301). Note that this is non-trivial consistency check of the result [182], since in order to fix the contact terms we used Ward identities which involve integrals of the even shape over  $\zeta$ , not just the  $\zeta \rightarrow 0$  and  $\zeta \rightarrow 1$  limits.

To summarize, the full two loop energy-energy correlator is given by (5.295), where  $c_0^{(2)}$  and  $c_1^{(2)}$  are given by (5.301). This completes the  $0 < \zeta < 1$  result of [182]. We checked numerically that the complete two-loop energy-energy correlator satisfies Ward identities (5.233) and (5.234). This check was also performed in [219].

### 5.7.6 Three loops

Recently the three loop the energy-energy correlator have been computed in [207]. The authors have verified that the leading  $\zeta$  asymptotic of their result agrees with our prediction (see section 5.7.7).<sup>38</sup> In this section we extend this check to contact terms at  $\zeta = 0$ , similarly to what we did at the two-loop level above. Namely, we will use the results of [207] and Ward identities to fix the contact terms at  $\zeta = 0$  and  $\zeta = 1$ , and then compare to the  $\zeta = 0$  contact terms predicted by the light-ray OPE. This provides a highly non-trivial consistency check of the results of [207], since the Ward identities involve integrals of  $\mathcal{F}_{\mathcal{E}}^{(3)}(\zeta)$  over  $\zeta$ .

We proceed as before, by writing

$$\begin{aligned} &4\mathcal{F}_{\mathcal{E}}^{(3)}(\zeta) \\ &= 4c_0^{(3)}\delta(\zeta) + \frac{1}{2} \left[ \frac{\log^2 \zeta}{\zeta} \right]_0 + \left( \frac{\pi^2}{3} - \zeta_3 - 5 \right) \left[ \frac{\log \zeta}{\zeta} \right]_0 + \left( 17 - \frac{4\pi^2}{3} + \frac{5\pi^4}{144} - \zeta_3 + \frac{3}{2}\zeta_5 \right) \left[ \frac{1}{\zeta} \right]_0 \\ &+ 4c_1^{(3)}\delta(y) - \frac{1}{8} \left[ \frac{\log^5 y}{y} \right]_1 - \frac{\pi^2}{6} \left[ \frac{\log^3 y}{y} \right]_1 - \frac{11\zeta_3}{4} \left[ \frac{\log^2 y}{y} \right]_1 - \frac{61\pi^4}{720} \left[ \frac{\log y}{y} \right]_1 - \left( \frac{7}{2}\zeta_5 + \frac{\pi^2}{3}\zeta_3 \right) \left[ \frac{1}{y} \right]_1 \\ &+ 4\mathcal{F}_{\mathcal{E}}^{(3),\text{reg}}(\zeta), \end{aligned} \quad (5.304)$$

where  $y = 1 - \zeta$  and  $\mathcal{F}_{\mathcal{E}}^{(3),\text{reg}}(\zeta)$  is integrable at  $\zeta = 0$  and  $\zeta = 1$ . We show the plot of  $\mathcal{F}_{\mathcal{E}}^{(3),\text{reg}}(\zeta)$  in the left panel of figure 5.13. Again, it only has integrable  $\log^k$  singular-

<sup>38</sup>This was also independently verified in [220] based on the two-loop result [182] and the energy Ward identity (5.233).

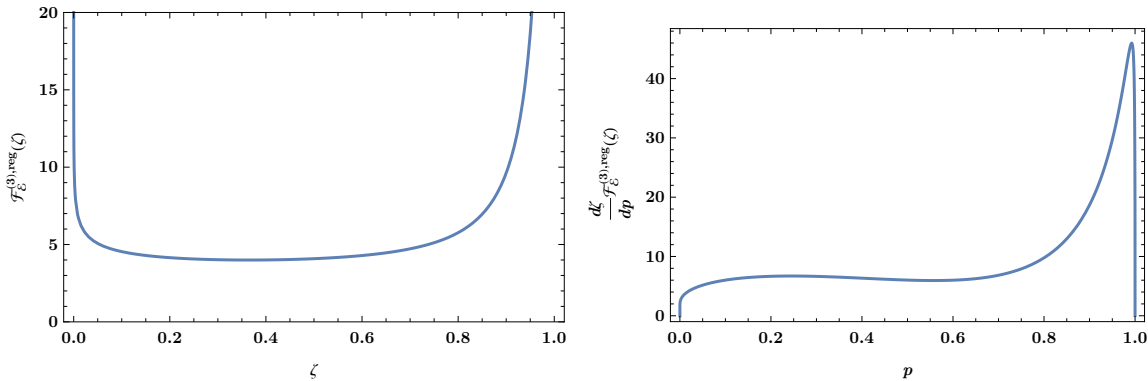


Figure 5.13: Integrable part  $\mathcal{F}_\varepsilon^{(3),\text{reg}}(\zeta)$  of the two-loop energy correlator. Left:  $\mathcal{F}_\varepsilon^{(3),\text{reg}}(\zeta)$  as a function of  $\zeta$ . Right:  $\frac{\partial \zeta}{\partial p} \mathcal{F}_\varepsilon^{(3),\text{reg}}(\zeta)$  as a function of  $p$ .

ities. In order to perform numerical integration of these singularities we change the variable from  $\zeta \in [0, 1]$  to  $p \in [0, 1]$  defined as

$$\zeta = \frac{(1-p)^2 + (1-p)^3}{\log^2 p} \left( 1 + \frac{p^5(1-p)}{\log^5(1-p)} \right). \quad (5.305)$$

This change of variables is designed so that the Jacobian  $\frac{\partial \zeta}{\partial p}$  has appropriate  $1/\log^k$  behavior to cancel  $\log^k$  singularities of  $\mathcal{F}_\varepsilon^{(3),\text{reg}}(\zeta)$  near  $\zeta = 0, 1$ . We show the plot of the resulting function  $\frac{\partial \zeta}{\partial p} \mathcal{F}_\varepsilon^{(3),\text{reg}}(\zeta)$  in the right panel of figure 5.13.

The singular part, except from the delta functions (and distributional interpretation of other pieces), can be obtained from the results of [207]. We can fix the coefficients  $c_i^{(3)}$  by requiring that the Ward identities (5.233) and (5.234) are satisfied. We find the equations

$$0 = c_0^{(3)} + c_1^{(3)} + \int d\zeta \mathcal{F}_\varepsilon^{(3),\text{reg}}(\zeta), \quad (5.306)$$

$$0 = -c_0^{(3)} + c_1^{(3)} + 4 - \frac{4\pi^2}{3} - \frac{\pi^4}{40} + \frac{11\zeta_3}{4} + \frac{\pi^2\zeta_3}{6} + \frac{5\zeta_5}{2} + \int d\zeta (2\zeta - 1) \mathcal{F}_\varepsilon^{(3),\text{reg}}(\zeta). \quad (5.307)$$

Integrating the result of [207], numerically we find

$$\begin{aligned} \int d\zeta \mathcal{F}_\varepsilon^{(3),\text{reg}}(\zeta) &\approx 9.53135, \\ \int d\zeta (2\zeta - 1) \mathcal{F}_\varepsilon^{(3),\text{reg}}(\zeta) &\approx 4.84686. \end{aligned} \quad (5.308)$$

In [207],  $\mathcal{F}_\varepsilon^{(3)}(\zeta)$  contains a piece expressed as a double integral, and the integrals above are therefore effectively triple integrals. Because of this, it is non-trivial to

control the numerical errors, and we have not attempted to get an a priori error estimate for (5.308). Based on the agreement with the light-ray OPE below, we expect that the errors in the numbers above are in the last digit.

Using this data, we find

$$\begin{aligned} c_0^{(3)} &\approx -4.20195, \\ c_1^{(3)} &\approx -5.32939. \end{aligned} \tag{5.309}$$

Using the same methods as above, and the OPE data described in section 5.7.7, we find the light-ray OPE prediction for  $c_0^{(3)}$ ,

$$\begin{aligned} c_0^{(3)} &= -\frac{49}{4} + \pi^2 - \frac{\pi^4}{576} - \frac{109\pi^6}{30240} + \frac{5\zeta_3}{4} - \frac{7}{24}\pi^2\zeta_3 + \frac{3\zeta_3^2}{16} + \frac{27\zeta_5}{8} \\ &= -4.2019873198181\dots \end{aligned} \tag{5.310}$$

This agrees well with (5.309), and based on the accuracy of the agreement, we expect for  $c_1^{(3)}$

$$c_1^{(3)} \approx -5.3294(1). \tag{5.311}$$

We show in appendix D.6 that  $c_1^{(3)}$  is given by

$$c_1^{(3)} = -\frac{197\pi^6}{40320} - \frac{7\zeta_3^2}{16} = -5.329425268\dots, \tag{5.312}$$

which precisely agrees with (5.311).<sup>39</sup> This numerical check was also done in [219].

To summarize, the complete three-loop energy-energy correlator, including contact terms, is given by (5.304), where  $c_0^{(3)}$  and  $c_1^{(3)}$  are given by (5.310) and (5.312), while  $\mathcal{F}_{\mathcal{E}}^{(3)}(\zeta)$  follows from its definition and results of [207]. We checked numerically that the complete three-loop energy-energy correlator satisfies Ward identities (5.233) and (5.234).

### 5.7.7 Four loops in the planar limit and finite coupling

Using known results for the OPE data of twist-2 operators, we can make new predictions for the leading small-angle asymptotics of the energy-energy correlator. At finite coupling the contribution of twist-two operators takes the form

$$\mathcal{F}_{\mathcal{E}}^{\text{twist-two}}(\zeta) = a_{2,-1}^{(+)} \frac{4\pi^4 \Gamma\left(3 + \gamma_{2,-1}^{(+)}\right)}{\Gamma\left(2 + \frac{\gamma_{2,-1}^{(+)}}{2}\right)^3 \Gamma\left(-1 - \frac{\gamma_{2,-1}^{(+)}}{2}\right)} f_{5+\gamma_{2,-1}^{(+)}}^{4,4}(\zeta), \tag{5.313}$$

<sup>39</sup>In deriving (5.312), we used the three-loop result for the so-called coefficient function  $H(a)$  [219].

where by (+) we indicate analytic continuation from even spin. Note that  $\gamma_{2,-1}^{(+)}$  can be computed at any 't Hooft coupling using integrability methods [198, 245]. At small angles we have  $f_{5+\gamma_{2,-1}^{(+)}}^{4,4}(\zeta) \approx \zeta^{\frac{\gamma_{2,-1}^{(+)}}{2}-1}$ . Therefore, at weak coupling (5.313) controls the small angle  $\zeta \rightarrow 0$  expansion of the EEC. When the coupling becomes large, operators with twist two at tree level become very heavy and the leading small-angle asymptotic is controlled by the approximately twist-four double trace operators. This transition happens at  $a \approx 2.645$ , see figure 5.14.

At finite coupling there is no contact term coming from (5.313), since the anomalous dimension of twist-two operators is finite. The term  $\xi(\zeta)$  in (5.232) is completely canceled by a contribution of a protected operator. This cancellation is the same as at strong coupling and is described in the next section. In summary, the event shape at finite coupling is integrable near  $\zeta = 0$  and the contact terms only appear at weak coupling through the expansion (5.215).

Using (5.313), we can easily make a planar four-loop prediction for the leading asymptotic of  $\mathcal{F}(\zeta)$ .<sup>40</sup> The relevant OPE data takes the form

$$\begin{aligned} \gamma_{2,-1}^{(+)} = & 2a + \left(-4 + \frac{\pi^2}{3} - \zeta_3\right) a^2 + \left(16 - \frac{4}{3}\pi^2 + \frac{\pi^4}{120} - 3\zeta_3 + 3\zeta_5\right) a^3 \\ & + \left(-80 + \frac{\pi^2}{6}[48 - 13\zeta_3 + \zeta_5] - \frac{1}{720}\pi^4[46 + 5\zeta_3] \right. \\ & \left. - \frac{107\pi^6}{15120} + 14\zeta_3 + \frac{9}{2}\zeta_3^2 + 16\zeta_5 - \frac{69}{8}\zeta_7\right) a^4 + \dots, \end{aligned} \quad (5.314)$$

$$\begin{aligned} \frac{a_{2,-1}^{(+)}}{a_{2,-1}^{(0)}} = & 1 - 2a + \left(12 - \frac{2\pi^2}{3} + \frac{11\pi^4}{360} + \frac{1}{2}\zeta_3\right) a^2 \\ & + \left(-80 + \pi^2\left(6 - \frac{7}{6}\zeta_3\right) - \frac{\pi^4}{24} - \frac{109}{7560}\pi^6 + 6\zeta_3 + \frac{3}{4}\zeta_3^2 + 12\zeta_5\right) a^3 + a_4 a^4 + \dots, \end{aligned} \quad (5.315)$$

where for our normalization of the four-point function the tree-level three-point function is  $a_{2,-1}^{(0)} = \frac{1}{32\pi^4}$ . Up to three loops, the results can be found in [247], where the three-loop correction to the structure constant was first explicitly computed.<sup>41</sup> For the four-loop anomalous dimensions, we combined the results of [249] and [250]. To analytically continue in spin, we used the HPL package [251] together with the supplement developed in [252].<sup>42</sup>

<sup>40</sup>Starting from the four loops there are non-planar corrections to the correlator [246].

<sup>41</sup>The currently available online version (arXiv v1) of [247] contains a typo. The corrected version

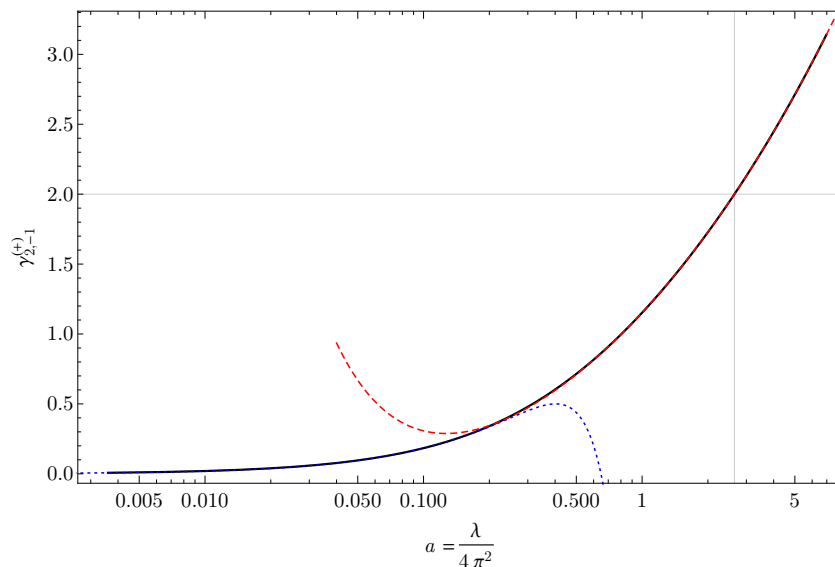


Figure 5.14:  $\gamma_{2,-1}^{(+)}$  as a function of the coupling constant  $a = \frac{\lambda}{4\pi^2}$ . The plot was kindly made for us by Nikolay Gromov. The actual numerics was done for  $J = -1 + 10^{-5}$ . The blue dotted line represents a four-loop weak coupling approximation to  $\gamma_{2,-1}^{(+)}$ , the red dashed line corresponds to the first four terms at the strong coupling expansion [245]. The solid line was obtained using the quantum spectral curve technique [245]. The curve intersects  $\gamma_{2,-1}^{(+)} = 2$  at  $a \approx 2.645$ . At this point the small angle expansion of the EEC becomes regular and dominated by the twist four double trace operators.

Plugging these results into (5.313), we easily obtain the leading small-angle expansion of the energy-energy correlator up to four loops. Due to the factor

$$\frac{1}{\Gamma\left(-1 - \frac{\gamma_{2,-1}^{(+)}}{2}\right)}, \quad (5.316)$$

only the three-loop correction to three-point coefficients is needed to compute the four-loop result for  $0 < \zeta < 1$ . At  $\zeta = 0$ ,  $\zeta = 1$ , there are contact terms that depend on additional data at four loops (discussed below). The first two terms in the expansion in the coupling reproduce the two-loop computation of [182]. The three- and four-loop predictions are new. Our three-loop prediction was recently independently confirmed in [207].

of the formula can be found for example in [248] which we used in our computation.

<sup>42</sup>In the papers cited above, the anomalous dimension and three-point coupling of  $\text{Tr}[ZD^J Z]$  operator are computed. These operators transform in the  $\mathbf{20}'$  representation and their dimensions and couplings are related to the anomalous dimension  $\gamma_{\tau=2,J}$  and  $a_{\tau=2,J}$  of the superconformal primaries that appear in (5.240) by a spin shift  $J \rightarrow J + 2$ , see e.g. [253]. Therefore, the formulas of [247] should be evaluated at  $J = 1$  for our purposes.

In more detail, we can write the following expression for the planar four-loop energy-energy correlator<sup>43</sup>

$$\begin{aligned}
\mathcal{F}_{\mathcal{E}}^{(4),\text{pl}}(\zeta) &= c_0^{(4)}\delta(\zeta) + \frac{1}{24} \left[ \frac{\log^3 \zeta}{\zeta} \right]_0 + \left( -\frac{7}{8} + \frac{1}{16}\pi^2 - \frac{3}{16}\zeta_3 \right) \left[ \frac{\log^2 \zeta}{\zeta} \right]_0 \\
&+ \frac{1}{4} \left( 31 - \frac{17}{6}\pi^2 + \frac{1}{15}\pi^4 - \frac{1}{6}\pi^2\zeta_3 + \frac{1}{4}\zeta_3^2 + 3\zeta_5 \right) \left[ \frac{\log \zeta}{\zeta} \right]_0 \\
&+ \frac{1}{4} \left( -111 + \frac{65}{6}\pi^2 - \frac{3}{16}\pi^4 - \frac{389}{30240}\pi^6 + 10\zeta_3 - 2\pi^2\zeta_3 \right. \\
&\quad \left. - \frac{3}{160}\pi^4\zeta_3 + 3\zeta_3^2 + 20\zeta_5 + \frac{1}{12}\pi^2\zeta_5 - \frac{69}{16}\zeta_7 \right) \left[ \frac{1}{\zeta} \right]_0 \\
&+ c_1^{(4)}\delta(y) + \frac{1}{192} \left[ \frac{\log^7 y}{y} \right]_1 + \frac{5}{384}\pi^2 \left[ \frac{\log^5 y}{y} \right]_1 + \frac{95}{192}\zeta_3 \left[ \frac{\log^4 y}{y} \right]_1 + \frac{29}{1920}\pi^4 \left[ \frac{\log^3 y}{y} \right]_1 \\
&+ \left( \frac{67}{192}\pi^2\zeta_3 + \frac{69}{16}\zeta_5 \right) \left[ \frac{\log^2 y}{y} \right]_1 + \left( \frac{367}{48384}\pi^4 + \frac{97}{32}\zeta_3^2 \right) \left[ \frac{\log y}{y} \right]_1 \\
&+ \left( \frac{187}{5760}\pi^4\zeta_3 + \frac{95}{192}\pi^2\zeta_5 + \frac{785}{128}\zeta_7 \right) \left[ \frac{1}{y} \right]_1 + \mathcal{F}_{\mathcal{E}}^{(4),\text{reg}}(\zeta), \tag{5.317}
\end{aligned}$$

where  $\mathcal{F}_{\mathcal{E}}^{(4),\text{reg}}(\zeta)$  is integrable at  $\zeta = 0, 1$ . We also included the leading terms in the  $\zeta \rightarrow 1$  limit, which we obtained using results of [182, 219, 254] as described in appendix D.6 (recall  $y = 1 - \zeta$ ).<sup>44</sup> The contact term coefficients  $c_0^{(4)}$  and  $c_1^{(4)}$  are equal to

$$\begin{aligned}
c_0^{(4)} &= \frac{1}{4} \left( -209 + \frac{37}{2}\pi^2 - \frac{23}{80}\pi^4 - \frac{389}{30240}\pi^6 + 20\zeta_3 - \frac{8}{3}\pi^2\zeta_3 - \frac{3}{160}\pi^4\zeta_3 \right. \\
&\quad \left. + \frac{11}{2}\zeta_3^2 + 14\zeta_5 + \frac{1}{12}\pi^2\zeta_5 - \frac{69}{16}\zeta_7 + a_4 \right), \\
c_1^{(4)} &= \frac{17}{144}\pi^2\zeta_3^2 + \frac{7}{2}\zeta_3\zeta_5 + \frac{1}{4}H_4, \tag{5.318}
\end{aligned}$$

where  $a_4$  is a four-loop correction to the three-point function at  $J = -1$ , see (5.315), and  $H_4$  is a four-loop correction to the coefficient function, see appendix D.6, which

<sup>43</sup>By planar we mean that it was obtained from the planar four-loop correlation function. Starting from four loops there are corrections to the energy correlator suppressed by  $\frac{1}{c}$ .

<sup>44</sup>Here we again made use of the three-loop result for  $H(a)$  [219].

are presently unknown. The Ward identities (5.233), (5.234) thus take the form

$$\begin{aligned}
c_0^{(4)} + c_1^{(4)} + \int_0^1 d\zeta \mathcal{F}_\mathcal{E}^{(4),\text{reg}}(\zeta) &= 0, \\
-c_0^{(4)} + c_1^{(4)} + \int_0^1 d\zeta (2\zeta - 1) \mathcal{F}_\mathcal{E}^{(4),\text{reg}}(\zeta) &= \frac{45}{2} - \frac{245}{24}\pi^2 - \frac{13}{240}\pi^4 - \frac{151}{17280}\pi^6 + \frac{39}{2}\zeta_3 \\
&\quad + \frac{37}{16}\pi^2\zeta_3 + \frac{107}{1440}\pi^4\zeta_3 - \frac{119}{16}\zeta_3^2 + \frac{35}{4}\zeta_5 \\
&\quad + \frac{91}{96}\pi^2\zeta_5 + \frac{923}{64}\zeta_7 \\
&\approx -9.784125919\dots
\end{aligned} \tag{5.319}$$

As was the case at three loops, these identities provide a nontrivial test for any future four-loop computation. Because we explicitly isolated all the distributional terms it is particularly suited for numerical tests. Alternatively, given a four-loop result for  $\mathcal{F}_\mathcal{E}^{(4),\text{pl}}$ , one can use (5.319) to predict  $a_4$  and  $H_4$ . These values can then be used to predict leading five-loop asymptotics at  $\zeta \rightarrow 0$  and  $\zeta \rightarrow 1$ .

### 5.7.8 Strong coupling in the planar limit

The four-point function at strong-coupling is simple enough that we can directly compute  $C^{+,\text{sugra}}(\Delta, J)$  and use the celestial block expansion to obtain the full scalar flow observable as a function of  $\zeta$ . The four-point function is [255]

$$\Phi^{(\text{sugra})}(u, v) = uv \bar{D}_{2422}(u, v). \tag{5.320}$$

For a review of  $\bar{D}$ -functions see e.g. [253].

As explained in [62], remarkably the tree-level supergravity answer is fixed by the protected half-BPS data and is given by

$$\text{dDisc}[G^{(105)}(z, \bar{z})] = \text{dDisc}\left[\frac{z\bar{z}}{(1-z)(1-\bar{z})}\right] f(z, \bar{z}), \tag{5.321}$$

where  $f(z, \bar{z})$  is regular at  $z, \bar{z} = 1$  and is symmetric under permutations of  $z$  and  $\bar{z}$ . The relation to the  $\mathcal{G}(z, \bar{z})$  used in [62] is  $G^{(105)}(z, \bar{z}) = c_{\frac{1}{2}} \frac{1}{(2\pi)^4} (z\bar{z})^2 \mathcal{G}(z, \bar{z})$ . Thus,

$$\begin{aligned}
C^{+,\text{sugra}}(\Delta, J) &= 2 \frac{\kappa_{\Delta+J}}{4} \int_0^1 \frac{dz}{z^2} \int_0^1 \frac{d\bar{z}}{\bar{z}^2} \frac{z - \bar{z}}{z\bar{z}} \\
&\quad \times (k_{\Delta+J}(z) k_{4+J-\Delta}(\bar{z}) - k_{\Delta+J}(\bar{z}) k_{4+J-\Delta}(z)) \frac{2(\sin \pi\delta)^2 z^{1+\delta} \bar{z}^{1+\delta}}{(1-z)^{1+\delta} (1-\bar{z})^{1+\delta}} f(z, \bar{z}) \Big|_{\delta \rightarrow 0},
\end{aligned} \tag{5.322}$$

where we have regulated the integral by introducing  $\delta$  in the same way as we did in section 5.7.3.



To isolate the contribution that survives as  $\delta \rightarrow 0$ , we rewrite  $z - \bar{z} = (1 - \bar{z}) - (1 - z)$ . By the symmetry of the integral under the exchange of  $z$  and  $\bar{z}$ , each of the terms produces an identical contribution, giving a factor of 2. We can rewrite the integral as

$$C^{+, \text{sugra}}(\Delta, J) = \frac{\kappa_{\Delta+J}}{(2\pi)^4} (\sin \pi \delta)^2 \int_0^1 \frac{dz}{z^2} \int_0^1 \frac{d\bar{z}}{\bar{z}^2} \left( \frac{1}{2} D(D-2) \frac{z \log z}{1-z} \right) \\ \times (k_{\Delta+J}(z) k_{4+J-\Delta}(\bar{z}) - k_{\Delta+J}(\bar{z}) k_{4+J-\Delta}(z)) \frac{\bar{z}^{1+\delta}}{(1-\bar{z})^{1+\delta}} \Big|_{\delta \rightarrow 0}, \quad (5.323)$$

where we set  $\bar{z} = 1$  in  $f(z, \bar{z})$  since it does not affect the  $\delta = 0$  result, and used  $f(z, 1) = \frac{1}{2} \frac{1}{(2\pi)^4} \left( -\frac{1}{2} D(D-2) \frac{z \log z}{1-z} \right)$ , see [62]. We have also introduced the differential operator

$$D = z^2 \partial_z (1-z) \partial_z, \quad (5.324)$$

which is the Casimir operator of which  $k_\beta(z)$  is an eigenfunction with eigenvalue  $\frac{\beta(\beta-2)}{4}$ . Doing the integrals, we get

$$C^{+, \text{sugra}}(\Delta, J) = \frac{\Gamma(\frac{\Delta+J}{2})^2}{64\pi^4 \Gamma(\Delta+J-1)} \left( -\tilde{I}(4+J-\Delta) + \frac{\Gamma(4+J-\Delta) \Gamma(\frac{\Delta+J}{2})^2}{\Gamma(\Delta+J) \Gamma(\frac{4+J-\Delta}{2})^2} \tilde{I}(\Delta+J) \right), \quad (5.325)$$

where

$$\tilde{I}(\beta) = \int_0^1 \frac{dz}{z^2} k_\beta(z) D(D-2) \frac{z \log z}{1-z} \\ = \frac{1}{16} (\beta+2) \beta (\beta-2) (\beta-4) \int_0^1 \frac{dz}{z^2} k_\beta(z) \frac{z \log z}{1-z} + \frac{\beta (\beta^2 - 2\beta - 10) \Gamma(1+\beta)}{16 \Gamma(1+\frac{\beta}{2})^2}, \quad (5.326)$$

where the second term in the second line comes from boundary terms when we integrate by parts. Its contribution to  $C^{+, \text{sugra}}(\Delta, -1)$  is equal to zero.

Specializing to  $J = -1$ , we find

$$C^{+, \text{sugra}}(\Delta, -1) \frac{4\pi^4 \Gamma(\Delta-2)}{\Gamma(\frac{\Delta-1}{2})^3 \Gamma(\frac{3-\Delta}{2})} = -\pi \frac{(\Delta+1)(\Delta-1)(\Delta-5) \Gamma(\frac{\Delta-1}{2})^2}{256 \Gamma(\Delta-3) \cos \frac{\pi \Delta}{2}}. \quad (5.327)$$

This provides the data needed to compute  $\mathcal{F}^{(\text{sugra})}$  using the celestial block expansion. Formula (5.228) gives an integral which we can evaluate by residues when  $0 < \zeta < 1$ ,

$$\begin{aligned} \mathcal{F}_{\mathcal{E}}^{(\text{sugra})}(\zeta) &= \int_{2-i\infty}^{2+i\infty} \frac{d\Delta}{2\pi i} C(\Delta, -1) \frac{4\pi^4 \Gamma(\Delta - 2)}{\Gamma(\frac{\Delta-1}{2})^3 \Gamma(\frac{3-\Delta}{2})} f_{\Delta}^{4,4}(\zeta) \\ &= \sum_{n=0}^{\infty} \frac{(-1)^n}{8} (n+1)(n+2)(n+3)(n+4) r_{n+3} f_{7+2n}^{4,4}(\zeta) \\ &= \frac{1}{2}, \quad 0 < \zeta < 1. \end{aligned} \tag{5.328}$$

where  $r_h$  was defined in (5.270). This answer coincides with the one obtained in [31]. Alternatively, we could have directly continued the known OPE decomposition of the correlation function to  $J = -1$ . Indeed, in the one-loop example above the sum above is equal to

$$\mathcal{F}_{\mathcal{E}}^{(\text{sugra})}(\zeta) = 2\pi^4 \sum_{n=0}^{\infty} (-1)^{n+1} \langle a_{\tau=4+2n,-1}^{(0)} \gamma_{\tau=4+2n,-1}^{(\text{sugra})} \rangle \frac{1}{r_{n+3}} f_{7+2n}^{4,4}(\zeta), \tag{5.329}$$

where the sum goes over the Regge trajectories of double trace operators with scaling dimension  $\Delta(J) = 4 + 2n + J + \gamma_{\tau=4+2n,J}^{(\text{sugra})}$ . Note that in our normalization  $a_{\tau=4+2n,-1}^{(0)} \sim O(c)$ , see (5.260), whereas  $\gamma_{\tau=4+2n,-1}^{(\text{sugra})} \sim O(\frac{1}{c})$ . After an appropriate overall rescaling related to the normalization of the conformal blocks the coefficients in the celestial block expansion (5.328) and (5.329) coincide with the analytic continuation of the OPE data worked out in [62] to  $J = -1$ .

The result (5.328) already satisfies Ward identities (5.233) and (5.234), so we do not need to add any distributional terms at  $\zeta = 0$  or  $\zeta = 1$ . Let us now check this using the light-ray OPE. Using (5.327) and formulas from 5.6.2 we find for the distributional terms at  $\zeta = 0$

$$\begin{aligned} & - \text{res}_{\Delta=3} C(\Delta, -1) \widehat{f}_3(\zeta) - \text{res}_{\Delta=5} C(\Delta, -1) \widehat{f}_5(\zeta) + \xi(\zeta) \\ &= \frac{1}{16\pi^4} (4\pi^4 \delta'(\zeta) - 2\pi^4 \delta(\zeta)) - \frac{3}{64\pi^4} 8\pi^4 \delta(\zeta) + \xi(\zeta) \\ &= \frac{1}{4} (\delta'(\zeta) - 2\delta(\zeta)) + \xi(\zeta) = 0. \end{aligned} \tag{5.330}$$

Similarly, to probe distributional terms at  $\zeta = 1$  we consider  $\int_0^1 d\zeta \zeta^N \mathcal{F}^{(\text{sugra})}(\zeta)$  and evaluate the integral over  $\Delta$ . The result is that distributional terms are absent.

To summarize, the complete strong coupling result takes the form

$$\mathcal{F}_{\mathcal{E}}^{(\text{sugra})}(\zeta) = \frac{1}{2}. \tag{5.331}$$

### 5.7.9 Comments on supergravity at one loop

Recently, the function  $G^{(105)}(u, v)$  was also computed at strong coupling to the  $\frac{1}{N^4}$  order [256], see also [62, 257, 258]. It corresponds to a one-loop computation in supergravity. It is therefore natural to ask if we can use it to compute the corresponding correction to the two-point energy correlator. As discussed in chapter 4, the existence of the two-point energy correlator is guaranteed in the non-perturbative theory as well as in the planar theory. This, however, does not have to be the case in  $\frac{1}{N^2}$  perturbation theory. Indeed, in this case the Regge behavior of the correlation function becomes more and more singular and the condition for the existence of the energy correlator  $J_0 < 3$  can be violated (here  $J_0$  is the Regge intercept of the correlator).

At infinite 't Hooft coupling and order  $\frac{1}{N^4}$ , we have  $J_0 = 3$  and thus the energy correlator becomes ill-defined. In other words, to compute it we have to first re-sum  $\frac{1}{N^2}$  corrections before doing the light transforms and taking the coincident limit, see chapter 4. It is very easy to see the manifestation of the problem at the level of the OPE as well. If we are to try to evaluate corrections to the spectrum at  $J = -1$  as we did above in section (5.7.5) we find a pole in  $\langle a_{\tau, -1}[\gamma_{\tau, -1}]^2 \rangle$ , see e.g. (3.15) in [62]. It is an interesting question how to compute subleading large  $N$  corrections to the energy correlator. We leave this question for the future.

### 5.7.10 Multi-point event shapes

It is also interesting to consider higher-point event shapes. To our knowledge, the only higher-point event shapes available in the literature are the ones due to Hofman and Maldacena [31] for planar  $\mathcal{N} = 4$  SYM at strong coupling. In principle, higher-point event shapes can be computed via repeated light-ray OPEs, in the same way that correlation functions of local operators can be computed by repeated local OPEs. (Alternatively, we can use the  $t$ -channel block decomposition introduced in chapter 4.) Although we have not developed the formalism for taking OPEs of completely general light-ray operators in this work, it is reasonable to conjecture that the light-ray OPE closes on the light-ray operators of [28]. This is already enough information to make nontrivial predictions about the small-angle limit of multi-point event shapes.

As a simplest nontrivial example, consider a three-point event shape of null-integrated scalars. We assume that the Regge behavior of the theory is such that the event shape

exists, and the null-integrated scalars commute. By taking consecutive OPEs, we have

$$\begin{aligned} \mathbf{L}[\phi_1](\vec{y}_1)\mathbf{L}[\phi_2](\vec{y}_2)\mathbf{L}[\phi_3](\vec{y}_3) &= \sum_i \mathcal{C}_{\Delta_i-1}(\vec{y}_{12}, \partial_{\vec{y}_2})\mathbb{O}_{i,-1}^+(\vec{y}_2)\mathbf{L}[\phi_3](\vec{y}_3) \\ &= \sum_{i,j} \mathcal{C}_{\Delta_i-1}(\vec{y}_{12}, \partial_{\vec{y}_2})\mathcal{C}_{\Delta_j-1}(\vec{y}_{23}, \partial_{\vec{y}_3})\mathbb{O}_{j,-2}^+(\vec{y}_3), \end{aligned} \quad (5.332)$$

where for simplicity we have ignored transverse spins in the second OPE and we are dropping overall constants. We have also abused notation and written the light-ray operators as a function of the transverse position  $\vec{y}$ , as opposed to  $x, z$  used in most of this work.

Inserting the above expression into an event shape, we obtain a sum of multi-point celestial blocks (which would be interesting to compute explicitly). In the limit  $|\vec{y}_{12}| \ll |\vec{y}_{23}| \ll 1$ , the product of operators is dominated by the lightest-dimension terms in each OPE

$$\begin{aligned} \lim_{\vec{y}_{23} \rightarrow 0} \lim_{\vec{y}_{12} \rightarrow 0} \mathbf{L}[\phi_1](\vec{y}_1)\mathbf{L}[\phi_2](\vec{y}_2)\mathbf{L}[\phi_3](\vec{y}_3) \\ \propto |\vec{y}_{12}|^{\Delta_{-1}^+ - \Delta_1 - \Delta_2 + 1} |\vec{y}_{23}|^{\Delta_{-2}^+ - \Delta_{-1}^+ - \Delta_3 + 1} \mathbb{O}_{\text{lightest}, -2}^+(\vec{y}_1), \end{aligned} \quad (5.333)$$

where  $\Delta_{-1}^+$  and  $\Delta_{-2}^+$  represent the lightest dimensions at spin  $-1$  and  $-2$ .

Similarly, we can take repeated OPE limits of an arbitrary number of scalar light-ray operators (assuming their products exist). This leads to a very simple formula for the multi-collinear limit of scalar event shapes

$$\begin{aligned} \lim_{\theta_{1k} \rightarrow 0} \cdots \lim_{\theta_{12} \rightarrow 0} \langle \mathbf{L}[\phi_1](\infty, z_1) \cdots \mathbf{L}[\phi_k](\infty, z_k) \rangle_{\psi(p)} \\ \propto |\theta_{1k}|^{\Delta_{1-k}^+ - \Delta_{2-k}^+ - (\Delta_k - 1)} \cdots |\theta_{12}|^{\Delta_{-1}^+ - \Delta_1 - \Delta_2 + 1}, \end{aligned} \quad (5.334)$$

where we have suppressed subleading terms and an overall proportionality constant that does not depend on relative angles.

Of course, a more physically interesting case is to consider multi-point energy correlators. A difference compared to the scalar case is that the OPE of ANEC operators contains light-ray operators transforming nontrivially under  $\text{SO}(d-2)$  (except for  $d=3$ ), see (5.149) and [31]. Let us ignore this for the moment. Repeated OPEs give

$$\lim_{\theta_{1k} \rightarrow 0} \cdots \lim_{\theta_{12} \rightarrow 0} \langle \mathcal{E}(z_1) \cdots \mathcal{E}(z_k) \rangle_{\psi(p)} \propto |\theta_{1k}|^{\tau_{k+1}^+ - \tau_k^+ + 2 - d} \cdots |\theta_{12}|^{\tau_3^+ + 4 - 2d}. \quad (5.335)$$

Here  $\tau_J^+$  represents the leading twist at spin  $J$ . When operators transform nontrivially under  $\text{SO}(d-2)$ , the overall scaling with respect to the corresponding small angle will not change — it will still be controlled by the minimal twist [31].

A fascinating property of repeated ANEC OPEs is that alternating steps are controlled by local operators. Specifically, after a single OPE, we obtain light-ray operators with even signature and spin 3. After taking an additional OPE with an ANEC operator, we obtain light-ray operators with even signature and spin 4. These are the quantum numbers of a light-transformed local operator. We expect that arguments like the ones in sections 5.4.1 and 5.4.2 establish that the resulting operator is indeed the light-transform of a local spin-4 operator. Thus, the structure of the light-ray OPE is<sup>45</sup>

$$\begin{aligned} \mathbf{L}[\text{local}] \times \mathbf{L}[\text{local}] &\sim (\text{nonlocal}) \\ (\text{nonlocal}) \times \mathbf{L}[\text{local}] &\sim \mathbf{L}[\text{local}]. \end{aligned} \tag{5.336}$$

We have already determined the form of the first line above. To understand OPEs for multi-point event shapes, it suffices to understand the second line.

## 5.8 Discussion and future directions

### 5.8.1 Generalizations

In this work, we derived an OPE for a product of null-integrated operators on the same null plane. There are several possible generalizations that would be interesting to consider.

One possibility is to derive OPEs of more general continuous-spin light-ray operators [28]. Such an OPE would enable repeated OPEs in multi-point event shapes. For example, a three-point energy correlator could be computed by applying the OPE in this paper to merge two ANEC operators into spin-3 light-ray operators, followed by a generalized OPE with the remaining ANEC operator to produce spin-4 light-ray operators. From symmetries, a multi-point OPE of  $n$  ANEC operators will produce light-ray operators with spin  $n + 1$ . The average null energy condition implies positivity of the leading light-ray operator in this product, which is presumably the lowest-twist light-ray operator with spin  $n + 1$ .<sup>46</sup> This gives an alternative derivation of the higher-even-spin ANEC [210] that additionally includes the case of odd spins, but is not as general as the continuous spin version in [28].

A possible application of repeated OPEs for multi-point event shapes is to set up a bootstrap program for event shapes similar to the bootstrap program for four-point

<sup>45</sup>In writing (5.336), we assumed that the nonlocal spin-3 operators that appear in the OPE of two ANEC operators commute with the ANEC operator. This is consistent with the fact that  $[\mathcal{E}(z_1)\mathcal{E}(z_2), \mathcal{E}(z_3)] = 0$ .

<sup>46</sup>We thank Clay Córdova for discussions on this point.

functions of local operators [9, 10].<sup>47</sup> Specifically, one could demand that the light-ray OPE is associative and use this condition to study the space of possible event shapes abstractly. One can also consider mixed light-ray and  $t$ -channel OPEs of the type discussed in chapter 4. With sufficient positivity conditions, perhaps one could apply numerical bootstrap techniques [11, 39, 54]. Even without deriving the details of the generalized light-ray OPE, it is reasonable to conjecture that it closes on the light-ray operators of [28], and thus multi-point event shapes should admit an expansion in multi-point celestial blocks (which would be interesting to compute).

A surprising property of the light-ray OPE is boundedness in transverse spin, i.e. in spin on the celestial sphere. This is a vast simplification compared to the naïve expectation that a product of point-like objects on the celestial sphere might result in arbitrarily high spin on the celestial sphere. Boundedness in transverse spin is a strong constraint on event shapes that would be interesting to test either analytically or experimentally. It also might have implications for the multi-point event-shape bootstrap. In the bootstrap of local operators, the presence of unbounded spin is important for associativity of the operator algebra [13–17, 20, 23]. It would be interesting to understand how this works for the light-ray OPE.

It would also be interesting to study OPEs of other types of null-integrated operators, such as those studied in [153, 154]. As explained in chapter 4, these can be viewed as descendants of light-transformed operators  $\mathbf{L}[\mathcal{O}]$ . Consider two such descendants inserted at the same point, say  $x = 0$ ,

$$(P^{k_1}\mathbf{L}[\mathcal{O}_1])(0, z_1)(P^{k_2}\mathbf{L}[\mathcal{O}_2])(0, z_2), \quad (5.337)$$

where we denoted the descendants schematically by  $P^{k_i}\mathbf{L}[\mathcal{O}_i]$  and suppressed polarizations associated to  $P$ . Acting on this with  $K^{k_1+k_2+1}$  we get 0, and so we must conclude that this product has an expansion in terms of descendants of light-ray operators at level at most  $k_1 + k_2$ . A conformally-invariant way to think about descendants  $P^{k_i}\mathbf{L}[\mathcal{O}_i]$  is in terms of weight-shifting operators [186, 214]. It is likely that the derivation of the light-ray OPE in this paper can be dressed appropriately with weight-shifting operators using methods described in [28, 186].

Another generalization is to allow null-integrated operators to be on different null planes that approach each other. It should still be possible to relate matrix elements of such a product to the Lorentzian inversion formula. We expect that light-ray operators with spin other than  $J_1 + J_2 - 1$  would appear.

---

<sup>47</sup>We discuss a different kind of bootstrap program for event shapes in the next subsection.

In chapter 4, we introduced shock amplitudes, which describe the flat-space limit of the bulk dual of a null-integrated operator. In theories with bounded Regge growth, it should be possible to analytically continue shock amplitudes in spin, giving a vast generalization of the amplitudes usually considered. This work suggests a simple way to partially achieve this generalization: one can take coincident limits of shock particles to produce other types of shocks with different (integer) spin. For example, a coincident limit of shock gravitons produces a spin-3 “stringy” shock, as studied by Hofman and Maldacena [31].

A more speculative possible direction is to derive a nonperturbative OPE for amplitudes, describing a convergent expansion around the collinear limit. Such an OPE expansion exists in planar  $\mathcal{N} = 4$  [259–264], relying on special properties of the theory like amplitude-Wilson-loop duality and integrability; it would be nice to generalize to a generic CFT. (Presumably, this would also require finding a good nonperturbative definition of an amplitude in a generic CFT.) Perhaps the conformal basis [265, 266] could be helpful for this. The soft limit of an external particle should correspond to the insertion of a null-integrated operator, so perhaps the hypothetical amplitudes OPE would be related to the light-ray OPE in this limit.

### 5.8.2 More applications to event shapes

It would be interesting to understand whether the light-ray OPE can be applied to asymptotically-free theories like QCD. The small angle behavior of the EEC in QCD was analyzed in [267]. A more general factorization formula describing the collinear limit  $\zeta \rightarrow 0$  and applicable to any weakly coupled gauge theory was derived in [220]. The energy-energy correlator (EEC) in QCD was recently computed at 2 loops (NLO) for arbitrary  $\zeta$  [208, 268]. The light-ray OPE gives a way to resum large logarithms using symmetries as opposed to RG equations. The celestial block expansion is ultimately a consequence of Lorentz symmetry, which is still present when conformal symmetry is broken. Thus, event shapes in any theory should admit a celestial block expansion. However, when dilatation symmetry is broken, the selection rule  $J = J_1 + J_2 - 1$  will no longer hold. Thus, we expect the celestial block expansion in asymptotically-free theories to involve light-ray operators with spin other than 3.<sup>48</sup>

In [31], it was shown how to relate the EEC to spin-3 moments of PDFs. Because these spin-3 moments compute matrix elements of spin-3 light-ray operators, it is natural to guess that spin- $J$  moments of PDFs for general  $J \in \mathbb{C}$  compute matrix

---

<sup>48</sup>We thank Ian Moutl for discussions on this point.

elements of general spin- $J$  light-ray operators.<sup>49</sup> It would be interesting to derive this connection directly.

The celestial block expansion suggests a way of “perturbatively bootstrapping” the EEC in the same sense as the perturbative bootstrap for amplitudes and Wilson loops in  $\mathcal{N} = 4$  SYM [269–275]. The idea of the perturbative bootstrap is to guess a basis of functions for the answer at some loop order (for example, by guessing the symbol alphabet). One then imposes consistency conditions to fix the coefficients in this basis. In the case of amplitudes in  $\mathcal{N} = 4$ , this program has been wildly successful, for example resulting in expressions for the 6-point gluon amplitude up to 7 loops [276]. There, consistency with the OPE for amplitudes [259–264] and data from integrability provide powerful constraints. The celestial block expansion can provide analogous constraints for the EEC. Furthermore, in chapter 4, we gave a different expansion for the EEC in terms of “ $t$ -channel blocks.” OPE data from integrability can be used in either channel to make predictions that could help bootstrap the EEC.

An important ingredient in the perturbative bootstrap is the presence of contact terms in perturbative event shapes at  $\zeta = 0$  and  $\zeta = 1$ . Because of Ward identities, the coefficients of contact terms serve as a check on the entire event shape. The light-ray OPE gives a systematic way to compute contact terms at  $\zeta = 0$ . Furthermore, it provides a connection between the  $\zeta = 0$  contact term at  $L$  loops and the leading non-contact term as  $\zeta \rightarrow 0$  at  $L + 1$  loops.<sup>50</sup>

It would also be interesting to understand event shapes in  $\mathcal{N} = 4$  SYM in a systematic expansion in  $1/\lambda$  and  $1/N$ . The leading  $1/\lambda$  corrections to energy-energy correlators were computed in [31], see also [104]. They take the form of a finite sum of the  $t$ -channel event-shape blocks defined in chapter 4. This suggests that  $t$ -channel blocks could be simple ingredients for setting up a perturbative expansion in  $1/\lambda$ . One advantage of the  $t$ -channel expansion is the absence of contributions from double-trace operators in the planar limit. (By contrast, the light-ray OPE discussed in this paper gets contributions from both single- and double-trace operators.) The extreme simplicity of the  $1/\lambda$  corrections in [31] stems from the fact that the string shockwave

---

<sup>49</sup>We thank Juan Maldacena and Aneesh Manohar for making this suggestion, and Ian Mould and Cyuan Han Chang for discussions.

<sup>50</sup>Meanwhile, the back-to-back expansion (D.85) provides a description of contact terms and leading non-contact terms at  $\zeta = 1$ , given knowledge of the hard function  $H(a)$  and cusp/collinear anomalous dimensions. Given this, one could imagine a poor-man’s version of the perturbative bootstrap, where one uses contact terms at  $L$  loops to predict leading non-contact terms at  $L + 1$  loops, fits the leading non-contact terms to a simple ansatz, integrates the ansatz to obtain contact terms at  $L + 1$  loops, and repeats.



$S$ -matrix, expanded to leading order in  $\alpha'$ , only mixes adjacent levels on the string worldsheet, see e.g. chapter 4.

The problem of developing a  $1/N$  expansion at large  $\lambda$  is conceptually interesting because the condition  $J_0 < 3$  for the event shape to be well-defined is violated in naïve  $1/N$  perturbation theory. To study  $1/N$  corrections, it will be necessary to re-sum the four-point function in the Regge regime.

### 5.8.3 Other applications and future directions

Null-integrated operators arise naturally in information-theoretic quantities in quantum field theory. For example, the full modular Hamiltonian in the vacuum state of a region bounded by a cut  $v = f(\vec{y})$  of the null plane  $u = 0$  is [153]

$$\begin{aligned} H_f &= 2\pi(K - P_f), \\ P_f &= \int d^{d-2}\vec{y} f(\vec{y}) \int_{-\infty}^{\infty} dv T_{vv}(u = 0, v, \vec{y}) = \int d^{d-2}\vec{y} f(\vec{y}) \mathbf{L}[T](\vec{y}), \end{aligned} \quad (5.338)$$

where  $K$  is the generator of a boost in the  $u$ - $v$  plane. Here, we have abused notation and written  $\mathbf{L}[T]$  as a function of the transverse position  $\vec{y}$ , instead of the usual arguments  $x, z$ .

The vacuum modular flow operator is  $U_f(s) = e^{-isH_f}$ . It is interesting to ask how  $U_f$  changes as we deform the cut  $f(\vec{y}) \rightarrow f(\vec{y}) + \delta f(\vec{y})$ . Because the ANEC operator  $\mathbf{L}[T]$  appears in the modular Hamiltonian, we can use the algebra of  $K$  and  $P_f$  together with the light-ray OPE to do perturbation theory in  $\delta f(\vec{y})$ :

$$\begin{aligned} U_{f+\delta f}(s)U_f(-s) &= \exp\left(-\frac{i}{2\pi}(e^{2\pi s} - 1)(H_{f+\delta f} - H_f)\right) \\ &= \exp\left(it \int d^{d-2}\vec{y} \delta f(\vec{y}) \mathbf{L}[T](\vec{y})\right) \\ &= 1 + it \int d^{d-2}\vec{y} \delta f(\vec{y}) \mathbf{L}[T](\vec{y}) \\ &\quad - (-i\pi) \frac{t^2}{2} \sum_i \int d^{d-2}\vec{y}_1 d^{d-2}\vec{y}_2 \delta f(\vec{y}_1) \delta f(\vec{y}_2) \mathcal{C}_{\Delta_i-1}(\vec{y}_{12}, \partial_{\vec{y}_2}) \mathbb{O}_{i,J=3}(\vec{y}) \\ &\quad + \dots, \end{aligned} \quad (5.339)$$

where  $t = e^{2\pi s} - 1$ . Similarly, at  $n$ -th order in  $\delta f$ , light-ray operators with spin  $J = n + 1$  will appear. The expression (5.339) gives a direct connection between the spectrum of a CFT and the shape dependence of the vacuum modular flow operator. It may be useful for understanding aspects of the quantum null energy condition (QNEC)

[209, 277–279]. Furthermore, it would be interesting to see whether it (or other manifestations of the light-ray OPE) has implications for bulk locality in holographic theories.

It would also be interesting to study the light-ray OPE for strongly-coupled theories like the 3d Ising model. With enough CFT data, it may be possible to compute event shapes and study modular flow quantitatively in this theory.

Particle colliders like the LHC have given us a wealth of data on event shapes in the Standard Model. In principle, it should be possible to measure event shapes in condensed matter systems using a tabletop collider. One must prepare a material in a state described by a QFT, excite it at a point, and measure the pattern of excitations on the boundary of the material. Several quantum critical points have both Euclidean and Lorentzian avatars in the laboratory. Traditionally, the most precise measurements are available for the Euclidean avatars, in the form of scaling dimensions of low-dimension operators. Event shapes for these systems could reveal intrinsically Lorentzian dynamics that would otherwise remain deeply hidden in the Euclidean measurements.

Finally, it could be interesting to study event shapes in gravitational theories in an asymptotically flat spacetime, see e.g. [280] and references therein.<sup>51</sup> In this case, physical measurements are performed at the future null infinity  $\mathcal{I}^+$ . As in a particle collider experiment, one can measure energy flux through the celestial sphere created in a gravitational collision. In addition to energy carried away by matter fields, there is a contribution due to gravity waves  $\mathcal{E}(\vec{n}) \sim \int_{\mathcal{I}^+} \text{News}^2$  which is quadratic in the so-called news tensor. In a gravitational theory, however, it is also natural to consider light-ray operators that are linear in the metric, similar to the ones measured in the current gravitational wave experiments. One such example is a memory light-ray operator  $\mathcal{M}(\vec{n}) \sim \int_{\mathcal{I}^+} \text{News}$  which measures the memory effect on the celestial sphere. As in the main body of the paper, we can consider multi-point gravitational event shapes and possibly study the corresponding light-ray OPE. One appealing feature of these observables is that they are IR safe — in other words all IR divergencies that arise in the computations of scattering amplitudes should cancel in the event shapes. BMS symmetry [281] and familiar soft theorems [282] should become statements that relate different gravitational event shapes.<sup>52</sup>

<sup>51</sup>The same comment applies to electromagnetism.

<sup>52</sup>For example, an integral of the energy flux operator over the celestial sphere is related to the insertion of the memory operator [283].

## Acknowledgements

We thank Mikhail Alfimov, Cyuan Han Chang, Clay Córdova, Lance Dixon, Claude Duhr, Tom Faulkner, Tom Hartman, Johannes Henn, Gregory Korchemsky, Adam Levine, Juan Maldacena, Ian Moulton, Gavin Salam, Amit Sever, Emery Sokatchev, and Kai Yan for discussions. We thank Lance Dixon, Ian Moulton, and Hua Xing Zhu for sharing a draft of their work before publication [220]. We also thank Gregory Korchemsky for sharing a draft of his work before publication [219]. We thank Nikolay Gromov for producing and sharing with us figure 5.14. DSD is supported by Simons Foundation grant 488657 (Simons Collaboration on the Nonperturbative Bootstrap), a Sloan Research Fellowship, and a DOE Early Career Award under grant No. DE-SC0019085. PK is supported by DOE grant No. DE-SC0009988. This research was supported in part by the National Science Foundation under Grant No. NSF PHY-1748958.

## QUANTUM VACUA OF 2D MAXIMALLY SUPERSYMMETRIC YANG-MILLS THEORY

<sup>1</sup>M. Koloğlu, “Quantum Vacua of 2d Maximally Supersymmetric Yang-Mills Theory”, *Journal of High Energy Physics* **11**, 140 (2017) [10.1007/JHEP11\(2017\)140](https://arxiv.org/abs/1609.08232), [arXiv:1609.08232](https://arxiv.org/abs/1609.08232) [[hep-th](#)].

### 6.1 Introduction and summary

Supersymmetric Yang-Mills theories (SYM) have been of central interest in string theory, especially since the advent of D-branes. In Type II string theories, the world-volume interactions of BPS  $Dp$ -branes at low energies are described by maximally supersymmetric Yang-Mills theories in  $(p + 1)$ -dimensions ( $\text{MSYM}_{p+1}$ ). These theories have 16 supersymmetries, inherited from the target-space supersymmetries left unbroken by the half-BPS D-branes. For a stack of  $N$  D-branes, the gauge group of the  $\text{MSYM}$  is  $U(N)$ . The gauge field arises from the open strings that stretch between pairs of branes, which carry  $U(N)$  Chan-Paton factors when the branes are coincident. The gauge theory is enhanced by the higher-form gauge fields and fluxes present in the string theory target space, which generalize the topological sectors of the theory. Properties of these gauge theories are intimately related to the interactions of D-branes. For example, topological sectors of the gauge theory are interpreted as the bound states of the branes with other objects in the string theory, including other D-branes of various dimensions and the fundamental string [284]. In fact, an entire non-perturbative formulation of M-theory was conjectured to arise from the  $N \rightarrow \infty$  limit of the  $\mathcal{N} = 16$  quantum mechanics  $\text{MSYM}_1$  describing the interactions of D0-branes [285].

In this article, we will focus on the two-dimensional (2d)  $\text{MSYM}$  theories with gauge group  $U(N)$  or  $SU(N)$ . In two dimensions, the weakly coupled gauge theory defined by the SYM Lagrangian is inherently the ultraviolet (UV) description, and such theories are asymptotically free. In the infrared (IR), the theory becomes strongly coupled. It is a difficult and interesting question to understand the infrared dynamics of  $\text{MSYM}_2$ . Both of the closely related theories with  $U(N)$  and  $SU(N)$  gauge group have been extensively analyzed, and much has been conjectured about their infrared description and quantum vacua [284, 286–289]. For example, in [286, 287],  $U(N)$

MSYM<sub>2</sub> theory was developed into matrix string theory, describing matrix theory compactified on a circle. It was proposed that the  $N \rightarrow \infty$  limit of this theory should provide a non-perturbative formulation of Type IIA string theory. Using M-theory and string duality considerations, the authors of [286] related the IR limit of MSYM<sub>2</sub> with gauge group  $U(N)$  to the supersymmetric sigma model into the symmetric orbifold  $\text{Sym}^N \mathbb{R}^8$ , identified as the sector of second quantized free Type IIA strings with light-cone momentum  $p_+ = N$ . However, exact computations or quantitative evidence have been elusive — a situation we seek to remedy.

The Lagrangian of MSYM<sub>2</sub> can be obtained by dimensional reduction from 10d  $\mathcal{N} = 1$  SYM, and for  $U(N)$  or  $SU(N)$  gauge group it is given by [286, 289]

$$\mathcal{L} = \text{Tr} \left( -\frac{1}{4} F_{\mu\nu}^2 - \frac{1}{2} (D_\mu X^i)^2 + i \chi^T \not{D} \chi + \frac{g^2}{4} [X^i, X^j]^2 - \sqrt{2} g \chi_L^T \gamma_i [X^i, \chi_R] \right). \quad (6.1)$$

The bosons  $X^i$ , the left-moving fermions  $\chi_L^\alpha$ , and the right moving fermions  $\chi_R^\alpha$  are in the  $\mathbf{8}_v$ ,  $\mathbf{8}_c$ , and  $\mathbf{8}_s$  representations, respectively, of the  $Spin(8)$  R-symmetry. The fields are also in the adjoint representation of the gauge group, so they are valued in  $\mathfrak{u}(N)$  ( $\mathfrak{su}(N)$ ) and can be realized as  $N \times N$  (traceless) Hermitian matrices for gauge group  $U(N)$  ( $SU(N)$ ). The theory has  $\mathcal{N} = (8, 8)$  supersymmetry generated by the transformations with 16 fermionic parameters ( $\epsilon_L^\alpha, \epsilon_R^\alpha$ ). We take the worldsheet directions to be  $\mu = 0, 9$ . The dimensional reduction of the Lagrangian and the supersymmetry transformations are reproduced in Appendix E.1.1.

The MSYM<sub>2</sub> theory was observed to have classical vacua determined by the zeroes of the bosonic potential  $V(X) = \frac{g^2}{4} [X^i, X^j]^2$ , which are commuting matrices  $X^i$ , modulo the Weyl group  $\mathbb{S}_N$  permuting the eigenvalues [284, 286]. For the  $U(N)$  theory on the worldsheet  $\mathbb{R}_t \times S^1$ , all the zero-energy configurations of the gauge field correspond to flat connections on the trivial  $U(N)$ -principal bundle, so in the quantum  $U(N)$  theory, the gauge field contributes a single trivial zero-energy state to the vacuum wavefunction, as elaborated in [290]. Therefore, it seems natural to conjecture that in the infrared limit, as  $g \rightarrow \infty$ , the theory flows to the supersymmetric sigma model into  $\text{Sym}^N(\mathbb{R}^8)$ , parametrized by the  $N$  eigenvalues of the  $X^i$  and fermionic partners [286]. Similar arguments could be made for the  $SU(N)$  theory, by removing the contributions for the free diagonal  $U(1)$  factor of the  $U(N)$  theory, leading to the supersymmetric sigma model into  $(\mathbb{R}^8)^{N-1}/\mathbb{S}_N$  as the conjectural IR limit.

However, this is not all of the vacua and therefore not the end of the story. In his analysis of bound states of fundamental strings and D-branes in Type II string theories, Witten [284] argued that the existence of  $(M, N)$ -string bound states in

Type IIB string theory requires the existence of various supersymmetric vacua for the  $SU(N)$   $\text{MSYM}_2$ . For the worldvolume theory of  $N$  D1-branes, the sector with  $M$  bound fundamental strings corresponds to a “charge at infinity” in the form of a Wilson loop in the  $M$ th tensor power of the fundamental representation of  $SU(N)$  [284]. Therefore, the  $(M, N)$ -string is naturally a superselection sector in the 2d quantum theory, and the vacuum in that sector is identified as the discrete  $\theta$  vacuum [291] (of the related  $SU(N)/\mathbb{Z}_N$  theory) with  $\theta$  angle specified by  $M \pmod{N}$  as

$$e^{i\theta} = e^{i\frac{2\pi M}{N}}. \quad (6.2)$$

Specifically, Witten argued that the case when  $M$  and  $N$  are relatively prime should correspond to a single supersymmetric vacuum of the  $SU(N)$  theory with a mass gap. This is because the center-of-mass motion of the branes decouples from the  $U(N)$  worldvolume theory as a free  $\mathcal{N} = (8, 8)$   $U(1)$  vector multiplet, corresponding to the determinant  $U(1)$  in  $U(N)$  (which decomposes as  $U(N) = (U(1) \times SU(N))/\mathbb{Z}_N$ ). In the case with  $M$  and  $N$  relatively prime, the center-of-mass dynamics encoded in the decoupled  $U(1)$  multiplet correspond to all of the massless physical degrees of freedom of the bound state in the string theory target space.

In the more general case when  $M$  and  $N$  are not relatively prime, Witten reasoned that there is no argument to indicate the corresponding vacuum should be massive. In fact, the  $(M, N)$ -string should be able to split up into  $D$  many  $(M/D, N/D)$ -string bound states without an energy barrier, where  $D = \text{gcd}(M, N)$ , as the eigenvalues of the scalars corresponding to the relative positions of these  $(M/D, N/D)$ -strings can take arbitrary expectation values at no cost in energy. It is then natural to expect that the vacuum corresponding to the  $(M, N)$ -string with  $D > 1$  should have massless excitations corresponding to the massless degrees of freedom of the relative motion of the  $(M/D, N/D)$ -strings. The relative positions of these bound states is just the configuration space of  $D$  indistinguishable strings in the transverse space  $\mathbb{R}^8$ , with the center-of-mass moduli excluded, which is described by the 2d symmetric-orbifold sigma model into  $(\mathbb{R}^8)^{D-1}/\mathbb{S}_D$ .

We would like to analyze the classical and the quantum theory, and determine to what extent these predictions hold. The main feature of the  $\text{MSYM}_2$  theory which gives rise to some important subtleties is that all the local fields are in the adjoint representation of the gauge group  $G$ . In particular, if  $G$  has a nontrivial center  $Z(G)$ , then there are no fields charged under it, so the  $Z(G)$  charge cannot be screened, giving rise to superselection sectors labeled by the  $Z(G)$  charge. For example, for

$G = SU(N)$ ,  $Z(G) = \mathbb{Z}_N$ , and there are  $N$  superselection sectors. Given a state in some sector, the emanation of a Wilson loop in some representation  $R$  of  $SU(N)$  with charge  $N_R$  under  $\mathbb{Z}_N$  will yield a state in another superselection sector, differing by  $N_R$  units modulo  $N$ . Since there are no fields charged under the center, we can also define the  $G/Z(G) = SU(N)/\mathbb{Z}_N$  theory that has the same Lagrangian. The  $SU(N)/\mathbb{Z}_N$  theory has the  $\theta$  angle parameter as additional discrete data, and for each of the  $N$  choices of  $\theta$ , the spectrum is a restriction of the  $SU(N)$  spectrum to one of the  $N$  superselection sectors. Likewise, one can define the  $SU(N)/\mathbb{Z}_K$  theory for  $K|N$ , which will have  $N/K$  superselection sectors with the same  $\mathbb{Z}_K \subset \mathbb{Z}_N$  charge for each of the  $K$  choices of the  $\theta$  angle.

Interestingly, when we consider the classical vacua of the  $SU(N)/\mathbb{Z}_N$  theory, we recover a spectrum consistent with the spectrum of relative positions of the  $(M/D, N/D)$ -strings. This requires analyzing the topological sectors of the theory. Let us recall that the discrete  $\theta$  vacua exist for the  $SU(N)/\mathbb{Z}_N$  theory because this gauge group has non-trivial fundamental group  $\pi_1(SU(N)/\mathbb{Z}_N) = \mathbb{Z}_N$ . Consequently, there are “instanton sectors” of the 2d theory corresponding to the topologically distinct  $SU(N)/\mathbb{Z}_N$ -principal bundles, labeled by elements in  $\pi_1(SU(N)/\mathbb{Z}_N)$  [291, 292]. We denote the  $\mathbb{Z}/N\mathbb{Z}$ -valued instanton number by  $k$ . As usual, the effect of the  $\theta$  angle in the path integral is to weigh the  $k$ -instanton sector by  $e^{i\theta k}$  in the sum over the instanton sectors. Naturally, the  $\theta$  angle takes values in the Pontryagin dual of the  $\pi_1$  of the gauge group, which is  $\mathbb{Z}_N$  once again for  $\pi_1(SU(N)/\mathbb{Z}_N) = \mathbb{Z}_N$ . The theory at a given  $\theta$  angle could be explicitly defined by including a surface operator constructed from the integral of a 2-form gauge field, as in [30]. When one puts the  $SU(N)/\mathbb{Z}_N$  theory on the two-torus  $T^2$ , the  $SU(N)/\mathbb{Z}_N$ -principal bundle  $P_{N,k}$  over  $T^2$  with instanton number  $k$  admits flat connections, with moduli space  $\mathcal{M}_{N,k}$ , so there are classical zero-energy configurations of the gauge field in each instanton sector. As all of the fields are in one  $\mathcal{N} = (8, 8)$  vector multiplet, the modes supersymmetric to the zero-energy modes of the gauge field are also classically zero-energy field configurations. The moduli space of flat connections  $\mathcal{M}_{N,k}$  turns out to have complex dimension  $d-1$ , where  $d = \gcd(k, N)$ . Thus, one expects on general supersymmetry grounds to have a  $8(d-1)$  real dimensional moduli space of vacua for the scalar fields, specifically  $(d-1)$  real moduli for the eigenvalues of each of the scalars  $X^i$ . Indeed, when  $d = 1$ ,  $\mathcal{M}_{N,k}$  is a point, and there is a single classical zero-energy field configuration with all

the scalars set to zero. When  $d > 1$ , the zero-energy scalar fields take the form

$$X^i = I_{N/d} \otimes \begin{pmatrix} x_1^i & & \\ & \ddots & \\ & & x_d^i \end{pmatrix}, \quad \text{with } \text{Tr} X^i = 0, \quad (6.3)$$

in the strong coupling limit  $g \rightarrow \infty$ , and the eigenvalues parametrize  $(\mathbb{R}^8)^{d-1}/\mathbb{S}_d$ . When  $d = N$ , we are in the trivial instanton sector with  $k = 0$ , with the classical vacua described by  $(\mathbb{R}^8)^{N-1}/\mathbb{S}_N$ , in agreement with [284, 286].

In the quantum theory, the wavefunction of a vacuum state spreads over all classical vacuum configurations, including the disconnected components. Although one expects that the quantum vacua should parallel the classical vacua in theories with high supersymmetry, one might be hesitant to reach this conclusion in our setting as it is *a priori* unclear how the sum over classical disconnected configurations reproduces the vacua wavefunctions. Nonetheless, the  $\theta$  angle isolates superselection sectors corresponding to  $(M, N)$ -strings, which have string theoretic descriptions strikingly in parallel with the classical vacua, supporting this conclusion. Here, a few relevant studies are crucial in guiding one's intuition. First of all, the  $SO(8)$  R-symmetry anomalies vanish for  $\text{MSYM}_2$  [284], so there are no anomaly arguments that rule out the existence of the various massive and massless vacua, unlike in theories with less supersymmetry. Also, in [288], it was argued that the IR description of  $\text{MSYM}_2$  could not be a non-trivial superconformal field theory with  $\mathcal{N} = (8, 8)$  supersymmetry, as there is no extension of this  $\mathcal{N} = (8, 8)$  supersymmetry algebra to a linear *superconformal* algebra [293].<sup>1</sup> This suggests that any scale invariant theories with massless excitations describing the IR fixed points should be free theories, or orbifolds thereof. Lastly, in [289],  $\text{MSYM}_2$  was analyzed using discrete light-cone quantization (DLCQ). There, numerical results were obtained in finite resolution of light-cone momentum indicating the absence of normalizable massless states and supporting the existence of a vacuum with mass gap for the  $SU(N)$  theory. By these considerations, the only possible choices for the IR limit of  $\text{MSYM}_2$  are massive vacua or orbifolds of free  $\mathcal{N} = (8, 8)$  sigma models. Given the favorable evidence, we conjecture that the quantum vacuum of the  $SU(N)/\mathbb{Z}_N$  theory with  $\theta = 2\pi M/N$  corresponding to the  $(M, N)$ -string should be described by the sigma model into  $(\mathbb{R}^8)^{D-1}/\mathbb{S}_D$ , and furthermore that the infrared fixed point of the theory with the given  $\theta$  angle is this sigma

---

<sup>1</sup>Non-linear  $\mathcal{N} = 8$  superconformal algebras have been constructed, however they are quite exceptional and do not seem to be relevant to  $\text{MSYM}_2$ . See [294] and the references therein for details.



model. We note that this description is invariant under the  $SL(2, \mathbb{Z})$  S-duality of the Type IIB string theory, which acts on the doublet  $(M, N)$  but leaves  $D$  invariant. Also, the vacua of the related  $SU(N)$  theory in one of its  $N$  superselection sectors is the vacuum of the  $SU(N)/\mathbb{Z}_N$  theory with the corresponding  $\theta$  parameter.

We provide strong evidence in favor of our claim by computing the  $\mathcal{N} = (8, 8)$  analog of the elliptic genus — or, index for short — of  $\text{MSYM}_2$  for  $SU(N)$  and  $SU(N)/\mathbb{Z}_N$  gauge group, for the latter also including the surface operator specifying the  $\theta$ -angle parameter. This index is a supersymmetric partition function on the Euclidean flat torus  $T^2$  (with conformal class  $\tau$ ), which counts states that are BPS with respect to a conjugate pair of right-moving supercharges. The choice of any such supercharge commutes with a  $Spin(6)$  subgroup of the  $Spin(8)$  R-symmetry, and we can refine the index with equivariant parameters  $a_{1,2,3} = \exp 2\pi i \xi_{1,2,3}$  coupling to the  $Spin(6)$  subgroup. This refinement keeps track of more information about the spectrum, as well as regulating the otherwise divergent sum over the infinitely many states contributed by the non-compact bosonic zero-modes. This index also agrees with the equivariant elliptic genus of the theory when viewed as a  $\mathcal{N} = (0, 2)$  supersymmetric theory — from which perspective the  $Spin(6)$  symmetry is just a flavor symmetry. Concretely, the index of an  $SU(N)/\mathbb{Z}_K$  theory is defined as the following trace in the Ramond-Ramond (RR) Hilbert space  $\mathcal{H}$  of the theory, which is a direct sum of  $K$  RR Hilbert spaces on the circle,  $\mathcal{H}_k$ , quantized in the given instanton background  $k$ :

$$\mathcal{I}^\theta(\tau|\xi) = \sum_k e^{i\theta k} \text{Tr}_{\mathcal{H}_k} (-1)^F a^f q^{H_L} \bar{q}^{H_R}. \quad (6.4)$$

Here,  $q = e^{2\pi i \tau}$ , and  $H_L$  and  $H_R$  are the left- and right-moving Hamiltonians. We show that the index of the  $SU(N)/\mathbb{Z}_N$  theory with the  $\theta(M) = 2\pi M/N$  vacuum is

$$\mathcal{I}_{SU(N)/\mathbb{Z}_N}^{\theta(M)}(\tau|\xi) = \frac{\mathcal{I}_D}{\mathcal{I}_1}(\tau|\xi), \quad (6.5)$$

where  $D = \text{gcd}(M, N)$ , and  $\mathcal{I}_D$  is the index of the supersymmetric sigma model into  $\text{Sym}^D(\mathbb{R}^8)$ . Of course, when  $D = 1$ ,  $\mathcal{I}_{SU(N)/\mathbb{Z}_N}^\theta = 1$ , which is the index of a single massive supersymmetric vacuum. When  $D > 1$ ,  $\mathcal{I}_D/\mathcal{I}_1$  is the index of the sigma model into  $(\mathbb{R}^8)^{D-1}/\mathbb{S}_D$ , since by factoring the diagonal copy of  $\mathbb{R}^8$ , we have  $\text{Sym}^D(\mathbb{R}^8) = \mathbb{R}^8 \times (\mathbb{R}^8)^{D-1}/\mathbb{S}_D$ . The expressions for  $\mathcal{I}_{SU(N)/\mathbb{Z}_N}^\theta(\tau|\xi)$  and  $\frac{\mathcal{I}_D}{\mathcal{I}_1}(\tau|\xi)$  are obtained through different methods, and it is non-trivial to show that they agree. Thankfully, both sets of functions enjoy multi-periodicity and  $SL(2, \mathbb{Z})$  modular invariance, and using these very restrictive properties we are able to establish (6.5) for  $N \leq 7$ . Since the index is an invariant of the theory under renormalization group

(RG) flow, which is furthermore a “strong” invariant in the sense that it contains data about the spectrum of the theory, matching the index computed in the UV with the index of our candidate IR fixed point is a powerful indication that the two theories are indeed related by RG flow.

From the  $SU(N)/\mathbb{Z}_N$  index, we infer the index of the  $SU(N)/\mathbb{Z}_K$  theory for any  $K|N$ ,

$$\mathcal{I}_{SU(N)/\mathbb{Z}_K}^{\theta(M)}(\tau|\xi) = \sum_{m \equiv M \pmod{K}} \frac{\mathcal{I}_{\text{gcd}(m,N)}}{\mathcal{I}_1}(\tau|\xi), \quad (6.6)$$

where the sum is over the  $N/K$  values of positive integers  $m$  between 1 and  $N$  equivalent to  $M$  modulo  $K$ . The terms being summed over are interpreted as the indices of the corresponding superselection sectors of the theory, and they are consistent with our earlier analysis of the superselection sectors.

Having understood the vacua  $SU(N)$   $\text{MSYM}_2$ , we would like to analyze the  $U(N)$  theory as well. Including the center of mass modes into our considerations of the  $SU(N)$  theory, one can readily conjecture that the  $U(N)$  theory also has vacua described by sigma models into  $\text{Sym}^D(\mathbb{R}^8)$  corresponding to the  $(M, N)$ -strings, as expected from string theory. However, the correct analysis of the full  $N$  D1-brane worldvolume theory is somewhat more complicated, and requires some discussion. For a standard 2d  $U(N)$  gauge theory with only adjoint fields, the  $U(1)$  degrees of freedom decouple, and the index of the standard  $U(N)$   $\text{MSYM}_2$  can be readily inferred from the  $SU(N)$  index as

$$\mathcal{I}_{U(N)}(\tau|\xi) = \mathcal{I}_{U(1)}\mathcal{I}_{SU(N)}(\tau|\xi) = \sum_{m=1}^N \mathcal{I}_{\text{gcd}(m,N)}(\tau|\xi). \quad (6.7)$$

But, this theory is not accurately taking into account the full structure of the  $(M, N)$ -string bound states. The true gauge theory describing the full worldvolume theory of the  $N$  D1-branes is not a standard  $U(N)$  gauge theory, but also has the Kalb-Ramond 2-form gauge field  $B$  coming from the Neveu-Schwarz (NS) sector of the string theory. The  $B$ -field has an Abelian gauge symmetry generated by a 1-form gauge transformation, under which the trace mode of the  $U(N)$ -connection  $A$  is also charged. Due to this additional 1-form gauge symmetry, the theory has generalized field content roughly described by  $U(1) \times SU(N)/\mathbb{Z}_N$  gauge bundles, and the structures of the classical and quantum vacua are different. Indeed, we find that the  $U(N)$   $\text{MSYM}_2$  with the 2-form  $B$ -field has sectors corresponding to the  $(M, N)$ -strings as sought. The  $M$ th sector has a net  $U(1)$  generalized electric flux of  $M$  units, which is interpreted as the flux of the  $M$  F-strings, as well as a  $\theta$  angle  $2\pi M/N$  in the  $SU(N)/\mathbb{Z}_N$  sector.

When  $M = 0$ , the net flux is zero, with correspondingly zero Yang-Mills energy, so the index is readily interpreted as

$$\mathcal{I}_{U(N)+B}^{M=0}(\tau|\xi) = \mathcal{I}_{U(1)}\mathcal{I}_{SU(N)/\mathbb{Z}_N}^{\theta=0}(\tau|\xi) = \mathcal{I}_N(\tau|\xi). \quad (6.8)$$

What about the other sectors with  $M \neq 0$ ? Although the bundles with non-zero field strength have non-zero Yang-Mills action, these  $(M, N)$ -string configurations are still half-BPS in the the string theory target space, and must still preserve 16 supersymmetries! Explicitly, the D1-brane worldvolume theory has non-linearly realized supersymmetries acting on the  $U(1)$  center of mass modes, which are the goldstinos of the spontaneously broken translation symmetry in the presence of the D-branes [295–297]. The action or energy of this flux should be considered as part of the binding energy of the  $(M, N)$ -string, or as the difference in the central charge of the two BPS sectors of the target-space supersymmetry algebra. The binding energy should be attributed to the DBI action [298] in the same sense as the tension of the  $N$  D1-branes is, and should be excluded from the vacuum describing the fluctuations of the bound state. In particular, we can modify the definition of the elliptic genus to count states that are BPS with respect to the supercharges preserved by the bound state, essentially by shifting the Hamiltonian by the central charge of the superalgebra. The corresponding BPS states are exactly the configurations with fixed electric flux  $M$  and minimal energy. Since the  $U(1)$  factor is free, the fields that contribute to the index are unaffected by this modification. Thus, we obtain the index of the  $U(N)$  theory for given sector with  $M$  units of electric flux,

$$\mathcal{I}_{U(N)+B}^M(\tau|\xi) = \mathcal{I}_D(\tau|\xi). \quad (6.9)$$

This strongly suggests that the vacuum describing the massless fluctuations of the  $(M, N)$ -string is given by the sigma model into  $\text{Sym}^D\mathbb{R}^8$ . Moreover, we also construct the index of the  $U(N) + B$  theory that sums over each  $(M, N)$ -string BPS sector, which is naturally refined by the  $U(1)$  holonomies of the  $B$ -field on the spacetime torus  $e^{iM\phi} = e^{iM \int_{T^2} B}$  with representations labeled by the F1-string winding number  $M$ ,

$$\mathcal{I}_{U(N)+B}(\tau|\xi) = \sum_{M \in \mathbb{Z}} e^{iM\phi} \mathcal{I}_{U(N)+B}^M(\tau|\xi) = \sum_{M \in \mathbb{Z}} e^{iM\phi} \mathcal{I}_D(\tau|\xi). \quad (6.10)$$

We note that this D1-brane index is invariant under the S-duality of the Type IIB string, which is generated by exchanging  $M$  and  $N$  and shifting  $M$  by a multiple of  $N$ , all the while leaving  $D$  invariant. By an S-duality followed by a T-duality on the circle wrapped by the D-string, the  $(M, N)$ -string is mapped to  $N$  F-strings bound

to  $M$  D0-branes [286]. Thus, the index (6.10) is also an index of the  $N$  Type IIA F-strings bound to D0-branes. Our result suggests that the world sheet theory of  $N$  F-strings bound to  $M$  D0-branes in the free string limit  $g_s = 0$  is given by the supersymmetric sigma model into  $\text{Sym}^D \mathbb{R}^8$ , and in particular,  $N/D$  F-strings bound to  $M/D$  D0-branes behave like free strings.

The paper is organized as follows. In Section 6.2, we analyze the structure of topological sectors of  $\text{MSYM}_2$  for  $SU(N)$  and  $U(N)$  gauge group, as well as the related  $SU(N)/\mathbb{Z}_K$  and  $U(N) + B$  theories, and determine the moduli space of flat connections and the classical vacua when the spacetime is  $T^2$ . In Section 6.3 we discuss how the elliptic genus generalizes for  $SU(N)/\mathbb{Z}_N$  gauge theories to include integration over the various components of the moduli space of flat connections. In Section 6.4, we compute the elliptic genus of  $SU(N)/\mathbb{Z}_K$   $\text{MSYM}_2$ , and infer the elliptic genus for the  $U(N)$  theory with and without the  $B$  field. Finally, in Section 6.5, we compute the elliptic genus of the  $\text{Sym}^N(\mathbb{R}^8)$  sigma model, and establish some of its properties which allow us to match it to the gauge theory elliptic genus. We also include Appendix E.1, which spells out some details about the action and supersymmetry transformations of  $\text{MSYM}_2$ .

## 6.2 The structure of vacua

Bound states of D1-branes with the F-strings in Type IIB string theory suggest that the  $\text{MSYM}_2$  with  $SU(N)$  gauge group should have  $N$  superselection sectors, and that the full worldvolume theory of the  $N$  D1-branes (with  $U(N)$  gauge group) should have topological sectors labeled by  $\mathbb{Z}$  [284]. A complete description of the vacua of the  $\text{MSYM}_2$  should account for the vacua in these additional sectors as well. Therefore, we will now task ourselves with hunting for them. We will discover that a rich story underlies the various vacua.

### 6.2.1 Topological sectors

Let us start by focusing on the  $SU(N)$  theory. It was shown in [284] that on a worldsheet with boundary, such as  $\mathbb{R}^{1,1}$  for concreteness, the sector with  $M$  F-strings attached to the stack of  $N$  D1-branes manifests itself as a Wilson loop “at infinity” in the  $M$ th tensor power of the fundamental representation of the gauge group. The vacua of superselection sectors of 2d non-abelian theories have been analyzed a long time ago by Witten [291]. Since  $\text{MSYM}_2$  contains only adjoint fields, the center of the gauge group acts trivially on all fields. In particular, the net charge under the center cannot be screened by local fields. For  $G = SU(N)$ , the center is  $Z(G) = \mathbb{Z}_N$ .

Therefore, we see that the  $N$  superselection sectors in the  $SU(N)$  theory are labeled by the background  $\mathbb{Z}_N$  charge. More precisely, the theory has a  $Z(G)$  1-form global symmetry, for which the charged objects are the Wilson loops in  $SU(N)$  representations [30], and the corresponding conserved  $\mathbb{Z}_N$  charge labels the superselection sectors. The creation of a Wilson loop in representation  $R$  will act as a domain wall between two superselection sectors of  $\mathbb{Z}_N$  charge differing by the charge under the center (or  $N$ -ality)  $N_R$  of the representation.

We would like to be able to identify and isolate the vacua. This is best done if one declares the gauge group to be  $G_{adj} = SU(N)/\mathbb{Z}_N$ , which we can do since all the fields are uncharged under the  $\mathbb{Z}_N$  center. Indeed, the  $\text{MSYM}_2$  Lagrangian (6.1) with the fields taken to be valued in  $\mathfrak{su}(N)$  does not uniquely define a quantum field theory, since one can declare the gauge group to be any Lie group with Lie algebra  $\mathfrak{su}(N)$ . This choice does not affect the local physics, but determines which non-local operators and instanton sectors are present in the theory. For example, the theory with  $SU(N)$  gauge group has Wilson loops in all  $SU(N)$  representations, whereas the  $SU(N)/\mathbb{Z}_N$  theory only has Wilson loops in representations for which  $N_R \equiv 0$ , but also has surface operators which have boundary Wilson loops in arbitrary  $SU(N)$  representations (we will revisit these surface operators shortly). Moreover, because  $\pi_1(SU(N)/\mathbb{Z}_N) = Z(SU(N)) = \mathbb{Z}_N$ , the  $SU(N)/\mathbb{Z}_N$  theory has a total of  $N$  instanton sectors. When the worldsheet is  $\mathbb{R}^{1,1}$ , the instanton sectors were described in [291]. More generally, if one considers the  $SU(N)/\mathbb{Z}_N$  gauge theory on a closed Riemann surface  $\Sigma$ , the instanton sectors are the  $N$   $SU(N)/\mathbb{Z}_N$ -principal bundles on  $\Sigma$ , labeled by discrete non-abelian 't Hooft electric flux [292] — or, mathematically, the second Stiefel-Whitney class of the bundle [299]

$$w_2(P) \in H^2(\Sigma, \pi_1(G_{adj})) = H^2(\Sigma, \mathbb{Z}_N). \quad (6.11)$$

The  $G_{adj}$  theory has additional data in the form of the discrete  $\theta$  angle, which takes values in the Pontryagin dual  $\mathbb{Z}_N$  of  $\pi_1(G_{adj})$ . For each of the  $N$  choices of the  $\theta$  angle, the theory isolates a corresponding superselection sector of the  $SU(N)$  theory, and the Hilbert space is a restriction of the  $SU(N)$  Hilbert space to that sector. This structure mirrors the structure of vacua in the closely related pure Yang-Mills theories with  $SU(N)$  and  $SU(N)/\mathbb{Z}_N$  gauge group [300].

The  $SU(N)/\mathbb{Z}_N$  and  $SU(N)$  theories are of course closely related. One can obtain the  $SU(N)/\mathbb{Z}_N$  theory from the  $SU(N)$  theory by gauging the 1-form symmetry generated by the center  $\mathbb{Z}_N = Z(SU(N))$  [30]. The procedure is illuminating, as

it allows one to explicitly construct the surface operator that detects  $w_2$ . One can first enhance the  $SU(N)$  gauge field to a  $U(N)$  gauge field by adding in the trace component  $\widehat{A}$ , and then impose the  $U(1)$  1-form gauge symmetry generated by

$$\widehat{A} \rightarrow \widehat{A} - N\lambda \quad (6.12)$$

which removes the field strength for  $\widehat{A}$  and also enhances the allowed gauge bundles to  $SU(N)/\mathbb{Z}_N$  bundles. In the resulting  $SU(N)/\mathbb{Z}_N$  theory, there are no Wilson loops in representations of  $SU(N)$  that transform nontrivially under the center  $\mathbb{Z}_N$ , unless they are the boundary of a surface operator constructed from  $d\widehat{A}$ , which is now a 2-form gauge field. The closed surface operator

$$e^{iM \int_{\Sigma} d\widehat{A}/N} \quad (6.13)$$

evaluates to  $e^{i2\pi Mk/N}$  for a bundle with 't Hooft flux  $\int_{\Sigma} w_2 = k$  around the two-cycle represented by  $\Sigma$ . The integral here is schematic, as  $d\widehat{A}$  is not a globally-defined 2-form, instead one should integrate it as a Deligne-Belinson cocycle (see [30] and references therein).<sup>2</sup> This operator can be inserted into the path integral to obtain the  $SU(N)/\mathbb{Z}_N$  theory with the discrete  $\theta$  angle equal to  $2\pi M/N$ . The parameter  $M$  is quantized in integer units, as required by invariance under large gauge transformations.

Even as classical theories, the  $G$  theory and the  $G_{adj}$  theory are different. In particular, the  $G_{adj}$  theory has additional classical field configurations corresponding to connections on  $G_{adj}$ -bundles, even for those which are not  $G$ -bundles. Each of these bundles admit flat connections, so the moduli space of classical vacua of Yang-Mills theory on Riemann surfaces is enlarged to include flat connections of  $G_{adj}$ -bundles on the Riemann surface. For theories with supersymmetry, one expects zero energy field configurations supersymmetric to flat connections for the non-trivial  $G_{adj}$ -bundles. We will describe these configurations in Section 6.2.2.2, and find a pleasant parallel to the string theory predictions for the vacua.

It is perhaps good practice to say a few words about the definition of a gauge theory with gauge group  $G$  and solidify our footing. In accordance with the literature [29], we take a general  $G$ -gauge theory to satisfy the following properties:

1. All local fields are in representations of  $G$ .

---

<sup>2</sup>Heuristically, given a cover  $U_i$  of the base, the transition functions  $\lambda_{ij}$  on double overlaps and the cocycle conditions on triple overlaps of  $d\widehat{A}$  encode the same information as the 't Hooft flux of the  $SU(N)/\mathbb{Z}_N$ -bundle [30]. The integral extracts that data.

2. Wilson lines in all representations of  $G$  are present.
3. The path integral sums over all  $G$ -bundles. There could be additional data that determines weights for the sum over  $G$ -bundles.

With these properties, the difference between a  $G$  and  $G/H$  theory where  $H \subset Z(G)$  is made explicit. We can go ahead and generalize our above analysis by also defining the  $SU(N)/\mathbb{Z}_K$   $\text{MSYM}_2$  theory with  $K|N$  accordingly. The 2d  $SU(N)/\mathbb{Z}_K$  theory has  $K$  instanton sectors, weighted by a  $\mathbb{Z}_K$  valued discrete  $\theta$  angle. Since the theory contains only adjoint fields, the charge under the center  $\mathbb{Z}_{N/K} = \mathbb{Z}_N/\mathbb{Z}_K$  will not be screened, and for each choice of the  $\theta$  angle the theory will have  $N/K$  superselection sectors corresponding to those superselection sectors of the  $SU(N)$  theory with  $\mathbb{Z}_N$  charge congruent modulo  $K$  to a given value determined by the choice of  $\theta$ .

Let us return to the  $U(N)$   $\text{MSYM}_2$ . The “standard”  $U(N)$   $\text{MSYM}_2$  has superselection sectors analogous to the  $SU(N)$   $\text{MSYM}_2$ . The pure  $U(N)$  Yang-Mills theory in 2d has  $N$  superselection sectors [300]. Similarly, a 2d  $U(N)$  gauge theory without fields charged under the center of the gauge group also has  $N$  superselection sectors, thus so does  $U(N)$   $\text{MSYM}_2$ . The  $U(N)$  theory has instanton sectors labeled by the integers corresponding to the quantized electric flux (or vortex number)  $c_1 \in H^2(\Sigma, \mathbb{Z})$ . Although one might hope to identify these sectors with the  $(M, N)$ -string sectors, this turns out to be not quite right. The true theory describing the interactions of  $N$  D1-branes is not just the  $U(N)$   $\text{MSYM}_2$  that we described above by the action (6.1), but also has a 2-form gauge field  $B$  coming from the restriction of the Kalb-Ramond field present in the NS-NS sector of the string theory target space to the brane world-volume. The  $B$ -field plays a subtle and important role, primarily by enhancing the classical field configurations of the theory. The  $B$ -field, being a 2-form gauge field, has Abelian 1-form gauge transformations under which the  $U(N)$  gauge field  $A$  also transforms [284],

$$B \rightarrow B + d\lambda, \tag{6.14}$$

$$A \rightarrow A - \lambda \mathbf{1}_N, \tag{6.15}$$

where  $\lambda$  is the 1-form gauge transformation parameter and  $\mathbf{1}_N$  is the  $N \times N$  identity matrix generating the center of the  $\mathfrak{u}(N)$  algebra. The correct gauge-invariant Lagrangian has the following kinetic term for the gauge field,

$$-\frac{1}{4} \text{Tr} (F_{\mu\nu} + B_{\mu\nu} \mathbf{1}_N)^2, \tag{6.16}$$

and  $\mathcal{F} = F + B\mathbf{1}_N$  is the appropriately modified field strength. Writing the  $U(N)$  gauge field as

$$A = \frac{1}{N}\widehat{A}\mathbf{1}_N + A', \quad (6.17)$$

with  $\widehat{A}$  the  $U(1)$  gauge field corresponding to the trace and  $A'$  the leftover  $SU(N)/\mathbb{Z}_N$  gauge field, we note that the 1-form gauge transformation above acts only on the  $U(1)$  gauge field  $\widehat{A}$ . Since all of the scalar and fermion fields are in the adjoint,  $\widehat{A}$  only appears in the gauge field kinetic term in the Lagrangian, and therefore none of the rest of the Lagrangian is modified with the inclusion of the  $B$ -field, as they are already gauge invariant under the 1-form gauge symmetry. The  $\mathcal{N} = (8, 8)$  supersymmetry remains intact once one modifies the supersymmetry transformations accordingly by replacing  $F$  with  $\mathcal{F}$ .

Now, let us consider what gauge bundles the theory has. As can be seen from the equation of motion for  $\widehat{A}$ ,  $\text{Tr}\mathcal{F}$  is constant, and has periods quantized in integer units when we impose the parameter  $\lambda$  generates the gauge group  $U(1)$  instead of  $\mathbb{R}$  [284]. So the theory considered on a Riemann surface  $\Sigma$  has a topological quantum number labeled by  $\tilde{c}_1 = [\text{Tr}\mathcal{F}/2\pi] \in H^2(\Sigma, \mathbb{Z})$  corresponding to the generalized  $U(1)$  electric flux. For an honest  $U(N)$  theory — without the  $B$ -field — the single Chern class  $c_1 = [\text{Tr}F/2\pi] \in H^2(\Sigma, \mathbb{Z})$  would classify all  $U(N)$ -principal bundles. A  $U(N)$ -bundle can be thought of as the data of a  $U(1)$ -bundle and an  $SU(N)/\mathbb{Z}_N$ -bundle, such that the Stiefel-Whitney class of the  $SU(N)/\mathbb{Z}_N$ -bundle  $w_2 \in H^2(\Sigma, \mathbb{Z}_N)$  is related to the  $U(1)$  characteristic class as  $\int w_2 = \int c_1 \pmod{N}$  [301]. This can be seen at the level of the transition functions for the gauge field. However, in the theory with the  $B$ -field, the additional 1-form symmetry enhances the transition functions and generalizes the allowed bundles and connections, as detailed in [30, 302]. The resulting generalized  $U(N)$ -connection admits an independent 't Hooft flux  $w_2$  in addition to the electric flux  $\tilde{c}_1$ . This type of gauge bundle would be more accurately described in the language of gerbes or 2-bundles, but we will not need to go into such territory here. Due to the particularly simple 2-group structure, practically speaking we can think of the allowed gauge bundles as  $U(1) \times SU(N)/\mathbb{Z}_N$ -bundles, with independently chosen characteristic classes  $(\tilde{c}_1, w_2) \in H^2(\Sigma, \mathbb{Z}) \times H^2(\Sigma, \mathbb{Z}_N)$ . The classical configurations of the scalar and fermion fields in the theory mimic the configurations in a  $U(1) \times SU(N)/\mathbb{Z}_N$  theory. It is important to emphasize that the theory is *not* a  $U(1) \times SU(N)/\mathbb{Z}_N$  gauge theory; for example the operator content — such as Wilson lines and surface operators — is different.



Configurations with  $\int_{\Sigma} \text{Tr}\mathcal{F}/2\pi = M$  correspond to the binding of  $M$  F-strings [284]. The  $M$  units of flux is interpreted as the NS-NS charge carried by the F-string, and  $\text{Tr}\mathcal{F}$  serves as a source for the  $B$ -field in the string target space. The generalized Yang-Mills action (or energy) of the flux is the binding energy of the  $(M, N)$ -string, measured as the difference from the mass of the  $N$  D-strings. If one considers the theory on the cylinder  $C = \mathbb{R}_t \times S^1$ , the presence of  $M$  units of  $\text{Tr}\mathcal{F}$  flux implies that there is a Wilson loop

$$e^{iM \oint_{\partial C} \widehat{A}/N} \quad (6.18)$$

at the boundary. However, this Wilson loop must also be complemented by the  $B$ -field to be gauge invariant. This can be seen by noting that the standard  $U(N)$  Wilson loops are not gauge invariant in this theory, instead one has the following surface operators considered in [30],

$$\left( \text{Tr}_R \mathcal{P} \exp \oint_{\partial \Sigma'} A \right) e^{iN_R \int_{\Sigma'} B} = \left( \text{Tr}_R \mathcal{P} \exp \oint_{\partial \Sigma'} A' \right) e^{iN_R \int_{\Sigma'} \frac{d\widehat{A}}{N} + B}. \quad (6.19)$$

Note that the inside and outside of this operator differ by  $N_R$  units of  $U(1)$  electric flux  $\text{Tr}\mathcal{F}$ . So, the sector with  $M$  units of electric flux has the operator

$$e^{iM \oint_{\partial C} \frac{\widehat{A}}{N}} e^{iM \int_C B} = e^{iM \int_C \frac{d\widehat{A}}{N}} e^{iM \int_C B} \quad (6.20)$$

turned on. As with the  $SU(N)/\mathbb{Z}_N$  theory, the integral of the 2-form gauge fields  $d\widehat{A}$  and  $B$  are not of global 2-forms. Upon quantizing the theory on the cylinder, these states with  $M$  units of electric field  $\text{Tr}\mathcal{F}$  are the  $(M, N)$ -string states. They fall into  $N$  superselection sectors determined by  $M \pmod{N}$ .

We are interested in the low-energy fluctuations of the  $(M, N)$ -string bound states. The path integral of the worldvolume  $U(N) + B$  theory on the Euclidean torus  $T^2$  is naturally a trace of the theory quantized on the cylinder  $C$ . The trace sums over the  $(M, N)$ -string sectors by summing over the flux  $\tilde{c}_1 \in H^2(T^2, \mathbb{Z})$ . Crucially, the  $U(N) + B$  theory has the operator

$$e^{iM \int_{T^2} d\widehat{A}/N} e^{iM \int_{T^2} B} \quad (6.21)$$

turned on in the sector with  $M$  units of electric flux. On a closed surface such as  $T^2$ , the first factor measures the 't Hooft flux in the  $SU(N)/\mathbb{Z}_N$  sector, since  $\int_{T^2} d\widehat{A} = \int_{T^2} w_2$  exactly as for the  $SU(N)/\mathbb{Z}_N$  theory discussed above. Once again, the presence of this term provides a discrete  $\theta$  angle  $2\pi M/N$  for the sum over the  $SU(N)/\mathbb{Z}_N$ -bundles. The second factor is simply the Wilson surface operator for the

$U(1)$  1-form gauge symmetry. The “charge”  $M$  is nothing but the F-string winding number once again. This closed Wilson surface operator measures the  $U(1)$ -valued holonomy of the background  $B$ -field.

We note that for the  $U(N)$  theory with or without the  $B$  field, one can also add a continuous  $\theta$ -angle term to the action proportional to  $\int \text{Tr} \mathcal{F}$  or  $\int \text{Tr} F$ , or in general a supersymmetric FI parameter. For the theory with the  $B$  field, this  $\theta$  angle is related to the axion of the Type IIB string theory [284]. However we will not consider including this term, as it does not affect the qualitative features of our discussion (or the elliptic genus).

### 6.2.2 Classical vacua on $T^2$

Motivated to perform a quantitative check of our conjectures regarding the structure and description of the vacua, we would like to compute the elliptic genera of the  $\text{MSYM}_2$  theory with the various gauge groups discussed above. The elliptic genus is a certain supersymmetric partition function on the 2-torus  $T^2$  [303], which counts (with a sign  $(-1)^F$ ) states in the cohomology of a conjugate pair of right-moving supercharges  $\mathcal{Q}_R^\pm$ .<sup>3</sup> States in the cohomology correspond to right-moving vacua tensored with left-moving BPS states. Elliptic genera have been extensively used to study  $\mathcal{N} = (2, 2)$  and more recently  $\mathcal{N} = (0, 2)$  theories; for a very restricted set of examples see [304–307]. It is often useful to refine the elliptic genus by other conserved charges in the theory that commute with  $\mathcal{Q}_R^\pm$ , which allows more information about the spectrum of the theory to be captured. For a theory with at least  $\mathcal{N} = (0, 2)$  supersymmetry, the elliptic genus can be schematically defined as

$$\mathcal{I} = \text{Tr} (-1)^F \prod_{J_L} y^{J_L} \prod_f x^f q^{H_L} \bar{q}^{H_R}, \quad (6.22)$$

where  $J_L$  stands for the generators of left-moving R-symmetry, and  $f$  stands for the generators of bosonic flavor symmetries, all commuting with the  $\mathcal{Q}_R^\pm$ . With this philosophy, the definition of the elliptic genus can be extended to theories with higher supersymmetry, as we will do so for theories with  $\mathcal{N} = (8, 8)$  supersymmetry in Sections 6.4 and 6.5. The trace can be taken in the Ramond or Neveu-Schwartz left- and right-moving Hilbert spaces of the theory on the spatial circle. We will specialize to the Ramond-Ramond sector. The elliptic genus is invariant under deformations of a theory preserving the right-moving supercharges, and therefore is a topological

---

<sup>3</sup>Elliptic genera can be defined for theories with  $\mathcal{N} = (0, 1)$  supersymmetry as well, with a single self-conjugate right moving supercharge  $\mathcal{Q}_R$ . However, one expects less control over the spectrum, as generically R- and flavor symmetries can be discrete.

index of theories. In particular, it is invariant under RG flow, which allows it to be computed in the free UV limit of a theory. For example, for Landau-Ginzburg theories it is sufficient to know the contributions from the field content of the theory in the free limit and impose the restrictions on R- and flavor symmetries coming from the superpotential [304].

For gauge theories the elliptic genus can be computed in the free limit of the theory by introducing fugacities for the gauge charges, which amounts to doing the path integral in the presence of a fixed but arbitrary background flat gauge connection, and then imposing Gauss' Law to project onto physical states by integrating over the moduli space of flat connections [305, 306, 308]. As discussed, for gauge theories with only adjoint fields such as  $\text{MSYM}_2$ , one has freedom in choosing the global form of the gauge group. For example, the theory with  $SU(N)$  gauge group differs from the theory with  $SU(N)/\mathbb{Z}_K$  gauge group for any  $K|N$ , despite having the same Lagrangian. Since  $\pi_1(SU(N)/\mathbb{Z}_K) = \mathbb{Z}_K$ , the  $SU(N)/\mathbb{Z}_K$  theory has additional classical field configurations on  $T^2$ , therefore both the moduli spaces of flat connections and the moduli space of classical vacua are enhanced to include various disconnected components. These additional components are crucial for the computation of the elliptic genus for such theories, as the path integral sums over them as well. We note that to compute the elliptic genus of the  $SU(N)$  theory and the  $U(N)$  theory without the  $B$  field, we only to integrate over the trivial moduli space of the  $SU(N)$  bundle. However, to compute the elliptic genus of the  $U(N)$  theory with the  $B$  field, we need to integrate over the full  $SU(N)/\mathbb{Z}_N$  moduli space. Also, once we have a description of the  $SU(N)/\mathbb{Z}_N$  moduli space, we can infer the  $SU(N)/\mathbb{Z}_K$  moduli space, and compute the elliptic genera for the  $SU(N)/\mathbb{Z}_K$  theories for free. To prime ourselves for computing the elliptic genera, we now turn to a description of the moduli space of flat  $SU(N)/\mathbb{Z}_N$ -connections on  $T^2$ . As an added bonus, we will be able to understand the classical field configurations on  $T^2$  for the various theories discussed, and discover the classical vacua.

### 6.2.2.1 Flat connections on $SU(N)/\mathbb{Z}_N$ -bundles over $T^2$

A treatment of the moduli spaces of flat connections for  $SU(N)/\mathbb{Z}_N$  bundles was given in [309], where in particular it was shown that the moduli spaces for the topologically non-trivial bundles with structure group  $G$  are isomorphic to moduli spaces of trivial bundles for a different structure group  $G^\omega$ . Here, we will give a self-contained, very explicit, and somewhat pedestrian account of the moduli spaces of flat connections

on  $T^2$ , specializing to the structure group  $G_{adj} = SU(N)/\mathbb{Z}_N$ .

Flat connections can be solved for by their holonomies, and the moduli space is given by

$$\mathcal{M}_{\text{flat}} = \text{Hom}(\pi_1(T^2), G_{adj})/G_{adj}. \quad (6.23)$$

Denoting elements of  $SU(N)/\mathbb{Z}_N$  as conjugacy classes  $[A]$  of elements  $A \in SU(N)$ , such homomorphisms for  $G_{adj} = SU(N)/\mathbb{Z}_N$  is the set of solutions to the equation

$$[A][B][A]^{-1}[B]^{-1} = 1 \quad (6.24)$$

modulo conjugation by  $SU(N)/\mathbb{Z}_N$  (or, equivalently, by  $SU(N)$  as the center acts trivially). For  $SU(N)$ , the analogous equation  $ABA^{-1}B^{-1} = 1$  implies  $A$  and  $B$  lie in the same maximal torus. While such commuting holonomies describe flat  $SU(N)/\mathbb{Z}_N$  connections, they are not the only solutions to (6.24). To find the rest of the solutions, we can lift (6.24) to  $SU(N)$ , and find solutions there. In  $SU(N)$ , we have  $N$  equations,

$$ABA^{-1}B^{-1} = \omega_N^k, \quad (6.25)$$

labeled by  $k \in \mathbb{Z}/N\mathbb{Z}$ , that project to the equation (6.24) in  $SU(N)/\mathbb{Z}_N$ . In (6.25),  $A$  and  $B$  are now in  $SU(N)$  and  $\omega_N$  is a primitive  $N$ th root of unity. We can use part of the gauge freedom to diagonalize  $B$ , leaving only the Weyl group, which reorders the eigenvalues. The equation now reads

$$SDS^\dagger = \omega_N^k D, \quad (6.26)$$

which is an eigenvalue equation for conjugacy action of  $SU(N)$  on a diagonal matrix. For each  $N$  and  $k$ , there is always a solution, constructed from the clock and shift matrices<sup>4</sup>

$$D_N = \begin{pmatrix} 1 & & & \\ & \omega_N & & \\ & & \ddots & \\ & & & \omega_N^{N-1} \end{pmatrix}, \text{ and } S_N = \begin{pmatrix} 0 & 1 & & \\ & 0 & 1 & \\ & & & \ddots & 1 \\ 1 & & & & 0 \end{pmatrix} \quad (6.27)$$

which satisfy

$$S_N^k D_N (S_N^k)^\dagger = \omega_N^k D_N. \quad (6.28)$$

---

<sup>4</sup>We note that as defined,  $D_N$  and  $S_N$  do not always have determinant equal to 1, and therefore are not always in  $SU(N)$ . This can easily be fixed by dividing by the  $N$ th root of the determinant in the definition. Since this overall phase decouples from the conjugation action, and so does not affect our calculations, we will drop it to avoid clutter.

Correspondingly, the pair of holonomies  $([S_N^k], [D_N])$  describes a flat  $SU(N)/\mathbb{Z}_N$  connection. Therefore, each  $k$  contributes a new component,  $\mathcal{M}_{N,k}$ , to the moduli space of flat  $SU(N)/\mathbb{Z}_N$  connections,  $\mathcal{M}_N$ . These components are disjoint, and labeled by discrete data  $k$ , so we can write

$$\mathcal{M}_N = \bigsqcup_{k=0}^{N-1} \mathcal{M}_{N,k}. \tag{6.29}$$

The principal  $SU(N)/\mathbb{Z}_N$  bundle  $P_{N,k}$  on  $T^2$ , with 't Hooft non-abelian flux  $k = \int_{T^2} w_2(P_{N,k})$ , has the moduli space of flat connection precisely  $\mathcal{M}_{N,k}$ .

Let's proceed to describe  $\mathcal{M}_{N,k}$  for given  $N$  and  $k$ . It will be useful to define  $d = \text{gcd}(N, k)$ , as  $\mathcal{M}_{N,k}$  will turn out to have complex dimension  $d - 1$ . In fact, for given  $N$  and any two  $k_1$  and  $k_2$  such that  $d = \text{gcd}(N, k_1) = \text{gcd}(N, k_2)$ , we will have the isomorphism  $\mathcal{M}_{N,k_1} \cong \mathcal{M}_{N,k_2}$ . This is not a surprise, since the bundles  $P_{N,k_1}$  and  $P_{N,k_2}$  are related by an automorphism of  $\pi_1(SU(N)/\mathbb{Z}_N) = \mathbb{Z}_N$  exchanging  $k_1$  and  $k_2$ . Motivated by this, we define  $\mathcal{M}_{N,d} \cong \mathcal{M}_{N,k}$ . Let's start with the case when  $N$  and  $k$  are relatively prime, so  $d = 1$ .

**Moduli space of bundles with  $d = 1$ :** We first note that for any pair of elements  $(A, B)$  in  $SU(N)$  satisfying some commutation relation, such as (6.25), there are a total of  $N^2$  points  $(\omega_N^a A, \omega_N^b B)$ , where  $a, b = 1, 2, \dots, N$ , that do so. (This is necessary for  $SU(N)$  solutions  $(A, B)$  to descend to  $SU(N)/\mathbb{Z}_N$  solutions  $([A], [B])$ .) So, we can work with representatives  $(A, B)$  of the conjugacy class  $([A], [B])$ .

To solve (6.25), we can diagonalize either  $A$  or  $B$ , and obtain the solutions  $(D_N^m, S_N^n)$  or  $(S_N^m, D_N^n)$ , for some  $mn = k$ . We note that  $S_N$  generates the  $\mathbb{Z}_N$  subgroup of the Weyl group  $\mathbb{S}_N$ , and therefore has the same eigenvalues as  $D_N$  (up to an irrelevant determinant factor). So,  $S_N$  and  $D_N$  are conjugate and the solutions  $(S_N^m, D_N^n)$  and  $(D_N^m, S_N^n)$  are identified by gauge transformations. Also, since we necessarily have  $\text{gcd}(m, N) = \text{gcd}(n, N) = 1$ , the solutions for various  $m, n$  only reorder the eigenvalues of  $D_N$  and  $S_N$  up to an overall cyclic ordering, and are related by the action of the Weyl group. We can partially fix the gauge by choosing  $m = k$  and  $n = 1$ , and we are left with  $N^2$  solutions in  $SU(N)$  given by  $(\omega_N^a S_N^k, \omega_N^b D_N)$ . But, precisely because  $S_N D_N S_N^\dagger = \omega_N D_N$ , these  $N^2$  points are also identified by gauge transformations generated by the simultaneous conjugation by  $D_N$  and by  $S_N$ ,

$$S_N(\omega_N^a S_N^k, \omega_N^b D_N) S_N^\dagger = (\omega_N^a S_N S_N^k S_N^\dagger, \omega_N^b S_N D_N S_N^\dagger) = (\omega_N^a S_N^k, \omega_N^{b+1} D_N) \tag{6.30}$$

$$D_N(\omega_N^a S_N^k, \omega_N^b D_N) D_N^\dagger = (\omega_N^a D_N S_N^k D_N^\dagger, \omega_N^b D_N D_N D_N^\dagger) = (\omega_N^{a-1} S_N^k, \omega_N^b D_N) \tag{6.31}$$

so there is a single solution in  $SU(N)$  up to conjugacy. Projecting to  $SU(N)/\mathbb{Z}_N$ , we still have a single point,  $([S_N^k], [D_N])$ , of  $SU(N)/\mathbb{Z}_N$  holonomies, but this point is fixed at order  $N^2$  by the  $\mathbb{Z}_N^2$  generated by simultaneous conjugation by  $[D_N]$  and by  $[S_N]$ ,

$$[S_N]([S_N^k], [D_N])[S_N]^\dagger = ([S_N^k], [D_N]) \quad (6.32)$$

$$[D_N]([S_N^k], [D_N])[D_N]^\dagger = ([S_N^k], [D_N]) \quad (6.33)$$

So, we finally have

$$\mathcal{M}_{N,k} = \{([S_N^k], [D_N])\}/\mathbb{Z}_N^2. \quad (6.34)$$

We see that

$$\mathcal{M}_{N,d=1} = \{([S_N], [D_N])\}/\mathbb{Z}_N^2, \quad (6.35)$$

and the isomorphism  $\mathcal{M}_{N,d=1} \cong \mathcal{M}_{N,k}$  is given by replacing the primitive  $N$ th root of unity  $\omega_N$  by its  $k$ th power.

**Moduli space of bundles with  $d > 1$ :** The essential observation for the  $d \neq 1$  cases is that

$$S_N^d = S_{N/d} \otimes I_d, \text{ and } D_N^d = D_{N/d} \otimes D_d^{d/N}. \quad (6.36)$$

Since the  $d$ -dimensional factors commute, one can turn on arbitrary eigenvalues in the corresponding  $d$ -dimensional subgroup of the Cartan torus. Explicitly, the solutions are generalized to

$$(e^{ih_{N,d}(\theta_s)} S_N^k, e^{ih_{N,d}(\theta_t)} D_N) = (S_{N/d} \otimes e^{ih_d(\theta_s)}, D_{N/d} \otimes e^{ih_d(\theta_t)} D_d^d), \quad (6.37)$$

where

$$e^{ih_{N,d}(\theta)} := I_{N/d} \otimes e^{ih_d(\theta)} := I_{N/d} \otimes \begin{pmatrix} e^{2\pi i \theta_1} & & & \\ & e^{2\pi i \theta_2} & & \\ & & \ddots & \\ & & & e^{2\pi i \theta_d} \end{pmatrix}, \quad (6.38)$$

as one can easily check that

$$\begin{aligned} & (e^{ih_{N,d}(\theta_s)} S_N^k)(e^{ih_{N,d}(\theta_t)} D_N)(e^{ih_{N,d}(\theta_s)} S_N^k)^\dagger \\ &= S_{N/d}^{k/d} D_{N/d} (S_{N/d}^{k/d})^\dagger \otimes e^{ih_d(\theta_s)} (e^{ih_d(\theta_t)} D_d^{d/N}) e^{-ih_d(\theta_s)} \\ &= \omega_{N/d}^{k/d} D_{N/d} \otimes e^{ih_d(\theta_t)} D_d^{d/N} \\ &= \omega_N^k (e^{ih_{N,d}(\theta_t)} D_N). \end{aligned} \quad (6.39)$$

The unitarity condition fixes  $(\theta_s)_i$  and  $(\theta_t)_i$  to be real, and the determinant condition fixes their sums to zero. Assigning the two holonomies to the spatial (along 1) and temporal (along  $\tau$ ) directions of the base torus, the moduli space inherits a natural complex structure, and is parametrized by complex coordinates  $u_i = (\theta_t)_i - \tau(\theta_s)_i$  which are periodic:  $u_i \sim u_i + 1 \sim u_i + \tau$ .

In choosing this presentation of the holonomies, we have used part of the gauge symmetry to write them as products of factors of size  $N/d$  and  $d$ . We are left with a  $\mathbb{Z}_{N/d}^2 \times \mathbb{S}_d$  subgroup of the gauge group. To see this, note that as far as the  $N/d$  by  $N/d$  factor is concerned, the situation is analogous to the  $d = 1$  case, wherein we have used part of the gauge symmetry to order the eigenvalues of  $S_{N/d}$  and  $D_{N/d}$  up to a cyclic ordering, and there is a remaining  $\mathbb{Z}_{N/d}^2$ , generated by simultaneous conjugation by  $S_{N/d} \otimes I_d$  and by  $D_{N/d} \otimes I_d$ , corresponding to the cyclic reordering of the eigenvalues, which acts on the solutions by identifying  $u_i \sim u_i + \frac{1}{N/d} \sim u_i + \frac{\tau}{N/d}$ . The  $d \times d$  block also has its eigenvalues permuted by the Weyl group  $\mathbb{S}_d$  of the  $d$ -dimensional Cartan subgroup. So, in  $SU(N)$ , the moduli space is  $\tilde{\mathfrak{M}}_{N,k}/\mathbb{S}_d$  where

$$\tilde{\mathfrak{M}}_{N,k} := \left\{ (S_{N/d}^{k/d} \otimes e^{i\hbar_d(\theta_s \cdot N/d)}, D_{N/d} \otimes e^{i\hbar_d(\theta_t \cdot N/d)}) \right\} \cong (T^2/\mathbb{Z}_{N/d}^2)^{d-1}. \quad (6.40)$$

Here,  $T^2$  is a copy of the base torus, with the same complex structure.

Once we project to  $SU(N)/\mathbb{Z}_N$ , the coordinates undergo the further identifications,  $u_i \sim u_i + \frac{1}{N} \sim u_i + \frac{\tau}{N}$ , so the solutions are fixed by the  $\mathbb{Z}_{N/d}^2$  action above. The moduli space is then

$$\mathcal{M}_{N,k} \cong \{([S_{N/d}^{k/d} \otimes e^{i\hbar_d(N\theta_s)}], [D_{N/d} \otimes e^{i\hbar_d(N\theta_t)}])\}/\mathbb{Z}_{N/d}^2 \times \mathbb{S}_d. \quad (6.41)$$

Once again, dependence on  $k$  is only through  $d$ , via the choice of an  $N/d$ th root of unity, and we can define

$$\mathcal{M}_{N,d} \cong (\mathfrak{M}_{N,d}/\mathbb{S}_d)/\mathbb{Z}_{N/d}^2, \quad (6.42)$$

where

$$\mathfrak{M}_{N,d} = \{(S_{N/d} \otimes e^{i\hbar_d(N\theta_s)}, D_{N/d} \otimes e^{i\hbar_d(N\theta_t)})\} \cong (T^2/\mathbb{Z}_N^2)^{d-1}, \quad (6.43)$$

and analogously for its lift to  $SU(N)$  via  $\tilde{\mathfrak{M}}_{N,d} \cong \tilde{\mathfrak{M}}_{N,k}$ . Note that  $\mathcal{M}_{N,d} \cong \mathcal{M}_{N/d,1} \times \mathcal{M}_{d,d}$ .

### 6.2.2.2 Classical vacua in instanton sectors

The classical zero energy configurations in the  $SU(N)/\mathbb{Z}_N$  theory are gauge invariant solutions to the BPS equations,

$$\begin{aligned} F_{\mu\nu} &= 0, \\ [X^i, X^j] &= 0, \\ D_\mu X^i &= 0, \end{aligned} \tag{6.44}$$

as can be seen from the fermionic supersymmetry variations, or directly from the action. In the IR limit as  $g \rightarrow \infty$ , we can think of a particular solution as the data of a flat connection  $A_\mu$ , and commuting constant bosons  $X^i$  satisfying  $[A_\mu, X^i] = 0$ . In the sector with trivial instanton number  $k = 0$ , the two components of  $A$  commute, so the  $X^i$  are all in the same Cartan subalgebra  $\mathfrak{h}$ , with the Weyl group  $W$  permuting the eigenvalues, so the eigenvalues parametrize  $(\mathfrak{h})^8/W = (\mathbb{R}^8)^{N-1}/\mathbb{S}_N$  [286]. However, in the presence of flat connections for non-trivial bundles, zero-energy configurations of the bosons are restricted further. To see directly from the above descriptions of the flat connections which  $X^i$  are zero energy, we can exponentiate the relation  $[A_\mu, X^i] = 0$  to the holonomies of  $A_\mu$  as  $e^{i\oint A} X^i e^{-i\oint A} = X^i$  for each of the two 1-cycles, the solutions to which are of the form (6.3), parametrizing  $(\mathbb{R}^8)^{d-1}/\mathbb{S}_d$  for the instanton sector with  $d = \text{gcd}(k, N)$ .

For the  $U(N)$  theory with the  $B$  field, classical field configurations are determined by picking  $(\tilde{c}_1, w_2)$ , which specifies a gauge 2-bundle. Given  $(\tilde{c}_1, w_2)$ , there will be minimal action configurations with constant field strength  $\mathcal{F}_{09} = 2\pi\frac{M}{N}\mathbf{1}_N$  and action proportional to  $M^2$ , where  $M = \int \tilde{c}_1$ , with the scalars parametrizing  $\text{Sym}^d \mathbb{R}^8$ . (In the Lorentzian theory, such configurations have  $M$  units of constant electric flux and energy  $g^2 M^2/N$ .) The naive “zero-energy” vacua have  $\tilde{c}_1 = 0$ , but, like the  $SU(N)/\mathbb{Z}_N$  theory, there are  $N$  disconnected components labeled by  $w_2$ .

What about the other choices for  $\tilde{c}_1$ ? In the brane picture, the  $U(N) + B$  MSYM theory is the leading approximation to the brane effective action. One can identify the energy of the flux  $\text{Tr}\mathcal{F}$  as the binding energy of F-strings to the D-strings [284, 286, 298]. These configurations are half-BPS in the target space, so the corresponding state in the MSYM theory should also preserve 16 supercharges. This is indeed the case, as the  $U(N) + B$  MSYM<sub>2</sub> theory has nonlinearly realized supersymmetries, which are the goldstinos of the breaking of translation symmetry in the presence of D-branes [295–297], so the supersymmetry variation (E.10) of the fermions is corrected to

$$\delta\Theta = \Gamma^{MN}\mathcal{F}_{MN}\epsilon_1 + \mathbf{1}_N\epsilon_2. \tag{6.45}$$



Here,  $\Theta = (\chi, 0)^T$  is the 10d Majorana spinor and  $\mathbf{1}_N$  is the generator of the center of the  $\mathfrak{u}(N)$  algebra. In particular, the BPS equations are generalized to

$$\begin{aligned}\mathcal{F}_{09} &= \Lambda \mathbf{1}_N, \\ [X^i, X^j] &= 0, \\ D_\mu X^i &= 0,\end{aligned}\tag{6.46}$$

by choosing  $\epsilon_2 = -2\Lambda\Gamma^{09}\epsilon_1$ . So, there are BPS sectors with constant  $\mathcal{F}_{09} = 2\pi\frac{M}{N}\mathbf{1}_N$  such that the minimal action configurations discussed above — with constant, commuting  $X^i$  parametrizing  $\text{Sym}^d(\mathbb{R}^8)$ , which are the solutions to the BPS equations for given bundle with  $w_2$  — preserve 16 appropriately chosen supersymmetries. Therefore, these configurations are “supersymmetric vacua”, but in a sector with a different central charge of the superalgebra.

We comment that it would be interesting to pursue the relation between the existence of the nonlinear supersymmetry to the presence of the  $B$  field.

### 6.3 Elliptic genera of $SU(N)/\mathbb{Z}_N$ gauge theories

We now delve into the task set upon in 6.2.2 of generalizing the elliptic genus when there are additional bundles to consider, such as for  $SU(N)/\mathbb{Z}_N$  theories, or for the  $U(N)$  theory with the  $B$ -field. Once again, as explored in [305, 306, 308], the elliptic genera of 2d gauge theories is a certain path integral on the torus, which due to localization can be calculated by integrating over the moduli space of flat connections. Let  $\tilde{G}$  be a simply-connected semi-simple Lie group with a discrete center  $Z(\tilde{G})$ . As discussed in the previous section, when one has a Lagrangian with gauge symmetry  $\tilde{G}$  and with all fields invariant under some subgroup  $H'$  of  $Z(\tilde{G})$ , one has several distinct choices of theories corresponding to a choice of the global form of the gauge group  $G = \tilde{G}/H$ , for each  $H \subset H'$ . These theories will generically have different choices of gauge bundles on the spacetime, and thus the choice of the gauge group will determine which bundles are being summed over by the path integral [29]. For such 2d theories, the elliptic genus is naturally also a sum over the path integrals for the sectors with different gauge bundles, each of which localizes to an integral over the moduli space of flat connections for that bundle. Furthermore, since  $\pi_1(G) = H$ , each 2d  $G$ -gauge theory carries additional discrete data in the form of a  $\theta$  angle dual to the relevant characteristic class  $w(P)$  of the bundle  $P$ , which specifies a weight for the sum over components. So, the elliptic genus can be written schematically as

$$\mathcal{I}^\theta = \sum_P e^{i\theta \int w(P)} Z_P,\tag{6.47}$$

where  $Z_P$  is the result of the path integral for the sector of the gauge theory with gauge bundle  $P$ .

Concretely, for 2d  $SU(N)/\mathbb{Z}_N$  theories, there are  $N$   $SU(N)/\mathbb{Z}_N$ -bundles  $P_{N,k}$ , and the relevant characteristic class is  $w_2(P) \in H^2(T^2, \mathbb{Z}_N)$ , with  $k = \int_{T^2} w_2(P_k)$ , so we write

$$\mathcal{I}_{SU(N)/\mathbb{Z}_N}^\theta = \sum_{k=0}^{N-1} e^{i\theta k} Z_{N,k}, \quad (6.48)$$

where  $\theta$  takes values in

$$\theta = 0, 2\pi \frac{1}{N}, 2\pi \frac{2}{N}, \dots, 2\pi \frac{N-1}{N}. \quad (6.49)$$

For  $U(N)$  MSYM<sub>2</sub>, there is an analogous but slightly more nuanced story. For a standard  $U(N)$  theory without the  $B$ -field, the gauge bundles are  $U(N)$ -bundles, which are classified by a single integer characteristic class  $c_1 \in H^2(\Sigma, \mathbb{Z})$ . Only the trivial bundle with  $c_1 = 0$  admits flat connections. Since the  $U(1)$  degrees of freedom are free and therefore decouple, the elliptic genus is computed as

$$\mathcal{I}_{U(N)} = \mathcal{I}_{U(1)} \mathcal{I}_{SU(N)}. \quad (6.50)$$

For the  $U(N)$  theory with the 2-form gauge field  $B$ , recall that there are additional field configurations corresponding to connections on gauge bundles with  $G_{adj} = U(1) \times SU(N)/\mathbb{Z}_N$  structure group. On a Riemann surface, these bundles are characterized by two independent classes,  $(\tilde{c}_1, w_2)$ , however, only certain bundles will contribute to the elliptic genus. For the theory taken at face value, flat connections are only present when  $\text{Tr} \mathcal{F} = 0$ , but there are still the  $SU(N)/\mathbb{Z}_N$ -bundles with flat connections to sum over, so we have the index

$$\mathcal{I}_{U(N)+B}^{\tilde{c}_1=0} = \mathcal{I}_{U(1)} \mathcal{I}_{SU(N)/\mathbb{Z}_N}^{\theta=0}. \quad (6.51)$$

Let us consider the other sectors, which require adding to the path integral the operator

$$e^{iM \int_\Sigma \frac{d\hat{A}}{N} + B}. \quad (6.52)$$

As we discussed in Section 6.2, this operator turns on a  $U(1)$  electric flux of  $M$  units, so we are in the sector with  $\tilde{c}_1 = M$ . For the  $SU(N)/\mathbb{Z}_N$  sector,  $w_2$  is unfixed, and is summed over with the discrete theta angle  $\theta = 2\pi M/N$  specified by the operator  $e^{iM \int_\Sigma \frac{d\hat{A}}{N}}$ . The definition of the elliptic genus for the sector with  $M$  strings needs

to be modified to take into account the non-linear supersymmetries, which shifts the central charge in the superalgebra. The corresponding elliptic genus localizes to states that saturate the BPS bound in this sector,  $\mathcal{F} = 2\pi \frac{M}{N} \mathbf{1}\omega$  with  $\omega$  the volume form, which specifies the bundle with  $\tilde{c}_1 = M$ . The scalar and fermionic fields in the  $U(1)$  multiplet, as well as the  $SU(N)/\mathbb{Z}_N$  sector of the theory are unaffected by this modification. Isolating the holonomy of the  $B$ -field  $e^{i\phi} = e^{i\int_{\Sigma} B}$ , we see that the elliptic genus of this sector is

$$e^{iM\phi} \mathcal{I}_{U(N)+B}^M = e^{iM\phi} \mathcal{I}_1 \mathcal{I}_{SU(N)}^{\theta=2\pi M/N}, \quad (6.53)$$

where  $\mathcal{I}_1$  is the contribution of the free center of mass modes. As a check, note that for the  $U(1)$  theory, the sector with  $M$  strings attached, which is the  $(M, 1)$ -string, has index  $\mathcal{I}_1$ . The S-dual  $(1, M)$  string indeed has the same index, if  $\mathcal{I}_{SU(N)}^{\theta} = 1$  for  $\theta = 2\pi/N$  which we will show to be the case. We can also construct the elliptic genus that sums over each BPS sector (labeled by the  $M$  units of flux),

$$\mathcal{I}_{U(N)+B} = \sum_{M \in \mathbb{Z}} e^{iM\phi} \mathcal{I}_{U(N)+B}^M. \quad (6.54)$$

To obtain each of the various indices, the crucial object we need to compute is  $\mathcal{I}_{SU(N)/\mathbb{Z}_N}^{\theta}$ . The computation requires some discussion, which we will now elaborate.

### 6.3.1 Integration over components of the moduli space of flat $SU(N)/\mathbb{Z}_N$ -connections

To compute  $\mathcal{I}_{SU(N)/\mathbb{Z}_N}^{\theta}$ , we need to calculate the path integrals  $Z_{N,k}$  for the  $SU(N)/\mathbb{Z}_N$  bundles, so let's analyze them. In general,  $Z_P$  is the path integral over all connections for  $P$ , so we can write

$$Z_P = \frac{1}{\text{Vol}(\mathcal{G}(P))} \int_{A \in \Omega^1(T^2, \text{ad}_P)} \mathcal{D}A Z(A). \quad (6.55)$$

Here,  $Z(A)$  is the result of the path integral over all other fields in the presence of a  $P$  connection  $A$ , and  $\mathcal{G}(P)$  is the group of gauge transformations (automorphisms) of the bundle  $P$ . The path integral for the elliptic genus localizes to a finite dimensional integral over the flat connections for the bundle  $P$ , but there are some global factors we need to worry about.

Let's consider the case when the moduli space of flat connections  $\mathcal{M}_P$  for a given bundle  $P$  is a point. After localization, there are no moduli to integrate over, so the path integral just becomes an evaluation of the torus partition function,  $Z_{1\text{-loop}}(u)$ , of

the fields in the theory in the background of the unique flat connection  $u \in \mathcal{M}_{N,1}$  (for a similar example, see the Abelian example in [305, §4.5]). If the point  $u$  is fixed by some finite group of gauge transformations, as is the case for  $u \in \mathcal{M}_{N,1} = \mathfrak{M}_{N,1}/\mathbb{Z}_N^2$ , we should divide by the order of this group. The bundles  $P_{N,k}$  with  $k \perp N$  (so  $d = 1$ ) are exactly of this type, and contribute  $Z_{N,k} = Z_{N,1}$  each, with

$$Z_{N,1} = Z_{1\text{-loop}}(u)|_{u \in \mathcal{M}_{N,1}} = \frac{1}{N^2} Z_{1\text{-loop}}(u)|_{u \in \mathfrak{M}_{N,1}}. \quad (6.56)$$

Next, let's consider the integral over the trivial  $SU(N)/\mathbb{Z}_N$ -bundle,  $P_{N,k=0}$ . Since the bundle  $P_{N,0}$  lifts to the (necessarily trivial)  $SU(N)$ -bundle  $\tilde{P}_N$ , we can lift the path integral over the  $SU(N)/\mathbb{Z}_N$ -connection to a path integral  $\tilde{Z}_{\tilde{P}}$  over an  $SU(N)$ -connection,  $\tilde{A}$ . As analyzed in [310, §4.1], the two path integrals are related by a factor of the ratio of the volume of gauge transformations of the bundles, which can be computed using the  $N : 1$  covering map  $\tilde{A} \rightarrow A$  to be

$$\frac{\text{Vol}(\mathcal{G}(\tilde{P}_N))}{\text{Vol}(\mathcal{G}(P_{N,0}))} = |\pi_1(SU(N)/\mathbb{Z}_N)|^{1-2g} \quad (6.57)$$

on a Riemann surface of genus  $g$ . Now, the  $SU(N)$  path integral is precisely what was shown in [306] to localize to a contour integral over the moduli space of flat  $SU(N)$ -connections,  $\tilde{\mathcal{M}}_N = \tilde{\mathfrak{M}}_N/\mathbb{S}_N$ . Therefore,

$$Z_{N,0} = \frac{1}{N} \tilde{Z}_{\tilde{P}_N} = \frac{1}{N} \frac{1}{|\mathbb{S}_N|} \oint_{\tilde{\mathfrak{M}}_N} Z_{1\text{-loop}}. \quad (6.58)$$

The contour integral is determined by the Jeffrey-Kirwan residue operation JK-Res. The integrand is once again  $Z_{1\text{-loop}}(u)$ , which is naturally a meromorphic function on the  $SU(N)/\mathbb{Z}_N$  moduli space  $\mathfrak{M}_{N,0}$  for a theory with no fields charged under the center. Since the  $SU(N)$  moduli space  $\tilde{\mathcal{M}}_N$  is an  $N^2 : 1$  cover of the moduli space  $\mathcal{M}_{N,0} = \mathfrak{M}_{N,0}/\mathbb{S}_N$  of  $P_{N,0}$ ,  $Z_{1\text{-loop}}$  extends to a periodic function on  $\tilde{\mathfrak{M}}_N$ . The contours specified by the JK-Res operation only depend on the charges of the fields giving rise to the poles, so the contours on the  $SU(N)$  moduli space are also periodic on the  $SU(N)/\mathbb{Z}_N$  moduli space for a theory with no fields charged under the center. In particular, the contour integral over  $\tilde{\mathfrak{M}}_N$  is just  $N^2$  times the contour integral on  $\mathfrak{M}_{N,0}$ . So, (6.58) can be simplified as

$$Z_{N,0} = N \frac{1}{|\mathbb{S}_N|} \oint_{\mathfrak{M}_{N,0}} Z_{1\text{-loop}}. \quad (6.59)$$

Finally, let's consider the case with general  $k \not\perp N$ , so  $d > 1$ . The moduli space in this case is  $\mathcal{M}_{N,k} \cong \mathcal{M}_{N,d} = \mathcal{M}_{N/d,1} \times \mathcal{M}_{d,d}$ , so flat connections are of the form  $A_\mu =$

$(A_{N/d} \otimes A_d)_\mu$ , with  $A_{N/d}$  the unique gauge-invariant flat connection on the bundle  $P_{N/d,k/d}$ , and  $A_d$  a flat connection on the bundle  $P_{d,0}$  which needs to be integrated over. Combining our arguments above leading to the formulas (6.56) and (6.59), the path integral for such  $P_{N,k}$  localizes to  $Z_{N,k} = Z_{N,d}$  with

$$Z_{N,d} = \frac{1}{(N/d)^2} d \frac{1}{|\mathbb{S}_d|} \oint_{\mathfrak{M}_{N,d}} Z_{1\text{-loop}}, \tag{6.60}$$

where  $\mathfrak{M}_{N,d}$  as given in (6.43). Once again, the contour is determined by the JK-Res operation.

Collecting our results in equations (6.56) and (6.60), the elliptic genus (6.48) is computed by the formula

$$\begin{aligned} \mathcal{I}_{SU(N)/\mathbb{Z}_N}^\theta &= \sum_{k=0}^{N-1} e^{i\theta k} \gcd(N, k) \frac{1}{|W_{N,k}|} \oint_{\mathfrak{M}_{N,k}} Z_{1\text{-loop}}(u) & (6.61) \\ &= \sum_{k \nmid N} e^{i\theta k} \gcd(N, k) \frac{1}{|W_{N,k}|} \sum_{u_* \in \mathfrak{M}_{N,d}^*} \text{JK-Res}(Q(u_*), \eta) Z_{1\text{-loop}}(u) \\ &\quad + \sum_{k \perp N} e^{i\theta k} \frac{1}{|W_{N,k}|} \sum_{u \in \mathfrak{M}_{N,1}} Z_{1\text{-loop}}(u) & (6.62) \end{aligned}$$

with  $W_{N,k} = \mathbb{Z}_{N/d}^2 \times \mathbb{S}_d$ . We will elaborate on the residue prescription JK-Res in Section 6.4.3 as part of the computation of the elliptic genus for  $\text{MSYM}_2$ .

### 6.3.2 Adjoint fields in the presence of background flat connections

To evaluate the contribution to the index from each of the components of the moduli space, we need to analyze how fields behave in the presence of background flat connections, and determine what  $Z_{1\text{-loop}}(u)$  is for each component. In line with our end goal, here we will determine  $Z_{1\text{-loop}}(u)$  for a theory with all fields in the adjoint representation.

First off, as is well known, background flat connections on  $T^2$  can be interchanged with boundary conditions around the two 1-cycles for fields charged under them. As a simple example, one could keep in mind that the choice of periodic or antiperiodic boundary conditions for fermions is equivalent to the choice of a background flat  $\mathbb{Z}_2$ -connection. Correspondingly, the boundary conditions determine the mode expansions of the fields into oscillators. Since the elliptic genus can be computed in the free field limit, the moding in the presence of arbitrary background flat connections can be easily determined by the charges of the fields.

Let's start by considering adjoint fields in the presence of a flat connection for the bundle  $P_{N,1}$  over  $T^2$ , described by a pair of  $SU(N)/\mathbb{Z}_N$  holonomies  $([S_N], [D_N])$ . Although the two matrices  $S_N$  and  $D_N$  do not commute, their actions by conjugation on  $N \times N$  matrices commute, since

$$S_N D_N A (S_N D_N)^\dagger = \omega_N D_N S_N A (\omega_N D_N S_N)^\dagger = D_N S_N A (D_N S_N)^\dagger. \quad (6.63)$$

Therefore, the matrices  $S_N$  and  $D_N$  acting on the Lie algebra  $\mathfrak{su}(N)$  by conjugation furnish an  $(N^2 - 1)$ -dimensional representation of  $\mathbb{Z}_N \times \mathbb{Z}_N$ , with eigenvalues  $(\omega_N^a, \omega_N^b)$ , where  $a, b = 0, 1, \dots, N - 1$ , and  $a$  and  $b$  both not 0 (as the mode with  $a = b = 0$  corresponds to the identity matrix, which is not in  $\mathfrak{su}(N)$ ). Explicitly, the eigenspace of the eigenvalue  $(\omega_N^a, \omega_N^b)$  is the 1-dimensional vector space of scalar multiples of the matrix  $S_N^{-b} D_N^a$ . For such a flat connection, adjoint fields will have gauge fugacities  $\exp 2\pi i \frac{a+(-1)^a b \tau}{N} = \omega_N^a q^{\frac{(-1)^a b}{N}}$ , where the charges  $a, b$  are taken from the set

$$\mathfrak{C}_N = \begin{cases} \left\{ -\frac{N-1}{2}, -\frac{N-1}{2} + 1, \dots, \frac{N-1}{2} \right\} & \text{for } N \text{ odd,} \\ \left\{ -\frac{N}{2}, -\frac{N}{2} + 1, \dots, \frac{N}{2}, \frac{N}{2} + 1 \right\} & \text{for } N \text{ even,} \end{cases} \quad (6.64)$$

but with the eigenvalue  $a = b = 0$  excluded. We had to be careful in picking the sign of the exponent of  $q$ , since we would like our expression to be charge conjugation invariant. This will be necessary later for evaluating the elliptic genus, which is a trace in the Ramond sector. These choices are also invariant under the modular S transformation of the base torus, which amounts to exchanging  $a$  and  $b$ . To summarize, if the contribution to the path integral of modes with gauge fugacity  $z = e^{2\pi i u}$  is  $\Xi(u)$ , the evaluation in (6.56) of  $Z_{1\text{-loop}}(u)$  at  $u \in \mathcal{M}_{N,1}$  is

$$Z_{1\text{-loop}}(u)|_{u \in \mathcal{M}_{N,1}} = \frac{1}{N^2} \prod_{\substack{a, b \in \mathfrak{C}_N \\ (a, b) \neq (0, 0)}} \Xi \left( \frac{a+(-1)^a b \tau}{N} \right). \quad (6.65)$$

The result is identical for all bundles  $P_{N,k}$  with  $k \perp N$ ; although the holonomies change to  $([S_N^k], [D_N])$ , the action on the Lie algebra is isomorphic — as expected, since they have isomorphic moduli spaces.

Next, we should consider the bundles with moduli spaces of positive dimension. We can study the holonomies  $([S_{N/d} \otimes e^{i\hbar(\theta_s)}], [D_{N/d} \otimes e^{i\hbar(\theta_i)}]) \in \mathcal{M}_{N,d}$ , and the result will be the same for all  $k$  with  $\gcd(k, N) = d$ . Similar to our above discussion, conjugation by  $S_{N/d}$  and  $D_{N/d}$  furnish  $d^2$  copies of a  $(N/d)^2$ -dimensional representation of  $\mathbb{Z}_{N/d}^2$ . Each of the  $d^2$  copies has the usual gauge charges for the adjoint representation of  $SU(d)$ . Explicitly, the matrices

$$S_{N/d}^a D_{N/d}^b \otimes (E_{(d)})_{i,j} \quad (6.66)$$

diagonalize the conjugation action, with eigenvalue

$$\left( \omega_{N/d}^b e^{2\pi i((\theta_s)_i - (\theta_s)_j)}, \omega_{N/d}^{-a} e^{2\pi i((\theta_t)_i - (\theta_t)_j)} \right), \quad (6.67)$$

where  $(E_{(d)})_{i,j}$  is the  $d \times d$  matrix with a 1 in the  $(i, j)$ th entry and zeroes everywhere else. So, for a flat connection on the torus with these holonomies, the adjoint fields have gauge fugacities  $\omega_{N/d}^a q^{\frac{(-1)^{ab}}{N/d} \frac{z_i}{z_j}}$ , where  $a, b \in \mathfrak{C}_{N/d}$ , and  $z_i = \exp(2\pi i u_i)$  with  $u_i = (\theta_t)_i - \tau(\theta_s)_i$ . One of the  $d$  modes with  $a = b = 0$  and  $i = j$  corresponds to the identity matrix, and should be excluded, as above for the  $d = 1$  case. Putting everything together, the contribution from a component of the moduli space isomorphic to  $\mathcal{M}_{N,d}$  is schematically

$$\int_{\mathcal{M}_{N,d}} Z_{1\text{-loop}} = d \frac{1}{(N/d)^2} \frac{1}{d!} \oint_{\mathfrak{M}_d} \left( \prod_i du_i \right) \frac{1}{\Xi(0)} \prod_{a,b \in \mathfrak{C}_{N/d}} \prod_{i,j=1}^d \Xi \left( \frac{a+(-1)^{ab}\tau}{N/d} + u_i - u_j \right), \quad (6.68)$$

where the  $1/\Xi(0)$  term serves to remove from the product the mode corresponding to the identity element in the Lie algebra. As a check, we see that this formula reproduces our earlier expression (6.65) for  $d = 1$ , and reproduces  $1/N$  times the expression for the integral over the  $SU(N)$  moduli space obtained by [305, 306, 308] for the integral over the moduli space of the trivial bundle with  $d = N$ , as can be seen by lifting  $\mathcal{M}_d$  to  $SU(N)$ .

## 6.4 Elliptic genus of MSYM<sub>2</sub>

### 6.4.1 Setup

We are now sufficiently equipped to turn to the computation of the elliptic genus of MSYM<sub>2</sub>. To compute the elliptic genus of a  $\mathcal{N} = (8, 8)$  supersymmetric theory, it is convenient to pick an  $\mathcal{N} = (0, 2)$  subalgebra of the  $\mathcal{N} = (8, 8)$  supersymmetry algebra and express the fields and the Lagrangian in representations of this  $\mathcal{N} = (0, 2)$  superalgebra. As elaborated in Appendix E.1, a choice of an  $\mathcal{N} = (0, 2)$  subalgebra is given by picking two right moving supercharges  $\mathcal{Q}_R^\pm$  that generate right-moving supersymmetry transformations  $\varepsilon_R^\pm \subset \varepsilon_R^\alpha$ , such that  $\varepsilon_R^\pm$  (and thus  $\mathcal{Q}_R^\pm$ ) are eigenstates of a weight of the  $\mathfrak{8}_s$  representation. To paraphrase the Appendix for convenience, this choice decomposes the R-symmetry group as  $Spin(8) \rightarrow Spin(2) \times Spin(6) \cong U(1)_R \times SU(4)$ , such that

$$\begin{aligned} \mathfrak{8}_s &\rightarrow \mathbf{1}_{+1} \oplus \mathbf{6}_0 \oplus \mathbf{1}_{-1} \\ \mathfrak{8}_c &\rightarrow \mathbf{4}_{-\frac{1}{2}} \oplus \bar{\mathbf{4}}_{+\frac{1}{2}} \\ \mathfrak{8}_v &\rightarrow \mathbf{4}_{+\frac{1}{2}} \oplus \bar{\mathbf{4}}_{-\frac{1}{2}}. \end{aligned} \quad (6.69)$$

Let  $\{\pm e^i\}_{i=1,\dots,4} \subset \mathfrak{h}^*$  be the weights of the  $\mathbf{8}_v$  representation of  $Spin(8)$ , and let  $\{K_j\}_{j=1,\dots,4} \subset \mathfrak{h}$  denote the Cartan generators with  $e^i(K_j) = \delta_j^i$ . A concrete choice of  $\varepsilon_R^\pm$  is given by the  $\mathbf{8}_s$  weights  $\pm r$  where  $r = \frac{1}{2}(e_1 + e_2 + e_3 + e_4)$ , for which  $U(1)_R$  is generated by the Cartan generator  $J_R = \frac{1}{2}(K_1 + K_2 + K_3 + K_4)$ .

Under such a split, the  $SU(4)$  factor commutes with the supercharges  $\mathcal{Q}_R^\pm$ ; therefore it is a flavor symmetry from the perspective of the  $\mathcal{N} = (0, 2)$  superalgebra. This allows us to define the index in the Ramond-Ramond sector via the  $\mathcal{N} = (0, 2)$  flavored elliptic genus [305, 306, 308]

$$\mathrm{Tr}_{\mathcal{H}}(-1)^F q^{H_L} \bar{q}^{H_R} \prod_A a_A^{f_A} \quad (6.70)$$

where  $f_A$  are the Cartan generators of  $Spin(6) \cong SU(4)$ . Generalizing the index to include the  $\theta$  angle, we obtain

$$\mathrm{Tr}_{\mathcal{H}} e^{i\theta \int w_2} (-1)^F q^{H_L} \bar{q}^{H_R} \prod_A a_A^{f_A} = \sum_k \mathrm{Tr}_{\mathcal{H}_k} e^{i\theta k} (-1)^F q^{H_L} \bar{q}^{H_R} \prod_A a_A^{f_A}. \quad (6.71)$$

Under the decomposition (6.69), the fields decompose into  $SU(4)$  representations as

$$\begin{aligned} \{X^i\} &\rightarrow \{\phi^A, \bar{\phi}_A\} \\ \{\chi_L^\alpha\} &\rightarrow \{\lambda_-, \bar{\lambda}_-, \psi_-^{AB}\} \\ \{\chi_R^{\dot{\alpha}}\} &\rightarrow \{\psi_+^A, \bar{\psi}_{+A}\}, \end{aligned} \quad (6.72)$$

which can be reorganized into  $\mathcal{N} = (0, 2)$  superfields  $\{\Phi^A, \bar{\Phi}_A, \Lambda, \bar{\Lambda}, \Psi^{A4}, \bar{\Psi}_{A4}\}$  as

$$\begin{aligned} \Phi^A &= \phi^A + \theta^+ \psi_+^A + \theta^+ \bar{\theta}^+ D_+ \phi^A \\ \Lambda &= \lambda_- + \theta^+ \frac{1}{\sqrt{2}} (D + iF_{09}) + \theta^+ \bar{\theta}^+ D_+ \lambda_- \\ \Psi^{A4} &= \psi_+^{A4} + \theta^+ G^{A4} + \bar{\theta}^+ E^{A4}(\Phi) + \theta^+ \bar{\theta}^+ D_+ \psi_+^{A4}. \end{aligned} \quad (6.73)$$

The Fermi multiplet  $\Lambda$  is the  $\mathcal{N} = (0, 2)$  vector multiplet, and carries the gauge field strength  $F_{09}$  (or  $\mathcal{F}_{09}$  for the  $U(N) + B$  theory). The  $E$ -type interaction term is  $E^{A4}(\Phi) = -i\sqrt{2}g[\Phi^A, \Phi^4]$ . There is also a  $J$ -term superpotential

$$ig \mathrm{Tr} \int d\theta^+ \Psi^{A4} J_A(\Phi) \Big|_{\bar{\theta}^+=0} + h.c. = ig \frac{\epsilon^{ABCA}}{3!} \mathrm{Tr} \int d\theta^+ \Psi^{A4} [\Phi^B, \Phi^C] \Big|_{\bar{\theta}^+=0} + h.c. \quad (6.74)$$

Perhaps the easiest way to derive these interactions is from the Lagrangian of 4d  $\mathcal{N} = 4$  SYM written in  $\mathcal{N} = 1$  supermultiplets. When dimensionally reduced to 2d, we get 2d  $\mathcal{N} = (8, 8)$  SYM, expressed in  $\mathcal{N} = (2, 2)$  vector and chiral superfields,



denoted  $\tilde{\Sigma}$  and  $\tilde{\Phi}^{1,2,3}$ , respectively, with the  $\mathcal{N} = 1$  superpotential descending to the  $\mathcal{N} = (2, 2)$  superpotential

$$ig\text{Tr} \int d\theta^2 \tilde{\Phi}^1 [\tilde{\Phi}^2, \tilde{\Phi}^3] + h.c.. \quad (6.75)$$

Now, we can decompose the  $\mathcal{N} = (2, 2)$  multiplets and the  $\mathcal{N} = (2, 2)$  superpotential into their  $\mathcal{N} = (0, 2)$  counterparts as described in [311]. The vector multiplet  $\tilde{\Sigma}$  decomposes into a chiral multiplet  $\Phi^4$  and the Fermi vector multiplet  $\Lambda$ . The chiral multiplet  $\tilde{\Phi}^A$  of  $\mathcal{N} = (2, 2)$  decomposes into a  $\mathcal{N} = (0, 2)$  chiral multiplet  $\Phi^A$  and Fermi multiplet  $\Psi^{A4}$ , where the Fermi multiplet has  $E$ -term  $\bar{\mathcal{D}}_+ \Psi^A = i\sqrt{2}g[\Phi^4, \Phi^A]$ . The  $\mathcal{N} = (2, 2)$  superpotential  $W(\Phi)$  descends to  $J_A(\Phi) = \frac{\partial W}{\partial \Phi^A}$ , which reproduces our expression above.

For the free  $U(1)$  theory, the index as defined vanishes due to the zero mode of  $\lambda_-$  and its conjugate, as usual. This is because  $\lambda_-$  and its conjugate are in the same eigenstate of bosonic symmetries as the  $\mathcal{N} = (0, 2)$  supercharges, including the R-symmetry, and have opposite fermion number, so their contributions cancel. But, following [312, 313], we can remove the contribution from the problematic zero modes by inserting a factor of  $J_R$  into the definition of the trace, as we will discuss in detail in Section 6.5. Then the index is simply the product of the one loop partition functions for each of the superfields

$$\mathcal{I}_{U(1)} = Z_\Lambda \prod_A Z_{\Phi^A} Z_{\Psi^{A4}} = \eta(\tau)^3 \frac{\prod_{A=1}^3 \theta_1(\tau|\xi_A + \xi_4)}{\prod_{A=1}^4 \theta_1(\tau|\xi_A)} \quad (6.76)$$

where  $\xi_A$  are holonomies for flat background gauge fields for the  $SU(4)$  “flavor” symmetry, coupling to fields via  $\rho(\xi) = \rho^A \xi_A$ , where  $\rho$  is a weight of the fundamental  $SU(4)$  representation. The holonomies  $\xi_A$  satisfy

$$\sum_A \xi_A = 0, \quad (6.77)$$

which is the determinant constraint of  $SU(4)$ , or equivalently the superpotential constraint. The Dedekind eta function is defined as

$$\eta(\tau) = q^{1/24} \prod_{n=1}^{\infty} (1 - q^n), \quad (6.78)$$

and the Jacobi theta function is defined as

$$\theta_1(\tau|u) = -iq^{1/8} z^{1/2} \prod_{n=1}^{\infty} (1 - q^n)(1 - zq^n)(1 - z^{-1}q^{n-1}), \quad (6.79)$$

with  $q = e^{2\pi i\tau}$  and  $z = e^{2\pi iu}$ .

Let's recall that in order to compute the index for the interacting gauge theory, one also needs to introduce gauge fugacities, and then impose Gauss' Law, which takes the form of a contour integral. Since the theory is free in the UV, and the index is scale invariant, we can do the computation in the free UV limit, so we only need the contribution from each free field. The integrand of the contour integral for the gauge theory index is then

$$Z_{1\text{-loop}}(\tau|u; \xi) = \prod_{\alpha} \Xi(\tau|\alpha(u); \xi), \quad (6.80)$$

where  $\Xi(\tau|\alpha(u); \xi)$  is the factor from the modes with charge  $\alpha$  in the presence of a background flat gauge connection specified by  $u$ , with  $\alpha(u)$  as discussed in Section 6.3.2 for the various components of the moduli space of flat connections. For  $\text{MSYM}_2$ , the free field index is

$$\Xi(\tau|u; \xi) := \frac{\theta_1(\tau|u) \prod_{A=1}^3 \theta_1(\tau|\xi_A + \xi_4 + u)}{\prod_{A=1}^4 \theta_1(\tau|\xi_A + u)}. \quad (6.81)$$

Note that we can recover the  $U(1)$  index as

$$\mathcal{I}_{U(1)}(\tau|\xi) = -\left. \frac{\partial}{\partial u} \right|_{u=0} \Xi(\tau|u; \xi). \quad (6.82)$$

The function  $\Xi(\tau|u; \xi)$  inherits the following periodicity properties from the theta function  $\theta_1(\tau|u)$ ,

$$\begin{aligned} \Xi(\tau|u + a + b\tau; \xi) &= e^{-2\pi i b(2\xi_4)} \Xi(\tau|u; \xi), \\ \Xi(\tau|u; \xi_1 + a + b\tau, \xi_2, \xi_3) &= e^{2\pi i b(2u)} \Xi(\tau|u; \xi), \end{aligned} \quad (6.83)$$

as well as the following modular transformation properties,

$$\begin{aligned} \Xi(\tau + 1|u; \xi) &= \Xi(\tau|u; \xi), \\ \Xi\left(-\frac{1}{\tau} \middle| \frac{u}{\tau}; \frac{\xi}{\tau}\right) &= e^{\frac{\pi i}{\tau}(4u\xi_4)} \Xi(\tau|u; \xi). \end{aligned} \quad (6.84)$$

These properties imply that the integrand  $Z_{1\text{-loop}}(\tau|u; \xi)$ , and therefore the index is a modular invariant symmetric Abelian (multi-periodic) function of the variables  $\xi_{1,2,3}$  with modular parameter  $\tau$ . We will explore such functions in Section 6.5, and their uniqueness properties will help us match the gauge theory index to the symmetric-orbifold index in Section 6.4.3.

### 6.4.2 Contribution from isolated flat connections

We are now ready to compute the various contributions to the  $SU(N)/\mathbb{Z}_N$  gauge theory index from the components of  $\mathcal{M}_{\text{flat}}$ . Let's start with the pointlike components, corresponding to isolated flat connections of the bundles  $P_{N,k}$  with  $k \perp N$ . Applying our earlier result (6.65), we have

$$Z_{1\text{-loop}}|_{\mathcal{M}_{N,1}} = \frac{1}{N^2} \prod_{\substack{a,b \in \mathfrak{C}_N \\ (a,b) \neq (0,0)}} \Xi(\tau | \frac{a+(-1)^a b \tau}{N}; \xi_A). \quad (6.85)$$

In fact, this expression simplifies quite a bit, due to the identity

$$\prod_{a,b \in \mathfrak{C}_N} \Xi(\tau | u + \frac{a+(-1)^a b \tau}{N}; \xi_A) = \Xi(\tau | Nu; N\xi_A). \quad (6.86)$$

We can now rewrite the contribution to the index as

$$Z_{1\text{-loop}}|_{\mathcal{M}_{N,1}} = \frac{1}{N^2} \lim_{u \rightarrow 0} \frac{\Xi(\tau | Nu; N\xi_A)}{\Xi(\tau | u; \xi_A)} = \frac{1}{N} \frac{\mathcal{I}_{U(1)}(\tau | N\xi_A)}{\mathcal{I}_{U(1)}(\tau | \xi_A)}. \quad (6.87)$$

### 6.4.3 Integral over flat connections on the trivial bundle

Let's move on to the contributions from components of  $\mathcal{M}_{\text{flat}}$  of positive dimension. We will start with the component corresponding to the trivial  $SU(N)/\mathbb{Z}_N$ -bundle  $P_{N,0}$ , which will be the bulk of our computation. As discussed in Section 6.3.1, we can lift the integral on the moduli space of flat connections  $\mathcal{M}_{N,N}$  of  $P_{N,0}$  to an integral on the moduli space of flat  $SU(N)$ -connections  $\tilde{\mathfrak{M}}/\mathbb{S}_N$ . This allows us to use the formula obtained by [306] (see also [305, 308]) and write the integral in (6.58) as

$$\oint_{\mathcal{M}_{N,N}} Z_{1\text{-loop}}(u) = \frac{1}{|\pi_1(SU(N)/\mathbb{Z}_N)|} \frac{1}{|\mathbb{S}_N|} \sum_{u_* \in \tilde{\mathfrak{M}}_{\text{sing}^*}} \text{JK-Res}(\mathcal{Q}(u_*), \eta) Z_{1\text{-loop}}(u), \quad (6.88)$$

where

$$Z_{1\text{-loop}} = (\mathcal{I}_{U(1)})^{N-1} \prod_{i \neq j} \frac{\theta_1(\tau | u_i - u_j) \prod_{A=1}^3 \theta_1(\tau | \xi_A + \xi_A + u_i - u_j)}{\prod_{A=1}^4 \theta_1(\tau | \xi_A + u_i - u_j)} \bigwedge_{i=2}^N du_i. \quad (6.89)$$

The authors of [306] give a detailed prescription for evaluating the JK-Res operation. Here, we will briefly recall parts of the prescription, and compute the residue. Let  $r$  denote the rank of the gauge group, so  $r = N - 1$  here for  $SU(N)$ . The integrand  $Z_{1\text{-loop}}$  is naturally a meromorphic  $(r, 0)$ -form on  $\tilde{\mathfrak{M}}$ , which is the torus  $\mathfrak{h}_{\mathbb{C}} / (Q^{\vee} + \tau Q^{\vee}) \cong (\mathbb{C}/\mathbb{Z} + \tau\mathbb{Z})^r$ , where  $\mathfrak{h}$  is the Cartan subalgebra of  $SU(N)$ , and  $Q^{\vee}$  is the

coroot lattice. We pick  $u_2, \dots, u_N$  as coordinates on  $\tilde{\mathfrak{M}}$  and solve for  $u_1$  using the trace constraint  $\sum_i u_i = 0$ . We observe that  $Z_{1\text{-loop}}$  is singular along the hyperplanes

$$H_{ij}^A = \{u_i - u_j + \xi_A = 0 \pmod{\mathbb{Z} + \tau\mathbb{Z}}\} \subset \tilde{\mathfrak{M}}. \quad (6.90)$$

Let  $Q_{ij}^A \in \mathfrak{h}^*$  denote the weight of the multiplet responsible for the hyperplane  $H_{ij}^A$ , which are the non-zero roots  $Q_{ij}^A(u) = u_i - u_j$ . Let  $\mathbf{Q}(u_*) = \{Q_{ij}^A \mid u_* \in H_{ij}^A\}$  denote the set of charges of the singular hyperplanes meeting at  $u_*$ . The collection of points  $u_*$  where at least  $r$  singular hyperplanes intersect is denoted by  $\tilde{\mathfrak{M}}_{\text{sing}^*}$ . When the charges  $\mathbf{Q}(u_*)$  of all singular hyperplanes meeting at a point are contained in a half-space of  $\mathfrak{h}^*$ , the arrangement of hyperplanes is termed ‘‘projective.’’ When there are exactly  $r$  singular hyperplanes intersecting at a point, labeled say  $H_{j_1}, \dots, H_{j_r}$ , the arrangement is termed ‘‘non-degenerate.’’ To evaluate the residue, we need to pick a covector  $\eta \in \mathfrak{h}^*$ , which for theories with only adjoint fields specifies a Weyl chamber. For a projective and non-degenerate arrangement, the residue is determined by the operation

$$\text{JK-Res}_{u=u_*}(\mathbf{Q}(u_*), \eta) \frac{du_1 \wedge \dots \wedge du_r}{Q_{j_1}(u - u_*) \dots Q_{j_r}(u - u_*)} = \begin{cases} \frac{1}{|\det(Q_{j_1} \dots Q_{j_r})|} & \text{if } \eta \in \text{Cone}(Q_{j_1} \dots Q_{j_r}), \\ 0 & \text{otherwise.} \end{cases} \quad (6.91)$$

Here,  $\text{Cone}(Q_{j_1} \dots Q_{j_r})$  stands for the positive cone generated by the charge rays  $Q_{j_1}, \dots, Q_{j_r}$ . When the arrangement is degenerate, so there are more than  $r$  singular hyperplanes intersecting, the JK-Res operation is more complicated, as one needs to specify the precise cycle to integrate on. However, for the case of interest for us, whenever the arrangement is degenerate, one can exploit the linearity of the JK-Res operation to determine the cycle relatively easily, as was pointed out in some examples in [306]. In any case, the JK-Res operation corresponds to a particular linear combination of iterated residues, and in our case we will be able express JK-Res explicitly as a somewhat simple prescription of iterated residues.

Let’s analyze which poles give non-zero contributions to the sum in (6.88). It simplifies the classification of poles to note that non-zero residues are from points  $u_*$  where  $s$  singular hyperplanes and  $s'$  zero hyperplanes intersect, such that  $s - s' = r$ . We see that  $Z_{1\text{-loop}}$  has zeroes along the hyperplanes defined by

$$\begin{aligned} N_{ij} &= \{u_i - u_j = 0 \pmod{\mathbb{Z} + \tau\mathbb{Z}}\}, \\ N_{ij}^{B4} &= \{u_i - u_j + \xi_B + \xi_4 = 0 \pmod{\mathbb{Z} + \tau\mathbb{Z}}\}, \end{aligned} \quad (6.92)$$

for  $i \neq j$  and  $B = 1, 2, 3$ . So, for example, at the  $N^2$  points where the hyperplanes  $H_{i+1,i}^A$  with  $i = 1, \dots, N-1$  and some fixed  $A$  intersect, there are no other singular or zero hyperplanes intersecting (for generic  $\xi_A$ ). These points therefore give non-zero contributions as long as  $\eta \in \text{Cone}(\{Q_{i+1,i}^A\}_{i=1,\dots,N-1})$ . However, whenever say  $H_{i,j}^A$  and  $H_{i',j}^A$  intersect, we have  $u_i = u_{i'}$ , at which point there is a double zero in the integrand, and such points don't contribute for generic  $\xi_A$ .

We note that sets of hyperplanes that contribute a non-zero residue always intersect at  $N^2$  points, and each of these points will contribute identical residues. This is coming from the fact that we have lifted the integral on the trivial  $SU(N)/\mathbb{Z}_N$ -bundle's moduli space to the  $SU(N)$  moduli space  $\tilde{\mathfrak{M}}$ , which as we discussed in Section 6.3.1 is an  $N^2 \rightarrow 1$  covering. For concreteness, we will continue the integral on  $\tilde{\mathfrak{M}}$  to make direct contact with the literature, and observe that we will obtain  $N^2$  times the integral over the  $SU(N)/\mathbb{Z}_N$  moduli space.

Let's return to the classification of poles. There are some points where a degenerate intersection occurs with the required number of zero hyperplanes for the residue to be non-zero. When this is the case, first of all, we need to determine what order of iterated residues JK-Res corresponds to. A second point that needs attention is as follows. We note that due to the constraint  $\sum \xi_A = 0$ , the second set of zero hyperplanes  $N_{ij}^{B4}$  can be written as

$$N_{ij}^{AB} = \{u_i - u_j + \xi_A + \xi_B = 0 \pmod{\mathbb{Z} + \tau\mathbb{Z}}\} \quad (6.93)$$

with  $A, B = 1, 2, 3, 4$ , but  $A \neq B$  — essentially, as an rank 2 antisymmetric tensor of  $SU(4)$ . Although the zeroes are totally symmetric in the  $\xi_A$  (as expected, since the integrand is totally symmetric in the  $\xi_A$ ), the signs of the factor in the integrand giving these hyperplanes differ for the pairs  $(A, B) \in \{(1, 4), (2, 4), (3, 4)\}$  versus  $(A, B) \in \{(1, 2), (1, 3), (2, 3)\}$ . This introduces a subtle sign in the computation of the residue, which we have to keep track of.

For concreteness, let's look closely at an example, as it will illuminate some of the subtleties in the computation. For  $N = 4$ , there are  $N^2 = 16$  points where four singular hyperplanes  $H_{12}^A, H_{13}^B, H_{24}^B$ , and  $H_{34}^A$  meet the zero hyperplane  $\{\epsilon(A, B)(u_1 - u_4) + \xi_A + \xi_B = 0\}$ . Here,  $\epsilon(A, B)$  is the sign that determines the correct zero hyperplane,  $N_{14}^{AB}$  or  $N_{14}^{BA}$ ; it is 1 if either of  $A$  or  $B$  is 4, and  $-1$  otherwise. The intersection occurs at the points

$$(u_2, u_3, u_4) = \frac{1}{2}(\xi_A - \xi_B, -\xi_A + \xi_B, \xi_A + \xi_B) + \frac{a + b\tau}{4}(1, 1, 1) \quad (6.94)$$

for  $a, b = 1, \dots, 4$ . A more suitable choice of coordinates is given by  $v_i = Q_{i1}(u) = u_i - u_1$  for  $i = 2, 3, 4$ . The intersection points in these coordinates are at

$$(v_2, v_3, v_4) = (\xi_A, \xi_B, \xi_A + \xi_B) + (a + b\tau)(1, 1, 1). \tag{6.95}$$

First of all, let's note that the integrand is doubly periodic in each of the variables  $v_i$  under translations by  $\mathbb{Z} + \tau\mathbb{Z}$ , so each of the poles contributes the same residue. Shifting the coordinates so that the intersection happens at  $v_i = 0$ , we need to evaluate

$$\text{JK-Res}_{v=0}(\mathbf{Q}_*, \eta) \frac{\epsilon(A, B)v_4}{v_2v_3(v_4 - v_2)(v_4 - v_3)} \frac{dv_2 \wedge dv_3 \wedge dv_4}{4}. \tag{6.96}$$

The set of charges  $\mathbf{Q}_*$  is  $\{Q_{12}, Q_{13}, Q_{24}, Q_{34}\}$ , which are

$$Q_{12} = (-1, 0, 0), \quad Q_{13} = (0, -1, 0), \quad Q_{24} = (1, 0, -1), \quad Q_{34} = (0, 1, -1) \tag{6.97}$$

in coordinates dual to  $v_i$ . We pick the convenient choice of  $\eta = (-1, -1, -1)$  in these coordinates. Now, we need to determine which cycle of integration JK-Res corresponds to for this  $\eta$ . As discussed in (6.88), there could be various such cycles, depending on which sub-chamber  $\eta$  sits in; however, the results are equivalent. By linearity of the JK-Res operation, if we find some cycle of integration such that when applied to the 3-form defined by

$$\omega_{234} = \left( \frac{a}{v_2v_3(v_4 - v_2)} + \frac{b}{v_2v_3(v_4 - v_3)} + \frac{c}{v_2(v_4 - v_2)(v_4 - v_3)} + \frac{d}{v_3(v_4 - v_2)(v_4 - v_3)} \right) \tag{6.98}$$

gives the correct residue for each of the linear pieces, as according to (6.91), then it is the right prescription for the degenerate case. Noting that for the four subsets of charges, only  $\text{Cone}(Q_{12}, Q_{13}, Q_{24})$  and  $\text{Cone}(Q_{12}, Q_{13}, Q_{34})$  contain  $\eta$ , the correct cycles are determined as  $\text{Res}_{v_4=0} \text{Res}_{v_3=0} \text{Res}_{v_2=0}$  and  $\text{Res}_{v_4=0} \text{Res}_{v_2=0} \text{Res}_{v_3=0}$ , as both evaluate to  $a + b$  when applied to  $\omega_{234}$ . Therefore, applying either of the iterated residues to (6.96), we see that it evaluates to  $\epsilon(A, B)/4$ . Such poles generalize to  $N > 4$  as Young tableaux along pairs  $(A, B)$  as one expects.

Another subtlety comes from poles containing ‘‘cubes,’’ which starts occurring for  $N \geq 8$ . Concretely, for  $N = 8$ , we have a pole at the point

$$(v_i)_{i=2, \dots, 8} = (\xi_1, \xi_2, \xi_3, \xi_1 + \xi_2, \xi_1 + \xi_3, \xi_2 + \xi_3, \xi_1 + \xi_2 + \xi_3). \tag{6.99}$$

There are 13 singular hyperplanes

$$H_{12}^1, H_{13}^2, H_{14}^3, H_{25}^1, H_{35}^2, H_{26}^3, H_{46}^1, H_{37}^3, H_{47}^2, H_{58}^3, H_{68}^2, H_{78}^1, H_{81}^4 \tag{6.100}$$

and 6 zero hyperplanes  $N_{51}^{34}, N_{61}^{24}, N_{71}^{14}, N_{82}^{14}, N_{83}^{24}, N_{84}^{34}$  meeting at this point. However, the charge vector  $Q_{81}$  coming from  $H_{81}^4$  points outside of any half-space containing all the other charge vectors, so the arrangement is not projective. As was pointed out in [306], we can deal with this situation by relaxing the constraint on the R-symmetry fugacities (which resolves the intersection into a bunch of projective ones), computing the residues, and then taking the limit  $\epsilon \rightarrow 0$ . Relaxing the constraint on  $\xi_A$  to  $\xi_1 + \xi_2 + \xi_3 + \xi_4 = \epsilon$ , the singular point is resolved to two points, at  $v_8 = \xi_1 + \xi_2 + \xi_3$  and at  $v_8 = -\xi_4 = -\xi_1 - \xi_2 - \xi_3 + \epsilon$  with  $v_2, \dots, v_7$  as before. For  $\eta = (-1, \dots, -1)$ , the second point does not contribute, and to obtain the contribution from the first point, we need to calculate

$$\text{JK-Res}_{v=0}(\mathbf{Q}_*, \eta) \frac{(v_5 + \epsilon)(v_6 + \epsilon)(v_7 + \epsilon)}{v_2 v_3 v_4 (v_5 - v_2)(v_5 - v_3)(v_6 - v_2)(v_6 - v_4)(v_7 - v_3)(v_7 - v_4)} \times \frac{(v_8 - v_2 + \epsilon)(v_8 - v_3 + \epsilon)(v_8 - v_4 + \epsilon) \bigwedge_{i=2}^8 dv_i}{(v_8 - v_5)(v_8 - v_6)(v_8 - v_7)(-\epsilon - v_8)} \quad (6.101)$$

We can determine possible choices of a cycle of integration for this degenerate arrangement as above, and once again the residue is independent of this choice. One choice is given by

$$\text{JK-Res}_{v=0}(\mathbf{Q}_*, \eta) \bigwedge_{i=2}^8 dv_i = \text{Res}_{v_8=0} \text{Res}_{v_7=0} \dots \text{Res}_{v_2=0}, \quad (6.102)$$

so (6.101) evaluates to  $-1/8$ . Note that this sign comes from the singular hyperplane  $H_{18}^4$  with the problematic charge covector which made the arrangement non-projective in the first place, and is separate from the sign coming from zero-hyperplanes discussed above. So, in general we need to keep track of both sources of sign for the residue.

Finally, we note that starting  $N \geq 16$ , there are poles containing ‘‘hypercubes,’’ with  $v_{16} = \xi_1 + \xi_2 + \xi_3 + \xi_4$ . Due to the constraint on  $\xi_A$ ,  $v_{16} = 0$  and there is a double zero from  $N_{16,1}$  and  $N_{1,16}$ , so such poles have vanishing residue.

We are now ready to compute the contour integral for general  $N$ . The contributing poles in any Weyl chamber are classified by certain 4d Young tableaux of size  $N$ .<sup>5</sup> A 4d Young tableau is a collection of  $N$  ‘‘nodes’’  $Y = (y_1, \dots, y_N) \in \mathbb{Z}_{\geq 0}^4$ , subject to the ‘‘stacking’’ condition: if the node  $x = (x^1, x^2, x^3, x^4) \in Y$ , then so do all the nodes  $y = (y^1, y^2, y^3, y^4)$  with  $0 \leq y^A \leq x^A$  for all  $A = 1, 2, 3, 4$  [314]. We also require that each node  $y_i$  have at most 3 non-zero coordinates  $y_i^A$ . We will denote

<sup>5</sup>4d Young tableaux of size  $N$  also classify solid (3d) partitions of  $N$ ,  $\sum_{i,j,k} n_{i,j,k} = N$ , where for each nonzero  $n_{ijk}$ , there are  $n_{ijk}$  corresponding nodes  $(i-1, j-1, k-1, l)$ , with  $0 \leq l < n_{ijk}$ . In [314], such partitions are denoted 4d partitions of  $N$ .

the collection of such 4d Young tableaux of size  $N$  by  $\mathcal{Y}_N$ . Each such 4d Young tableau  $Y$  of size  $N$  describes  $N! \cdot N^2$  poles of the integrand, at coordinates given by solutions to  $u_i - u_j = y_{\sigma(i)}^A \xi_A$ , for some choice of  $j$  and the  $(N - 1)!$  orderings  $\sigma(i)$  of the remaining  $u_i$  with  $i \neq j$ .<sup>6</sup> The choice of  $j$  is related to the choice of a Weyl chamber; for any choice of  $\eta$  only  $(N - 1)! \cdot N^2$  poles survive the JK-Res operation, corresponding to some fixed  $j$ . For concreteness, we fix  $j = 1$  with the convenient choice of  $\eta = (-1, -1, \dots, -1)$  in coordinates  $(u_2, u_3, \dots, u_N)$ . Since the integrand is symmetric in the  $u_i$ , the  $(N - 1)!$  orderings  $\sigma(i)$  contribute identically, cancelling part of the factor coming from the order of the Weyl group. We define  $v_i = Q_{i1}(u) = u_i - u_1$  for  $i = 2, \dots, N$ , noting the relation  $\sum u_i = 0$ . Contributing poles are at points  $v(Y)$  given by coordinates  $v_i = y_i^A \xi_A + a + b\tau$ , for  $a, b = 1, \dots, N$ . Due to the periodicity structure of the integrand, the sum over  $a, b$  is trivial and produces a factor of  $N^2$ .

We introduce the following partial ordering  $\preceq$  on the nodes of 4d Young tableaux,

$$y_i \preceq y_j \quad \text{if } y_i^A \leq y_j^A \text{ for all } A, \tag{6.103}$$

which keeps track of the stacking of the nodes. The operation JK-Res for a pole  $Y = (y_1, \dots, y_N)$ , partially ordered such that  $y_i \preceq y_j$  if  $i < j$ , is given explicitly by the iterated residue

$$\text{JK-Res}_{u=u_*}(\mathbf{Q}_*, \eta) \bigwedge du_i = \frac{1}{N} \text{Res}_{v_N=y_N^A \xi_A} \cdots \text{Res}_{v_3=y_3^A \xi_A} \text{Res}_{v_2=y_2^A \xi_A} \cdot \tag{6.104}$$

The integral over the moduli space is then

$$\oint_{\mathcal{M}_{N,N}} Z_{1\text{-loop}} = \frac{1}{N} \sum_{Y \in \mathcal{Y}_N} N^2 \text{JK-Res}_{v_i=y_i^A \xi_A}(\mathbf{Q}_*, \eta) Z_{1\text{-loop}}(u) \tag{6.105}$$

$$= \frac{1}{N} \sum_{Y \in \mathcal{Y}_N} \epsilon(Y) \lim_{\delta \rightarrow 0} \frac{1}{\Xi(\tau|\delta; \xi)} \prod_{i,j} \Xi(\tau|y_i^A \xi_A - y_j^A \xi_A + \delta; \xi), \tag{6.106}$$

where we have introduced an auxiliary variable  $\delta$  to simplify the expressions of the residues. The coefficient  $\epsilon(Y)$  is a sign due to degenerate and non-projective intersections, and is determined as follows. Let  $c_3(Y)$  be the number of nodes in  $Y$  with at least 2 nonzero entries in the first 3 coordinates, and let  $c_4(Y)$  be the number of nodes in  $Y$  with exactly 3 nonzero coordinates, or

$$\begin{aligned} c_3(Y) &= \#\{y_i \in Y \mid y_i^B = 0 \text{ for at most one } B, \text{ with } B \in \{1, 2, 3\}\} \\ c_4(Y) &= \#\{y_i \in Y \mid y_i^A = 0 \text{ for exactly one } A, \text{ with } A \in \{1, 2, 3, 4\}\} \end{aligned} \tag{6.107}$$

---

<sup>6</sup>We have picked  $y_j^A = 0$  which we are free to do for any  $Y$ .



Then, the sign  $\epsilon(Y)$  is given by

$$\epsilon(Y) = (-1)^{c_3(Y)+c_4(Y)}. \quad (6.108)$$

We conjecture that the sum over the residues greatly simplifies to the expression

$$\frac{1}{N} \sum_{|Y|=N} \epsilon(Y) \lim_{\delta \rightarrow 0} \frac{1}{\Xi(\tau|\delta; \xi)} \prod_{i,j} \Xi(\tau|y_i^A \xi_A - y_j^A \xi_A + \delta; \xi) = \frac{1}{N} \sum_{s|N} s \frac{\mathcal{I}_{U(1)}(\tau|\frac{N}{s}\xi)}{\mathcal{I}_{U(1)}(\tau|\xi)}. \quad (6.109)$$

This is a highly nontrivial simplification to check analytically, as the summands on the left-hand side grow in number and complexity very quickly in  $N$ . Fortunately, the functions on both sides of this equation are very special, and they enjoy some very restrictive properties, which allows us to make some exact statements. Specifically, they are modular invariant symmetric Abelian (multi-periodic) functions of the variables  $\xi_{1,2,3}$  with the modulus  $\tau$  and period as in (6.134), of the kind explored in detail in Section 6.5. This follows from the periodicity and modular transformation properties of  $\Xi(\tau|u; \xi)$  and  $\mathcal{I}_{U(1)}(\tau|\xi)$ ; as the integrand (6.89) is such a function, so is the integral. We will explore some key properties of such functions in Section 6.5, leading up to Lemma 6.5.1 which states that such functions are completely determined by the rational function in variables  $a_{1,2,3} = \exp 2\pi i \xi_{1,2,3}$  obtained by setting  $\tau = i\infty$  (or  $q = 0$ ), corresponding to the constant term in the Fourier expansion in  $q$ . This dramatically simplifies the effort of checking (6.109), since if we can show the equality for  $q = 0$ , the full equality follows exactly! We were able to show this for  $N \leq 7$  by using *Mathematica* to simplify the sum over the residues with  $q = 0$ . For larger  $N$ , up to  $N \leq 12$ , we checked that the pole structure of the rational functions obtained by setting  $q = 0$  on both sides agrees, as well as by performing some numerical checks.

#### 6.4.4 Integral over flat connections on generic bundles

Having computed the integral on the moduli space of the trivial bundle, turns out we can infer the integral on each of the other components of  $\mathcal{M}_{\text{flat}}$ . We first note that we can use the identity (6.86) to simplify the integrand in (6.68),

$$\begin{aligned} & \int_{\mathcal{M}_{N,d}} Z_{1\text{-loop}} \\ &= \frac{d^2}{N} \frac{\mathcal{I}_{U(1)}(\tau|\frac{N}{d}\xi)}{\mathcal{I}_{U(1)}(\tau|\xi)} \frac{1}{d!} \oint_{\mathfrak{M}_d} \left( \prod_i du_i \right) \left( \frac{N}{d} \mathcal{I}_{U(1)} \left( \tau|\frac{N}{d}\xi \right) \right)^{d-1} \prod_{\substack{i,j=1 \\ i \neq j}}^d \Xi\left(\tau|\frac{N}{d}(u_i - u_j); \frac{N}{d}\xi\right). \end{aligned} \quad (6.110)$$

We recognize the first factor as the contribution from  $\mathcal{M}_{N/d,1}$ . The integral is the same as the integral over  $\mathcal{M}_{d,d}$ , but with scaled flavor charges  $\xi \rightarrow \frac{N}{d}\xi$ . Quoting our result above, we have

$$\int_{\mathcal{M}_{N,d}} Z_{1\text{-loop}} = \frac{1}{N} \frac{\mathcal{I}_{U(1)}(\tau|\frac{N}{d}\xi)}{\mathcal{I}_{U(1)}(\tau|\xi)} \sum_{s|d} s \frac{\mathcal{I}_{U(1)}(\tau|\frac{d}{s}\frac{N}{d}\xi)}{\mathcal{I}_{U(1)}(\tau|\frac{N}{d}\xi)} = \frac{1}{N} \sum_{s|d} s \frac{\mathcal{I}_{U(1)}(\tau|\frac{N}{s}\xi)}{\mathcal{I}_{U(1)}(\tau|\xi)}. \quad (6.111)$$

#### 6.4.5 Putting the pieces together

Adding up the contributions from each of the components of the moduli space of flat connections, we obtain the index

$$\mathcal{I}_{SU(N)/\mathbb{Z}_N}^\theta(\tau|\xi) = \frac{1}{N} \sum_{k=1}^N e^{i\theta k} \sum_{s|\gcd(k,N)} s \frac{\mathcal{I}_{U(1)}(\tau|\frac{N}{s}\xi)}{\mathcal{I}_{U(1)}(\tau|\xi)}. \quad (6.112)$$

In fact, we can evaluate the sum over  $k$  with given  $\theta = \frac{2\pi M}{N} \pmod{2\pi}$

$$\mathcal{I}_{SU(N)/\mathbb{Z}_N}^{\theta=\frac{2\pi M}{N}}(\tau|\xi) = \sum_{s|D} \frac{\mathcal{I}_{U(1)}(\tau|s\xi)}{\mathcal{I}_{U(1)}(\tau|\xi)} = \frac{\mathcal{I}_D}{\mathcal{I}_1}(\tau|\xi) \quad (6.113)$$

where  $D = \gcd(M, N)$ . Thus we establish that the index for the  $SU(N)/\mathbb{Z}_N$   $\mathbf{MSYM}_2$  theory at theta angle  $\theta = \frac{2\pi M}{N}$  is equal to the index of the sigma model into  $(\mathbb{R}^8)^{D-1}/\mathbb{S}_D$ , providing strong evidence that the IR limit of the gauge theory with the corresponding theta parameter is described by this sigma model.

We can also easily infer the index of the  $SU(N)$  and  $SU(N)/\mathbb{Z}_K$  theories for each  $K|N$  with our results thus far. For each such theory, the contributing bundles are a subset of the  $SU(N)/\mathbb{Z}_N$ -bundles, with the moduli space of flat connections lifted appropriately. For the  $SU(N)$  theory only the trivial bundle contributes, so we have the index

$$\mathcal{I}_{SU(N)} = \sum_{s|N} s \frac{\mathcal{I}_{U(1)}(\tau|\frac{N}{s}\xi)}{\mathcal{I}_{U(1)}(\tau|\xi)} = \sum_{k=1}^N \frac{\mathcal{I}_{\gcd(k,N)}}{\mathcal{I}_1}(\tau|\xi), \quad (6.114)$$

which is the sum of the index of each of the  $N$  superselection sectors in the theory, with the  $k$ th superselection sector described by the sigma model into  $(\mathbb{R}^8)^{d-1}/\mathbb{S}_d$  with  $d = \gcd(k, N)$ . For a  $SU(N)/\mathbb{Z}_K$  theory, there are  $K$  bundles to sum over, corresponding to those  $SU(N)/\mathbb{Z}_N$  bundles with  $w_2$  liftable to  $H^2(T^2, \mathbb{Z}_K)$  where  $\mathbb{Z}_K \subset \mathbb{Z}_N$  — essentially those with  $K|w_2$ . Accounting for the volume of gauge transformations and adding in the  $\mathbb{Z}_K$ -valued  $\theta$  angle  $\theta = 2\pi M/N$  with  $M \in \mathbb{Z}_N/\mathbb{Z}_{N/K} \cong \mathbb{Z}_K$ , we obtain

the index

$$\mathcal{I}_{SU(N)/\mathbb{Z}_K}^{\theta=\frac{2\pi M}{N}}(\tau|\xi) = \frac{1}{K} \sum_{k=1}^{N/K} e^{i\theta kK} \sum_{s|\gcd(kK,N)} s \frac{\mathcal{I}_{U(1)}(\tau|\frac{N}{s}\xi)}{\mathcal{I}_{U(1)}(\tau|\xi)} \quad (6.115)$$

$$= \sum_{k \equiv M \pmod{K}} \sum_{s|\gcd(k,N)} \frac{\mathcal{I}_{U(1)}(\tau|s\xi)}{\mathcal{I}_{U(1)}(\tau|\xi)} \quad (6.116)$$

$$= \sum_{k \equiv M \pmod{K}} \frac{\mathcal{I}_{\gcd(k,N)}}{\mathcal{I}_1}(\tau|\xi). \quad (6.117)$$

For each of the  $K$  values of  $\theta$ , the index is the sum of the indices of the  $N/K$  superselection sectors of the  $SU(N)$  theory with the same  $\mathbb{Z}_K$  charge.

As discussed, the index of the  $U(N)$  theory can be inferred from that of the  $SU(N)$  theory, and is

$$\mathcal{I}_{U(N)}(\tau|\xi) = \mathcal{I}_{U(1)} \mathcal{I}_{SU(N)}(\tau|\xi) = \sum_{k=1}^N \mathcal{I}_{\gcd(k,N)}(\tau|\xi). \quad (6.118)$$

The  $U(N)$  theory has  $N$  superselection sectors, as expected.

The index of the  $N$  D1-branes worldvolume theory with  $U(N)$  gauge field and the  $B$ -field in the sector with  $M$  units of flux  $\tilde{c}_1$  is

$$\mathcal{I}_{U(N)+B}^M(\tau|\xi) = \mathcal{I}_{U(1)}^{\tilde{c}_1=M} \mathcal{I}_{SU(N)}^{\theta=\frac{2\pi M}{N}}(\tau|\xi) = \mathcal{I}_D(\tau|\xi). \quad (6.119)$$

We have used the fact that the  $U(1)$  factor is free, and since the field strength does not contribute to the index,  $\mathcal{I}_{U(1)}^{\tilde{c}_1} = \mathcal{I}_1$  in the appropriate topological sector of the supersymmetry algebra. The index summing over all flux sectors (and therefore all BPS sectors) is

$$\mathcal{I}_{U(N)+B}(\tau|\xi) = \sum_{M \in \mathbb{Z}} e^{iM\phi} \mathcal{I}_D(\tau|\xi). \quad (6.120)$$

Once again, we note that the D1-brane index is invariant under the S-duality of the Type IIB string, which is generated by exchanging  $M$  and  $N$  and shifting  $M$  by a multiple of  $N$ , while leaving  $D$  invariant.

### 6.5 Elliptic genera of $\mathcal{N} = (8, 8)$ sigma models

We have thus far computed an  $\mathcal{N} = (8, 8)$  analog of the elliptic genus of the  $SU(N)$  and the  $U(N)$  MSYM<sub>2</sub>, and claimed that they are equal to the corresponding elliptic genus of some symmetric orbifolds of the supersymmetric sigma model into  $\mathbb{R}^8$ . In this section, we will compute the elliptic genus of the orbifold sigma model, and establish some of its key properties that allow us to match it with the gauge theory elliptic genus.

### 6.5.1 Elliptic genus of the $\mathbb{R}^8$ sigma model

For brevity, we will denote the supersymmetric sigma model into  $\mathbb{R}^8$  by  $\mathcal{C}$ .  $\mathcal{C}$  is a free theory. When viewed as a non-supersymmetric theory,  $\mathcal{C}$  carries 3  $Spin(8)$  flavor symmetry groups, labeled  $K_b$ ,  $K_l$ , and  $K_r$ , each acting separately on the 8 real bosons, the 8 real left-moving fermions, and the 8 real right-moving fermions. When viewed as a  $\mathcal{N} = (8, 8)$  supersymmetric theory, these actions are combined into a single copy of  $Spin(8)$ ,  $K$ , which is the R-symmetry identified as the rotation symmetry of the target space, with the bosons, the left-moving fermions, and the right-moving fermions transforming in the  $\mathbf{8}_v$ ,  $\mathbf{8}_s$ , and  $\mathbf{8}_c$  representations, respectively (up to  $Spin(8)$  triality). We can pick the representations of the fields under  $K_b \times K_l \times K_r$  as

$$(\mathbf{8}_v, \mathbf{1}, \mathbf{1}) \oplus (\mathbf{1}, \mathbf{8}_s, \mathbf{1}) \oplus (\mathbf{1}, \mathbf{1}, \mathbf{8}_c). \quad (6.121)$$

With this choice,  $K$  is identified as the diagonal combination of  $K_b \times K_l \times K_r$ .

The philosophy for computing the flavored elliptic genus is to pick an  $\mathcal{N} = (0, 2)$  supersymmetry, and insert into the trace fugacities for every bosonic charge which commutes with the chosen supersymmetry. We can think of  $\mathcal{C}$  as an  $\mathcal{N} = (0, 8)$  theory with R-symmetry  $K_r$ , which has flavor symmetry  $K_b \times K_l$ . Any choice of an  $\mathcal{N} = (0, 2)$  subalgebra gives the free theory with 4 chiral and 4 Fermi complex  $\mathcal{N} = (0, 2)$  superfields. The flavored elliptic genus in the RR sector of this theory is then

$$Z_1(\tau|\xi_A, \tilde{\zeta}_{\tilde{A}}) = \text{Tr}_{RR}(-1)^F q^{H_L} \bar{q}^{H_R} \prod_{A=1}^4 a_A^{K_{b,A}} \prod_{\tilde{A}=1}^4 b_{\tilde{A}}^{K_{l,\tilde{A}}} = \frac{\theta_1(\tilde{\zeta}_1)\theta_1(\tilde{\zeta}_2)\theta_1(\tilde{\zeta}_3)\theta_1(\tilde{\zeta}_4)}{\theta_1(\xi_1)\theta_1(\xi_2)\theta_1(\xi_3)\theta_1(\xi_4)} \quad (6.122)$$

where  $\xi_A$  and  $\tilde{\zeta}_{\tilde{A}}$  are eigenvalues of flat background gauge fields for  $K_b$  and  $K_l$  corresponding to the Cartan generators  $K_{b,A}$  and  $K_{l,\tilde{A}}$ , with

$$a_A = e^{2\pi i \xi_A}, \quad \tilde{b}_{\tilde{A}} = e^{2\pi i \tilde{\zeta}_{\tilde{A}}}. \quad (6.123)$$

We have used the superscript tildes for the  $K_l$  Cartan to denote the basis in which the  $\mathbf{8}_s$  weights are diagonal. The transformation to the basis in which the  $\mathbf{8}_v$  weights are diagonal is given by

$$K_{l,\tilde{A}} = M_{\tilde{A}}^A K_{l,A}, \quad \text{where} \quad M_{\tilde{A}}^A = \frac{1}{2} \begin{pmatrix} 1 & 1 & 1 & 1 \\ 1 & -1 & -1 & 1 \\ -1 & 1 & -1 & 1 \\ -1 & -1 & 1 & 1 \end{pmatrix}. \quad (6.124)$$

However, this  $K_b \times K_l$  flavor symmetry only commutes with the action of a  $\mathcal{N} = (0, 8)$  superalgebra, and does not respect the full  $\mathcal{N} = (8, 8)$  supersymmetry of the theory. If we insist that  $\mathcal{C}$  is indeed an  $\mathcal{N} = (8, 8)$  supersymmetric theory, there is a single  $K = Spin(8)$  R-symmetry, which is not respected by the backgrounds considered above. As described in Section 6.4.1 and Appendix E.1.2, once an  $\mathcal{N} = (0, 2)$  subalgebra of the  $\mathcal{N} = (8, 8)$  algebra is chosen, the supersymmetry generators  $\mathcal{Q}^\pm$  are eigenstates of a corresponding  $Spin(2)$  subgroup of  $K$ , and there is only a  $Spin(6) \cong SU(4)$  symmetry commuting with it. In this case, we can define an index with fugacities for the  $SU(4)$  ‘‘flavor’’ symmetry, which we label  $K'$ ,

$$Z_1(\tau|\xi'_B) = \text{Tr}_{RR}(-1)^F q^{H_L} \bar{q}^{H_R} \prod_{B=1}^3 a'^{K'_B}, \quad (6.125)$$

with  $K'_B$  the Cartan generators of  $K'$ . But the left-moving fermions and the right-moving supersymmetry generators transform in the same representation,  $\mathbf{8}_s$ , of  $K$ . So, for any choice of an  $\mathcal{N} = (0, 2)$  subalgebra, there will be left-moving fermions which are eigenstates of the  $Spin(2)$  R-symmetry, and therefore uncharged under the  $SU(4)$  flavor symmetry. The index as defined in (6.125) vanishes due to the contributions of these fermion zero modes, as was the case for the free  $U(1)$  multiplet as discussed in the paragraph leading up to equation (6.76).

Once again, as is commonly done in the literature, we can remove the contributions from the uncharged fermion zero modes by slightly modifying the index (6.125). This is done by (re)introducing fugacities for symmetries the fermions with problematic fermion zero modes are charged under (so that the modified index has a zero when the fugacities are turned off), taking appropriate derivatives to get rid of the zero, and then turning off the fugacities, as in [313] (see also [312]). We can do this by relating (6.122) to (6.125). First, we identify  $K_b$  and  $K_l$  diagonally, and write the reduced  $\mathcal{N} = (0, 8)$  index

$$Z_1(\tau|\xi_A) = \frac{\theta_1\left(\frac{\xi_1+\xi_2+\xi_3+\xi_4}{2}\right)\theta_1\left(\frac{\xi_1-\xi_2-\xi_3+\xi_4}{2}\right)\theta_1\left(\frac{-\xi_1+\xi_2-\xi_3+\xi_4}{2}\right)\theta_1\left(\frac{-\xi_1-\xi_2+\xi_3+\xi_4}{2}\right)}{\theta_1(\xi_1)\theta_1(\xi_2)\theta_1(\xi_3)\theta_1(\xi_4)}. \quad (6.126)$$

The  $\mathcal{N} = (8, 8)$  index (6.125) can be computed from (6.126) by further identifying  $K_r$  with  $K_b$  and  $K_l$  diagonally (so  $K_A = K_{b,A} + K_{l,A} + K_{r,A}$ ), and turning off the fugacity corresponding to the  $Spin(2)$  R-symmetry of the  $\mathcal{N} = (0, 2)$  subalgebra. Choosing the  $\mathcal{N} = (0, 2)$  superalgebra as in Section 6.4.1 and equation (E.15), with the R-symmetry generated by  $J_R = M_1^A K_A = \frac{1}{2}(K_1 + K_2 + K_3 + K_4)$ , we identify

$$K'_B = M_{B+1}^A K_A, \quad B = 1, 2, 3 \quad (6.127)$$

as the Cartan generators of  $K'$ . Practically, turning off the fugacity for  $J_R$  can be realized by having the  $\xi_A$  descend to eigenvalues of background flat  $SU(4)$ -connections, which satisfy the trace constraint

$$\xi_1 + \xi_2 + \xi_3 + \xi_4 = 0. \quad (6.128)$$

The  $\mathcal{N} = (0, 8)$  index (6.126) has a first-order zero at exactly this constraint due to fermion zero-modes, as it should by our argument above. To remove this zero, we simply take the derivative with respect to  $b_1 = \exp(2\pi i \tilde{\zeta}_1) = \exp(2\pi i \frac{\xi_1 + \xi_2 + \xi_3 + \xi_4}{2}) = \sqrt{a_1 a_2 a_3 a_4}$ , and set  $b_1 = 1$ ,

$$\mathcal{I}_1(\tau|\xi_A) := -\frac{\partial}{\partial b_1} Z_1(\tau|\xi_A) \Big|_{b_1=1} \quad (6.129)$$

$$= \frac{\eta^3(\tau) \theta_1(\tau|\xi_1 + \xi_4) \theta_1(\tau|\xi_2 + \xi_4) \theta_1(\tau|\xi_3 + \xi_4)}{\theta_1(\tau|\xi_1) \theta_1(\tau|\xi_2) \theta_1(\tau|\xi_3) \theta_1(\tau|\xi_4)}. \quad (6.130)$$

In this expression, it is understood that the  $\xi_A$  satisfy the constraint above. One could explicitly plug in  $\xi_4 = -\xi_1 - \xi_2 - \xi_3$ , if desired. We note that this is exactly the index for the (necessarily free)  $U(1)$   $\mathcal{N} = (8, 8)$  vector multiplet with the vanishing gaugino zero-mode contributions removed, which is a good check that the two definitions of the index for the gauge theory and the sigma model agree.

More generally, for any  $\mathcal{N} = (8, 8)$  theory, this index is defined as

$$\mathcal{I}(\tau|\xi_A) = -\frac{\partial}{\partial b_1} \Big|_{b_1=1} \text{Tr}_{RR}(-1)^F q^{H_L} \bar{q}^{H_R} \prod_{A=1}^4 a_A^{K_A} \quad (6.131)$$

$$= \text{Tr}_{RR}(-1)^F J_R q^{H_L} \bar{q}^{H_R} \prod_{B=1}^3 a_B^{K'_B}. \quad (6.132)$$

**Fourier expansion of  $\mathcal{I}_1$ .** The index  $\mathcal{I}_1$  enjoys a number of very special properties. For definiteness, we will solve for the  $SU(4)$  (or, really,  $SL(4, \mathbb{C})$ ) constraint by setting  $\xi_4 = -\xi_1 - \xi_2 - \xi_3$  explicitly in this section.

- (Abelian function.)  $\mathcal{I}_1$  is holomorphic in  $\tau \in \mathbb{H}/SL(2, \mathbb{Z})$  (including at the cusp  $q = 0$  or  $\tau = i\infty$ ), and meromorphic in each  $\xi_A \in \mathbb{C}/(\mathbb{Z} + \tau\mathbb{Z})$ . Moreover,  $\mathcal{I}_1$  is doubly periodic in each  $\xi_A$  under translations by the lattice  $\mathbb{Z} + \tau\mathbb{Z}$ , i.e.

$$\mathcal{I}_1(\tau|\xi + \Omega \cdot n) = \mathcal{I}_1(\tau|\xi), \quad (6.133)$$

where  $n \in \mathbb{Z}^6$  and  $\Omega$  is the period matrix

$$\Omega = \begin{pmatrix} 1 & \tau & 0 & 0 & 0 & 0 \\ 0 & 0 & 1 & \tau & 0 & 0 \\ 0 & 0 & 0 & 0 & 1 & \tau \end{pmatrix}. \quad (6.134)$$

- (Symmetric function.)  $\mathcal{I}_1$  is symmetric in  $\xi_A$ .
- (Modularity.)  $\mathcal{I}_1$  is modular invariant, i.e. under  $SL(2, \mathbb{Z})$  transformations  $\tau \rightarrow \frac{a\tau+b}{c\tau+d}$ , we have,

$$\mathcal{I}_1 \left( \frac{a\tau + b}{c\tau + d} \middle| \frac{\xi_A}{c\tau + d} \right) = \mathcal{I}_1(\tau | \xi_A), \quad \begin{pmatrix} a & b \\ c & d \end{pmatrix} \in SL(2, \mathbb{Z}). \tag{6.135}$$

It follows from these properties that  $\mathcal{I}_1$  is an honest map  $(\mathbb{H}/SL(2, \mathbb{Z})) \times (\mathbb{C}/\mathbb{Z} + \tau\mathbb{Z})^3 \rightarrow \mathbb{C}$ , and also a 3 variable Jacobi form (function) of weight 0 and index  $(0, 0, 0)$ . The periodicity in  $\tau \rightarrow \tau + 1$  and  $\xi_A \rightarrow \xi_A + 1$  allows for a Fourier expansion, of the form

$$\mathcal{I}_1(\tau | \xi_A) = \sum_m q^m f_m(\xi) = \sum_{m \geq 0, l} c(m, l) q^m \prod_A a_A^{l_A}. \tag{6.136}$$

Since the function is holomorphic in  $q$ , the coefficients  $f_m(\xi)$  of  $q^m$  are unique and well-defined. But since the  $f_m$  are meromorphic functions themselves, they might have multiple Fourier expansions. For example, we can easily determine

$$\begin{aligned} \mathcal{I}_1|_{q=0}(\xi) &:= \mathcal{I}_1(\tau = i\infty | \xi) = \frac{(1 - a_1 a_2)(1 - a_1 a_3)(1 - a_2 a_3)}{(1 - a_1)(1 - a_2)(1 - a_3)(1 - a_1 a_2 a_3)} \\ &= 1 + \frac{a_1}{1 - a_1} + \frac{a_2}{1 - a_2} + \frac{a_3}{1 - a_3} - \frac{a_1 a_2 a_3}{1 - a_1 a_2 a_3}. \end{aligned} \tag{6.137}$$

The function  $\mathcal{I}_1|_{q=0}(\xi)$  has different Fourier expansions in different regions of convergence of the  $a_A$ . Now, we can use the periodicity in  $\xi_A \rightarrow \xi_A + \tau$  to find a recursion relation for  $c(m, l_A)$ , which, when combined with modular invariance, determines  $\mathcal{I}_1$  completely given  $\mathcal{I}_1|_{q=0} := \mathcal{I}_1(\tau = i\infty | \xi)$ . Explicitly, we have

$$\mathcal{I}_1(\tau | \xi) = \mathcal{I}_1|_{q=0}(\xi) + \sum_{m=1}^{\infty} q^m \sum_{s|m} \chi(s\xi) \tag{6.138}$$

where  $\chi(\xi)$  is the  $SL(4, \mathbb{C})$  character

$$\chi(\xi_A) = \chi_{\square}(\xi_A) - \chi_{\wedge^3 \square}(\xi_A) = a_1 + a_2 + a_3 + a_4 - \frac{1}{a_1} - \frac{1}{a_2} - \frac{1}{a_3} - \frac{1}{a_4}. \tag{6.139}$$

To see this, note that the periodicity of  $\mathcal{I}_1$  under  $\xi_1 \rightarrow \xi_1 + \tau$  implies the identity,

$$\sum_{m \geq 0, l_A} c(m, l_1, l_2, l_3) q^m a_1^{l_1} a_2^{l_2} a_3^{l_3} = \sum_{m \geq 0, l_A} c(m, l_A) q^{m+l_1} a_1^{l_1} a_2^{l_2} a_3^{l_3}, \tag{6.140}$$

and similarly for  $\xi_2$  and  $\xi_3$ . To retain a holomorphic series expansion in  $q$ , we must choose  $c(0, l)$  to be the coefficients of the expansion of  $\mathcal{I}_1|_{q=0}$  in positive powers of  $a_A$ , i.e. the expansion convergent in the region  $|a_A| < 1$ . From here, for each  $A = 1, 2, 3$  and  $m \geq 0$ , we infer the following relations

$$c(m, l_1, l_2, l_3) = \begin{cases} 0 & \text{if } m > 0 \text{ and, } m + l_A < 0 \text{ or } m - l_A < 0, \\ c(m + l_A, l_1, l_2, l_3) & \text{if } m + l_A > 0. \end{cases} \quad (6.141)$$

The case with  $l_A < 0$  such that  $m + l_A = 0$  should be handled with more care. In that case, for say  $A = 1$ , we have

$$\mathcal{I}_1|_{q=0}(\xi) = \sum_{l_1 \leq 0, l_2, l_3} c(-l_1, l_1, l_2, l_3) a_1^{l_1} a_2^{l_2} a_3^{l_3}, \quad (6.142)$$

which determines  $c(-l_A, l_1, l_2, l_3) = \tilde{c}(0, l_1, l_2, l_3)$  where  $\tilde{c}$  are the coefficients of  $\mathcal{I}_1|_{q=0}$  in the expansion with negative powers of  $a_A$ . Putting it together, we have<sup>7</sup>

$$c(m, l_1, l_2, l_3) = \begin{cases} c(0, l_1, l_2, l_3) & \text{if } l_A > 0 \text{ and } l_A | m \text{ for some } A, \\ \tilde{c}(0, l_1, l_2, l_3) & \text{if } l_A < 0 \text{ and } l_A | m \text{ for some } A, \\ c(m, 0, 0, 0) & \text{if } l_A = 0 \text{ for all } A, \\ 0 & \text{otherwise.} \end{cases} \quad (6.143)$$

The only coefficients that are not determined by these relations are those of the form  $c(m, 0, 0, 0)$ , implying that the function is determined up to a holomorphic function of  $q$ . Requiring the function to be modular invariant fixes this ambiguity, since the only holomorphic modular invariant functions are constants. For  $\mathcal{I}_1$ ,  $c(m, 0, 0, 0) = 0$  for  $m > 0$ , and we obtain (6.138).

It is important to note that our discussion above proves that if any Abelian, modular invariant function  $f(\tau|\xi)$  with the same period matrix  $\Omega$  as  $\mathcal{I}_1(\tau|\xi)$  agrees with  $\mathcal{I}_1$  at  $q = 0$ , then it must equal  $\mathcal{I}_1$ . More generally, we have the following result.

**Lemma 6.5.1.** *Let  $f(\tau|\xi_A)$  be a modular invariant, Abelian function with periods 1 and  $\tau$  for each  $\xi$ , holomorphic in  $\tau$  (including at the cusp,  $q = 0$ ) and meromorphic in  $\xi_A$ . Then  $f(\tau|\xi_A)$  is completely determined by  $f|_{q=0}(\xi_A) = f(\tau = i\infty|\xi_A)$ .*

A particularly useful class of such functions for us turn out to be  $\mathcal{I}_1(\tau|N\xi)$ , which satisfy the same properties as  $\mathcal{I}_1(\tau|\xi)$ .

<sup>7</sup>We should note that for the general case, the first two cases should be generalized to hold for the conditional  $n^A l_A = m$  for some integers  $n^A$ , rather than just  $l_A | m$ . But for the specific case of  $\mathcal{I}_1$ , since  $c(0, l)$  is only nonzero when  $l = (l_1, l_2, l_3)$  is of the form  $(l, 0, 0)$ ,  $(0, l, 0)$ ,  $(0, 0, l)$ , or  $(l, l, l)$ , the notions coincide.



### 6.5.2 Elliptic genus of the $\text{Sym}^N(\mathbb{R}^8)$ sigma model

There are various equivalent methods of computing the partition function  $Z_N$  of a symmetric product theory given the partition function of the base theory  $Z_1$ . We list three prominent methods here.

- Summing over  $\mathbb{S}_N$  connections and twisted sectors

$$Z_N = \frac{1}{|\mathbb{S}_N|} \sum_{gh=hg} (Z_1^N)^{g,h} \quad (6.144)$$

- The DMVV formula [315]

$$\mathcal{Z} := 1 + \sum_{N \geq 1} p^N Z_N(q, \vec{a}) = \prod_{n>0, m \geq 0, \vec{l}} \frac{1}{(1 - p^n q^m \vec{a}^{\vec{l}})^{c(nm, \vec{l})}}. \quad (6.145)$$

- Hecke operators [313]

$$\log \mathcal{Z} = \sum_{M=1}^{\infty} p^M T_M Z_1, \quad (6.146)$$

so in particular

$$Z_N = T_N Z_1 + \cdots + \frac{1}{N!} (T_1 Z_1)^N \quad (6.147)$$

where

$$T_M Z_1(\tau | \vec{\xi}) := \frac{1}{M} \sum_{d|M, d=1}^M \sum_{b=0}^{M/d-1} Z_1 \left( \frac{d\tau + b}{M/d} \middle| d\vec{\xi} \right). \quad (6.148)$$

The Hecke operators turn out to be the most straightforward to extract a closed-form expression for  $Z_N$ , given one for  $Z_1$ . For the index we are interested in, we need to perform the “index operation” to remove zero-mode contributions,

$$\mathcal{I}_N := - \frac{\partial}{\partial b_1} \bigg|_{b_1=1} Z_N, \quad (6.149)$$

like we did to obtain  $\mathcal{I}_1$ . Analogous to the case in [313], only the term linear in  $Z_1$  survives this operation, as all the other terms have zeroes of order greater than 1 at  $b_1 = 1$ . Thus,

$$\mathcal{I}_N = - \frac{\partial}{\partial b_1} \bigg|_{b_1=1} T_N Z_1 = \frac{1}{N} \sum_{d|N} \sum_{b=0}^{N/d-1} d \mathcal{I}_1 \left( \frac{d\tau + b}{N/d} \middle| d\xi_A \right). \quad (6.150)$$

Specializing to the sigma model into  $\text{Sym}^N(\mathbb{R}^8)$ , turns out we can simplify further,

$$\mathcal{I}_N = \sum_{d|N} \mathcal{I}_1(\tau|d\xi_A). \quad (6.151)$$

This last simplification is nontrivial, but can be seen in two ways. One can notice that the  $q = 0$  piece of the two expressions in (6.150) and (6.151) agree, and they are both periodic functions on  $(\mathbb{C}/\mathbb{Z} + \tau\mathbb{Z})^3$ ; therefore they are equal by Lemma 6.5.1. Alternatively, one can directly compute from the Fourier expansion:

$$\begin{aligned} \frac{1}{N} \sum_{d|N} \sum_{b=0}^{N/d-1} d \mathcal{I}_1 \left( \frac{d\tau + b}{N/d} \middle| d\xi_A \right) &= \sum_{d|N} \mathcal{I}_1|_{q=0}(d\xi_A) + \sum_{d|N} \sum_{m=1}^{\infty} q^{dm} \sum_{s|\frac{N}{d}m} \chi(sd\xi_A) \\ &= \sum_{d|N} \mathcal{I}_1(\tau = i\infty|d\xi_A) + \sum_{k=1}^{\infty} q^k \sum_{d'|N} \sum_{s'|k} \chi(s'd'\xi_A) \\ &= \sum_{d|N} \mathcal{I}_1(\tau|d\xi_A). \end{aligned} \quad (6.152)$$

## 6.6 Conclusions and future directions

We have computed the elliptic genera of the  $SU(N)/\mathbb{Z}_K$   $\text{MSYM}_2$  and  $U(N)$   $\text{MSYM}_2$  with and without the  $B$  field, with each corresponding choice of the discrete  $\theta$  angle, and matched it with the elliptic genus of a corresponding  $\mathcal{N} = (8, 8)$  sigma model into a symmetric orbifold of  $\mathbb{R}^8$ , which we claim describes the IR fixed point in that sector. While the main focus of this work was in answering questions about the vacua of  $\text{MSYM}_2$ , the elliptic genera we have computed as part of our analysis are interesting objects in their own rights. For example, they are related to the supersymmetric partition function of the free second quantized Type IIA string as explored in [315], if one performs the sum over the string winding number  $N$ ;

$$\mathcal{Z}_0(\tau, \sigma|\xi) = 1 + \sum_{N \geq 1} p^N \mathcal{I}_N(\tau|\xi), \quad (6.153)$$

where  $p = e^{2\pi i\sigma}$ . One needs to modify this expression with an appropriate factor to obtain the T-duality invariant partition function  $\mathcal{Z}(\tau, \sigma|\xi)$  [315]. T-duality exchanges string winding number and oscillator number, so acts by interchanging  $p$  and  $q$ , which can be used to determine  $\mathcal{Z}$ . One could try to extract information about the strongly coupled limit of the string, which is M-theory, using the topological invariance of this function. It would also be an interesting question to understand the automorphic properties of  $\mathcal{Z}$ , *a la* [316]. One might also consider replacing  $\mathcal{I}_N$  with the full D1-

brane index  $\mathcal{I}_{U(N)+B}$ , which in the Type IIA picture sums over the bound states with D0-branes as well.

This work was inspired by the 4d-2d correspondence explored in [311], as well as by recent developments in the computation of flavored elliptic genera for 2d gauge theories. In particular,  $\text{MSYM}_2$  can be obtained by considering M5-branes on a four-dimensional torus  $T^4$  and letting the volume of the  $T^4$  shrink to zero. On the other hand, considering M5-branes on  $T^6 = T^2 \times T^4$ , and compactifying first on the  $T^2$  factor taken to be the worldvolume of the  $\text{MSYM}_2$ , one obtains 4d  $\mathcal{N} = 4$  SYM. Following the general idea of [311], the elliptic genus of  $\text{MSYM}_2$  is then related to the Vafa-Witten partition function of the 4d  $\mathcal{N} = 4$  theory on  $T^4$ , as well as to an appropriate supersymmetric partition function of the 6d  $\mathcal{N} = (2, 0)$  theory on  $T^6$ . We will be exploring this relation in upcoming works.

## APPENDICES TO CHAPTER 2

Appendices to chapter 2 are attached here.

### A.1 Estimating $b_T$ from $Z_{S^1_\beta \times S^{d-1}}$

As discussed in section 2.2.1.3, estimating thermal one-point functions by taking a limit of correlation functions on  $S^1_\beta \times S^{d-1}$  is challenging. In general, one needs to know the spectrum  $\Delta_{\mathcal{O}}$  and OPE coefficients  $f_{\mathcal{O}\mathcal{O}'}$  for arbitrarily high dimension operators  $\mathcal{O}'$  (not to mention the one-point blocks for all tensor structures appearing in  $\langle \mathcal{O}\mathcal{O}'\mathcal{O} \rangle$ ). In the next appendix, we give slightly more detail in  $d = 2$ .

However, in any  $d$ , the observable  $b_T$  is special in that it depends only on the spectrum of the theory.<sup>1</sup> This is because the expectation value of the stress-tensor on  $S^1_\beta \times S^{d-1}$  is proportional to a derivative of the partition function,

$$\langle T^{00} \rangle_{S^1_\beta \times S^{d-1}} = \frac{1}{S_d} \frac{\partial}{\partial \beta} \log Z_{S^1_\beta \times S^{d-1}}, \quad (\text{A.1})$$

where  $S_d = \text{vol}(S^{d-1}) = \frac{2\pi^{d/2}}{\Gamma(d/2)}$ . Thus, we can compute  $b_T$  via the limit

$$b_T = \lim_{\beta \rightarrow 0} \frac{\beta^d}{1 - 1/d} \langle T^{00} \rangle_{S^1_\beta \times S^{d-1}} = \frac{1}{S_d(1 - 1/d)} \lim_{\beta \rightarrow 0} \beta^d \frac{\partial}{\partial \beta} \log Z_{S^1_\beta \times S^{d-1}}. \quad (\text{A.2})$$

The partition function can be expanded in characters

$$Z_{S^1_\beta \times S^{d-1}} = \sum_{\mathcal{O}} \chi_{\Delta, \rho}(e^{-\beta}), \quad (\text{A.3})$$

where  $\Delta, \rho$  are the dimension and  $\text{SO}(d)$  representation, respectively, of  $\mathcal{O}$ , and we sum over primaries only. In practice, even if we don't know the full spectrum of a theory, we can try to estimate  $b_T$  by truncating the sum over characters at some  $\Delta_{\max}$ . More precisely, let us define

$$g_{\Delta_{\max}}(\beta) = \frac{1}{S_d(1 - 1/d)} \beta^d \frac{\partial}{\partial \beta} \log \sum_{\Delta \leq \Delta_{\max}} \chi_{\Delta, \rho}(e^{-\beta}). \quad (\text{A.4})$$

---

<sup>1</sup>We thank Chris Beem, Scott Collier, Liam Fitzpatrick, and Slava Rychkov for discussions that inspired the calculations in this appendix.

We can then try to extrapolate  $g_{\Delta_{\max}}(\beta)$  towards  $\beta = 0$ . The actual value of  $g_{\Delta_{\max}}(0)$  will always be 0, because  $\beta^d$  will dominate over the contribution of a finite number of characters at sufficiently small  $\beta$ . However, perhaps we can estimate  $b_T$  by evaluating  $g_{\Delta_{\max}}(\beta)$  at a small, nonzero value of  $\beta$ .

As a check on this idea, let us study the free boson, where we know the spectrum exactly. For concreteness, we work in  $d = 3$ . The partition function is given by

$$Z_{\text{free}}(q) = \prod_{j=0}^{\infty} \frac{1}{(1 - q^{j+1/2})^{2j+1}}, \quad (\text{A.5})$$

where  $q = e^{-\beta}$ .<sup>2,3</sup> It can be decomposed into conformal characters as

$$\begin{aligned} Z_{\text{free}}(q) &= 1 + \chi^{\text{free}}(q) + \sum_{\ell=2,4,\dots} \chi_{\ell}^{\text{short}}(q) + Z_{\text{long}}(q), \\ \chi^{\text{free}}(q) &= \chi_{1/2,0}(q) - \chi_{1/2+2,0}(q), \\ \chi_{\ell}^{\text{short}}(q) &= \chi_{\ell+1,\ell}(q) - \chi_{\ell+2,\ell-1}(q), \\ \chi_{\Delta,\ell}(q) &= \frac{q^{\Delta}(2\ell+1)}{(1-q)^3}. \end{aligned} \quad (\text{A.6})$$

Here,  $\chi_{\Delta,\ell}(q)$  is the character of a long multiplet, and the first three terms in  $Z_{\text{free}}(q)$  correspond to the unit operator, the boson  $\phi$  itself, and a tower of higher-spin currents. The long multiplet content is

$$Z_{\text{long}}(q) = \chi_{1,0}(q) + \chi_{3/2,0}(q) + \chi_{2,0}(q) + \dots \quad (\text{A.7})$$

To determine the quantum numbers and multiplicities of long multiplets, we can include a fugacity for angular momentum and decompose the full partition function with this fugacity into conformal characters. This is a standard exercise and we do not include the details here.

Using our knowledge of the spectrum, we can plot  $g_{\Delta_{\max}}(\beta)$  for various values of  $\Delta_{\max}$  in the free boson theory (figure A.1). The function with  $\Delta_{\max} = \infty$  (black dotted

<sup>2</sup>This expression comes from counting states that can be built from arbitrary products of the basic words  $\partial_{\mu_1} \cdots \partial_{\mu_j} \phi$ . The dimension of a word is  $j + 1/2$ . Because  $\partial^2 \phi = 0$ , the words transform as traceless symmetric tensors, so there are  $2j + 1$  of them for a given  $j$ . This leads to the above product representation of the partition function.

<sup>3</sup>There is no Casimir energy contribution to the partition function on  $S^1 \times S^{d-1}$  in odd dimensions. One way to understand this is to start on  $S^d$  and perform a Weyl transformation to a long capped cylinder with length  $L$ . Because there is no Weyl anomaly in odd dimensions, the partition function does not develop any interesting dependence on  $L$  at large  $L$ , and hence the Casimir energy is zero. In 4 and higher even dimensions, the Casimir energy on  $S^{d-1}$  is scheme-dependent, since it can be shifted by a counterterm proportional to powers of the scalar curvature. Thus, there is only a universal scheme-independent Casimir energy in  $d = 2$ . (The story is different in supersymmetric theories [317].)

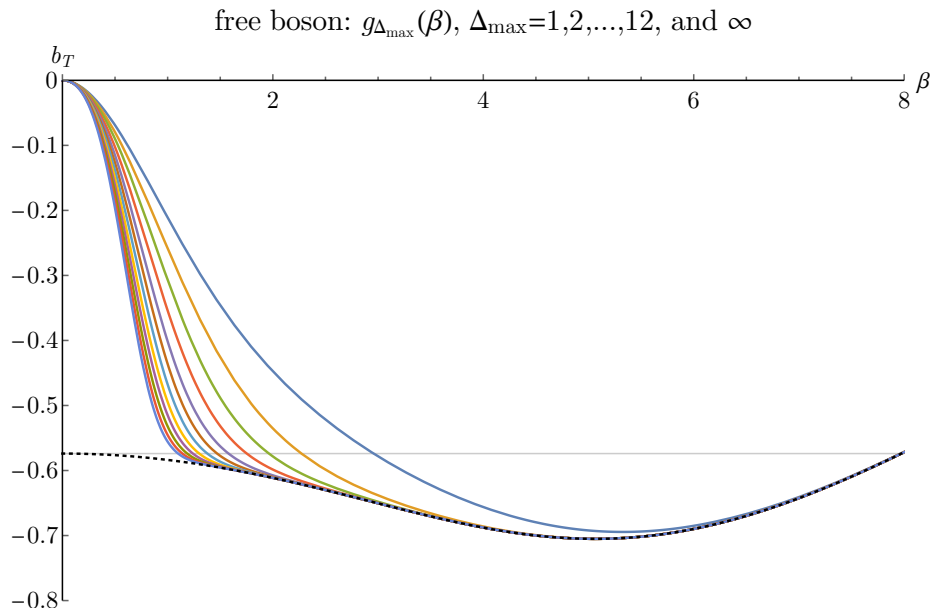


Figure A.1: The function  $g_{\Delta_{\max}}(\beta)$  in the free boson theory in 3d, plotted for the values  $\Delta_{\max} = 1, 2, \dots, 12$  (colors), and  $\Delta_{\max} = \infty$  (black dotted line). The value of  $b_T$  in the free theory (gray horizontal line) is  $-\frac{3\zeta(3)}{2\pi} \approx -0.574$ .

line) decays as  $e^{-\beta/2}$  for large  $\beta$  (coming from the contribution of the lowest-dimension operator  $\phi$ ). It reaches a minimum near  $\beta = 5$ , and then smoothly approaches the value  $b_T = -\frac{3\zeta(3)}{2\pi} \approx -0.574$  as  $\beta \rightarrow 0$ . The curves with finite  $\Delta_{\max}$  move closer to the  $\Delta_{\max} = \infty$  curve, with longer and longer plateaus near  $b_T$  before eventually going to 0 at  $\beta = 0$ .

The 3d Ising model is a nonperturbative theory where we don't know the full spectrum, but we do know a large part of it to reasonable precision from numerical bootstrap computations [20, 41, 43, 54–56, 318]. In particular, the spectrum of operators appearing in the  $\sigma \times \sigma$ ,  $\sigma \times \epsilon$ , and  $\epsilon \times \epsilon$  OPEs are known up to dimension 8 [20]. Some additional low-twist families are known up to very high dimension, but these are a small portion of the high-dimension spectrum. The lowest-dimension operator not appearing in the above OPEs is expected to be a  $\mathbb{Z}_2$ -even vector with dimension approximately 6, though its dimension is not known to high precision [319]. Thus, our knowledge of the spectrum begins to fade when  $\Delta_{\max} \approx 6$ . Nevertheless, in figure A.2, we estimate  $g_{\Delta_{\max}}(\beta)$  by including the known operators with dimension  $\Delta \leq \Delta_{\max}$ .

Despite our ignorance of the high-dimension spectrum, the plot in figure A.2 already shows similar structure to the free scalar case, with a plateau beginning to form near  $b_T \approx -0.45$ , close to the value  $b_T \approx -0.459$  determined via Monte Carlo simulations

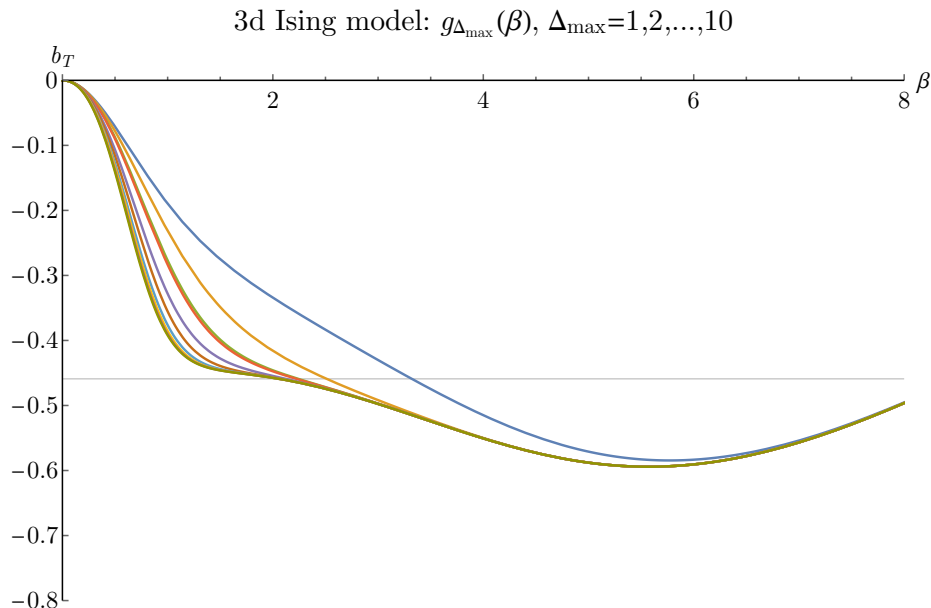


Figure A.2: The function  $g_{\Delta_{\max}}(\beta)$  in the 3d Ising model, estimated using known operators only, and plotted for the values  $\Delta_{\max} = 1, 2, \dots, 10$ . The value of  $b_T$  determined from Monte Carlo simulations is  $-0.459$  (gray horizontal line, [74–76]).

[74–76]. It would be interesting to understand whether figure A.2 can be turned into a rigorous estimate, perhaps by understanding better the analytic structure of  $g_{\infty}(\beta)$ . It would also be interesting to understand whether the existence of a minimum, seen as the “dip” in these plots, is a feature shared by all CFTs.

## A.2 One-point functions on $S_{\beta}^1 \times \mathbb{R}^{d-1}$ from one-point functions on $S_{\beta}^1 \times S^{d-1}$

Here we make some basic comments about the challenges in determining  $b_{\mathcal{O}}$  by passage from  $S_{\beta}^1 \times S_L^{d-1}$ , for generic operators  $\mathcal{O}$ . The strategy is to expand the one-point function in  $S_{\beta}^1 \times S_L^{d-1}$  conformal blocks, and take the large  $L$  limit. In (2.28), we gave the conformal block expansion for  $\langle \mathcal{O} \rangle_{S_{\beta}^1 \times S_L^{d-1}}$ . We focus here on  $d = 2$  for simplicity. In this case, the thermal blocks factorize,

$$F(h_{\mathcal{O}}, \bar{h}_{\mathcal{O}}; h_{\mathcal{O}'}, \bar{h}_{\mathcal{O}'} | \beta) = |\mathbf{g}(h_{\mathcal{O}}, h_{\mathcal{O}'} | \beta)|^2 \quad (\text{A.8})$$

where  $|f(h)|^2 \equiv f(h)f(\bar{h})$ , and (e.g. [320, 321])

$$\mathbf{g}(h_{\mathcal{O}}, h_{\mathcal{O}'} | \beta) = \frac{q^{h_{\mathcal{O}'}}}{(1-q)^{h_{\mathcal{O}}}} {}_2F_1(2h_{\mathcal{O}'} - h_{\mathcal{O}}, 1 - h_{\mathcal{O}}; 2h_{\mathcal{O}'}; q) \quad (\text{A.9})$$

where  $q \equiv e^{-\beta}$ . (A.8) generalizes in the obvious way to unequal left- and right-moving temperatures. Using the connection formulae for hypergeometric functions, we may

rewrite the left-moving block (for generic  $(h_{\mathcal{O}}, h_{\mathcal{O}'})$ ) as

$$\begin{aligned} & \mathfrak{g}(h_{\mathcal{O}}, h_{\mathcal{O}'}|\beta) \\ &= \frac{q^{h_{\mathcal{O}'}}}{(1-q)^{h_{\mathcal{O}}}} \left[ \frac{\Gamma(2h_{\mathcal{O}'})\Gamma(2h_{\mathcal{O}}-1)}{\Gamma(h_{\mathcal{O}})\Gamma(2h_{\mathcal{O}'}+h_{\mathcal{O}}-1)} {}_2F_1(2h_{\mathcal{O}'}-h_{\mathcal{O}}, 1-h_{\mathcal{O}}; 2-2h_{\mathcal{O}}; 1-q) \right. \\ & \quad \left. + (1-q)^{2h_{\mathcal{O}'-1}} \frac{\Gamma(2h_{\mathcal{O}'})\Gamma(1-2h_{\mathcal{O}})}{\Gamma(2h_{\mathcal{O}'}-h_{\mathcal{O}})\Gamma(1-h_{\mathcal{O}})} {}_2F_1(h_{\mathcal{O}}, 2h_{\mathcal{O}'}+h_{\mathcal{O}}-1; 2h_{\mathcal{O}}; 1-q) \right]. \end{aligned} \tag{A.10}$$

As  $\beta \rightarrow 0$ , there are two branches:

$$\mathfrak{g}(h_{\mathcal{O}}, h_{\mathcal{O}'}|\beta) \sim \beta^{-h_{\mathcal{O}}} \frac{\Gamma(2h_{\mathcal{O}'})\Gamma(2h_{\mathcal{O}}-1)}{\Gamma(h_{\mathcal{O}})\Gamma(2h_{\mathcal{O}'}+h_{\mathcal{O}}-1)} + \beta^{h_{\mathcal{O}'-1}} \frac{\Gamma(2h_{\mathcal{O}'})\Gamma(1-2h_{\mathcal{O}})}{\Gamma(2h_{\mathcal{O}'}-h_{\mathcal{O}})\Gamma(1-h_{\mathcal{O}})}. \tag{A.11}$$

Combining the left- and right-moving blocks yields the full scaling behavior of the torus one-point blocks at high temperature.<sup>4</sup>

It is remarkable that, for  $h_{\mathcal{O}} \geq 1/2$ , the leading term in (A.11) exhibits the same scaling of the full one-point function on  $S_{\beta}^1 \times \mathbb{R}$ , for all intermediate operators  $\mathcal{O}'$ . For instance, for scalar  $\mathcal{O}$  with  $\Delta_{\mathcal{O}} = 2h_{\mathcal{O}} > 1$ ,

$$F(h_{\mathcal{O}}, \bar{h}_{\mathcal{O}}; h_{\mathcal{O}'}, \bar{h}_{\mathcal{O}'}|\beta) \sim \beta^{-2h_{\mathcal{O}}} \left| \frac{\Gamma(2h_{\mathcal{O}'})\Gamma(2h_{\mathcal{O}}-1)}{\Gamma(h_{\mathcal{O}})\Gamma(2h_{\mathcal{O}'}+h_{\mathcal{O}}-1)} \right|^2. \tag{A.12}$$

This leads to a formal expression for the  $S_{\beta}^1 \times \mathbb{R}^{d-1}$  one-point function  $b_{\mathcal{O}}$  as a sum over states, in the limit of high temperature:

$$b_{\mathcal{O}} = \frac{\Gamma^2(2h_{\mathcal{O}}-1)}{\Gamma^2(h_{\mathcal{O}})} \sum_{\text{Primary } \mathcal{O}'} f_{\mathcal{O}\mathcal{O}'\mathcal{O}'} \left| \frac{\Gamma(2h_{\mathcal{O}'})}{\Gamma(2h_{\mathcal{O}'}+h_{\mathcal{O}}-1)} \right|^2 \quad \left( h_{\mathcal{O}} > \frac{1}{2} \right). \tag{A.13}$$

Note that the summand is not, in general, sign-definite, and receives contributions from all spins and arbitrarily high energies.<sup>5</sup> On the other hand, for low-dimension operators  $\mathcal{O}$ , with  $h_{\mathcal{O}} < 1/2$ , the second term of (A.11) dominates, and even the recovery of the requisite  $\beta^{-2h_{\mathcal{O}}}$  scaling at high temperature is sensitive to the details of the full sum. For any value of  $h_{\mathcal{O}}$ , one can approximate  $b_{\mathcal{O}}$  using the asymptotics of  $f_{\mathcal{O}\mathcal{O}'\mathcal{O}'}$  for  $h_{\mathcal{O}'} \gg 1$ , which are often determined by eigenstate thermalization.

<sup>4</sup>The  $d > 2$  one-point blocks have similar behavior. In fact, there is a third branch in that case. We thank Alex Maloney for sharing the results of [80] with us.

<sup>5</sup>One can instead use Virasoro conformal blocks, although these are not known in full generality. At large central charge  $c$ , the torus one-point Virasoro block is simply the the global block (A.8) times the Virasoro vacuum character,  $\chi_{vac}(\beta) = q^{(1-c)/24}(1-q)\eta^{-1}(q)$ , where  $\eta(q)$  is the Dedekind eta function. At high temperature,  $\chi_{vac}(\beta) \sim \beta^{3/2}$ . This implies that at  $c \rightarrow \infty$ , the sum (A.13) must, in general, diverge.



### A.3 Thermal mass in the $O(N)$ model at large $N$

Our starting point is the Lagrangian (2.90). By integrating out the fields  $\phi_i$ , the partition function is given by,

$$Z = \int D\sigma e^{-\frac{N}{2} \text{Tr} \log(-\nabla^2 + \sigma)}. \quad (\text{A.14})$$

As  $N \rightarrow \infty$  the partition function is dominated by the saddle-point solution for  $\sigma$ . On  $\mathbb{R}^3$ , due to Poincare symmetry, the saddle-point solution can be argued to be  $\sigma = 0$ . However, on  $\mathbb{R}^2 \times S^1_\beta$ , the saddle-point solution is nonzero. The saddle point equation is

$$\frac{\partial}{\partial \sigma} \text{Tr} \log(-\nabla^2 + \sigma) = \sum_{n=-\infty}^{\infty} \int \frac{d^2 p}{(2\pi)^2} \frac{1}{\omega_n^2 + p^2 + \sigma} = 0, \quad (\text{A.15})$$

where  $\omega_n = 2\pi n/\beta$  are the Matsubara frequencies. Doing the sum over  $n$ , we reduce this equation to

$$\int_0^\Lambda \frac{p dp}{2\pi} \frac{1}{2\sqrt{p^2 + \sigma}} \coth \frac{\sqrt{p^2 + \sigma}}{2T} = 0. \quad (\text{A.16})$$

Now make the change of variables  $x = \sqrt{p^2 + \sigma}/2T$ . The integral of  $\coth x$  is  $\log \sinh x$ . The upper limit gives  $\log \sinh[\Lambda/2T] \approx \Lambda/2T - \log 2$ . The linear UV divergence is subtracted out by hand, and the  $\log 2$  is left over. Alternatively, we could replace the integrand  $\coth x$  by  $\coth x - 1$ , which is equivalent to a Pauli-Villars regulator. Thus, overall we get the equation

$$\log \left[ 2 \sinh \frac{\sqrt{\sigma}}{2T} \right] = 0, \quad (\text{A.17})$$

whose solution is (2.91).

### A.4 Subtleties in dimensional reduction of CFTs

The dimensional reduction of a  $d$ -dimensional CFT on  $S^1$  does not always give a well-defined theory in  $d - 1$ -dimensions. For example, a problem occurs if we try to compactify the free boson CFT in 3d down to 2d (with periodic boundary conditions around the  $S^1$ ).<sup>6</sup> Naively, we should get the 2d free boson with noncompact target space, but this theory is pathological because correlations grow logarithmically with distance. Another way to see the problem is that if we try to compute the propagator using the method of images, the sum over images diverges.<sup>7</sup>

<sup>6</sup>Conformal invariance requires that the free boson CFT have a noncompact target space in 3d.

<sup>7</sup>It is interesting to ask what happens if we have a physical system that has an EFT description in terms of a 3d free boson, and we place it at finite temperature. In this case, the thermal physics

We expect this issue to arise whenever we compactify a 3d CFT with a nontrivial moduli space of vacua down to 2d, as long as the boundary conditions do not destroy the moduli space. For example, supersymmetric compactifications of 3d SCFTs with Higgs or Coulomb branches should be treated with care. One way to study such theories is to introduce twisted boundary conditions that remove the zero mode from the path integral.<sup>8</sup> Correlation functions in the twisted setting then share many similar properties to those we discuss in this work (for example an OPE and crossing equation). It would be interesting to adapt the techniques in this work to deal with general twisted boundary conditions. In our case, thermal compactification does the job because it breaks supersymmetry and generically lifts the moduli space.

### A.5 Fixed point of self-corrections of double-twist families

Let's consider the self-corrections of the  $[\phi\phi]_0$  family in  $\langle\phi\phi\rangle_\beta$ . To leading order in large  $\bar{h}$ , self-correction is the linear map

$$S : a_{[\phi\phi]_0} \mapsto a_{[\phi\phi]_0} + \sum_{n=0}^{\infty} \alpha_0^{\text{even}} \left[ \frac{\delta^n}{n!} a_{[\phi\phi]_0}, \delta, h_e \right] (1 + (-1)^J) K_J S_{h_f - h_e, h_e}^{(n)}(\bar{h}). \quad (\text{A.18})$$

Self-corrections of  $a_{[\phi\phi]_0}$  take the general form

$$a_{[\phi\phi]_0}(J) = a_{[\phi\phi]_0}^0(J) + (1 + (-1)^J) K_J \sum_{m=0}^{\infty} f_m S_{h_f - h_e, h_e}^{(m)}(\bar{h}) \quad (\text{A.19})$$

with some initial  $a_{[\phi\phi]_0}^0(J)$ , and some coefficients  $f_m$ . Inserting this form into the self-correction map, we get

$$S[a_{[\phi\phi]_0}] = a_{[\phi\phi]_0} + (1 + (-1)^J) K_J \sum_{n=0}^{\infty} \left( \lambda_n + \sum_{m=0}^{\infty} f_m T_n^m \right) S_{h_f - h_e, h_e}^{(n)}, \quad (\text{A.20})$$

where we have defined the vector

$$\lambda_n = \alpha_0^{\text{even}} \left[ \frac{\delta^n}{n!} a_{[\phi\phi]_0}^0, \delta, h_e \right] \quad (\text{A.21})$$

and matrix

$$T_n^m = \alpha_0^{\text{even}} \left[ \frac{\delta^n}{n!} S_{h_f - h_e, h_e}^{(m)}, \delta, h_e \right], \quad (\text{A.22})$$

---

can depend on UV details that are not directly captured by the 3d effective CFT. For example, if the 3d boson is the Goldstone boson of a broken  $U(1)$  symmetry with symmetry breaking scale  $\Lambda$ , its dimensional reduction is better described as a 2d boson with compact target space, where the radius is  $R \propto \sqrt{\beta\Lambda}$ .

<sup>8</sup>We thank Nati Seiberg for discussions on this point.

of coefficients. To evaluate these coefficients, we need to evaluate sums of  $S_{c,\Delta}^{(m)}(\bar{h})$ , which is easily obtained by generalizing our treatment of the sums of  $S_{c,\Delta}(\bar{h})$  by taking derivatives of  $c$ . The fixed point of the map  $S$  satisfies  $S[a] = a$ , which from (A.20) is the solution to the linear equation

$$\lambda_n + f_m T_n^m = 0. \quad (\text{A.23})$$

Inverting this equation, the fixed point is determined by

$$f_m = \lambda_n (T^{-1})_m^n. \quad (\text{A.24})$$

In practice, one can work order-by-order in the small anomalous dimensions of the family, effectively truncating the  $m$  and  $n$  to some finite order, thus avoiding having to compute an infinite number of coefficients and to invert an infinite matrix. Finally, let's note that it is possible to generalize this method to the  $[\phi\phi]_n$  families, and even potentially to considering collections of families at once.

## APPENDIX TO CHAPTER 3

Appendix to chapter 3 is attached here.

**B.1 Details of the Monte-Carlo simulation**

To compute the thermal two-point function  $\langle \sigma \sigma \rangle_\beta$  using Monte-Carlo integration, we implemented Wolff's cluster algorithm on a periodic square lattice of size  $40 \times 500 \times 500$ . We used the spin-spin coupling  $\beta_{\text{critical}} = 0.22165463(8)$  from [126]. The periodic direction of size 40 represents the thermal circle, while the directions of size 500 approximate noncompact  $\mathbb{R}^2$ . The MC integration was performed over  $4 \times 10^8$  iteration steps.

As usual, there are three main sources of error: statistical error, finite-size effects (IR), and lattice-size effects (UV). One of the nice properties of thermal correlators is that finite-size effects are much easier to control than for flat-space correlators. The reason is that we can imagine dimensionally reducing our system along the thermal circle. The result is a theory with thermal mass  $m_{\text{th}} \sim 1/\beta$ , and consequently fluctuations in the noncompact directions die off like  $e^{-x/\beta}$ . Thus, on a torus with lengths  $\beta \times L \times L$ , we expect corrections from the finiteness of  $L$  to be suppressed by  $e^{-L/\beta} \sim 4 \times 10^{-6}$ . By contrast, to compute flat-space two-point functions, one must consider torii with size  $L \times L \times L$ . In that case, finite-size effects go like  $(L/x)^{-\Delta_{\mathcal{O}}}$ , where  $\mathcal{O}$  is the leading operator appearing in the OPE.

Thus, we expect that finite-size effects are negligible. Our main sources of error are statistical (visible as jitteriness in figure 3.5) and lattice effects which cause the simulation to become inaccurate near the coincident point singularity.

## APPENDICES TO CHAPTER 4

Appendices to chapter 4 are attached here.

**C.1 More on superconvergence in flat space****C.1.1 Commutativity and the Regge Limit**

It is also very easy to see the connection between the Regge limit and commutativity at the level of the four-point function. As the simplest example, consider  $\phi^3$  theory where we write different couplings in different channels. The amplitude takes the form

$$\mathcal{A}(s, t) = \frac{\alpha_s}{s} + \frac{\alpha_t}{t} + \frac{\alpha_u}{u}, \quad (\text{C.1})$$

where  $s + t + u = 0$ .

Let us consider the Regge limit of (C.1),  $t \rightarrow \infty$  and  $s$  fixed. The amplitude takes the form

$$\mathcal{A}(s, t) = \frac{\alpha_s}{s} + \frac{\alpha_t - \alpha_u}{t} + \dots \quad (\text{C.2})$$

For the superconvergence sum rule to hold, the amplitude should decay faster than  $\frac{1}{t}$ . We see that it implies  $\alpha_s = 0$  and  $\alpha_t = \alpha_u$ , the latter condition being the analog of shock commutativity.

A different example is to consider the scattering of a vector particle against the scalar shocks. The amplitude takes the form

$$\mathcal{A}(s, t, \epsilon_3, \epsilon_4) = \left( \alpha_t \frac{p_1 \cdot p_3}{p_1 \cdot p_2} + \alpha_u \frac{p_2 \cdot p_3}{p_1 \cdot p_2} \right) \left( \epsilon_3 \cdot \epsilon_4 + \frac{\epsilon_3 \cdot p_1 \epsilon_4 \cdot p_2}{p_1 \cdot p_3} + \frac{\epsilon_3 \cdot p_2 \epsilon_4 \cdot p_1}{p_2 \cdot p_3} \right), \quad (\text{C.3})$$

where the form of the amplitude is fixed by unitarity and we introduced different couplings for the  $t$ - and  $u$ -channel residues. The second bracket in (C.3) is manifestly symmetric under permutations of the shocks  $1 \leftrightarrow 2$ . On the other hand, we can rewrite the first bracket as

$$\mathcal{A}(s, t, \epsilon_3, \epsilon_4) \sim \left( \alpha_t \frac{u}{s} + \alpha_u \frac{t}{s} \right) \rightarrow (\alpha_u - \alpha_t)t, \quad t \rightarrow \infty, \quad s \text{ fixed}. \quad (\text{C.4})$$

Again, we explicitly see the relation between the commutativity of shocks and the Regge limit.

### C.1.2 Scalar-graviton elastic scattering

Let us consider a four-point amplitude of scalar-graviton elastic scattering in General Relativity. The scattering amplitude takes the form [322]

$$\mathcal{A} = -\frac{1}{2} \frac{p_1 \cdot p_3 p_2 \cdot p_3}{p_1 \cdot p_2} \left( \frac{1}{p_1 \cdot p_3} \epsilon_1 \cdot p_3 \epsilon_2 \cdot p_4 + \frac{1}{p_2 \cdot p_3} \epsilon_1 \cdot p_4 \epsilon_2 \cdot p_3 - \epsilon_1 \cdot \epsilon_2 \right)^2, \quad (\text{C.5})$$

where gravitons have momenta  $p_1$  and  $p_2$  and scalars have momenta  $p_3$  and  $p_4$ .

We evaluate this amplitude in the shockwave kinematics (4.17). The result takes the form

$$\mathcal{A}_{\phi g^* \rightarrow \phi g^*} = 2(p^u)^3 \frac{\vec{q}_1 \cdot \vec{q}_2}{p^v (p^u p^v - 2\vec{q}_1 \cdot \vec{q}_2)}. \quad (\text{C.6})$$

As expected from the discussion in the main text, at large  $p^v$  (or  $t$ ) this goes as  $\mathcal{A}_{\phi g^* \rightarrow \phi g^*} \sim \frac{1}{t^2}$ , in particular we can write the superconvergence sum rule. Upon taking the discontinuity at  $t = 0$ , we reproduce (4.42).

Let us contrast this behavior with the kinematics used in [96] which describes a high-energy scattering with physical transverse momenta and polarizations

$$\begin{aligned} p_1 &= \left(-\frac{\vec{q}^2}{p^v}, -p^v, \vec{q}\right), & p_2 &= \left(\frac{\vec{q}^2}{p^v}, p^v, \vec{q}\right), \\ p_3 &= \left(p^u, \frac{\vec{q}^2}{p^u}, -\vec{q}\right), & p_4 &= \left(-p^u, -\frac{\vec{q}^2}{p^u}, -\vec{q}\right), \end{aligned} \quad (\text{C.7})$$

and polarizations

$$\epsilon_1 = \left(-2\frac{\vec{e}_1 \cdot \vec{q}}{p^v}, 0, \vec{e}_1\right), \quad \epsilon_2 = \left(2\frac{\vec{e}_2 \cdot \vec{q}}{p^v}, 0, \vec{e}_2\right). \quad (\text{C.8})$$

The scattering amplitude then evaluates to

$$\mathcal{A}_{\phi g \rightarrow \phi g} = (\vec{e}_1 \cdot \vec{e}_2)^2 \frac{(p^u p^v)^2}{16\vec{q}^2} \left(1 - \frac{\vec{q}^2}{p^u p^v}\right)^2 \left(1 + \frac{\vec{q}^2}{p^u p^v}\right)^2. \quad (\text{C.9})$$

This time the amplitude grows as  $\mathcal{A}_{\phi g \rightarrow \phi g} \sim t^2$  consistent with the usual intuition about the high energy behavior of gravitational scattering. In this case, it is not possible to write the superconvergence sum rule. The difference in the high energy behavior of (C.6) and (C.9) is  $\frac{1}{t^{J_1+J_2}} = \frac{1}{t^4}$  as discussed in the main text.

### C.1.3 Gravitational sum rule in a generic theory

In this section, we describe the superconvergence sum rule for commutativity of coincident shocks in a generic tree-level theory of gravity. Firstly, a shock three-point

amplitude for a massive graviton  $\tilde{g}$  with mass  $m$  takes the form

$$\begin{aligned} \mathcal{A}_{g_1 g_3 \tilde{g}}^{\mu\nu} &= \tilde{\alpha}_2 [\epsilon_1^\mu p_3^\nu (\epsilon_3 \cdot p_1) + \epsilon_3^\mu p_1^\nu (\epsilon_1 \cdot p_3) - p_1^\mu p_3^\nu (\epsilon_1 \cdot \epsilon_3) - \epsilon_1^\mu \epsilon_3^\nu (p_1 \cdot p_3)] \\ &\quad \times [(\epsilon_1 \cdot \epsilon_3)(p_1 \cdot p_3) - (\epsilon_3 \cdot p_1)(\epsilon_1 \cdot p_3)] \\ &\quad - \tilde{\alpha}_4 p_1^\mu p_3^\nu [(\epsilon_1 \cdot p_3)(\epsilon_3 \cdot p_1) - (\epsilon_1 \cdot \epsilon_3)(p_1 \cdot p_3)]^2, \end{aligned} \quad (\text{C.10})$$

where the  $\mu\nu$  indices should be contracted with the polarization tensor of the massive graviton. The massive graviton can appear as an intermediate state in the propagation of a graviton through two shocks. Its contribution to the shock commutator is given by

$$\Delta \mathcal{Q}_{J=2} = \frac{2\pi}{p^u} \left( \mathcal{A}_{g_1 g_3 \tilde{g}}^{\mu\nu} \Pi_{\mu\nu, \rho\sigma}^{\tilde{g}} \mathcal{A}_{g_2 g_4 \tilde{g}}^{\rho\sigma} - \mathcal{A}_{g_2 g_3 \tilde{g}}^{\mu\nu} \Pi_{\mu\nu, \alpha\beta}^{\tilde{g}} \mathcal{A}_{g_1 g_4 \tilde{g}}^{\alpha\beta} \right), \quad (\text{C.11})$$

where

$$\begin{aligned} \Pi_{\mu\nu, \alpha\beta}^{\tilde{g}} &= \frac{1}{2} (P_{\mu\alpha} P_{\nu\beta} + P_{\mu\beta} P_{\nu\alpha}) - \frac{1}{D-1} P_{\mu\nu} P_{\alpha\beta}, \\ P_{\alpha\beta} &= \eta_{\alpha\beta} + \frac{p_\alpha p_\beta}{m^2}. \end{aligned} \quad (\text{C.12})$$

The explicit result for (C.11) is

$$\begin{aligned} \Delta \mathcal{Q}_{J=2} &\sim \frac{1}{2} \tilde{\alpha}_2^2 \vec{e}_3 \cdot \vec{e}_4 \vec{q}_1 \cdot \vec{q}_2 (\vec{e}_3 \cdot \vec{q}_1 \vec{e}_4 \cdot \vec{q}_2 - \vec{e}_3 \cdot \vec{q}_2 \vec{e}_4 \cdot \vec{q}_1) \\ &\quad - \tilde{\alpha}_2 \tilde{\alpha}_4 \vec{q}_1 \cdot \vec{q}_2 (\vec{e}_3 \cdot \vec{q}_1 \vec{e}_4 \cdot \vec{q}_2 - \vec{e}_3 \cdot \vec{q}_2 \vec{e}_4 \cdot \vec{q}_1) (\vec{e}_3 \cdot \vec{q}_1 \vec{e}_4 \cdot \vec{q}_1 + \vec{e}_3 \cdot \vec{q}_2 \vec{e}_4 \cdot \vec{q}_2) \\ &\quad + \left( \tilde{\alpha}_4^2 [(\vec{q}_1 \cdot \vec{q}_2)^2 - \frac{1}{2} m^2 \vec{q}_1 \cdot \vec{q}_2] + \frac{\frac{D-2}{4} m^4 \tilde{\alpha}_4^2 - (D-4) m^2 \tilde{\alpha}_2 \tilde{\alpha}_4 + (D-10) \tilde{\alpha}_2^2}{4(D-1)} \right) \\ &\quad [(\vec{e}_3 \cdot \vec{q}_1)^2 (\vec{e}_4 \cdot \vec{q}_2)^2 - (\vec{e}_3 \cdot \vec{q}_2)^2 (\vec{e}_4 \cdot \vec{q}_1)^2]. \end{aligned} \quad (\text{C.13})$$

From this form of the commutator, it is immediately obvious that massive spin-2 particles cannot cancel the contributions of higher-derivative gravitational interactions.

For higher spin particles, the shock three-point amplitude has the same structure, with extra polarization indices contracted with the momentum  $\frac{1}{m^{J-2}} \epsilon_{\mu_1 \mu_2 \mu_3 \dots \mu_s} p_3^{\mu_3} \dots p_3^{\mu_J}$ . An extra structure takes the form

$$\begin{aligned} \mathcal{A}_{g g \tilde{g}} &= \frac{1}{m^{J-4}} \tilde{\alpha}_0^J \epsilon_{\mu\nu\rho\sigma} \cdot p_3 \dots p_3 [\epsilon_1^\mu p_3^\nu (\epsilon_3 \cdot p_1) + \epsilon_3^\mu p_1^\nu (\epsilon_1 \cdot p_3) - p_1^\mu p_3^\nu (\epsilon_1 \cdot \epsilon_3) - \epsilon_1^\mu \epsilon_3^\nu (p_1 \cdot p_3)] \\ &\quad [\epsilon_1^\rho p_3^\sigma (\epsilon_3 \cdot p_1) + \epsilon_3^\rho p_1^\sigma (\epsilon_1 \cdot p_3) - p_1^\rho p_3^\sigma (\epsilon_1 \cdot \epsilon_3) - \epsilon_1^\rho \epsilon_3^\sigma (p_1 \cdot p_3)], \end{aligned} \quad (\text{C.14})$$

where we added the proper powers of mass to have the same dimensionality for different couplings that will contribute to the superconvergence sum rules.

To compute the blocks we simply need to square these and sum over intermediate states in our kinematics. A convenient way to do that is to first contract a spin- $J$  symmetric traceless projection operator with null vectors. The result takes the form

$$\begin{aligned}\Pi_J(p, z_1, z_2) &= z_1^{\mu_1} \dots z_1^{\mu_J} \Pi_{\mu_1 \dots \mu_J; \nu_1 \dots \nu_J} z_2^{\nu_1} \dots z_2^{\nu_J} \\ &= \frac{\Gamma(J+1)\Gamma(\frac{D-3}{2})}{2^J \Gamma(\frac{D-3}{2} + J)} (-p^2)^{-J} (z_1 \cdot p)^J (z_2 \cdot p)^J C_J^{(\frac{D-3}{2})}(\eta),\end{aligned}\quad (\text{C.15})$$

where

$$\eta = 1 - \frac{p^2 z_1 \cdot z_2}{(z_1 \cdot p)(z_2 \cdot p)}.\quad (\text{C.16})$$

The commutator is then given by

$$\begin{aligned}\Delta \mathcal{Q}_J &= \frac{2\pi}{p^u} \left( \mathcal{A}_{g_1 g_3 \tilde{g}}^{\mu_1 \mu_2 \mu_3 \mu_4} \Pi_{\mu_1 \mu_2 \mu_3 \mu_4; \nu_1 \nu_2 \nu_3 \nu_4}(-p_1 - p_3; p_3, p_4) \mathcal{A}_{g_2 g_4 \tilde{g}}^{\nu_1 \nu_2 \nu_3 \nu_4} \right. \\ &\quad \left. - \mathcal{A}_{g_2 g_3 \tilde{g}}^{\mu_1 \mu_2 \mu_3 \mu_4} \Pi_{\mu_1 \mu_2 \mu_3 \mu_4; \nu_1 \nu_2 \nu_3 \nu_4}(-p_2 - p_3; p_3, p_4) \mathcal{A}_{g_1 g_4 \tilde{g}}^{\nu_1 \nu_2 \nu_3 \nu_4} \right),\end{aligned}\quad (\text{C.17})$$

where we defined

$$\Pi_{\mu_1 \mu_2 \mu_3 \mu_4; \nu_1 \nu_2 \nu_3 \nu_4} = D_{\mu_1}^{(1)} D_{\mu_2}^{(1)} D_{\mu_3}^{(1)} D_{\mu_4}^{(1)} D_{\nu_1}^{(2)} D_{\nu_2}^{(2)} D_{\nu_3}^{(2)} D_{\nu_4}^{(2)} \Pi_J(p, z_1, z_2)\quad (\text{C.18})$$

with  $D_\mu = (\frac{D}{2} - 1 + z \cdot \partial_z) \partial_\mu - \frac{1}{2} z_\mu \partial^2$  being the standard Thomas-Todorov operator. In both channels, the argument of the Gegenbauer polynomial becomes  $\eta = 1 + \frac{4\vec{q}_1 \cdot \vec{q}_2}{m^2}$ . The final superconvergence sum rule holds for any  $\vec{q}_1 \cdot \vec{q}_2$ .

The result for the commutator takes the form

$$\begin{aligned}\Delta \mathcal{Q}_J &= \vec{e}_3 \cdot \vec{e}_4 \vec{q}_1 \cdot \vec{q}_2 (\vec{e}_3 \cdot \vec{q}_1 \vec{e}_4 \cdot \vec{q}_2 - \vec{e}_3 \cdot \vec{q}_2 \vec{e}_4 \cdot \vec{q}_1) \Delta \mathcal{Q}_J^{(1)}(\eta) \\ &\quad + \vec{q}_1 \cdot \vec{q}_2 (\vec{e}_3 \cdot \vec{q}_1 \vec{e}_4 \cdot \vec{q}_2 - \vec{e}_3 \cdot \vec{q}_2 \vec{e}_4 \cdot \vec{q}_1) (\vec{e}_3 \cdot \vec{q}_1 \vec{e}_4 \cdot \vec{q}_1 + \vec{e}_3 \cdot \vec{q}_2 \vec{e}_4 \cdot \vec{q}_2) \Delta \mathcal{Q}_J^{(2)}(\eta) \\ &\quad + [(\vec{e}_3 \cdot \vec{q}_1)^2 (\vec{e}_4 \cdot \vec{q}_2)^2 - (\vec{e}_3 \cdot \vec{q}_2)^2 (\vec{e}_4 \cdot \vec{q}_1)^2] \Delta \mathcal{Q}_J^{(3)}(\eta),\end{aligned}\quad (\text{C.19})$$

where  $\Delta \mathcal{Q}_J^{(i)}$  are computable polynomials of  $\eta$  of maximal power  $\eta^J$  and quadratic functions of the couplings  $(\tilde{\alpha}_0^J, \tilde{\alpha}_2^J, \tilde{\alpha}_4^J)$ . We get three superconvergence sum rules, each should be satisfied identically for any  $\eta$ .

Let us go back to the non-commutativity introduced by the Gauss-Bonnet coupling  $\alpha_2$ . Adding a spin four particle with  $\tilde{\alpha}_2^J = \tilde{\alpha}_4^J = 0$  leads to

$$\begin{aligned}\Delta \mathcal{Q}_4^{(1)}(\eta) &\sim -(\tilde{\alpha}_0^4)^2, \\ \Delta \mathcal{Q}_4^{(3)}(\eta) &\sim -(\tilde{\alpha}_0^4)^2, \\ \Delta \mathcal{Q}_4^{(2)}(\eta) &= 0,\end{aligned}\quad (\text{C.20})$$



where we omitted irrelevant positive-definite  $D$ -dependent coefficients. We see that by adding to the Gauss-Bonnet theory a single spin four particle and a non-minimally coupled scalar, we can satisfy the superconvergence relations in flat space. With one spin four particle in the spectrum, the theory would still have pathological Regge behavior which should become visible in a slightly different kinematics, see e.g. [96].

## C.2 Noncommutativity of light-transformed scalars

Let us consider a simple model that illustrates some of the subtleties involved in computations of light transforms at coincident points. Imagine four free complex scalar fields of different masses in AdS. The dual theory is a version of generalized free field theory with scalar operators  $\phi_k$  with dimensions  $\Delta_k$ . We consider the following correlator<sup>1</sup>

$$\mathcal{O}_1 = \phi_a \phi_b, \quad \mathcal{O}_2 = \phi_b^\dagger \phi_d^\dagger, \quad \mathcal{O}_3 = \phi_c^\dagger \phi_d, \quad \mathcal{O}_4 = \phi_a^\dagger \phi_c, \quad (\text{C.21})$$

where  $\mathcal{O}_{1,2}$  model detectors and  $\mathcal{O}_{3,4}$  model sinks. The four-point function takes the form

$$\langle \mathcal{O}_4 \mathcal{O}_1 \mathcal{O}_2 \mathcal{O}_3 \rangle = \frac{1}{x_{12}^{2\Delta_b} x_{34}^{2\Delta_c}} \frac{1}{x_{14}^{2\Delta_a} x_{23}^{2\Delta_d}}. \quad (\text{C.22})$$

An immediate observation about this four-point function is that

$$\langle [\mathcal{O}_4, \mathcal{O}_2][\mathcal{O}_1, \mathcal{O}_3] \rangle = 0. \quad (\text{C.23})$$

Therefore, doing the light transform and taking the coincident limit for the  $\mathbf{L}[\mathcal{O}_2]\mathbf{L}[\mathcal{O}_1]$  ordering of light ray operators always exist and is trivially equal to zero.

For the other ordering of operators, we get

$$\langle [\mathcal{O}_4, \mathcal{O}_1][\mathcal{O}_2, \mathcal{O}_3] \rangle = \frac{4 \sin \pi \Delta_a \sin \pi \Delta_d \operatorname{sgn}[x_{14}^0] \theta(-x_{14}^2) \operatorname{sgn}[x_{23}^0] \theta(-x_{23}^2)}{x_{12}^{2\Delta_b} x_{34}^{2\Delta_c} (-x_{14}^2)^{\Delta_a} (-x_{23}^2)^{\Delta_d}}. \quad (\text{C.24})$$

To do the light transforms, it is convenient to specialize to simple kinematics in the lightcone coordinates  $(u, v, \vec{y})$  for which we get

$$\begin{aligned} & \langle \Omega | \mathcal{O}_4(1, -1, \vec{0}) \mathcal{O}_1(-\delta u, v_1, -\vec{y}) \mathcal{O}_2(\delta u, v_2, \vec{y}) \mathcal{O}_3(-1, 1, \vec{0}) | \Omega \rangle \\ &= \frac{1}{(2\delta u(v_1 - v_2 - i\epsilon) + 4\vec{y}^2)^{\Delta_b} 4^{\Delta_c}} \frac{1}{((1 + \delta u)(v_1 + 1 + i\epsilon) + \vec{y}^2)^{\Delta_a} ((1 + \delta u)(1 - v_2 + i\epsilon) + \vec{y}^2)^{\Delta_d}}, \end{aligned} \quad (\text{C.25})$$

<sup>1</sup>See fig. 3 in [229], where this model of detector cross-talk is discussed.

where we explicitly wrote the  $i\epsilon$  prescription dictated by the ordering of operators and introduced a small separation in the  $u$ -direction between the detector operators.

Let us first analyze the integral (4.147) which guarantees both the existence and commutativity of the coincident limit. To do that we set  $\delta u = 0$  in (C.25) and perform the integral over  $v_1$  and  $v_2$

$$\int_{-\infty}^{\infty} dv_1 dv_2 \frac{1}{(4\bar{y}^2)^{\Delta_b} 4^{\Delta_c}} \frac{1}{(v_1 + 1 + \bar{y}^2 + i\epsilon)^{\Delta_a} (1 - v_2 + \bar{y}^2 + i\epsilon)^{\Delta_d}}. \quad (\text{C.26})$$

This integral is zero for  $\Delta_a, \Delta_d > 1$  and diverges otherwise. Let us check that it agrees with the sufficient conditions for the existence of the integral derived in the main text. For the local operators at hand, we have  $J_1 = J_2 = 0$  and  $\Delta_1 = \Delta_a + \Delta_b$  and  $\Delta_2 = \Delta_b + \Delta_d$ . The Euclidean OPE, light-cone OPE, and the Regge limit are all controlled by the leading operator that appears in the OPE of  $\mathcal{O}_1$  and  $\mathcal{O}_2$ , which has dimension  $\Delta_a + \Delta_d$  and spin 0. The strongest constraint comes from the light-cone OPE (4.155) which for the case at hand becomes

$$-|\Delta_a - \Delta_d| > 2 - (\Delta_a + \Delta_d). \quad (\text{C.27})$$

This can be rewritten as

$$4(\Delta_a - 1)(\Delta_d - 1) > 0, \quad (\text{C.28})$$

which indeed coincides with the direct analysis above. Note also that in this case, the behavior of the double discontinuity (C.24) is no different from the behavior of the original Wightman function. Using the analysis from the main text, we again conclude that the sufficient condition for the existence of the coincident limit of the light transform is  $\Delta_a, \Delta_d > 1$ .

Let us now do the light transform first, while keeping  $\delta u \neq 0$ . Again it is clear from the position of poles that the result depends on the ordering of the operators  $\mathcal{O}_1$  and  $\mathcal{O}_2$ , one of them trivially producing zero in agreement with (C.23). For the nontrivial ordering, we get

$$\begin{aligned} & \int_{-\infty}^{\infty} dv_1 dv_2 \langle \Omega | \mathcal{O}_4(1, -1, \vec{0}) \mathcal{O}_1(-\delta u, v_1, -\vec{y}) \mathcal{O}_2(\delta u, v_2, \vec{y}) \mathcal{O}_3(-1, 1, \vec{0}) | \Omega \rangle \quad (\text{C.29}) \\ & = (2\pi i)^2 e^{-i\pi(\Delta_a + \Delta_d)} \frac{\Gamma(\Delta_a + \Delta_b + \Delta_d - 2)}{\Gamma(\Delta_a)\Gamma(\Delta_b)\Gamma(\Delta_d)4^{\Delta_c}} (2\delta u)^{\Delta_a + \Delta_d - 2} (4\bar{y}^2)^{2 - \Delta_a - \Delta_b - \Delta_d}. \end{aligned}$$

Next, we take the  $\delta u \rightarrow 0$  limit for the nontrivial ordering of light ray operators  $\mathbf{L}[\mathcal{O}_1]\mathbf{L}[\mathcal{O}_2]$ . We see that the result is zero for  $\Delta_a + \Delta_d > 2$ , finite and non-trivial for

$\Delta_a + \Delta_d = 2$ , and divergent for  $\Delta_a + \Delta_d < 2$ . Thus, we observe that the coincident limit exists beyond the range found by the sufficient conditions described in the text.

Apart from variations of the correlator above where subtleties related to the coincident limit of the light-ray operators can be demonstrated, one can also consider exchange Witten diagrams in AdS where similar subtleties occur. This can be easily seen using the Mellin space approach used to efficiently compute light transforms in [147].

### C.3 Fourier transform of two-point functions

In this appendix we compute the Fourier transform of the two-point function, which in Euclidean signature takes the form

$$\langle \mathcal{O}_J(x_1, z_1) \mathcal{O}_J(x_2, z_2) \rangle = \frac{(z_1 \cdot I(x_{12}) \cdot z_2)^J}{x_{12}^{2\Delta}}. \quad (\text{C.30})$$

Continuation to Lorentzian signature for

$$\langle \mathcal{O} | \mathcal{O}_J(0, z_1) \mathcal{O}_J(x, z_2) | \mathcal{O} \rangle \quad (\text{C.31})$$

amounts to using the Euclidean expression for spacelike  $x$  and the  $i\epsilon$  prescription  $x^0 \rightarrow x^0 + i\epsilon$  for analytic continuation to timelike  $x$ .

The basic strategy is the same as for three-point functions. We first decompose into harmonic functions (4.379)

$$(z_1 \cdot I(x) \cdot z_2)^J = \sum_{k=0}^J \beta_k (z_1 \cdot z_2)^k (-x^2)^{k-J} [z_1^{J-k} z_2^{J-k} |x], \quad (\text{C.32})$$

with

$$\beta_k = \frac{2^{J-k} J! (\frac{d-2}{2} + J - k)_{J-k+1}}{k! (J-k)! (\frac{d-2}{2} + J)_{J-k+1}}. \quad (\text{C.33})$$

Therefore, for  $x > 0$  the Wightman two-point function (C.31) takes form

$$\langle \mathcal{O} | \mathcal{O}_J(0, z_1) \mathcal{O}_J(x, z_2) | \mathcal{O} \rangle = \sum_{k=0}^J e^{i\pi\Delta} \beta_k (z_1 \cdot z_2)^k (-x^2)^{k-J-\Delta} [z_1^{J-k} z_2^{J-k} |x]. \quad (\text{C.34})$$

Using (4.382) we find that the Fourier transform is given by

$$\begin{aligned} & \langle \mathcal{O} | \mathcal{O}_J(0, z_1) \mathcal{O}_J(p, z_2) | \mathcal{O} \rangle \\ &= \sum_k e^{i\pi\Delta} \beta_k \widehat{\mathcal{F}}_{2\Delta, 2J-2k} (-p^2)^{\Delta-J+k-d} (z_1 \cdot z_2)^k [z_1^{J-k} z_2^{J-k} |p] \theta(p) \\ &= e^{i\pi\Delta} \widehat{\mathcal{F}}_{2\Delta, 2J} 2^J (-z_1 \cdot p)^J (-z_2 \cdot p)^J \\ & \quad \times {}_2F_1 \left( -J, \Delta - 1; \Delta - J - \frac{d-2}{2}; \frac{1}{2} \frac{p^2 (z_1 \cdot z_2)}{(z_1 \cdot p)(z_2 \cdot p)} \right) (-p^2)^{\Delta-d/2-J} \theta(p), \quad (\text{C.35}) \end{aligned}$$

where  $\widehat{\mathcal{F}}$  is given by (4.329).

We would now like to understand its decomposition into  $\text{SO}(d-1)$  projectors. For this, we set  $p = (1, 0, \dots)$ ,  $z_i = (1, n_i)$ , and decompose into  $(d-1)$ -dimensional Gegenbauer polynomials of  $\eta = (n_1 \cdot n_2)$ . In particular, we have

$$\begin{aligned} & {}_2F_1\left(-J, \Delta-1; \Delta-J-\frac{d-2}{2}; \frac{1-\eta}{2}\right) \\ &= \sum_{s=0}^J \frac{2^{-2J} J! (d+J-2)_J (d-2)_J (d-\Delta-1)_J}{\left(\frac{d-1}{2}\right)_J \left(\frac{d-2\Delta}{2}\right)_J} \frac{(-1)^s (d+2s-3)}{(J-s)! (d-3)_{J+s+1}} \frac{(\Delta-1)_s}{(d-\Delta-1)_s} C_s^{\left(\frac{d-3}{2}\right)}(\eta). \end{aligned} \quad (\text{C.36})$$

Plugging this into (C.35) and by using (4.276), we reproduce the claimed result (4.279).

#### C.4 Details on the light-transform of three-point structures

In this section we fix the overall normalization in our light-transform ansatz (4.300)

$$\langle 0 | \mathcal{O}'_2 \mathbf{L}[\phi_1] \mathcal{O}'_3 | 0 \rangle \propto \frac{V_{1,23}^{1-\Delta_\phi} V_{2,31}^{J'_2} V_{3,12}^{J'_3} f\left(\frac{H_{12}}{V_{1,23} V_{2,31}}, \frac{H_{13}}{V_{1,23} V_{3,12}}\right)}{X_{12}^{\frac{\bar{\tau}'_1 + \bar{\tau}'_2 - \bar{\tau}'_3}{2}} X_{13}^{\frac{\bar{\tau}'_1 + \bar{\tau}'_3 - \bar{\tau}'_2}{2}} X_{23}^{\frac{\bar{\tau}'_2 + \bar{\tau}'_3 - \bar{\tau}'_1}{2}}}. \quad (\text{C.37})$$

We have fixed the form of the function  $f$  in (4.306). To fix the coefficient, we will compute this light-transform in special kinematics. In particular, we take  $x_2 = 0$ ,  $x_3 = \infty$ , and  $x_1 = x$  in the absolute past of 0. Since light transform annihilates the vacuum state, we have

$$\langle 0 | \mathcal{O}'_2 \mathbf{L}[\phi_1] \mathcal{O}'_3 | 0 \rangle = \langle 0 | [\mathcal{O}'_2, \mathbf{L}[\phi_1]] \mathcal{O}'_3 | 0 \rangle, \quad (\text{C.38})$$

and the integral in  $\mathbf{L}$  in the right-hand side is only over positions of  $\phi_1$  which are in the past of  $\mathcal{O}'_2$ . The rest of the integral over  $\phi_1$  is spacelike from  $\mathcal{O}'_2$  and the commutator vanishes.

Therefore, we first need to find  $\langle 0 | [\mathcal{O}'_2, \phi_1] \mathcal{O}'_3 | 0 \rangle$  in the configuration where  $(2 > 1) \approx 3$ , starting from the Euclidean expression (4.299). We obtain

$$\langle 0 | \mathcal{O}'_2 \phi_1 \mathcal{O}'_3 | 0 \rangle = \frac{e^{-i\pi \frac{\bar{\tau}_1 + \bar{\tau}_2 - \bar{\tau}_3}{2}} V_{2,31}^{J'_2} V_{3,12}^{J'_3}}{(-X_{12})^{\frac{\bar{\tau}_1 + \bar{\tau}_2 - \bar{\tau}_3}{2}} X_{13}^{\frac{\bar{\tau}_1 + \bar{\tau}_3 - \bar{\tau}_2}{2}} X_{23}^{\frac{\bar{\tau}_2 + \bar{\tau}_3 - \bar{\tau}_1}{2}}}. \quad (\text{C.39})$$

We then specialize to our kinematics, which gives (using also  $\bar{\tau}_2 = \bar{\tau}'_2$  and  $\bar{\tau}_3 = \bar{\tau}'_3$ )

$$\langle 0 | \mathcal{O}'_2 \phi_1 \mathcal{O}'_3 | 0 \rangle = \frac{e^{-i\pi \frac{\bar{\tau}_1 + \bar{\tau}'_2 - \bar{\tau}'_3}{2}} (-x \cdot z_2)^{J'_2} (x^{-2} (x \cdot z_3))^{J'_3}}{(-x^2)^{\frac{\bar{\tau}_1 + \bar{\tau}'_2 - \bar{\tau}'_3}{2}}}. \quad (\text{C.40})$$

We can further set  $z_2 = z_3 = z$  to get

$$\langle 0 | \mathcal{O}'_2 \phi_1 \mathcal{O}'_3 | 0 \rangle = \frac{e^{-i\pi \frac{\bar{\tau}_1 + \bar{\tau}_2 - \bar{\tau}_3}{2}} (-x \cdot z)^{J'_2 + J'_3}}{(-x^2)^{\frac{\bar{\tau}_1 + \bar{\tau}'_2 - \bar{\tau}'_3 + 2J'_3}{2}}}. \quad (\text{C.41})$$

The opposite ordering comes with the opposite phase, and so

$$\langle 0 | [\mathcal{O}'_2, \phi_1] \mathcal{O}'_3 | 0 \rangle = -\frac{2i \sin\left(\pi \frac{\bar{\tau}_1 + \bar{\tau}_2 - \bar{\tau}_3}{2}\right) (-x \cdot z)^{J'_2 + J'_3}}{(-x^2)^{\frac{\bar{\tau}_1 + \bar{\tau}'_2 - \bar{\tau}'_3 + 2J'_3}{2}}}. \quad (\text{C.42})$$

We can evaluate the light transform  $\mathbf{L}[\phi_1]$  at  $z_1 = z$ ,

$$\langle 0 | [\mathcal{O}'_2, \mathbf{L}[\phi_1]] \mathcal{O}'_3 | 0 \rangle = -\int_{-\infty}^{2(z \cdot x)/x^2} d\alpha (-\alpha)^{-\bar{\tau}_1} \frac{2i \sin\left(\pi \frac{\bar{\tau}_1 + \bar{\tau}_2 - \bar{\tau}_3}{2}\right) (-x \cdot z)^{J'_2 + J'_3}}{(-x^2 + 2(x \cdot z)/\alpha)^{\frac{\bar{\tau}_1 + \bar{\tau}'_2 - \bar{\tau}'_3 + 2J'_3}{2}}}, \quad (\text{C.43})$$

where the upper bound of integration is due to the vanishing of the commutator. The integral is easy to perform, and by comparing to the ansatz (C.37), we can fix the overall coefficient. After some simple manipulations, the result is

$$\begin{aligned} \langle 0 | \mathcal{O}'_2 \mathbf{L}[\phi_1] \mathcal{O}'_3 | 0 \rangle &= -2\pi i \frac{2^{J'_1} \Gamma(-J'_1)}{\Gamma\left(\frac{\tau'_1 + \tau'_2 - \tau'_3}{2}\right) \Gamma\left(\frac{\tau'_1 - \tau'_2 + \tau'_3}{2}\right)} \frac{(-V_{1,23})^{J'_1} (-V_{2,31})^{J'_2} (-V_{3,12})^{J'_3}}{(-X_{12})^{\frac{\bar{\tau}'_1 + \bar{\tau}'_2 - \bar{\tau}'_3}{2}} X_{13}^{\frac{\bar{\tau}'_1 + \bar{\tau}'_3 - \bar{\tau}'_2}{2}} X_{23}^{\frac{\bar{\tau}'_2 + \bar{\tau}'_3 - \bar{\tau}'_1}{2}}} \\ &\times f\left(\frac{H_{12}}{V_{1,23} V_{2,31}}, \frac{H_{13}}{V_{1,23} V_{3,12}}\right) \quad ((2 > 1) \approx 3), \end{aligned} \quad (\text{C.44})$$

which holds for causal relations  $(2 > 1) \approx 3$ . Note that the explicit  $(-)$  signs are inserted so that there are no phase ambiguities in this causal configuration. Other causal configurations may be obtained by analytic continuation using the appropriate  $i\epsilon$  prescription.

In particular, we need to send point 1 to spatial infinity, which corresponds to  $1 \approx 2, 3$ , and we'll also choose  $3 > 2$ . During the corresponding analytic continuation, one can check that all  $V$  structures go from being negative back to being negative, with trivial monodromy around 0.<sup>2</sup> Then, the only phases come from the distances  $x_{ij}^2$  in the denominator, and it is easy to see that after the analytic continuation, we find

$$\begin{aligned} \langle 0 | \mathcal{O}'_2 \mathbf{L}[\phi_1] \mathcal{O}'_3 | 0 \rangle &= -2\pi i \frac{e^{i\pi \bar{\tau}'_2} 2^{J'_1} \Gamma(-J'_1)}{\Gamma\left(\frac{\tau'_1 + \tau'_2 - \tau'_3}{2}\right) \Gamma\left(\frac{\tau'_1 - \tau'_2 + \tau'_3}{2}\right)} \frac{(-V_{1,23})^{J'_1} (-V_{2,31})^{J'_2} (-V_{3,12})^{J'_3}}{X_{12}^{\frac{\bar{\tau}'_1 + \bar{\tau}'_2 - \bar{\tau}'_3}{2}} X_{13}^{\frac{\bar{\tau}'_1 + \bar{\tau}'_3 - \bar{\tau}'_2}{2}} (-X_{23})^{\frac{\bar{\tau}'_2 + \bar{\tau}'_3 - \bar{\tau}'_1}{2}}} \\ &\times f\left(\frac{H_{12}}{V_{1,23} V_{2,31}}, \frac{H_{13}}{V_{1,23} V_{3,12}}\right) \quad ((3 > 2) \approx 1). \end{aligned} \quad (\text{C.45})$$

<sup>2</sup>This really only matters for  $V_{1,23}$  and it is a general result that the value of this structure cannot wind around 0 with the  $i\epsilon$  prescriptions corresponding to the Wightman ordering in question [28].

This can also be derived by observing that if  $(2 > 1) \approx 3$ , then  $(3 > 2^-) \approx 1$ , which is the desired ordering if we replace  $2 \rightarrow 2^+$ . Using the fact that  $\langle 0 | \mathcal{O}'_2 \mathcal{T}^{-1} = e^{-i\pi\bar{\tau}'_2} \langle 0 | \mathcal{O}'_2$ , where  $\mathcal{T}$  is defined in [28], we can arrive at the same result.

### C.5 Structures for the sum rule

In this appendix, we describe the tensor structures  $\{2, 2|\lambda|2, 2\}_t$  and  $\{2, 2|\lambda|2, 2\}_s$  used in the main text. We start with  $\{2, 2|\lambda|2, 2\}_t$ . In principle, these structures are harmonic polynomials of  $n_i$  with appropriate homogeneity degree 2. To describe them, it is convenient to restrict to complex  $n_i$  subject to  $n_i^2 = 0$ . For example, the structure  $\{2, 2|0|2, 2\}_t$  is given in main text as

$$\left( (n_1 \cdot n_4)^2 - \frac{1}{d-1} \right) \left( (n_2 \cdot n_3)^2 - \frac{1}{d-1} \right). \quad (\text{C.46})$$

We can first restore homogeneity as

$$\left( (n_1 \cdot n_4)^2 - \frac{n_1^2 n_4^2}{d-1} \right) \left( (n_2 \cdot n_3)^2 - \frac{n_2^2 n_3^2}{d-1} \right), \quad (\text{C.47})$$

and then set  $n_i^2 \rightarrow 0$  to get

$$(n_1 \cdot n_4)^2 (n_2 \cdot n_3)^2, \quad (\text{C.48})$$

which is a more economical encoding of the original structure.

Using this convention, we have

$$\begin{aligned} \{2, 2|0|2, 2\}_t &= n_{14}^2 n_{23}^2, \\ \{2, 2|2|2, 2\}_t &= 4n_{14}n_{23} \left( \frac{n_{12}n_{34} + n_{13}n_{24} - n_{14}n_{23}}{2} - \frac{n_{14}n_{23}}{d-1} \right), \\ \{2, 2|4|2, 2\}_t &= 6 \left( \frac{8n_{14}^2 n_{23}^2}{(d+1)(d+3)} - \frac{8n_{14} (n_{13}n_{24} + n_{12}n_{34}) n_{23}}{d+3} + n_{13}^2 n_{24}^2 \right. \\ &\quad \left. + n_{12}^2 n_{34}^2 + 4n_{12}n_{13}n_{24}n_{34} \right), \\ \{2, 2|(1, 1)|2, 2\}_t &= \frac{8n_{14}^2 n_{23}^2}{d^2 - 5d + 6} - \frac{8n_{14} (n_{13}n_{24} + n_{12}n_{34}) n_{23}}{d-3} + 4(n_{13}n_{24} - n_{12}n_{34})^2, \\ \{2, 2|(2, 2)|2, 2\}_t &= 2n_{14}n_{23} (n_{12}n_{34} - n_{13}n_{24}), \\ \{2, 2|(3, 1)|2, 2\}_t &= -\frac{4(n_{13}n_{24} - n_{12}n_{34}) ((d+1)(n_{13}n_{24} + n_{12}n_{34}) - 4n_{14}n_{23})}{d+1}, \end{aligned} \quad (\text{C.49})$$

where  $n_{ij} = (n_i \cdot n_j)$ .

The structures  $\{2, 2|0|2, 2\}_s$  are obtained from  $\{2, 2|0|2, 2\}_t$  by exchanging  $2 \leftrightarrow 4$ .

## APPENDICES TO CHAPTER 5

Appendices to chapter 5 are attached here.

**D.1 Notation**

In this appendix, we summarize some of our notation. Many of our conventions are taken from [28].

It is useful to distinguish between physical correlation functions and conformally invariant structures. A correlation function in the state  $|\Omega\rangle$  represents a physical correlation function in a CFT. For example,

$$\langle\Omega|\mathcal{O}_1\cdots\mathcal{O}_n|\Omega\rangle \tag{D.1}$$

is a Wightman  $n$ -point function in a physical theory, and

$$\langle\mathcal{O}_1\cdots\mathcal{O}_n\rangle_\Omega \tag{D.2}$$

is a time-ordered  $n$ -point function in a physical theory.

Two- or three-point functions in the fictitious state  $|0\rangle$  represent conformally-invariant functions that are fixed by conformal invariance. If conformal symmetry allows a finite set of possible tensor structures, then we index the possibilities by a label  $(a)$ ,  $(b)$ , etc.. For example,

$$\langle 0|\mathcal{O}_1\mathcal{O}_2\mathcal{O}_3|0\rangle^{(a)} \tag{D.3}$$

represents a conformally-invariant tensor structure for the representations of  $\mathcal{O}_1, \mathcal{O}_2, \mathcal{O}_3$ , and  $a$  runs over the possible solutions to the conformal Ward identities. The above structure has an  $i\epsilon$  prescription appropriate for a Wightman function. Meanwhile,

$$\langle\mathcal{O}_1\mathcal{O}_2\mathcal{O}_3\rangle^{(a)} \tag{D.4}$$

represents a conformally-invariant structure with the  $i\epsilon$  prescription of a time-ordered correlator.

Primary operators are labeled by weights  $(\Delta, \rho)$  with respect to the conformal group  $\widetilde{\text{SO}}(d, 2)$ . Here,  $\Delta \in \mathbb{C}$  and  $\rho$  is an irreducible representation of  $\text{SO}(d - 1, 1)$ . ( $\Delta$  is

constrained to be real and sufficiently positive for local operators in unitary theories.) The weights of  $\rho$  can be further decomposed into  $\rho = (J, \lambda)$ , where  $J$  is a positive integer for local operators, but in general  $J \in \mathbb{C}$  can be continuous in Lorentzian signature. Here,  $\lambda$  is a finite-dimensional representation of  $\text{SO}(d-2)$ . We can think of  $J$  as the length of the first row of the Young diagram of  $\rho$ , while  $\lambda$  encodes the remaining rows. Altogether, we specify a conformal representation by the triplet  $(\Delta, J, \lambda)$ .

We often use the symbol  $\mathcal{O}$  to stand for the conformal representation with quantum numbers  $(\Delta, J, \lambda)$ . We use  $\phi$  to represent a scalar operator with quantum numbers  $(\Delta_\phi, 0, \bullet)$ , where  $\bullet$  is the trivial representation. (An exception is in section 5.7, where  $\mathcal{O}^{IJ}$  refers to a  $\mathbf{20}'$  operator in  $\mathcal{N} = 4$  SYM.)

If  $\mathcal{O}$  is a local operator, then  $\rho$  is a finite-dimensional representation. In this case, we define shadow and Hermitian conjugate representations as follows:

$$\begin{aligned}\tilde{\mathcal{O}} &: (d - \Delta, \rho^R), \\ \mathcal{O}^\dagger &: (\Delta, (\rho^R)^*),\end{aligned}\tag{D.5}$$

where  $\rho^R$  denotes the reflection of  $\rho$  and  $(\rho^R)^*$  is the dual of  $\rho^R$ .

For continuous-spin operators,  $\rho = (J, \lambda)$  is infinite-dimensional. The light transform turns a local operator into a continuous spin operator

$$\mathbf{L}[\mathcal{O}] : (1 - J, 1 - \Delta, \lambda) .\tag{D.6}$$

To define a conformally-invariant pairing for continuous spin operators we define

$$\begin{aligned}\mathcal{O}^S &: (d - \Delta, 2 - d - J, \lambda), \\ \mathcal{O}^{S\dagger} &: (d - \Delta, 2 - d - J, \lambda^*).\end{aligned}\tag{D.7}$$

Similarly, we define  $\mathcal{O}^F$  as an operator that can be paired with  $\mathbf{L}[\mathcal{O}]$  (upon Hermitian conjugation)

$$\begin{aligned}\mathcal{O}^F &: (J + d - 1, \Delta - d + 1, \lambda), \\ \mathcal{O}^{F\dagger} &: (J + d - 1, \Delta - d + 1, \lambda^*).\end{aligned}\tag{D.8}$$

To describe the causal relation between two points, we use the following symbols:

- $x \approx y$  if  $x$  and  $y$  are space-like;



- $x > y$  ( $x < y$ ) if  $x$  lies in the future (past) light-cone of  $y$ ;
- $x \gtrsim y$  ( $x \lesssim y$ ) if  $x$  is on the future (past) null cone of  $y$ .

In section 5.3, we extensively use Euclidean and Lorentzian pairings between the 2-, 3- and 4-point functions. These are described in detail in appendix C and D of [28] correspondingly.

## D.2 Representations of orthogonal groups

### D.2.1 General index-free notation

A finite-dimensional representation of  $\text{SO}(d)$  is labeled by a sequence

$$\mathbf{m}_d = (m_{d,1}, \dots, m_{d,n}) \quad (\text{D.9})$$

such that

$$m_{d,1} \geq m_{d,2} \geq \dots \geq m_{d,n-1} \geq |m_{d,n}| \quad d = 2n \quad (\text{D.10})$$

$$m_{d,1} \geq m_{d,2} \geq \dots \geq m_{d,n} \geq 0 \quad d = 2n + 1 \quad (\text{D.11})$$

The  $m_{d,i}$  are either all integers (in the case of tensor representations) or all half-integers. When they are integers, we can think of them as lengths of rows of a Young diagram. See [71] for a recent review.

A spin- $J$  traceless symmetric tensor has labels  $\mathbf{m}_d = (J, 0, \dots, 0)$ , corresponding to a single-row Young diagram with length  $J$ . More generally, an object in the representation  $\mathbf{m}_d$  is a tensor with indices

$$f^{\mu_1 \dots \mu_{m_{d,1}} \nu_1 \dots \nu_{m_{d,2}} \dots \rho_1 \dots \rho_{m_{d,n}}}. \quad (\text{D.12})$$

For a given Young diagram, we can choose to make either symmetry of the rows manifest or antisymmetry of the columns manifest. We choose to make symmetry of the rows manifest. Thus,  $f$  is symmetric in each of its  $n$  groups of indices

$$f^{\mu_1 \dots \mu_{m_{d,1}} \nu_1 \dots \nu_{m_{d,2}} \dots \rho_1 \dots \rho_{m_{d,n}}} = f^{(\mu_1 \dots \mu_{m_{d,1}})(\nu_1 \dots \nu_{m_{d,2}}) \dots (\rho_1 \dots \rho_{m_{d,n}})}. \quad (\text{D.13})$$

Furthermore, it is traceless in all pairs of indices. Antisymmetrization of columns of the Young diagram is reflected in the fact that if we try to symmetrize too many indices, we get zero. For example,

$$f^{(\mu_1 \dots \mu_{m_{d,1}} \nu_1) \nu_2 \dots \nu_{m_{d,2}} \dots \rho_1 \dots \rho_{m_{d,n}}} = 0. \quad (\text{D.14})$$

It is useful to encode the tensor  $f$  using index-free notation. We introduce polarization vectors  $z_1, \dots, z_n \in \mathbb{C}^d$  for each row of the Young diagram and contract them with the corresponding indices to form a polynomial

$$f(z_1, \dots, z_n) \equiv f^{\mu_1 \dots \mu_{m_{d,1}} \nu_1 \dots \nu_{m_{d,2}} \dots \rho_1 \dots \rho_{m_{d,n}}} z_{1\mu_1} \dots z_{1\mu_{m_{d,1}}} z_{2\nu_1} \dots z_{2\nu_{m_{d,2}}} \dots z_{n\rho_1} \dots z_{n\rho_{m_{d,n}}}. \quad (\text{D.15})$$

By construction,  $f(z_i)$  is homogeneous in each polarization vector

$$f(\alpha_1 z_1, \dots, \alpha_n z_n) = \alpha_1^{m_{d,1}} \dots \alpha_n^{m_{d,n}} f(z_1, \dots, z_n) \quad (\alpha_i \in \mathbb{C}). \quad (\text{D.16})$$

Because  $f$  is traceless, we can impose the conditions

$$z_i^2 = 0, \quad z_i \cdot z_j = 0. \quad (\text{D.17})$$

These conditions mean that shifting  $f$  by anything proportional to  $\delta^{\mu\nu}$  leads to the same polynomial  $f(z_i)$ . The traceless tensor  $f$  can thus be recovered from the polynomial  $f(z_i)$  by choosing any tensor leading to the correct polynomial and subtracting traces.

In index-free notation, the antisymmetrization condition (D.14) becomes

$$f(z_1, z_2 + \beta z_1, z_3, \dots, z_n) = f(z_1, z_2, z_3, \dots, z_n). \quad (\text{D.18})$$

In other words,  $f$  is gauge-invariant under shifts  $z_2 \rightarrow z_2 + \beta z_1$ . (Note that this gauge-redundancy is consistent with the orthogonality conditions (D.17).) More general antisymmetrization conditions show that  $f$  is invariant under the gauge redundancies

$$\begin{aligned} z_2 &\rightarrow z_2 + \#z_1 \\ z_3 &\rightarrow z_3 + \#z_2 + \#z_1 \\ &\vdots \\ z_n &\rightarrow z_n + \#z_{n-1} + \dots + \#z_1. \end{aligned} \quad (\text{D.19})$$

Finally, in even dimensions, the tensor  $f$  can satisfy

$$\begin{aligned} &\epsilon^{\mu_1 \dots \rho_1}_{\mu_0 \dots \rho_0} f^{\mu_0 \mu_2 \dots \mu_{m_{d,1}} \dots \rho_0 \rho_2 \dots \rho_{m_{d,n}}} z_{1\mu_1} \dots z_{1\mu_{m_{d,1}}} z_{2\nu_1} \dots z_{2\nu_{m_{d,2}}} \dots z_{n\rho_1} \dots z_{n\rho_{m_{d,n}}} \\ &= \pm p_n f(z_1, \dots, z_n) \end{aligned} \quad (\text{D.20})$$

where  $p_n$  is a constant depending only on  $n$ . This is equivalent to imposing an (anti-)self-duality condition on the polarization vectors

$$\epsilon^{\mu_1 \dots \rho_1}_{\mu_0 \dots \rho_0} z_{1\mu_1} \dots z_{n\rho_1} = \pm p_n n! z_{[1\mu_0} \dots z_{n\rho_0]}. \quad (\text{D.21})$$

To summarize, the representation  $\mathbf{m}_d$  is equivalent to the space of homogeneous polynomials of polarization vectors  $z_1, \dots, z_n \in \mathbb{C}^d$  with degrees  $m_{d,1}, \dots, m_{d,n}$ , satisfying the orthogonality conditions (D.17), duality condition (D.21) in even dimensions, and subject to gauge-redundancy (D.19).

We have essentially arrived at the Borel-Weil theorem, specialized to orthogonal groups. The theorem states that each irreducible finite-dimensional representation of a reductive Lie group  $G$  is equivalent to the space of global sections of a holomorphic line bundle on the flag manifold  $G/B$ , where  $B \subset G$  is a Borel subgroup. In the case  $G = \text{SO}(d)$ , the flag manifold  $G/B$  is the projectivization of the space of vectors  $z_1, \dots, z_n$  satisfying the above conditions and gauge-redundancies. A section of a line bundle on this space is a homogeneous polynomial of the polarization vectors.

It is sometimes useful to use mixed index-free notation, where only some of the polarization vectors are contracted. For example, we could consider

$$f^{\nu_1 \dots \nu_{m_{d,2}} \dots \rho_1 \dots \rho_{m_{d,n}}}(z_1) \equiv f^{\mu_1 \dots \mu_{m_{d,1}} \nu_1 \dots \nu_{m_{d,2}} \dots \rho_1 \dots \rho_{m_{d,n}}} z_{1\mu_1} \dots z_{1\mu_{m_{d,1}}}. \quad (\text{D.22})$$

The object  $f^{\nu_1 \dots \nu_{m_{d,2}} \dots \rho_1 \dots \rho_{m_{d,n}}}(z_1)$  is a tensor on the null cone  $z_1^2 = 0$ . Its indices satisfy all the symmetry conditions appropriate for the Young diagram  $(m_{d,2}, \dots, m_{d,n})$  obtained by discarding the first row of the Young diagram  $(m_{d,1}, m_{d,2}, \dots, m_{d,n})$ . Furthermore, antisymmetry conditions like (D.14) mean that if we contract any of the indices of (D.22) with  $z_1$ , the result is zero. We say that (D.22) is “transverse.”

### D.2.2 Poincare patches

We can think of the polarization vector  $z_1$  as an embedding-space coordinate in  $d-2$  dimensions. It is natural to ask what the function  $f(z_1, \dots, z_n)$  looks like in flat coordinates. Let us write the metric on  $\mathbb{C}^d$  as

$$z \cdot z = -z^+ z^- + z^\perp \cdot z^\perp, \quad (\text{D.23})$$

where  $z^\perp \in \mathbb{C}^{d-2}$ . For generic  $z_1$ , we can use homogeneity to set

$$z_1 = (z_1^+, z_1^-, z_1^\perp) = (1, (y^\perp)^2, y^\perp), \quad y^\perp \in \mathbb{C}^{d-2}. \quad (\text{D.24})$$

Using the gauge redundancies (D.19), we can set  $z_2^+ = \dots = z_n^+ = 0$ . The orthogonality conditions (D.17) then imply that the other  $z_i$  take the form

$$z_i = (0, 2z_i^\perp \cdot y^\perp, z_i^\perp), \quad z_i^\perp \in \mathbb{C}^{d-2}, \quad (\text{D.25})$$

where

$$z_i^\perp \cdot z_j^\perp = 0 \quad (i, j = 2, \dots, n). \quad (\text{D.26})$$

Thus, we obtain a function

$$f^\downarrow(y^\perp; z_2^\perp, \dots, z_n^\perp) \equiv f(z_1, \dots, z_n) \Big|_{\substack{z_1=(1, \vec{y}^{\perp 2}, y^\perp) \\ z_i=(0, 2z_i^\perp \cdot y^\perp, z_i^\perp)}} \quad (\text{D.27})$$

The function  $f^\downarrow$  is not homogeneous in  $y^\perp$ , but it is a homogeneous polynomial in the remaining arguments  $z_2^\perp, \dots, z_n^\perp \in \mathbb{C}^{d-2}$ . Furthermore, the  $z_2^\perp, \dots, z_n^\perp$  are subject to the same orthogonality and gauge redundancies as before, except now in 2-fewer dimensions. Thus,  $f^\downarrow$  is equivalent to a tensor field on  $\mathbb{C}^{d-2}$ , transforming in the  $\text{SO}(d-2)$  representation  $(m_{d,2}, \dots, m_{d,n})$

$$f^\downarrow(y^\perp; z_2^\perp, \dots, z_n^\perp) = f^{\downarrow\alpha_1 \dots \alpha_{m_{d,2}} \dots \beta_1 \dots \beta_{m_{d,n}}}(y^\perp) z_{2\alpha_1}^\perp \dots z_{2\alpha_{m_{d,2}}}^\perp \dots z_{n\beta_1}^\perp \dots z_{n\beta_{m_{d,n}}}^\perp, \quad (\text{D.28})$$

where  $\alpha_i, \beta_i$  are vector indices in  $d-2$ -dimensions. This is the usual procedure of restricting to a Poincare patch in the embedding formalism.

The function  $f(z_1, \dots, z_n)$  can easily be recovered from  $f^\downarrow(y^\perp; z_2^\perp, \dots, z_n^\perp)$  by imposing the correct homogeneity and gauge redundancy

$$\begin{aligned} f(z_1, \dots, z_n) &= (f^\downarrow)^\uparrow(z_1, \dots, z_n) \\ &= (z_1^+)^{m_1} f^\downarrow \left( \frac{z_1^\perp}{z_1^+}; z_2^\perp - \frac{z_2^+}{z_1^+} z_1^\perp, \dots, z_n^\perp - \frac{z_n^+}{z_1^+} z_1^\perp \right). \end{aligned} \quad (\text{D.29})$$

This is the usual procedure of lifting to the embedding space.

If we would like, restriction to a Poincare patch can be iterated again to obtain a tensor field on  $\mathbb{C}^{d-2} \times \mathbb{C}^{d-4}$  with indices valued in the  $\text{SO}(d-4)$  representation  $(m_{d,3}, \dots, m_{d,n})$ ,

$$\begin{aligned} &f^{\downarrow\downarrow}(y^\perp, x^{\perp\perp}; z_3^{\perp\perp}, \dots, z_n^{\perp\perp}), \\ &= f^{\downarrow\downarrow\alpha_1 \dots \alpha_{m_{d,3}} \dots \beta_1 \dots \beta_{m_{d,n}}}(y^\perp, x^{\perp\perp}) z_{3\alpha_1}^{\perp\perp} \dots z_{3\alpha_{m_{d,3}}}^{\perp\perp} \dots z_{n\beta_1}^{\perp\perp} z_{n\beta_{m_{d,n}}}^{\perp\perp} \quad x^{\perp\perp}, z_j^{\perp\perp} \in \mathbb{C}^{d-4}. \end{aligned} \quad (\text{D.30})$$

Here,  $\alpha_i, \beta_i$  are vector indices in  $d-4$  dimensions. Similarly, we can obtain  $f^{\downarrow\downarrow\downarrow}$  which is a tensor field on  $\mathbb{C}^{d-2} \times \mathbb{C}^{d-4} \times \mathbb{C}^{d-6}$ , etc. All of these functions can be lifted back to the original homogeneous polynomial  $f(z_1, \dots, z_n)$ .

### D.2.3 Application to CFT

Most of the above constructions still work when some of the weights  $m_{d,i}$  become continuous. We can now no longer demand that  $f$  is a polynomial in the polarization vectors with continuous weights. However, we can still demand that  $f$  is a homogeneous function. Such homogeneous functions yield infinite-dimensional representations of  $\text{SO}(d)$ .<sup>1</sup>

We are interested in studying infinite-dimensional representations of  $\widetilde{\text{SO}}(d, 2)$ , corresponding to operators in CFT. These are labeled by a weight

$$\mathbf{m}_{d+2} = (-\Delta, m_{d,1}, \dots, m_{d,n}), \quad (\text{D.31})$$

where  $\Delta$  is not necessarily a negative integer. To describe light-ray operators, we must additionally allow  $m_{d,1} = J$  to be non-integer. We often use the notation

$$\begin{aligned} \mathbf{m}_{d+2} &= (-\Delta, J, \lambda), \\ \lambda &= (m_{d,2}, \dots, m_{d,n}), \end{aligned} \quad (\text{D.32})$$

where  $\lambda$  are weights of a finite-dimensional representation of  $\text{SO}(d-2)$ . When  $J$  is an integer satisfying  $J \geq m_{d,2}$ , we can also define the finite-dimensional representation of  $\text{SO}(d-1, 1)$

$$\rho = (J, m_{d,2}, \dots, m_{d,n}). \quad (\text{D.33})$$

The elements of the representation with weights  $\mathbf{m}_{d+2}$  are homogeneous functions of the kind described in section D.2.1. Here, we simply introduce some specialized notation for the case at hand. The functions are

$$\mathcal{O}(X, Z, W_1, \dots, W_{n-1}), \quad X, Z \in \mathbb{R}^{d,2}, \quad W_i \in \mathbb{C}^{d+2}, \quad (\text{D.34})$$

where the vectors  $X, Z, W_i$  are null and mutually orthogonal. Furthermore, they satisfy gauge redundancies

$$\begin{aligned} Z &\sim Z + \#X \\ W_1 &\sim W_1 + \#Z + \#X \\ &\vdots \\ W_{n-1} &\sim W_{n-1} + \#W_{n-2} + \dots + \#X. \end{aligned} \quad (\text{D.35})$$

---

<sup>1</sup>An index-free formalism for CFT operators in general tensor representations was introduced in [323]. That formalism introduces fermionic polarization vectors, and essentially differs from the one here by privileging the columns of Young tableaux instead of the rows.

The homogeneity condition is

$$\mathcal{O}(\alpha X, \beta Z, \alpha_1 W_1, \dots, \alpha_{n-1} W_{n-1}) = \alpha^{-\Delta} \beta^J \alpha_1^{m_{d,2}} \dots \alpha_{n-1}^{m_{d,n}} \mathcal{O}(X, Z, W_1, \dots, W_{n-1}). \quad (\text{D.36})$$

Furthermore,  $\mathcal{O}$  is constrained to be a polynomial in the  $W_i$ 's (but not in  $X, Z$ ).

The restriction of  $\mathcal{O}$  to a Poincare patch is given by

$$\mathcal{O}^\downarrow(x, z, w_1, \dots, w_{n-1}) = \mathcal{O}(X, Z, W_1, \dots, W_{n-1}) \Big|_{\substack{X=(1, x^2, x) \\ Z=(0, 2x \cdot z, z) \\ W_i=(0, 2x \cdot w_i, w_i)}}. \quad (\text{D.37})$$

Here,  $z, w_i$  are mutually orthogonal null vectors, subject to the gauge redundancies

$$\begin{aligned} w_1 &\sim w_1 + \#z \\ w_2 &\sim w_2 + \#w_1 + \#z \\ &\vdots \\ w_{n-1} &\sim w_{n-1} + \#w_{n-2} + \dots + \#z. \end{aligned} \quad (\text{D.38})$$

The function  $\mathcal{O}^\downarrow$  satisfies the homogeneity condition

$$\mathcal{O}^\downarrow(x, \beta z, \alpha_1 w_1, \dots, \alpha_{n-1} w_{n-1}) = \beta^J \alpha_1^{m_{d,2}} \dots \alpha_{n-1}^{m_{d,n}} \mathcal{O}^\downarrow(x, z, w_1, \dots, w_{n-1}). \quad (\text{D.39})$$

The transverse coordinates  $\vec{y}$  discussed in section 5.2.1 come about when we do an additional restriction to a Poincare patch in the  $z$  variable:

$$\mathcal{O}^{\downarrow\downarrow}(x, \vec{y}; \vec{w}_1, \dots, \vec{w}_{n-1}) = \mathcal{O}^\downarrow(x, z, w_1, \dots, w_{n-1}) \Big|_{\substack{z=(1, \vec{y}^2, \vec{y}) \\ w_i=(0, 2\vec{y} \cdot \vec{w}_i, \vec{w}_i)}}, \quad (\text{D.40})$$

where

$$x \in \mathbb{R}^{d-1,1}, \quad \vec{y} \in \mathbb{R}^{d-2}, \quad \vec{w}_i \in \mathbb{C}^{d-2}. \quad (\text{D.41})$$

We can equivalently think of  $\mathcal{O}^{\downarrow\downarrow}(x, \vec{y})$  as a tensor field on  $\mathbb{R}^{d-1,1} \times \mathbb{R}^{d-2}$  transforming in the  $\text{SO}(d-2)$  representation  $\lambda$ . When  $\mathcal{O}$  is a traceless symmetric tensor (i.e.  $\lambda$  is trivial), we have

$$\int_{-\infty}^{\infty} \mathcal{O}_{v\dots v}(u=0, v, \vec{y}) \propto \mathbf{L}[\mathcal{O}]^{\downarrow\downarrow}(-\infty z_0, \vec{y}), \quad (\text{D.42})$$

where  $z_0 = (1, 1, 0, \dots, 0)$  is a null vector in the  $v$  direction.

We almost always abuse notation and drop the  $\downarrow$  superscripts, relying on the arguments of  $\mathcal{O}$  to distinguish between the embedding-space function and its restrictions

to Poincare patches. We also often use mixed index-free notation, where we strip off the  $w_i$ 's to obtain a tensor operator

$$\mathcal{O}(x, z, w_1, \dots, w_{n-1}) = \mathcal{O}^{\mu_1 \dots \mu_{m_{d,2}} \dots \nu_1 \dots \nu_{m_{d,n}}}(x, z) w_{1\mu_1} \dots w_{1\mu_{m_{d,2}}} \dots w_{n-1\nu_1} \dots w_{n-1\nu_{m_{d,n}}}. \quad (\text{D.43})$$

The tensor  $\mathcal{O}^{\mu_1 \dots \mu_{m_{d,2}} \dots \nu_1 \dots \nu_{m_{d,n}}}(x, z)$  has indices symmetrized using the Young tableau  $\lambda = (m_{d,2}, \dots, m_{d,n})$ , and furthermore all its indices are transverse to  $z$ . Finally, we often suppress tensor indices and simply write  $\mathcal{O}(x, z)$ , where it is understood that  $\mathcal{O}$  can carry indices transverse to  $z$ .

All of these different formalisms for representing  $\mathcal{O}$  are equivalent, and they are convenient for different purposes. For example, to define the celestial map in section 5.3.4.4, it is convenient to use embedding-space operators  $\mathcal{O}(X, Z, W_1, \dots, W_{n-1})$ . To define the Lorentzian pairings (5.95) and (5.97), it is convenient to use the object  $\mathcal{O}^{\mu_1 \dots \mu_{m_{d,2}} \dots \nu_1 \dots \nu_{m_{d,n}}}(x, z)$  which carries a finite set of indices transverse to  $z$ . We move freely between the different formalisms as needed.

### D.3 More on analytic continuation and even/odd spin

In this section, we give more detail on the relationship between CRT and the generalized Lorentzian inversion formula. In particular, we explain how to go from the formula in [28] to the formula (5.92) in the main text.

The formula derived in [28] is

$$\begin{aligned} C_{ab}^\pm(\Delta, J, \lambda) = & -\frac{1}{2\pi i} \int_{\substack{4>1 \\ 2>3}} \frac{d^d x_1 \dots d^d x_4}{\text{vol}(\widetilde{\text{SO}}(d, 2))} \langle \mathcal{O}[[\mathcal{O}_4, \mathcal{O}_1][\mathcal{O}_2, \mathcal{O}_3]] \mathcal{O} \rangle \\ & \times \frac{\mathcal{T}_2^{-1} \mathcal{T}_4^{-1} (\mathcal{T}_2 \langle \mathcal{O}_1 \mathcal{O}_2 \mathbf{L}[\mathcal{O}^\dagger] \rangle^{(a)})^{-1} (\mathcal{T}_4 \langle \mathcal{O}_4 \mathcal{O}_3 \mathbf{L}[\mathcal{O}] \rangle^{(b)})^{-1}}{\langle \mathbf{L}[\mathcal{O}] \mathbf{L}[\mathcal{O}^\dagger] \rangle^{-1}} \\ & + (1 \leftrightarrow 2). \end{aligned} \quad (\text{D.44})$$

It involves light-transforms of time-ordered structures  $\langle \mathcal{O}_1 \mathcal{O}_2 \mathbf{L}[\mathcal{O}^\dagger] \rangle^{(a)}$  and  $\langle \mathcal{O}_3 \mathcal{O}_4 \mathbf{L}[\mathcal{O}] \rangle^{(b)}$ .<sup>2</sup> Time-ordered structures only make sense for integer  $J$  (see appendix A of [28]), so we must give a prescription for how to analytically continue (D.44) in  $J$ . Such a

<sup>2</sup>By a ‘‘time-ordered structure,’’ we mean a conformally-invariant function of positions, with the  $i\epsilon$  prescription appropriate for a time-ordered correlator. By a ‘‘Wightman structure,’’ we mean a conformally-invariant function of positions, with the  $i\epsilon$  prescription appropriate for a Wightman function with the given ordering.

prescription was described in [28].<sup>3</sup> However, for our purposes, it will be helpful to phrase it in a different way. In particular, this requires clarifying the role of the  $\pm$  sign in the definition of  $\mathcal{O}_{\Delta, J, \lambda}^{\pm}$ .

Note that there are two terms in the Lorentzian inversion formula. The  $t$ -channel term written explicitly in (D.44) depends on

$$\mathcal{T}_2 \langle \mathcal{O}_1 \mathcal{O}_2 \mathbf{L}[\mathcal{O}^\dagger](x_0, z_0) \rangle^{(a)} = \mathcal{T}_2 \langle 0 | \mathcal{O}_2 \mathbf{L}[\mathcal{O}^\dagger](x_0, z_0) \mathcal{O}_1 | 0 \rangle^{(a)} \quad ((1 > 2) \approx 0), \quad (\text{D.45})$$

$$\mathcal{T}_4 \langle \mathcal{O}_3 \mathcal{O}_4 \mathbf{L}[\mathcal{O}](x_0, z_0) \rangle^{(b)} = \mathcal{T}_4 \langle 0 | \mathcal{O}_4 \mathbf{L}[\mathcal{O}](x_0, z_0) \mathcal{O}_3 | 0 \rangle^{(b)} \quad ((3 > 4) \approx 0). \quad (\text{D.46})$$

On the right, we indicate the causal relationship between points for which the structure is needed. We also give light-transformed Wightman structures that equal the light-transformed time-ordered structures when those causal relationships hold. Meanwhile, the  $u$ -channel term ( $1 \leftrightarrow 2$ ) depends on

$$\mathcal{T}_1 \langle \mathcal{O}_1 \mathcal{O}_2 \mathbf{L}[\mathcal{O}^\dagger](x_0, z_0) \rangle^{(a)} = \mathcal{T}_1 \langle 0 | \mathcal{O}_1 \mathbf{L}[\mathcal{O}^\dagger](x_0, z_0) \mathcal{O}_2 | 0 \rangle^{(a)} \quad ((2 > 1) \approx 0), \quad (\text{D.47})$$

instead of (D.45).

We see from (D.45) and (D.47) that the Lorentzian inversion formula actually depends on a pair of Wightman structures

$$\langle 0 | \mathcal{O}_2 \mathcal{O}^\dagger(x_0, z_0) \mathcal{O}_1 | 0 \rangle^{(a)}, \quad \langle 0 | \mathcal{O}_1 \mathcal{O}^\dagger(x_0, z_0) \mathcal{O}_2 | 0 \rangle^{(a)}. \quad (\text{D.48})$$

It is easy to separately analytically continue each Wightman structure in spin. However, we should take care to preserve the correct relationship between the structures. Let us describe this relationship when  $J$  is an integer, and then generalize to non-integer  $J$ .

The simplest way to relate the structures (D.48) for integer  $J$  is to demand that they are equal when all operators are spacelike separated. Unfortunately, this type of relationship does not generalize to non-integer  $J$  due to branch cuts in the spacelike region [28].

A different way to state the relationship between the structures (D.48) for integer  $J$  is to say how they transform under a combination of CRT and Hermitian conjugation. Recall that CRT is an anti-unitary symmetry that takes  $x = (x^0, x^1, x^2, \dots, x^{d-1})$  to

---

<sup>3</sup>It is as follows: we should first compute  $\langle \mathcal{O}_1 \mathcal{O}_2 \mathbf{L}[\mathcal{O}^\dagger] \rangle^{(a)}$  for general nonnegative integer  $J$  (where  $J$  is the spin of  $\mathcal{O}$ ). The result is no longer a time-ordered structure (e.g. it has  $\theta$ -functions of positions). It can then be analytically continued from even or odd  $J$ , depending on whether we are computing  $C_{ab}^+(\Delta, J, \lambda)$  or  $C_{ab}^-(\Delta, J, \lambda)$ . The analytic continuations are fixed by demanding that they are well-behaved in the right-half  $J$ -plane.



its Rindler reflection  $\bar{x} = (-x^0, -x^1, x^2, \dots, x^{d-1})$ . Its action on a local operator is given by

$$(\text{CRT})\mathcal{O}_{\text{local}}^\alpha(x)(\text{CRT}) = \left( (e^{-i\pi\mathcal{M}^{01}})^\alpha_\beta \mathcal{O}_{\text{local}}^\beta(\bar{x}) \right)^\dagger, \quad (\text{D.49})$$

where  $\alpha, \beta$  are indices for the Lorentz representation of  $\mathcal{O}$ , and  $\mathcal{M}^{01}$  is the generator of a boost in the 01 plane. (We assume  $\mathcal{O}_{\text{local}}$  is bosonic, for simplicity.) In general, we define the ‘‘Rindler conjugate’’ of any (not necessarily local) operator  $\mathcal{O}$  by

$$\bar{\mathcal{O}} \equiv (\text{CRT})\mathcal{O}(\text{CRT}). \quad (\text{D.50})$$

Note that Rindler conjugation preserves operator ordering, since it is simply conjugation by a symmetry.

If we combine Rindler conjugation with Hermitian conjugation, we obtain a linear map that reverses operator ordering

$$\mathcal{O} \rightarrow \bar{\mathcal{O}}^\dagger. \quad (\text{D.51})$$

For local operators, this is equivalent to a rotation by  $\pi$  in the plane spanned by  $x^1$  and Euclidean time  $ix^0$ ,

$$\overline{\mathcal{O}_{\text{local}}^\alpha(x)}^\dagger = (e^{-i\pi\mathcal{M}^{01}})^\alpha_\beta \mathcal{O}_{\text{local}}^\beta(\bar{x}). \quad (\text{D.52})$$

(One way to understand why this reverses operator ordering is that such a rotation reverses all the  $i\epsilon$ 's.) However, for non-local operators, (D.51) cannot be described in terms of a Euclidean rotation. We call the eigenvalue of an operator under (D.52) its ‘‘signature.’’

Let  $z_0 = (1, 1, 0, \dots, 0)$  be a null vector satisfying  $\bar{z}_0 = -z_0$ . Given a local operator  $\mathcal{O}_{\text{local}}$  with dimension  $\Delta$  and spin- $J$ , it is easy to check using (D.49) that  $\mathbf{L}[\mathcal{O}_{\text{local}}](-\infty z_0, z_0)$  has signature  $(-1)^J$ ,

$$\overline{\mathbf{L}[\mathcal{O}_{\text{local}}](-\infty z_0, z_0)}^\dagger = (-1)^J \mathbf{L}[\mathcal{O}_{\text{local}}](-\infty z_0, z_0). \quad (\text{D.53})$$

However, more general light-ray operators can have a signature that is not necessarily related to  $J$ , and this is what the superscript  $\pm$  encodes:

$$\overline{\mathbb{O}_{\Delta, J}^\pm(-\infty z_0, z_0)}^\dagger = \pm \mathbb{O}_{\Delta, J}^\pm(-\infty z_0, z_0). \quad (\text{D.54})$$

Let us understand how signature is encoded in the inversion formula. Since (D.51) acts as a complexified Lorentz transformation (D.52) on local operators, it is an

operator-order-reversing “symmetry” of three-point functions of local operators. Let  $\mathcal{O}_1, \mathcal{O}_2$  be any local operators. We have

$$\begin{aligned} \langle 0 | \mathcal{O}_1 \mathcal{O}_{\text{local}}^\dagger(x, z) \mathcal{O}_2 | 0 \rangle &= \langle 0 | \overline{\mathcal{O}_2^\dagger} \overline{\mathcal{O}_{\text{local}}^\dagger(x, z)}^\dagger \overline{\mathcal{O}_1^\dagger} | 0 \rangle \\ &= \langle 0 | \overline{\mathcal{O}_2^\dagger} \mathcal{O}_{\text{local}}^\dagger(\bar{x}, \bar{z}) \overline{\mathcal{O}_1^\dagger} | 0 \rangle \\ &= (-1)^J \langle 0 | \overline{\mathcal{O}_2^\dagger} \mathcal{O}_{\text{local}}^\dagger(\bar{x}, -\bar{z}) \overline{\mathcal{O}_1^\dagger} | 0 \rangle. \end{aligned} \quad (\text{D.55})$$

In the last line, we used that  $\mathcal{O}_{\text{local}}^\dagger(x, z)$  is a degree- $J$  polynomial in  $z$  to give it a future-pointing polarization vector  $-\bar{z}$ . Here,  $\overline{\mathcal{O}_{1,2}^\dagger}$  are given by (D.49).

The natural generalization to non-integer  $J$  is that the Wightman structures (D.48) should be related by

$$\langle 0 | \mathcal{O}_1 \mathcal{O}^\dagger(x, z) \mathcal{O}_2 | 0 \rangle^{(a)} = \pm \langle 0 | \overline{\mathcal{O}_2^\dagger} \mathcal{O}^\dagger(\bar{x}, -\bar{z}) \overline{\mathcal{O}_1^\dagger} | 0 \rangle^{(a)}, \quad (\text{D.56})$$

where  $\pm$  indicates whether we have analytically continued from even or odd spin. Again,  $\overline{\mathcal{O}_i^\dagger}$  is given by (D.52). Plugging this in to (D.44) gives equation (5.92).

#### D.4 Checking the celestial map with triple light transforms

For symmetric traceless tensors  $\mathcal{O}_1$  and  $\mathcal{O}_2$ , our OPE formula (5.139) relies on the computation of the coefficient  $q_{\delta,j}^{(a)}$  defined by the triple light-transform in (5.135). For more general representations of  $\mathcal{O}_1$  and  $\mathcal{O}_2$ , our formula (5.149) requires computation of the map defined by (5.148). We claim that this map is determined by the celestial map (5.151). In this appendix, we will prove the celestial map for operators in symmetric traceless tensor representations. We leave proving it for more general representations for the future.

Let  $\mathcal{O}_1$  and  $\mathcal{O}_2$  be symmetric traceless tensors of spins  $J_1$  and  $J_2$ , and consider the three-point structures

$$\langle 0 | \mathcal{O}_1(X_1, Z_1) \mathcal{O}_2(X_2, Z_2) \mathcal{O}(X_0, Z_0) | 0 \rangle^{(a)}. \quad (\text{D.57})$$

For simplicity, we consider the case with  $\mathcal{O}$  in a symmetric traceless tensor representation,  $(\Delta, J = J_1 + J_2 - 1, \lambda = \bullet)$ , as well. Then, the relevant three-point structures were classified in [192]. In embedding space, we can use the following basis of tensor structures:

$$\langle 0 | \mathcal{O}_1(X_1, Z_1) \mathcal{O}_2(X_2, Z_2) \mathcal{O}(X_0, Z_0) | 0 \rangle^{(a)} = \frac{\prod_i (-2V_i)^{m_i} \prod_{i < j} (-2H_{ij})^{n_{ij}}}{X_{12}^{\frac{\bar{\tau}_1 + \bar{\tau}_2 - \bar{\tau}_0}{2}} X_{20}^{\frac{\bar{\tau}_2 + \bar{\tau}_0 - \bar{\tau}_1}{2}} X_{01}^{\frac{\bar{\tau}_0 + \bar{\tau}_1 - \bar{\tau}_2}{2}}}, \quad (\text{D.58})$$

where  $i, j = 0, 1, 2$ ,  $\bar{\tau}_i = \Delta_i + J_i$  and the basis index ( $a$ ) is determined by six numbers  $\{m_i, n_{ij}\}$  satisfying

$$m_i + \sum_{j \neq i} n_{ij} = J_i. \quad (\text{D.59})$$

Recall that  $X_{ij} \equiv -2X_i \cdot X_j$ . The building blocks for the structures are [192]

$$\begin{aligned} X_{ij} &\equiv -2X_i \cdot X_j, \\ V_{i,jk} &\equiv \frac{Z_i \cdot X_j X_i \cdot X_k - Z_i \cdot X_k X_i \cdot X_j}{X_j \cdot X_k}, \\ H_{ij} &\equiv -2(Z_i \cdot Z_j X_i \cdot X_j - Z_i \cdot X_j Z_j \cdot X_i). \end{aligned} \quad (\text{D.60})$$

For brevity, we define  $V_i \equiv V_{i,jk}$  for  $\{i, j, k\}$  in cyclic order. We have shown in [214] that

$$\langle 0 | \mathcal{O}_2 \mathbf{L}[\mathcal{O}] \mathcal{O}_1 | 0 \rangle^{(a)} = (-2V_0)^{m_0} \prod_{i < j} (-2H_{ij})^{n_{ij}} \langle 0 | \mathcal{O}'_2 \mathbf{L}[\phi] \mathcal{O}'_1 | 0 \rangle^{(a')}. \quad (\text{D.61})$$

The new structure  $\langle 0 | \mathcal{O}'_2 \phi \mathcal{O}'_1 | 0 \rangle^{(a')}$  is the unique one that has

$$n'_{ij} = 0, \quad m'_0 = 0, \quad m'_1 = m_1, \quad m'_2 = m_2. \quad (\text{D.62})$$

The new formal operators  $\mathcal{O}'_i$  have spin  $J'_i = m_i$  and dimension  $\Delta'_i = \Delta_i + J_i - m_i$ . (Note that  $\bar{\tau}_i = \bar{\tau}'_i$ .) The formal scalar  $\phi$  has dimension  $\Delta_\phi = \bar{\tau}$ . The light-transform of the structure ( $a'$ ) is [214]

$$\begin{aligned} &\langle 0 | \mathcal{O}'_2 \mathbf{L}[\phi] \mathcal{O}'_1 | 0 \rangle^{(a')} \\ &= L(\mathcal{O}'_1 \mathcal{O}'_2[\phi]) \frac{(-2V_0)^{1-\bar{\tau}} (-2V_1)^{m_1} (-2V_2)^{m_2}}{(-X_{02})^{\frac{\bar{\tau}L + \bar{\tau}_2 - \bar{\tau}_1}{2}} X_{01}^{\frac{\bar{\tau}L + \bar{\tau}_1 - \bar{\tau}_2}{2}} X_{12}^{\frac{\bar{\tau}_1 + \bar{\tau}_2 - \bar{\tau}L}{2}}} \\ &\quad \times f\left(-\frac{H_{01}}{2V_0V_1}, -\frac{H_{02}}{2V_0V_2}\right) \quad ((2 > 0) \approx 1), \end{aligned} \quad (\text{D.63})$$

where  $\bar{\tau}^L = (1 - J) + (1 - \Delta) = 2 - \bar{\tau}$ ,

$$L(\mathcal{O}'_1 \mathcal{O}'_2[\phi]) = -2\pi i \frac{\Gamma(\Delta_\phi - 1)}{\Gamma\left(\frac{\Delta_\phi + \tau'_1 - \tau'_2}{2}\right) \Gamma\left(\frac{\Delta_\phi - \tau'_1 + \tau'_2}{2}\right)}, \quad (\text{D.64})$$

and

$$f(x, y) = F_2(\bar{\tau} - 1; -m_1, -m_2; \frac{1}{2}(\bar{\tau} + \tau'_1 - \tau'_2), \frac{1}{2}(\bar{\tau} - \tau'_1 + \tau'_2); x, y). \quad (\text{D.65})$$

$F_2$  is the Appell hypergeometric function

$$F_2(\alpha; \beta, \beta'; \gamma, \gamma'; x, y) \equiv \sum_{k=0}^{\infty} \sum_{l=0}^{\infty} \frac{(\alpha)_{k+l} (\beta)_k (\beta')_l}{k! l! (\gamma)_k (\gamma')_l} x^k y^l. \quad (\text{D.66})$$

Now, we'd like to specialize  $X_0 = (1, 0, 0)$  and compute the remaining light transforms  $\mathbf{L}^-[\mathcal{O}_1](X_\infty, Z_1)$  and  $\mathbf{L}^+[\mathcal{O}_2](X_\infty, Z_2)$ .

$$\begin{aligned} & \frac{\langle 0 | \mathbf{L}^+[\mathcal{O}_2](X_\infty, Z_2) \mathbf{L}[\mathcal{O}](X_0, Z_0) \mathbf{L}^-[\mathcal{O}_1](X_\infty, Z_1) | 0 \rangle^{(a)}}{\text{vol SO}(1, 1)} \\ &= \frac{1}{\text{vol SO}(1, 1)} \int_0^\infty d\alpha_2 \int_{-\infty}^0 d\alpha_1 (2V_0)^{m_0} \prod_{i < j} (-2H_{ij})^{n_{ij}} \langle \mathcal{O}'_1 \mathbf{L}[\phi] \mathcal{O}'_2 \rangle^{(a')} \\ &= \frac{1}{\text{vol SO}(1, 1)} \int_0^\infty d\alpha_2 \int_{-\infty}^0 d\alpha_1 \prod_{i < j} (-2H_{ij})^{n_{ij}} L(\mathcal{O}'_1 \mathcal{O}'_2[\phi]) \\ & \quad \times \frac{(2V_0)^{1-\bar{\tau}+m_0} (2V_1)^{m_1} (2V_2)^{m_2}}{(-X_{02})^{\frac{\bar{\tau}L+\bar{\tau}_1-\bar{\tau}_2}{2}} X_{01}^{\frac{\bar{\tau}L+\bar{\tau}_2-\bar{\tau}_1}{2}} X_{12}^{\frac{\bar{\tau}_1+\bar{\tau}_2-\bar{\tau}L}{2}}} f\left(-\frac{H_{01}}{2V_0V_1}, -\frac{H_{02}}{2V_0V_2}\right). \end{aligned} \quad (\text{D.67})$$

Inside the integral, the light-transform instructs us to replace

$$\begin{aligned} X_1 &\rightarrow Z_1 - \alpha_1 X_\infty = (0, -\alpha_1, z_1) \\ X_2 &\rightarrow Z_2 - \alpha_2 X_\infty = (0, -\alpha_2, z_2) \\ Z_{1,2} &\rightarrow -X_\infty = (0, -1, \vec{0}) \end{aligned} \quad (\text{D.68})$$

where  $Z_i = (0, 0, z_i)$ , and accordingly,

$$\begin{aligned} V_1 &= -\frac{z_1 \cdot z_2}{\alpha_2} \\ V_2 &= \frac{z_1 \cdot z_2}{\alpha_1} \\ V_0 &= \frac{\alpha_2 z_1 \cdot z_0 - \alpha_1 z_2 \cdot z_0}{2z_1 \cdot z_2} \\ H_{01} &= z_0 \cdot z_1 \\ H_{02} &= z_0 \cdot z_2 \\ H_{12} &= 0. \end{aligned} \quad (\text{D.69})$$

Since  $H_{12} = 0$ , only structures with  $n_{12} = 0$  will survive. In that case, the selection rule  $J = J_1 + J_2 - 1$  implies

$$m_0 = m_1 + m_2 - 1. \quad (\text{D.70})$$

Expanding the Appell  $F_2$  sum, we evaluate the integral for each term;

$$\begin{aligned}
& \int_0^\infty d\alpha_2 \int_{-\infty}^0 d\alpha_1 \frac{(-2H_{01})^{J_1-m_1+k} (-2H_{02})^{J_2-m_2+l} (2V_0)^{1-\bar{\tau}+m_0-k-l} (2V_1)^{m_1-k} (2V_2)^{m_2-l}}{(-X_{02})^{\frac{\bar{\tau}L+\bar{\tau}_1-\bar{\tau}_2}{2}} X_{01}^{\frac{\bar{\tau}L+\bar{\tau}_2-\bar{\tau}_1}{2}} X_{12}^{\frac{\bar{\tau}_1+\bar{\tau}_2-\bar{\tau}L}{2}}} \\
&= \frac{z_{01}^{k+J_1-m_1} z_{02}^{l+J_2-m_2}}{z_{12}^{\frac{\bar{\tau}_1+\bar{\tau}_2-\bar{\tau}}{2}}} \int_0^\infty d\alpha_2 \int_{-\infty}^0 d\alpha_1 \frac{(\alpha_2 z_{01} - \alpha_1 z_{02})^{1-\bar{\tau}-k-l+m_0}}{\alpha_2^{\frac{\bar{\tau}L-\bar{\tau}_1+\bar{\tau}_2}{2}-k+m_1} (-\alpha_1)^{\frac{\bar{\tau}L+\bar{\tau}_1-\bar{\tau}_2}{2}-l+m_2}} \\
&= \frac{\Gamma(\frac{\delta+\delta_{12}}{2} + J_1 - m_1 + k) \Gamma(\frac{\delta+\delta_{21}}{2} + J_2 - m_2 + l)}{\Gamma(\delta + J - m_0 + k + l)} \left( \int_0^\infty \frac{d\alpha_2}{\alpha_2} \right) \langle \mathcal{P}_{\delta_1}(z_1) \mathcal{P}_{\delta_2}(z_2) \mathcal{P}_\delta(z_0) \rangle.
\end{aligned} \tag{D.71}$$

Combining with the remaining factors, we have

$$\frac{\langle 0 | \mathbf{L}^+[\mathcal{O}_2](X_\infty, Z_2) \mathbf{L}[\mathcal{O}](X_0, Z_0) \mathbf{L}^-[\mathcal{O}_1](X_\infty, Z_1) | 0 \rangle^{(a)}}{\text{vol SO}(1, 1)} = q_{\delta,0}^{(a)} \langle \mathcal{P}_{\delta_1}(z_1) \mathcal{P}_{\delta_2}(z_2) \mathcal{P}_\delta(z_0) \rangle \tag{D.72}$$

with

$$\begin{aligned}
q_{\delta,0}^{(a)} &= -2\pi i \delta_{n_{12},0} \frac{(\delta + J - m_0)_{m_0}}{(\frac{\delta+\delta_1-\delta_2}{2} + J_1 - m_1)_{m_2} (\frac{\delta+\delta_2-\delta_1}{2} + J_2 - m_2)_{m_1}} \\
&\times \sum_{k,l=0}^\infty \frac{1}{k! l!} \frac{(-m_1)_k (-m_2)_l (\delta + J)_{k+l} (\frac{\delta+\delta_1-\delta_2}{2} + J_1 - m_1)_k (\frac{\delta+\delta_2-\delta_1}{2} + J_2 - m_2)_l}{(\delta + J - m_0)_{k+l} (\frac{\delta+\delta_1-\delta_2}{2} + J_1 - m_1 + m_2)_k (\frac{\delta+\delta_2-\delta_1}{2} + J_2 - m_2 + m_1)_l}.
\end{aligned} \tag{D.73}$$

Quite remarkably, this sum completely simplifies, yielding a pair of Kronecker delta functions. Finally, we have

$$\begin{aligned}
q_{\delta,0}^{(a)} &= -2\pi i \delta_{n_{12},0} \frac{(\delta + J - m_0)_{m_0}}{(\frac{\delta+\delta_1-\delta_2}{2} + J_1 - m_1)_{m_2} (\frac{\delta+\delta_2-\delta_1}{2} + J_2 - m_2)_{m_1}} \delta_{m_1,0} \delta_{m_2,0} \\
&= -2\pi i \frac{1}{\delta + J} \delta_{n_{12},0} \delta_{m_1,0} \delta_{m_2,0}.
\end{aligned} \tag{D.74}$$

Recalling that

$$r_{\delta,0} = -\frac{2\pi i}{\delta + J}, \tag{D.75}$$

the OPE differential on the celestial sphere is given by

$$\mathcal{D}_{\delta,0}^{(a)}(z_1, z_2, \partial_{z_2}) = \frac{q_{\delta,0}^{(a)}}{r_{\delta,0}} \mathcal{C}_{\delta,0} = \delta_{n_{12},0} \delta_{m_1,0} \delta_{m_2,0} \mathcal{C}_{\delta,0}. \tag{D.76}$$

In other words, the differential is  $\mathcal{C}_{\delta,0}$  if  $(a)$  is the structure

$$(a) = \{m_0, m_1, m_2, n_{01}, n_{02}, n_{12}\} = \{-1, 0, 0, J_1, J_2, 0\} \tag{D.77}$$

proportional to

$$V_0^{-1} H_{01}^{J_1} H_{02}^{J_2}, \tag{D.78}$$

and zero otherwise. This precisely agrees with the celestial map (5.151).

### D.5 Swapping the integral and $t$ -channel sum in the inversion formula

We would like to argue that

$$C^\pm(\Delta, J) = \sum_{\Delta', J'} p_{\Delta', J'} \mathcal{B}^\pm(\Delta, J; \Delta', J') \quad (\text{D.79})$$

is a convergent sum, where  $\mathcal{B}^\pm(\Delta, J; \Delta', J')$  is the Lorentzian inversion of a single  $t$ -channel block, and we have  $J > J_0$  and  $\Delta = \frac{d}{2} + i\nu$ . We can argue for this using the Fubini-Tonelli theorem. The theorem implies that we can exchange the sum over  $\Delta', J'$  and the integral over  $z, \bar{z}$  in the Lorentzian inversion formula if the result after replacing each term with its absolute value is finite:

$$\int_0^1 \int_0^1 dz d\bar{z} \frac{|z - \bar{z}|^{d-2}}{(z\bar{z})^d} |G_{J+d-1, \Delta-d+1}(z, \bar{z})| \times \sum_{\Delta', J'} \left| p_{\Delta', J'} d\text{Disc}_t \left[ \left( \frac{z\bar{z}}{(1-z)(1-\bar{z})} \right)^{\Delta_\phi} G_{\Delta', J'}(1-z, 1-\bar{z}) \right] \right| < \infty. \quad (\text{D.80})$$

Because  $p_{\Delta', J'}$  is positive and  $d\text{Disc}_t[\dots]$  is as well, we can write this condition more simply as

$$\int_0^1 \int_0^1 dz d\bar{z} \frac{|z - \bar{z}|^{d-2}}{(z\bar{z})^d} |G_{J+d-1, \Delta-d+1}(z, \bar{z})| d\text{Disc}_t[g](z, \bar{z}) < \infty. \quad (\text{D.81})$$

Note that the Lorentzian inversion formula converges for  $J > J_0$  and  $\Delta = \frac{d}{2} + i\nu$  on the principal series [25, 26]. Thus, it suffices to bound the integral (D.81) by a constant times the Lorentzian inversion formula with  $\Delta = \frac{d}{2}$  (which is on the principal series). Specifically, we will argue that

$$\frac{|G_{J+d-1, \Delta-d+1}(z, \bar{z})|}{G_{J+d-1, \frac{d}{2}-d+1}(z, \bar{z})} < \text{const}, \quad z, \bar{z} \in [0, 1], \quad \Delta = \frac{d}{2} + i\nu, \quad (\text{D.82})$$

where the constant can depend on  $\Delta$  and  $J$ , but is independent of  $z, \bar{z}$ . Because the functions in the numerator and denominator of (D.82) are smooth and nonzero in the interior of the square, it suffices to argue that their ratio is bounded in a neighborhood of the boundary of the square. By symmetry, it suffices to consider  $z \leq \bar{z}$ .

When  $z \ll \bar{z}$ , the ratio takes the form

$$\frac{|G_{J+d-1, \Delta-d+1}(z, \bar{z})|}{G_{J+d-1, \frac{d}{2}-d+1}(z, \bar{z})} \sim \frac{\left| z^{\frac{J-\Delta+2d-2}{2}} k_{\Delta+J}(\bar{z}) \right|}{z^{\frac{J-\frac{d}{2}+2d-2}{2}} k_{\frac{d}{2}+J}(\bar{z})} = \frac{|k_{\Delta+J}(\bar{z})|}{k_{\frac{d}{2}+J}(\bar{z})}, \quad z \ll \bar{z} \quad (\text{D.83})$$

where  $k_\beta(x)$  is an  $\text{SL}_2$  block. The above ratio is equal to 1 (and hence bounded) when  $\bar{z} = 0$ . Since both  $\text{SL}_2$  blocks behave like  $\log(1 - \bar{z})$  near  $\bar{z} = 1$ , their ratio is bounded near  $\bar{z} = 1$  as well. Because the numerator and denominator are smooth and nonzero for  $0 < \bar{z} < 1$ , the ratio (D.83) is bounded by a  $\bar{z}$ -independent constant.

In the Regge limit  $z, \bar{z} \ll 1$  with  $z/\bar{z}$  fixed, (D.82) is

$$\frac{|G_{J+d-1, \Delta-d+1}(z, \bar{z})|}{G_{J+d-1, \frac{d}{2}-d+1}(z, \bar{z})} \sim \frac{|C_{\Delta-d+1}(x)|}{C_{\frac{d}{2}-d+1}(x)}, \quad z, \bar{z} \ll 1, \quad (\text{D.84})$$

where  $C_J(x)$  is a Gegenbauer function and  $x = \frac{z+\bar{z}}{2\sqrt{z\bar{z}}}$  ranges from 1 to  $\infty$ . Again, by examining the limits  $x \rightarrow 1$  and  $x \rightarrow \infty$ , one finds that the above ratio is bounded.

The  $\bar{z} \rightarrow 1$  limit of a conformal block can be studied by solving the Casimir equation. Again in this case, one finds that the numerator and denominator of (D.82) both behave as the same function of  $1 - \bar{z}$ , times functions of  $z$  whose ratios are bounded. This completes our argument.

## D.6 Contact terms at $\zeta = 1$ in $\mathcal{N} = 4$ SYM

In the main text, we described how one can recover the contact terms in the energy-energy correlator  $\mathcal{F}_E(\zeta)$  in  $\mathcal{N} = 4$  SYM at  $\zeta = 0$  and  $\zeta = 1$  using Ward identities (5.233) and (5.234). We were also able to recover the  $\zeta = 0$  contact terms using the light-ray OPE formula (5.227). In this appendix we explain how the  $\zeta = 1$  contact terms can be obtained by another independent argument.

In the back-to-back region, the energy-energy correlator in  $\mathcal{N} = 4$  SYM takes the following form [182, 219, 254]:

$$\mathcal{F}_E(\zeta) \sim_{\zeta \rightarrow 1} \frac{H(a)}{8y} \int_0^\infty e^{-\frac{1}{2}\Gamma_{\text{cusp}}(a) \log^2\left(\frac{b^2}{yb_0^2}\right) - \Gamma_{\text{coll}}(a) \log\left(\frac{b^2}{yb_0^2}\right)} b J_0(b) db, \quad (\text{D.85})$$

where  $y = 1 - \zeta$ ,  $b_0 = 2e^{-\gamma_E}$ ,  $\Gamma_{\text{cusp}}(a)$  is the cusp anomalous dimension and  $\Gamma_{\text{coll}}(a)$  is the so-called collinear anomalous dimension. Both  $\Gamma_{\text{cusp}}(a)$  and  $\Gamma_{\text{coll}}(a)$  are known at any coupling  $a$  from integrability [324]. Note that starting from four loops there are non-planar corrections to  $\Gamma_{\text{cusp}}(a)$  and  $\Gamma_{\text{coll}}(a)$  which we do not write here [325–327].

At weak coupling,  $\Gamma_{\text{cusp}}(a)$  is given by the following expansion [328]:

$$\Gamma_{\text{cusp}}(a) = a - \frac{1}{2}\zeta_2 a^2 + \frac{11}{8}\zeta_4 a^3 - \left(\frac{1}{8}\zeta_3^2 + \frac{219}{64}\zeta_6\right) a^4 + \dots, \quad (\text{D.86})$$

$\Gamma_{\text{coll}}(a)$  is the collinear anomalous dimension given by [329, 330]

$$\Gamma_{\text{coll}}(a) = -\frac{3}{2}\zeta_3 a^2 + \left(\frac{1}{2}\zeta_2 \zeta_3 + \frac{5}{2}\zeta_5\right) a^3 - \left(\frac{21}{16}\zeta_3 \zeta_4 + \frac{5}{8}\zeta_2 \zeta_5 + \frac{175}{32}\zeta_7\right) a^4 + \dots, \quad (\text{D.87})$$

and  $H(a)$  is the so-called coefficient function given by<sup>4</sup> [207, 219]

$$H(a) = 1 - \zeta_2 a + 2\zeta_2^2 a^2 + \left(-\frac{33}{8}\zeta_2^3 - \frac{1}{4}\zeta_4\zeta_2 - \frac{17}{12}\zeta_3^2 + \frac{1}{64}\zeta_6\right) a^3 + H_4 a^4 + \dots \quad (\text{D.88})$$

The coefficient  $H_4$  is at present unknown.

At finite  $a$ , (D.85) is integrable near  $y = 0$ , and so does not have any contact terms. It is possible that even at finite coupling there is an extra contact term that has to be added to (D.85). We assume that this is not the case, and that there are no contact terms at  $\zeta = 1$  at finite coupling. Under this assumption, we can therefore obtain perturbative contact terms at  $\zeta = 1$  if we carefully expand (D.85) in powers of  $a$ . Naïve expansion yields terms of the form  $y^{-1} \log^k y$ . In our conventions for the distributional part of  $\mathcal{F}_{\mathcal{E}}(\zeta)$ , we interpret these terms as  $[y^{-1} \log y]_1$ , which satisfy

$$\int_0^1 d\zeta \left[ \frac{\log^k(1-\zeta)}{1-\zeta} \right]_1 = 0. \quad (\text{D.89})$$

Therefore, to determine the coefficient of  $\delta(y) = \delta(1-\zeta)$  in (D.85), it suffices to integrate (D.85) from 0 to 1, and expand the result as a power series in  $a$ .

The  $y$  integral we need to perform is

$$\begin{aligned} \mathcal{I}_a(b) &= \int_0^1 dy y^{-1+2\Gamma_{\text{cusp}}(a) \log \frac{b}{b_0} + \Gamma_{\text{coll}}(a)} e^{-\frac{1}{2}\Gamma_{\text{cusp}}(a) \log^2 y} \\ &= e^{\frac{(2\Gamma_{\text{cusp}}(a) \log \frac{b}{b_0} + \Gamma_{\text{coll}}(a))^2}{2\Gamma_{\text{cusp}}(a)}} \frac{\sqrt{\pi} \operatorname{erfc}\left(\frac{2\Gamma_{\text{cusp}}(a) \log \frac{b}{b_0} + \Gamma_{\text{coll}}(a)}{\sqrt{2\Gamma_{\text{cusp}}(a)}}\right)}{\sqrt{2\Gamma_{\text{cusp}}(a)}}. \end{aligned} \quad (\text{D.90})$$

This can be expanded in powers of  $a$ , with  $b$ -dependence entering as powers  $\log \frac{b}{b_0}$ . Note that naïvely this function has an expansion in powers of  $\sqrt{a}$ . However, all non-integer powers of  $a$  will go away after performing  $b$ -integral.

We now want to perform the  $a$ -expansion of the integral

$$\int_0^\infty \mathcal{I}_a(b) e^{-2\Gamma_{\text{coll}}(a) \log \frac{b}{b_0}} e^{-2\Gamma_{\text{cusp}}(a) \log^2 \frac{b}{b_0}} b J_0(b) db. \quad (\text{D.91})$$

The product

$$\mathcal{I}_a(b) e^{-2\Gamma_{\text{coll}}(a) \log \frac{b}{b_0}} \quad (\text{D.92})$$

can be expanded in  $a$  with coefficients polynomial in  $\log \frac{b}{b_0}$ . This is legal since the integral still converges after the expansion. This means that it suffices to compute

---

<sup>4</sup>We thank Grisha Korchemsky for sharing the coefficient of  $a^3$  in  $H(a)$  with us.



the integrals

$$\int_0^\infty \log^k \frac{b}{b_0} e^{-2\Gamma_{\text{cusp}} \log^2 \frac{b}{b_0}} b J_0(b) db, \quad (\text{D.93})$$

where we treat  $\Gamma_{\text{cusp}}$  as arbitrary parameter. It suffices only to compute this in the case  $k = 0, 1$  since to get higher  $k$ , we can simply take derivatives with respect to  $\Gamma_{\text{cusp}}$ . Let us consider the case  $k = 0$ ;  $k = 1$  is completely analogous. We first integrate by parts,

$$\begin{aligned} \int_0^\infty e^{-2\Gamma_{\text{cusp}} \log^2 \frac{b}{b_0}} b J_0(b) db &= \int_0^\infty e^{-2\Gamma_{\text{cusp}} \log^2 \frac{b}{b_0}} d(b J_1(b)) \\ &= 4\Gamma_{\text{cusp}} \int_0^\infty \log \frac{b}{b_0} e^{-2\Gamma_{\text{cusp}} \log^2 \frac{b}{b_0}} J_1(b) db. \end{aligned} \quad (\text{D.94})$$

Now the integral converges even for  $\Gamma_{\text{cusp}} = 0$ , so we can expand the exponential since  $\Gamma_{\text{cusp}} \in O(a)$ . This way, we reduce to integrals

$$\int_0^\infty \log^k \frac{b}{b_0} J_1(b) db = \left( \partial_\nu^k \int_0^\infty \left( \frac{b}{b_0} \right)^\nu J_1(b) db \right)_{\nu=0} = \left( \partial_\nu^k \left( \frac{2}{b_0} \right)^\nu \frac{\Gamma(1 + \frac{\nu}{2})}{\Gamma(1 - \frac{\nu}{2})} \right)_{\nu=0}. \quad (\text{D.95})$$

Using this algorithm we find that the coefficient  $c_1$  in front of  $\delta(1 - \zeta)$  is given by

$$\begin{aligned} c_1 &= \frac{H(a)}{8} (2 - 4[\Gamma_{\text{coll}}(a)\Gamma_{\text{cusp}}(a)\zeta_3 + \frac{5}{3}\Gamma_{\text{cusp}}(a)^3\zeta_3^2] \\ &\quad + 12\zeta_5[\Gamma_{\text{coll}}(a)\Gamma_{\text{cusp}}(a)^2 + \frac{14}{3}\Gamma_{\text{cusp}}(a)^4\zeta_3] + O(a^5)) \\ &= \frac{H(a)}{8} (2 - \frac{2}{3}\zeta_3^2 a^3 + (28\zeta_3\zeta_5 + 5\zeta_2\zeta_3^2) a^4 + O(a^5)) \\ &= \frac{1}{4} - \frac{1}{4}\zeta_2 a + \frac{1}{2}\zeta_2^2 a^2 - \left( \frac{197\pi^6}{40320} + \frac{7\zeta_3^2}{16} \right) a^3 + \frac{1}{144} (17\pi^2\zeta_3^2 + 504\zeta_3\zeta_5 + 36H_4) a^4 + O(a^5). \end{aligned} \quad (\text{D.96})$$

## APPENDICES TO CHAPTER 6

Appendices to chapter 6 are attached here.

**E.1 Action and supersymmetry transformations of MSYM<sub>2</sub>****E.1.1 Dimensional reduction from 10d to 2d**

The Lagrangian for the  $\mathcal{N} = (8, 8)$  super Yang-Mills theory in 2 dimensions can be obtained by dimensionally reducing the 10 dimensional  $\mathcal{N} = 1$  SYM action

$$\int d^{10}x \text{Tr} \left( -\frac{1}{4} F_{MN} F^{MN} + \frac{i}{2} \bar{\Theta} \Gamma^M D_M \Theta \right) \quad (\text{E.1})$$

where

$$D_M = \partial_M + ig[A_M, \cdot] \quad (\text{E.2})$$

$$F_{MN} = \frac{1}{ig} [D_M, D_N] = \partial_M A_N - \partial_N A_M + ig[A_M, A_N]. \quad (\text{E.3})$$

The dimensionally reduced Lagrangian is [286, 289]

$$\mathcal{L} = \text{Tr} \left( -\frac{1}{2} (D_\mu X^i)^2 + i\chi^T \not{D}\chi - \frac{1}{4} F_{\mu\nu}^2 + \frac{g^2}{4} [X^i, X^j]^2 - \sqrt{2} g \chi_L^T \gamma_i [X^i, \chi_R] \right). \quad (\text{E.4})$$

We will summarize the derivation presented in [289], but adopt a “mostly plus” metric signature in contrast. We use the 10 dimensional metric

$$g_{MN} = \eta_{\mu\nu} \oplus \delta_{ij} \quad (\text{E.5})$$

where  $\mu, \nu = 0, 9$ , and  $i, j = 1, 2, \dots, 8$ , and  $\eta_{\mu\nu} = \text{diag}(-1, +1)$ . We can write the following 10d Majorana-basis (purely imaginary) gamma matrices satisfying  $\{\Gamma^M, \Gamma^N\} = -2g^{MN}$

$$\begin{aligned} \Gamma^0 &= \sigma_2 \otimes I_{16} & \gamma^i &= \begin{pmatrix} 0 & \beta_i \\ \beta_i^T & 0 \end{pmatrix}, \\ \Gamma^i &= i\sigma_1 \otimes \gamma^i & & \\ \Gamma^9 &= i\sigma_1 \otimes \gamma^9, & \gamma^9 &= \begin{pmatrix} I_8 & 0 \\ 0 & -I_8 \end{pmatrix}, \end{aligned} \quad (\text{E.6})$$

where the  $\sigma_a$  are the usual Pauli matrices,

$$\sigma_1 = \begin{pmatrix} 0 & 1 \\ 1 & 0 \end{pmatrix}, \quad \sigma_2 = \begin{pmatrix} 0 & -i \\ i & 0 \end{pmatrix}, \quad \sigma_3 = \begin{pmatrix} 1 & 0 \\ 0 & -1 \end{pmatrix}, \quad (\text{E.7})$$

and the  $\gamma^i$  are  $16 \times 16$   $SO(8)$  gamma matrices of the reducible  $\mathbf{8}_s \oplus \mathbf{8}_c$  representation, with the  $\beta_i$  satisfying  $\{\beta_i, \beta_j^T\} = 2\delta_{ij}$ . The 10d spinor  $\Theta$  is Majorana, and has real components in the Majorana basis we have chosen above, thus we can identify the charge conjugation matrix  $\mathcal{C} = -\Gamma^0$ .  $\Theta$  also satisfies the Weyl condition  $\Theta = \Gamma^{11}\Theta$ , where  $\Gamma^{11} = \Gamma^0 \cdots \Gamma^9 = \sigma_3 \otimes I_{16}$  is the 10d chirality matrix, which allows us to write  $\Theta = (\chi, 0)^T$ . The 8d chirality matrix  $\gamma^9$  allows us to decompose further as  $\chi = (\chi_L, \chi_R)$ .

Dimensionally reducing on the  $1, 2, \dots, 8$  directions, we define scalars  $X^i := A^i$ , and obtain the action

$$S_{\text{MSYM}_2} = \int dx^2 \text{Tr} \left( -\frac{1}{2} (D_\mu X^i)^2 + \frac{i}{2} \chi_L^T (D_0 + D_9) \chi_L + \frac{i}{2} \chi_R^T (D_0 - D_9) \chi_R - \frac{1}{4} F_{\mu\nu}^2 + \frac{g^2}{4} [X^i, X^j]^2 - g \chi_L^\alpha \gamma_{\alpha\dot{\beta}}^i [X^i, \chi_R^{\dot{\beta}}] \right). \quad (\text{E.8})$$

We are interested in the theory with gauge group  $U(N)$  or  $SU(N)$ . The scalars  $X^i$  and the fermions  $\chi = (\chi_L^\alpha, \chi_R^{\dot{\alpha}})$  are in the adjoint of the gauge group. The Lagrangian manifestly possesses a  $Spin(8)$  R-symmetry, interpreted as rotations in the 8 transverse directions, under which the scalars  $X^i$  and the spinors  $\chi_L^\alpha$ , and  $\chi_R^{\dot{\alpha}}$  transform in the  $\mathbf{8}_v$ ,  $\mathbf{8}_s$ , and  $\mathbf{8}_c$  representations, respectively.

The supersymmetry transformations can be deduced from the 10d SYM transformations [331]:

$$\delta A_M = i\bar{\varepsilon} \Gamma_M \Theta \quad (\text{E.9})$$

$$\delta \Theta = \Gamma_{MN} F^{MN} \varepsilon. \quad (\text{E.10})$$

After dimensional reduction, they are given by

$$\delta A_\mu = i\varepsilon^T \Gamma^0 \Gamma_\mu \chi \quad (\text{E.11})$$

$$\delta X^i = i\varepsilon_L^\alpha \gamma_{\alpha\dot{\alpha}}^i \chi_R^{\dot{\alpha}} + i\varepsilon_R^{\dot{\alpha}} \gamma_{\dot{\alpha}\alpha}^i \chi_L^\alpha \quad (\text{E.12})$$

$$\delta \chi_L^\alpha = 4c \left[ (+F_{09} \delta_{\alpha\beta} - \frac{ig}{2} [X_i, X_j] \gamma_{\alpha\rho}^i \gamma_{\rho\beta}^j) \varepsilon_L^\beta + (D_0 - D_9) X_i \gamma_{\alpha\beta}^i \varepsilon_R^\beta \right] \quad (\text{E.13})$$

$$\delta \chi_R^{\dot{\alpha}} = 4c \left[ (-F_{09} \delta_{\dot{\alpha}\dot{\beta}} - \frac{ig}{2} [X_i, X_j] \gamma_{\dot{\alpha}\rho}^i \gamma_{\rho\dot{\beta}}^j) \varepsilon_R^{\dot{\beta}} + (D_0 + D_9) X_i \gamma_{\dot{\alpha}\beta}^i \varepsilon_L^\beta \right] \quad (\text{E.14})$$

where  $c$  is the constant in  $\Gamma^{MN} = c[\Gamma^M, \Gamma^N]$ , and is determined as  $c = \frac{1}{4}$  by imposing  $\Gamma^{MN} \Gamma_{MN} = -2 \binom{10}{2}$ . In the  $U(N) + B$  theory, one should replace  $F_{09}$  with the generalized field strength  $\mathcal{F}_{09}$ .

### E.1.2 Supersymmetry subalgebras and superspace formulation

For the purpose of computing the index of  $\text{MSYM}_2$ , it is convenient to express fields and the Lagrangian in  $\mathcal{N} = (0, 2)$  or  $\mathcal{N} = (2, 2)$  superspace. This can be done by considering the representations of the fields and supersymmetries under the  $Spin(8)$  R-symmetry. The 16 supersymmetry generators  $(\varepsilon_L^\dot{\alpha}, \varepsilon_R^\alpha)$  are in the representation  $\mathbf{8}_c \oplus \mathbf{8}_s$  of  $Spin(8)$ . A choice of a  $\mathcal{N} = (0, 2)$  subalgebra of the supersymmetry algebra is generated by  $\varepsilon_R^\pm := \varepsilon_R^1 \pm i\varepsilon_R^2$  corresponding to a pair of antiparallel weights of the  $\mathbf{8}_s$  representation. Letting  $\{\pm e_i\} \subset \mathfrak{h}^*$  be the weights of the fundamental representation  $\mathbf{8}_v$ , we pick the two weights  $\pm r$  of  $\mathbf{8}_s$  where

$$r := \frac{1}{2}(e_1 + e_2 + e_3 + e_4). \quad (\text{E.15})$$

Note that  $\pm r$  are eigenvalues for the action of the Cartan generator  $J = \frac{1}{2}(K_1 + K_2 + K_3 + K_4)$  on the weightspaces of  $\pm r$ , where  $e_i(K_k) = \delta_{ik}$ . With this choice, the  $Spin(8)$  representations reduce as

$$\begin{aligned} \mathbf{8}_s &\rightarrow \mathbf{1}_{+1} \oplus \mathbf{6}_0 \oplus \mathbf{1}_{-1} \\ \mathbf{8}_c &\rightarrow \mathbf{4}_{-\frac{1}{2}} \oplus \bar{\mathbf{4}}_{+\frac{1}{2}} \\ \mathbf{8}_v &\rightarrow \mathbf{4}_{+\frac{1}{2}} \oplus \bar{\mathbf{4}}_{-\frac{1}{2}} \end{aligned} \quad (\text{E.16})$$

under the decomposition  $U(1)_R \times SU(4) \cong Spin(2) \times Spin(6) \subset Spin(8)$ , where  $U(1)_R$  is generated by  $J$ . The supersymmetry generators are now  $(\varepsilon_L^\dot{\alpha}, \varepsilon_R^\alpha) = (\varepsilon_L^A, (\varepsilon_L)_A, \varepsilon_R^\pm, \varepsilon_R^{AB})$ , where  $A, B = 1, 2, 3, 4$  are  $SU(4)$  indices for the fundamental representation  $\mathbf{4}$ . The field content of the theory is organized into  $\mathcal{N} = (0, 2)$  superfields as in (6.73) in the main text, with the Lagrangian given by the standard D-terms and the superpotential (6.74).

To get an  $\mathcal{N} = (2, 2)$  subalgebra, one can to pick  $l := \frac{1}{2}(e_1 + e_2 + e_3 - e_4)$ . Then, the vector and axial R-symmetries are determined by

$$R_V = r + l = e_1 + e_2 + e_3, \quad R_A = r - l = e_4. \quad (\text{E.17})$$

This choice further decomposes the R-symmetry to  $U(1)_R \times U(1)_L \times SU(3) \subset Spin(8)$ , with the representations decomposing as

$$\begin{aligned} \mathbf{8}_s &\rightarrow \mathbf{1}_{+1, +\frac{1}{2}} \oplus \mathbf{3}_{0, +\frac{1}{2}} \oplus \bar{\mathbf{3}}_{0, -\frac{1}{2}} \oplus \mathbf{1}_{-1, -\frac{1}{2}} \\ \mathbf{8}_c &\rightarrow \mathbf{3}_{-\frac{1}{2}, 0} \oplus \mathbf{1}_{-\frac{1}{2}, -1} \oplus \bar{\mathbf{3}}_{+\frac{1}{2}, 0} \oplus \mathbf{1}_{+\frac{1}{2}, +1} \\ \mathbf{8}_v &\rightarrow \mathbf{3}_{+\frac{1}{2}, +\frac{1}{2}} \oplus \mathbf{1}_{+\frac{1}{2}, -\frac{1}{2}} \oplus \bar{\mathbf{3}}_{-\frac{1}{2}, -\frac{1}{2}} \oplus \mathbf{1}_{-\frac{1}{2}, +\frac{1}{2}} \end{aligned} \quad (\text{E.18})$$

The supersymmetries are generated by  $(\varepsilon_L^\pm, \varepsilon_L^A, (\varepsilon_L)_A, \varepsilon_R^\pm, \varepsilon_R^A, (\varepsilon_R)_A)$ . In  $\mathcal{N} = (2, 2)$  superspace, the  $SU(3)$  singlets correspond to the components of the vector multiplet  $\tilde{\Sigma}$  and its conjugate, and the  $\mathbf{3} \oplus \bar{\mathbf{3}}$  correspond to the components of the chiral fields  $\tilde{\Phi}^B$  and its conjugate, with the superpotential as in (6.75).

## BIBLIOGRAPHY

- <sup>1</sup>D. Simmons-Duffin, “The Conformal Bootstrap”, in [Proceedings, Theoretical Advanced Study Institute in Elementary Particle Physics: New Frontiers in Fields and Strings \(TASI 2015\): Boulder, CO, USA, June 1-26, 2015](#) (2017), pp. 1–74, [10.1142/9789813149441\\_0001](#), [arXiv:1602.07982 \[hep-th\]](#).
- <sup>2</sup>J. L. Cardy, *Scaling and renormalization in statistical physics*, Cambridge lecture notes in physics: 3 (Cambridge, UK: Univ. Pr., 1996).
- <sup>3</sup>J. Lipa, J. Nissen, D. Stricker, D. Swanson, and T. Chui, “Specific heat of liquid helium in zero gravity very near the lambda point”, *Phys.Rev.* **B68**, 174518 (2003) [10.1103/PhysRevB.68.174518](#).
- <sup>4</sup>M.-C. Cha, M. P. A. Fisher, S. M. Girvin, M. Wallin, and A. P. Young, “Universal conductivity of two-dimensional films at the superconductor-insulator transition”, *Phys. Rev. B* **44**, 6883–6902 (1991) [10.1103/PhysRevB.44.6883](#).
- <sup>5</sup>J. Smakov and E. Sorensen, “Universal scaling of the conductivity at the superfluid-insulator phase transition”, *Phys. Rev. Lett.* **95**, 180603 (2005) [10.1103/PhysRevLett.95.180603](#).
- <sup>6</sup>J. M. Maldacena, “The Large N limit of superconformal field theories and supergravity”, *Int. J. Theor. Phys.* **38**, [Adv. Theor. Math. Phys.2,231(1998)], 1113–1133 (1999) [10.1023/A:1026654312961](#), [10.4310/ATMP.1998.v2.n2.a1](#), [arXiv:hep-th/9711200 \[hep-th\]](#).
- <sup>7</sup>E. Witten, “Anti-de Sitter space and holography”, *Adv. Theor. Math. Phys.* **2**, 253–291 (1998) [10.4310/ATMP.1998.v2.n2.a2](#), [arXiv:hep-th/9802150 \[hep-th\]](#).
- <sup>8</sup>R. Streater and A. Wightman, *Pct, spin and statistics, and all that*, Princeton Landmarks in Mathematics and Physics (Princeton University Press, 2016).
- <sup>9</sup>S. Ferrara, A. F. Grillo, and R. Gatto, “Tensor representations of conformal algebra and conformally covariant operator product expansion”, *Annals Phys.* **76**, 161–188 (1973) [10.1016/0003-4916\(73\)90446-6](#).
- <sup>10</sup>A. M. Polyakov, “Nonhamiltonian approach to conformal quantum field theory”, *Zh. Eksp. Teor. Fiz.* **66**, [Sov. Phys. JETP39,9(1974)], 23–42 (1974).
- <sup>11</sup>D. Poland, S. Rychkov, and A. Vichi, “The Conformal Bootstrap: Theory, Numerical Techniques, and Applications”, *Rev. Mod. Phys.* **91**, 15002 (2019) [10.1103/RevModPhys.91.015002](#), [arXiv:1805.04405 \[hep-th\]](#).
- <sup>12</sup>L. F. Alday and J. M. Maldacena, “Comments on operators with large spin”, *JHEP* **11**, 019 (2007) [10.1088/1126-6708/2007/11/019](#), [arXiv:0708.0672 \[hep-th\]](#).
- <sup>13</sup>A. L. Fitzpatrick, J. Kaplan, D. Poland, and D. Simmons-Duffin, “The Analytic Bootstrap and AdS Superhorizon Locality”, *JHEP* **1312**, 004 (2013) [10.1007/JHEP12\(2013\)004](#), [arXiv:1212.3616 \[hep-th\]](#).

- <sup>14</sup>Z. Komargodski and A. Zhiboedov, “Convexity and Liberation at Large Spin”, *JHEP* **1311**, 140 (2013) [10.1007/JHEP11\(2013\)140](https://doi.org/10.1007/JHEP11(2013)140), [arXiv:1212.4103](https://arxiv.org/abs/1212.4103) [[hep-th](#)].
- <sup>15</sup>L. F. Alday, A. Bissi, and T. Lukowski, “Large spin systematics in CFT”, *JHEP* **11**, 101 (2015) [10.1007/JHEP11\(2015\)101](https://doi.org/10.1007/JHEP11(2015)101), [arXiv:1502.07707](https://arxiv.org/abs/1502.07707) [[hep-th](#)].
- <sup>16</sup>L. F. Alday and A. Zhiboedov, “Conformal Bootstrap With Slightly Broken Higher Spin Symmetry”, *JHEP* **06**, 091 (2016) [10.1007/JHEP06\(2016\)091](https://doi.org/10.1007/JHEP06(2016)091), [arXiv:1506.04659](https://arxiv.org/abs/1506.04659) [[hep-th](#)].
- <sup>17</sup>L. F. Alday and A. Zhiboedov, “An Algebraic Approach to the Analytic Bootstrap”, *JHEP* **04**, 157 (2017) [10.1007/JHEP04\(2017\)157](https://doi.org/10.1007/JHEP04(2017)157), [arXiv:1510.08091](https://arxiv.org/abs/1510.08091) [[hep-th](#)].
- <sup>18</sup>A. Kaviraj, K. Sen, and A. Sinha, “Analytic bootstrap at large spin”, *JHEP* **11**, 083 (2015) [10.1007/JHEP11\(2015\)083](https://doi.org/10.1007/JHEP11(2015)083), [arXiv:1502.01437](https://arxiv.org/abs/1502.01437) [[hep-th](#)].
- <sup>19</sup>A. Kaviraj, K. Sen, and A. Sinha, “Universal anomalous dimensions at large spin and large twist”, *JHEP* **07**, 026 (2015) [10.1007/JHEP07\(2015\)026](https://doi.org/10.1007/JHEP07(2015)026), [arXiv:1504.00772](https://arxiv.org/abs/1504.00772) [[hep-th](#)].
- <sup>20</sup>D. Simmons-Duffin, “The Lightcone Bootstrap and the Spectrum of the 3d Ising CFT”, *JHEP* **03**, 086 (2017) [10.1007/JHEP03\(2017\)086](https://doi.org/10.1007/JHEP03(2017)086), [arXiv:1612.08471](https://arxiv.org/abs/1612.08471) [[hep-th](#)].
- <sup>21</sup>L. F. Alday, “Solving CFTs with Weakly Broken Higher Spin Symmetry”, (2016), [arXiv:1612.00696](https://arxiv.org/abs/1612.00696) [[hep-th](#)].
- <sup>22</sup>L. F. Alday and A. Bissi, “Crossing symmetry and Higher spin towers”, (2016), [arXiv:1603.05150](https://arxiv.org/abs/1603.05150) [[hep-th](#)].
- <sup>23</sup>L. F. Alday, “Large Spin Perturbation Theory for Conformal Field Theories”, *Phys. Rev. Lett.* **119**, 111601 (2017) [10.1103/PhysRevLett.119.111601](https://doi.org/10.1103/PhysRevLett.119.111601), [arXiv:1611.01500](https://arxiv.org/abs/1611.01500) [[hep-th](#)].
- <sup>24</sup>L. F. Alday, J. Henriksson, and M. van Loon, “Taming the  $\epsilon$ -expansion with Large Spin Perturbation Theory”, (2017), [arXiv:1712.02314](https://arxiv.org/abs/1712.02314) [[hep-th](#)].
- <sup>25</sup>S. Caron-Huot, “Analyticity in Spin in Conformal Theories”, *JHEP* **09**, 078 (2017) [10.1007/JHEP09\(2017\)078](https://doi.org/10.1007/JHEP09(2017)078), [arXiv:1703.00278](https://arxiv.org/abs/1703.00278) [[hep-th](#)].
- <sup>26</sup>D. Simmons-Duffin, D. Stanford, and E. Witten, “A spacetime derivation of the Lorentzian OPE inversion formula”, *JHEP* **07**, 085 (2018) [10.1007/JHEP07\(2018\)085](https://doi.org/10.1007/JHEP07(2018)085), [arXiv:1711.03816](https://arxiv.org/abs/1711.03816) [[hep-th](#)].
- <sup>27</sup>G. Mack, “All Unitary Ray Representations of the Conformal Group  $SU(2, 2)$  with Positive Energy”, *Commun.Math.Phys.* **55**, 1 (1977) [10.1007/BF01613145](https://doi.org/10.1007/BF01613145).
- <sup>28</sup>P. Kravchuk and D. Simmons-Duffin, “Light-ray operators in conformal field theory”, *JHEP* **11**, [236(2018)], 102 (2018) [10.1007/JHEP11\(2018\)102](https://doi.org/10.1007/JHEP11(2018)102), [arXiv:1805.00098](https://arxiv.org/abs/1805.00098) [[hep-th](#)].
- <sup>29</sup>O. Aharony, N. Seiberg, and Y. Tachikawa, “Reading between the lines of four-dimensional gauge theories”, *JHEP* **08**, 115 (2013) [10.1007/JHEP08\(2013\)115](https://doi.org/10.1007/JHEP08(2013)115), [arXiv:1305.0318](https://arxiv.org/abs/1305.0318) [[hep-th](#)].

- <sup>30</sup>A. Kapustin and N. Seiberg, “Coupling a QFT to a TQFT and duality”, *JHEP* **04**, 001 (2014) [10.1007/JHEP04\(2014\)001](https://doi.org/10.1007/JHEP04(2014)001), [arXiv:1401.0740](https://arxiv.org/abs/1401.0740) [[hep-th](#)].
- <sup>31</sup>D. M. Hofman and J. Maldacena, “Conformal collider physics: Energy and charge correlations”, *JHEP* **05**, 012 (2008) [10.1088/1126-6708/2008/05/012](https://doi.org/10.1088/1126-6708/2008/05/012), [arXiv:0803.1467](https://arxiv.org/abs/0803.1467) [[hep-th](#)].
- <sup>32</sup>E. Katz, S. Sachdev, E. S. Sorensen, and W. Witczak-Krempa, “Conformal field theories at nonzero temperature: Operator product expansions, Monte Carlo, and holography”, *Phys. Rev.* **B90**, 245109 (2014) [10.1103/PhysRevB.90.245109](https://doi.org/10.1103/PhysRevB.90.245109), [arXiv:1409.3841](https://arxiv.org/abs/1409.3841) [[cond-mat.str-el](#)].
- <sup>33</sup>F. Kos, D. Poland, D. Simmons-Duffin, and A. Vichi, “Bootstrapping the O(N) Archipelago”, *JHEP* **11**, 106 (2015) [10.1007/JHEP11\(2015\)106](https://doi.org/10.1007/JHEP11(2015)106), [arXiv:1504.07997](https://arxiv.org/abs/1504.07997) [[hep-th](#)].
- <sup>34</sup>Y. Nakayama, “Bootstrapping critical Ising model on three-dimensional real projective space”, *Phys. Rev. Lett.* **116**, 141602 (2016) [10.1103/PhysRevLett.116.141602](https://doi.org/10.1103/PhysRevLett.116.141602), [arXiv:1601.06851](https://arxiv.org/abs/1601.06851) [[hep-th](#)].
- <sup>35</sup>C. Hasegawa and Yu. Nakayama, “ $\epsilon$ -Expansion in Critical  $\phi^3$ -Theory on Real Projective Space from Conformal Field Theory”, *Mod. Phys. Lett.* **A32**, 1750045 (2017) [10.1142/S0217732317500456](https://doi.org/10.1142/S0217732317500456), [arXiv:1611.06373](https://arxiv.org/abs/1611.06373) [[hep-th](#)].
- <sup>36</sup>C. Hasegawa and Y. Nakayama, “Three ways to solve critical  $\phi^4$  theory on  $4 - \epsilon$  dimensional real projective space: perturbation, bootstrap, and Schwinger-Dyson equation”, (2018), [arXiv:1801.09107](https://arxiv.org/abs/1801.09107) [[hep-th](#)].
- <sup>37</sup>S. S. Gubser, I. R. Klebanov, and A. M. Polyakov, “Gauge theory correlators from noncritical string theory”, *Phys. Lett.* **B428**, 105–114 (1998) [10.1016/S0370-2693\(98\)00377-3](https://doi.org/10.1016/S0370-2693(98)00377-3), [arXiv:hep-th/9802109](https://arxiv.org/abs/hep-th/9802109) [[hep-th](#)].
- <sup>38</sup>S. El-Showk and K. Papadodimas, “Emergent Spacetime and Holographic CFTs”, *JHEP* **1210**, 106 (2012) [10.1007/JHEP10\(2012\)106](https://doi.org/10.1007/JHEP10(2012)106), [arXiv:1101.4163](https://arxiv.org/abs/1101.4163) [[hep-th](#)].
- <sup>39</sup>R. Rattazzi, V. S. Rychkov, E. Tonni, and A. Vichi, “Bounding scalar operator dimensions in 4D CFT”, *JHEP* **12**, 031 (2008) [10.1088/1126-6708/2008/12/031](https://doi.org/10.1088/1126-6708/2008/12/031), [arXiv:0807.0004](https://arxiv.org/abs/0807.0004) [[hep-th](#)].
- <sup>40</sup>D. Poland, D. Simmons-Duffin, and A. Vichi, “Carving Out the Space of 4D CFTs”, *JHEP* **05**, 110 (2012) [10.1007/JHEP05\(2012\)110](https://doi.org/10.1007/JHEP05(2012)110), [arXiv:1109.5176](https://arxiv.org/abs/1109.5176) [[hep-th](#)].
- <sup>41</sup>S. El-Showk, M. F. Paulos, D. Poland, S. Rychkov, D. Simmons-Duffin, and A. Vichi, “Solving the 3d Ising Model with the Conformal Bootstrap II. c-Minimization and Precise Critical Exponents”, *J. Stat. Phys.* **157**, 869 (2014) [10.1007/s10955-014-1042-7](https://doi.org/10.1007/s10955-014-1042-7), [arXiv:1403.4545](https://arxiv.org/abs/1403.4545) [[hep-th](#)].
- <sup>42</sup>M. F. Paulos, “JuliBootS: a hands-on guide to the conformal bootstrap”, (2014), [arXiv:1412.4127](https://arxiv.org/abs/1412.4127) [[hep-th](#)].
- <sup>43</sup>D. Simmons-Duffin, “A Semidefinite Program Solver for the Conformal Bootstrap”, *JHEP* **06**, 174 (2015) [10.1007/JHEP06\(2015\)174](https://doi.org/10.1007/JHEP06(2015)174), [arXiv:1502.02033](https://arxiv.org/abs/1502.02033) [[hep-th](#)].



- <sup>44</sup>P. Liendo, L. Rastelli, and B. C. van Rees, “The Bootstrap Program for Boundary CFT<sub>d</sub>”, *JHEP* **1307**, 113 (2013) [10.1007/JHEP07\(2013\)113](https://doi.org/10.1007/JHEP07(2013)113), [arXiv:1210.4258](https://arxiv.org/abs/1210.4258) [[hep-th](#)].
- <sup>45</sup>F. Gliozzi, P. Liendo, M. Meineri, and A. Rago, “Boundary and Interface CFTs from the Conformal Bootstrap”, *JHEP* **05**, 036 (2015) [10.1007/JHEP05\(2015\)036](https://doi.org/10.1007/JHEP05(2015)036), [arXiv:1502.07217](https://arxiv.org/abs/1502.07217) [[hep-th](#)].
- <sup>46</sup>L. Rastelli and X. Zhou, “The Mellin Formalism for Boundary CFT<sub>d</sub>”, *JHEP* **10**, 146 (2017) [10.1007/JHEP10\(2017\)146](https://doi.org/10.1007/JHEP10(2017)146), [arXiv:1705.05362](https://arxiv.org/abs/1705.05362) [[hep-th](#)].
- <sup>47</sup>M. Billò, V. Gonçalves, E. Lauria, and M. Meineri, “Defects in conformal field theory”, *JHEP* **04**, 091 (2016) [10.1007/JHEP04\(2016\)091](https://doi.org/10.1007/JHEP04(2016)091), [arXiv:1601.02883](https://arxiv.org/abs/1601.02883) [[hep-th](#)].
- <sup>48</sup>A. Gadde, “Conformal constraints on defects”, (2016), [arXiv:1602.06354](https://arxiv.org/abs/1602.06354) [[hep-th](#)].
- <sup>49</sup>P. Liendo and C. Meneghelli, “Bootstrap equations for  $\mathcal{N} = 4$  SYM with defects”, *JHEP* **01**, 122 (2017) [10.1007/JHEP01\(2017\)122](https://doi.org/10.1007/JHEP01(2017)122), [arXiv:1608.05126](https://arxiv.org/abs/1608.05126) [[hep-th](#)].
- <sup>50</sup>E. Lauria, M. Meineri, and E. Trevisani, “Radial coordinates for defect CFTs”, (2017), [arXiv:1712.07668](https://arxiv.org/abs/1712.07668) [[hep-th](#)].
- <sup>51</sup>M. Lemos, P. Liendo, M. Meineri, and S. Sarkar, “Universality at large transverse spin in defect CFT”, (2017), [arXiv:1712.08185](https://arxiv.org/abs/1712.08185) [[hep-th](#)].
- <sup>52</sup>F. Gliozzi and A. Rago, “Critical exponents of the 3d Ising and related models from Conformal Bootstrap”, *JHEP* **1410**, 42 (2014) [10.1007/JHEP10\(2014\)042](https://doi.org/10.1007/JHEP10(2014)042), [arXiv:1403.6003](https://arxiv.org/abs/1403.6003) [[hep-th](#)].
- <sup>53</sup>S. Hikami, “Conformal Bootstrap Analysis for Yang-Lee Edge Singularity”, (2017), [arXiv:1707.04813](https://arxiv.org/abs/1707.04813) [[hep-th](#)].
- <sup>54</sup>S. El-Showk, M. F. Paulos, D. Poland, S. Rychkov, D. Simmons-Duffin, and A. Vichi, “Solving the 3D Ising Model with the Conformal Bootstrap”, *Phys. Rev.* **D86**, 025022 (2012) [10.1103/PhysRevD.86.025022](https://doi.org/10.1103/PhysRevD.86.025022), [arXiv:1203.6064](https://arxiv.org/abs/1203.6064) [[hep-th](#)].
- <sup>55</sup>F. Kos, D. Poland, and D. Simmons-Duffin, “Bootstrapping Mixed Correlators in the 3D Ising Model”, *JHEP* **11**, 109 (2014) [10.1007/JHEP11\(2014\)109](https://doi.org/10.1007/JHEP11(2014)109), [arXiv:1406.4858](https://arxiv.org/abs/1406.4858) [[hep-th](#)].
- <sup>56</sup>F. Kos, D. Poland, D. Simmons-Duffin, and A. Vichi, “Precision Islands in the Ising and  $O(N)$  Models”, *JHEP* **08**, 036 (2016) [10.1007/JHEP08\(2016\)036](https://doi.org/10.1007/JHEP08(2016)036), [arXiv:1603.04436](https://arxiv.org/abs/1603.04436) [[hep-th](#)].
- <sup>57</sup>V. N. Gribov, “Partial waves with complex orbital angular momenta and the asymptotic behavior of the scattering amplitude”, *Sov. Phys. JETP* **14**, [Zh. Eksp. Teor. Fiz.41,1962(1961)], 1395 (1962).
- <sup>58</sup>M. Froissart, “Asymptotic behavior and subtractions in the Mandelstam representation”, *Phys. Rev.* **123**, 1053–1057 (1961) [10.1103/PhysRev.123.1053](https://doi.org/10.1103/PhysRev.123.1053).

- <sup>59</sup>L. F. Alday, A. Bissi, and E. Perlmutter, “Holographic Reconstruction of AdS Exchanges from Crossing Symmetry”, *JHEP* **08**, 147 (2017) [10.1007/JHEP08\(2017\)147](https://doi.org/10.1007/JHEP08(2017)147), [arXiv:1705.02318](https://arxiv.org/abs/1705.02318) [[hep-th](#)].
- <sup>60</sup>P. Dey, K. Ghosh, and A. Sinha, “Simplifying large spin bootstrap in Mellin space”, *JHEP* **01**, 152 (2018) [10.1007/JHEP01\(2018\)152](https://doi.org/10.1007/JHEP01(2018)152), [arXiv:1709.06110](https://arxiv.org/abs/1709.06110) [[hep-th](#)].
- <sup>61</sup>J. Henriksson and T. Lukowski, “Perturbative Four-Point Functions from the Analytic Conformal Bootstrap”, (2017), [arXiv:1710.06242](https://arxiv.org/abs/1710.06242) [[hep-th](#)].
- <sup>62</sup>L. F. Alday and S. Caron-Huot, “Gravitational S-matrix from CFT dispersion relations”, *JHEP* **12**, 017 (2018) [10.1007/JHEP12\(2018\)017](https://doi.org/10.1007/JHEP12(2018)017), [arXiv:1711.02031](https://arxiv.org/abs/1711.02031) [[hep-th](#)].
- <sup>63</sup>M. van Loon, “The Analytic Bootstrap in Fermionic CFTs”, *JHEP* **01**, 104 (2018) [10.1007/JHEP01\(2018\)104](https://doi.org/10.1007/JHEP01(2018)104), [arXiv:1711.02099](https://arxiv.org/abs/1711.02099) [[hep-th](#)].
- <sup>64</sup>J. Henriksson and M. van Loon, “Critical  $O(N)$  model to order  $\epsilon^4$  from analytic bootstrap”, (2018), [arXiv:1801.03512](https://arxiv.org/abs/1801.03512) [[hep-th](#)].
- <sup>65</sup>G. J. Turiaci and A. Zhiboedov, “Veneziano Amplitude of Vasiliev Theory”, (2018), [arXiv:1802.04390](https://arxiv.org/abs/1802.04390) [[hep-th](#)].
- <sup>66</sup>S. Sachdev, “Polylogarithm identities in a conformal field theory in three-dimensions”, *Phys. Lett.* **B309**, 285–288 (1993) [10.1016/0370-2693\(93\)90935-B](https://doi.org/10.1016/0370-2693(93)90935-B), [arXiv:hep-th/9305131](https://arxiv.org/abs/hep-th/9305131) [[hep-th](#)].
- <sup>67</sup>M. A. Vasiliev, “Higher spin gauge theories: Star product and AdS space”, (1999) [10.1142/9789812793850\\_0030](https://doi.org/10.1142/9789812793850_0030), [arXiv:hep-th/9910096](https://arxiv.org/abs/hep-th/9910096) [[hep-th](#)].
- <sup>68</sup>I. Klebanov and A. Polyakov, “AdS dual of the critical  $O(N)$  vector model”, *Phys.Lett.* **B550**, 213–219 (2002) [10.1016/S0370-2693\(02\)02980-5](https://doi.org/10.1016/S0370-2693(02)02980-5), [arXiv:hep-th/0210114](https://arxiv.org/abs/hep-th/0210114) [[hep-th](#)].
- <sup>69</sup>S. Giombi and X. Yin, “The Higher Spin/Vector Model Duality”, *J. Phys.* **A46**, 214003 (2013) [10.1088/1751-8113/46/21/214003](https://doi.org/10.1088/1751-8113/46/21/214003), [arXiv:1208.4036](https://arxiv.org/abs/1208.4036) [[hep-th](#)].
- <sup>70</sup>W. Witczak-Krempa, “Constraining Quantum Critical Dynamics: (2+1)D Ising Model and Beyond”, *Phys. Rev. Lett.* **114**, 177201 (2015) [10.1103/PhysRevLett.114.177201](https://doi.org/10.1103/PhysRevLett.114.177201), [arXiv:1501.03495](https://arxiv.org/abs/1501.03495) [[cond-mat.str-el](#)].
- <sup>71</sup>P. Kravchuk, “Casimir recursion relations for general conformal blocks”, *JHEP* **02**, [164(2017)], 011 (2018) [10.1007/JHEP02\(2018\)011](https://doi.org/10.1007/JHEP02(2018)011), [arXiv:1709.05347](https://arxiv.org/abs/1709.05347) [[hep-th](#)].
- <sup>72</sup>H. Osborn and A. C. Petkou, “Implications of conformal invariance in field theories for general dimensions”, *Annals Phys.* **231**, 311–362 (1994) [10.1006/aphy.1994.1045](https://doi.org/10.1006/aphy.1994.1045), [arXiv:hep-th/9307010](https://arxiv.org/abs/hep-th/9307010) [[hep-th](#)].
- <sup>73</sup>A. V. Chubukov, S. Sachdev, and J. Ye, “Theory of two-dimensional quantum Heisenberg antiferromagnets with a nearly critical ground state”, *Phys. Rev.* **B49**, 11919–11961 (1994) [10.1103/PhysRevB.49.11919](https://doi.org/10.1103/PhysRevB.49.11919).

- <sup>74</sup>O. Vasilyev, A. Gambassi, A. Maciolek, and S. Dietrich, “Universal scaling functions of critical casimir forces obtained by monte carlo simulations”, *Phys. Rev. E* **79**, 041142 (2009) [10.1103/PhysRevE.79.041142](https://doi.org/10.1103/PhysRevE.79.041142).
- <sup>75</sup>M. Krech and D. P. Landau, “Casimir effect in critical systems: a monte carlo simulation”, *Phys. Rev. E* **53**, 4414–4423 (1996) [10.1103/PhysRevE.53.4414](https://doi.org/10.1103/PhysRevE.53.4414).
- <sup>76</sup>M. Krech, “Casimir forces in binary liquid mixtures”, *Phys. Rev. E* **56**, 1642–1659 (1997) [10.1103/PhysRevE.56.1642](https://doi.org/10.1103/PhysRevE.56.1642).
- <sup>77</sup>P. Di Francesco, P. Mathieu, and D. Senechal, *Conformal Field Theory*, Graduate Texts in Contemporary Physics (Springer-Verlag, New York, 1997), [10.1007/978-1-4612-2256-9](https://doi.org/10.1007/978-1-4612-2256-9).
- <sup>78</sup>M. Gaberdiel, “A General transformation formula for conformal fields”, *Phys. Lett. B* **325**, 366–370 (1994) [10.1016/0370-2693\(94\)90026-4](https://doi.org/10.1016/0370-2693(94)90026-4), [arXiv:hep-th/9401166](https://arxiv.org/abs/hep-th/9401166) [[hep-th](#)].
- <sup>79</sup>B. Chen, J. Long, and J.-j. Zhang, “Holographic Renyi entropy for CFT with W symmetry”, *JHEP* **04**, 041 (2014) [10.1007/JHEP04\(2014\)041](https://doi.org/10.1007/JHEP04(2014)041), [arXiv:1312.5510](https://arxiv.org/abs/1312.5510) [[hep-th](#)].
- <sup>80</sup>Y. Gobeil, A. Maloney, G. S. Ng, and J.-q. Wu, “Thermal Conformal Blocks”, (2018), [arXiv:1802.10537](https://arxiv.org/abs/1802.10537) [[hep-th](#)].
- <sup>81</sup>F. M. Haehl, R. Loganayagam, P. Narayan, A. A. Nizami, and M. Rangamani, “Thermal out-of-time-order correlators, KMS relations, and spectral functions”, *JHEP* **12**, 154 (2017) [10.1007/JHEP12\(2017\)154](https://doi.org/10.1007/JHEP12(2017)154), [arXiv:1706.08956](https://arxiv.org/abs/1706.08956) [[hep-th](#)].
- <sup>82</sup>V. K. Dobrev, G. Mack, V. B. Petkova, S. G. Petrova, and I. T. Todorov, “Harmonic Analysis on the n-Dimensional Lorentz Group and Its Application to Conformal Quantum Field Theory”, *Lect. Notes Phys.* **63**, 1–280 (1977) [10.1007/BFb0009678](https://doi.org/10.1007/BFb0009678).
- <sup>83</sup>M. F. Paulos, J. Penedones, J. Toledo, B. C. van Rees, and P. Vieira, “The S-matrix Bootstrap III: Higher Dimensional Amplitudes”, (2017), [arXiv:1708.06765](https://arxiv.org/abs/1708.06765) [[hep-th](#)].
- <sup>84</sup>J. Maldacena, S. H. Shenker, and D. Stanford, “A bound on chaos”, *JHEP* **08**, 106 (2016) [10.1007/JHEP08\(2016\)106](https://doi.org/10.1007/JHEP08(2016)106), [arXiv:1503.01409](https://arxiv.org/abs/1503.01409) [[hep-th](#)].
- <sup>85</sup>O. Aharony, L. F. Alday, A. Bissi, and E. Perlmutter, “Loops in AdS from Conformal Field Theory”, *JHEP* **07**, 036 (2017) [10.1007/JHEP07\(2017\)036](https://doi.org/10.1007/JHEP07(2017)036), [arXiv:1612.03891](https://arxiv.org/abs/1612.03891) [[hep-th](#)].
- <sup>86</sup>D. Stanford, “Many-body chaos at weak coupling”, *JHEP* **10**, 009 (2016) [10.1007/JHEP10\(2016\)009](https://doi.org/10.1007/JHEP10(2016)009), [arXiv:1512.07687](https://arxiv.org/abs/1512.07687) [[hep-th](#)].
- <sup>87</sup>A. L. Fitzpatrick and J. Kaplan, “Unitarity and the Holographic S-Matrix”, *JHEP* **1210**, 032 (2012) [10.1007/JHEP10\(2012\)032](https://doi.org/10.1007/JHEP10(2012)032), [arXiv:1112.4845](https://arxiv.org/abs/1112.4845) [[hep-th](#)].
- <sup>88</sup>A. V. Chubukov, S. Sachdev, and J. Ye, “Theory of two-dimensional quantum heisenberg antiferromagnets with a nearly critical ground state”, *Physical Review B* **49**, 11919 (1994).

- <sup>89</sup>J. Zinn-Justin, *Quantum Field Theory and Critical Phenomena*, 1054 p. (Oxford, England: Clarendon Pr., 2002).
- <sup>90</sup>E. D. Skvortsov, “On (Un)Broken Higher-Spin Symmetry in Vector Models”, in *Proceedings, International Workshop on Higher Spin Gauge Theories: Singapore, Singapore, November 4-6, 2015* (2017), pp. 103–137, [10.1142/97898131444101\\_0008](https://doi.org/10.1142/97898131444101_0008), [arXiv:1512.05994](https://arxiv.org/abs/1512.05994) [hep-th].
- <sup>91</sup>V. E. Didenko and M. A. Vasiliev, “Static BPS black hole in 4d higher-spin gauge theory”, *Phys. Lett.* **B682**, [Erratum: *Phys. Lett.*B722,389(2013)], 305–315 (2009) [10.1016/j.physletb.2013.04.021](https://doi.org/10.1016/j.physletb.2013.04.021), [10.1016/j.physletb.2009.11.023](https://doi.org/10.1016/j.physletb.2009.11.023), [arXiv:0906.3898](https://arxiv.org/abs/0906.3898) [hep-th].
- <sup>92</sup>V. E. Didenko and E. D. Skvortsov, “Exact higher-spin symmetry in CFT: all correlators in unbroken Vasiliev theory”, *JHEP* **04**, 158 (2013) [10.1007/JHEP04\(2013\)158](https://doi.org/10.1007/JHEP04(2013)158), [arXiv:1210.7963](https://arxiv.org/abs/1210.7963) [hep-th].
- <sup>93</sup>M. A. Vasiliev, “Invariant Functionals in Higher-Spin Theory”, *Nucl. Phys.* **B916**, 219–253 (2017) [10.1016/j.nuclphysb.2017.01.001](https://doi.org/10.1016/j.nuclphysb.2017.01.001), [arXiv:1504.07289](https://arxiv.org/abs/1504.07289) [hep-th].
- <sup>94</sup>V. E. Didenko, N. G. Misuna, and M. A. Vasiliev, “Charges in nonlinear higher-spin theory”, *JHEP* **03**, 164 (2017) [10.1007/JHEP03\(2017\)164](https://doi.org/10.1007/JHEP03(2017)164), [arXiv:1512.07626](https://arxiv.org/abs/1512.07626) [hep-th].
- <sup>95</sup>C. Iazeolla, E. Sezgin, and P. Sundell, “On Exact Solutions and Perturbative Schemes in Higher Spin Theory”, *Universe* **4**, 5 (2018) [10.3390/universe4010005](https://doi.org/10.3390/universe4010005), [arXiv:1711.03550](https://arxiv.org/abs/1711.03550) [hep-th].
- <sup>96</sup>X. O. Camanho, J. D. Edelstein, J. Maldacena, and A. Zhiboedov, “Causality Constraints on Corrections to the Graviton Three-Point Coupling”, *JHEP* **02**, 020 (2016) [10.1007/JHEP02\(2016\)020](https://doi.org/10.1007/JHEP02(2016)020), [arXiv:1407.5597](https://arxiv.org/abs/1407.5597) [hep-th].
- <sup>97</sup>N. Afkhami-Jeddi, T. Hartman, S. Kundu, and A. Tajdini, “Einstein gravity 3-point functions from conformal field theory”, *JHEP* **12**, 049 (2017) [10.1007/JHEP12\(2017\)049](https://doi.org/10.1007/JHEP12(2017)049), [arXiv:1610.09378](https://arxiv.org/abs/1610.09378) [hep-th].
- <sup>98</sup>M. S. Costa, T. Hansen, and J. Penedones, “Bounds for OPE coefficients on the Regge trajectory”, *JHEP* **10**, 197 (2017) [10.1007/JHEP10\(2017\)197](https://doi.org/10.1007/JHEP10(2017)197), [arXiv:1707.07689](https://arxiv.org/abs/1707.07689) [hep-th].
- <sup>99</sup>D. Meltzer and E. Perlmutter, “Beyond  $a = c$ : gravitational couplings to matter and the stress tensor OPE”, *JHEP* **07**, 157 (2018) [10.1007/JHEP07\(2018\)157](https://doi.org/10.1007/JHEP07(2018)157), [arXiv:1712.04861](https://arxiv.org/abs/1712.04861) [hep-th].
- <sup>100</sup>R. C. Myers, T. Sierens, and W. Witczak-Krempa, “A Holographic Model for Quantum Critical Responses”, *JHEP* **05**, [Addendum: *JHEP09,066(2016)*], 073 (2016) [10.1007/JHEP09\(2016\)066](https://doi.org/10.1007/JHEP09(2016)066), [10.1007/JHEP05\(2016\)073](https://doi.org/10.1007/JHEP05(2016)073), [arXiv:1602.05599](https://arxiv.org/abs/1602.05599) [hep-th].
- <sup>101</sup>C. Cordova, J. Maldacena, and G. J. Turiaci, “Bounds on OPE Coefficients from Interference Effects in the Conformal Collider”, *JHEP* **11**, 032 (2017) [10.1007/JHEP11\(2017\)032](https://doi.org/10.1007/JHEP11(2017)032), [arXiv:1710.03199](https://arxiv.org/abs/1710.03199) [hep-th].

- <sup>102</sup>K. A. Intriligator, “Bonus symmetries of  $N=4$  superYang-Mills correlation functions via AdS duality”, *Nucl. Phys.* **B551**, 575–600 (1999) [10.1016/S0550-3213\(99\)00242-4](#), [arXiv:hep-th/9811047 \[hep-th\]](#).
- <sup>103</sup>S. S. Gubser, I. R. Klebanov, and A. W. Peet, “Entropy and temperature of black 3-branes”, *Phys. Rev.* **D54**, 3915–3919 (1996) [10.1103/PhysRevD.54.3915](#), [arXiv:hep-th/9602135 \[hep-th\]](#).
- <sup>104</sup>V. Gonçalves, “Four point function of  $\mathcal{N} = 4$  stress-tensor multiplet at strong coupling”, *JHEP* **04**, 150 (2015) [10.1007/JHEP04\(2015\)150](#), [arXiv:1411.1675 \[hep-th\]](#).
- <sup>105</sup>A. Belin, J. de Boer, J. Kruthoff, B. Michel, E. Shaghoulian, and M. Shyani, “Universality of sparse  $d > 2$  conformal field theory at large  $N$ ”, *JHEP* **03**, 067 (2017) [10.1007/JHEP03\(2017\)067](#), [arXiv:1610.06186 \[hep-th\]](#).
- <sup>106</sup>A. Belin, J. de Boer, and J. Kruthoff, “Comments on a state-operator correspondence for the torus”, (2018), [arXiv:1802.00006 \[hep-th\]](#).
- <sup>107</sup>S. Giombi, S. Minwalla, S. Prakash, S. P. Trivedi, S. R. Wadia, and X. Yin, “Chern-Simons Theory with Vector Fermion Matter”, *Eur. Phys. J.* **C72**, 2112 (2012) [10.1140/epjc/s10052-012-2112-0](#), [arXiv:1110.4386 \[hep-th\]](#).
- <sup>108</sup>O. Aharony, G. Gur-Ari, and R. Yacoby, “ $d=3$  Bosonic Vector Models Coupled to Chern-Simons Gauge Theories”, *JHEP* **03**, 037 (2012) [10.1007/JHEP03\(2012\)037](#), [arXiv:1110.4382 \[hep-th\]](#).
- <sup>109</sup>S. Jain, S. P. Trivedi, S. R. Wadia, and S. Yokoyama, “Supersymmetric Chern-Simons Theories with Vector Matter”, *JHEP* **10**, 194 (2012) [10.1007/JHEP10\(2012\)194](#), [arXiv:1207.4750 \[hep-th\]](#).
- <sup>110</sup>O. Aharony, S. Giombi, G. Gur-Ari, J. Maldacena, and R. Yacoby, “The Thermal Free Energy in Large  $N$  Chern-Simons-Matter Theories”, *JHEP* **03**, 121 (2013) [10.1007/JHEP03\(2013\)121](#), [arXiv:1211.4843 \[hep-th\]](#).
- <sup>111</sup>G. Gur-Ari, S. A. Hartnoll, and R. Mahajan, “Transport in Chern-Simons-Matter Theories”, *JHEP* **07**, 090 (2016) [10.1007/JHEP07\(2016\)090](#), [arXiv:1605.01122 \[hep-th\]](#).
- <sup>112</sup>J. Maldacena and A. Zhiboedov, “Constraining Conformal Field Theories with A Higher Spin Symmetry”, (2011), [arXiv:1112.1016 \[hep-th\]](#).
- <sup>113</sup>J. Maldacena and A. Zhiboedov, “Constraining conformal field theories with a slightly broken higher spin symmetry”, *Class.Quant.Grav.* **30**, 104003 (2013) [10.1088/0264-9381/30/10/104003](#), [arXiv:1204.3882 \[hep-th\]](#).
- <sup>114</sup>E. Hijano, P. Kraus, E. Perlmutter, and R. Snively, “Semiclassical Virasoro blocks from  $AdS_3$  gravity”, *JHEP* **12**, 077 (2015) [10.1007/JHEP12\(2015\)077](#), [arXiv:1508.04987 \[hep-th\]](#).

- <sup>115</sup>E. Hijano, P. Kraus, E. Perlmutter, and R. Snively, “Witten Diagrams Revisited: The AdS Geometry of Conformal Blocks”, *JHEP* **01**, 146 (2016) [10.1007/JHEP01\(2016\)146](#), [arXiv:1508.00501 \[hep-th\]](#).
- <sup>116</sup>A. L. Fitzpatrick, J. Kaplan, M. T. Walters, and J. Wang, “Eikonalization of Conformal Blocks”, *JHEP* **09**, 019 (2015) [10.1007/JHEP09\(2015\)019](#), [arXiv:1504.01737 \[hep-th\]](#).
- <sup>117</sup>M. Hasenbusch, “Private correspondence”.
- <sup>118</sup>N. Lashkari, A. Dymarsky, and H. Liu, “Eigenstate Thermalization Hypothesis in Conformal Field Theory”, (2016), [arXiv:1610.00302 \[hep-th\]](#).
- <sup>119</sup>D. Jafferis, B. Mukhametzhanov, and A. Zhiboedov, “Conformal Bootstrap At Large Charge”, (2017), [arXiv:1710.11161 \[hep-th\]](#).
- <sup>120</sup>A. L. Fitzpatrick, J. Kaplan, D. Li, and J. Wang, “On information loss in AdS<sub>3</sub>/CFT<sub>2</sub>”, *JHEP* **05**, 109 (2016) [10.1007/JHEP05\(2016\)109](#), [arXiv:1603.08925 \[hep-th\]](#).
- <sup>121</sup>R. Kubo, “Statistical-Mechanical Theory of Irreversible Processes. I”, *Journal of the Physical Society of Japan* **12**, 570–586 (1957) [10.1143/JPSJ.12.570](#).
- <sup>122</sup>R. Kubo, M. Yokota, and S. Nakajima, “Statistical-Mechanical Theory of Irreversible Processes. II. Response to Thermal Disturbance”, *Journal of the Physical Society of Japan* **12**, 1203–1211 (1957) [10.1143/JPSJ.12.1203](#).
- <sup>123</sup>R. Kubo, “The fluctuation-dissipation theorem”, *Reports on Progress in Physics* **29**, 255 (1966).
- <sup>124</sup>S. A. Hartnoll, A. Lucas, and S. Sachdev, “Holographic quantum matter”, (2016), [arXiv:1612.07324 \[hep-th\]](#).
- <sup>125</sup>L. P. Kadanoff and P. C. Martin, “Hydrodynamic equations and correlation functions”, *Annals of Physics* **24**, 419–469 (1963) [10.1016/0003-4916\(63\)90078-2](#).
- <sup>126</sup>M. Hasenbusch, “Finite size scaling study of lattice models in the three-dimensional Ising universality class”, *Phys.Rev.* **B82**, 174433 (2010) [10.1103/PhysRevB.82.174433](#), [arXiv:1004.4486 \[cond-mat\]](#).
- <sup>127</sup>S. Hellerman, “A Universal Inequality for CFT and Quantum Gravity”, *JHEP* **08**, 130 (2011) [10.1007/JHEP08\(2011\)130](#), [arXiv:0902.2790 \[hep-th\]](#).
- <sup>128</sup>F. Gliozzi, “More constraining conformal bootstrap”, *Phys. Rev. Lett.* **111**, 161602 (2013) [10.1103/PhysRevLett.111.161602](#), [arXiv:1307.3111 \[hep-th\]](#).
- <sup>129</sup>S. Caron-Huot, “Talk at analytic bootstrap workshop, Azores 2018”, (2018).
- <sup>130</sup>D. Poland and D. Simmons-Duffin, “Bounds on 4D Conformal and Superconformal Field Theories”, *JHEP* **05**, 017 (2011) [10.1007/JHEP05\(2011\)017](#), [arXiv:1009.2087 \[hep-th\]](#).
- <sup>131</sup>S. El-Showk and M. F. Paulos, “Bootstrapping Conformal Field Theories with the Extremal Functional Method”, *Phys. Rev. Lett.* **111**, 241601 (2013) [10.1103/PhysRevLett.111.241601](#), [arXiv:1211.2810 \[hep-th\]](#).

- <sup>132</sup>O. Nachtmann, “Positivity constraints for anomalous dimensions”, *Nucl.Phys.* **B63**, 237–247 (1973) [10.1016/0550-3213\(73\)90144-2](https://doi.org/10.1016/0550-3213(73)90144-2).
- <sup>133</sup>M. Campostrini, A. Pelissetto, P. Rossi, and E. Vicari, “Improved high temperature expansion and critical equation of state of three-dimensional Ising - like systems”, *Phys. Rev.* **E60**, 3526–3563 (1999) [10.1103/PhysRevE.60.3526](https://doi.org/10.1103/PhysRevE.60.3526), [arXiv:cond-mat/9905078](https://arxiv.org/abs/cond-mat/9905078) [[cond-mat](#)].
- <sup>134</sup>M. Krech and D. P. Landau, “Casimir effect in critical systems: a monte carlo simulation”, *Phys. Rev. E* **53**, 4414–4423 (1996) [10.1103/PhysRevE.53.4414](https://doi.org/10.1103/PhysRevE.53.4414).
- <sup>135</sup>M. Krech, “Casimir forces in binary liquid mixtures”, *Phys. Rev. E* **56**, 1642–1659 (1997) [10.1103/PhysRevE.56.1642](https://doi.org/10.1103/PhysRevE.56.1642).
- <sup>136</sup>L. Iliesiu, M. Kologlu, R. Mahajan, E. Perlmutter, and D. Simmons-Duffin, “The Conformal Bootstrap at Finite Temperature”, *Journal of High Energy Physics* **10**, 070 (2018) [10.1007/JHEP10\(2018\)070](https://doi.org/10.1007/JHEP10(2018)070), [arXiv:1802.10266](https://arxiv.org/abs/1802.10266) [[hep-th](#)].
- <sup>137</sup>J. Bros and D. Buchholz, “Relativistic KMS condition and Kallen-Lehmann type representations of thermal propagators”, in *Thermal field theories and their applications. Proceedings, 4th International Workshop, Dalian, P.R. China, August 5-10, 1995* (1995), pp. 103–110, [arXiv:hep-th/9511022](https://arxiv.org/abs/hep-th/9511022) [[hep-th](#)].
- <sup>138</sup>C. M. Will, “The Confrontation between General Relativity and Experiment”, *Living Rev. Rel.* **17**, 4 (2014) [10.12942/lrr-2014-4](https://doi.org/10.12942/lrr-2014-4), [arXiv:1403.7377](https://arxiv.org/abs/1403.7377) [[gr-qc](#)].
- <sup>139</sup>S. Gao and R. M. Wald, “Theorems on gravitational time delay and related issues”, *Class. Quant. Grav.* **17**, 4999–5008 (2000) [10.1088/0264-9381/17/24/305](https://doi.org/10.1088/0264-9381/17/24/305), [arXiv:gr-qc/0007021](https://arxiv.org/abs/gr-qc/0007021) [[gr-qc](#)].
- <sup>140</sup>D. M. Hofman, “Higher Derivative Gravity, Causality and Positivity of Energy in a UV complete QFT”, *Nucl. Phys.* **B823**, 174–194 (2009) [10.1016/j.nuclphysb.2009.08.001](https://doi.org/10.1016/j.nuclphysb.2009.08.001), [arXiv:0907.1625](https://arxiv.org/abs/0907.1625) [[hep-th](#)].
- <sup>141</sup>M. Kulaxizi, A. Parnachev, and A. Zhiboedov, “Bulk Phase Shift, CFT Regge Limit and Einstein Gravity”, *JHEP* **06**, 121 (2018) [10.1007/JHEP06\(2018\)121](https://doi.org/10.1007/JHEP06(2018)121), [arXiv:1705.02934](https://arxiv.org/abs/1705.02934) [[hep-th](#)].
- <sup>142</sup>V. D. Alfaro, S. Fubini, G. Rossetti, and G. Furlan, “Sum rules for strong interactions”, *Physics Letters* **21**, 576–579 (1966) [https://doi.org/10.1016/0031-9163\(66\)91306-0](https://doi.org/10.1016/0031-9163(66)91306-0).
- <sup>143</sup>I. G. Aznauryan and L. D. Soloviev, *Dubna Report E-2544* (1966).
- <sup>144</sup>C. L. Basham, L. S. Brown, S. D. Ellis, and S. T. Love, “Electron - Positron Annihilation Energy Pattern in Quantum Chromodynamics: Asymptotically Free Perturbation Theory”, *Phys. Rev.* **D17**, 2298 (1978) [10.1103/PhysRevD.17.2298](https://doi.org/10.1103/PhysRevD.17.2298).
- <sup>145</sup>C. L. Basham, L. S. Brown, S. D. Ellis, and S. T. Love, “Energy Correlations in electron-Positron Annihilation in Quantum Chromodynamics: Asymptotically Free Perturbation Theory”, *Phys. Rev.* **D19**, 2018 (1979) [10.1103/PhysRevD.19.2018](https://doi.org/10.1103/PhysRevD.19.2018).

- <sup>146</sup>C. L. Basham, L. S. Brown, S. D. Ellis, and S. T. Love, “Energy Correlations in electron - Positron Annihilation: Testing QCD”, *Phys. Rev. Lett.* **41**, 1585 (1978) [10.1103/PhysRevLett.41.1585](#).
- <sup>147</sup>A. V. Belitsky, S. Hohenegger, G. P. Korchemsky, E. Sokatchev, and A. Zhiboedov, “From correlation functions to event shapes”, *Nucl. Phys.* **B884**, 305–343 (2014) [10.1016/j.nuclphysb.2014.04.020](#), [arXiv:1309.0769 \[hep-th\]](#).
- <sup>148</sup>R. C. Brower, J. Polchinski, M. J. Strassler, and C.-I. Tan, “The Pomeron and gauge/string duality”, *JHEP* **12**, 005 (2007) [10.1088/1126-6708/2007/12/005](#), [arXiv:hep-th/0603115 \[hep-th\]](#).
- <sup>149</sup>L. Cornalba, “Eikonal methods in AdS/CFT: Regge theory and multi-reggeon exchange”, (2007), [arXiv:0710.5480 \[hep-th\]](#).
- <sup>150</sup>M. S. Costa, V. Goncalves, and J. Penedones, “Conformal Regge theory”, *JHEP* **1212**, 091 (2012) [10.1007/JHEP12\(2012\)091](#), [arXiv:1209.4355 \[hep-th\]](#).
- <sup>151</sup>T. Hartman, S. Jain, and S. Kundu, “Causality Constraints in Conformal Field Theory”, *JHEP* **05**, 099 (2016) [10.1007/JHEP05\(2016\)099](#), [arXiv:1509.00014 \[hep-th\]](#).
- <sup>152</sup>T. Faulkner, R. G. Leigh, O. Parrikar, and H. Wang, “Modular Hamiltonians for Deformed Half-Spaces and the Averaged Null Energy Condition”, *JHEP* **09**, 038 (2016) [10.1007/JHEP09\(2016\)038](#), [arXiv:1605.08072 \[hep-th\]](#).
- <sup>153</sup>H. Casini, E. Teste, and G. Torroba, “Modular Hamiltonians on the null plane and the Markov property of the vacuum state”, *J. Phys.* **A50**, 364001 (2017) [10.1088/1751-8121/aa7eaa](#), [arXiv:1703.10656 \[hep-th\]](#).
- <sup>154</sup>C. Córdova and S.-H. Shao, “Light-ray Operators and the BMS Algebra”, *Phys. Rev.* **D98**, 125015 (2018) [10.1103/PhysRevD.98.125015](#), [arXiv:1810.05706 \[hep-th\]](#).
- <sup>155</sup>X. O. Camanho, *Unpublished notes* (2015).
- <sup>156</sup>I. Heemskerk, J. Penedones, J. Polchinski, and J. Sully, “Holography from Conformal Field Theory”, *JHEP* **0910**, 079 (2009) [10.1088/1126-6708/2009/10/079](#), [arXiv:0907.0151 \[hep-th\]](#).
- <sup>157</sup>A. Belin, D. M. Hofman, and G. Mathys, “Einstein gravity from ANEC correlators”, (2019), [arXiv:1904.05892 \[hep-th\]](#).
- <sup>158</sup>P. C. Aichelburg and R. U. Sexl, “On the Gravitational field of a massless particle”, *Gen. Rel. Grav.* **2**, 303–312 (1971) [10.1007/BF00758149](#).
- <sup>159</sup>G. ’t Hooft, “Graviton Dominance in Ultrahigh-Energy Scattering”, *Phys. Lett.* **B198**, 61–63 (1987) [10.1016/0370-2693\(87\)90159-6](#).
- <sup>160</sup>G. Papallo and H. S. Reall, “Graviton time delay and a speed limit for small black holes in Einstein-Gauss-Bonnet theory”, *JHEP* **11**, 109 (2015) [10.1007/JHEP11\(2015\)109](#), [arXiv:1508.05303 \[gr-qc\]](#).



- <sup>161</sup>G. T. Horowitz and A. R. Steif, “Space-Time Singularities in String Theory”, *Phys. Rev. Lett.* **64**, 260 (1990) [10.1103/PhysRevLett.64.260](https://doi.org/10.1103/PhysRevLett.64.260).
- <sup>162</sup>C. Schmid, “Construction of the  $\pi \pi$  scattering amplitude from superconvergence”, *Physics Letters B* **28**, 348–352 (1968) [https://doi.org/10.1016/0370-2693\(68\)90128-7](https://doi.org/10.1016/0370-2693(68)90128-7).
- <sup>163</sup>C.-H. Fu, J.-C. Lee, C.-I. Tan, and Y. Yang, “BCFW Deformation and Regge Limit”, (2013), [arXiv:1305.7442 \[hep-th\]](https://arxiv.org/abs/1305.7442).
- <sup>164</sup>H. Kawai, D. C. Lewellen, and S. H. H. Tye, “A Relation Between Tree Amplitudes of Closed and Open Strings”, *Nucl. Phys.* **B269**, 1–23 (1986) [10.1016/0550-3213\(86\)90362-7](https://doi.org/10.1016/0550-3213(86)90362-7).
- <sup>165</sup>Y. Cai and C. A. Nunez, “Heterotic String Covariant Amplitudes and Low-energy Effective Action”, *Nucl. Phys.* **B287**, 279 (1987) [10.1016/0550-3213\(87\)90106-4](https://doi.org/10.1016/0550-3213(87)90106-4).
- <sup>166</sup>D. Amati and C. Klimcik, “Strings in a shock wave background and generation of curved geometry from flat-space string theory”, *Physics Letters B* **210**, 92–96 (1988) [10.1016/0370-2693\(88\)90355-3](https://doi.org/10.1016/0370-2693(88)90355-3).
- <sup>167</sup>G. T. Horowitz and A. R. Steif, “Strings in Strong Gravitational Fields”, *Phys. Rev.* **D42**, 1950–1959 (1990) [10.1103/PhysRevD.42.1950](https://doi.org/10.1103/PhysRevD.42.1950).
- <sup>168</sup>H. J. de Vega and N. G. Sanchez, “Space-time singularities in string theory and string propagation through gravitational shock waves”, *Phys. Rev. Lett.* **65**, 1517 (1990) [10.1103/PhysRevLett.65.1517](https://doi.org/10.1103/PhysRevLett.65.1517).
- <sup>169</sup>G. Horowitz and A. Steif, “Reply to ‘Space-time singularities in string theory and string propagation through gravitational shock waves.’”, *Phys. Rev. Lett.* **65**, 1518 (1990) [10.1103/PhysRevLett.65.1518](https://doi.org/10.1103/PhysRevLett.65.1518).
- <sup>170</sup>H. J. de Vega and N. G. Sanchez, “QUANTUM STRING PROPAGATION THROUGH GRAVITATIONAL SHOCK WAVES”, *Phys. Lett.* **B244**, 215–219 (1990) [10.1016/0370-2693\(90\)90058-E](https://doi.org/10.1016/0370-2693(90)90058-E).
- <sup>171</sup>H. J. de Vega and N. G. Sanchez, “Mass and energy momentum tensor of quantum strings in gravitational shock waves”, *Int. J. Mod. Phys.* **A7**, 3043–3064 (1992) [10.1142/S0217751X92001368](https://doi.org/10.1142/S0217751X92001368).
- <sup>172</sup>H. J. de Vega, M. Ramon Medrano, and N. G. Sanchez, “Superstring propagation through supergravitational shock waves”, *Nucl. Phys.* **B374**, 425–445 (1992) [10.1016/0550-3213\(92\)90361-E](https://doi.org/10.1016/0550-3213(92)90361-E).
- <sup>173</sup>A. Martin, “Extension of the axiomatic analyticity domain of scattering amplitudes by unitarity. 1.”, *Nuovo Cim.* **A42**, 930–953 (1965) [10.1007/BF02720568](https://doi.org/10.1007/BF02720568).
- <sup>174</sup>G. Mahoux and A. Martin, “Extension of axiomatic analyticity properties for particles with spin, and proof of superconvergence relations”, *Phys. Rev.* **174**, 2140–2150 (1968) [10.1103/PhysRev.174.2140](https://doi.org/10.1103/PhysRev.174.2140).

- <sup>175</sup>C. de Rham, S. Melville, A. J. Tolley, and S.-Y. Zhou, “UV complete me: Positivity Bounds for Particles with Spin”, *JHEP* **03**, 011 (2018) [10.1007/JHEP03\(2018\)011](https://doi.org/10.1007/JHEP03(2018)011), [arXiv:1706.02712 \[hep-th\]](https://arxiv.org/abs/1706.02712).
- <sup>176</sup>Z. Komargodski, M. Kulaxizi, A. Parnachev, and A. Zhiboedov, “Conformal Field Theories and Deep Inelastic Scattering”, *Phys. Rev.* **D95**, 065011 (2017) [10.1103/PhysRevD.95.065011](https://doi.org/10.1103/PhysRevD.95.065011), [arXiv:1601.05453 \[hep-th\]](https://arxiv.org/abs/1601.05453).
- <sup>177</sup>N. Afkhami-Jeddi, T. Hartman, S. Kundu, and A. Tajdini, “Shockwaves from the Operator Product Expansion”, (2017), [arXiv:1709.03597 \[hep-th\]](https://arxiv.org/abs/1709.03597).
- <sup>178</sup>A. Buchel, J. Escobedo, R. C. Myers, M. F. Paulos, A. Sinha, and M. Smolkin, “Holographic GB gravity in arbitrary dimensions”, *JHEP* **03**, 111 (2010) [10.1007/JHEP03\(2010\)111](https://doi.org/10.1007/JHEP03(2010)111), [arXiv:0911.4257 \[hep-th\]](https://arxiv.org/abs/0911.4257).
- <sup>179</sup>X. O. Camanho and J. D. Edelstein, “Causality constraints in AdS/CFT from conformal collider physics and Gauss-Bonnet gravity”, *JHEP* **04**, 007 (2010) [10.1007/JHEP04\(2010\)007](https://doi.org/10.1007/JHEP04(2010)007), [arXiv:0911.3160 \[hep-th\]](https://arxiv.org/abs/0911.3160).
- <sup>180</sup>R. C. Myers, M. F. Paulos, and A. Sinha, “Holographic studies of quasi-topological gravity”, *JHEP* **08**, 035 (2010) [10.1007/JHEP08\(2010\)035](https://doi.org/10.1007/JHEP08(2010)035), [arXiv:1004.2055 \[hep-th\]](https://arxiv.org/abs/1004.2055).
- <sup>181</sup>G. T. Horowitz and N. Itzhaki, “Black holes, shock waves, and causality in the AdS / CFT correspondence”, *JHEP* **02**, 010 (1999) [10.1088/1126-6708/1999/02/010](https://doi.org/10.1088/1126-6708/1999/02/010), [arXiv:hep-th/9901012 \[hep-th\]](https://arxiv.org/abs/hep-th/9901012).
- <sup>182</sup>A. V. Belitsky, S. Hohenegger, G. P. Korchemsky, E. Sokatchev, and A. Zhiboedov, “Energy-Energy Correlations in N=4 Supersymmetric Yang-Mills Theory”, *Phys. Rev. Lett.* **112**, 071601 (2014) [10.1103/PhysRevLett.112.071601](https://doi.org/10.1103/PhysRevLett.112.071601), [arXiv:1311.6800 \[hep-th\]](https://arxiv.org/abs/1311.6800).
- <sup>183</sup>G. Mack, “Convergence of Operator Product Expansions on the Vacuum in Conformal Invariant Quantum Field Theory”, *Commun. Math. Phys.* **53**, 155 (1977) [10.1007/BF01609130](https://doi.org/10.1007/BF01609130).
- <sup>184</sup>D. Pappadopulo, S. Rychkov, J. Espin, and R. Rattazzi, “OPE Convergence in Conformal Field Theory”, *Phys.Rev.* **D86**, 105043 (2012) [10.1103/PhysRevD.86.105043](https://doi.org/10.1103/PhysRevD.86.105043), [arXiv:1208.6449 \[hep-th\]](https://arxiv.org/abs/1208.6449).
- <sup>185</sup>H. Casini, “Wedge reflection positivity”, *J. Phys.* **A44**, 435202 (2011) [10.1088/1751-8113/44/43/435202](https://doi.org/10.1088/1751-8113/44/43/435202), [arXiv:1009.3832 \[hep-th\]](https://arxiv.org/abs/1009.3832).
- <sup>186</sup>D. Karateev, P. Kravchuk, and D. Simmons-Duffin, “Weight Shifting Operators and Conformal Blocks”, *JHEP* **02**, [91(2017)], 081 (2018) [10.1007/JHEP02\(2018\)081](https://doi.org/10.1007/JHEP02(2018)081), [arXiv:1706.07813 \[hep-th\]](https://arxiv.org/abs/1706.07813).
- <sup>187</sup>A. W. Knap and E. M. Stein, “Intertwining operators for semisimple groups”, *Ann. of Math. (2)* **93**, 489–578 (1971) [10.2307/1970887](https://doi.org/10.2307/1970887).
- <sup>188</sup>A. W. Knap and E. M. Stein, “Intertwining operators for semisimple groups. II”, *Invent. Math.* **60**, 9–84 (1980) [10.1007/BF01389898](https://doi.org/10.1007/BF01389898).

- <sup>189</sup>M. Gillioz, “Momentum-space conformal blocks on the light cone”, (2018), [arXiv:1807.07003 \[hep-th\]](#).
- <sup>190</sup>D. Simmons-Duffin, “Projectors, Shadows, and Conformal Blocks”, *JHEP* **1404**, 146 (2014) [10.1007/JHEP04\(2014\)146](#), [arXiv:1204.3894 \[hep-th\]](#).
- <sup>191</sup>P. Kravchuk and D. Simmons-Duffin, “Counting Conformal Correlators”, *JHEP* **02**, 096 (2018) [10.1007/JHEP02\(2018\)096](#), [arXiv:1612.08987 \[hep-th\]](#).
- <sup>192</sup>M. S. Costa, J. Penedones, D. Poland, and S. Rychkov, “Spinning Conformal Correlators”, *JHEP* **1111**, 071 (2011) [10.1007/JHEP11\(2011\)071](#), [arXiv:1107.3554 \[hep-th\]](#).
- <sup>193</sup>M. S. Costa, J. Penedones, D. Poland, and S. Rychkov, “Spinning Conformal Blocks”, *JHEP* **1111**, 154 (2011) [10.1007/JHEP11\(2011\)154](#), [arXiv:1109.6321 \[hep-th\]](#).
- <sup>194</sup>D. Karateev, P. Kravchuk, and D. Simmons-Duffin, “Harmonic Analysis and Mean Field Theory”, (2018), [arXiv:1809.05111 \[hep-th\]](#).
- <sup>195</sup>N. J. Vilenkin and A. U. Klimyk, *Representation of lie groups and special functions*, Vol. 3 (Springer Netherlands, 1992).
- <sup>196</sup>F. A. Dolan and H. Osborn, “Conformal four point functions and the operator product expansion”, *Nucl. Phys.* **B599**, 459–496 (2001) [10.1016/S0550-3213\(01\)00013-X](#), [arXiv:hep-th/0011040 \[hep-th\]](#).
- <sup>197</sup>N. Gromov, V. Kazakov, and P. Vieira, “Exact Spectrum of Anomalous Dimensions of Planar  $N=4$  Supersymmetric Yang-Mills Theory”, *Phys. Rev. Lett.* **103**, 131601 (2009) [10.1103/PhysRevLett.103.131601](#), [arXiv:0901.3753 \[hep-th\]](#).
- <sup>198</sup>N. Gromov, V. Kazakov, S. Leurent, and D. Volin, “Quantum Spectral Curve for Planar  $\mathcal{N} = 4$  Super-Yang-Mills Theory”, *Phys. Rev. Lett.* **112**, 011602 (2014) [10.1103/PhysRevLett.112.011602](#), [arXiv:1305.1939 \[hep-th\]](#).
- <sup>199</sup>N. Gromov, V. Kazakov, S. Leurent, and D. Volin, “Quantum spectral curve for arbitrary state/operator in  $AdS_5/CFT_4$ ”, *JHEP* **09**, 187 (2015) [10.1007/JHEP09\(2015\)187](#), [arXiv:1405.4857 \[hep-th\]](#).
- <sup>200</sup>J. Maldacena, D. Simmons-Duffin, and A. Zhiboedov, “Looking for a bulk point”, *JHEP* **01**, 013 (2017) [10.1007/JHEP01\(2017\)013](#), [arXiv:1509.03612 \[hep-th\]](#).
- <sup>201</sup>S. H. Shenker and D. Stanford, “Black holes and the butterfly effect”, *JHEP* **03**, 067 (2014) [10.1007/JHEP03\(2014\)067](#), [arXiv:1306.0622 \[hep-th\]](#).
- <sup>202</sup>A. Kitaev and S. J. Suh, “The soft mode in the Sachdev-Ye-Kitaev model and its gravity dual”, *JHEP* **05**, 183 (2018) [10.1007/JHEP05\(2018\)183](#), [arXiv:1711.08467 \[hep-th\]](#).
- <sup>203</sup>T. Faulkner, M. Li, and H. Wang, “A modular toolkit for bulk reconstruction”, (2018), [arXiv:1806.10560 \[hep-th\]](#).

- <sup>204</sup>A. Dymarsky, F. Kos, P. Kravchuk, D. Poland, and D. Simmons-Duffin, “The 3d Stress-Tensor Bootstrap”, *JHEP* **02**, [343(2017)], 164 (2018) [10.1007/JHEP02\(2018\)164](https://doi.org/10.1007/JHEP02(2018)164), [arXiv:1708.05718](https://arxiv.org/abs/1708.05718) [[hep-th](#)].
- <sup>205</sup>N. Beisert et al., “Review of AdS/CFT Integrability: An Overview”, *Lett. Math. Phys.* **99**, 3–32 (2012) [10.1007/s11005-011-0529-2](https://doi.org/10.1007/s11005-011-0529-2), [arXiv:1012.3982](https://arxiv.org/abs/1012.3982) [[hep-th](#)].
- <sup>206</sup>B. Basso, S. Komatsu, and P. Vieira, “Structure Constants and Integrable Bootstrap in Planar N=4 SYM Theory”, (2015), [arXiv:1505.06745](https://arxiv.org/abs/1505.06745) [[hep-th](#)].
- <sup>207</sup>J. M. Henn, E. Sokatchev, K. Yan, and A. Zhiboedov, “Energy-energy correlations at next-to-next-to-leading order”, (2019), [arXiv:1903.05314](https://arxiv.org/abs/1903.05314) [[hep-th](#)].
- <sup>208</sup>L. J. Dixon, M.-X. Luo, V. Shtabovenko, T.-Z. Yang, and H. X. Zhu, “Analytical Computation of Energy-Energy Correlation at Next-to-Leading Order in QCD”, *Phys. Rev. Lett.* **120**, 102001 (2018) [10.1103/PhysRevLett.120.102001](https://doi.org/10.1103/PhysRevLett.120.102001), [arXiv:1801.03219](https://arxiv.org/abs/1801.03219) [[hep-ph](#)].
- <sup>209</sup>F. Ceyhan and T. Faulkner, “Recovering the QNEC from the ANEC”, (2018), [arXiv:1812.04683](https://arxiv.org/abs/1812.04683) [[hep-th](#)].
- <sup>210</sup>T. Hartman, S. Kundu, and A. Tajdini, “Averaged Null Energy Condition from Causality”, *JHEP* **07**, 066 (2017) [10.1007/JHEP07\(2017\)066](https://doi.org/10.1007/JHEP07(2017)066), [arXiv:1610.05308](https://arxiv.org/abs/1610.05308) [[hep-th](#)].
- <sup>211</sup>C. Cordova and K. Diab, “Universal Bounds on Operator Dimensions from the Average Null Energy Condition”, *JHEP* **02**, 131 (2018) [10.1007/JHEP02\(2018\)131](https://doi.org/10.1007/JHEP02(2018)131), [arXiv:1712.01089](https://arxiv.org/abs/1712.01089) [[hep-th](#)].
- <sup>212</sup>L. V. Delacrétaz, T. Hartman, S. A. Hartnoll, and A. Lewkowycz, “Thermalization, Viscosity and the Averaged Null Energy Condition”, *JHEP* **10**, 028 (2018) [10.1007/JHEP10\(2018\)028](https://doi.org/10.1007/JHEP10(2018)028), [arXiv:1805.04194](https://arxiv.org/abs/1805.04194) [[hep-th](#)].
- <sup>213</sup>D. Meltzer, “Higher Spin ANEC and the Space of CFTs”, (2018), [arXiv:1811.01913](https://arxiv.org/abs/1811.01913) [[hep-th](#)].
- <sup>214</sup>M. Koloğlu, P. Kravchuk, D. Simmons-Duffin, and A. Zhiboedov, “Shocks, Superconvergence, and a Stringy Equivalence Principle”, (2019), [arXiv:1904.05905](https://arxiv.org/abs/1904.05905) [[hep-th](#)].
- <sup>215</sup>J. Polchinski, *String theory*, Vol. 1, Cambridge Monographs on Mathematical Physics (Cambridge University Press, 1998), [10.1017/CB09780511816079](https://doi.org/10.1017/CB09780511816079).
- <sup>216</sup>D. M. McAvity and H. Osborn, “Conformal field theories near a boundary in general dimensions”, *Nucl. Phys.* **B455**, 522–576 (1995) [10.1016/0550-3213\(95\)00476-9](https://doi.org/10.1016/0550-3213(95)00476-9), [arXiv:cond-mat/9505127](https://arxiv.org/abs/cond-mat/9505127) [[cond-mat](#)].
- <sup>217</sup>A. V. Belitsky, S. Hohenegger, G. P. Korchemsky, and E. Sokatchev, “N=4 superconformal Ward identities for correlation functions”, *Nucl. Phys.* **B904**, 176–215 (2016) [10.1016/j.nuclphysb.2016.01.008](https://doi.org/10.1016/j.nuclphysb.2016.01.008), [arXiv:1409.2502](https://arxiv.org/abs/1409.2502) [[hep-th](#)].

- <sup>218</sup>G. P. Korchemsky and E. Sokatchev, “Four-point correlation function of stress-energy tensors in  $\mathcal{N} = 4$  superconformal theories”, *JHEP* **12**, 133 (2015) [10.1007/JHEP12\(2015\)133](#), [arXiv:1504.07904 \[hep-th\]](#).
- <sup>219</sup>G. Korchemsky, *Energy correlations in the end-point region* (To appear, IPhT-T19/041, 2019).
- <sup>220</sup>L. J. Dixon, I. Moulton, and H. X. Zhu, *The Collinear Limit of the Energy-Energy Correlator* (To appear, SLAC-PUB-17427, 2019).
- <sup>221</sup>L. F. Alday, B. Eden, G. P. Korchemsky, J. Maldacena, and E. Sokatchev, “From correlation functions to Wilson loops”, *JHEP* **09**, 123 (2011) [10.1007/JHEP09\(2011\)123](#), [arXiv:1007.3243 \[hep-th\]](#).
- <sup>222</sup>P. A. M. Dirac, “Wave equations in conformal space”, *Annals Math.* **37**, 429–442 (1936) [10.2307/1968455](#).
- <sup>223</sup>G. Mack and A. Salam, “Finite component field representations of the conformal group”, *Annals Phys.* **53**, 174–202 (1969) [10.1016/0003-4916\(69\)90278-4](#).
- <sup>224</sup>D. G. Boulware, L. S. Brown, and R. D. Peccei, “Deep-inelastic electroproduction and conformal symmetry”, *Phys. Rev.* **D2**, 293–298 (1970) [10.1103/PhysRevD.2.293](#).
- <sup>225</sup>S. Ferrara, R. Gatto, and A. F. Grillo, “Conformal algebra in space-time and operator product expansion”, *Springer Tracts Mod. Phys.* **67**, 1–64 (1973) [10.1007/BFb0111104](#).
- <sup>226</sup>L. Cornalba, M. S. Costa, and J. Penedones, “Deep Inelastic Scattering in Conformal QCD”, *JHEP* **03**, 133 (2010) [10.1007/JHEP03\(2010\)133](#), [arXiv:0911.0043 \[hep-th\]](#).
- <sup>227</sup>S. Weinberg, “Six-dimensional Methods for Four-dimensional Conformal Field Theories”, *Phys. Rev.* **D82**, 045031 (2010) [10.1103/PhysRevD.82.045031](#), [arXiv:1006.3480 \[hep-th\]](#).
- <sup>228</sup>K. Akiyama et al., “First M87 Event Horizon Telescope Results. I. The Shadow of the Supermassive Black Hole”, *Astrophys. J.* **875**, L1 (2019) [10.3847/2041-8213/ab0ec7](#).
- <sup>229</sup>A. V. Belitsky, S. Hohenegger, G. P. Korchemsky, E. Sokatchev, and A. Zhiboedov, “Event shapes in  $\mathcal{N} = 4$  super-Yang-Mills theory”, *Nucl. Phys.* **B884**, 206–256 (2014) [10.1016/j.nuclphysb.2014.04.019](#), [arXiv:1309.1424 \[hep-th\]](#).
- <sup>230</sup>J. Liu, E. Perlmutter, V. Rosenhaus, and D. Simmons-Duffin, “ $d$ -dimensional SYK, AdS Loops, and  $6j$  Symbols”, *JHEP* **03**, 052 (2019) [10.1007/JHEP03\(2019\)052](#), [arXiv:1808.00612 \[hep-th\]](#).
- <sup>231</sup>F. Dolan and H. Osborn, “Conformal four point functions and the operator product expansion”, *Nucl.Phys.* **B599**, 459–496 (2001) [10.1016/S0550-3213\(01\)00013-X](#), [arXiv:hep-th/0011040 \[hep-th\]](#).

- <sup>232</sup>F. Dolan and H. Osborn, “Conformal partial waves and the operator product expansion”, *Nucl.Phys.* **B678**, 491–507 (2004) [10.1016/j.nuclphysb.2003.11.016](#), [arXiv:hep-th/0309180 \[hep-th\]](#).
- <sup>233</sup>J. Maldacena and D. Stanford, “Remarks on the Sachdev-Ye-Kitaev model”, *Phys. Rev.* **D94**, 106002 (2016) [10.1103/PhysRevD.94.106002](#), [arXiv:1604.07818 \[hep-th\]](#).
- <sup>234</sup>B. Eden, P. S. Howe, and P. C. West, “Nilpotent invariants in N=4 SYM”, *Phys. Lett.* **B463**, 19–26 (1999) [10.1016/S0370-2693\(99\)00705-4](#), [arXiv:hep-th/9905085 \[hep-th\]](#).
- <sup>235</sup>P. S. Howe, C. Schubert, E. Sokatchev, and P. C. West, “Explicit construction of nilpotent covariants in N=4 SYM”, *Nucl. Phys.* **B571**, 71–90 (2000) [10.1016/S0550-3213\(99\)00768-3](#), [arXiv:hep-th/9910011 \[hep-th\]](#).
- <sup>236</sup>J. Drummond, C. Duhr, B. Eden, P. Heslop, J. Pennington, and V. A. Smirnov, “Leading singularities and off-shell conformal integrals”, *JHEP* **08**, 133 (2013) [10.1007/JHEP08\(2013\)133](#), [arXiv:1303.6909 \[hep-th\]](#).
- <sup>237</sup>B. Eden, P. Heslop, G. P. Korchemsky, and E. Sokatchev, “Hidden symmetry of four-point correlation functions and amplitudes in N=4 SYM”, *Nucl. Phys.* **B862**, 193–231 (2012) [10.1016/j.nuclphysb.2012.04.007](#), [arXiv:1108.3557 \[hep-th\]](#).
- <sup>238</sup>J. L. Bourjaily, P. Heslop, and V.-V. Tran, “Amplitudes and Correlators to Ten Loops Using Simple, Graphical Bootstraps”, *JHEP* **11**, 125 (2016) [10.1007/JHEP11\(2016\)125](#), [arXiv:1609.00007 \[hep-th\]](#).
- <sup>239</sup>C. Beem, L. Rastelli, and B. C. van Rees, “More  $\mathcal{N} = 4$  superconformal bootstrap”, (2016), [arXiv:1612.02363 \[hep-th\]](#).
- <sup>240</sup>J. Henriksson and T. Lukowski, “Perturbative Four-Point Functions from the Analytic Conformal Bootstrap”, *JHEP* **02**, 123 (2018) [10.1007/JHEP02\(2018\)123](#), [arXiv:1710.06242 \[hep-th\]](#).
- <sup>241</sup>B. Eden, C. Schubert, and E. Sokatchev, “Three loop four point correlator in N=4 SYM”, *Phys. Lett.* **B482**, 309–314 (2000) [10.1016/S0370-2693\(00\)00515-3](#), [arXiv:hep-th/0003096 \[hep-th\]](#).
- <sup>242</sup>M. Bianchi, S. Kovacs, G. Rossi, and Y. S. Stanev, “Anomalous dimensions in  $\mathcal{N} = 4$  SYM theory at order  $g^4$ ”, *Nucl. Phys.* **B584**, 216–232 (2000) [10.1016/S0550-3213\(00\)00312-6](#), [arXiv:hep-th/0003203 \[hep-th\]](#).
- <sup>243</sup>F. Dolan and H. Osborn, “Conformal partial wave expansions for  $\mathcal{N} = 4$  chiral four point functions”, *Annals Phys.* **321**, 581–626 (2006) [10.1016/j.aop.2005.07.005](#), [arXiv:hep-th/0412335 \[hep-th\]](#).
- <sup>244</sup>A. V. Kotikov and V. N. Velizhanin, “Analytic continuation of the Mellin moments of deep inelastic structure functions”, (2005), [arXiv:hep-ph/0501274 \[hep-ph\]](#).

- <sup>245</sup>N. Gromov, F. Levkovich-Maslyuk, G. Sizov, and S. Valatka, “Quantum spectral curve at work: from small spin to strong coupling in  $\mathcal{N} = 4$  SYM”, *JHEP* **07**, 156 (2014) [10.1007/JHEP07\(2014\)156](https://doi.org/10.1007/JHEP07(2014)156), [arXiv:1402.0871 \[hep-th\]](https://arxiv.org/abs/1402.0871).
- <sup>246</sup>B. Eden, P. Heslop, G. P. Korchemsky, and E. Sokatchev, “Constructing the correlation function of four stress-tensor multiplets and the four-particle amplitude in  $\mathcal{N}=4$  SYM”, *Nucl. Phys.* **B862**, 450–503 (2012) [10.1016/j.nuclphysb.2012.04.013](https://doi.org/10.1016/j.nuclphysb.2012.04.013), [arXiv:1201.5329 \[hep-th\]](https://arxiv.org/abs/1201.5329).
- <sup>247</sup>B. Eden, “Three-loop universal structure constants in  $\mathcal{N}=4$  susy Yang-Mills theory”, (2012), [arXiv:1207.3112 \[hep-th\]](https://arxiv.org/abs/1207.3112).
- <sup>248</sup>L. F. Alday and A. Bissi, “Higher-spin correlators”, *JHEP* **10**, 202 (2013) [10.1007/JHEP10\(2013\)202](https://doi.org/10.1007/JHEP10(2013)202), [arXiv:1305.4604 \[hep-th\]](https://arxiv.org/abs/1305.4604).
- <sup>249</sup>A. V. Kotikov, L. N. Lipatov, A. Rej, M. Staudacher, and V. N. Velizhanin, “Dressing and wrapping”, *J. Stat. Mech.* **0710**, P10003 (2007) [10.1088/1742-5468/2007/10/P10003](https://doi.org/10.1088/1742-5468/2007/10/P10003), [arXiv:0704.3586 \[hep-th\]](https://arxiv.org/abs/0704.3586).
- <sup>250</sup>Z. Bajnok, R. A. Janik, and T. Lukowski, “Four loop twist two, BFKL, wrapping and strings”, *Nucl. Phys.* **B816**, 376–398 (2009) [10.1016/j.nuclphysb.2009.02.005](https://doi.org/10.1016/j.nuclphysb.2009.02.005), [arXiv:0811.4448 \[hep-th\]](https://arxiv.org/abs/0811.4448).
- <sup>251</sup>D. Maitre, “HPL, a mathematica implementation of the harmonic polylogarithms”, *Comput. Phys. Commun.* **174**, 222–240 (2006) [10.1016/j.cpc.2005.10.008](https://doi.org/10.1016/j.cpc.2005.10.008), [arXiv:hep-ph/0507152 \[hep-ph\]](https://arxiv.org/abs/hep-ph/0507152).
- <sup>252</sup>N. Gromov, F. Levkovich-Maslyuk, and G. Sizov, “Pomeron Eigenvalue at Three Loops in  $\mathcal{N} = 4$  Supersymmetric Yang-Mills Theory”, *Phys. Rev. Lett.* **115**, 251601 (2015) [10.1103/PhysRevLett.115.251601](https://doi.org/10.1103/PhysRevLett.115.251601), [arXiv:1507.04010 \[hep-th\]](https://arxiv.org/abs/1507.04010).
- <sup>253</sup>F. Dolan and H. Osborn, “Superconformal symmetry, correlation functions and the operator product expansion”, *Nucl.Phys.* **B629**, 3–73 (2002) [10.1016/S0550-3213\(02\)00096-2](https://doi.org/10.1016/S0550-3213(02)00096-2), [arXiv:hep-th/0112251 \[hep-th\]](https://arxiv.org/abs/hep-th/0112251).
- <sup>254</sup>J. C. Collins and D. E. Soper, “Back-To-Back Jets in QCD”, *Nucl. Phys.* **B193**, [Erratum: *Nucl. Phys.*B213,545(1983)], 381 (1981) [10.1016/0550-3213\(81\)90339-4](https://doi.org/10.1016/0550-3213(81)90339-4).
- <sup>255</sup>G. Arutyunov and S. Frolov, “Four point functions of lowest weight CPOs in  $\mathcal{N}=4$  SYM(4) in supergravity approximation”, *Phys. Rev.* **D62**, 064016 (2000) [10.1103/PhysRevD.62.064016](https://doi.org/10.1103/PhysRevD.62.064016), [arXiv:hep-th/0002170 \[hep-th\]](https://arxiv.org/abs/hep-th/0002170).
- <sup>256</sup>F. Aprile, J. M. Drummond, P. Heslop, and H. Paul, “Quantum Gravity from Conformal Field Theory”, *JHEP* **01**, 035 (2018) [10.1007/JHEP01\(2018\)035](https://doi.org/10.1007/JHEP01(2018)035), [arXiv:1706.02822 \[hep-th\]](https://arxiv.org/abs/1706.02822).
- <sup>257</sup>F. Aprile, J. M. Drummond, P. Heslop, and H. Paul, “Loop corrections for Kaluza-Klein AdS amplitudes”, *JHEP* **05**, 056 (2018) [10.1007/JHEP05\(2018\)056](https://doi.org/10.1007/JHEP05(2018)056), [arXiv:1711.03903 \[hep-th\]](https://arxiv.org/abs/1711.03903).

- <sup>258</sup>L. F. Alday and A. Bissi, “Loop Corrections to Supergravity on  $AdS_5 \times S^5$ ”, *Phys. Rev. Lett.* **119**, 171601 (2017) [10.1103/PhysRevLett.119.171601](https://doi.org/10.1103/PhysRevLett.119.171601), [arXiv:1706.02388](https://arxiv.org/abs/1706.02388) [[hep-th](#)].
- <sup>259</sup>L. F. Alday, D. Gaiotto, J. Maldacena, A. Sever, and P. Vieira, “An Operator Product Expansion for Polygonal null Wilson Loops”, *JHEP* **04**, 088 (2011) [10.1007/JHEP04\(2011\)088](https://doi.org/10.1007/JHEP04(2011)088), [arXiv:1006.2788](https://arxiv.org/abs/1006.2788) [[hep-th](#)].
- <sup>260</sup>B. Basso, A. Sever, and P. Vieira, “Spacetime and Flux Tube S-Matrices at Finite Coupling for  $N=4$  Supersymmetric Yang-Mills Theory”, *Phys. Rev. Lett.* **111**, 091602 (2013) [10.1103/PhysRevLett.111.091602](https://doi.org/10.1103/PhysRevLett.111.091602), [arXiv:1303.1396](https://arxiv.org/abs/1303.1396) [[hep-th](#)].
- <sup>261</sup>B. Basso, A. Sever, and P. Vieira, “Space-time S-matrix and Flux tube S-matrix II. Extracting and Matching Data”, *JHEP* **01**, 008 (2014) [10.1007/JHEP01\(2014\)008](https://doi.org/10.1007/JHEP01(2014)008), [arXiv:1306.2058](https://arxiv.org/abs/1306.2058) [[hep-th](#)].
- <sup>262</sup>B. Basso, A. Sever, and P. Vieira, “Space-time S-matrix and Flux-tube S-matrix III. The two-particle contributions”, *JHEP* **08**, 085 (2014) [10.1007/JHEP08\(2014\)085](https://doi.org/10.1007/JHEP08(2014)085), [arXiv:1402.3307](https://arxiv.org/abs/1402.3307) [[hep-th](#)].
- <sup>263</sup>B. Basso, A. Sever, and P. Vieira, “Collinear Limit of Scattering Amplitudes at Strong Coupling”, *Phys. Rev. Lett.* **113**, 261604 (2014) [10.1103/PhysRevLett.113.261604](https://doi.org/10.1103/PhysRevLett.113.261604), [arXiv:1405.6350](https://arxiv.org/abs/1405.6350) [[hep-th](#)].
- <sup>264</sup>B. Basso, A. Sever, and P. Vieira, “Space-time S-matrix and Flux-tube S-matrix IV. Gluons and Fusion”, *JHEP* **09**, 149 (2014) [10.1007/JHEP09\(2014\)149](https://doi.org/10.1007/JHEP09(2014)149), [arXiv:1407.1736](https://arxiv.org/abs/1407.1736) [[hep-th](#)].
- <sup>265</sup>S. Pasterski, S.-H. Shao, and A. Strominger, “Flat Space Amplitudes and Conformal Symmetry of the Celestial Sphere”, *Phys. Rev.* **D96**, 065026 (2017) [10.1103/PhysRevD.96.065026](https://doi.org/10.1103/PhysRevD.96.065026), [arXiv:1701.00049](https://arxiv.org/abs/1701.00049) [[hep-th](#)].
- <sup>266</sup>S. Pasterski and S.-H. Shao, “Conformal basis for flat space amplitudes”, *Phys. Rev.* **D96**, 065022 (2017) [10.1103/PhysRevD.96.065022](https://doi.org/10.1103/PhysRevD.96.065022), [arXiv:1705.01027](https://arxiv.org/abs/1705.01027) [[hep-th](#)].
- <sup>267</sup>K. Konishi, A. Ukawa, and G. Veneziano, “Jet Calculus: A Simple Algorithm for Resolving QCD Jets”, *Nucl. Phys.* **B157**, 45–107 (1979) [10.1016/0550-3213\(79\)90053-1](https://doi.org/10.1016/0550-3213(79)90053-1).
- <sup>268</sup>M.-X. Luo, V. Shtabovenko, T.-Z. Yang, and H. X. Zhu, “Analytic Next-To-Leading Order Calculation of Energy-Energy Correlation in Gluon-Initiated Higgs Decays”, (2019), [arXiv:1903.07277](https://arxiv.org/abs/1903.07277) [[hep-ph](#)].
- <sup>269</sup>L. J. Dixon, J. M. Drummond, and J. M. Henn, “Bootstrapping the three-loop hexagon”, *JHEP* **11**, 023 (2011) [10.1007/JHEP11\(2011\)023](https://doi.org/10.1007/JHEP11(2011)023), [arXiv:1108.4461](https://arxiv.org/abs/1108.4461) [[hep-th](#)].
- <sup>270</sup>L. J. Dixon, J. M. Drummond, M. von Hippel, and J. Pennington, “Hexagon functions and the three-loop remainder function”, *JHEP* **12**, 049 (2013) [10.1007/JHEP12\(2013\)049](https://doi.org/10.1007/JHEP12(2013)049), [arXiv:1308.2276](https://arxiv.org/abs/1308.2276) [[hep-th](#)].



- <sup>271</sup>L. J. Dixon and M. von Hippel, “Bootstrapping an NMHV amplitude through three loops”, *JHEP* **10**, 065 (2014) [10.1007/JHEP10\(2014\)065](https://doi.org/10.1007/JHEP10(2014)065), [arXiv:1408.1505](https://arxiv.org/abs/1408.1505) [[hep-th](#)].
- <sup>272</sup>J. M. Drummond, G. Papathanasiou, and M. Spradlin, “A Symbol of Uniqueness: The Cluster Bootstrap for the 3-Loop MHV Heptagon”, *JHEP* **03**, 072 (2015) [10.1007/JHEP03\(2015\)072](https://doi.org/10.1007/JHEP03(2015)072), [arXiv:1412.3763](https://arxiv.org/abs/1412.3763) [[hep-th](#)].
- <sup>273</sup>L. J. Dixon, J. M. Drummond, C. Duhr, M. von Hippel, and J. Pennington, “Bootstrapping six-gluon scattering in planar  $N=4$  super-Yang-Mills theory”, *PoS LL2014*, 077 (2014) [10.22323/1.211.0077](https://doi.org/10.22323/1.211.0077), [arXiv:1407.4724](https://arxiv.org/abs/1407.4724) [[hep-th](#)].
- <sup>274</sup>J. Golden and M. Spradlin, “A Cluster Bootstrap for Two-Loop MHV Amplitudes”, *JHEP* **02**, 002 (2015) [10.1007/JHEP02\(2015\)002](https://doi.org/10.1007/JHEP02(2015)002), [arXiv:1411.3289](https://arxiv.org/abs/1411.3289) [[hep-th](#)].
- <sup>275</sup>S. Caron-Huot, L. J. Dixon, A. McLeod, and M. von Hippel, “Bootstrapping a Five-Loop Amplitude Using Steinmann Relations”, *Phys. Rev. Lett.* **117**, 241601 (2016) [10.1103/PhysRevLett.117.241601](https://doi.org/10.1103/PhysRevLett.117.241601), [arXiv:1609.00669](https://arxiv.org/abs/1609.00669) [[hep-th](#)].
- <sup>276</sup>S. Caron-Huot, L. J. Dixon, F. Dulat, M. von Hippel, A. J. McLeod, and G. Papathanasiou, “Six-Gluon Amplitudes in Planar  $\mathcal{N} = 4$  Super-Yang-Mills Theory at Six and Seven Loops”, Submitted to: *J. High Energy Phys.* (2019), [arXiv:1903.10890](https://arxiv.org/abs/1903.10890) [[hep-th](#)].
- <sup>277</sup>R. Bousso, Z. Fisher, S. Leichenauer, and A. C. Wall, “Quantum focusing conjecture”, *Phys. Rev.* **D93**, 064044 (2016) [10.1103/PhysRevD.93.064044](https://doi.org/10.1103/PhysRevD.93.064044), [arXiv:1506.02669](https://arxiv.org/abs/1506.02669) [[hep-th](#)].
- <sup>278</sup>R. Bousso, Z. Fisher, J. Koeller, S. Leichenauer, and A. C. Wall, “Proof of the Quantum Null Energy Condition”, *Phys. Rev.* **D93**, 024017 (2016) [10.1103/PhysRevD.93.024017](https://doi.org/10.1103/PhysRevD.93.024017), [arXiv:1509.02542](https://arxiv.org/abs/1509.02542) [[hep-th](#)].
- <sup>279</sup>S. Balakrishnan, T. Faulkner, Z. U. Khandker, and H. Wang, “A General Proof of the Quantum Null Energy Condition”, (2017), [arXiv:1706.09432](https://arxiv.org/abs/1706.09432) [[hep-th](#)].
- <sup>280</sup>A. Strominger, “Lectures on the Infrared Structure of Gravity and Gauge Theory”, (2017), [arXiv:1703.05448](https://arxiv.org/abs/1703.05448) [[hep-th](#)].
- <sup>281</sup>A. Strominger, “On BMS Invariance of Gravitational Scattering”, *JHEP* **07**, 152 (2014) [10.1007/JHEP07\(2014\)152](https://doi.org/10.1007/JHEP07(2014)152), [arXiv:1312.2229](https://arxiv.org/abs/1312.2229) [[hep-th](#)].
- <sup>282</sup>T. He, V. Lysov, P. Mitra, and A. Strominger, “BMS supertranslations and Weinberg’s soft graviton theorem”, *JHEP* **05**, 151 (2015) [10.1007/JHEP05\(2015\)151](https://doi.org/10.1007/JHEP05(2015)151), [arXiv:1401.7026](https://arxiv.org/abs/1401.7026) [[hep-th](#)].
- <sup>283</sup>A. Strominger and A. Zhiboedov, “Gravitational Memory, BMS Supertranslations and Soft Theorems”, *JHEP* **01**, 086 (2016) [10.1007/JHEP01\(2016\)086](https://doi.org/10.1007/JHEP01(2016)086), [arXiv:1411.5745](https://arxiv.org/abs/1411.5745) [[hep-th](#)].
- <sup>284</sup>E. Witten, “Bound states of strings and  $p$ -branes”, *Nucl. Phys.* **B460**, 335–350 (1996) [10.1016/0550-3213\(95\)00610-9](https://doi.org/10.1016/0550-3213(95)00610-9), [arXiv:hep-th/9510135](https://arxiv.org/abs/hep-th/9510135) [[hep-th](#)].

- <sup>285</sup>T. Banks, W. Fischler, S. H. Shenker, and L. Susskind, “M theory as a matrix model: A conjecture”, *Phys. Rev.* **D55**, 5112–5128 (1997) [10.1103/PhysRevD.55.5112](#), [arXiv:hep-th/9610043 \[hep-th\]](#).
- <sup>286</sup>R. Dijkgraaf, E. P. Verlinde, and H. L. Verlinde, “Matrix string theory”, *Nucl. Phys.* **B500**, 43–61 (1997) [10.1016/S0550-3213\(97\)00326-X](#), [arXiv:hep-th/9703030 \[hep-th\]](#).
- <sup>287</sup>L. Motl, “Proposals on nonperturbative superstring interactions”, (1997), [arXiv:hep-th/9701025 \[hep-th\]](#).
- <sup>288</sup>N. Seiberg, “Notes on theories with 16 supercharges”, *Nucl. Phys. Proc. Suppl.* **67**, 158–171 (1998) [10.1016/S0920-5632\(98\)00128-5](#), [arXiv:hep-th/9705117 \[hep-th\]](#).
- <sup>289</sup>F. Antonuccio, O. Lunin, S. Pinsky, H.-C. Pauli, and S. Tsujimaru, “The DLCQ spectrum of  $\mathcal{N} = (8, 8)$  super Yang-Mills”, *Phys. Rev.* **D58**, 105024 (1998), eprint: [hep-th/9806133](#).
- <sup>290</sup>R. Dijkgraaf, “Fields, strings, matrices and symmetric products”, in *Moduli of curves and abelian varieties* (Springer, 1999), pp. 151–199, [arXiv:hep-th/9912104 \[hep-th\]](#).
- <sup>291</sup>E. Witten, “ $\theta$  vacua in two-dimensional quantum chromodynamics”, *Nuovo Cim.* **A51**, 325 (1979) [10.1007/BF02776593](#).
- <sup>292</sup>G. ’t Hooft, “A property of electric and magnetic flux in nonabelian gauge theories”, *Nucl. Phys.* **B153**, 141–160 (1979) [10.1016/0550-3213\(79\)90595-9](#).
- <sup>293</sup>W. Nahm, “Supersymmetries and their representations”, *Nucl. Phys.* **B135**, 149 (1978) [10.1016/0550-3213\(78\)90218-3](#).
- <sup>294</sup>M. Gunaydin and S. V. Ketov, “Seven sphere and the exceptional N=7 and N=8 superconformal algebras”, *Nucl. Phys.* **B467**, 215–246 (1996) [10.1016/0550-3213\(96\)00088-0](#), [arXiv:hep-th/9601072 \[hep-th\]](#).
- <sup>295</sup>J. A. Harvey and G. W. Moore, “On the algebras of BPS states”, *Commun. Math. Phys.* **197**, 489–519 (1998) [10.1007/s002200050461](#), [arXiv:hep-th/9609017 \[hep-th\]](#).
- <sup>296</sup>Z. Guralnik and S. Ramgoolam, “Torons and D-brane bound states”, *Nucl. Phys.* **B499**, 241–252 (1997) [10.1016/S0550-3213\(97\)00286-1](#), [arXiv:hep-th/9702099 \[hep-th\]](#).
- <sup>297</sup>Z. Guralnik and S. Ramgoolam, “From 0-branes to torons”, *Nucl. Phys.* **B521**, 129–138 (1998) [10.1016/S0550-3213\(98\)00070-4](#), [arXiv:hep-th/9708089 \[hep-th\]](#).
- <sup>298</sup>W. Taylor, “Lectures on D-branes, gauge theory and M(atrices)”, in *2nd Trieste Conference on Duality in String Theory Trieste, Italy, June 16-20, 1997* (1997), [arXiv:hep-th/9801182 \[hep-th\]](#).

- <sup>299</sup>M. Henningson and N. Wyllard, “Low-energy spectrum of  $\mathcal{N} = 4$  super-Yang-Mills on  $T^3$ : Flat connections, bound states at threshold, and  $S$ -duality”, *JHEP* **06**, 001 (2007) [10.1088/1126-6708/2007/06/001](#), [arXiv:hep-th/0703172](#) [HEP-TH].
- <sup>300</sup>A. Lawrence, “ $\theta$ -angle monodromy in two dimensions”, *Phys. Rev.* **D85**, 105029 (2012) [10.1103/PhysRevD.85.105029](#), [arXiv:1203.6656](#) [hep-th].
- <sup>301</sup>M. F. Atiyah and R. Bott, “The Yang-Mills equations over Riemann surfaces”, *Philosophical Transactions of the Royal Society of London A: Mathematical, Physical and Engineering Sciences* **308**, 523–615 (1983) [10.1098/rsta.1983.0017](#).
- <sup>302</sup>A. Kapustin, “D-branes in a topologically nontrivial B field”, *Adv. Theor. Math. Phys.* **4**, 127–154 (2000), [arXiv:hep-th/9909089](#) [hep-th].
- <sup>303</sup>E. Witten, “Elliptic Genera and Quantum Field Theory”, *Commun. Math. Phys.* **109**, 525 (1987) [10.1007/BF01208956](#).
- <sup>304</sup>E. Witten, “On the Landau-Ginzburg description of  $\mathcal{N} = 2$  minimal models”, *Int. J. Mod. Phys.* **A9**, 4783–4800 (1994) [10.1142/S0217751X9400193X](#), [arXiv:hep-th/9304026](#) [hep-th].
- <sup>305</sup>F. Benini, R. Eager, K. Hori, and Y. Tachikawa, “Elliptic genera of two-dimensional  $\mathcal{N} = 2$  gauge theories with rank-one gauge groups”, *Lett.Math.Phys.* **104**, 465–493 (2014) [10.1007/s11005-013-0673-y](#), [arXiv:1305.0533](#) [hep-th].
- <sup>306</sup>F. Benini, R. Eager, K. Hori, and Y. Tachikawa, “Elliptic genera of 2d  $\mathcal{N} = 2$  gauge theories”, *Commun. Math. Phys.* **333**, 1241–1286 (2015) [10.1007/s00220-014-2210-y](#), [arXiv:1308.4896](#) [hep-th].
- <sup>307</sup>A. Gadde, S. Gukov, and P. Putrov, “(0,2) trialities”, *JHEP* **03**, 076 (2014) [10.1007/JHEP03\(2014\)076](#), [arXiv:1310.0818](#) [hep-th].
- <sup>308</sup>A. Gadde and S. Gukov, “2d index and surface operators”, *JHEP* **1403**, 080 (2014) [10.1007/JHEP03\(2014\)080](#), [arXiv:1305.0266](#) [hep-th].
- <sup>309</sup>C. Schweigert, “On moduli spaces of flat connections with nonsimply connected structure group”, *Nucl. Phys.* **B492**, 743–755 (1997) [10.1016/S0550-3213\(97\)00152-1](#), [arXiv:hep-th/9611092](#) [hep-th].
- <sup>310</sup>E. Witten, “Two-dimensional gauge theories revisited”, *J. Geom. Phys.* **9**, 303–368 (1992) [10.1016/0393-0440\(92\)90034-X](#), [arXiv:hep-th/9204083](#) [hep-th].
- <sup>311</sup>A. Gadde, S. Gukov, and P. Putrov, “Fivebranes and 4-manifolds”, (2013), [arXiv:1306.4320](#) [hep-th].
- <sup>312</sup>S. Cecotti, P. Fendley, K. A. Intriligator, and C. Vafa, “A new supersymmetric index”, *Nucl. Phys.* **B386**, 405–452 (1992) [10.1016/0550-3213\(92\)90572-S](#), [arXiv:hep-th/9204102](#) [hep-th].
- <sup>313</sup>S. Gukov, E. Martinec, G. W. Moore, and A. Strominger, “An index for 2D field theories with large  $\mathcal{N} = 4$  superconformal symmetry”, (2004), [arXiv:hep-th/0404023](#) [hep-th].

- <sup>314</sup>A. O. L. Atkin, P. Bratley, I. G. Macdonald, and J. K. S. McKay, “Some computations for  $m$ -dimensional partitions”, in *Mathematical proceedings of the cambridge philosophical society*, Vol. 63, 04 (Cambridge Univ Press, 1967), pp. 1097–1100.
- <sup>315</sup>R. Dijkgraaf, G. W. Moore, E. P. Verlinde, and H. L. Verlinde, “Elliptic genera of symmetric products and second quantized strings”, *Commun. Math. Phys.* **185**, 197–209 (1997) [10.1007/s002200050087](https://doi.org/10.1007/s002200050087), [arXiv:hep-th/9608096](https://arxiv.org/abs/hep-th/9608096) [hep-th].
- <sup>316</sup>R. E. Borcherds, “Automorphic forms on  $O_{s+2,2}(R)$  and infinite products”, *Inventiones mathematicae* **120**, 161–213 (1995) [10.1007/BF01241126](https://doi.org/10.1007/BF01241126).
- <sup>317</sup>B. Assel, D. Cassani, L. Di Pietro, Z. Komargodski, J. Lorenzen, and D. Martelli, “The Casimir Energy in Curved Space and its Supersymmetric Counterpart”, *JHEP* **07**, 043 (2015) [10.1007/JHEP07\(2015\)043](https://doi.org/10.1007/JHEP07(2015)043), [arXiv:1503.05537](https://arxiv.org/abs/1503.05537) [hep-th].
- <sup>318</sup>Z. Komargodski and D. Simmons-Duffin, “The Random-Bond Ising Model in 2.01 and 3 Dimensions”, *J. Phys.* **A50**, 154001 (2017) [10.1088/1751-8121/aa6087](https://doi.org/10.1088/1751-8121/aa6087), [arXiv:1603.04444](https://arxiv.org/abs/1603.04444) [hep-th].
- <sup>319</sup>S. Meneses, S. Rychkov, J. M. V. P. Lopes, and P. Yvernay, “A structural test for the conformal invariance of the critical 3d Ising model”, (2018), [arXiv:1802.02319](https://arxiv.org/abs/1802.02319) [hep-th].
- <sup>320</sup>L. Hadasz, Z. Jaskolski, and P. Suchanek, “Recursive representation of the torus 1-point conformal block”, *JHEP* **01**, 063 (2010) [10.1007/JHEP01\(2010\)063](https://doi.org/10.1007/JHEP01(2010)063), [arXiv:0911.2353](https://arxiv.org/abs/0911.2353) [hep-th].
- <sup>321</sup>P. Kraus, A. Maloney, H. Maxfield, G. S. Ng, and J.-q. Wu, “Witten Diagrams for Torus Conformal Blocks”, *JHEP* **09**, 149 (2017) [10.1007/JHEP09\(2017\)149](https://doi.org/10.1007/JHEP09(2017)149), [arXiv:1706.00047](https://arxiv.org/abs/1706.00047) [hep-th].
- <sup>322</sup>N. E. J. Bjerrum-Bohr, J. F. Donoghue, and P. Vanhove, “On-shell Techniques and Universal Results in Quantum Gravity”, *JHEP* **02**, 111 (2014) [10.1007/JHEP02\(2014\)111](https://doi.org/10.1007/JHEP02(2014)111), [arXiv:1309.0804](https://arxiv.org/abs/1309.0804) [hep-th].
- <sup>323</sup>M. S. Costa and T. Hansen, “Conformal correlators of mixed-symmetry tensors”, *JHEP* **1502**, 151 (2015) [10.1007/JHEP02\(2015\)151](https://doi.org/10.1007/JHEP02(2015)151), [arXiv:1411.7351](https://arxiv.org/abs/1411.7351) [hep-th].
- <sup>324</sup>L. Freyhult, “Review of AdS/CFT Integrability, Chapter III.4: Twist States and the cusp Anomalous Dimension”, *Lett. Math. Phys.* **99**, 255–276 (2012) [10.1007/s11005-011-0483-z](https://doi.org/10.1007/s11005-011-0483-z), [arXiv:1012.3993](https://arxiv.org/abs/1012.3993) [hep-th].
- <sup>325</sup>R. H. Boels, T. Huber, and G. Yang, “Four-Loop Nonplanar Cusp Anomalous Dimension in  $N=4$  Supersymmetric Yang-Mills Theory”, *Phys. Rev. Lett.* **119**, 201601 (2017) [10.1103/PhysRevLett.119.201601](https://doi.org/10.1103/PhysRevLett.119.201601), [arXiv:1705.03444](https://arxiv.org/abs/1705.03444) [hep-th].
- <sup>326</sup>R. H. Boels, T. Huber, and G. Yang, “The nonplanar cusp and collinear anomalous dimension at four loops in  $\mathcal{N} = 4$  SYM theory”, *PoS RADCOR2017*, 042 (2017) [10.22323/1.290.0042](https://doi.org/10.22323/1.290.0042), [arXiv:1712.07563](https://arxiv.org/abs/1712.07563) [hep-th].
- <sup>327</sup>J. M. Henn, T. Peraro, M. Stahlhofen, and P. Wasser, “Matter dependence of the four-loop cusp anomalous dimension”, (2019), [arXiv:1901.03693](https://arxiv.org/abs/1901.03693) [hep-ph].

- <sup>328</sup>N. Beisert, B. Eden, and M. Staudacher, “Transcendentality and Crossing”, *J. Stat. Mech.* **0701**, P01021 (2007) [10.1088/1742-5468/2007/01/P01021](https://doi.org/10.1088/1742-5468/2007/01/P01021), [arXiv:hep-th/0610251](https://arxiv.org/abs/hep-th/0610251) [[hep-th](#)].
- <sup>329</sup>L. Freyhult, A. Rej, and M. Staudacher, “A Generalized Scaling Function for AdS/CFT”, *J. Stat. Mech.* **0807**, P07015 (2008) [10.1088/1742-5468/2008/07/P07015](https://doi.org/10.1088/1742-5468/2008/07/P07015), [arXiv:0712.2743](https://arxiv.org/abs/0712.2743) [[hep-th](#)].
- <sup>330</sup>L. J. Dixon, “The Principle of Maximal Transcendentality and the Four-Loop Collinear Anomalous Dimension”, *JHEP* **01**, 075 (2018) [10.1007/JHEP01\(2018\)075](https://doi.org/10.1007/JHEP01(2018)075), [arXiv:1712.07274](https://arxiv.org/abs/1712.07274) [[hep-th](#)].
- <sup>331</sup>L. Brink, J. H. Schwarz, and J. Scherk, “Supersymmetric Yang-Mills theories”, *Nucl. Phys.* **B121**, 77–92 (1977) [10.1016/0550-3213\(77\)90328-5](https://doi.org/10.1016/0550-3213(77)90328-5).